R&D 6274-CH-01

(2)

# PROCEEDINGS THIRD SYMPOSIUM ON ANALYSIS AND DETECTION OF EXPLOSIVES

AD-A213 614

DTIC
ELECTE
SEP 20 1989
S D
D

DISTRIBUTION STATEMENT A
Approved for public release;
Distribution Unlimited

Organized by
Fraunhofer-Institut für
Chemische Technologie (ICT)

Bundesakademie für
Wehrverwaltung und
Wehrtechnik (BAkWVT)

DTIC FILE COPY

89 9 20 112

# PROCEEDINGS THIRD SYMPOSIUM ON ANALYSIS AND DETECTION OF EXPLOSIVES

DAJA45-89-M-0225

Sponsored by:
Ministry of Defense, FRG

US Army Research and Development
and Standardization Group, London, UK

Office of Naval Research
European Office, US Navy, London, UK

Organized by
Fraunhofer-Institut für
Chemische Technologie (ICT)

Bundesakademie für
Wehrverwaltung und
Wehrtechnik (BAkWVT)

Accesion For
NTIS CRA&I ☑
DTIC TAB ☐
Unannounced ☐
Justification
By per form 50
Distribution /
Availability Codes
Dist | Avail and / or Special
A-1

*Herausgeber/Editor:*

Fraunhofer-Institut für Chemische Technologie (ICT)
*vormals:*
Fraunhofer-Institut für Treib- und Explosivstoffe
Joseph-von-Fraunhofer-Straße, Postfach 1240
D-7507 Pfinztal 1 (Berghausen)
Bundesrepublik Deutschland
Telefon (0721) 4640-0
Telex 7826909 ict d
Telefax (0721) 4640-111

*Herstellung:* dws, Karlsruhe
Printed in Germany

1989

## PREFACE

The Third Symposium is held at the Bundesakademie für Wehrverwaltung und Wehrtechnik (BakWVT), Mannheim, FRG, from July 10 to 13, 1989.

This Symposium is one of a series started in 1983 in Quantico, VA, USA. The Second Symposium was held in Neurim, Israel, 1986.

The Symposia have international attendance. The main purpose of these Symposia is to provide a forum for the discussion of the special problems in the field of analysis and detection of explosives: fundamental studies, applications, development of instrumentation and methods and their evaluation and the improvement of established techniques.

About 20 countries are expected to be represented at the Symposium. 48 papers have been submitted. Of these papers four have been withdrawn.

The Symposium also includes the display of instrumentation and equipment specialized for the needs of the analysis and detection of explosives research community.

Professor Jehuda Yinon of The Weizmann Institute of Science, Rehovot, Israel and Dr. Frank Conrad of Sandia National Laboratory, Albuquerque, NM, USA, have been invited as Keynote Speakers.

For the first time we have managed to have the Proceedings published in a hardbound volume prior to starting the Symposium. We hope this meets with your approval. This does, however, require strict adherence to deadlines for publishing. For those who have submitted the manuscript too late, we offer the possibility of publication in our Journal "Propellants, Explosives and Pyrotechniques".

Thank you all for your kind attendance. We wish you a most informative and enjoyable meeting.

Fred Volk, Fraunhofer Institut für Chemische Technologie, Pfinztal, FRG

H. Lehmann, Bundesakademie für Wehrverwaltung und Wehrtechnik, Mannheim, FRG

Forum-3rd Symposium Explosives Detectors; (KT)

TABLE OF CONTENTS


| PAPER | | PAGE |
|---|---|---|
| V 1 | *Keynote Lecture:* TECHNIQUES FOR THE DETECTION OF EXPLOSIVES<br>F. Conrad | 1-1 |
| V 2 | *Keynote Lecture:* ENVIRONMENTAL AND BIOMEDICAL APPLICATIONS OF ANALYSIS OF EXPLOSIVES<br>J. Yinon | 2-1 |
| V 3 | SYSTEMATIZED DIFFERENTIATION OF SMOKELESS POWDERS<br>R.A. Strobel, C.M. Selavka, R.O. Keto, R.E. Tontarski | 3-1 |
| V 4 | THE IDENTIFICATION OF MUSK AMBRETTE DURING A ROUTINE TEST FOR EXPLOSIVES<br>Y. Bamberger, S. Levy, T. Tamiri, S. Zitrin | 4-1 |
| V 5 | TRACE ANALYSIS OF EXPLOSIVES BY MASS SPECTROMETRY<br>M. Lee, D. Hwang, C. Tang | 5-1 |
| V 6 | APPLICATION OF CHROMATOGRAPHIC METHODS FOR IDENTIFICATION AND SEPARATION OF EXPLOSIVES, THEIR DEGRADATION AND BYPRODUCTS IN DIFFERENT MATRICES E.G. FORMULATIONS, WATER, SOIL AND AIR<br>H. Köhler | 6-1 |
| V 7 | EXPLOSIVES DETECTION USING ENERGETIC PHOTONS<br>J.R. Clifford, R.B. Miller, Wm.F. McCullough, Wm.K. Tucker | 7-1 |
| V 8 | MS/MS OF ENERGETIC COMPOUNDS. A COLLISION INDUCED DISSOCIATION STUDY OF SOME POLYNITROBIPHENYL-2-AMINES<br>J. Yinon, R.W. Read | 8-1 |

TABLE OF CONTENTS


| PAPER | | PAGE |
|---|---|---|
| V 9 | DETECTION AND PERSISTANCE OF TRACES OF SEMTEX AND SOME OTHER EXPLOSIVES ON SKIN SURFACES<br>J.B.F. Lloyd, R.M. King | 9-1 |
| V 10 | ANALYSIS OF PORTUGUESE EXPLOSIVES<br>J.M. de Morais Anes | 10-1 |
| V 11 | ANALYSIS OF THE EASTERN BLOC EXPLOSIVE SEMTEX<br>R.O. Keto | 11-1 |
| V 12 | ANALYSIS OF REACTION PRODUCTS OF PROPELLANTS AND HIGH EXPLOSIVES<br>F. Volk | 12-1 |
| V 13 | FUMÉES DE TIR: L'EXPÉRIENCE DU CERCHAR AVEC UNE CHAMBRE ÉTANCHE DE 15 $m^3$<br>D. Gaston, C. Michot | 13-1 |
| V 14 | THE DETERMINATION OF NITRIC OXIDES IN THE POST-DETONATION FUMES OF INDUSTRIAL EXPLOSIVES<br>R.B. Zimmermann | 14-1 |
| V 15 | DETERMINATION OF NITROGEN DIOXIDE GENERATED IN PROPELLANTS AND EXPLOSIVES BY POLAROGRAPHY AND HPLC WITH ELECTROCHEMICAL DETECTION<br>A. Bergens, J. Asplund | 15-1 |
| V 16 | PROCESSING THE POST-BLAST SCENE: AN INTEGRATED APPROACH<br>J.S. Deak, H. Clark, C. Dagens, J.J. Gaudet, B.W. Richardson | 16-1 |

TABLE OF CONTENTS


| PAPER | | PAGE |
|---|---|---|
| V 17 | IDENTIFICATION AND CHARACTERIZATION OF FLASH POWDERS<br><br>Ch.R. Midkiff, Jr. | 17-1 |
| V 18 | POST-BLAST RESIDUE ANALYSIS IN THE R.C.M.P. LABORATORIES<br><br>J.S. Deak, H. Clark, C. Dagensis, S. Jones, B.W. Richardson | 18-1 |
| V 19 | DETECTION AND ANALYSIS OF INORGANIC ANIONS IN EXPLOSIVE RESIDUES BY REVERSED-PHASE ION-PAIR CHROMATOGRAPHY<br><br>D. Woolfson-Bartfeld, E. Grushka, S. Abramovich-Bar, Y. Bamberger | 19-1 |
| V 20 | A FIELD TRIAL OF EXPLOSIVES DETECTORS FOR PERSONNEL AND BAGGAGE SEARCH<br><br>T. Sheldon | 20-1 |
| V 21 | NUCLEAR ACTIVATION ANALYSIS AND SCANNING ELECTRON MICROSCOPY IN FORENSIC GUNSHOT RESIDUE DETERMINATION: A CRITICAL EVALUATION<br><br>A. Brandone, M. Signori, F. DeFerrari, P. Pelliza | 21-1 |
| V 22 | FINGERPRINTING OF GUN POWDER<br><br>A. Brandone, M. Signori, F. DeFerrari, P. Pelliza | 22-1 |
| V 23 | DETECTION OF THE FOUR POLYMORPHS OF HMX, BOTH QUANTITATIVE AND QUALITATIVE USING DIFFERENCE METHODS<br><br>F. Hopfgarten | 23-1 |
| V 24 | POST EXPLOSION ANALYSIS BY NMR SPECTROSCOPY<br><br>Y. Bamberger, S. Zitrin, Y. Margalit | 24-1 |

TABLE OF CONTENTS


| PAPER | | PAGE |
|---|---|---|
| V 25 | EXPLOSIVE DETECTION WITH AN ION TRAP SPECTROMETER<br>S.A. McLuckey, G.L. Glish, B.C. Grant, | 25-1 |
| V 26 | IDENTIFICATION AND CONFIRMATION OF SOME NITROCAGE COMPOUNDS AND EXPLOSIVES BY DEMPS<br>T.H. Chen, C. Campbell | 26-1 |
| V 27 | THE HPLC DETERMINATION OF SOME PROPELLANT ADDITIVES<br>P. DeBruyne, J. Arijs, H. DeBisschop | 27-1 |
| V 28 | DETECTION AND IDENTIFICATION OF IMPURITIES IN EXPLOSIVES BY NMR-TECHNIQUE<br>M. Kaiser | 28-1 |
| V 29 | MULTICOMPONENT ANALYSIS OF EXPLOSIVES<br>F. Ark, T.H. Chen | 29-1 |
| V 30 | DIFFUSION ASPECTS OF TRACEABLE MATERIALS FOR EXPLOSIVES DETECTION<br>J.D. Gilbert | 30-1 |
| V 31 | GUNSHOT DISTANCE DETERMINATION BY MEANS OF NEUTRON ACTIVATION ANALYSIS AND AUTORADIOGRAPHY<br>A. Brandone, M. Signori, F. DeFerrari, P. Pelliza | 31-1 |
| V 32 | DETECTION OF EXTREMELY LOW CONCENTRATIIONS OF ULTRA PURE TNT BY RAT<br>S. Weinstein, R. Drozdenko, C. Weinstein | 32-1 |

TABLE OF CONTENTS


| PAPER | | PAGE |
|---|---|---|
| V 33 | FBI LABORATORY EVALUATION OF PORTABLE EXPLOSIVES VAPOR DETECTORS<br><br>D. Fetterolf | 33-1 |
| V 34 | AIRPORT TESTS OF FEDERAL AVIATION ADMINISTRATION THERMAL NEUTRON ACTIVATION EXPLOSIVE DETECTION SYSTEMS<br><br>Ch. Seher | 34-1 |
| V 35 | THE EVALUATION OF THE OAK RIDGE MS/MS EXPLOSIVES DETECTOR<br><br>F.J. Conrad, D.W. Hannum, B.C. Grant, S.A. McLuckey, H.S. McKnown, | 35-1 |
| V 36 | NUCLEAR BASED TECHNIQUES FOR EXPLOSIVE DETECTION - 1989 STATUS<br><br>T. Gozani, R. Morgado, Ch. Seher | 36-1 |
| V 37 | APPLICATION OF A DESORPTION-CONCENTRATION-INJECTION DEVICE (D.C.I. PLATINE) TO EXPLOSIVES DETECTION<br><br>J.C. Sarthou | 37-1 |
| V 38 | A MODEL OF EXPLOSIVE VAPOR CONCENTRATION<br><br>Th.A. Griffy | 38-1 |
| V 39 | DESIGN OF A HIGH PERFORMANCE GAS-PHASE EXPLOSIVES VAPOR PRECONCENTRATOR<br><br>D.P. Lucero | 39-1 |
| V 40 | SPECIFICITY AND INTERFERENT CHARACTERISTICS OF A BIOLUMINISCENT VAPOR DETECTION AND IDENTIFICATION SYSTEM<br><br>Elaine M. Boncyk | 40-1 |

TABLE OF CONTENTS


| PAPER | | PAGE |
|---|---|---|
| V 41 | COMPARISON OF DIFFERENT TECHNIQUES FOR THE HEAD SPACE ANALYSIS OF EXPLOSIVES<br>J.R. Hobbs, E. Conde | 41-1 |
| V 42 | DEVELOPMENT OF A MOBILE EXPLOSIVES DETECTION SYSTEM<br>R. Jackson, E.E.A. Bromberg | 42-1 |
| V 43 | LABORATORY EVALUATION OF PORTABLE AND WALK-THROUGH EXPLOSIVES VAPOR DETECTORS<br>L. Elias, P. Neudorfl | 43-1 |
| V 44 | PYROTECHNIC FLASH COMPOSITIONS<br>U. Krone, H. Treumann | 44-1 |
| V 45 | VERFAHREN ZUR ENTSCHÄRFUNG VON BOMBEN BZW. BOMBENBLINDGÄNGERN UNTER ANWENDUNG DER LOW-ORDER-SPRENGTECHNIK<br>M. Volk, W. Spyra | 45-1 |

# TECHNIQUES FOR THE DETECTION OF EXPLOSIVES

Mister Chairman

Esteemed Colleagues

Ladies and Gentlemen

Truly I feel privileged to have been asked to deliver the keynote address to this conference. I thank you.

I personally hope that the tone of this conference will be the exchange of information, ideas, and techniques of analysis and detection. I tell you that this conference is significant for many reasons, but for me one of the greatest reasons is that I do not have to try to explain concepts, numbers, properties and actions of molecules to governmental people who do not understand, and explain these in such a way that they think that they do understand. Do you have that problem also? Take my word--it is a treat to talk to people who understand the problem.

The title of this address, "Techniques for the Detection of Explosives," brings to my mind an automatic separation into Bulk Detection and Vapor Detection. There has been much research in the USA in both fields in the last few years. Since my area of interest is vapor detection, we will first consider the research in the bulk detection and then get to the interesting stuff.

In the area of X-ray the main developments have been in the computer enhancement of the images. Many of the regular instruments use color enhancement to assist the operators in detecting suspicious articles in baggage. However, some of the newer X-ray units work differently. One unit works by

differentiating the compton scattering of organic materials from the photoelectric attenuation of inorganic materials as well as the transmitted view on the video screen. This particular unit colors the different effects with different colors. Another unit uses backscattering to give additional information about the organic materials in bags and cases. One of the problems with this technique is the thickness of bags and possible shielding material attenuating the backscattered signal. One choice for a fix of this problem is to put in a forward scattered detector along with the backscattered detector which they have done.

A new technique for checked luggage is the Thermal Neutron Analysis (TNA) device. Although TNA itself is not new the use of the technique as a check for nitrogen in a bag at an airport is quite a departure from what has been acceptable in the near past. Extensive testing of this device has been carried out in airports in our state of California, which is our state with the most stringent safety standards, and the test results are impressive.

The technique of Nuclear Magnetic Resonance (NMR) has been studied for detecting explosives in baggage for a number of years. The obvious problem is when metal is introduced into the magnetic field. You know you have a problem when a bag passes through the magnetic field and the identification tag stands straight up at the end of its metal chain. Although there are problems using the technique there is still interest in NMR applications.

There is a possibility of developing a low power microwave detector as an explosives detector. Using the correct frequency to get the right 1/4 wave length one can measure the conductance and determine the dielectric constant of materials through other materials such as cloth, wall board, thin steel, etc. This could allow explosives and other materials of concern to be detected without dismantling the vehicle or disrobing the individual. One example of the operation of this device is to monitor bodily functions such as watching a heart move within a chest cavity in real time without operating. A few years ago the Lovelace Foundation in Albuquerque,

New Mexico, did some work on monitoring heart functions through a wall without the patient knowing and being disturbed by the monitoring.

Now let us look at the interesting science! Let's look at vapor detection of explosives. The techniques that we discussed before were just application of known technology. Now we are entering an unknown space where everything is not cut and dried but we must learn new material. At this time let me apologize to any "dog" people who might be here because I have not addressed their problem at all.

Although we have made great strides in vapor detection in the past few years we still have many problems. One main problem is the pressure that is being applied by the recent incidents in the airline industry. Since most of us got here by airplane, no one has to explain the urgency of developing an explosives detector that detects all the explosives of interest.

Since we cannot actively probe people with neutrons, X-rays, or whatever, we must concentrate on "sniffing" the vapors. As one looks at the complete field of vapor detection it is evident that there is a logical division of the field. The array divides into those situations that require "hand-held" sampling and those that require "portal" sampling. For example, searching a building for a bomb would at this time be a hand-held job where searching passengers entering an airport would be a portal scenario. In effect both the hand-held and the portal scenarios have identical requirements, i.e., getting the sample or sampling, separating the explosives molecules from air and interfering compounds or preconcentration, and having a detector that is sensitive enough to detect the molecules.

Any investigation obviously starts with the detector. If the detector is not sensitive enough to detect what is collected the enhancement of the other factors will not help. I feel there are currently four detectors to choose from depending on the scenario

for use. The four are an Electron Capture Detector with a Gas Chromatographic separator (GC-ECD), a Mass Spec/Mass Spec (MS/MS), an Ion Mobility Spectrometer (IMS), and a Chemiluminescence Detector. The GC-ECD and the IMS detectors are logical choices for hand-held devices with possible applications in other scenarios. The Chemiluminescence and MS/MS detectors are for larger installations. Let us say something about each of the detectors individually.

All of us who have GC with ECD detectors in our labs know that the commercial explosives detectors are not using the potential of the combination. The main problem is that since these molecules are sticky, the sample never reaches the detector and therefore cannot be detected. Look for a new GC-ECD detector in less than a year which under ideal conditions will detect all the molecules of interest.

In a paper that will be given at this conference we will describe an evaluation of the Oak Ridge MS/MS which was built for sampling mail. This unit was very easy to use and had a Limit Of Detection (LOD) of 3 ppt (30 femtograms/cc air in 6.4 cc air/sec) using the quartz sample tube as a preconcentrator.

The IMS detector as represented by the PC-100 sold by PCP Inc., West Palm Beach, Florida, has increased in sensitivity tremendously over the last few years. We mention the name only because this unit is the only IMS unit that we have numbers on. Recently we repeated the Limit Of Detection (LOD) determination on this unit and found it to be 0.3 ppt RDX (3 femtograms/cc in 3 cc/sec flow) in air. The LOD for the unit with a quartz tube preconcentrator and background subtraction is a factor of 10 lower than the above figure.

The chemilumimescence detector is a sensitive detector. Upon the addition of a GC column the detection unit becomes also specific and selective. I do not have the exact numbers for the sensitivity of the most recent unit. I can say there has been a tremendous

amount of work done with the technique in the last two years and there are people here who can give more information on the technique.

Next let us discuss sampling of an explosives vapor from a person in a portal configuration. A study was done at Sandia on this subject. The conclusion was that the best way to take a sample from an individual was with an air flow down across the head of the individual to the feet and to pick up the sample below the floor through a widely spaced grid. It seems the body is a reasonably good airfoil and the air flow follows the contours of the body (some contours easier than others) and picks up these molecules. These molecules are large and are greatly affected by air flows. In these tests they showed a strong preference to flow in a downward direction and with the flow of the air. Recent studies in Canada confirm the propensity of these molecules to follow the air flow. After the molecules pass through the grid they can be trapped on a preconcentrator or transferred in the air flow through the largest tube possible to the preconcentrator. We have already alluded to the "stickiness" of these molecules and their action can be simply stated that if they touch anything they stick to it. However, if they do not touch they can be transported to the preconcentrator. We do not propose to tell you that our way is the only way to sample because we see that most portal units sample from the side. We wonder how much of that decision was from science and how much from politics. One purveyor of commercial equipment admitted that his loss going to the side flow was only a factor of 5 or 6. I happen to think that we need every factor we can get our hands on. When we get to where we have extra factors of sensitivity, then we can afford to throw them away, but not now. To summarize this section it is sufficient to say that there remains much to be done in portal sampling of explosives vapors.

Now let us discuss a preconcentrator. A simple definition of an explosives preconcentrator is a selective filter that picks explosives molecules from a large air flow and holds them while dumping almost everything else overboard. These trapped molecules

are then released into a smaller flow resulting in a compression of the sample and therefore enhanced sensitivity. From studies at the University of Texas at Austin it was learned that silicon dioxide is a neutral oxide and is the most favorable material of all the materials studied for a preconcentrator. We have used quartz extensively as a preconcentrating material. We have just completed a study that evaluated a 6 mm O.D. quartz tube with a 6.4 mm quartz wool plug as a preconcentrator. It is an amazing device at low flows. Previous work had proven that 3.2 cm O.D. glass tube 7.6 cm long filled with glass melting point capillary tubing works well as a preconcentrator at flows of 1000 L/min. with a retention factor of approximately 30 percent.

Most of the other preconcentrators in use benefit from Sandia's experience in preconcentrators in that they use some form of silicon dioxide coating even if the units are covered with a GC coating.

We have discussed a number of problems that we have with these explosives molecules. However, there are a couple of additional characteristics of these molecules that should be discussed in this presentation and the first one is their adsorption from solutions. We had noticed previously when standard solutions were added to different glasses we obtained different concentrations when the resulting solutions were analyzed. Very simply stated we do not have standard solutions of these molecules because some of the molecules adsorb onto the walls of the volumetric containers. After studying this problem at Sandia, it was found that different glasses adsorb different quantities of explosives molecules from various solvents. In each case where the molecules were in solution in a solvent the coverage on the glass was limited to one monolayer as compared to multilayer coverage on glass surfaces when the molecules were adsorbed from vapor. When the glass surfaces were silylized there was no adsorption from the solutions studied. We find, however, that silylization of glass surfaces has little or no effect when capturing explosives vapors in a preconcentrator.

The second chacteristic that should be discussed is the diffusion of these molecules from boxes and bags. We will not spend much time on this subject because Professor Thomas Griffy will give us the theoretical equations for the diffusion of these molecules. The tests that we have done indicate that the diffusion times calculated by the professor for these molecules are reasonable. However, if one expects to detect explosives vapors from bags or boxes by sampling the outsides of the containers near cracks and holes, the times will be inordinately long.

In closing, I must say, "let us not be complacent and think the job has been done". Actually, we have almost succeeded in defining the problems. I think we can all agree on several points, the first being that explosive molecules are difficult to work with, when you can find them. The physical problems of sampling have had to be deciphered and solved. Yet there still remains some questions, particularly in the area of personnel sampling in booths. Secondly, preconcentration is a virtual necessity for vapor detection of explosives. Again, a great deal of effort by many groups has focused on this problem and although the problems may seem to have been solved for the most part there is additional work to do. We still must strive toward the impossible goal of 100% collection efficiency. Lastly, perhaps the most difficult problems have been encountered in the techniques for explosives detection because of the very low vapor pressure of most explosives. Again, technology has been developed which can detect most explosives under controlled conditions. However, there remains much to be done in this area because the limit of detection of these systems simply are not good enough yet to meet the demands of detecting devices prepared by technically competent terrorists.

Thank you.

# ENVIRONMENTAL AND BIOMEDICAL APPLICATIONS OF ANALYSIS OF EXPLOSIVES

Jehuda Yinon

Weizmann Institute of Science
76100 Rehovot, Israel

## ABSTRACT

The analysis of explosives and their metabolites in body fluids is of great importance because of the toxicity of many explosives. Personnel working in explosives and ammunition manufacturing plants are exposed to these toxic compounds which present a major health hazard. Periodical analysis of blood and urine of such personnel has to be made in order to detect traces of explosives and/or their metabolites.

In the environmental field, disposal of obsolete ammunition and discharge of waste waters from explosives manufacturing plants may cause serious contamination problems. Trace analysis of water and soil for the detection of explosives and their degradation products is therefore of great importance.

Examples of analytical methods including GC, HPLC, GC/MS and LC/MS for the analysis of explosives in body fluids, in water and in soil will be presented.

## 1. INTRODUCTION

All of us know about the destructive properties of explosives when detonated. However, the toxicity of many explosives present a major health hazard for ammunition workers and military personnel exposed to explosives [1]. For example, during the first seven and a half months of World War I, 17,000 TNT poisoning cases, including 475 deaths, occurred in munition factories in the U.S. [2]. However in World War II, during a period of 4 years, the total number of fatalities reported from all government-owned explosive plants in the U.S. amounted to 22 [3]. This lower rate of explosives poisoning fatalities was believed to be the direct result of a better understanding of the toxicity, diagnosis and prevention of explosives poisoning.

Several cases of intoxication with composition C-4, containing RDX, occurred during the Vietnam war and after it. Because it is a malleable solid, burns without explosion, and is relatively insensitive to impact and friction, composition C-4 can be easily transported and stored without special precautions. It was therefore used as a field cooking fuel which was the origin of many cases of intoxication [4].

Many studies were undertaken to determine the channels of absorption of explosives by the human body and the symptoms and clinical manifestations of poisoning by various explosives. In all these studies analyses of body fluids of animals and humans exposed to explosives were done in order to detect traces of these compounds and their metabolites. Periodical analysis of the body fluids of personnel working in explosives manufacturing plants is therefore necessary in order to detect traces of these explosives and their metabolites in the body fluids.

In the environmental field, disposal of explosives and their degradation products from munitions manufacturing plants and disposal sites, presents a serious and potentially hazardous contamination problem [5]. For example, a single TNT manufacturing plant can generate as much as 500,000 gallons of waste water per day which contain TNT as well as other nitrocompounds. Upon exposure to sunlight some of these compounds undergo chemical transformation, producing highly colored substances. In shell-loading plants large volumes of water are used to wash out residual explosives. All these waste waters are disposed of by discharging them into rivers or streams. Trace analysis of soil and water for explosives and their degradation products is of great importance in order to reveal the level of explosives contamination.

## 2. TOXIC EFFECTS OF EXPLOSIVES

Many of the widely used explosives have various toxic effects, and accordingly the symptoms and clinical manifestations are different.

### A. 2,4,6-Trinitrotoluene (TNT)

(1). Dermatitis. Typical signs and symptoms of dermatitis are irritation of the skin producing staining, redness, hardening and scaliness of the skin [6]. The initial lesion is usually noted on the exposed hands and forearms. TNT stains the skin of the hands a light yellow and discolors the hair to a reddish blond [7].

(2). Gastritis. Gastric complaints include nausea, vomiting, a feeling of fullness and occasionally a rather typical peptic ulcer syndrome [8]. It appears that complaints about gastrointestinal disorders such as distress, nausea, vomiting, loss of appetite and diarrhea are among the first signs and symptoms of severe TNT poisoning involving the liver [9].

(3). Cyanosis. One of the typical signs of TNT poisoning is cyanosis, which shows itself by a darkening of the blood color and in a palor of the skin with blueness of the lips [9]. Cyanosis is due to a chemical change in the hemoglobin of the red blood corpuscles, forming a mixture of methemoglobin and NO-hemoglobin and a consequent damage to the oxygen-carrying functions of the blood [10].

(4). Toxic jaundice. Toxic jaundice is a sign of advanced TNT poisoning and indicates severe liver damage. It carries a 30% mortality [10]. The symptoms include subcutaneous hemorrhages and pain in the area of the liver. Although toxic jaundice is usually associated with less serious symptoms, such as nausea, vomiting and cyanosis, it may occur suddenly without any other signs of poisoning [2].

(5). Aplastic anemia. Aplastic anemia is an advanced and severe type of TNT intoxication which is nearly always fatal. In aplastic anemia the blood-forming organs fail in function and a progressive loss of the blood elements results. Aplastic anemia may or may not be preceded by jaundice [10,11]. The signs and symptoms of aplastic anemia may be noticed only at a very late stage. These are palor, fatigue, giddiness, breathlessness on exertion, loss of appetite and weight, mild cough and bleeding from the nose and gums [3,12].

(6). Other symptoms. Signs and symptoms of TNT poisoning in the nervous system consist of dizziness, headache, fatigue and sleepiness [9]. In severe cases delirium, convulsions and coma may appear [13]. Cataract was diagnosed in long-term TNT workers [14].

B. 1,3,5-Trinitro-1,3,5-triazacyclohexane (hexogen, RDX)

Symptoms and clinical manifestations include convulsions followed by loss of consciousness. Additional clinical symptoms observed in humans poisoned by RDX included muscular cramps, dizziness, headache, nausea and vomiting [15,16]. The most frequent abnormal laboratory finding was a transient elevation of the white blood count [17].

C. Tetryl

(1). Dermatitis. Dermatitis is the most common symptom of tetryl poisoning. The dermatitis generally occurs between the second and third week of exposure [10,18]. Tetryl dermatitis begins nearly always on the face. First there is a slight itching and irritation, followed by puffiness around the eyes and a reddening, drying and cracking of the skin.

(2). Gastric tract. The main symptoms of gastric disorder due to tetryl poisoning are nausea and anorexia [19]. Other symptoms observed are epigastric pain, vomiting, diarrhea or constipation [20].

(3). Other symptoms. Additional symptoms observed in tetryl workers included headache, fatigue, vertigo, nervousness, sweating, insomnia, depression and apathy [20].

D. Nitroglycerin (NG)

The threshold for producing symptoms is so low, that the mere standing near a worker with traces of NG on his body or clothes is sufficient to induce prompt manifestations [21]. The most common symptoms of NG poisoning - mainly due to reduction of blood pressure - are headache, throbbing in the head, palpitation of the heart, nausea, vomiting and flushing. In severe cases, the signs are not due entirely to lowering of blood pressure. The heart muscle is affected directly and the heart beats are weakened. There may be delirium and convulsions or sudden collapse. The breathing is at first quickened and deepened, the respirations become slower and shallower, and death finally occurs from asphyxia due to paralysis of the respiratory center [22]. Mental disturbances due to NG exposure include drowsiness, stupor, insomnia, mental confusion, dizziness, hallucinations and maniacal manifestations [22]. After continuous exposure to NG for a number of years, an interruption of the exposure may be followed by pains in the chest. The pains resemble attacks of angina pectoris but do not occur in relation to exercise or emotional stimuli. These symptoms are called "withdrawal symptoms" and may sometimes result in death [23]. Several cases of sudden death in workers exposed to NG have been reported [24]. Death occurred on the weekends or on Monday morning, 30-72 hours after previous exposure to NG.

## 3. ANALYSIS OF EXPLOSIVES IN BODY FLUIDS

Analysis of traces of explosives and their metabolites in urine, blood and plasma has been carried out by a variety of methods including gas chromatography (GC), high performance liquid chromatography (HPLC), gas chromatography/mass spectrometry (GC/MS) and liquid chromatography/mass spectrometry (LC/MS). An integral and important part of such an analysis is the extraction of the explosive and/or metabolites from the body fluid before the actual analysis. Several examples of such analyses will be described for various explosives.

### A. Gas chromatography (GC)

Hexane extraction of NG in plasma and analysis by GC with electron capture detection was used by Hennig and Benecke [25]. They used a 1 m×3 mm I.D. silanized glass column packed with 3% OV-17 and 3.9% QF-1 on Chromosorb WAW-DMCS with nitrogen as carrier gas at a flow rate of 85 ml/min. Temperatures of injector, column and detector were 150°, 110° and 150°C respectively. Calibration and quantitation were done with dinitrobenzene (DNB) as internal standard. The lowest detection limit of NG in plasma was 0.1 ng/ml and the linearity range was 0.2 to 30 ng/ml.

Capillary column GC has been used extensively for the analysis of NG and its metabolites from plasma extracts. Lee et al. [26] used capillary GC with an electron capture detector and on column injection for the determination of NG and its dinitrate metabolites in human plasma. 1 ml-plasma samples were spiked with 2,6-dinitrotoluene as internal standard and extracted with 10 ml of a mixture of methylene chloride-pentane (30:70). The column was a 25 m×0.32 mm I.C. fused silica capillary column HP-1. The carrier gas was hydrogen at a flow rate of 15 ml/min. Column temperature was held at 96°C for 9 min and then increased at 4°C/min to 126°C. The limits of detection for NG, 1,2-dinitroglycerin and 1,3-dinitroglycerin in plasma were 0.025, 0.1 and 0.1 ng/ml respectively.

### B. High-performance liquid chromatography (HPLC)

A method, described by Turley and Brewster [27], uses HPLC with UV detection at 240 nm to detect RDX in serum and urine. The internal standard was 1 mg/ml of p-nitroacetanilide (PNA) in water. The samples were eluted with 0.5 ml of methanol through C-18 bonded-phase columns at a

pressure of 30-40 kPa (in order to separate RDX from interfering compounds), then evaporated to a volume of 0.1 ml of which 0.05 ml was injected into the HPLC. The column was a reversed-phase 30 cm × 3.9 mm I.D. μ Bondapack C-18 column. The mobile phase was methanol-water (35:65) at a flow rate of 1.8 ml/min. Figure 1 shows an HPLC chromatogram of urine containing RDX, the internal standard PNA and phenobarbital, which was used as an anticonvulsant for seizures produced by RDX poisoning. The lowest limit of detection of RDX was found to be 0.1 mg/l.

Fine et al. [28] used HPLC with a thermal energy analyzer (TEA®) detector for the analysis of RDX in blood. The HPLC column was a 30 cm × 3.9 mm I.D. μ Bondapack CN column. The mobile phase was isooctane-methylene chloride-methanol (60:30:10) at a flow rate of 1.5 ml/min. 5 ml of plasma spiked with RDX at the 5 ppb level was extracted with 16 ml of methylene chloride and pentane (1:1), filtered and concentrated to 0.2 ml, and analyzed by injecting 25 μl into the HPLC-TEA®. The minimal detectable amount of RDX was estimated to be about 100 pg/ml of plasma.

C. Gas chromatography/mass spectrometry (GC/MS)

Several groups used GC/MS with negative-ion chemical ionization (NICI) with single-ion monitoring for the determination of NG and its metabolites in plasma. Ottoila et al. [29] used BTN as internal standard. Extraction from plasma was done with pentane. The GC column was a 25 m × 0.3 mm I.D. fused silica capillary column with a 0.5μ thick SE-30 liquid film. Helium flow rate was 2 ml/min. After a splitless injection of 0.5 μl of plasma extract at 40°C, the column temperature was raised to 150°C. GC/MS interface and ion source temperatures were 150° and 130°C respectively. Methane was used as CI reagent gas. The ion monitored was $(^{15}O_3)^-$ at m/z 62. The lowest detection limit was 50 pg/ml and the linearity obtained was in the range of 50-1600 pg/ml.

D. Liquid chromatography/mass spectrometry (LC/MS)

LC/MS was used for the detection and identification of TNT and its metabolites in urine and blood (30-34). For example, the toluene extracts from a series of urine samples taken from TNT munition workers were analyzed by micro-LC/MS [33]. The system consisted of a micro-HPLC system interfaced to a magnetic sector mass spectrometer by a direct liquid

introduction LC/MS interface. The column used was a reversed-phase RP-8 (C-8) microbore column, 10 cm × 2.1 mm I.D. Mobile phases were acetonitrile-water (37:63) and methanol-acetonitrile-water (20:18:62) at a flow rate of 120 µl/min. In this system the whole HPLC effluent (sample and mobile phase) was introduced into the ion source of the mass spectrometer. Chemical ionization (CI) was the mode of ionization, the mobile phase serving as CI reagent. A UV detector with a microbore cell, operating at 214 nm, was on line between the HPLC and the mass spectrometer. Two separate isocratic separations were used, one to separate 2-amino-4,6-dinitrotoluene (2-A), 4-amino-2,6-dinitrotoluene (4-A) and TNT (Figure 2), and the second to separate 2,4-diamino-6-nitrotoluene (2,4-DA) and 2,6-diamino-4-nitrotoluene (2,6-DA) (Figure 3). The LC/MS mass spectrum of the separated 4-A fraction is shown in Figure 4.

## 4. ANALYSIS OF EXPLOSIVES IN WATER AND SOIL

### A. Analysis of explosives and their degradation products in water

Contaminated groundwater by filtered wastes derived from TNT at an ammunition depot was analyzed by GC with a Ni-63 electron capture detector [5]. Groundwater samples were extracted with benzene and chromatographed isothermally at 180°C on a 6 ft × 1/4 inch glass column packed with 3% OV-101 or Gas Chrom Q. Ar-$CH_4$ (95:5) was used as carrier gas at a flow rate of 60 ml/min. Compounds identified included TNT, 2,4-DNT, 2-A and 4-A.

Jenkins et al. [35] diluted aqueous samples of munitions wastewater with methanol-acetonitrile (76:24), filtered them through a 0.4µ polycarbonate membrane and analyzed them by HPLC, using a Supelco LC-8 25 cm × 4.6 mm I.D. column. The mobile phase was methanol-acetonitrile-water (38:12:50) at a flow rate of 1.5 ml/min. A UV detector was used at 254 nm. Detection limit for RDX in water was estimated to be 22 µg/l.

Heller et al. [36] developed a rapid on-site device for the detection of TNT in effluent water from ammunition plants. The indicator tube consisted of a basic oxide section to convert the TNT to its Meisenheimer anions, followed by an alkyl quaternary ammonium chloride ion exchange resin which collected the colored anions. The length of the resultant stain was proportional to the concentration of TNT in the wastewater. Lower detection limit of TNT in water was 0.1 ppm.

B. Analysis of explosives in soil

Bongiovanni et al. [37] developed a method for the preparation and analysis of explosive-contaminated soils for trace amounts of 2,4-DNT, 2,6-DNT, TNT, RDX, HMX and tetryl. Extraction of tetryl, for example, was done with acetonitrile. In order to enhance the extraction and obtain uniformity of samples, soils were stabilized at 20-30% moisture and samples were homogenized. Analysis was performed by HPLC with UV detection at 254 nm. The column was a reversed-phase C-18 Radial-Pak$^R$ cartridge column. The mobile phase was methanol-water (40:60) at a flow rate of 2 ml/min. The detection limit was 4.59 ppm.

Another method, developed by Jenkins and Walsh [38], was used to determine the concentrations of RDX, HMX, TNT, 2,4-DNT and tetryl in soil. The method involved the extraction of a 2-g sample with 50 ml of acetonitrile using an ultrasonic bath procedure. A 10 ml portion of the extract was diluted with an equal amount of water and analyzed by reversed-phase HPLC with a UV detector at 254 nm and using 25 cm × 4.6 mm I.D. LC-18 and LC-CN columns. The mobile phase was water-methanol (50:50) at a flow rate of 1.5 ml/min. The detection limit for tetryl was 5.5 μg/g.

5. CONCLUSIONS

As some explosives are highly toxic compounds, munition workers and other personnel in continuous contact with explosives should take appropriate precautions to minimize that contact. The modes of absorption of most explosives are by inhalation, ingestion and skin absorption. Therefore adequate ventilation should be installed in such environments and protective hygiene measures should be enforced. Periodical analysis of urine and blood of munition workers should be carried out in order to detect traces of explosives and their metabolites before an irreversible damage has occurred.

In the environmental field it is necessary to perform analyses of groundwater and soil to detect explosives and their degradation products. Such analyses may reveal the contamination state of areas suspected to be contaminated by improper disposal of obsolete explosives or by waste waters from ammunition plants.

**REFERENCES**


1. J.A. Hathaway, J. Occ. Med., 19, 341, 1977.
2. A. McCausland and R.F. Hawkins, Virginia Med. Month., 71, 242, 1944.
3. W.J. McConnel and R.H. Flinn, J. Indust. Hyg. Toxicol., 28, 76, 1946.
4. A.I. Hollander and E.M. Colbach, Military Medicine, 134, 1529, 1969.
5. W.E. Pereira, D.L. Short, D.B. Manigold and F.K. Roscio, Bull. Environ. Contam. Toxicol., 21, 554, 1979.
6. S.R. Haythorn, J. Industr. Hygiene, 2, 298, 1920/21.
7. N.I. Sax, "Dangerous Properties of Industrial Materials", 4th edition, Var Nostrand Reinhold, New York, 1209-1210, 1975.
8. J.H. Eddy, J. Am. Med. Assoc., 125, 1169, 1944.
9. W.F. Van Oettingen, U.S. Public Health Bull., 271, 106, 1941.
10. J. Hilton and C.N. Swanston, Brit. Med. J., 509, October 11, 1941.
11. G.R. Minot, J. Industr. Hyg., 1, 301, 1919.
12. A.D. Crawford, Brit. Med. J. 430, August 21, 1954.
13. A. Livingstone-Learmonth and B.M. Cunningham, Lancet, 261, 1916.
14. P. Hassman, V. Hassmanova, D. Borovska, O. Preininoerovn, H. Hanus, J. Juran and J. Sverac, Cesk. Neurol. Neurochir., 41, 372, 1978.
15. M. Barsotti and G. Crotti, Med. Lavoro, 40, 107, 1949.
16. R.C Woody, G.L. Kearns, M.A. Brewster, C.P. Turley, G.B. Sharp and R.S. Lake, J. Toxicol. Clin. Toxicol., 24, 305, 1986.
17. W.B. Ketel and J.R. Hughes, Neurology, 22, 871, 1972.
18. L.J. Witkowski, C.N. Fisher and H.D. Murdock, J. Am. Med. Assoc., 119, 1406, 1942.
19. H.B. Troup, Brit. J. Ind. Med., 3, 20, 1946.
20. L. Noro, Wien Med. Wochschr., 91, 969, 1941.
21. A.N. Shoun, J. Am. Med. Assoc., 119, 1536, 1942.
22. I.M. Rabinowitch, Canad. Med. Assoc. J., 50, 199, 1944.
23. R.P. Lund, J. Heggendal and G. Johnsson, Brit. J. Industr. Med., 25, 136, 1968.
24. C. Hogstedt and K. Andersson, J. Occup. Med., 21, 553, 1979.
25. B. Hennig and R. Benecke, Pharmazie, 42, 507, 1987.
26. F.W. Lee, N. Watari, J. Rigod and L.Z. Benet, J. Chromatogr. Biom. Appl., 426, 259, 1988.
27. C.P. Turley and M.A. Brewster, J. Chromatogr. Biom. Appl., 421, 430, 1987.
28. D.H. Fine, W.C. Yu, E.U. Goff, E.C. Bender and D.J. Reutter, J. Forensic Sci., 29, 732, 1984.

29. P. Ottoila, J. Taskinen and A. Sothman, Biom. Mass Spectr., 9, 108, 1982.

30. J. Yinon and D.-G. Hwang, J. Chromatogr. Biom. Appl., 339, 127, 1985.

31. J. Yinon and D.-G. Hwang, Toxicol. Letters, 26, 205, 1985.

32. J. Yinon and D.-G. Hwang, J. Chromatogr. Biom. Appl., 375, 154, 1986.

33. J. Yinon and D.-G. Hwang, Biom. Chromatogr., 1, 123, 1986.

34. J. Yinon and D.-G. Hwang, J. Chromatogr., 394, 257, 1987.

35. T.F. Jenkins, D.C. Leggett, C.L. Grant and C.F. Bauer, Anal. Chem., 58, 170, 1986.

36. C.A. Heller, S.R. Greni and E.D. Erickson, Anal. Chem., 54, 286, 1982.

37. R. Bongiovanni, G.E. Podolak, L.D. Clark and D.T. Scarborough, Am. Ind. Hyg. Assoc. J., 45, 222, 1984.

38. T.F. Jenkins and M.E. Walsh, Development of an Analytical Method for Explosive Residues in Soil, Report No. CRREL 87-7, U.S. Army Cold Regions Research and Engineering Laboratory, Hanover, NH 03755, June 1987.

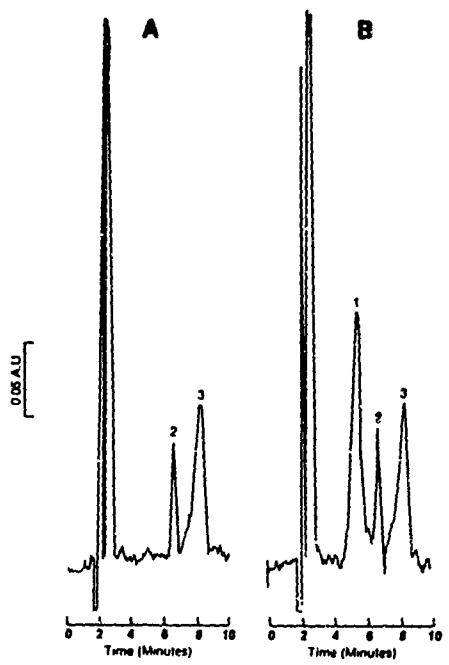


Fig. 1. Chromatograms of urine containing 5.0 mg/l RDX (peak 1), 20 mg/l phenobarbitol (peak 2) and the internal standard, PNA (peak 3). (A) Urine containing no RDX; (B) urine containing RDX. (C.P. Turley and M.A. Brewster, J. Chromatogr. 421, 430 (1987).

COLUMN: RP-8 MICROCOLUMN 2.1 mm I.D. × 10 cm
MOBILE PHASE ACETONITRILE-WATER (37.63)
FLOW RATE: 120 μl/min
UV WAVELENGTH: 214 nm

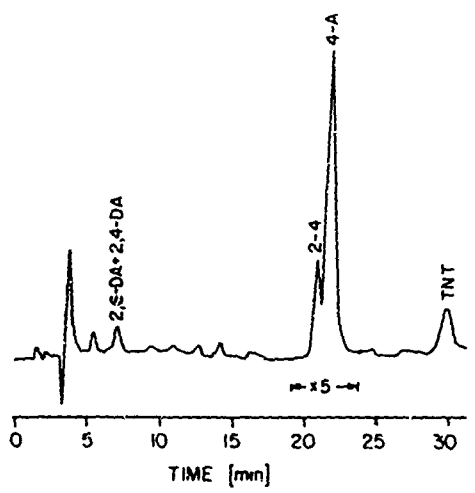


Figure 2. HPLC-UV chromatogram of a urine sample (J. Yinon and D.-G. Hwang, Biom. Chromatogr. 1, 123, 1986).

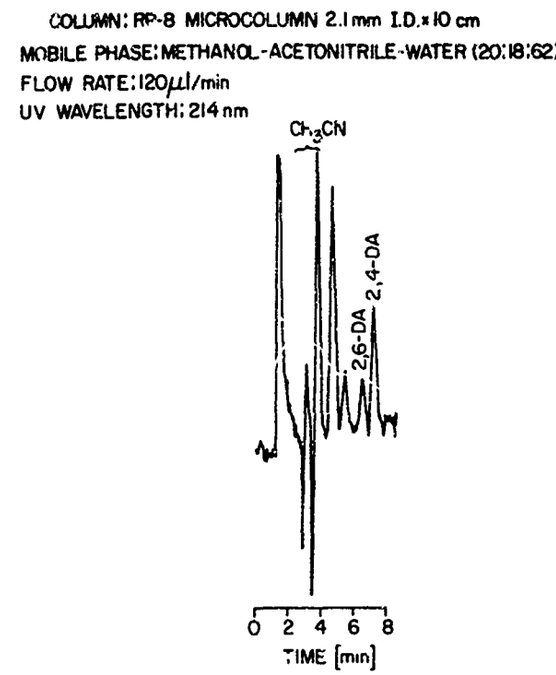


Figure 3. HPLC-UV chromatogram of urine sample showing the separation of 2,4-DA and 2,6-DA.

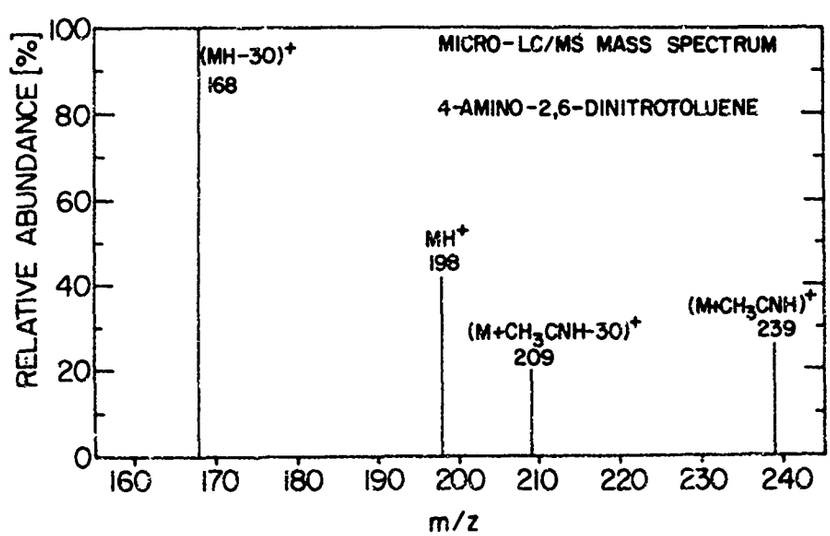


Figure 4. LC/MS mass spectrum of separated 4-A fraction from a urine sample.

# THE SYSTEMATIC IDENTIFICATION OF SMOKELESS POWDERS: AN UPDATE

Carl M. Selavka, Ph.D.

Forensic Toxicology Drug Testing Laboratory
Tripler Army Medical Center
Honolulu, Hawaii 96859-5000

Richard A. Strobel, B.S.
Richard E. Tontarski, M.F.S.*

Bureau of Alcohol, Tobacco and Firearms
National Laboratory Center
1401 Research Boulevard, Rockville, MD 20850

*Presenting Author, to Whom Correspondence Should Be Addressed

## Abstract

Smokeless powders are commonly recovered in post-blast debris from bombing scenes, or intact following seizures related to bomb incident investigations. Maximizing the amount of information obtained during the forensic examination of such

evidence is facilitated by comparison of the recovered particles of smokeless powder to a collection of known powder. This manuscript describes improvements in a systematic approach for the identification of canister smokeless powders developed at the Bureau of Alcohol, Tobacco and Firearms National Laboratory Center. The powders are readily available over the counter for ammunition reloading. The approach relies on simple stereo-microscopic examination of the evidence for determination of class (and, for many powders, individual) characteristics of the recovered powder, with subsequent instrumental and chromatographic tests used to further pare the list of possible sources, when needed. The basis for individualization is correlation of physical and chemical aspects of the unknown with those of a reference powder in the ATF's library of commercially available powders. As little material as a single particle of the questioned powder can be used to identify the powder. The library database search, previously validated in single-blind studies, has been simplified by improved computer search techniques. The discriminating power for flattened ball powders has been increased by the addition of ion chromatography and gas chromatography to the systematic scheme. Finally, the method has been used to advantage in a number of actual cases, and should find general applicability in any laboratory in which smokeless powders are examined during the performance of casework.

## Introduction

Significant progress has been made with respect to the systematic identification of high explosives, even in challenging crime scenes and on a multitude of post-blast media [1-5]. However, the bulk of the cases investigated in the United States by the Bureau of Alcohol, Tobacco and Firearms involve the use of devices containing either improvised explosives (such as sugar-chlorate mixtures) or commercially available low explosives (black powder, flash powder, and smokeless powders).

This reality has been the motivation for a number of studies that we have performed to try to improve the analytical power of conventional methods for the identification of low explosives [6-9]. However, we have been continually frustrated by the problems associated with the examination of smokeless powders, and the lack of sufficient literature methods to routinely identify the manufacturer of an unknown powder discovered during examination of evidence. For this reason, a research project was initiated to concretely define and develop a rapid, workable approach for systematically identifying smokeless powders.

The results of this project were first reported at the American Academy of Forensic Sciences Annual Meeting in 1988 [10], and the initial manuscripts for this work are being prepared for publication [11, 12]. The present manuscript is

designed to update the original report procedures, to describe work with ion chromatography that has enhanced differentiation of some ball and flattened ball powders, and to document changes made in the way he computer search is performed. A brief discussion of the original research will be offered, to provide the reader with a background for understanding these advances.

Review of the literature led us to the belief that most of the analyses previously proposed as forensic methods of choice would not allow for inexpensive, rapid and routine individualization of smokeless powders. And, it was our opinion that the failure of most of these previous methods was due to a lack of regard for the fundamentals of smokeless powder design, composition and manufacturing. However, a glimmer of the possibilities uncovered in our studies was found in the work of Zack and House in 1978 [13].

Table 1 lists typical primary formulations for single-, double- and triple-based smokeless powders. The differentiation of these three classes is usually based on the presence of nitrocellulose (NC) (single base), nitroglycerin (NG) and NC (double base), or nitroguanidine (NGu), NG and NC (triple base). Plasticizers assist in the formation of a dough-like mass from the base components during manufacturing, stabilizers prolong the shelf-life of powders by acting as scavengers of nitrous acid formed by thermal decomposition of nitro-compounds during storage, while most modifiers retard burning rates and reduce

muzzle flash during firing. Deterrents, plasticizers, ignition aids, flash suppressants and graphite are coated onto the grains in rotating drums during the manufacturing process. The resulting chemical composition within a group of morphologically comparable powders may often be similar.

**TYPICAL SMOKELESS POWDER FORMULATIONS**

| SINGLE BASE | DOUBLE BASE |
|---|---|
| NC-base component | NC-base component |
| EC-deterrent plasticizer | NG-base component |
| DBP-deterrent plasticizer | EC-deterrent plasticizer |
| DPA-stabilizer | DBP-deterrent plasticizer |
| DNT-burn modifier | 2-NDPA-stabilizer |
| Pot. Sulfate-burn modifier | DNT-burn modifier |
| | Pot. Sulfate-flash suppressant |
| | Pot. Nitrate-ignition aid |

TRIPLE BASE

NC-base component
NG-base component
NGu-base component
EC-deterrent plasticizer
DBP-deterrent plasticizer
2-NDPA-stabilizer

Table 1-Typical formulations for single-base, double-base and triple-base smokeless powders.

For our purposes, it is important to consider that the burning characteristics of commercially available canister powders are affected by both their chemical composition and morphology. The early studies of nitrocellulose by Vieille [14], and subsequent experiments by Belayev and Zeldovich [14], defined and described the burning process of nitrocellulose as occurring in a series of steps, in parallel layers of the grain. The

chemical composition is only one factor influencing the performance characteristics of the powder. The nature (progressive, neutral or degressive) and the duration (controlled by the smallest physical aspect of the powder grain because of the laminar burning process) of the burning is of critical importance to the manufacturer, and is predominantly controlled by the morphology of the powder.

The way that the manufacturer decides to fashion the morphology of a particular powder is influenced by his manufacturing capabilities, available materials, cost factors, and bias with respect to what may only be characterized as the aesthetics of the finished product. In most cases, a manufacturer will start with a given general manufacturing process, for example; Olin makes ball-grain powders, while Hercules uses extruded processing. They then alter physical dimensions and chemical composition until the full range of products demanded by reloaders and ammunition manufacturers has been covered. In and of itself, this fact allows for some simple categorization of powders from their gross morphology.

Figures 1 and 2 illustrate the gross morphological classes into which we have divided smokeless powders. These classes include lamel, disc, perforated disc, tube, rod, ball, flattened ball, agglomerated ball, irregular flake, and clump. Of these, only ball, flattened ball and agglomerated ball powders are manufactured using the ball-grain process; the others are

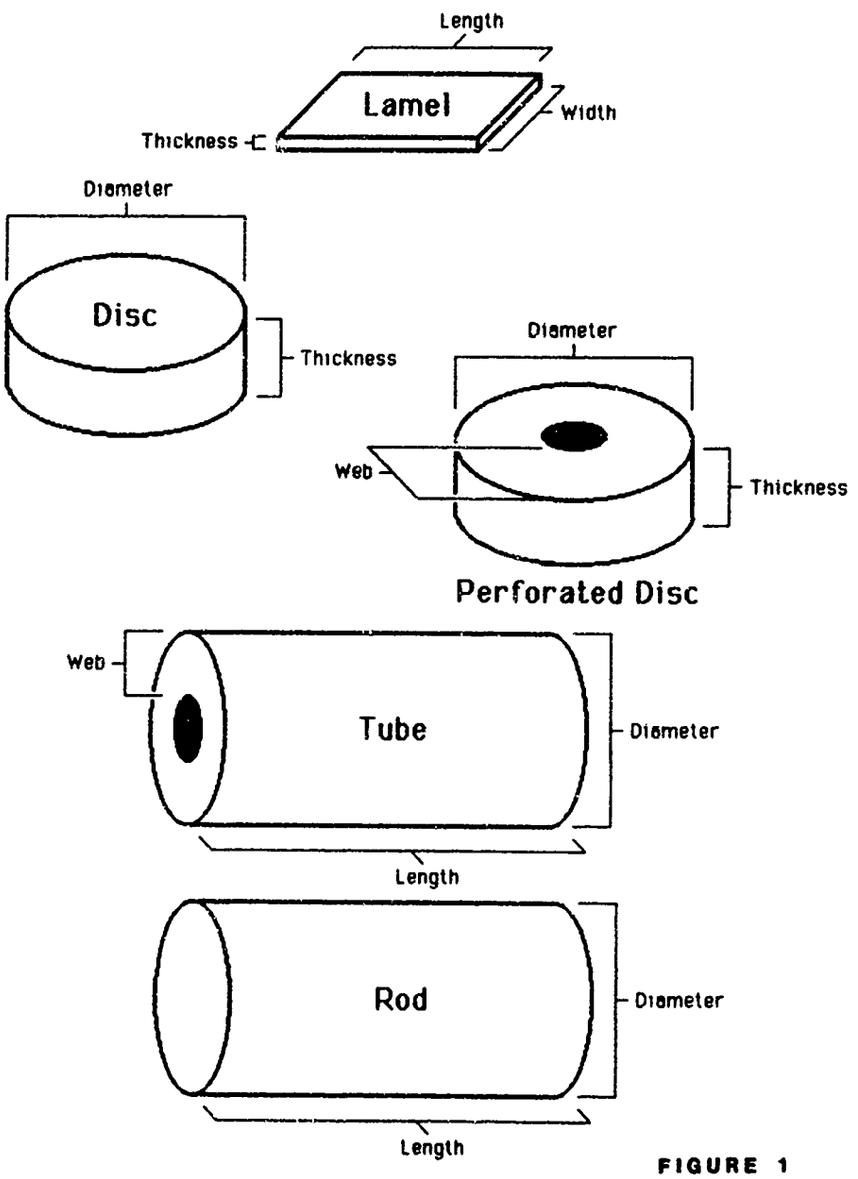
Length
Lamel
Width
Thickness
Diameter
Disc
Thickness
Diameter
Web
Thickness
Perforated Disc
Web
Tube
Diameter
Length
Rod
Diameter
Length

FIGURE 1

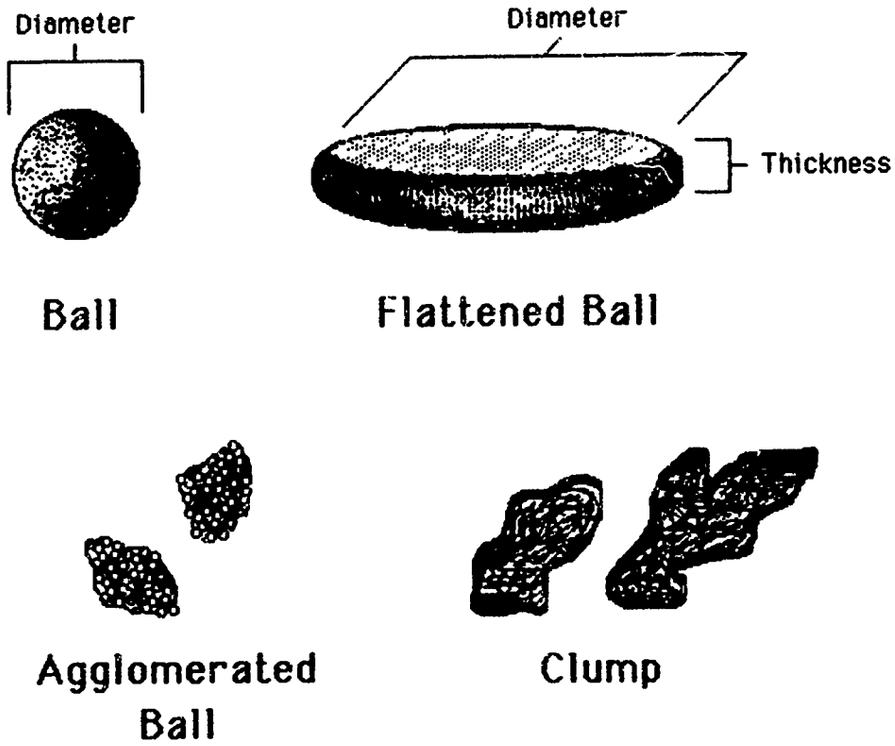
Diameter
Diameter
Thickness
Ball
Flattened Ball
Agglomerated Ball
Clump

FIGURE 2

produced by extrusion or rolling, followed by cutting and sizing. Morphological aspects found to provide high potential for discrimination are also shown in Figures 1 and 2. In addition, Table 2 lists the morphologies, manufacturers and distributors for smokeless powders currently available in the United States.

**Canister Powders Available in the United States, 1989**

| Manufacturer | Morphology | Marketed By |
|---|---|---|
| Olin (USA) | Flattened Ball<br>Ball | Winchester Western<br>Hodgdon Powder Co. (primarily surplus)<br>Accurate Arms (surplus) |
| Expro (Canada) (formerly DuPont) | Tube<br>Disc | IMR Powder Co. (formerly DuPont)<br>Hodgdon Powder Co. (surplus) |
| ICI Nobel (Scotland) | Tube<br>Lamel<br>Disc | Hodgdon Powder Co.<br>Smith & Wesson/Alcan<br>Scot Powder Co. |
| Hercules (USA) | Disc<br>Tube | Hercules |
| IMI (Israel) | Flattened Ball | Accurate Arms |
| Nobel | Tube | Hercules |

Table 2-Manufacturers, Morphologies and Distributors of Smokeless Powders in the United States

One of the most important experimental findings in our initial work was that propellent manufacturers maintain very tight control of the physical aspects of a given brand of powder, with automation and quality control insuring low lot-to-lot

variability in dimensions, chemical content and ballistic properties. Therefore, we were able to generate a database whose intra-brand morphological variabilities are significantly smaller than inter-brand variabilities. All database values use an identifying range of the mean measurement plus or minus two standard deviations (SD). This was generated from the measurement of dimensions for 50 particles, chosen at random from agitated canisters of the powder under examination. For all of the powders in our library, the measurement of appropriate physical aspects, determination of single- or double-base category of the powder (using TLC), and computerized searching of the database, quickly eliminate all but a few possible sources for a powder of unknown identity and source. In addition, many searches will bring up only a single possible source for an unknown recovered particle.

The one "problem class" of powders in the initial studies were the ball and flattened ball powders. Physical properties such as the inside and outside color of the powder and texture (the hardness or softness of the grain) allowed for further discrimination, but the analyst error rate involved with using such properties led to difficulties when the search was subjected to single-blind testing. Some initial studies using SEM-EDAX had indicated that there were differences in the inorganic content of many of the ball and flattened ball powders. For this reason, ion chromatography (IC) has been evaluated as another secondary segregating method. In addition, continued communication with

the manufacturers of ball-grain powders led to the re-evaluation of flattened ball particle diameter as a discriminating aspect. Finally, gas chromatographic determination of stabilizers and plasticizers was added to the testing methodology for some groups of similar powders. These modifications of the systematic analysis scheme are described in this report.

## Experimental

### Materials

All measurements of microscopic aspects were made using a Bausch & Lomb stereo-microscope (for smaller aspects), with an eyepiece calibrated to 2.5-um (at 70x), or an EPOi comparator (for larger measurements), calibrated to 10-um. Thin layer chromatography for nitroglycerin was performed using pre-scored, 5- x 25cm silica gel GHL plates (Analtech - Newark, DE), and a benzene:hexane (1:1) solvent system. Ion Chromatography (IC) was performed using a DIONEX Model 16, with eluents of 0.005N HCl for cations and 0.004M sodium bicarbonate/0.0024M sodium carbonate for anions with suppressed conductivity detection. GC-FID for plasticizers and stabilizers was performed on a Perkin-Elmer Sigma 3B, with a 0.25-mm x 15-m DB-1 (methyl silicone) capillary column (1.0um bonded phase thickness). Average linear gas flow rate was 73.5 cm/second of helium. The split ratio was 20 to 1.

Analysis conditions were: initial temperature 190 degrees C, ramp 10 degrees/minute to a final temperature of 230 degrees C with a 10 minute final hold.

## Procedures

Microscopic measurements of recovered or questioned particle aspects are performed by mounting the sample on common adhesive tape, using fine forceps for manipulation. The gross morphology of the unknown is determined first, and then the appropriate aspects for individualizing powders in that gross morphological class are measured (see Figures 1 and 2). Whenever possible, up to 10 recovered particles exhibiting identical gross morphology should be included in the examination of individualizing aspects, and the mean should be used in the database search. The database search statements required in our first report [12] have now been replaced by an R:Base ("prompt by example") search module, which is described below. Any additional discriminating factors required to more conclusively identify the unknown (e.g. identifying colored particles, single/double base) are evaluated either before the search begins, or after the list of possible sources has been pared to a few choices. The latter approach is often used when a search based on simple microscopic measurements reveals that there are differences in additional discriminators that could be used to advantage.

When further characterization of the chemical components are required, 1 to 3 particles of recovered powder are dissolved in acetone or dichloromethane (DCM), TLC is used to determine whether the powder extract contains nitroglycerine, which is characteristic of double-base smokeless powders. IC analyses are performed on 1mL aqueous extracts of 1 to 3 particles. Sodium, potassium, sulfate and nitrate may be used to characterize the presence or absence of a drying agent (sodium sulfate), ignition aid (potassium nitrate), or flash suppressant coating (potassium sulfate). Six to ten particles are extracted with 5 mL of DCM. Three to five uL injections are made on the GC-FID for characterization of ethyl centralite (EC) and dibutylphthalate (DBP) in flattened ball powders. HPLC is no longer used for the characterization of plasticizers and stabilizers.

## RESULTS AND DISCUSSION

The addition of IC and GC to the systematic method has improved our ability to routinely differentiate between powders in the ball and flattened ball group (e.g. those manufactured by Olin and Israeli Military Industries (IMI)). The systematic method has continually demonstrated strong discriminating ability for the remaining powder morphologies. In these cases, measurements of the appropriate aspects, and database searching,

quickly lead to a few or even a single potential source for the unknown. Table 3 lists the measurements taken for each type of powder.

Lamel
- *Width
- *Thickness
- +Width Range Hi/Lo
- +Thickness Range Hi/Lo

Disk
- *Diameter
- *Thickness
- *Idents
- *Base
- +Diameter Range Hi/Lo
- +Thickness Range Hi/Lo

Perforated Disc
- *Diameter
- *Thickness
- *Idents
- *Base
- *Web
- +Diameter Range Hi/Lo
- +Thickness Range Hi/Lo
- +Web Range Hi/Lo

Tube
- *Diameter
- *Base
- *Web
- *Length
- +Diameter Range Hi/Lo
- +Web Range Hi/Lo
- +Length Range Hi/Lo

Rod
- *Diameter
- *Base
- *Length
- +Diameter Range Hi/Lo
- +Length Range Hi/Lo

Ball
- *Diameter
- *Base
- +Ball Diameter Hi/Lo

Flattened Ball
- *Diameter
- *Thickness
- *Idents
- *Base
- +Diameter Range Hi/lo
- +Thickness Range Hi/Lo
- +Ball Diameter Hi/Lo

Agglomerated Ball
- *Diameter (agglomerate)
- *Ball Diameter
- *Thickness
- *Idents
- *Base
- +Diameter Range Hi/Lo
- +Thickness Range Hi/Lo
- +Ball Diameter Hi/Lo

*=examiner measured value  Base=single or double
+=computer calculated value from SD  Idents=colored markers
**Note**: one "clump" powder is available from Dupont; two "irregular flake" powders are available from Hodgdon

Table 3-Measurement Taken and derived for smokeless powder types

Flattened ball and ball powders continue to be the most difficult morphological class to differentiate. The thickness of flattened ball powder is determined by the gap set between two heavy rollers, through which sieved spherical powders fall during one of the final steps of the manufacturing process. It was our initial impression that thickness was the only useful dimensional aspect of measurement for differentiating these powders. However, continued examination of morphologically similar flattened ball powders, and continued communication with representatives at Olin and Accurate Arms, led to a re-evaluation of the measurement of flattened-ball diameter for added discrimination. Diameter is defined as shown in Figure 1.

Before the particle diameter measurement step is performed, an important particle selection step must occur. In this step, the only particles chosen for diameter measurement are those that were formed from a single particle of spherical powder entering the rollers. Any flattened ball particle that was formed by the agglomeration, or overlapping, of two or more spherical particles in the rolling process is not included in the measurement of this aspect. Typically, three or more particles of uniform diameter (each produced by the rolling of a single spherical powder grain) are measured, and the mean diameter is used in the database search.

On its face, it would appear that flattened-ball diameter would not be a useful criterion for characterizing an unknown particle. Because the thickness is typically the smallest physical dimension of flattened ball powders, and since the duration of burning of a grain of powder is predominantly affected by the smallest aspect, it would seem that the diameter of the flattened ball would be relatively unimportant to the ballistic properties of the product. However, the tolerance on the sieving of the ball powder grains preceding the rolling stage for these powders is very tightly controlled. As a result the spherical particles presented to the rollers for flattening have a narrow diameter range. In addition, the viscosity, porosity, plasticizer penetration depth, and formulation composition are tightly controlled. The result is that particles having nominally identical spherical dimensions, and rolled using identical roller gaps and pressures, will tend to give uniform particle thicknesses and diameters. Therefore, flattened ball diameters can improve differentiation of unknown particles having very similar particle thickness ranges.

By including the routine measurements of flattened ball diameter, the original flattened ball groups have been pared to a smaller number of groups, several of which contain fewer members (see Table 4). For example, Hodgdon H414 and Winchester Western 780 have similar thickness, but have significantly different diameters.

SMOKELESS POWDER DATABASE---

Search Results for:

PRINT SMOKEOUT SORTED BY NAME WHERE MORPH1 EQ "Flattened Ball" AND THRNGHI GE ".40" AND THRNGLO LE ".40"

Page 1

| Name | Current | Base | Type | Measurements Mean | SD | Low | High |
|---|---|---|---|---|---|---|---|
| Morphologies | Identifiers | | | | | | |
| AccArms AA-2460 | Yes | D | Thickness: | 0.35 | 0.03 | 0.29 | 0.41 |
| flattened ball | | | Diameter: | 0.63 | 0.05 | 0.53 | 0.73 |
| Ball | None | | Web: | ... | ... | ... | ... |
| | | | Length: | ... | ... | ... | ... |
| | | | Width: | ... | ... | ... | ... |
| Comments\\\ | | | Ball Diam: | ... | ... | 0.35 | 0.9 |
| Group 2 Flattened/Ball; see Group sheet for further analyses. | | | | | | | |
| Hodgdon H414 | Yes | D | Thickness: | 0.42 | 0.03 | 0.36 | 0.48 |
| flattened ball | | | Diameter: | 0.63 | 0.08 | 0.47 | 0.79 |
| | None | | Web: | ... | ... | ... | ... |
| | | | Length: | ... | ... | ... | ... |
| | | | Width: | ... | ... | ... | ... |
| Comments\\\ | | | Ball Diam: | ... | ... | 0.59 | 0.99 |
| Group 3 Flattened/Ball: see Group sheet for further analyses. | | | | | | | |
| Hodgdon H450 | Yes | D | Thickness: | 0.46 | 0.05 | 0.36 | 0.56 |
| flattened ball | | | Diameter: | 0.79 | 0.05 | 0.69 | 0.89 |
| | None | | Web: | ... | ... | ... | ... |
| | | | Length: | ... | ... | ... | ... |
| | | | Width: | ... | ... | ... | ... |
| Comments\\\ | | | Ball Diam: | ... | ... | 0.54 | 1.11 |
| Group 3 Flattened/Ball: see Group sheet for further analyses. | | | | | | | |
| WinchWest 780 | No | D | Thickness: | 0.39 | 0.03 | 0.33 | 0.45 |
| flattened ball | | | Diameter: | 0.95 | 0.09 | 0.77 | 1.13 |
| Ball | None | | Web: | ... | ... | ... | ... |
| | | | Length: | ... | ... | ... | ... |
| | | | Width: | ... | ... | ... | ... |
| Comments\\\ | | | Ball Diam: | ... | ... | 0.45 | 1.23 |
| Group 3 Flattened/Ball: see Group sheet for further analyses. | | | | | | | |
| WinchWest 785 | Yes | D | Thickness: | 0.42 | 0.02 | 0.38 | 0.46 |
| flattened ball | | | Diameter: | 0.94 | 0.07 | 0.8 | 1.08 |
| Ball | None | | Web: | ... | ... | ... | ... |
| | | | Length: | ... | ... | ... | ... |
| | | | Width: | ... | ... | ... | ... |
| Comments\\\ | | | Ball Diam: | ... | ... | 0.53 | 1.32 |
| Black matte outer finish. Group 3 Flattened/Ball: see Group sheet for further analyses. | | | | | | | |

TABLE 4A

SMOKELESS POWDER DATABASE---

Search Results for:

PRINT SMOKEOUT SORTED BY NAME WHERE MORPH1 EQ "Flattened Ball" AND THRNGHI GE ".40" AND THRNGLO LE ".40" AND DIRNGHI GE ".65" AND DIRNGLO LE ".65"

Page 1

| Name | Current | Base | Type | Measurements Mean | SD | Low | High |
|---|---|---|---|---|---|---|---|
| Morphologies | Identifiers | | | | | | |
| AccArms AA-2460 | Yes | D | Thickness: | 0 35 | 0.03 | 0.29 | 0.41 |
| flattened ball | | | Diameter: | 0.63 | 0.05 | 0.53 | 0.73 |
| Ball | None | | Web: | ... | ... | ... | ... |
| | | | Length: | ... | ... | .. | ... |
| | | | Width: | ... | ... | ... | ... |
| Comments\\\ | | | Ball Diam: | ... | ... | 0.35 | 0.9 |
| Group 2 Flattened/Ball; see Group sheet for further analyses. | | | | | | | |
| Hodgdon H414 | Yes | D | Thickness: | 0.42 | 0.03 | 0.36 | 0.48 |
| flattened ball | | | Diameter: | 0.63 | 0.08 | 0.47 | 0.79 |
| | None | | Web: | ... | ... | ... | ... |
| | | | Length: | ... | ... | ... | ... |
| | | | Width: | ... | ... | ... | ... |
| Comments\\\ | | | Ball Diam: | ... | .. | 0.59 | 0.99 |
| Group 3 Flattened/Ball: see Group sheet for further analyses. | | | | | | | |

TABLE 4B

The use of IC for discrimination of ball and flattened ball powders that exhibit similar morphological aspects has met with some success. The basis for the differences in measured levels of sulfate, nitrate, sodium and potassium ions in these powders is due to the use of sodium and potassium salts of these oxidizers as drying aids and flash suppression coatings. Most flattened ball products contain residual traces of sulfate, left over from the use of sodium sulfate in a dehydration step during the early stages of nitrocellulose processing. However, powders that have been coated with potassium sulfate as a flash suppressant during the final steps of processing will have significantly higher sulfate levels than those arising from the residual source. Using five particles and 1mL aqueous extracts, we have observed a sulfate level higher than observed with sodium sulfate alone. This establishes the presence of potassium sulfate in the powder being examined. Table 5 provides examples of flattened ball powders that are in the same morphological group, but which can be discriminated using IC determination of sulfate.

| POWDER | NO3 | SO4 | K | Na |
|---|---|---|---|---|
| AA-9 | W | - | M | M |
| AA No. 2 | W | - | - | W |
| WW 540 | M | M | M | M |
| WW 571 | S | M | M | M |

W=weak
M=medium
S=strong

AA=Accurate Arms
WW=Winchester Western

Table 5-Examples of observed IC results for ball and flattened ball powders

The original HPLC method used for the characterization of plasticizers, deterrents, stabilizers and their nitroso- and nitro-derivatives (formed by scavenging of nitrous acid by the stabilizers during propellent ageing), did not significantly help discriminate the powders. For this reason, a simple GC method has been incorporated for the determination of ethyl centralite (EC) and dibutylphthalate (DBP). The predominant segregating power offered by measurement of these two analytes is in the discrimination of Winchester-Western (Olin) ball and flattened ball powders from those manufactured in Israel for Accurate Arms. Higher nitroglycerin content smokeless powders manufactured by Olin tend to have less or no DBP. Any DBP observed may be from re-working powders. Accurate Arms powders tend to have appreciable amounts of DBP in all the powders examined. Examples of morphologically similar powders that can be differentiated using GC determination of EC and DBP are listed in Table 6.

| POWDER | EC | DBP |
|---|---|---|
| AA-9 | - | S |
| AA No. 2 | - | S |
| WW 231 | M | W |
| WW 680 | M | - |

EC=ethyl centralite
DBP=dibutylphthalate

W=weak
M=medium
S=strong

AA=Accurate Arms
WW=Winchester Western

Table 6-Examples of observed GC results for ball and flattened ball powders

One of the more frustrating characteristics of the database search, as originally described [12], was a rather complicated conditional statement had to be used to manually search the nested R:Base fields. As is typical with such manual search statements, a single transposition error, or lacking unit of punctuation, would lead to an error message. Laboratory personnel using the system found error messages and cryptic diagnostic codes frustrating.

With the introduction of the "prompt by example" mode of searching the R:Base smokeless powder data set, practical operation is substantially simplified. In this search mode, criteria for the conditional statements are loaded by the operator into a statement framework (see Examples 1a and 1b), and each is chosen by scrolling through a displayed menu of potential criteria. Following this simple procedure, the individual criteria are loaded with prompting. The final product is the same conditional search statement previously used, but is now generated by concatenation of the individually selected search criteria. An example of the screen displays, and operator selections, involved with the "prompt by example" R:Base search for determining the identity of an unknown disc powder is shown in Example 2.

```
MORPHOLOGY   SMOKELESS POWDER DATABASE SEARCH
Agglomerated Ball
Ball
Clump
Disc
Flattened Ball
Irregular Flake
Perforated Disc
Rod
Lamel
Tube
EVERYTHING
QUIT
```

EXAMPLE 1A

```
SEARCH ON   SMOKELESS POWDER DATABASE SEARCH
Start Search
Diameter
Thickness
Base
Identifiers
Redo
MORPHOLOGY

Current Morphology
Disc

Current Search Selections

Diameter (mm) 1.51
```

EXAMPLE 1B

SMOKELESS POWDER DATABASE---

Search Results for:

PRINT SMOKEOUT SORTED BY NAME WHERE MORPH1 EQ "Disc" AND DIRNGHI GE "1.51" AND DIRNGLO LE "1.51" AND THRNGHI GE "0.2" AND THRNGLO LE "0.2"

Page 1

| Name | Current | Base | Type | Measurements Mean | SD | Low | High |
|---|---|---|---|---|---|---|---|
| Herc Green Dot | Yes | D | Thickness: | 0.14 | 0.03 | 0.08 | 0.2 |
| Disc | | | Diameter: | 1.59 | 0.08 | 1.43 | 1.75 |
| | Green | | Web: | ... | ... | ... | ... |
| | | | Length: | ... | ... | ... | ... |
| | | | Width: | ... | ... | ... | ... |
| Comments\\\ | | | Ball Diam: | ... | ... | ... | ... |
| Some bias-cut edges. Group 1 Disc; see Group sheet for further analyses. | | | | | | | |
| Herc Herco | Yes | D | Thickness: | 0.17 | 0.03 | 0.11 | 0.23 |
| Disc | | | Diameter: | 1.49 | 0.07 | 1.35 | 1.63 |
| | None | | Web: | ... | ... | ... | ... |
| | | | Length: | ... | ... | ... | ... |
| | | | Width: | ... | ... | ... | ... |
| Comments\\\ | | | Ball Diam: | ... | ... | ... | ... |
| Some bias-cut edges. Group 1 Disc; see Group sheet for further analyses. | | | | | | | |
| Herc Unique | | D | Thickness: | 0.21 | 0.07 | 0.07 | 0.35 |
| Disc | | | Diameter: | 1.6 | 0.1 | 1.4 | 1.8 |
| | None | | Web: | ... | ... | ... | ... |
| | | | Length: | ... | ... | ... | ... |
| | | | Width: | ... | ... | ... | ... |
| Comments\\\ | | | Ball Diam: | ... | ... | ... | ... |
| Bias-cut not apparent. Group 1 Disc; see Group sheet for further analyses. | | | | | | | |

EXAMPLE 2

## Conclusions and Future Directions

In this manuscript, several improvements are described which make the systematic identification of smokeless powders easier, more accurate, and more definitive. The list of commercially available smokeless powders seems to change almost annually. Older products are phased out, newer products introduced, new importers enter the American market with new product lines, and changes are made in the corporate ownership of smokeless powder manufacturers. Despite this flux, ATF has made a commitment to continue our efforts with smokeless powders, due to the major role that these materials play as explosive fillers in recovered and detonated improvised explosive devices. Studies are planned to establish the possibility of differentiating powder lots within a brand, and to determine whether "single canister" identification is possible from nitroso- and nitro-analogue profiles in questioned and known powders. It is our desire to provide a clearinghouse for information and data useful for performing smokeless powder identification.

Work is continuing in IC, GC, and HPLC to further differentiate powders that remain in morphologically similar groups.

## Acknowledgments

The authors wish to acknowledge the contribution that Gregory P. Czarnopys and Cynthia Wallace made to the work described in this manuscript. We also appreciate the cooperation that we have received from other laboratories involved with bomb investigation and gunshot residue determinations. Thanks must also go to the propellent manufacturers who provided the information that has made this work possible.

## References


1. Beveridge, A.D., Payton, S.F., Audette, R.J., Lambertus, A.J. and Shaddick, R.C., "Systematic analysis of explosive residues", J. Forensic Sci., 20: 431-454 (1975).

2. Midkiff, C.R. and Washington, W.D., "Systematic approach to the detection of explosive residues. IV. Military explosives", J. Assoc. Off. Anal. Chem., 59: 1357-1374 (1976).

3. Washington, W.D. and Midkiff, C.R., "Explosive residues in bombing-scene investigations. New technology applied to their detection and identification", in Forensic Science 2d Ed. (G. Davies, Ed.), Washington, DC: American Chemical Society (1986),pp. 259-278.

4. Yinon, J. and Zitrin, S., The Analysis of Explosives, New York: Pergamon Press (1981).

5. J.Energetic Mat. 4 (1986). (Proceedings of the Second International Symposium on the Analysis and Detection of Explosives).

6. Meyers, R.E. "A systematic approach to the forensic examination of flash powders", J. Forensic Sci. 23: 66-73 (1978).

7. Meyers, R.E. and Meyers, J.A., "Instrumental techniques utilized in the identification of smokeless powders, proton magnetic resonance (PMR) and gas chromatography (GC)", in Proceedings of the First International Symposium on the Analysis and Detection of Explosives, Washington, D.C.: U.S. Government Printing Office (1984), pp. 93-106.

8. Keto, R.O., "Characterization of smokeless powder by pyrolysis capillary gas chromatography", J. Forensic Sci., 24: 74-82 (1988).

9. Selavka, C.M. and Strobel, R.A. "Evaporation method for retention of integrity of ionic explosive traces in post-blast debris extracts", (to be submitted for publication in J. Forensic Sci., 1989).

10. Selavka, C.M., Strobel, R.A., Keto, R.O. and Tontarski, R.E., "Systematized differentiation of smokeless powders", presented to the American Academy of Forensic Sciences Annual Meeting, Philadelphia, PA, FEB 88, paper 880089.

11. Selavka, C.M., Strobel, R.A. and Tontarski, R.E., "Generation of a systematic method for the differentiation of smokeless powders, 1. Historical data." (in preparation for submission to J. Forensic Sci. 1989).

12. Selavka, C.M., Strobel, R.A. and Tontarski, R.E., "Generation of a systematic method for the differentiation of smokeless powders, II. Analytical procedures." (in preparation for submission to J. Forensic Sci. 1989).

13. Zack, P.J. and House, J.E., "Propellant Identification by particle size measurement," J. Forensic Sci. 23: 74-77 (1978).

14. Urbanski, T., Chemistry and Technology of Explosives, Vol. 3, Chapters VII and VIII, Pergamon Press New York, reprinted 1985, pp. 528-668.

# THE IDENTIFICATION OF MUSK AMBRETTE DURING A ROUTINE TEST FOR EXPLOSIVES

Y. Bamberger, S. Levy, T. Tamiri and S. Zitrin

Division of Criminal Identification, Israel National Police,

Police Headquarters, Jerusalem, Israel

## ABSTRACT

Light yellow crystals were found on a man entering Israel from Jordan. In the border station, the material was tested with an explosives testing kit ("ETK") and the result was positive: a violet color, similar to that obtained with TNT, was formed. The material was then sent for a complete laboratory analysis. This is the normal procedure following a positive result in a field test. The material was analysed by TLC, IR, GC/MS (EI and CI modes) and NMR. It was subsequently identified as 1-tert-butyl-2-methoxy-3,5-dinitro-4-methylbenzene. This compound, known as "musk ambrette", is one of several artificial musks which are used in perfumes and related preparations.

## 1. INTRODUCTION

An unknown sample in the form of light yellow crystals was received in the analytical laboratory of the Israel National Police. The material was found during a search on a man entering Israel from Jordan through one of the bridges on the Jordan River. It was suspected by border security personnel to be an explosive after it had reacted positively to the Explosive Testing Kit ("ETK"). This kit (1) is used in the field to detect traces of explosives on suspects and also for preliminary tests of unknown materials in border stations. The material reacted to the first reagent in the ETK, giving a purple color which was similar to the color obtained with TNT.

This paper describes the identification of this material in our laboratory.

## 2. EXPERIMENTAL

Thin layer chromatography (TLC) plates were 10 x 20 cm aluminium plates precoated with silica gel 0.2 mm thick (SI F Riedel de Haen). The standard developing solvent was petrol ether : ethyl acetate (9:1) and the developed plates were sprayed with 3% KOH in ethanol (2).

Infrared (IR) spectra were recorded on an Analect model FX6160 Fourier transform IR spectrophotometer. A Wilks 1/2 in. (12.7 mm) diameter pellet holder was used to prepare the KBr pellets.

Gas chromatography/mass spectrometry (GC/MS) was carried out on a Finnigan 4500 quadrupole mass spectrometer. The GC column was a J&W fused silica capillary column, 15m x 0.25 mm (I.D.) with 0.25 mm coating of DB-5. GC temperatures were programmed from 70°C to 270°C at 15°C/min. Ion source temperature was 140°C. Scan range was 40-500 in the electron impact (EI) mode and 100-500 in the chemical ionization (CI) mode. Electron energy was 70eV. Helium was the GC carrier gas and methane was used as CI reagent gas.

Nuclear Magnetic Resonance (NMR) for protons was carried out on a BRUKER WP 200 instrument, operating at 200 MHz. The solvent was deuteriochloroform.

## 3. RESULTS AND DISCUSSION

TLC was performed on the unknown sample, using a standard TLC system for the analysis of explosives (see EXPERIMENTAL). A spot at Rf = 0.54 was observed under a UV lamp. It turned yellow after spraying with KOH solution and heating. 2,4,6 - TNT gave a purple color at Rf = 0.3 under these conditions. Color reactions with KOH and other bases could indicate the presence of a polynitroaromatic compound. These color reactions have been attributed to the formation of colored Mesenheimer complexes but other explanations have also been suggested (3).

The IR spectrum of the unknown sample is shown in Figure 1. The two characteristic bands of the aromatic nitro group (4), $\nu_s$ at 1350 $cm^{-1}$ and $\nu_{as}$ at 1527 $cm^{-1}$, are clearly present. This led us to assume that the sample contained a nitroaromatic compound. This assumption was further supported by similarities between the IR spectrum of the unknown and that of TNT (Figure 2).

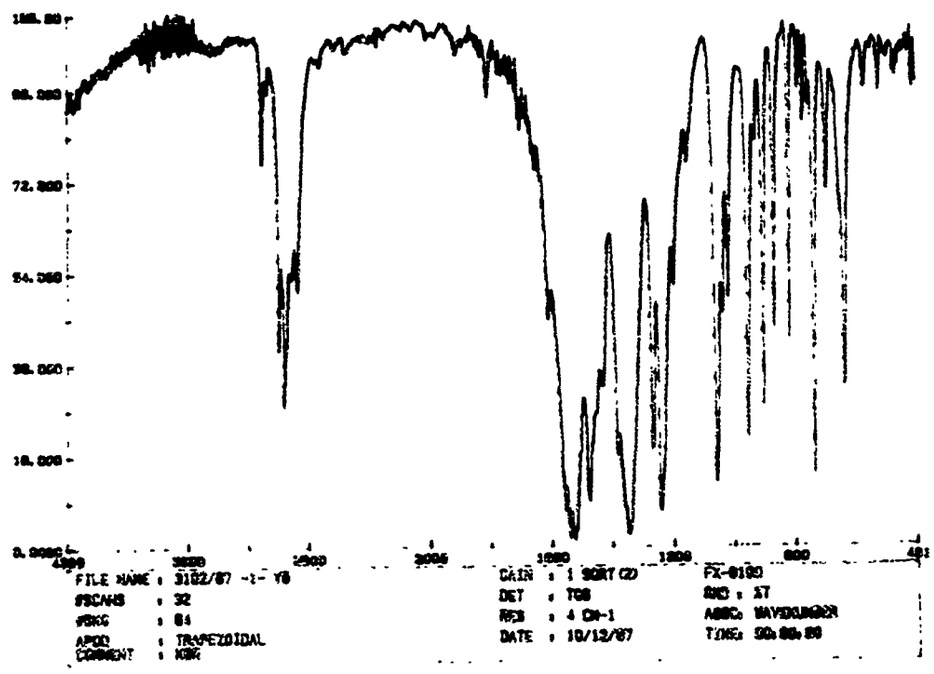


FIGURE 1: The IR spectrum of the unknown sample.

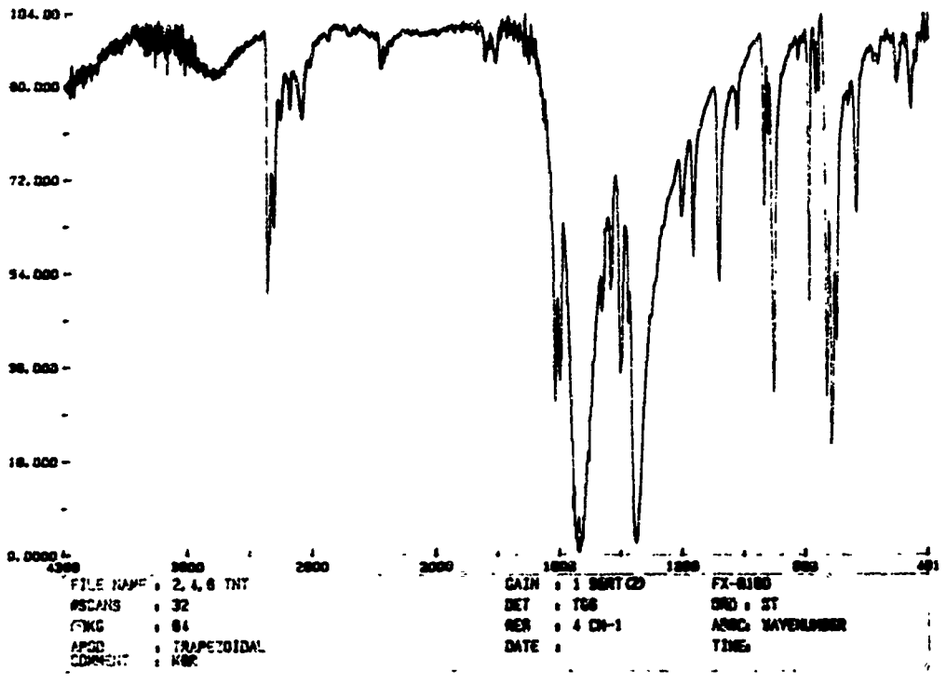


FIGURE 2: The IR spectrum of 2, 4, 6 - TNT.

Next the sample was analysed by GC/MS, using both EI and CI (methane) modes. In both modes a molecular weight of 268 was indicated. Being an even number, this molecular weight corresponds to an even number of nitrogen atoms in the molecule. The EI mass spectrum, shown in Figure 3, confirmed the presence of an aromatic ring (typical ions appeared at m/z 91, 77 and 51). This supported the proposed nitroaromatic structure. The base peak at m/z 253 corresponded to the loss of a methyl group from the molecular ion.

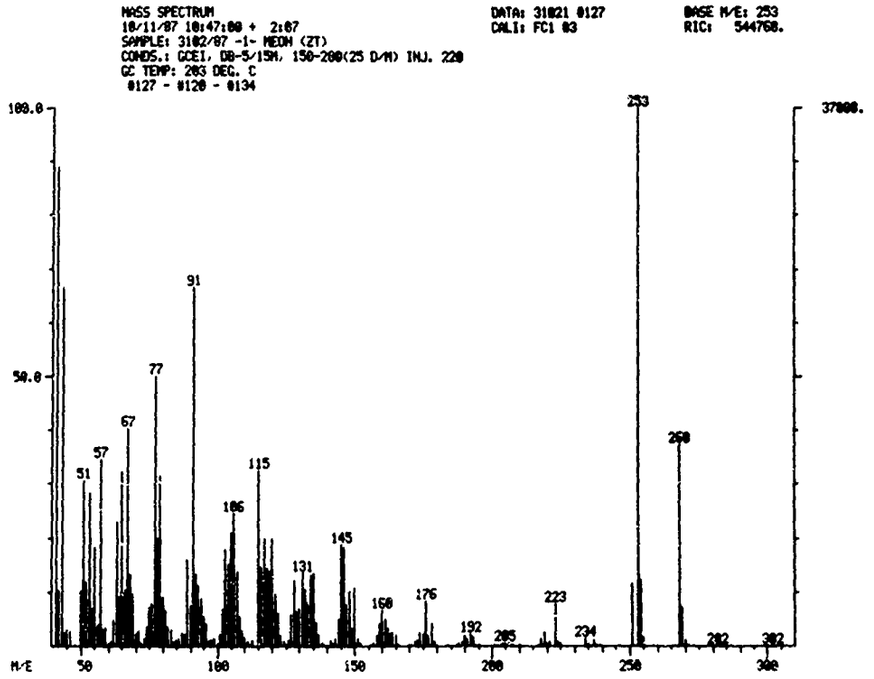


FIGURE 3: The EI mass spectrum of the unknown sample.

Explosives, like other compounds of forensic interest, are listed in our laboratory according to their molecular weights. We could not find in our lists an explosive with a molecular weight of 268. The Table of Molecular Weights published by Merck (5) did not include a compound whose spectral data were compatible with those of the unknown sample.

Finally, we recorded the proton NMR spectrum of our sample. We obtained an interesting spectrum shown in Figure 4, which included only four singlets. Their chemical shifts were 1.4 ppm, 2.4 ppm, 3.9 ppm and 8 ppm with integration ratio of 9:3:3:1, respectively. These data could correspond to the following functional groups: $(CH_3)_3C$, $OCH_3$, $CH_3$ and H. As no coupling was observed we assumed that each group was attached directly to the aromatic ring. The presence of a t-butyl group was compatible with the major process of a loss of a methyl group from the molecular ion in the EI mass spectrum.

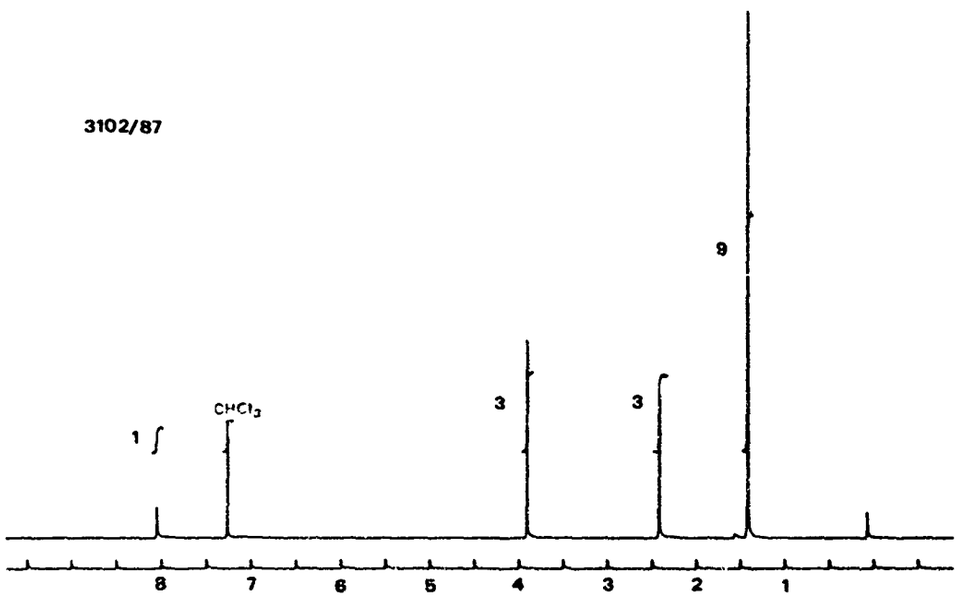


FIGURE 4: The proton NMR spectrum of the unknown sample.

Bearing in mind the molecular weight of 268, the nitroaromatic character, the even number of nitrogen atoms and the four substituents we proposed the structure shown in Figure 5, in which the positions of the functional groups on the aromatic ring have not been assigned.

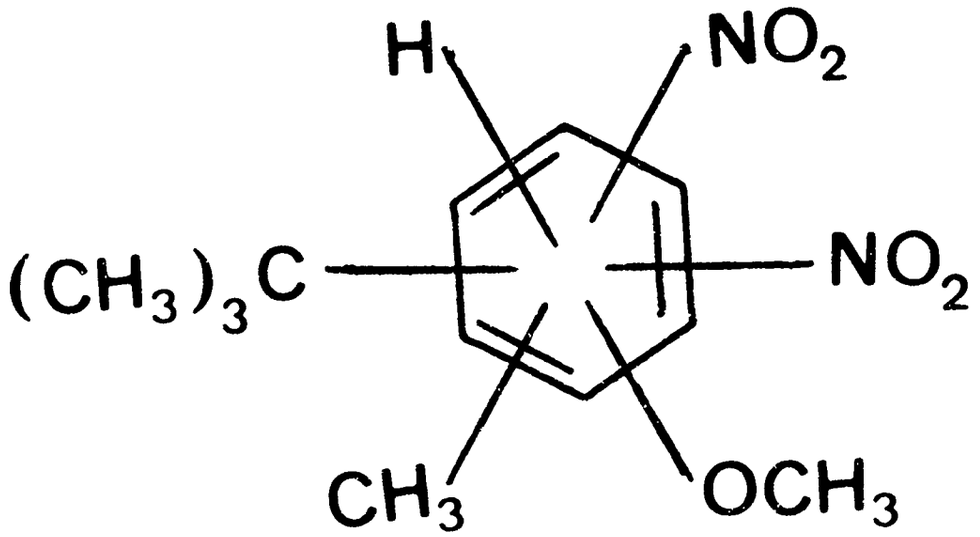


FIGURE 5: Possible substituents on the aromatic ring of the unknown sample.

Literature survey through the Chemical Abstracts showed that 1-t-butyl-2-methoxy-3,5-dinitro-4-methylbenzene (Figure 6), known as "musk ambrette" has been used as a "synthetic musk". Synthetic musks are used as fragrances in soaps, lotions and other cosmetic products (6). Musk ambrette is one of several synthetic musks having a nitroaromatic structure (unlike muscone, the odorous compound in natural musk, whose structure is macrocyclic). The EI mass spectra of synthetic musks have been reported (7,8). Their possible interference in tests for explosives as well as some analytical properties have also been discussed (9).

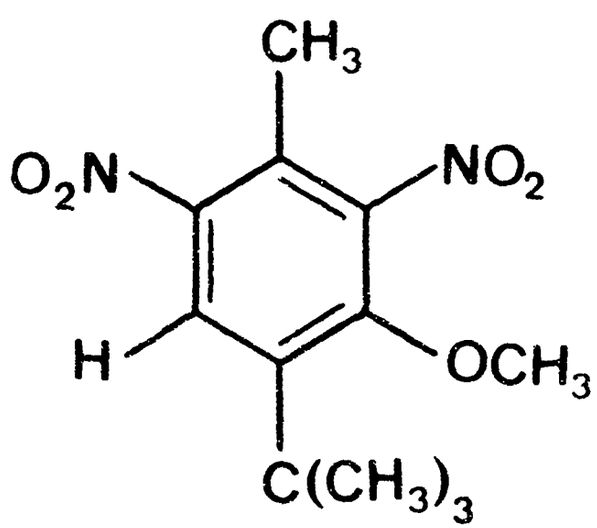


**MUSK AMBRETTE**

FIGURE 6: Musk ambrette (1-t-butyl-2-methoxy-3,5-dinitro-4-methylbenzene).

All the spectral data of our unknown sample were completely identical with those reported for musk ambrette.

## 4. CONCLUSIONS

Nitroaromatic synthetic musks could interfere with some tests for explosives. This is especially relevant when field tests based on color reactions are used as a preliminary indication for the presence of explosives.

## 5. REFERENCES


1. J. Almog, S. Kraus and B. Glattstein, J. Energetic Materials, 4 , 159 (1986).
2. M. A. Kaplan and S. Zitrin, J. Assoc. Off. Anal. Chem. 60 , 619 (1977).
3. J. Yinon and S. Zitrin,"The Analysis of Explosives", Pergamon Press, Oxford, U.K. 1981, Chapter 2 , pp 30-37.
4. J. F. Brown, Jr. J. Am. Chem. Soc. 77, 6341 (1955).
5. Table of Molecular Weights, Merck & Co., Inc. Rahway, N.J. U.S.A. (1978).
6. D.L.J. Opdyke, Food Cosmet. Toxicol. 13, Suppl. 875 (1975).
7. M.P. Yurawecz and B.J. Puma, J. Assoc. Off. Anal. Chem. 66 , 241 (1983).
8. C.L. Goh and S. F. Kwok, Contact Dermatitis, 14, 53 (1986).
9. J.M.F. Douse and R.N.Smith, J. Energetic Materials, 4, 169 (1986).

# TRACE ANALYSIS OF EXPLOSIVES BY MASS SPECTROMETRY

Maw-Rong Lee, Dau-Gwei Hwang and Chia-Pin Tang
Chung-Shan Institute of Science and Technology
P.O.Box 90008-17, Lung-Tan, Taiwan 32526, R.O.C.

## ABSTRACT

Quantification analysis by mass spectspcctrometry seems to be a powerful technique for the explosives detection. A series of nitrate ester explosives ,namely pentaerythritol tetranitrate (PETN) , 1,2,4-butanetriol trinitrate (BTTN), nitroglycerine (NG) , triethylene-glycol dinitrate (TEGN) , propylene - 1,2-glycol dinitrate (PGDN) , and 1,1,1-trimenthylolethane trinitrate (TMETN) were systematically studied.

Election impact , positive and negative chemical ionization methods were applied . Quantification of these niitrate esters were carried out by GC/MS with the selected ion monitoring (SIM) as well as by GC/MS/MS selected ion reaction monitoring (SRM). The adduct ions formed by these different ionization methods in MS and the limits of detection (LOD) obtained with various ionization modes in GC/MS-SIM and GC/MS/MS-SRM are discussed.

## 1. INTRODUCTION

The identification and quantification of the components of explosive formulations are beneficial to both manufacturers and forensic scientists . Several analytical methodologies including thin-layer chromatography , gas chromatography, and spot tests etc. have been developed for

analyzing explosives [1] . Mass spectrometry is considered to be one of the most powerful tools available to the analytical chemists for the characterization of unknown materials . By virtual of its high sensitivity and specificity, MS is the most suitable technique in the identification of explosives . A review of its application in the field of explosives analysis has been reported [2].

Trace analysis of explosives is of importance in forensic science . The analytical problems encountered in this field involve the detection of nanogram quantities of explosives in the extracts obtained from the post-explosion residues . In order to find out a suitable trace analytical method by mass spectrometry , various ionization methods , including positive and negative chemical ionizations (PCI/NCI) as well as electron impact (EI) were used . A series of nitrate ester explosives including PETN , BTTN , NG , TEGN , PGDN and TMETN were studied . Their structural formula are shown in Figure 1.

## 2. EXPERIMENTAL

All mass spectra were generated via a Finnigan Model 4023 combined gas chromatograph / mass spectrometer (GC/MS) equipped with a dual CI/EI source. A Finnigan MAT TSQ 46 triple stage quadrupole GC/MS/MS sytatem was used for acquisition of daughter ion mass spectrometric data. Ultra-high purity methane , isobutane and ammonia ( Matheson , Morrow, CA ,USA ) were used as the CI reagent gases and Ar was used as the collision gas.

The explosives PETN , BTTN , TEGN , TMETN and PGDN were specially purified for using as standards . Solutions of explosives were freshly prepared in acetone (Merck) and

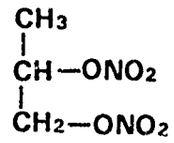

Propylene-1,2-glycol dinitrate

(PGDN)

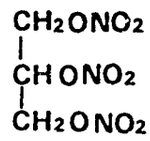

Nitroglycerin

(NG)

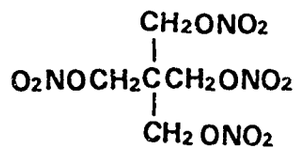

Pentaerythritol tetranitrate

(PETN)

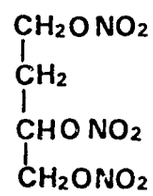

1,2,4-Butanetriol trinitrate

(BTTN)

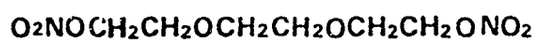

Triethylene glycol dinitrate

(TEGN)

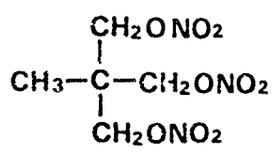

1,1,1-Trimethylolethane trinitrate

(TMETN)

Figure 1. Structure of nitrate ester explosives.

diluted with acetone to provide a series of different concentrations . Sample solution was eluted on a two-meter-long DB-5 fused silica capillary column using a helium carrier at the head pressure 8 psig. The GC temperature was programmed from 40℃ to 250℃ at a rate of 30℃ /Min . Injector temperature was 180℃ . Ion source temperature was 250℃ for EI and 150℃ for CI techniques. Tandem mass spectrometry (MS/MS) was performed with a collision energy of 20 eV and collision gas pressure of 3 milliitorr. Electron energy was 70 eV in EI mode and changed to 100 eV in CI modes. Triplicate 1.0 $\mu$l injections of each sample solution were made.

Quantitative studies were performed by using the highly selective selected ion monitoring (SIM) technique in GC/MS and selected ion reaction monitoring (SRM) technique in GC/MS/MS with sample introduction via a short capillary column. The quantification signal was obtained by integrating the ion current over the scans during elution of sample to obtain the GC peak area. The limit of detection (LOD) was calculated as the amount of samaple necessary to give a signal- to-noise (S/N) ratio of 3 .

## 3. RESULTS AND DISCUSSION

### 3.1 Mass Spectrometry of The Nitrate Ester Explosives

The EI mass spectra of all above nitrate esters have shown the $(M+NO)^+$ , $(M+NO_2)^+$ adduct ions and quasi-molecular ion $(M+H)^+$ (Table 1) . Adduct ions seem due to the addition of $NO^+$ or $NO_2^+$ fragment ions and neutral sample molecules in the high pressure ion source chamber. Example of the EI mass spectrum of TMETN is shown in Figure 2. The base peak at m/z 46 is due to $NO_2^+$ . This base peak is found in all the EI mass spectra of

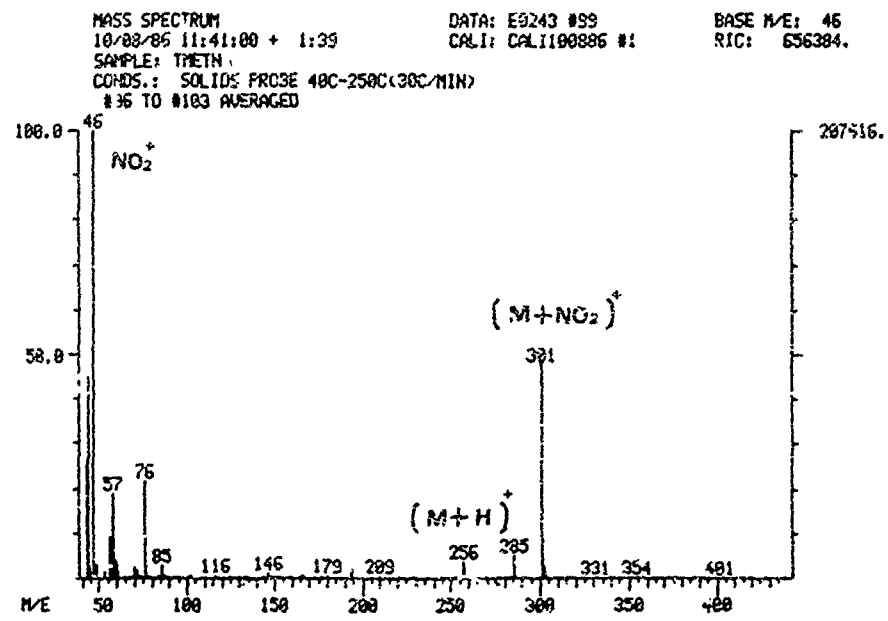


Figure 2. EI mass spectrum of TMETN.

Table 1. The relative abundance of addition ions in the EI mass spectra of nitrate ester explosives.

| Compound | Molecular weight (a.m.u) | Addition ions in m/z (%) | | |
|---|---|---|---|---|
| | | $(M + H)^+$ | $(M + NO)^+$ | $(M + NO_2)^+$ |
| PGDN | 166 | 167(0.3) | 196(1.2) | 212(8.7) |
| NG | 227 | 228(1.1) | 257(0.7) | 273(8.0) |
| PETN | 316 | 317(0.03) | 346(0.05) | 362(0.4) |
| BTTN | 241 | 242(1.6) | 271(2.4) | 287(21.4) |
| TEGN | 240 | 241(25.5) | 270(2.6) | 286(12.0) |
| TMETN | 255 | 256(3.7) | 285(5.2) | 301(47.8) |

these compounds .

The PCI technique with $CH_4$ ( or $i\text{-}C_4H_{10}$ ) as the reagent gases, the observed major ions are similar to those in the EI mass spectrometry. The most abundant ions found in the PCI-$CH_4$ mass spectra are the $(M + H)^+$ ion for PETN, TEGN, and TMETN, and the adduct ion, $(M + NO_2)^+$, for PGDN, NG and BTTN (Table 2). As $NH_3$ to be the reagent gas, the major ions is $(M + NH_4)^+$.

With NCI technique, despite of which reagent gas is used, the most abundant ion , except TEGN, is $(M + NO_2)^-$ (Table 3). In TEGN mass spectrum , the observed most abundant ion is $(M + NO_3)^-$ . This may be due to the linear molecular structure of TEGN.

## 3.2 Selected Ion Monitoring (SIM)

In order to increase the sensitivity of mass spectrometry , selected ion monitoring (SIM) of the most abundant ion was used to determine the detection limit in GC/MS method [3]. The base peak ion of nitrate ester explosive was determined from the mass spectra in which samples were introduced via GC.

The selected ions monitored in different modes and the optimized quantitation conditions are listed in Table 4. The LODs are in the range of 8 ~40 ng for EI, 2 ~17 ng for PCI-$CH_4$ and 0.008 ~0.8 ng for NCI-$CH_4$ . The relative standard deviations of integrated signals for the triplicate analyses having S/N ratio greater than 3 are ranged from 6 to 27 % for the PCI technique and 4 to 20 % for NCI.

From Table 4, it is found that the detection limits are dependent upon nitrate ester explosives and mass spectrometric techniques. The detection limits obtainable for PCI are of the same order as for EI. The sensitivity in NCI is increased by one or two orders of magnitute higher than that

Table 2. Summary of methane positive chemical ionization mass spectra of nitrate ester explosives.

| Compound | Molecular weight (a.m.u) | Prominent loss / Addition ions in m/z (%) | | | | | | |
|---|---|---|---|---|---|---|---|---|
| | | $(M - NO_2)^+$ | $M^+$ | $(M + H)^+$ | $(M + NO)^+$ | $(M + NO_2)^+$ | $(M + NO_3)^+$ | $(2M-NO_2)^+$ |
| PGDN | 166 | 104(25) | 166(0) | 167(1.4) | 196(9.4) | 212(100) | 228(0) | 170(0) |
| NG | 227 | 165(0.6) | 227(0) | 228(20.8) | 257(13.2) | 273(100) | 289(0) | 392(4) |
| PETN | 316 | 254(56) | 316(0.7) | 317(100) | 346(3.7) | 362(8.4) | 378(0) | 570(0) |
| BTTN | 241 | 179(2.7) | 241(0) | 242(7.6) | 271(10) | 287(100) | 303(0) | 420(0) |
| TEGN | 240 | 178(13.1) | 240(0) | 241(100) | 270(6.1) | 286(38.1) | 302(0) | 418(0.3) |
| TMETN | 255 | 193(38) | 255(1.1) | 256(100) | 285(6.9) | 301(51.6) | 317(0.5) | 448(0) |

Table 3. Summary of methane positive chemical ionization mass spectra of nitrate ester explosives.

| Compound | Molecular weight (a.m.u) | Prominent loss / Addition ions in m/z (%) | | | | | |
|---|---|---|---|---|---|---|---|
| | | $(NO_3)^-$ | $M^-$ | $(M + H)^-$ | $(M + NO)^-$ | $(M + NO_2)^-$ | $(M + NO_3)^-$ |
| PGDN | 166 | 62(71.6) | 166(0) | 167(0.2) | 196(0) | 212(42.0) | 228(100) |
| NG | 227 | 62(49.8) | 227(0) | 228(1.1) | 257(0) | 273(0.8) | 289(100) |
| PETN | 316 | 62(100.0) | 316(0) | 317(0.2) | 346(0) | 362(1.0) | 378(71.9) |
| BTTN | 241 | 62(26.2) | 241(0) | 242(0.4) | 271(0) | 287(5.6) | 303(100) |
| TEGN | 240 | 62(16.1) | 240(0) | 241(0) | 270(0.01) | 286(100) | 302(19.4) |
| TMETN | 255 | 62(50.0) | 255(0) | 256(1.1) | 285(0) | 301(19.9) | 317(100) |

Table 4. Comparion of different methods with short capillary column GC/MS (SIM) for determination of TMETN, BTTN, TEGN, PETN and PGDN.

| Compound | Reagent gas | Reagent gas pressure (torr) | Technique | Ion monitored | LOD (ng) |
|---|---|---|---|---|---|
| TMETN | — | — | EI | 46 | 15 |
| | $CH_4$ | 0.3 | PCI | 256 | 8 |
| | $CH_4$ | 0.3 | NCI | 62 | 0.30 |
| BTTN | — | — | EI | 46 | 40 |
| | $CH_4$ | 0.3 | PCI | 242 | 14 |
| | $CH_4$ | 0.3 | NCI | 62 | 0.8 |
| TEGN | — | — | EI | 46 | 29 |
| | $CH_4$ | 0.3 | PCI | 241 | 9 |
| | $CH_4$ | 0.3 | NCI | 62 | 0.04 |
| PETN | — | — | EI | 46 | 20 |
| | $CH_4$ | 0.3 | PCI | 317 | 17 |
| | $CH_4$ | 0.3 | NCI | 62 | 7 |
| PGDN | — | — | EI | 46 | 8 |
| | $CH_4$ | 0.3 | PCI | 212 | 2 |
| | $CH_4$ | 0.3 | NCI | 62 | 0.008 |

Table 5. Comparion of different methods with short capillary column GC/MS/MS (SRM) for determination of TMETN and BTTN.

| Compound | Reagent gas | Technique | Reaction monitored | CAD Pressure (mtorr) | CAD Energy (ev) | LOD (ng) |
|---|---|---|---|---|---|---|
| TMETN | $CH_4$ | PCI | $256^+ \rightarrow 46^+$ | 2.5 | 20 | 4 |
| | $CH_4$ | NCI | $62^- \rightarrow 46^-$ | .. | .. | 0.43 |
| BTTN | $CH_4$ | PCI | $242^+ \rightarrow 46^+$ | .. | .. | 7 |
| | $CH_4$ | NCI | $62^- \rightarrow 46^-$ | .. | .. | 0.17 |

obtained in EI and PCI . This is similar to the results reported in the literature [4]. The most sensitive LOD with 0.008 ng of PGDN is obtained in NCI mode .

### 3.3 Selected Ion Reaction Monitoring (SRM) [5]

For PCI-SRM, the quasi-molecular ion of TMETN or BTTN was selected as the parent ion by the first quadrupole and fragmented by an inert collision gas Ar in the central quadrupole. Only the most abundant daughter ion, m/z 46 , was allowed to pass through the third quadrupole. The quanitation signal was obtained by integrating the ion current over the scans during elution of TMETN or BTTN. The daughter spectrum of the $(MH)^+$ ion, m/z 256, of TMETN is shown in Figure 3.

For NCI-SRM, the most abundant ion $NO_3^-$ , m/z 62 , in TMETN and BTTN was selected as the parent ion , the daughter ion at m/z 46 was monitored . The daughter spectrum of $NO_3^-$ at m/z 62 of TMETN is shown in Figure 4.

Results of the quantitative studies of TMETN and BTTN using highly selective selected ion reaction monitoring technique of MS/MS under the optimized conditions are summarized in Table 5. The LODs obtained in the PCI-SRM are 4 ng for TMETN and 7 ng for BTTN , whereas in NCI-SRM , 0.43 ng for TMETN and 0.17 ng for BTTN .

The sensitivity for NCI is increased by one order of magnitute higher than that obtained in PCI. This is similar to the result obtained in the SIM technique.

Although the fragmentation efficiency for parent ion to daughter ion will affect the sensitiviy of SRM technique, but as a matter of fact that the LODs for SRM and SIM are similar . This indicates that a partial loss of sensitivity inherent in SRM is compensated by the decrease in " chemical noise " . The daughter ion spectrum in the GC/MS/MS-SRM can provide a method for the identification

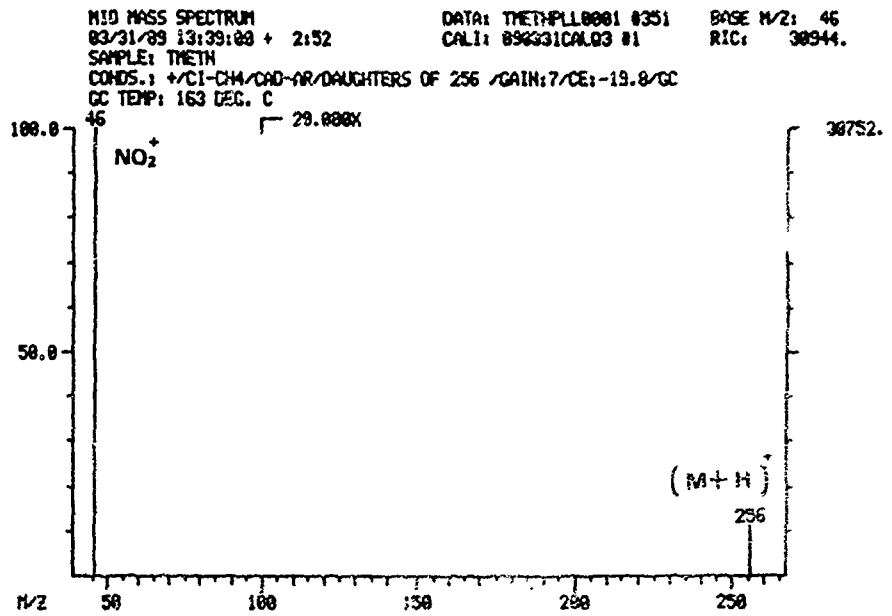


Figure 3. Daughter spectrum of ion $(M+H)^+$, m/z 256 of TMETN produced by PCI ($CH_4$).

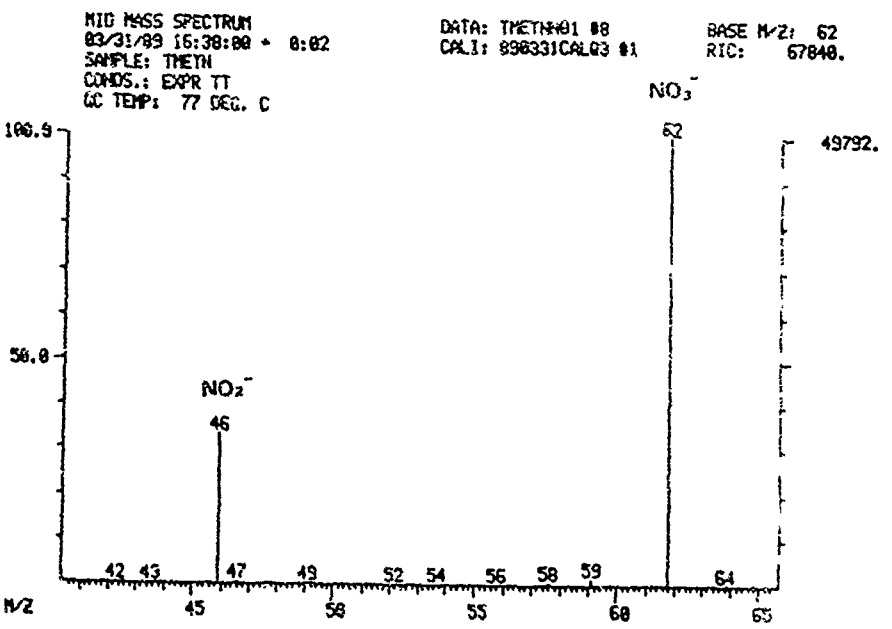


Figure 4. Daughter spectrum of ion $NO_3^-$, m/z 62 of TMETN produced by NCI ($CH_4$).

of compounds in a complex matrix without previous separation.

Application of these detection techniques is to be studied in our laboratory for trace analysis of explosives in post-explosion debris.

## 4. CONCLUSIONS

4.1 The combination of EI, PCI and NCI ionzation methods of mass spectrometry provides a very powerfully analytical system which is capable of giving clear positive identification of nitrate ester explosives.

4.2 Comparing various MS monitoring modes , the best monitoring mode for determination of nitrate ester explosives seems to be the NCI-$CH_4$ with selected ion monitoring or with selected ion reaction monitoring .

4.3 The lowest PGDN detection limit obtained with short capillary column GC/NCI-SIM is 0.008 ng. The situation of PETN seems rather different among all determined nitrate esters, since the LOD can not be lower with the same experimental conditions.

REFERENCES

1. J Yinon
" The Analysis of Explosives.", Pergmon Press, Oxford, 1981.

2. J Yinon
Mass Spectrometry of Explosives : Nitro Compounds, Nitrate Esters and Nitroamines . Mass Spectrometry Revivs . 1 . 257-307 .1982 .

3. B J Millard
" Quantative Mass Spectrometry " , London . Heyden . 1978 .

4. D F Hunt et al.
Pulsed Positive Negative Ion Chemical Ionization Mass Spectrometry . Anal. Chem. 48 . 2098-2105 . 1976 .

5. J V Johnson et al.
Tandem Mass Spectrometry for Trace Analysis . Anal. Chem. 57, 758A-768A . 1985.

# APPLICATION OF CHROMATOGRAPHIC METHODS FOR IDENTIFICATION AND SEPARATION OF EXPLOSIVES, THEIR DEGRADATION- AND BY-PRODUCTS IN DIFFERENT MATRICES E.G. FORMULATIONS, WATER, SOIL AND AIR.

H. Köhler
Dynamit Nobel AG, Werk Schlebusch
Leverkusen-Schlebusch, Kalkstraße 218
F.R.G.

## ABSTRACT

In the first part of this contribution a survey is given of well established methods of analysis of explosives described in the literature (1-4). Analysis of explosives is mainly done by high pressure liquid chromatography, the application of g.l.c. and t.l.c. is used for special applications.

In the second part of this paper the application of chromatographic methods will be discussed using examples of actual analysis from a typical explosives-factory.

In particular the sample preparation is important to obtain correct and reproducible results because of the possible interferences of the matrices.

The following applications are discussed in detail:

1.) Analysis of mono-, di- and trinitrotoluene in water and soil.
2.) Analysis of glyceroltrinitrate, -dinitrate, -mononitrate in water and soil.
3.) Analysis of glyceroltrinitrate and glycoldinitrate in air.
4.) Analysis of pharmaceutical preparations of glyceroltrinitrate, isosorbide-mononitrate and -dinitrate.

5.) Analysis of coal-mining explosives.

6.) HPLC-methods for separating some of the most common explosives and stabilizers in one or two runs of a chromatogram.

Table of contents:

1.0.0 Introduction

1.1.0 Methods for identification and separation of explosives in general

1.2.0 Aim of this contribution

2.0.0 Analysis of explosives

2.1.0 Sample preparation

2.1.1 Air

2.1.2 Water

2.1.3 Soil

2.1.4 Pharmaceutical formulations

2.1.5 Coal mining explosives, powders and propellents

2.2.0 Chromatographic methods

2.2.1 Gas chromatography

2.2.2 High performance liquid chromatography

2.2.3 Calibration methods

2.3.0 Chromatograms

2.3.1 Determination of GTN and EGDN in air

2.3.2 Determination of tri-, di- and mononitrotoluenes in water

2.3.3 Analysis of GTN, EGDN and Glycolmononitrate in water

2.3.4 Separation of 1,2-Glycerol-di-nitrate and 1,3-Glycerol-di-nitrate

2.3.5 Separation of 2-ISMO, 5-ISMO, $NO_2^-$ and $NO_3^-$

2.3.6 Determination of GTN in GTN/lactose trituration

2.3.7 GTN and EGDN in coal-mining explosives

2.3.8 Chromatogram of mixture of different explosives

3.0.0 Dicussion and conclusions
3.1.0 Reproducibility
3.2.0 Minimum detectable concentration range

4.0.0 Table of analysed explosives and substances

5.0.0 Literature cited

1.0.0 Introduction:

1.1.0 Survey: Common methods of analysis of explosives

For the analysis of most classes of organic compounds, it is usually possible to use most chromatographic techniques in combination with a wide variety of detectors.
However, in the case of explosives, the very nature of these materials requires the application of certain important chromatographic methods. Medium or high temperature gas chromatography is generally impossible to employ with most explosives exepted some nitroaromates.
Thin layer chromatography (TLC) has often been employed along with organic spray reagents for rapid identification of explosives. This technique makes their detection very simple, but their quantitation still suffers a bit from some nonreproducible effects.
The progress of analysis of explosive materials has shown in the past 10 years that the analysis of explosives with a high degree of accuracy and precision both qualitative and quantitative, has mainly been proceeded by the application of high performance liquid chromatography (HPLC). HPLC can be utilized for the combined analysis of both volatile and nonvolatile materials, and is nondestructive all cases, because this method is generally conducted at ambient temperatures.
Most HPLC applications can readily be automated, thus permitting the routine analysis of a large number of samples in a short period of time. Recent progress in analytical instrumentation have brought commercially available sensitive and highly selective detectors such

as electrochemical detection, the coupling of HPLC/MS detection, or application of a nitrosyl-specific detector, variable wavelength UV-detector and diode-array UV-VIS detectors. Chromatography is mainly a separating method, but by the application of the obove mentioned specific detectors can also be used for identification purposes. (1)

1.2.0 Aim of this contribution

In this paper are shown with some typical examples the possibilities of HPLC methods, developed in an analytic laboratory of an explosives factory. Most of these methods were elaborated because of the necessity to perform quality control of products, to solve environmental and industrial hygiene problems.

Roughly ten years ago, when our laboratory came into contact with the new HPLC methods, the commercially available columns or separating materials were based on special normal phase silicagel. Therefore our first methods dealing with the analysis of explosives were performed with normal phase columns and organic solvents.

These methods involved many separations with solvent-gradient programming which brought successful analysis. (2)

However, solvent gradient HPLC-methods were time consuming in respect of postrun equilibration of the column. This had also an effect on reproducibility and sensitivity of the following analysis.

Organic-solvent gradient HPLC-methods are very sensitive to a constant amount of water in the system stationary phase/mobile phase. Sensitivity was relatively poor; a late eluting small peak in a gradient programme was difficult to integrate and gave poor quantitative, not good reproducible results.

Another problem ten years ago was the lack of sufficient sensitive UV-detectors. In our very first beginning we had a fixed wavelength detector which operated at 254 nm. This was good for analysis of some nitroaromatic based explosives, but not sufficient for aliphatic nitrate esters.

Fortunately in a relative short time good reversed phase stationary phases were available, in the same time UV-VIS Detectors for HPLC with variable wavelength came on to the market. Therefore our laboratory redeveloped all previous methods.

Nowadays we do HPLC analysis of explosives practically exclusively with reversed-phase chromatography and water/methanol or water/acetonitrile mixtures as mobile phase. A breakthrough in sensitivity and reproducibility was achieved by the application of isocratic separation and the possibility to have detection wavelength at 205 nm for nitrate esters.
Before starting with the report on the practical examples of analysis, a few words over the concentration range in which quantitative analysis is performed in our laboratory:
We do analysis normally on products which contain explosives in the percent range, e.g. pharmaceutical formulations and coal-mining explosives. The analysis of by-products and degradation products covers ca. 1000 to 10 ppms. Environmental analysis requires methods where the concentration of some explosives is in the 0,01 ppm to the 1 ppb range.
The following discussion will be divided in three parts:
At first, sampling methods are described in general. In the second part chromatographic methods and calibration is discussed. The third part gives technical details on HPLC- and G.C.-apparatus, columns, mobile phase and will show some typical chromatograms with chromatogaphic conditions.

## 2.0.0 Analysis of explosives

### 2.1.0 Sample preparation

Reproducible and correct analytical data depend highly on the sample preparation which has to be specific for the matrix, in which the explosives are to be determined.

#### 2.1.1 Air

Starting from 1980, in Germany the MAK-values (TLV-values) at working places were drastically lowered from 5 mg/m³ to 0,5 mg/m³ for GTN and from 1,6 mg/m³ to 0,3 mg/m³ for EGDN, creating a demand for a method for separating the two explosives which is sensitive enough for the control of the lowered TLV-values.
This was achieved by application of a special construction of impingers, which allow to pump the air through a volume of 10 ml of isopropanol.

The impingers are cooled during pumping the air through with a mixture of solid carbon dioxide with methanol, maintaining temperatures at -70°C (203 K). The pumping velocity is 2 l/min. up to 2,5 l/min. Sampling takes between 2 h to 8 h, depending on the amount of the nitrate esters being present in the air. Normally a sampling volume of 500 l to 1000 l air is sufficient. The isopropanol solution is directly injected into the HPLC (10 ul).

Sampling trinitrotoluene (TNT) in air must follow two different intentions of analysis:

a) Determining TNT in form of vapour phase and dust particles, sampling is done by pumping the air through bubblers which contain trichloroethylene. Sampled volume is between 500 l and 1000 l air. To increase sensitivity the trichloroethylene solution can be concentrated by destillation and then diluted with methylenechloride.

b) Determining the TNT dust in the air requires another sampling method: The air is pumped through 8 micron membrane filters with the aid of a dust collecting device. The filter material is nitrocellulose, the device we apply is the dust sampler MD 8 by Sartorius. After sampling the membrane filters are extracted with methylene chloride. This solution is is used for HPLC analysis.

2.1.2 Water

The determination of GTN, EGDN and their decomposition product in waste water of the nitration factory or in water solutions for pharmaceutical use needs no special sample preparation, excepted microfiltration for removing particulate matter to avoid clogging of the HPLC-columms. Because of the poor solubility of the nitrate esters in water, (ca. 0,1 %) these water solutions are in the proper concentration for HPLC-analysis. Different from this is the sample preparation for the determination of the trinitro-, dinitro- and mononitrotoluenes in ground water. For these analyses which are performed by glass-capillary gaschromatography with flame ionisation detection in the ppb-range, direct injection of the water is not possible. Sample preparation is performed by extraction of 1 liter of underground water with 20 ml of pure chloroform. This is done by vigourus stirring and mixing the two phases in a 1 liter glass stoppered glass bottle during one hour. The organic phase can directly be injected

into the gas chromatograph.

2.1.3 Soil

Samples of contaminated soils or sands are extracted with chloroform, when TNT and the by-products are present. Ca. 100 g sample is treated with 50 ml of solvent in an ultrasonic bath.

If nitrate esters are supposed to be present in soil the extraction is done with acetonitrile, treating ca. 100 g sample with 50 to 20 ml of acetonitrile in an ultrasonic bath.

2.1.4 Pharmaceutical formulations

Nitrate esters like GTN, Isosorbidedinitrate and 5-Isosorbidemononitrate are delivered in harmless, phlegmatized formulations in the form of bulk ware. The most important bulk ware formulations are triturations with sugars, mixture with fatty oils, solutions in alcohols, alcohol/water or water solutions and spray formulations.

Sample preparation for trituration in sugars like lactose or glucose of nitrate esters is done by treating the samples with acetonitrile (HPLC-grade) in an ultrasonic bath. After 10-15 minutes the sample vials are centrifugated. The clear solution is then ready for injection. Solutions of nitrate esters in alcohols are diluted to an adequate concentration. Mixtures with fatty oils are treated in the same manner like the sugar-triturations.

A special method of sample preparation is when analysis of GTN-Spray is required for determiningthe GTN-content of a spray-shot-dose. Spraying into volumetric flasks filled with solvent gives no reproducible results because the volatile, chlorotrifluorohydrocarbon propellant takes to much GTN away. We therefore put the spray bottle into a sealable polyethylene bag. After 10 times pressing the valve of the spray bottle from the outer side of the flexible bag and after waiting for five minutes, through a tiny opening 50 ml of methanol are pipetted into the bag, closed again and well agitated. After a few minutes, the bag is openend and the solution is transferred into sealable sample vials.

2.1.5 Coal mining explosives, powder and propellents

The coal mining explosives are mainly mixtures of inorganic salts with ca. 10 % of GTN/EGDN blend. Sample preparation is done by extraction of 50 g of explosives in a soxhlet apparatus using glass filter extraction devices with diethylether. After 3 hours extraction time the diethylether is allowed to evaporate under a hood at room temperature. The remaining residue can be directly analysed by HPLC, weighing in aliquots and diluting with acetonitrile.

Another more direct approach is done by weighing in the explosive into a volumetric flask, filling up with acetonitrile and then filtering to obtain a clear solution. Powders and propellants, which contain different explosives, nitrocellulose and stabilizers, are extracted during 48 h in a soxhlet apparatus with methylenechloride in the ratio a 2,5 g sample and 100 ml solvent. The obtained solution is evaporated to dryness at 40°C under vacuum.

This residue is rinsed with acetonitrile or adequate solvents into volumetric flasks. This solution is ready for analysis. (3)

2.2.0 Chromatographic conditions and calibrating methods

2.2.1 Gas chromatography

Apparatus: Hewlett Packard 5880 equipped with flame ionisation detector. Column is a 12 m 0,2 mm internal diameter glass capillary coated with deactivated carbowax OV 101.

Injection is splitless, the run is temperature programmed from 60°C to 150°C end temperature.

Integration is done by using HP-System Level four.

2.2.2 High performance liquid chromatography (HPLC)

Apparatus:

Analysis of the nitrate esters and their formulations were performed using HPLC-equipment manufactured by Varian, Darmstadt, West Germany. Two models are in use: Model 5020 with Vista 401 Data-System and model 5040 with computing integrator Hitachi/Merck D 2000.

For detection variable wavelength UV detectors were used (Varian UV 100 and UV 2050). Ready packed columns form different suppliers were

used. Separations were performed on RP-8 columns (Merck,Darmstadt), Varian RP-18 Mikropac columns and Macherey and Nagel RP-18 columns. Particle size of the stationary phase varied between 5; 7 and 10 microns. All solvent are HPLC-grade (Baker).

Most of the separations were isocratic runs with simple mixtures of water/methanol or acetonitrile/water. Two special methods need to be described more detailed:

1.) Separation of the two isomeric isosorbide mononitrates 2-ISMO, 5-ISMO and inorganic $NO_2^-$ and $NO_3^-$ was not possible with the above mentionend mixtures. The problem was solved by trying "ion pair" chromatography. Literature describes that ion pair chromatography influences the retentention times only of ionic substances, whereas nonionic substances should not be affected. (4)
   In contrast to this, good separations were achieved on RP-18 columns with tetrabutylammoniumhydrogensulphate in water/acetonitrile as mobile phase.

2.) For the separation of a mixture of different types of explosives, isocratic runs are not applicable. Therefore gradient programming of the mobile phase was necessary to achieve separation in a rational time.
   An example will be shown in chromatogram. (8)

2.2.3 Calibration methods

Sample introduction for HPLC separations was always done by sample loops. Therefore all our calibration for quantitative determinations was done by the external standard method using the solutions of pure explosives in adequate concentration which meet the concentration range of the substance to be analysed.

We achieved best reproducible results when determining the assay of nitrate esters in pharmaceutical formulations with "matrix calibration". For example when GTN-lactose triturations have to be analysed, an external standard is prepared by mixing a known amount of GTN with an exactly weighed amount of lactose. This mixture is treated in the same manner of sample preparation like the formulation to be analysed. The following example emphazises the need of matrix calibration for obtaining correct quantitetive results. When a 0,1 % solution of GTN in water is analysed by HPLC, using as external standard an acetonitrile-GTN

solution, the result is 0,14 % GTN. When using GTN-water solution as external standard, the correct result of 0,1 % is obtained. The cause of this difference is the fact, that GTN-water and GTN-acetonitrile solutions of the same concentration have a different UV extinction coefficient. We have proved this by measuring the UV spectra.
For the determination of nitrotoluenes an internal standard method is used. The calibration solution is a mixture of known amounts of the mono-, di- and trinitrotoluenes. The internal standard is hexadecane, as shown in chromatogram. (2)

2.3.0 Chromatograms

2.3.1 Determination of GTN and EGDN in air

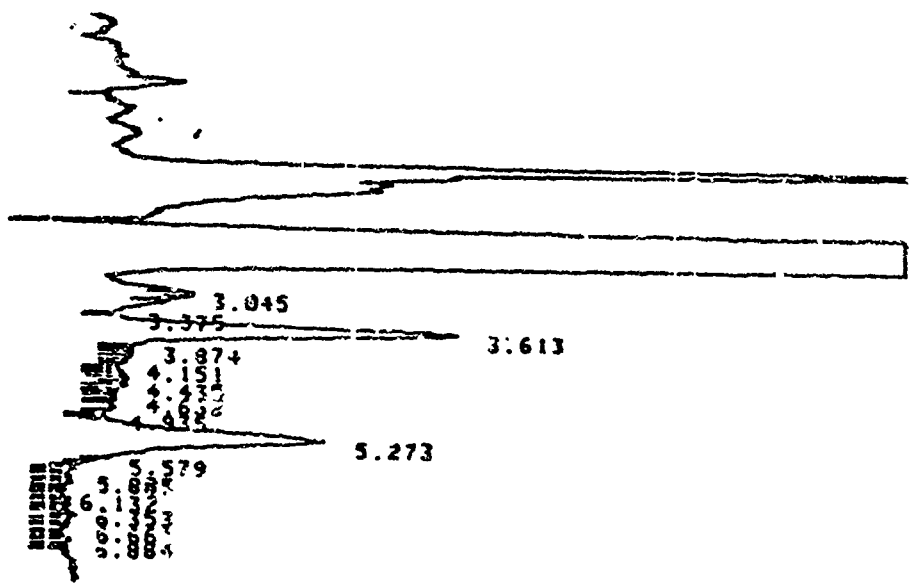


EGDN at 3,6 min., GTN at 5,3 min.
Column RP-18, mobile phase water/acetonitrile 1:1,
flow 1 ml/min., detection UV 210 nm

2.3.2 Determination of Tri-, di- and mononitrotoluenes in water

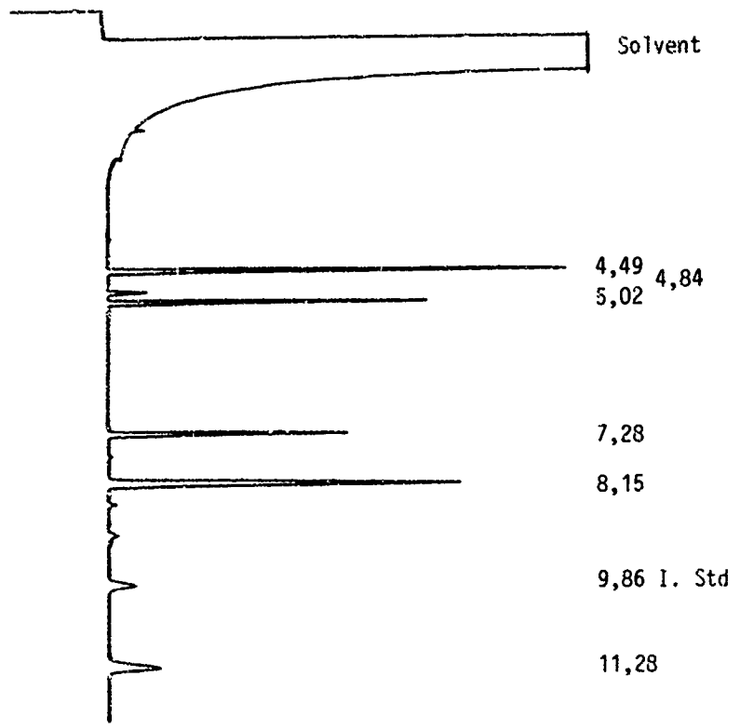


Glass capillary 12 m CV 101, i.d. 0,2 mm
Oven temperature 60°C/1 min. to 150°C, rate 15°C/min.
F.I.D. Splitless injection. Injector temperature 230°C,
Detector temperature 250°C.
Substances are eluted in increasing times as follows:
o-mono-, m-mono-, p-mono-, 2,6-di-, 2,4-dinitrotoluene
hexadecane, trinitrotoluene.

2.3.3 Analysis of GTN, EGDN and glycolmononitrate in water

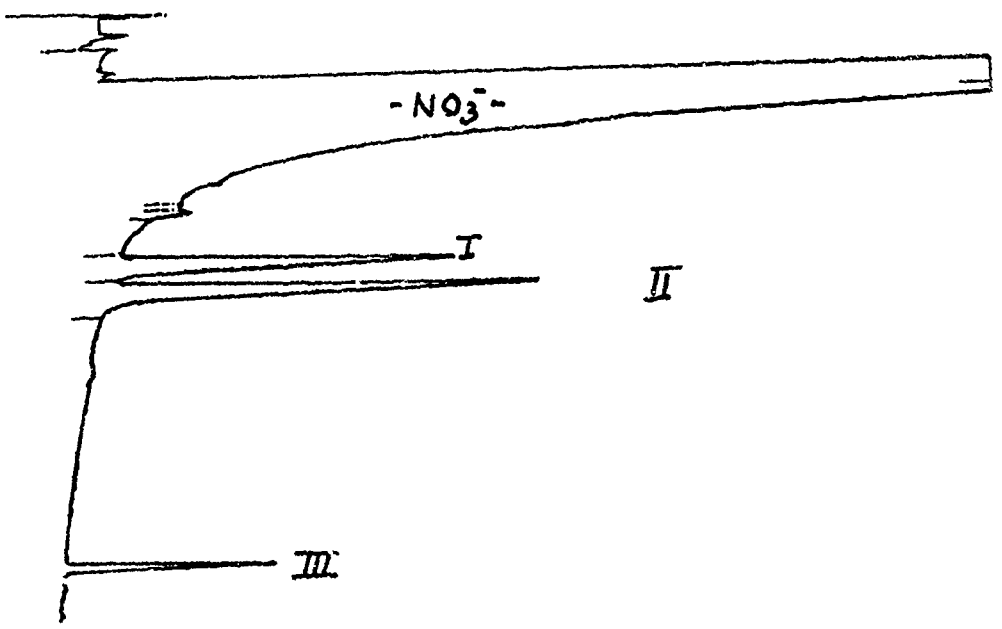


I = Glycolmononitrate at 7,[illegible] min.
II = EGDN at 7,9 min.
III = GTN at 17,1 min.

Column: RP-C 18; 60/40 water/acetonitrile
Detection: UV 210 nm; flow 1 ml/min.

2.3.4 Separation of 1,2-GDN and 1,3-GDN

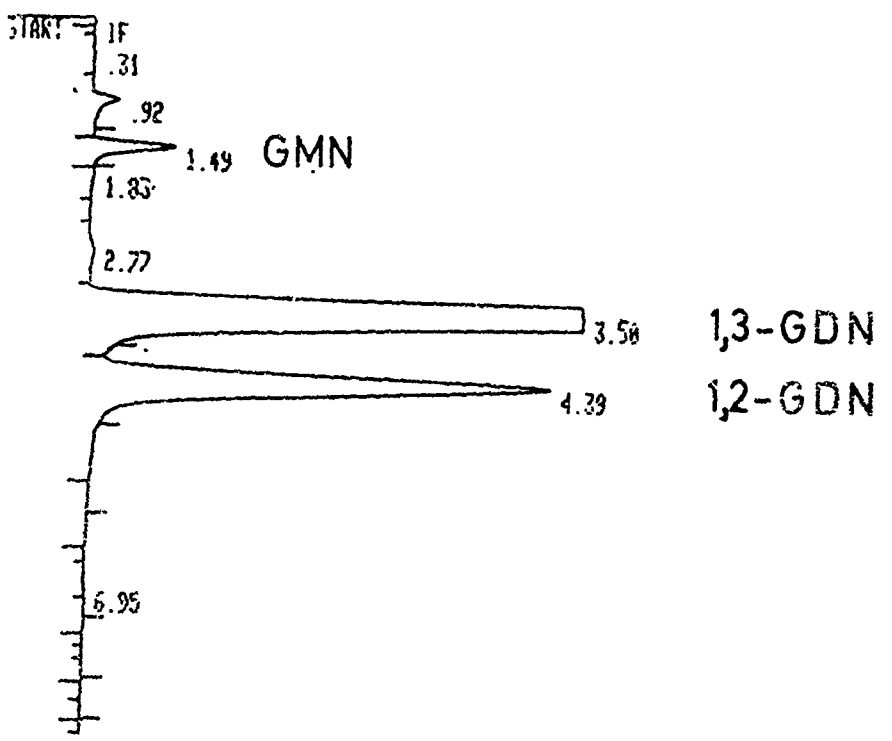


Column RP-18, mobile phase: water/acetonitrole 80/20
Detection UV 210 nm, flow rate 1,5 ml/min.
1,3-GDN at 3,5 min., 1,2-GDN at 1,4 min.

2.3.5 Separation of 2-ISMO, 5-ISMO, $NO_3^-$ and $NO_2^-$

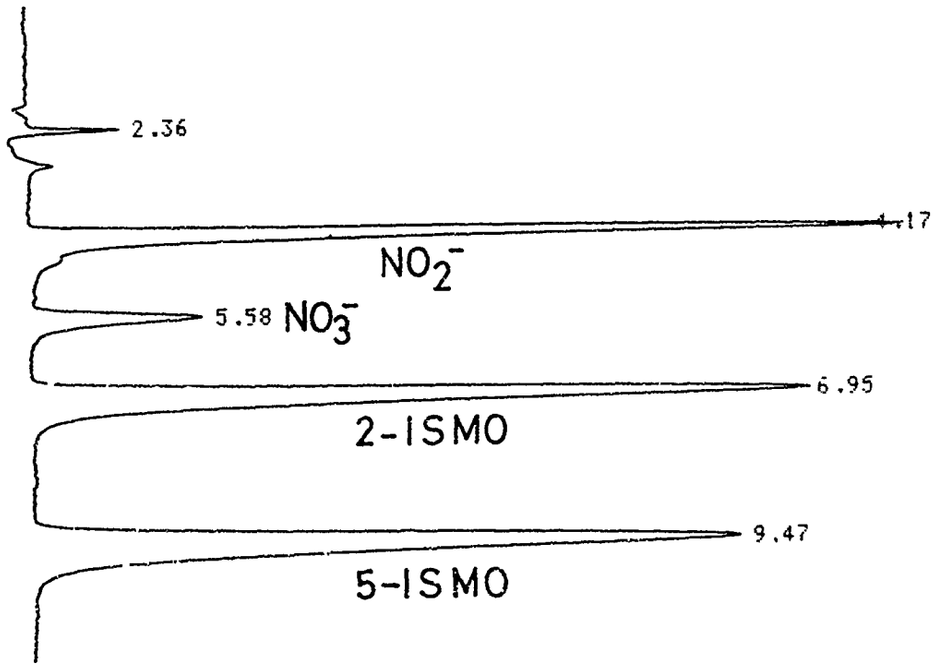


Column: RP-8, mobile phase: 0,005 m tetrabutylammonium hydrogenesulphate in water with buffer solution pH 6,5 and acetonitrile mixture 90:10 by volume
Detection UV 210 nm, flow rate 1 ml/min.

2.3.6 Determination of GTN in GTN/lactose triturations

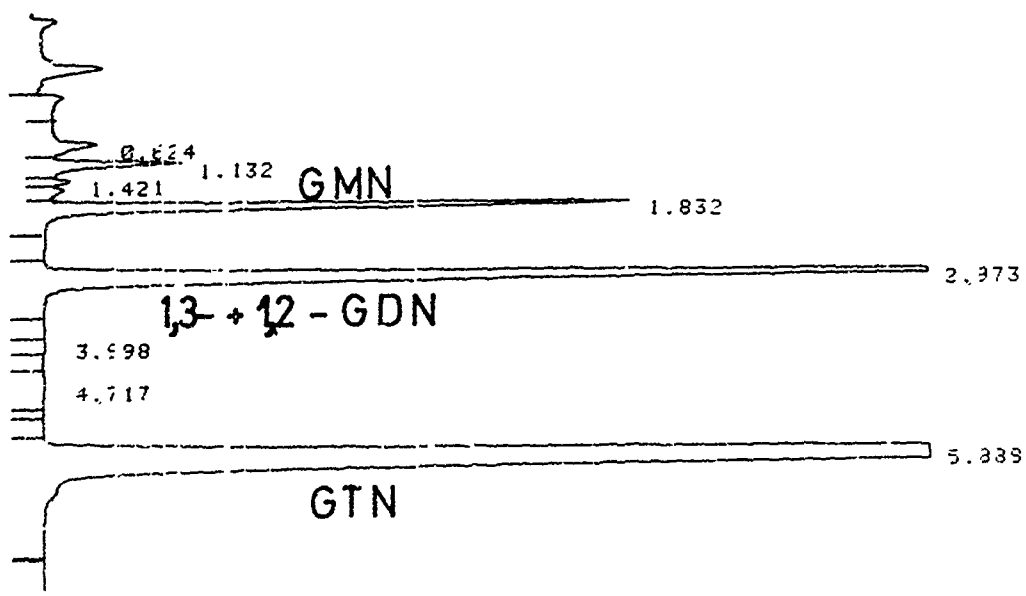


Column: RP-18, mobile phase acetonitrile/water,
50:50 by volume, detection UV at 210 nm
flow rate 1,5 ml/min.
GMN at 1,8 min.; 1,3- + 1,2-GDN at 2,9 min.
GTN at 5,9 min.

2.3.7 Determination of EGDN and GTN in coal mining explosives

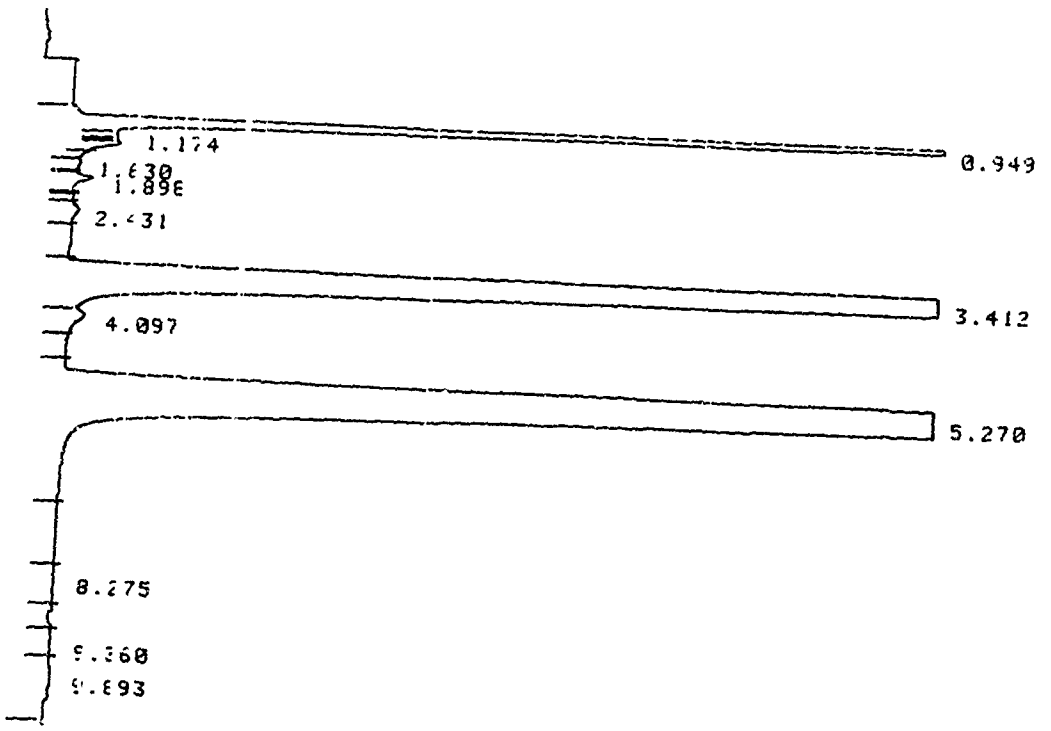


Column: RP-18, mobile phase water/acetonitrile 50:50 by volume, detection UV 230 nm, flow 1,0 ml/min.
EGDN at 3,6 min., GTN at 5,3 min.

2.3.8 Chromatogram of mixture of different explosives with gradient and flow programming

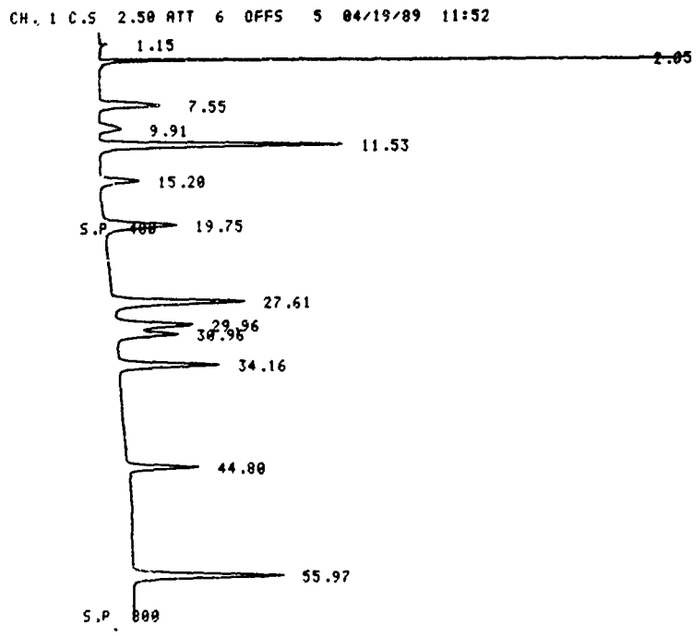


Column: RP-18, mobile phase: gradient program
with water/acetonitrile: Time O: Water = 95 %,
time 5 min.: water = 95 %, time 45 min.: water = 60 %
time 60 min.: water = 60 %
Flow program: Time O: 1,1 ml/min., time 5 min.:
1,1 ml/min.; time 45 min.: 1,6 ml/min., time 60 min.: 1,6 ml/min.
Detection UV at 210 nm
Elution order:

| | | | |
|---|---|---|---|
| Nitroguanidine: | 2,8 min. | Hexogene: | 27,6 min. |
| 2-ISMO: | 7,6 min. | Octogene: | 29,9 min. |
| 5-ISMO: | 9,9 min. | DEGDN: | 31,0 min. |
| 1,3-GDN: | 11,5 min. | ISDN: | 34,2 min |
| 1,2-GDN: | 15,2 min. | GTN: | 44,8 min. |
| EGDN. | 19,8 min. | Centralit I: | 56,0 min. |

3.3.0 Discussion and conclusions

3.1.0 Reproducibility and accuracy

The described methods of analysing explosives by chromatographic methods are used mainly for quantitative determinations. When doing assay for the products containing explosives in the percent range, we achieved in routine analysis an overall relative standard deviation of ± 0,5 % to ± 1 % of the results. The determination of GTN and EGDN in air to control the TLV-values gives relative standard deviations up to ± 5 %. This arises from the fact that the concentrations are very low and therefore the noise is higher than in other separations. For the determination of nitrotoluenes in the ppb range, the relative standard deviation is ± 10 %.
Qualitative analysis shows deviation in the retention times in the range of 5 %. Since the commercial available prepacked HPLC columns have been greatly improved, the retention times and the separation behaviour does only show miniumum changes.
When a new column is installed test runs with calibration solutions are done.

3.2.0 Sensitivity and minium detectable concentration range

In HPLC separations detection limit with the used equipment is in the 10-5 nanogram range absolute when analysing GTN and other nitrate ester. In some cases, sensitivity can be increased by overloading the column when the separation of the by products form the main products is good. For example in the determination of inorganic nitrates and 2-ISMO in 5-ISMO, solutions of 1 g per 100 ml are analysed.
The analysis of nitrotoluenes with glass capillary GC with flame ionisation detection has also detection limits of 5 to 10 nanograms absolute.
The chromatograms which were shown as practical examples do not cover all our work but were selected to show typical simple and reliable methods. With slight variations or modifications of the mobile phase these methods can be used for various problems which arise in the daily work of an analytical laboratory of an explosives plant.

4.0.0 Table of analysed components:

| | | |
|---|---|---|
| Centralit I | = | Diethyldiphenylurea |
| DEGDN | = | Diglycoldinitrate |
| 1,2-GDN | = | 1,2-Glyceroldinitrate |
| 1,3-GDN | = | 1,3-Glyceroldinitrate |
| GTN | = | Glyceroltrinitrate |
| EGDN | = | Glycoldinitrate |
| Glycolmononitrate | | |
| 2-ISMO | = | Isosorbide-2-mononitrate |
| 5-ISMO | = | Isosorbide-5-mononitrate |
| ISDN | = | Isosorbidedinitrate |
| o-Mononitrotoluene | | |
| m-Mononitrotoluene | | |
| p-Mononitrotoluene | | |
| 2,4-Dinitrotoluene | | |
| 2,6-Dinitrotoluene | | |
| 2,4,6-Trinitrotoluene | | |
| Nitroguanidine | | |
| Hexogen = RDX | = | Cyclotrimethylenetrinitramine |
| Octogen = HMX | = | Cyclotetramethylenetetranitramine |

5.0.0 Literature cited

(1) I.S. Krull, M.J. Camp, International Laboratory, May/June 1980, p. 15-20

(2) M. Fariwar-Mohsenie, E. Ripper, K.H. Habermann, Fresenius Z. Anal.Chem., 296, 152-155 (1979)

(3) H.Köhler in Proceedings of the 15th International Conference of ICT, Karlsruhe 1984

(4) H. Engelhardt, High Performance Liquid Chromatographie, Springer Verlag Berlin, Heidelberg, New York, 1977, p. 183

(5) H.Köhler in Proceedings of the 18th International Conference of ICT, Karlsruhe 1986

# EXPLOSIVES DETECTION USING ENERGETIC PHOTONS

Jerome R. Clifford, R. Bruce Miller, Wm. F. McCullough, and Wm. K. Tucker*

TITAN Technologies, P. O. Box 4399
Albuquerque, NM 87196
USA

## ABSTRACT

TITAN Technologies is testing a new technique called EXDEP (EXplosive Detection with Energetic Photons) for detecting explosives. The technique uses an intense x-ray beam to photoactivate the nitrogen in an explosive. Following the activation, the resulting nitrogen isotope decays with a 10-minute half-life emitting a positively charged positron. The positron annihilates producing two 511-keV photons which are counted using sodium iodide scintillation detectors.

EXDEP works because most commercial and military explosives contain ≥18% nitrogen. Possible signal contaminants which also undergo photoactivation generally have short half-lives or reaction threshold energies above 15 MeV. Because the nitrogen reaction threshold is 10.6 MeV, the signal-to-background can be enhanced by tuning the accelerator to around 14 MeV. Copper, zinc and silver which also produce annihilation photons can be distinguished using conventional x-rays to determine the higher metal density.

Experiments, supported by the Defense Advanced Research Projects Agency, have shown that EXDEP can detect several hundred grams of mock TNT explosives. The experimental results agree with our model calculations, and the model has been used to determine the optimum accelerator and detector parameters to achieve >99.8% detection probability with a <0.2% false alarm probability. TITAN, under Sandia National Laboratories funding, is designing, constructing, and testing a prototype EXDEP system including the RF LINAC and detector components.

The EXDEP technique can be used to search for unexploded ordnance and terrorist devices. It can be configured with a computer tomography x-ray unit to inspect luggage at airports or parcels at bulk mail facilities. A portable EXDEP unit can be used by bomb squads to determine the presence of explosives in packages or confined spaces.

* Sandia National Laboratories, Albuquerque, NM 87185

# MS/MS OF ENERGETIC COMPOUNDS. A COLLISION INDUCED DISSOCIATION (CID) STUDY OF SOME POLYNITROBIPHENYL-2-AMINES

Jehuda Yinon* and R.W. Read**

*Department of Isotope Research
Weizmann Institute of Science
76100 Rehovot, Israel

**Department of Organic Chemistry
University of New South Wales
Kensington, N.S.W. 2033, Australia

## ABSTRACT

In an effort to design energetic materials with improved properties, polyaminopolynitroaromatic compounds have become the subject of renewed investigation. As part of this effort we have investigated the fragmentation processes of a series of polynitrobiphenyl-2-amines, previously synthesized, using tandem mass spectrometry (MS/MS) with collision induced dissociation (CID). Major fragmentations included loss of OH from the molecular ion, second loss of OH from the $(M-OH)^+$ ion, loss of NO and loss of $NO_2$. Fragmentation processes in relation to molecular structure are discussed.

## 1. INTRODUCTION

Although polyaminopolynitroaromatic compounds have been used as explosives for many years, only recently have they become the subject of renewed interest. Amino substitution has been used as a way of modifying the properties of nitroaromatic compounds in an effort to decrease the impact sensitivity (1,2). As part of this effort to design energetic materials with improved properties, a series of polynitrobiphenyl-2-amines were synthesized (3). It was found that the amino group can raise the melting point and density of a nitroaromatic compound, because of its ability to undergo strong hydrogen bonding with a neighboring nitro group and its ability to strengthen the $C-NO_2$ bond of an ortho or para nitro group (3).

In order to better understand the mass spectral fragmentation reactions and pathways of these compounds a collision induced dissociation (CID) study was carried out using a tandem mass spectrometer (MS/MS).

In CID, when using magnetic sector instruments, a beam of precursor ions having translational kinetic energies of several keV collides with an inert gas, which transforms some of the translational energy of the ions into internal excitation energy. Because of the similarity between CID and electron impact (EI) spectra, it is assumed that the CID mass spectrum is related to the precursor ion structure in the same way as the EI mass spectrum is related to the molecular structure (4). Fragmentation pathways of several energetic compounds have been previously determined by MS/MS CID (5-10).

Thus, we have studied the MS/MS CID spectra of a series of polynitrobiphenyl-2-amines in order to determine the fragmentation processes of these compounds. The investigated compounds included 2'-nitrobiphenyl-2-amine (1), 2',4',6'-trinitrobiphenyl-2-amine (2), 2',3',4',5-tetranitrobiphenyl-2-amine (3), 2',3,5,6'-tetranitrobiphenyl-2-amine (4), 2',4,4',6,6'-pentanitrobiphenyl-2-amine and (5), and 2',3,4',5,6'-pentanitrobiphenyl-2-amine (6).

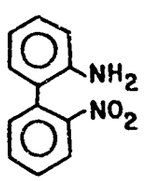


1

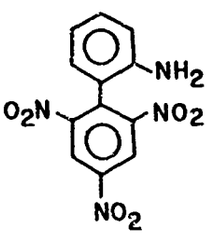


2

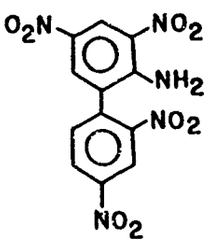


3

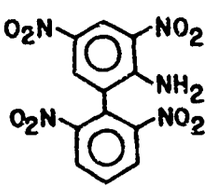


4

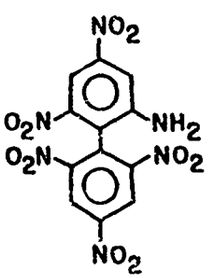


5

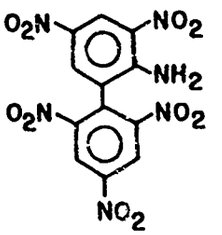


6

## 2. EXPERIMENTAL

The tandem mass spectrometer (MS/MS) consists of two magnetic sector analyzers with a collision cell located in the region between the two analyzers. A full description of the instrument is given elsewhere (9). Argon was used as collision gas. The pressure of the argon was adjusted so that the precursor ion beam intensity was reduced to half of its initial value.

The ionization mode was EI at 70 eV. The ion source was operated at a temperature of 150–250°C. Samples were introduced through the solid probe inlet, using the in-beam EI technique (11,12). To obtain in-beam EI spectra, the sample was loaded on the tip of the modified solid probe (13). The probe was not heated separately.

The synthesis of the investigated compounds is described in Reference 3.

## 3. RESULTS AND DISCUSSION

Table 1 lists the abundances of the major ions observed in the CID spectra of the molecular ions as well as of the highly abundant fragment ions. The daughter ion abundances are expressed as a percentage of the abundance of the largest daughter ion. Six examples of CID spectra are shown in Figures 1-6, which depict the CID spectra of the molecular ions of the six investigated compounds.

All six compounds are characterized by a molecular ion in their EI mass spectrum. Loss of OH from the molecular ion is typical to all 6 compounds, probably due to an ortho effect. Second loss of OH from the $(M-OH)^+$ ion occurs only in the 2'-nitro and the 2',3,4',5-tetranitro compounds. These two compounds are the only ones which do not have a nitro group in the 6' position, which might be the reason of the exclusion of this process.

Loss of NO occurs mainly after loss of OH. Only in the 2',3,4',5,6'-pentanitro compound, does the loss of NO occur after loss of $NO_2$. The losses of NO might be a measure of $C-NO_2$ to C-ONO rearrangement. Isotopic labeled compounds could give an indication concerning the origin of the NO loss.

Loss of $NO_2$ (or loss of $HNO_2$ in the 2'-nitro compound) is a major loss in the investigated compounds. Loss of a second nitro group (either simultaneously with the first one or consecutively after loss of the first one) is a minor process in these compounds.

The results reported herein are only preliminary results. More work on CID of amino nitro biphenyls has to be carried out in order to come to conclusions regarding the stability of these molecules as function of amino and nitro groups.

REFERENCES

1. S. Iyer, J. Energetic Materials 2, 151 (1984).
2. C.D. Hutchinson, V. Krishna Mohan and R.W. Millar, Prop. Explos. Pyrotech. 9, 161 (1984).
3. A.J. Bell and R.W. Read, Aust. J. Chem. 40, 1813 (1987).
4. P.F. Bente III and F.W. McLafferty, in "Mass Spectrometry", edited by C. Merrit, Jr. and C.N. McEwen, Part B, p. 253, Marcel Dekker, New York (1980).
5. J. Yinon, D.J. Harvan and J.R. Hass, Org. Mass Spectrom. 17, 321 (1982).
6. W.R. Carper, R.C. Dorey, K.B. Tomer and F.W. Crow, Org. Mass Spectrom. 19, 623 (1984).
7. J. Yinon and S. Bulusu, Org. Mass Spectrom. 21, 529 (1986).
8. J. Yinon and S. Bulusu, J. Energetic Materials 4, 115 (1986).
9. J. Yinon, Org. Mass Spectrom. 22, 501 (1987).
10. J. Yinon, Org. Mass Spectrom. 23, 274 (1988).
11. B. Soltmann, C.C. Sweeley and J.F. Holland, Anal. Chem. 49, 1164 (1977).
12. M. Ohashi, S. Yamada, H. Kudo and N. Nakayama, Biomed. Mass Spectrom. 5, 578 (1978).
13. J. Yinon, Org. Mass Spectrom. 15, 637 (1980).

Table 1. CID ions of polynitrobiphenyl-2-amines

| | COMPOUND | PRECURSOR ION m/z | DAUGHTER IONS | | | | | | | |
|---|---|---|---|---|---|---|---|---|---|---|
| | | | $(P\text{-}OH)^+$ | $(P\text{-}NO)^+$ | $(P\text{-}2OH)^-$ | $(P\text{-}NO_2)^+$ | $(P\text{-}HNO_2)^+$ | $(P\text{-}OH\text{-}NO_2)^+$ | $(P\text{-}2NO_2)^+$ | OTHER IONS |
| 1 | 2'-NITROBIPHENYL-2-AMINE M.W. 214 | $214(M)^{+\cdot}$<br>$197(M\text{-}OH)^+$<br>$167(M\text{-}HNO_2)^{+\cdot}$ | 197(42)<br>180(100) | | 180(14) | | 167(100) | | | 152(5)<br>166(5),139(100) |
| 2 | 2',4',6'-TRINITROBIPHENYL-2-AMINE M.W. 304 | $304(M)^{+\cdot}$<br>$287(M\text{-}OH)^+$<br>$258(M\text{-}NO_2)^+$ | 287(100)<br>241(100) | | | 258(71)<br>241(100)<br>212(73) | | 241(28) | | |
| 3 | 2',3,4',5-TETRANITROBIPHENYL-2-AMINE M.W. 349 | $349(M)^{+\cdot}$<br>$332(M\text{-}OH)^+$<br>$303(M\text{-}NO_2)^+$<br>$286(M\text{-}OH\text{-}NO_2)^+$ | 332(100)<br>315(35)<br>286(100) | 256(100) | | 303(16)<br>286(100)<br>240(27) | | 286(12) | 240(27) | |
| 4 | 2',3,5,6'-TETRANITROBIPHENYL-2-AMINE M.W. 349 | $349(M)^{-\cdot}$<br>$332(M\text{-}OH)^+$<br>$303(M\text{-}NO_2)^+$<br>$286(M\text{-}OH\text{-}NO_2)^-$ | 332(100)<br>286(100) | 256(100) | | 303(42)<br>286(100)<br>257(11)<br>240(45) | | 286(68 ) | 257(11)<br>240(10) | |
| 5 | 2',4,4',6,6'-PENTANITROBIPHENYL-2-AMINE M.W. 394 | $394(M)^{+\cdot}$<br>$377(M\text{-}OH)^+$ | 377(100) | 347(100) | | 348(38) | | | 302(11) | |
| 6 | 2',3,4',5,6'-PENTANITROBIPHENYL-2-AMINE M.W. 394 | $394(M)^{+\cdot}$<br>$377(M\text{-}OH)^+$<br>$348(M\text{-}NO_2)^+$ | 377(100) | 364(21)<br>318(100) | | 348(25)<br>331(100)<br>302(80) | | 331(35) | 302(9)<br>285(37) | |

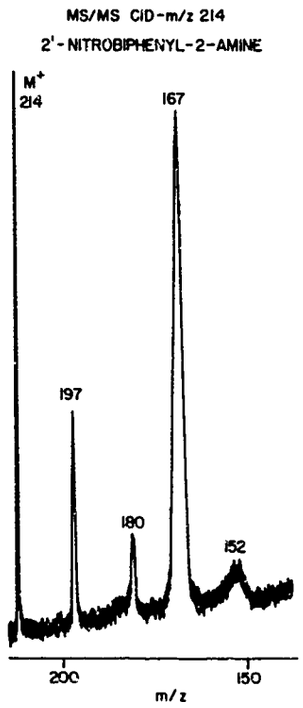


Figure 1. CID spectrum of the molecular ion of 2'-nitrobiphenyl-2-amine.

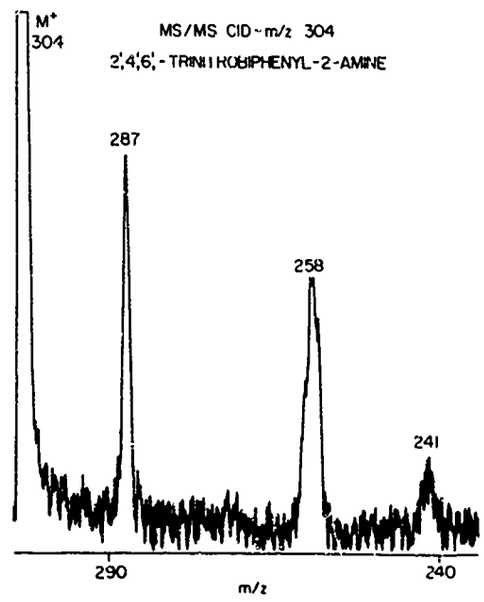


Figure 2. CID spectrum of the molecular ion of 2',4',6'-trinitrobiphenyl-2-amine.

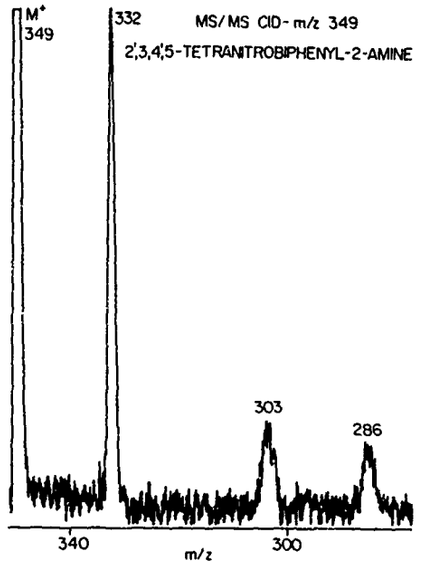


Figure 3. CID spectrum of the molecular ion of 2',3,4',5-tetranitrobiphenyl-2-amine.

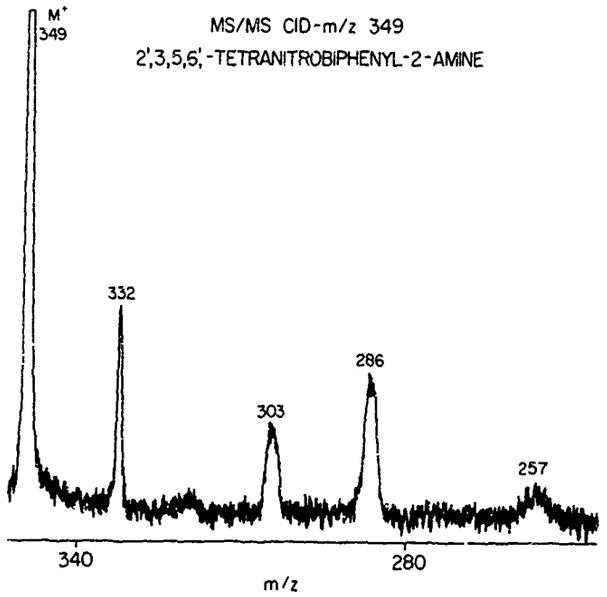


Figure 4. CID spectrum of the molecular ion of 2',3,5,6'-tetranitrobiphenyl-2-amine.

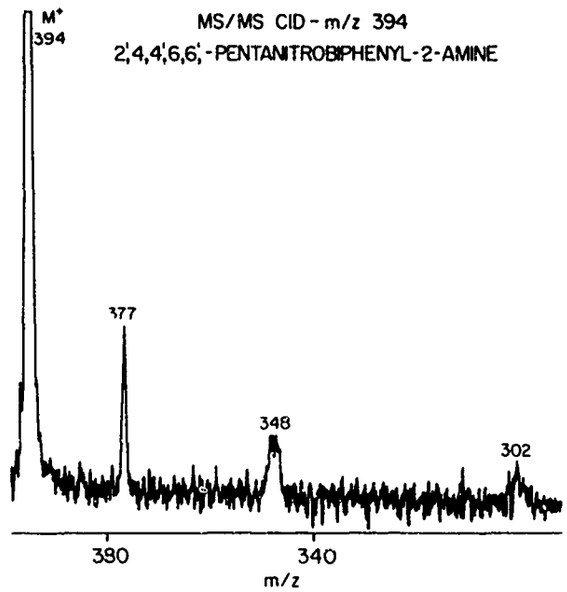


Figure 5. CID spectrum of the molecular ion of 2',4,4',6,6'-pentanitrobiphenyl-2-amine.

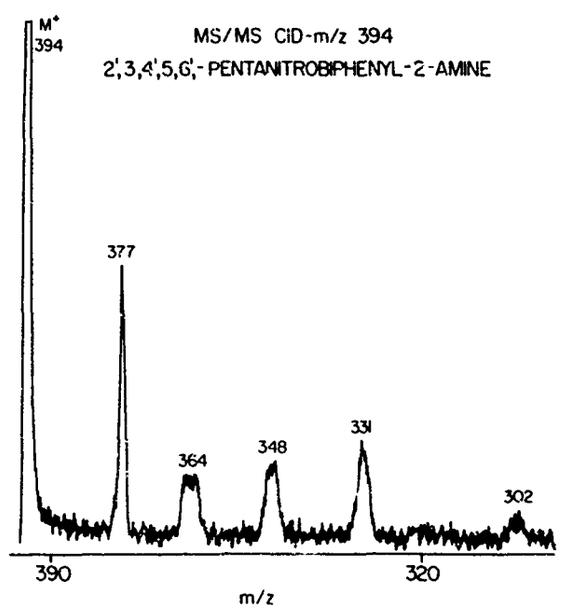


Figure 6. CID spectrum of the molecular ion of 2',3,4',5,6'-pentanitrobiphenyl-2-amine.

# DETECTION AND PERSISTENCE OF TRACES OF SEMTEX AND SOME OTHER EXPLOSIVES ON SKIN SURFACES

J B F Lloyd and R M King

Home Office Forensic Science Laboratory, Gooch Street North, Birmingham B5 6QQ, U.K.

(British Crown copyright reserved)

## ABSTRACT

It is shown that with the described swabbing procedures and analytical techniques, relatively slight skin-contact with Semtex may be detected for at least a week afterwards. During this time some secondary transfer may occur. Other common explosives are much less strongly retained.

## INTRODUCTION

Previous work employing gas chromatography (GC) [1] and high-performance liquid chromatography (HPLC) [2] techniques has demonstrated that nitroglycerin (NG) traces remaining from a contact with gelignite explosives may be detected on the hands for up to 48 hr following the initial contact. During this time strongly retained metabolites appear on the skin surface in amounts finally similar to the amount of the remaining NG. Apart from their greatly increasing the specificity of a result, these

residues give an indication of the time sin. contact with an explosive [2].

Because of the now common association of the plastic explosive Semtex with terrorist activity, it seemed pertinent to extend the earlier work to this material. The explosive components of Semtex are PETN (pentaerythritol tetranitrate) and RDX (cyclotrimethylene trinitramine), the individual persistences of which, from contact with military explosives, have been studied by Twibell et al. [3]. Their results (from GC, electron capture detection) were that RDX could be detected 24 hr after contact at the 30 ng/swab level. None was detected after 48 hr although by extrapolation it was estimated that identifiable amounts should remain after two to three days. The behaviour of PETN was reported to be similar to RDX.

## EXPERIMENTAL

### Explosive

The sample of Semtex was obtained from the Royal Armaments Research and Development Establishment, U.K.; HPLC analysis indicated the presence of RDX (40%) and PETN (43%). For the administration of controlled amounts to skin surfaces the explosive was dissolved in ethyl acetate.

### Swabs and swab processing

The swabbing material was a non-woven cotton cloth (Litex-10, 4 * 6 cm, LIC Hygiene) [4] wetted with isopropanol containing 20% v/v water. The samples from the hands were collected by a vigorous scrubbing of the palm

and finger surfaces with the swabs. These were returned to the containers (disposable polypropylene centrifuge tubes) in which most of the subsequent processing was conducted by already-described techniques [5]. Essentially, centrifugates of the swabs were diluted with water and extracted onto loose Chromosorb-104 (10 mg). This was transferred to 1-mm i.d. microcolumns prepacked with Amberlite XAD-4 (5 mg), from which the explosives components were eluted in acetonitrile : water (25 : 12, v/v) at 1 µl/s. The 35-90 s fraction was collected.

Analytical details

Small portions of the microcolumn eluates were examined by reversed-phase HPLC with electrochemical reductive detection at a pendent mercury drop electrode (-1.0 V vs Ag/AgCl; and -0.7 V in the event of an initial positive result) according to well-established procedures [6]. For confirmation of their identities the weaker HPLC peaks of interest were diverted to a 65-mm microcolumn of Chromosorb-104, connected through a 4-port valve installed at the outlet of the HPLC column. The collected peaks were eluted with ethyl acetate : acetonitrile (3 : 2, v/v) into the 20 µl following the void volume. These eluates were examined by capillary GC with Thermal Energy Analyser (GC/TEA) detection under conditions similar to published procedures [7] excepting that the time constant of the TEA electronics (Thermo Electron, #543 Analyser) had been reduced by the replacement of a capacitor in the

circuitry, and the output signal was smoothed by a purposely-built active filter [8]. The pyrolysis tube (Thermo Electron, #610 furnace) was held at 850 °C. The GC column (5 m, 0.32 mm i.d., SE52) was preceded by a retention gap (2 m of 0.32 mm i.d. unmodified silica tubing), which enabled the injection of up to 4-µl samples. (Hence, there was no need to employ an evaporation step in the sample work-up.) All the chromatograms were temperature-programmed from 60-230 °C at 25 °C/min, with an inlet carrier gas (He) pressure of 1 Kg/cm².

The reported quantitative results are from HPLC analyses calibrated against solutions of the standard compounds. Each set of analyses included swabs taken from subjects who had had no known contact with explosives. None of these swabs gave any response attributable to explosives.

## RESULTS AND DISCUSSION

The swabbing materials and procedures used were, respectively, the same as those now issued in kits and now employed on a routine basis in the areas covered by all of the Home Office forensic science laboratories. Prepacked, prewetted swabs are included in the kits, which are used for both explosives and firearms residue traces. The used kits are returned to a central unit that provides an analytical service based on the techniques applied in this investigation, with the additions as needed of GC/mass spectrometry and scanning electron microscopy.

In general, 1 ng/swab of an explosive is a more than adequate amount for its detection and confirmation. In Figs. 1 and 2 are chromatograms from a swab found to contain RDX, 2.5 ng, and PETN, 21 ng. In the HPLC result shown (Fig. 1) the main peak is due to an internal standard (1,3-dinitrobenzene, 10 ng/swab); but apart from this and the weakly retained material only the explosives peaks are prominent. Just a small fraction of the sample is required for the HPLC: the RDX peak here corresponds to a 50-pg amount. The remainder of the sample is available to confirmatory techniques, which are restricted specifically to the HPLC effluent containing the compounds of interest. This minimizes the ambiguity arising otherwise in whether or not the different techniques applied are responding to the same compound. Also, very clean samples are produced by the trapping technique, as the GC/TEA result in Fig. 2 shows.

Details of the persistence experiments conducted on five male subjects are given in Table 1. The results quoted are of the quantities of explosives recovered from the swabs. No account has been taken of the swabbing efficiency, processing losses, or the effects in some instances of the earlier swabbings. Hence, the values given are substantial underestimates of the amounts actually present. The intermediate amount applied to the hands - 500 µg of the explosive - is of the order of the amount transferred when plastic explosive is handled [3]. Some cursory experiments in the present work indicated

that if the hands are washed immediately afterwards not more than 10% remains immediately retrievable to swabbing. Even so, as Table 1 shows, sufficient remains to give a substantial response several days later. An HPLC result obtained a week after a 500-µg contamination is given in Fig. 3. In this instance only a slight response attributable to PETN remained, but as the chromatogram shows there remained substantial amounts of RDX.

Usually the RDX component tended to be more persistent than the PETN but the effect was weak. The results were dominated by the large between-subject variation characteristic of this type of experiment, particularly when there can be no control of the mechanisms responsible for the loss of explosives from the hands (2). The variation is particularly apparent in Fig. 4 where results from Table 1 have been plotted as depletion ratios at various times after the initial contamination. It is also apparent, however, that after the initial loss over the first day almost a week may elapse before a similar further loss has occurred.

Included in Fig. 4 are the approximate depletions found after 24 hr in experiments conducted on TNT-contaminated hands and in earlier work on NG (2). The ordering of the depletion ratios is the reverse of the volatility of the compounds. For NG, and the more volatile explosives generally, volatilisation is undoubtedly a major depletion mechanism; but from the extreme persistence of RDX in particular it seems that a specific affinity for a

skin component might be involved. Unlike the case of NG no evidence has been found in this work of a substantial accumulation of any metabolic degradation product of the other explosives on the skin surface. Partly nitrated products from the analogous PETN as well as from TNT [9] are well-known, and the presence of significant amounts of them should have been detected.

Some determinations were made of the extent to which secondary transfer of the Semtex components might occur. The results, from members of the family of each primary contact, are collected in Table 2. From three out of the seven possible recipients a positive result was obtained. The amounts of explosives found were small, but clearly more substantial amounts could be transferred from a heavily contaminated skin surface, or from any other heavily contaminated source.

## CONCLUSIONS

A transfer to the hands of microgram amounts of Semtex may result in the presence of RDX and PETN in detectable amounts on the hands for at least as long as a week afterwards. The detection of traces of explosive, especially of RDX alone, is not a necessary consequence of a direct contact with Semtex or with a related explosive, although a contact of some kind - perhaps indirect but none the less significant - with an explosives-containing environment must have occurred. A sampling of possible origins might be needed to clarify the position.

Surroundings containing heavily contaminated items may act as a reservoir of skin contamination over a prolonged time. Even so, the overall conclusion remains that under the kind of circumstances with which this paper is concerned Semtex is the most readily detected of the high explosives commonly available to terrorism.

## REFERENCES


1. J D Twibell, J M Home, K W Smalldon & D G Higgs
   The Quantities of Nitroglycerine Recovered from Hands after Contact with Commercial Explosives,
   J. Forens. Sci., 27, 783-791, 1982.

2. J B F Lloyd
   Glyceryl Dinitrates in the Detection of Skin-contact with Explosives and Related Materials of Forensic Science Interest,
   J. Forens. Sci. Soc., 26, 341-348, 1986.

3. J D Twibell, S L Turner, K W Smalldon & D G Higgs
   The Persistence of Military Explosives on the Hands,
   J. Forens. Sci., 29, 284-290, 1984.

4. L W Russell
   The Universal Hand-swab - Does it Exist?
   J. Forens. Sci. Soc., 24, 349, 1984.

5. J B F Lloyd & R M King
   (submitted for publication).

6. J B F Lloyd
   Liquid Chromatography of Firearms Propellants Traces,
   J. Energetic Materials, 4, 239-271, 1986; and references therein.

7. J M F Douse
   Improved Method for the Trace Analysis of Explosives by Silica Capillary Column Gas Chromatography with Thermal Energy Analyser Detection,
   J. Chromatogr., 410, 181-189, 1987.

8. D A Collins
   (submitted for publication).

9. J Yinon & D -G Hwang
   Detection of TNT and its Metabolites in Body Fluids of Laboratory Animals and in Occupational Exposed Humans,
   J. Energetic Materials, 4, 305-313, 1986.

TABLE 1: Recovery of RDX and PETN from hands contaminated with Semtex.

| Semtex contamination | Subject | Time (hr) | RDX found/ng | | PETN found/ng | |
|---|---|---|---|---|---|---|
| | | | Left | Right. | Left | Right |
| 2.5 mg in solution to each hand. | A | 16 | 4710 (total) | | 4750 (total) | |
| | | 43* | 774 | 743 | 233 | 207 |
| 500 µg in solution to each hand (at 113 hr, B's left hand, dry swab used). | B | 64 | 98 | 91 | 49 | 52 |
| | | 113* | 16 | 30 | nd** | 1.4 |
| | | 161* | 27 | 21 | 2.2 | nd |
| | C | 64 | 34 | 9.1 | 3.0 | nd |
| | | 161* | nd | 0.6 | nd | nd |
| Piece between palms 10 s, hands immediately washed. | A | 65 | 21 | 22 | 25 | 30 |
| | B | 65 | 4.6 | 1.9 | nd | nd |
| | C | 65 | 5.9 | 0.6 | 1.3 | nd |
| 50 µg in solution to each hand. | D | 68 | 29 | 30 | nd | nd |
| | E | 94 | 0.8 | 3.6 | 1.0 | 3.9 |

*Reswabbings.
**nd = not detected.

TABLE 2: Secondary transfer from Semtex-contaminated hands (initial primary contamination, ca. 50 µg/hand).

| Subject | Time since primary contamination (hr) | Relationship of contact | Total recovered, hands of contact (ng) | |
|---|---|---|---|---|
| | | | RDX | PETN |
| A | 75 | Wife | 12 | nd* |
| B | 75 | Wife | nd | nd |
| C | 75 | Wife | 11 | 11 |
| D | 68 | Mother | 2.0 | nd |
| | | Sister | nd | nd |
| E | 94 | Wife | nd | nd |
| | | Daughter | nd | nd |

*nd = not detected.

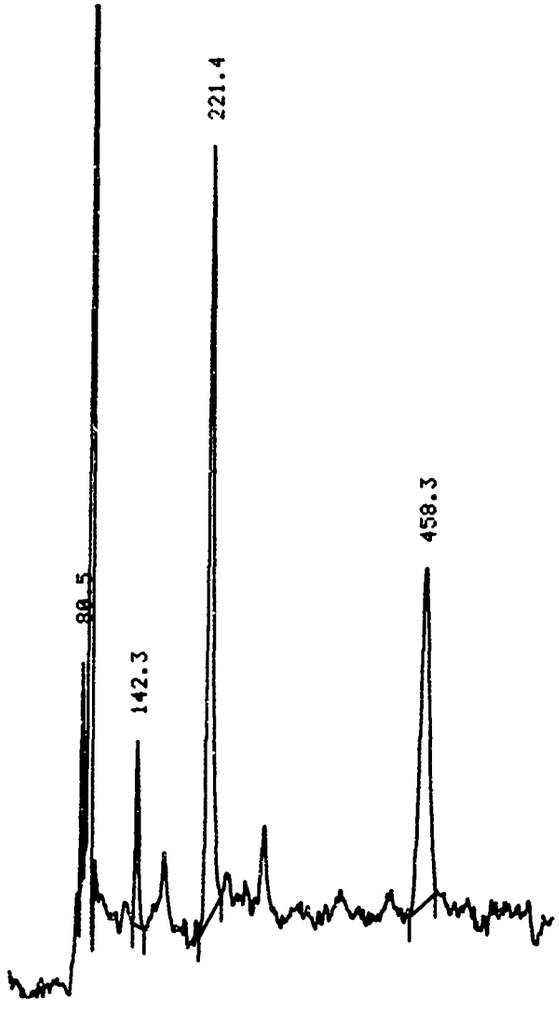


FIGURE 1: HPLC result from a hand swab. The retention times (s) are superscripted on the peaks. RDX and PETN are apparent at 142.3 s and 458.3 s respectively (within 0.4% of the standard compounds), with peak amplitudes of 0.24 nA and 1.0 nA. The peak at 221.4 s is an internal standard (1,3-dinitrobenzene). The respective amounts of RDX and PETN found in the swab are 2.5 ng and 21 ng. Approximately 1/50th of the swab is represented in the chromatogram.

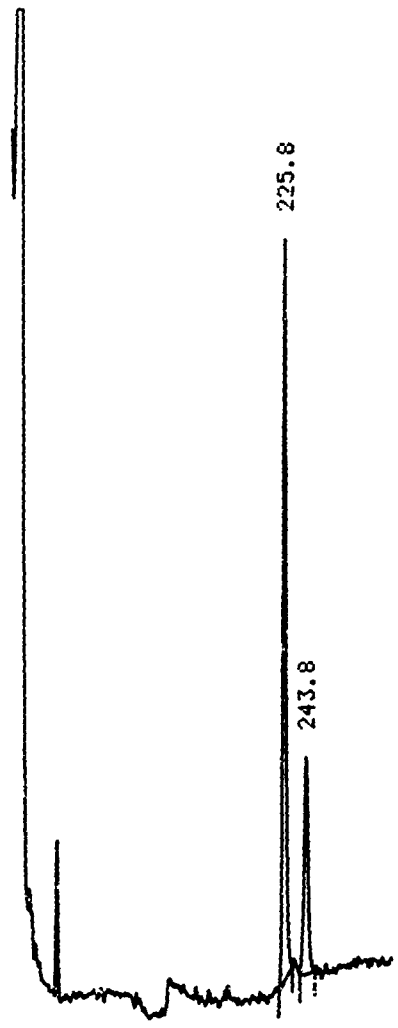


FIGURE 2: GC/TEA result from the RDX and PETN peaks trapped by HPLC from the swab extract shown in Fig. 1. The respective retention times (within 0.5% of standard compounds) are 243.8 s and 225.8 s.

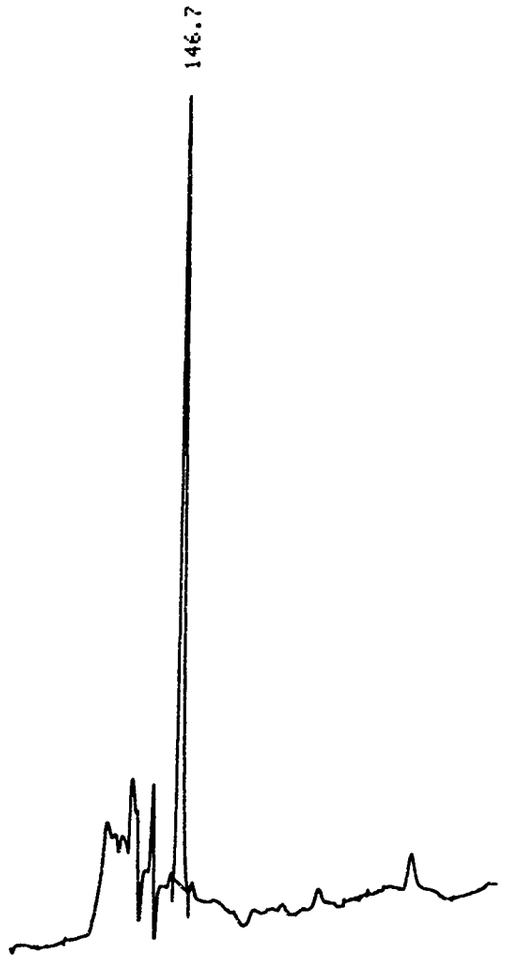


FIGURE 3: LC result from a hand swab taken 7 days after contact with Semtex. RDX is present at 146.7 s (the retention time is within 0.1 s of the standard compound; a less aqueous eluent was used here relative to Fig. 1); the peak amplitude is 3.0 nA. The peak is equivalent to an amount of 27 ng recovered from the swab.

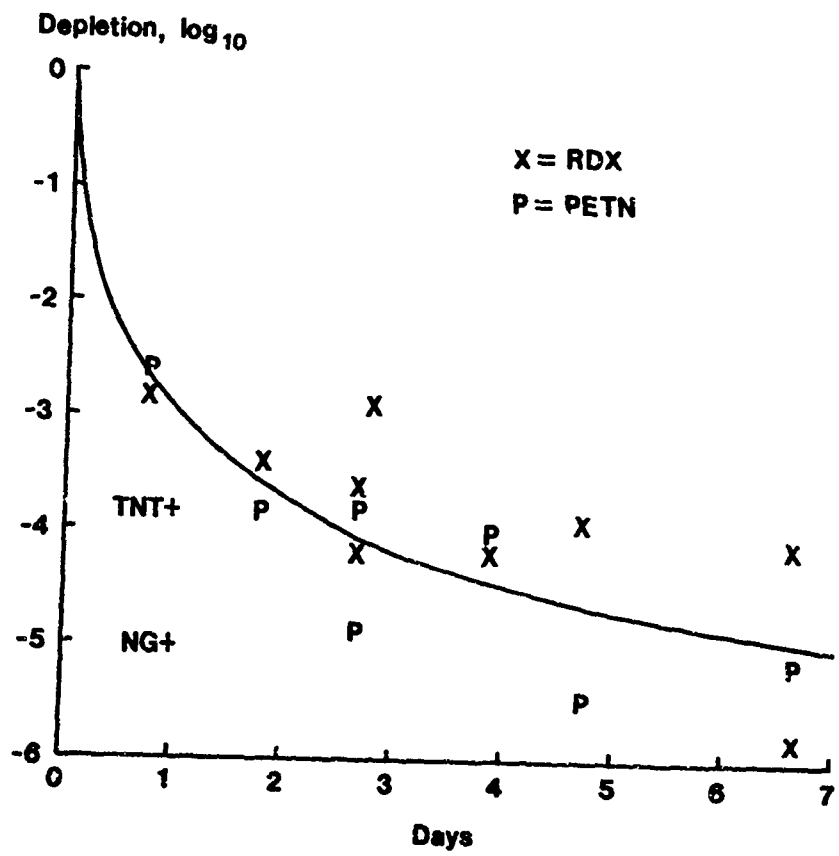


FIGURE 4: Variation of depletion factors with time of RDX and PETN on hands contaminated with Semtex. The approximate depletions of TNT and NG after 1 day are also indicated.

# ANALYSIS OF PORTUGUESE EXPLOSIVES

José Manuel de Morais Anes
Portuguese Forensic Laboratory

## ABSTRACT

The portuguese explosives which are produced by two factories near Lisbon - SPEL and ET - are now being used in criminal activities in other countries (Spain, France etc.).

We present a qualitative and quantitative analysis of these explosives ("dynamites", plastic etc.). We also give information on the morphological aspects, inscriptions, marks, colours, etc., in order to permit a quick identification of the non-exploded portuguese explosives.

# ANALYSIS OF THE EASTERN BLOC EXPLOSIVE SEMTEX-H

Raymond O. Keto

Forensic Science Laboratory
National Laboratory Center
Bureau of Alcohol, Tobacco, and Firearms
Rockville, Maryland 20850, USA

## ABSTRACT

Terrorist use of high explosives such as Semtex-H is a growing problem world wide. The identification of an explosive through its composition, and the linking of similar explosives through chemical analysis are tasks for the forensic chemist. This paper describes procedures used in the instrumental analysis of Semtex-H, and possible "finger-printing" techniques that could be useful in linking samples of Semtex-H from different incidents.

## INTRODUCTION

Semtex-H is an orange colored plastic high explosive manufactured in Czechoslovakia. It can be considered as the Eastern Bloc equivalent to Western plastic explosives such as the U.S. military C-4 and the British PE-4, in terms of consistency, moldability, and brisance. Semtex has been implicated in a number of terrorist activities in recent years, including the recent downing of Pan American Flight 103 over Scotland.

The identification of Semtex requires that the forensic

chemist have knowledge of the explosive compounds and other components present. Occasionally, he may be asked to determine whether two or more suspect samples can be associated through chemical analysis. More than one type of Semtex appear to be available to the terrorist at present. To date, this laboratory has had experience with an developed analytical techniques for the Semtex-"H" variety only. This paper describes preliminary approaches we have used to characterize this type of Semtex.

High Performance Liquid Chromatography (HPLC):

The two high explosive components in Semtex-H are pentaerythritol tetranitrate (PETN) and hexahydro-1,3,5 trinitro-S-triazine (RDX). The ratio of these explosives has been found to vary, and appears to fall into a few broad categories (i.e., 1:1, 1:3, 2:3, etc.). The determination of the exact ratio can be useful in associating a suspect sample with a source. This determination is readily performed by HPLC, using the instrumental parameters listed in Table 1. (Note: These parameters were developed for a ten milligram sample of Semtex-H. It is advisable to use a larger sample, if available, and dilute accordingly to increase the precision of the method.)

Approximately 10 mg of Semtex-H were placed in a 1-dram (3.7ml) glass vial with 1 ml tetrahydrofuran (THF) and stirred on a magnetic stirrer until no solid particles remained. The solution was transferred quantitatively to a 25 ml volumetric flask with a Pasteur pipet. Two subsequent .5 ml THF rinsings of the vial were also transferred to the flask with the pipet. The solution was then diluted to the mark with acetonitrile. (The solution developed a cloudiness due to the insolubility of the non-explosive components in acetonitrile. These insolubles must be removed to prevent clogging of the HPLC system.) 15 microliters of toluene (internal standard) were accurately

measured with a Hamilton #802 syringe, added to the flask, and mixed thoroughly. A 1 to 2 ml aliquot was removed and filtered through a 1 micron Gelman Acrodisc membrane filter for HPLC analysis.

Four standard solutions were prepared individually by accurately weighing portions of recrystallized PETN and RDX and dissolving in the same manner. The dilution volumes were such that the final solutions contained approximately .05, .1, .2, and .4 mg of each explosive per ml.

The chromatogram (Figure 1) showed good peak symmetry, baseline resolution, and a total elution time of less than 5 minutes. Peak areas were computed on a Perkin-Elmer Chromatographics Intelligent Terminal Model 3600 data station. The calibration curve (Figure 2) is a plot of concentration versus the ratio of the peak area to the toluene peak area. Though slightly non-linear, the curves were reproducible and were used as-is. (In subsequent work, we may attempt to identify the cause of this curvature and correct it.)

The relative standard deviation for the determination of PETN and RDX in five replicate 10 mg samples of Semtex-H was +/- 4%. The magnitude of this number may be associated with the limited sample size used and the degree of inhomogeneity in each sample. A larger sample size would tend to minimize compositional variations and lead to a smaller relative standard deviation.

<u>Gel Permeation Chromatography/Fourier Transform Infrared Spectroscopy (GPC/FTIR):</u>

Gel permeation chromatography (size exclusion chromatography) was investigated as a means of separating other

components present in Semtex-H. The GPC operating parameters are listed in Table 2. Figure 3 shows the gel permeation chromatogram. The total exclusion volume for this system occurs at about 5 minutes; the entire sample elutes between this point and the total permeation volume (approximately 10 min.). The numbered peaks were collected in separate vials for subsequent identification by Fourier transform infrared spectroscopy. Samples were prepared for FTIR examination by allowing a few drops of each fraction to evaporate on a KRS-5 window (Wilks #6012). The non-volatile residues were analyzed by transmission on a Digilab UMA-300 microscope attached to a Digilab FTS-40 F.T.I.R. spectrometer.

Peak 1 (Figure 4) was identified as a styrene-butadiene copolymer. This is the binder in Semtex-H. The relative intensities for the styrene and butadiene absorptions indicate a low (less than 50%) styrene-to-butadiene ratio. This material elutes at the total exclusion volume for the 100 Å column. Separation on a larger pore column (Waters Associates linear mixed bed) showed a molecular weight distribution centered at approximately 150,000 daltons.

Peak 2 (Figure 5) was identified as dilauryl thiodipropionate, an antioxidant having a molecular weight of 517. Peak 3 (Figure 6) and Peak 4 (Figure 7) were identified as the two explosives PETN (molecular weight 316) and RDX (molecular weight 222), respectively. (Figure 7 shows some contamination of the RDX by the PETN due to an uncalibrated "delay" volume between the detector and the collection point. This carry-over did not compromise the identification of the RDX).

Because it contains a highly resolved separation pattern for both explosives and two other major ingredients, the gel permeation chromatogram could be an excellent "fingerprint" of

the particular lot of Semtex-H being examined. Given appropriate standards, this method could be used to quantify all four components, giving more information with less sample preparation than with the HPLC technique previously discussed.

Thin-Layer Chromatography:

The orange colorant in Semtex-H is Sudan-I (Color Index 12055, Solvent Yellow 14). It is a common colorant for oils, fats, waxes, shoe and floor polishes, candles, styrene resins, and soap, and dissolves in a variety of organic solvents including alcohol, acetone, ethyl acetate, toluene, and pyridine.

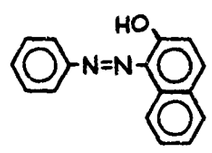


SUDAN - I
M.W. 248

Thin layer chromatography of Sudan-I can be performed on silica (E. Merck HPTLC) using a mobile phase of either chloroform or hexane/ethyl acetate 9:1. It is identified by its color and retention relative to a known sample of Sudan-I.

Gas Chromatography (G.C.):

An aliphatic oil fraction, evident by the FTIR spectrum in Figure 8, was extracted from Semtex-H with hexane. This fraction was analyzed by gas chromatography using the instrumental parameters listed in Table 3. The resulting chromatogram is shown.

a hydrocarbon distribution similar to that for a 10W-40 multiviscosity motor oil (Figure 9). The sharp peaks that are superimposed on the chromatogram (at approximately 3.7, 8.8, and 11.3 minutes) have not been further characterized. Their presence and relative heights, as well as the appearance of the rest of the G.C. pattern, may provide yet another means of linking suspect samples of Semtex-H.

Determination of RDX Type:

There are two types of technical grade RDX specified in the United States, depending on the method of manufacture. Type A is pure RDX, and is manufactured by the nitration of hexamine. Type B contains an impurity of 8 to 12 percent HMX (Octahydro-1,3,5,7-tetranitro-1,3,5,7-tetrazocine), along with a few other side products, and is manufactured by the acetic anhydride or Bachman process (1). The HPLC method listed in Table 4 was used to discern small amounts of HMX in the presence of RDX. The 8 to 12 percent HMX present in the U.S. plastic explosive C-4 was easily detected by this method. No HMX was found in the few Semtex-H samples analyzed to date.

Conclusions:

To date the ATF Laboratory has identified the following ingredients in Semtex-H:

| | | | |
|---|---|---|---|
| Explosives | = | PETN ) | In varying |
| | | RDX ) | ratios |
| Polymer binder | = | Styrene-Butadiene Rubber | |

1. Encyclopedia of Explosives and Related Items, Vol. 3, pp. C611-C624, Picatinny Arsenal, Dover, Delaware, USA, 1966

**Additives**

| | | |
|---|---|---|
| Hydrocarbon Oil | | |
| Antioxidant | = | Dilauryl Thiodipropionate |
| Colorant | = | Sudan-I |

In addition, several chromatographic techniques that show potential for lot identification have been developed. These include HPLC for PETN/RDX ratio: GPC for relative amounts of binder, preservative, and both explosives; and G.C. for hydrocarbon oil characterization. Further work would have to be done on known samples of Semtex-H to establish the validity of lot determination based on these techniques.

TABLE 1

HPLC SEPARATION PARAMETERS

| | | |
|---|---|---|
| Pump | : | Waters Associates M-600A |
| Injector | : | Waters Associates U6K |
| Column | : | Waters Associates Radial Compression C-18, 8mm x 10cm, 4 micron particle size |
| Eluant | : | 70 $CH_3CN$ / 30 $H_2O$ |
| Flow rate | : | 1.0 ML./Min. |
| Detector | : | Schoeffel Model 770 @ 210 nM |
| Sample | : | 15 micro-liters @ 0.5 mg SEMTEX / ml |
| Internal Std. | : | Toluene @ 0.6 micro-liters/ml |

**TABLE 2**

SIZE - EXCLUSION CHROMATOGRAPHY

| | | |
|---|---|---|
| Column | : | Waters Associates Ultrastyragel 100° A Pore Size |
| Eluant | : | THF @ 1.0 ml/min |
| Detector | : | Waters Associates R401 Refractive Index |

**TABLE 3**

GAS CHROMATOGRAPHIC CONDITIONS

| | | |
|---|---|---|
| Instrument | : | Perkin-Elmer Sigma 1-B |
| Column | : | Quadrex High-Temperature Al-Clad Capillary 15M x .25 MM ("400" Methyl Silicone) |
| Carrier | : | He @ 25 PSIG |
| Program | : | $100^{\circ}$ c to $350^{\circ}$ c @ $20^{\circ}$ /Min |
| Injector | : | Modified for Capillary $350^{\circ}$ c |
| Detector | : | F.I.D. @ $350^{\circ}$ c |

## TABLE 4

### CHARACTERIZATION OF RDX BY HPLC

| | | |
|---|---|---|
| Column | : | Supelco LC-CN (cyanopropyl banded phase), 4.6 mm x 7.5 cm, 3 micron particle size |
| Eluant | : | 50 $CH_2CL_2$ / 50 isooctane, by vol. |
| FLow rate | : | 2.0 ml/min |
| Detector | : | Thermo-Electron Corporation TEA Model 510 |
| Sample | : | 1.0 microliter $CH_2CL_2$ extract |
| Elution times | : | PETN, RDX < 5 min; HMX @ 10 min |

## HPLC OF SEMTEX

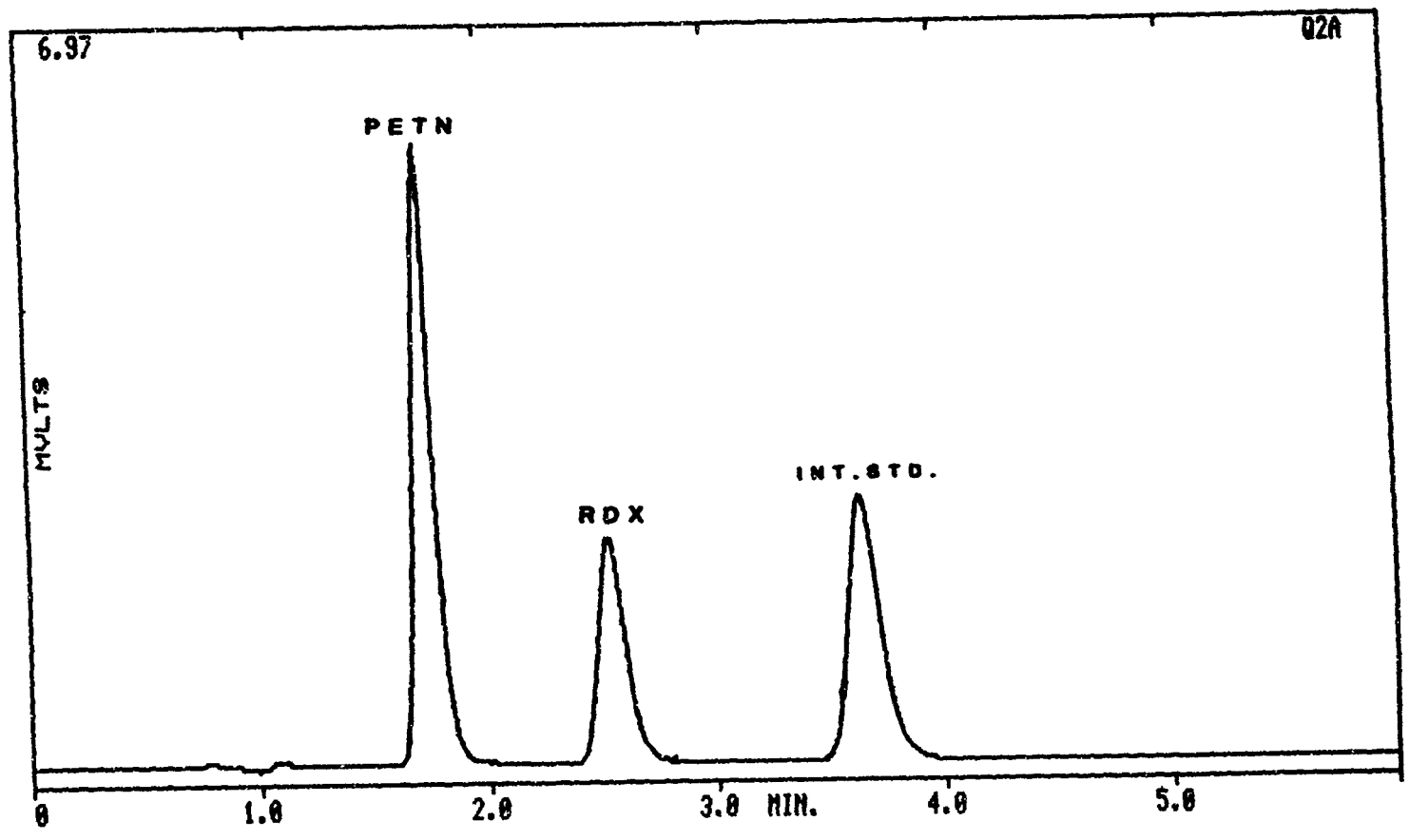


**FIGURE 1**

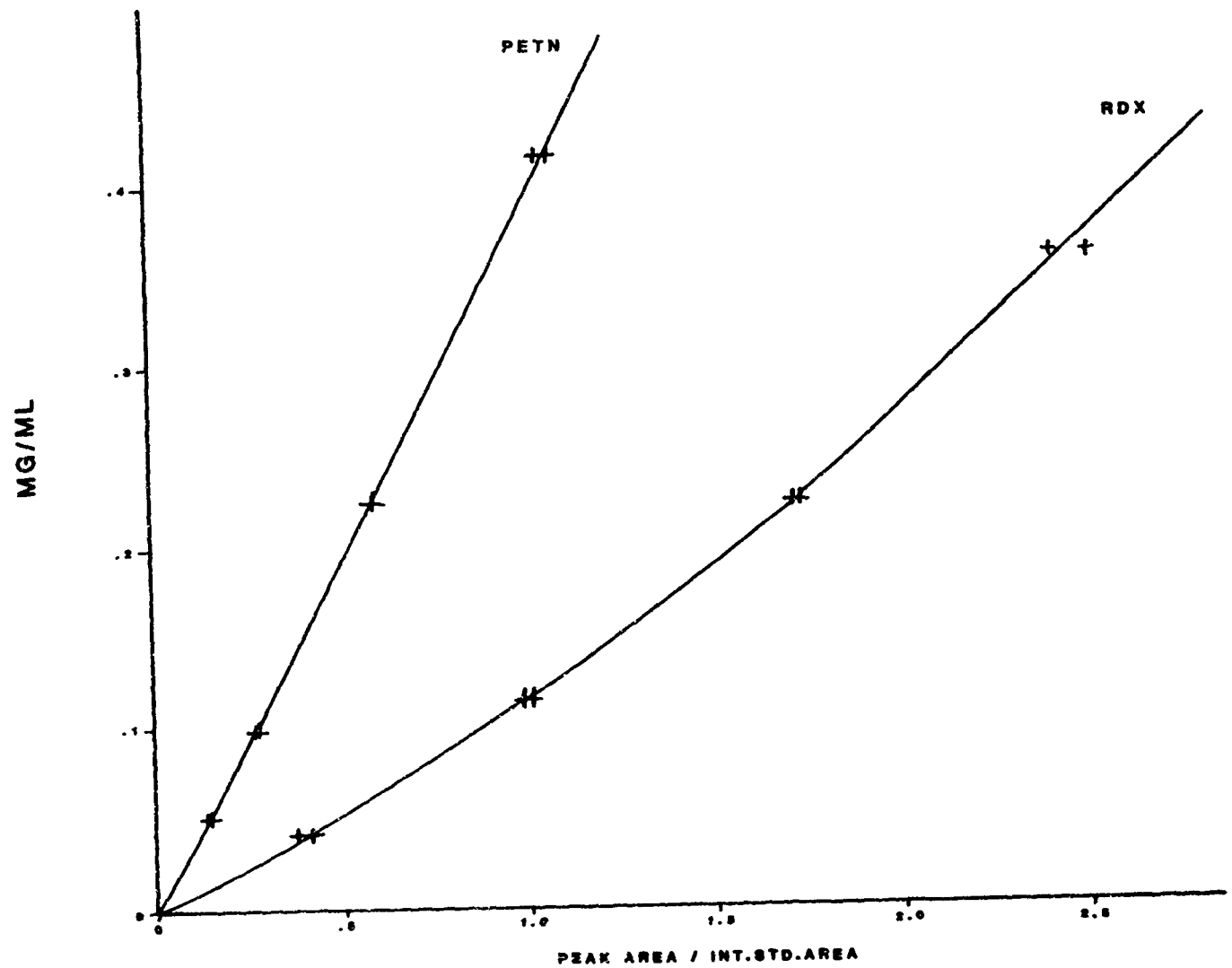


FIGURE 2

GPC OF SEMTEX

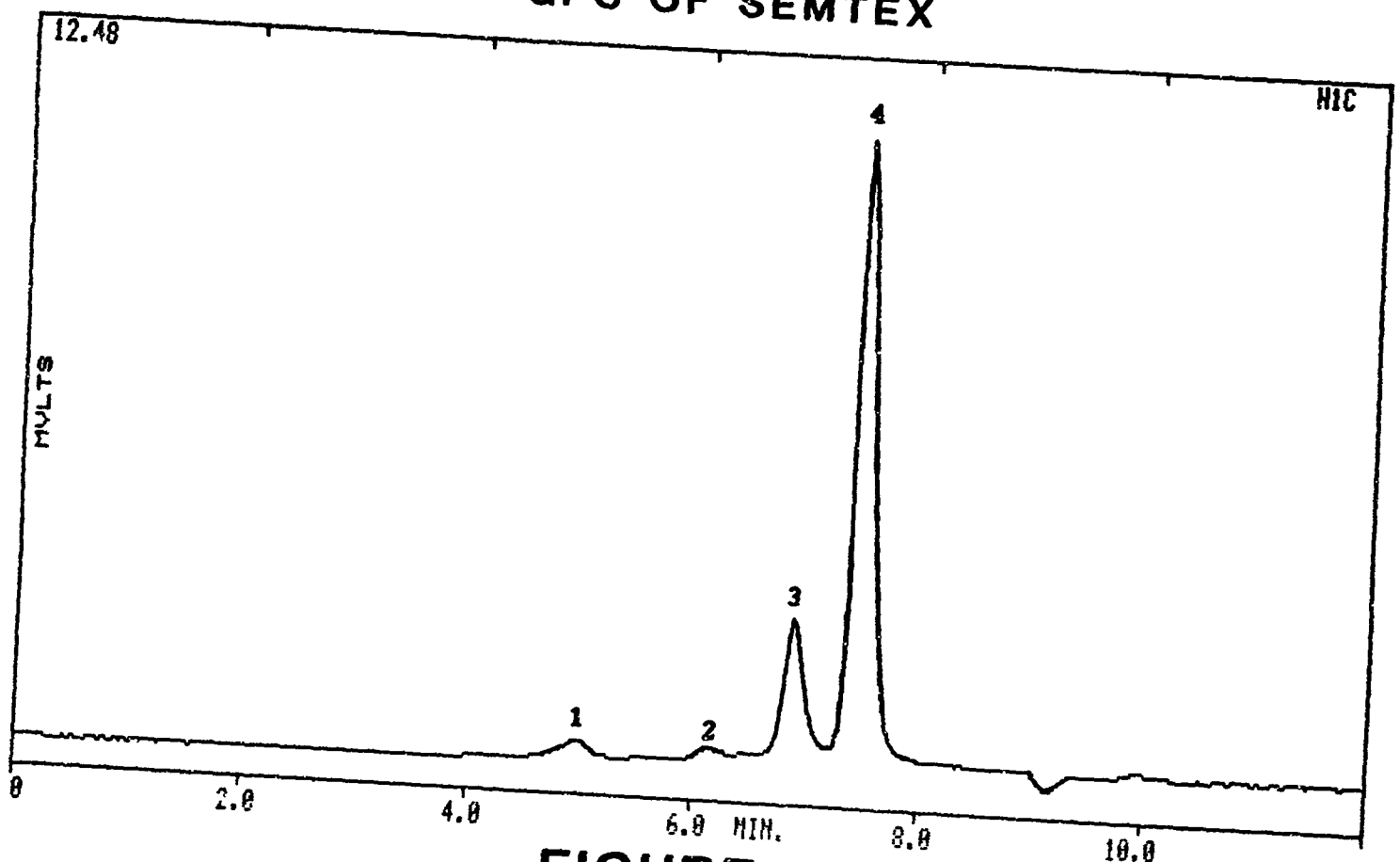


FIGURE 3

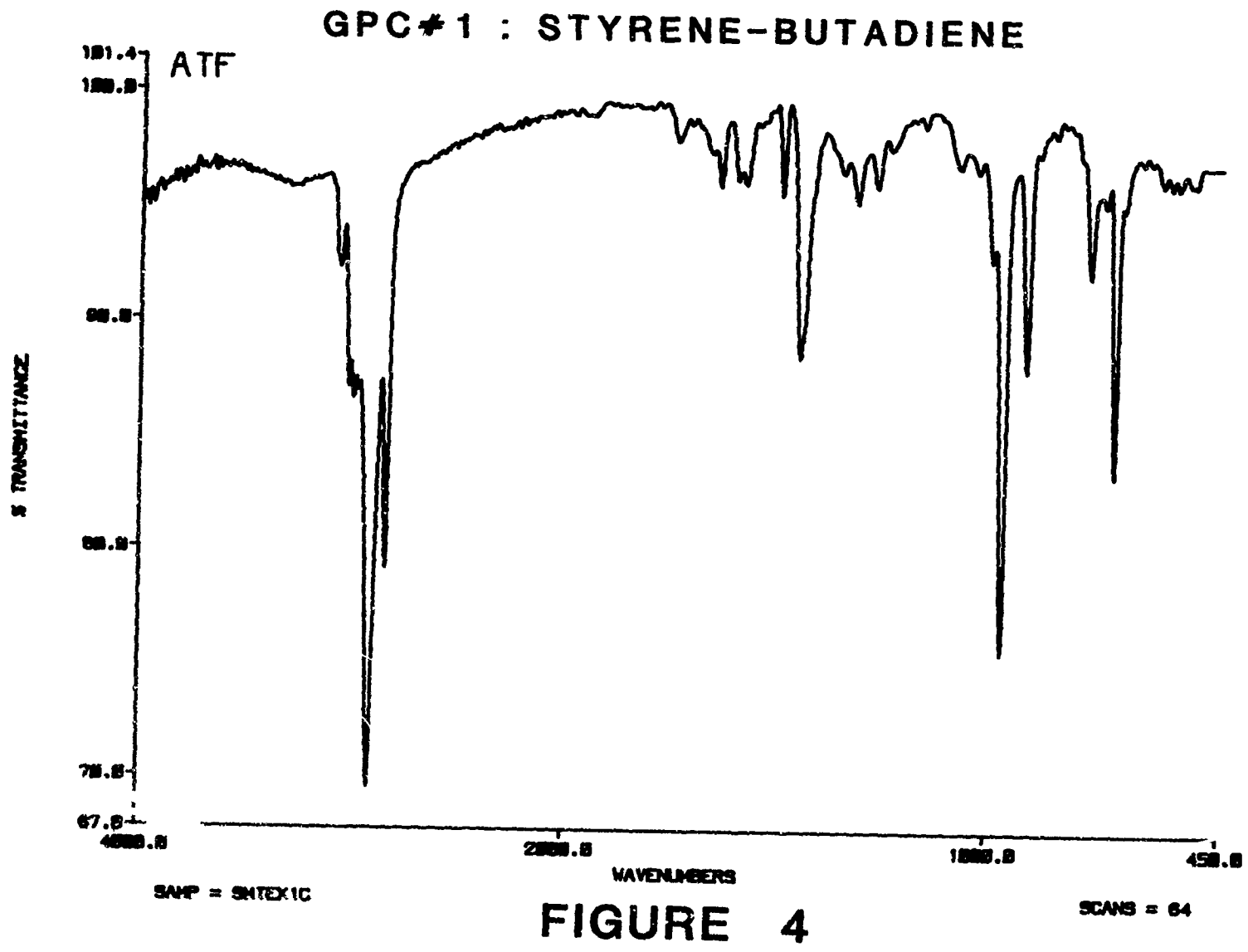
GPC#1 : STYRENE-BUTADIENE
ATF
% TRANSMITTANCE
WAVENUMBERS
SAMP = SNTEX1C
SCANS = 64

FIGURE 4

GPC#2 : DILAURYL THIODIPROPIONATE

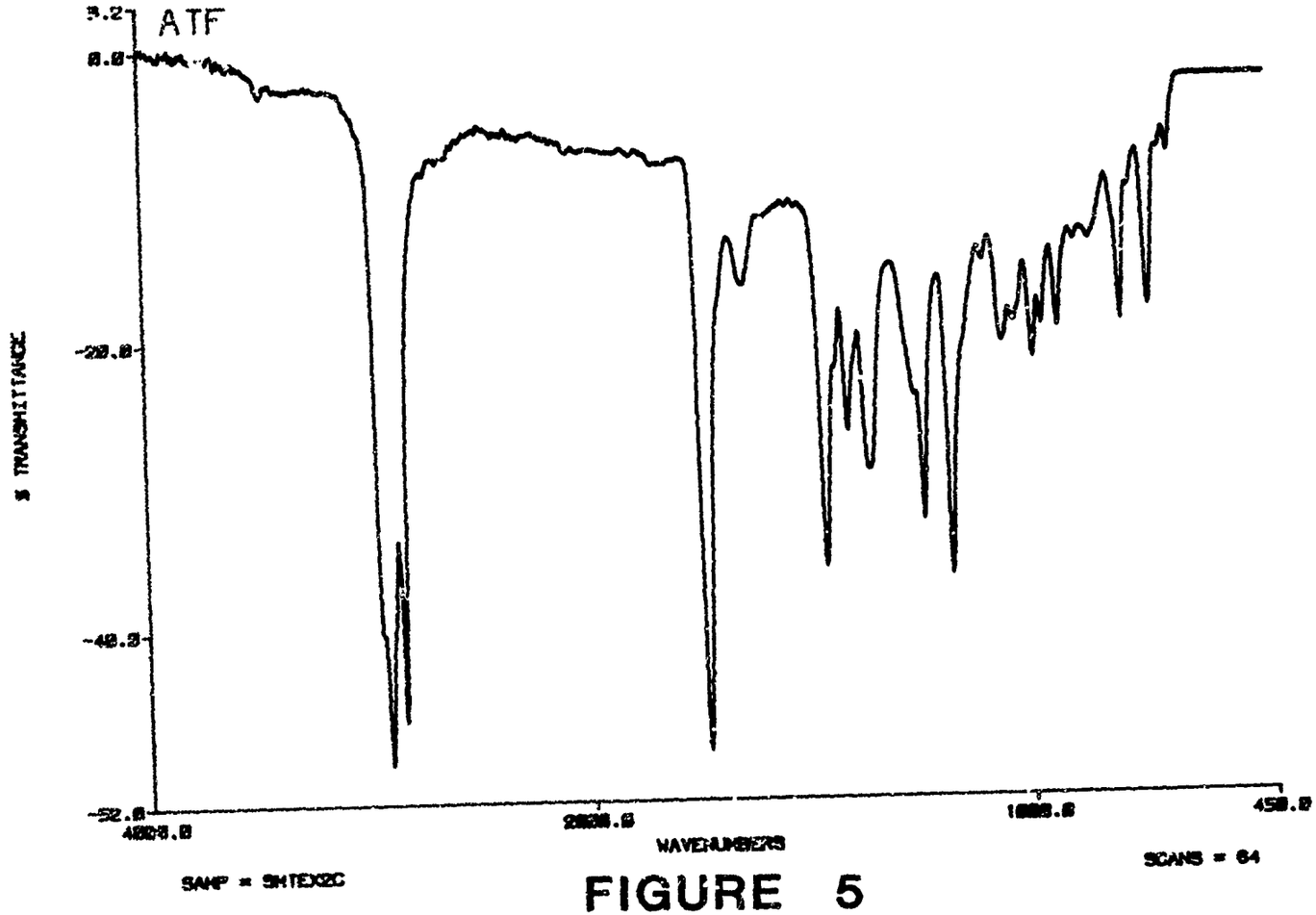


FIGURE 5

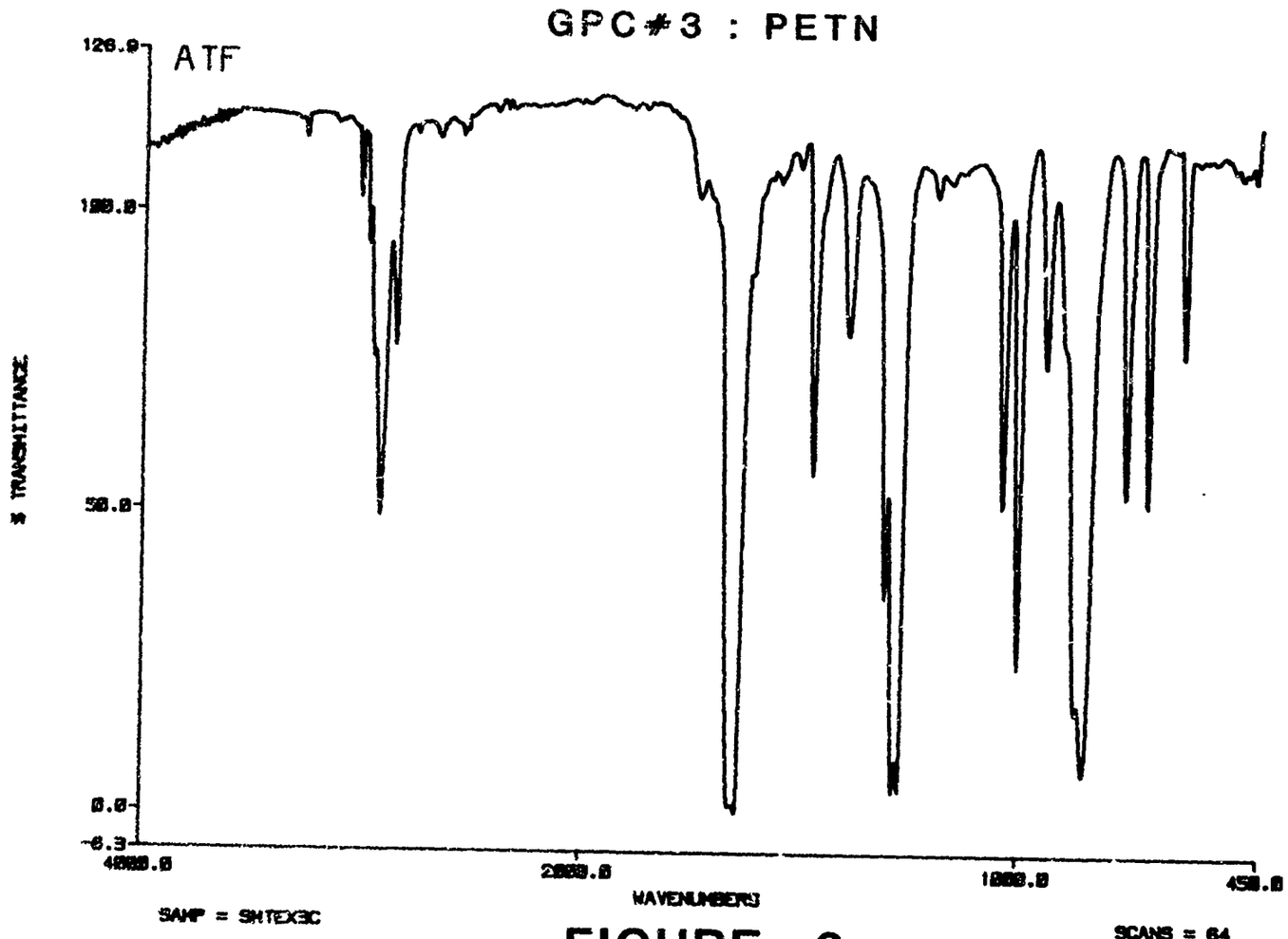
GPC#3 : PETN
ATF
126.0
100.0
50.0
0.0
-6.3
% TRANSMITTANCE
4000.0
2000.0
1000.0
450.0
WAVENUMBERS
SAMP = SNTEX3C
SCANS = 64

FIGURE 6

GPC#4 : RDX

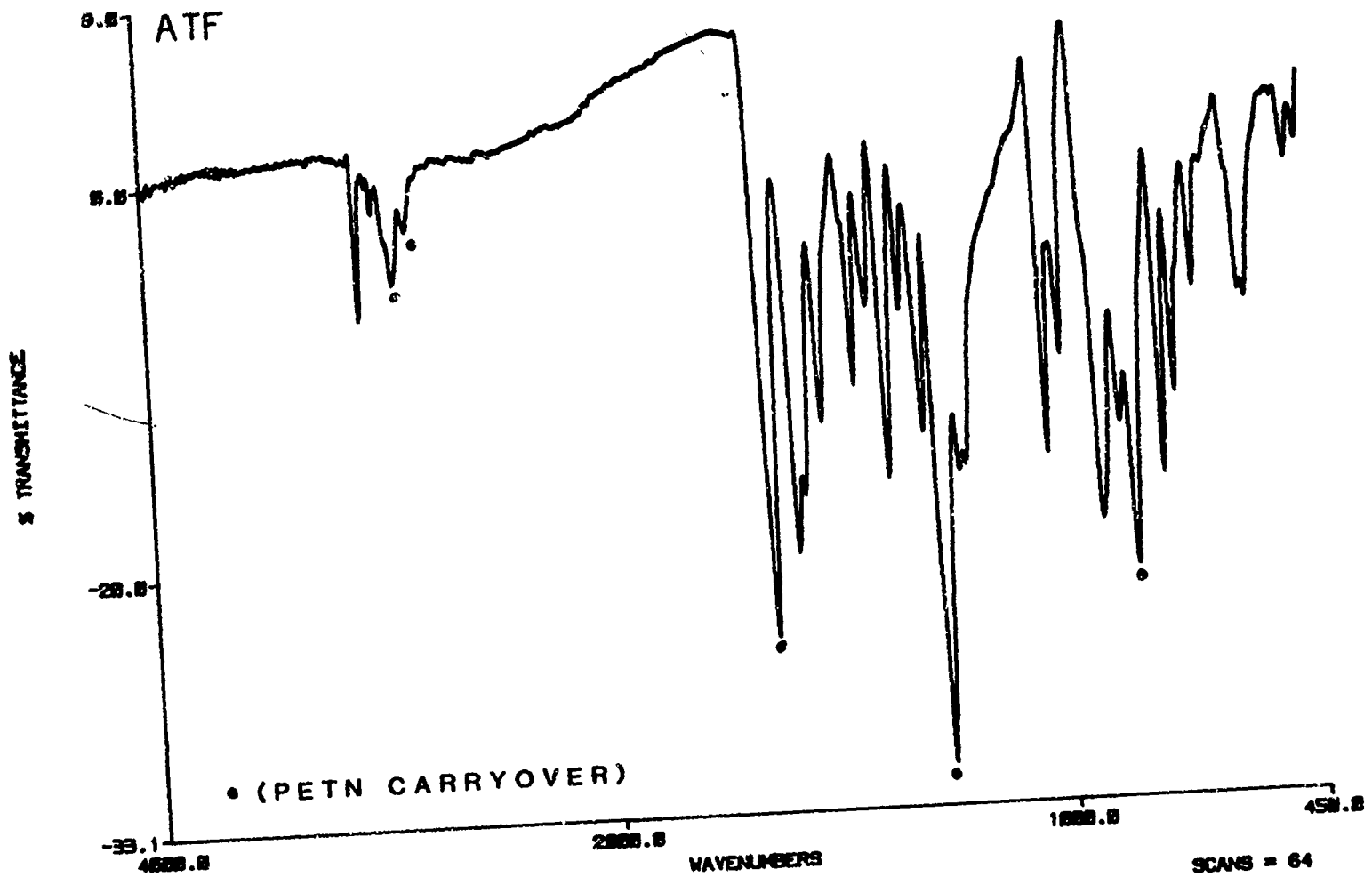


SAMP = SNTEX4C

FIGURE 7

SEMTEX HEXANE EXTRACT

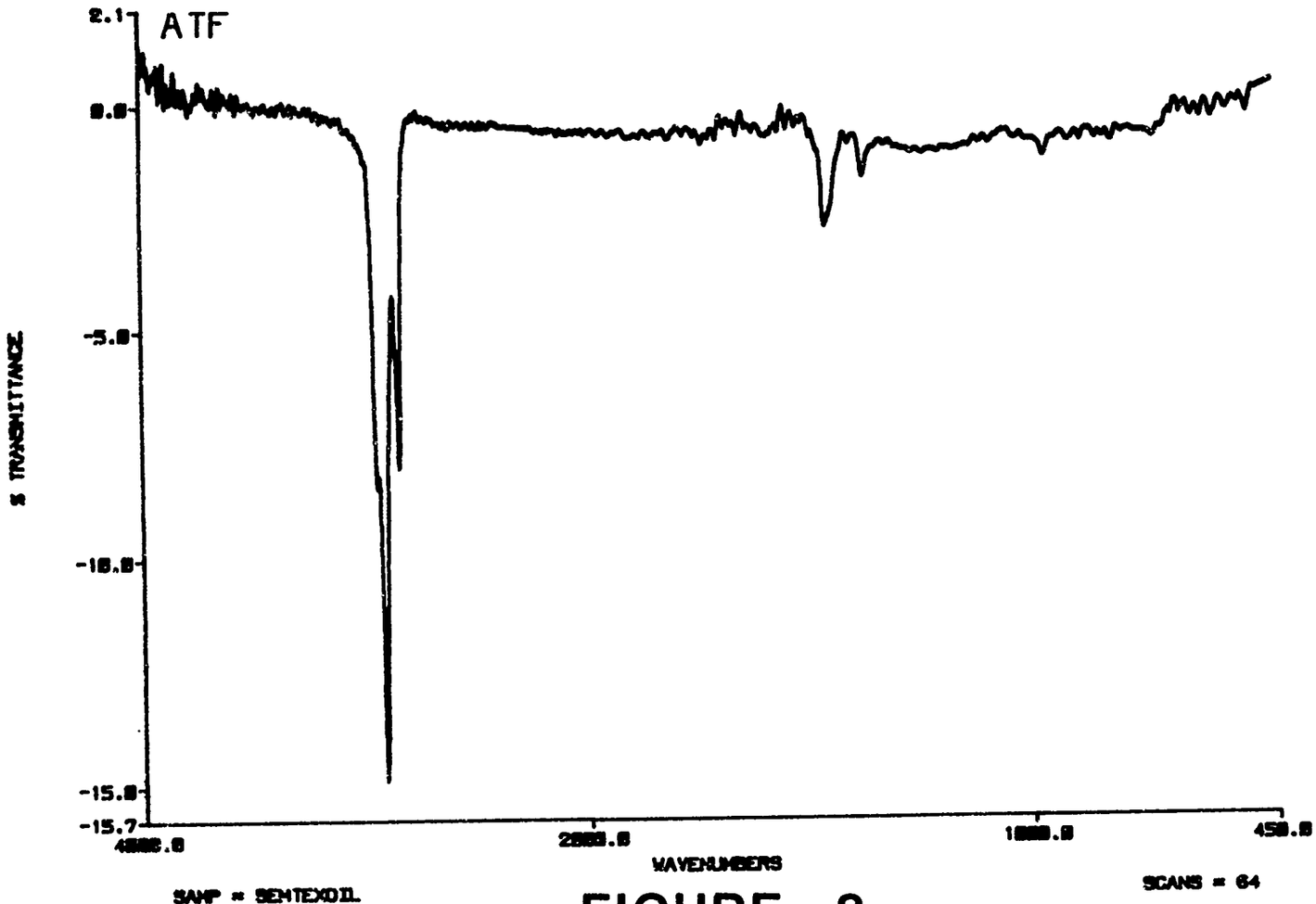


FIGURE 8

# GAS CHROMATOGRAPHY

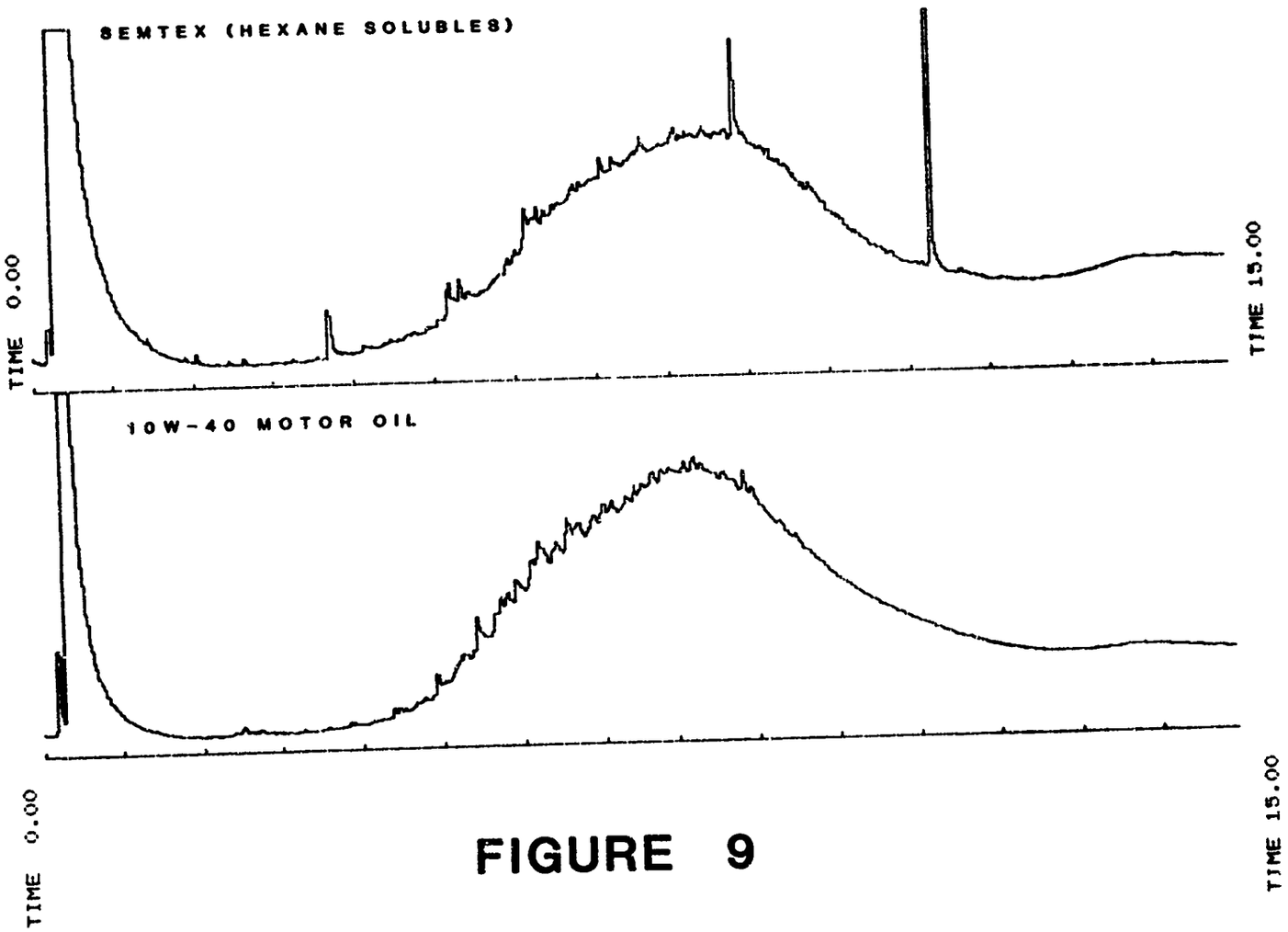


FIGURE 9

# ANALYSIS OF REACTION PRODUCTS OF PROPELLANTS AND HIGH EXPLOSIVES

F. Volk
Fraunhofer-Institut für Chemische
Technologie, ICT, 7507 Pfinztal, FRG

## ABSTRACT

The reaction products of propellants and high explosives are dependent on the pressure and therefore also on the confinement under which the combustion or detonation reaction proceeds. In order to evaluate this influence, different propellants were burned under atmospheric pressure and heavily confined in a closed vessel.

In addition high explosives containing TNT were initiated in an evacuated metal containment and under atmospheric pressure of argon. In all cases, the products were analysed to find out the completeness of the combustion and detonation reaction. The gaseous products were analysed by mass spectrometry and gas-chromatography, the residues by CHN-analysis and by high performance liquid chromatography. The combustion of propellants at atmospheric pressure formed uncomplete reaction gases with a high content of NO.

The investigation of the detonation products of unconfined high explosives has shown that unreacted TNT could be analysed in the solid residue, when the initiating booster was not optimized.

## 1 INTRODUCTION

The knowledge of the reaction products of combustion and detonation processes is important for different reasons:

a) to learn more in the field of the reaction kinetics or of equilibrium or non-equilibrium burning

b) to study the heat output
c) to evaluate the completeness of reactions and to find out if components of the original propellant or high explosive can be analysed in the residue.
d) In connection with the disposal of energetic materials, it is also of interest, if the combustion leads to toxic or cancerogenic reaction products.

The last point is of main interest for the disposal of ammunition, whereas in the case of c) the analysis of explosive residue allows us to find out the kind of explosive which was used by terrorists.

## 2 AIM

It is the aim of this investigation to analyse the reaction products of some propellants with different heats of explosion. In each case the combustion reaction was started under a different confinement: a) low pressure resp. unconfined, b) heavily confined which leads to a high combustion pressure.

When high explosives were investigated, a containment of steel was used, which could be evacuated. So it was possible to analyse the detonation products formed under vacuum or under a different pressurization. Additonally, the influence of different initiating booster explosives on the completeness of the detonation reaction could be analysed.

## 3 COMBUSTION EXPERIMENTS

### 3.1 Combustion of ambient pressure

For the low pressure experiments a 1,5 l glass vessel was used in which air could be replaced by argon by evacuation. About 1 g of the propellant was ignited using a filament igniter. After the combustion, the products gas were analysed by mass spectrometry.

Typical reaction gases consist of:
$H_2$, $N_2$, CO, $CO_2$, NO, $N_2O$, HCN, $H_2O$ and $CH_4$ with small amounts of $NH_3$, $C_2H_4$ and $C_2H_2$. Usually solid reaction products such as carbon were formed.

### 3.2 Combustion in Confinement

For the combustion in confinement, a high pressure vessel was used in which also the heat of combustion of substances could be measured, when placed into a calorimeter. The volume of the calorimetric bomb was 25 $cm^3$. Up to 2,5 g of the propellant were ignited, also by using a filament. Because of the heavily confined reaction, in all cases an equilibrium burning takes place, which produced gases such as $H_2$, $N_2$, CO, $CO_2$, $H_2O$ and $CH_4$. Carbon was formed in high pressure vessel only when propellants were burned with a very negative oxygen balance.

The above mentioned gases with the exception of $H_2O$ could be analysed by gas-chromatography.

### 3.3 Propellants investigated

For measuring the combustion products, the following propellants were taken into consideration:

a) Black Powder (75 % $KNO_3$/15 % Charcoal, 10 % Sulfur)
b) A gun propellant with a low heat of explosion: Single base gun propellant A 5020
c) A gun propellant with a high heat of explosion: Double base propellant H 518

## 4 DETONATION EXPERIMENTS

The detonation experiments were carried out in a containment of stainless steel with a volume of 1,5 $m^3$, which could be evacuated in order to detonate under vacuum or to replace air by an inert gaseous atmosphere such as argon.

Cylindrical high explosive charges of about 300 g were used. The high explosive was initiated by a detonator cap No. 8 together with an RDX booster of 10 g.

In order to determine the influence of the booster strength on the completeness of the reaction, in some cases an additional booster was used (18 g) having the same diameter as the main explosive charge (50 mm). After the detonation, gas samples were taken for the mass spectrometric analysis. In addition, the solid residue was collected to analyse it for the CHN-content and for unreacted explosive components such as TNT.

Two different kinds of experiments have been conducted:

- Measuring the influence of the initiation strength on the completeness of the detonation reaction
- Measuring the pressurization on the detonation products.

4.1 High Explosives investigated for measuring the initiation strength on the completeness of the detonation reaction

The following high explosives were investigated:

a) Compound B and

Cast high explosive charges consisting of

b) 60 % TNT/40 % Nitroguanidine (NQ)
c) 50 % TNT/30 % Nitroguanidine/20 % Mg
d) 50 % TNT/50 % Ammoniumnitrate (AN)
e) 60 % TNT/40 % Nitroguanidine (NQ)
f) 50 % TNT/50 % Nitroguanidine (NQ)
g) 50 % TNT/50 % Triaminotrinitrobenzene (TATB)

### 4.2 High Explosives investigated for measuring the influence of prepressurization on the detonation products

The influence of prepressurization was tested by the initiation of unconfined charges in:

- Vacuum
- in 0,5 bar argon and
- 1,0 bar argon

Additionally, three charges of the same size and the same composition, but in a glass confinement with a thickness of 9 mm were investigated under the same conditions.

For all these tests, the composition of the explosive charges was as follows:
45 % TNT/55 % Nitroguanidine (NQ)

## 5 RESULTS

### 5.1 Combustion Processes

#### 5.1.1 Black Powder

The black powder, which has been tested, consisted of:
- 75 % potassium nitrate ($KNO_3$)
- 15 % charcoal (79 %)
- 10 % sulfur

The heat of explosion of this type of black powder was about 2850 kJ/kg. A mass of 2,5 g of black powder was burned in the closed bomb. The reaction gas was analysed by using a double focusing mass spectrometer of Varion MAT.

Black powder burns basically according to the following empirical formula /1/.

$$16\ KNO_3 + 21\ C + 5\ S \rightleftharpoons 5\ K_2CO_3 + K_2SO_4 + 2\ K_2S_2 + 13\ CO_2 + 3\ CO + 8\ N_2$$

About 43 wt. % of gases and 57 wt. % of condensed reaction products are developed during this burning process. Depending on the development of the burning and on test conditions, the following reactions will take place in a more or less complete form:

$$K_2CO_3 + H_2S \rightleftharpoons K_2S + H_2O + CO_2;\ \Delta H = +62.8\ kJ$$

$$2\ H_2S + 2\ K_2CO_3 \rightleftharpoons K_2SO_4 + K_2S + CH_4 + CO_2;\ \Delta H = +7{,}1\ kJ$$

An incomplete equilibrium will have no strong effect on the heat balance because of the low reaction enthalpy, however, it gives rise to a change of the reaction products.

The composition of the reaction products without $H_2O$ may be seen from Table 1. The first column contains the result of a very low loading density 25 g/l. The next three columns are the result of the higher loading densities 100 g/l, 200 g/l and 300 g/l.

As the most important result of our investigation it should be stressed that between loading density 100 g/l and 300 g/l the burning of the black powder is almost independent on the loading density. In contrast with this result, however, it is found that in the lower range of loading densities (25 g/l) the composition of gas is different from the higher range of loading densities.

With regard to the solid residue, the formation of solid products such as potassium carbonate, potassium sulfate and potassium sulfide is characteristic for black powder.

### 5.1.2 Gun Propellant A 5020

The gun propellant A 5020, which exhibits a heat of explosion of about 3584 kJ/kg and an oxygen balance of -42,2 g $O_2$/100 g propellant was tested under a very low loading density which was 0.33 g/l. The propellant was burned in glass vessel of 1,5 l, containing argon as an inert gas.

In addition, the same propellant was ignited in a stainless steel vessel of only 25 $cm^3$ burning volume. By using 2.5 g of the propellant, the loading density was 0,1 g/$cm^3$ or 100 g/l. The results of both tests may be seen in Table 2. For the loading densities mentioned very different reaction gases were formed: Very large amounts of nitric oxide (NO) in the lower range and nearly no nitric oxide in the higher loading density. The different gases are responsible for the different heat outputs ($Q_{ex}$ = heat of explosion).

As we see, the reaction gases at the loading density of 100 g/l agree very well with the equilibrium gases, which were thermodynamically calculated /2/ using the ICT-computer-programm.

The formation of carbon was only seen by burning the propellant in the lower pressure range. But there was no other residue which could be characteristic for detection of the original propellant.

### 5.1.3 Gun Propellant H 518

The gun propellant H 518, which contains a high amount of nitroglycerine, exhibits a very high heat of explosion of 5132 kJ/kg. The oxygen balance is -22,5 g $O_2$/100 g propellant. It was tested under the same conditions as A 5020. At first it was burned in an argon atmosphere of about 1 bar; secondly heavily confined in a closed bomb, see the results in Table 3.

Compared with the cooler propellant A 5020, the nitric oxide content of the low pressure burning experiment is clearly higher: 19,3 mol %. But the carbon formation is lower because of the higher oxygen content. On the other hand, the combustion in the closed bomb leads to high contents of $CO_2$ and $H_2O$; both values are responsible for the very high heat of explosion of the propellant H 518. It is understandable that no solid residue has been formed.

## 5.2 Detonation Processes

The first part of these investigations has the objective to determine the influence of the initiation strength on the effectivity of the detonation reaction. This means, it should be found out if it is possible to analyse explosive components in the detonation residue under the precondition that the initiating booster was too small or not optimized.

The second part has to examine what kind of influence on the reaction products of TNT containing high explosives will cause a detonation in vacuum, in argon atmosphere or if the explosive is confined in a glass tube.

### 5.2.1 Influence of Initiation Strength

For all the experiments described, we used high explosive charges of about 300 g with 50 mm in diameter and 80 to 90 mm in length. For the initiation different boosters were used:

1) A booster with a low initiation strength which consisted of 10 g RDX (Type I). The cylindrical shape of these booster had a diameter of about 20 mm and a length of about 20 mm.

   In this connection it should be pointed out that the diameter of the RDX-booster is much smaller than the diameter of the explosive charge, see Fig. 1.

2) The second booster type consisted on 18 g explosive sheets (type II) with the same diameter as the main charge explosive. We expect that the increased initiation strength of both types of boosters gives rise to a more complete detonation reaction with the result that no more explosive components can be identified in the post-blast residue, see Fig. 2.

The results of the examination of the initiation strength of the two different boosters may be seen from the following table. In the post-blast residues, which contain a large amount of carbon, TNT was determined quantitatively by High Performance Liquid Chromatography (HPLC).

| Initiating Booster | | | High Explosive Charge | TNT in Residue wt. % |
|---|---|---|---|---|
| | Type I 10 g RDX | Type II 18 g Expl.Sheets | | |
| a) | + | - | 40 % TNT/60 % RDX (Compound B) | - |
| b) | + | - | 60 % TNT/40 % NQ | 1,5 |
| c) | + | - | 50 % TNT/30 % NQ/20 % Mg | 6,0 |
| d) | + | - | 50 % TNT/50 % AN | 2,0 |
| e) | + | + | 60 % TNT/40 % NQ | - |
| f) | + | + | 50 % TNT/50 % NQ | - |
| g) | + | + | 50 % TNT/50 % TATB | - |

In this table it is shown that compound B, which is much more easily to initiate, reacts completely by using the booster type I alone.In contrast to this, nitroguanidine (NQ) and ammonium nitrate (AN) containing high explosive charges, which need a higher initiation strength, leave unreacted TNT. The same holds for the charge containing additionally magnesium (Mg). On the other side, a complete detonation reaction is shown by using both types of boosters: no TNT could by analysed.

### 5.2.2 Influence of Ambient Gas on the Detonation Products

When detonating high explosives in different atmospheric conditions, it is of interest to know if the energy output will change. In order to investigate this behavior, we analysed the reaction products of explosive charges consisting of 45 % TNT and 55 % Nitroguanidine (NQ) initiated in different pressures of argon and in vacuum. Argon was used as an inert gas to avoid a reaction of the detonation products with air. The results of the unconfined charges are recorded in Table 5.

From Table 5 we see that the detonation products change very clearly going from vacuum to 1,0 bar of argon (0,1 MPa). The content of $H_2$ and CO decrease, whereas $CO_2$, $H_2O$ and carbon increase. The heat of detonation increase in the same direction. This means that a detonation under a pressure of 1 bar is much more powerfullo than in vacuum or at low pressures.

In order to evaluate the influence of a confinement, three charges of the same composition and the same weight were cast into glass tubes of 9 mm wall thickness. The results are listed in Table 6.

It is shown that the glass confined charge exhibits very different products from the unconfined charge if we compare the vacuum shots. The confined charge produces in vacuum nearly the same reaction products as the unconfined explosive charge at 0.5 and 1,0 bar argon. The same holds also for the enthalpy of detonation. The conclusion which can be drawn from these experiments is that ambient argon behaves as a confinement.

## 6 CONCLUSION

Black powder and two gun propellants with different heats of explosion were burned under different pressures. Only black powder produces solid reaction products which can be used for the identification of the propellant.

The initiation of high explosives with different boosters has shown that components of the origin explosive charges could be analysed in the post-blast residue, when the initiating booster was not optimized.

The influence of an ambient atmosphere and of confinement could be demonstrated by examining the reaction products in vacuum, under 0,5 bar and 1,0 bar argon. It was found that 1,0 bar argon behaves as a confinement.

## 7 REFERENCES

/1/ R. Escales
Schwarzpulver und Sprengsalpeter
Leipzig 1514, Verlag von Veit u. Comp.

/2/ H. Bathelt, F. Volk
Computer Program for Performance
Calculation of Rocket and Gun Propellants and
Gaseous Explosives
ICT Report 4/85

/3/ F. Volk, H. Bathelt, F. Schedlbauer, J. Wagner
Detonation Products of Insensitive Cast High
Explosives
Proc. 8th Symp. (Int.) on Detonation
July 15-19, 1985, Albuquerque, NM, USA,
p. 577-586

/4/ F. Volk
Detonation Gases and Residues of Composite
Explosives
Journal of Energetic Materials 4 (1986) 93-113

/5/ F. Volk, F. Schedlbauer
Detonation Products of Less Sensitiv High Explosives
Formed Under Different Pressures of Argon and in
Vacuum
Preprints of papers to be presented of the 9th Smyp.
(Int.) on Detonation to be held in
August 28-September 1, 1989, Portland, Oregon, USA

Table 1: Reaction Products of Black Powder

| Load Density g/l | 25 | 100 | 200 | 300 |
|---|---|---|---|---|
| Combustion Condition | Closed Vessel | Closed Vessel | Closed Vessel | Closed Vessel |
| Products in Vol % | | | | |
| $H_2$ | 0,7 | 3,5 | 2,9 | 4,1 |
| $N_2$ | 32,9 | 27,7 | 30,7 | 28,9 |
| CO | 4,6 | 10,6 | 10,2 | 9,2 |
| $CO_2$ | 52,4 | 52,5 | 50,4 | 53,3 |
| $H_2S$ | 8,2 | 5,5 | 5,9 | 5,6 |
| $SO_2$ | 0,1 | 0,1 | 0,1 | 0,1 |
| COS | 1,1 | 0,2 | 0,2 | 0,2 |
| $CS_2$ | 0,04 | - | - | - |
| $CH_4$ | 0,04 | - | - | - |
| Residue analysis in wt. % | | | | |
| C | not analysed | 3,6 | 3,6 | 3,5 |
| $K_2CO_3$ | | 56,6 | 56,1 | 54,5 |
| $K_2SO_4$ | | 16,5 | 17,4 | 17,1 |
| $K_2S$ + Others | | 23,3 | 22,9 | 24,9 |

Table 2: Reaction products of Single Base Gun Propellant A 5020

| TLP A 5020 | Experiment | | Calculation without CH4 | Calculation including CH4 |
|---|---|---|---|---|
| O2-Balance [%] | -42.2 | -42.2 | -42.2 | -42.2 |
| Load. Density [g/l] | 0.33 | 100 | 100 | 100 |
| Comb. Condition | 1 bar | Closed Vessel | - | - |
| Products [Mol %] | | | | |
| H2 | 1.8 | 18.4 | 19.2 | 15.8 |
| CH4 | 0.6 | 0.1 | - | 2.1 |
| CO | 17.0 | 42.7 | 42.4 | 40.2 |
| CO2 | 7.0 | 12.6 | 12.5 | 14.7 |
| N2 | 4.4 | 10.1 | 10.4 | 10.9 |
| N2O | - | - | - | - |
| NO | 11.1 | - | 0.0018*) | - |
| HCN | 0.2 | - | 0.013 | 0.01 |
| C2H4 | - | - | - | - |
| NH3 | - | 0.85 | 0.14 | 0.10 |
| H2O | 30.3 | 15.2 | 15.4 | 16.2 |
| C s | 27.6 | - | - | - |
| Qex [J/g] | 2696 | 3360 | 3472 | 3679 |
| Kp (T) | 40.88 | 2.799 | 2.72 | 2.80 |

*) (NO)x - Analyzer

Table 3: Reaction Products of Double Base Gun Propellant H 518

| TLP H518 | Experiment | | Calculation |
|---|---|---|---|
| O2-Balance [%] | -22.5 | -22.5 | -22.5 |
| Load. Density [g/l] | 0.33 | 100 | 100 |
| Comb. Condition | 1 bar | Closed Vessel | - |
| Products [Mol %] | | | |
| H2 | 1.9 | 10.2 | 10.0 |
| CH4 | 0.4 | - | 0.2 |
| CO | 22.5 | 28.5 \ 50.8 | 26.9 \ 50.8 |
| CO2 | 6.3 | 22.3 / | 23.9 / |
| N2 | 3.4 | 14.4 | 14.6 |
| N2O | - | - | - |
| NO | 19.3 | 0.09 | - |
| HCN | 0.6 | 0.03 | 0.002 |
| C2H4 | - | - | - |
| NH3 | - | - | 0.05 |
| H2O | 28.8 | 24.4 | 24.4 |
| C s | 16.8 | - | - |
| Qex [J/g] | 2548 | 5044 | 5219 |
| Kp (T) | 54.1 | 3.06 | 2.75 |

Table 4: Detonation Products of the Unconfined Charges of 45 % TNT/55 % NQ

| TABLE 4: CHARGES OF 45% TNT / 55% NQ IN DIFFERENT AR PRESSURES | | | |
|---|---|---|---|
| Sample No. | 1450/1c | 1450/2c | 1450/3c |
| Ar pressure, Mpa | Vac. | 0.05 | 0.1 |
| Composition | 45% TNT/ 55% NQ | | |
| O2-Balance, % | -47.6 | | |
| Charge Weight, g | 331 | 332 | 331 |
| $\Delta H_f$, KJ/Kg | -661 | -662 | -657 |
| Products, Mol%: H2 | 20.7 | 8.3 | 5.0 |
| CH4 | 0.04 | 0.1 | 0.24 |
| CO | 32.1 | 17.9 | 14.3 |
| CO2 | 3.7 | 7.9 | 10.3 |
| N2 | 27.5 | 26.1 | 25.6 |
| NO | 0.1 | 0.1 | 0.13 |
| HCN | 0.3 | 3.2 | 3.6 |
| NH3 | 0.5 | 3.0 | 4.9 |
| C2H2 | 0.02 | 0.03 | 0.1 |
| H2O | 10.7 | 19.6 | 20.0 |
| $C_s$ | 4.4 | 13.8 | 15.9 |
| $\Delta H_{det}$, KJ/Kg | 2999 | 3653 | 3763 |
| C in Residue [% of total C] | 10.8 | 32.2 | 35.7 |
| Gas formation [mol/Kg] | 44.5 | 37.9 | 35.7 |

Table 5: Detonation Products of the Glass Confined Charges of 45 % TNT/55 % NQ in Different Argon Pressures and in Vacuum

| TABLE 5: CHARGES OF 45% TNT / 55% NQ IN GLASS CONFINEMENT AND DIFFERENT AR PRESSURES | | | | |
|---|---|---|---|---|
| Sample No. | | 1451/1 | 1451/2 | 1451/3 |
| Ar pressure, Mpa | | Vac. | 0.05 | 0.1 |
| Composition | | 45% TNT/ 55% NQ | | |
| O2-Balance, % | | -47.6 | | |
| Charge Weight, g | | 332 | 335 | 332 |
| $\Delta H_f$, KJ/Kg | | -656 | -658 | -658 |
| Products, Mol%: | H2 | 8.7 | 4.2 | 3.1 |
| | CH4 | 0.2 | 0.4 | 0.44 |
| | CO | 15.9 | 10.2 | 9.3 |
| | CO2 | 7.9 | 11.9 | 12.7 |
| | N2 | 27.3 | 26.0 | 25.6 |
| | NO | 0.06 | 0.05 | 0.14 |
| | HCN | 1.35 | 2.4 | 1.1 |
| | NH3 | 1.15 | 4.7 | 5.3 |
| | C2H2 | 0.07 | 0.1 | 0.13 |
| | H2O | 20.5 | 20.7 | 21.0 |
| | $C_s$ | 16.8 | 19.2 | 21.3 |
| $\Delta H_{det}$, KJ/Kg | | 3779 | 3960 | 4003 |
| C in Residue [% of total C] | | 39.8 | 43.3 | 47.2 |
| Gas formation [mol/Kg] | | 37.1 | 34.4 | 33.0 |

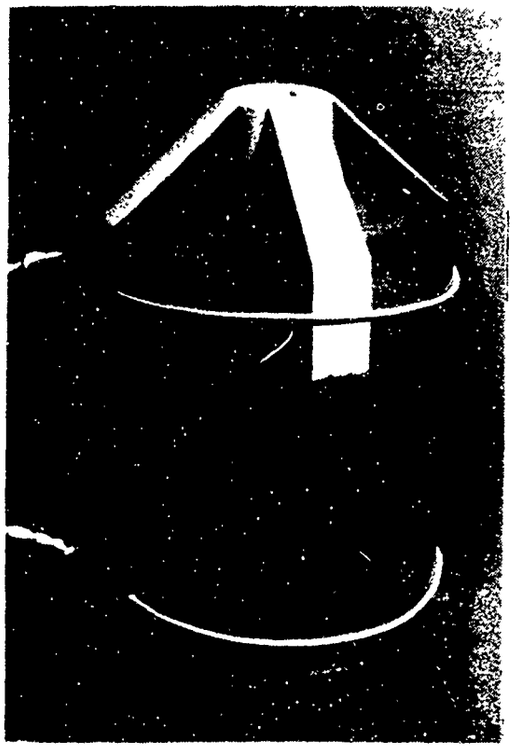

Fig. 1

a = RDX - booster

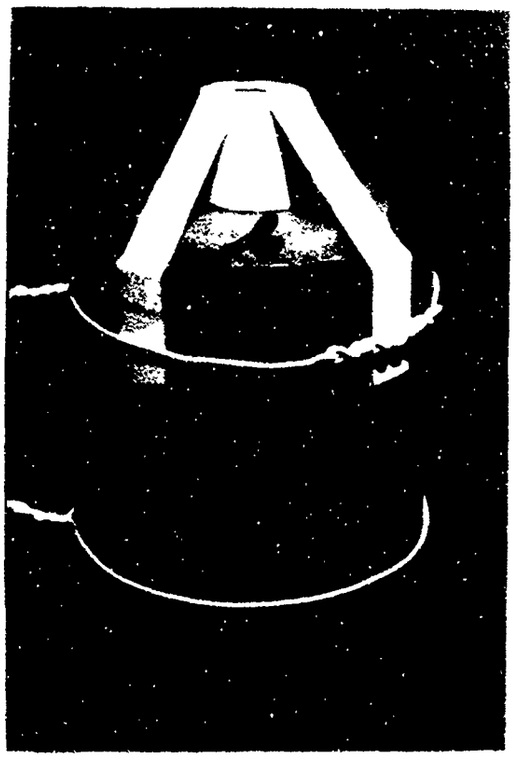

Fig. 2

a = RDX - booster

b = Detonation Sheets - booster

ABSTRACT FOR THE 3 rd INTERNATIONAL SYMPOSIUM
ON ANALYSIS AND DETECTION OF EXPLOSIVES
July 10-13, 1989
MANNHEIM-NEUOSTHEIM (RFA)

---

# CERCHAR 15 m3 chamber for the assesment of the toxicity of blast fumes

---

D. GASTON - C. MICHOT

---

Centre d'Etudes et Recherches de Charbonnages de France
(CERCHAR)
B.P. 2
60550 VERNEUIL-EN-HALATTE (France)

---

Two methods are available at CERCHAR to assess the toxicity of blast fumes: the 115 liters bomb and the 15 m3 chamber. The last one developped for more than fifteen years appear to give relevant results, close with the pratice in underground works. Furthemore the corresponding facility offer large possibilities for investigating the influence of crucial parameters such as confinement and surround of the charge, nature of the atmosphere. Interesting observations have been derived from the results, especially concerning the participation of nitrogen in air in the formation of nitrous oxides and the relationship between the toxicity of fumes and the reactivity of the constituents of a granular ammonium nitrate based explosive

# Fumées de tir : l'expérience du CERCHAR

# avec une chambre étanche de 15 m3

---

**D. GASTON et C. MICHOT**

---

Ingénieurs au Groupe "Substances Explosives et

Sécurité Explosions" du CERCHAR,

B.P. 2, 60550 VERNEUIL-EN-HALATTE (France)

---

**RESUME :**

Deux méthodes sont utilisées au CERCHAR pour déterminer la toxicité des fumées de tir : une bombe de 115 l et une chambre de 15 m3. Cette derniere installation est utilisée depuis plus d'une quinzaine d'années. Elle donne des résultats proches des mesures réalisées en mine. Elle permet également d'étudier l'influence de paramètres importants tels le confinement de la charge, la nature de l'atmosphère et des matériaux au contact de l'explosif, les propriétés de l'explosif, ....

Des observations intéressantes issues des essais ont été réalisées. On peut citer notamment le rôle de l'air dans la formation de vapeurs nitreuses, la relation entre la toxicité des fumées et la réactivité des constituants d'un explosif nitraté, ...

## I / PRESENTATION - HISTORIQUE :

Depuis plus d'une trentaine d'années, le CERCHAR s'est intéressé à différentes methodes pour l'évaluation des productions de gaz libéres lors des tirs en mine. En ce qui concerne les conditions d'essais, aprés avoir utilisé régulièrement pendant une dizaine d'années une bombe de 115 litres, il préfère actuellement realiser des essais dans une chambre étanche de 15 m3. Cette installation de taille , intermédiaire entre le matériel de laboratoire et les conditions pratiques en mines souterraines est unique (1).

De nombreux travaux ont été réalisés pour la mise au point de la methode et pour la validation des résultats. Parmi les études les plus importantes nous pouvons citer trois études à financement CECA(2,3,4) et des travaux internes pour la définition d'une épreuve codifiée retenue en France dans la Réglementation pour l'utilisation des explosifs dans les mines souterraines de combustibles solides (5,6,7). Plus de 1500 tirs avec des explosifs industriels ou des produits de laboratoires, dans des configurations très différentes, ont ainsi été réalisés.

La figure 1 représente schématiquement la chambre de 15 m3. Pour sa réalisation, on a utilisé une citerne en acier qui a été modifiée : augmentation du diamètre du trou d'homme qui est équipé d'une porte étanche à fermeture rapide; adjonction de plusieurs tubulures qui sont fermées par des plaques d'acier boulonnées, l'étanchéité étant assurée par des joints de caoutchouc. La citerne a ensuite été noyée dans un massif de béton.

L'intérieur de la chambre est équipé d'un chemin de roulement permettant d'introduire un mortier d'acier, d'un blindage qui protège le fond de la citerne et d'un ventilateur électrique pour le brassage des gaz. Le volume intérieur est ainsi ramené à 14,5 m3 environ.

Des passages étanches sont réalisés au travers des plaques fermant les tubulures pour l'introduction de la ligne de tir, de la ligne d'alimentation du ventilateur, et des thermocouples qui permettent d'apprécier la température moyenne des gaz ainsi que pour le passage de tuyaux qui servent à mesurer la pression ou à prélever les gaz pour l'analyse.

La masse de la charge d'explosif tiré dans la chambre est de 750 g. Cette charge est réalisée dans un étui léger, généralement en papier kraft et elle est amorcée par un détonateur étalon à charge de 0,6 g de penthrite, dans le cas d'un produit sensible au détonateur, ou par un relais d'explosif dont le bilan en oxygène est nul, pour un produit moins sensible.

Aprés tir, l'atmosphère de la chambre est brassée, et on détermine l'évolution au cours du temps des concentrations en vapeurs nitreuses (NO et NO2) à l'aide d'un appareil à chimiluminescence. Les concentrations en oxydes de carbone, en methane, en hydrogène et en azote sont déterminées par chromatographie en phase gazeuse sur des échantillons prélevés en ampoules de verre 30 minutes aprés le tir.

Le résultat d'un essai est l'ensemble des productions des gaz cités précédemment, exprimées en litre par kg d'explosif, dans les conditions normales de température et de pression (273 °K, 760 mm Hg soit $10^5$ Pa). On indique également la quantité totale de gaz secs, calculée à partir de la surpression et de la température mesurées aprés tir.

## II / EXEMPLES D'ETUDES REALISEES:

### II - 1 - Influence du confinement (mode de tir) :

II - 1 - 1 - Introduction :

Les explosifs de mine classiques (nitratés et dynamites) sont composés essentiellement d'un mélange de nitrate d'ammonium et d'un sensibilisant. Lors de la détonation de ces explosifs, la décomposition est plus ou moins incomplète. On distingue (7) :

- des réactions primaires qui se produisent dans la zone de réaction et qui peuvent être plus ou moins développées suivant le diamètre de la charge et le confinement de celle-ci;
- des réactions secondaires qui peuvent se produire ensuite en arrière de la

zone de détonation, dans la mesure où les fumées restent suffisamment confinées.

Lors d'un tir à l'air libre sans confinement, seules les réactions primaires se produisent et la composition des fumées que l'on détermine dans ces conditions est proche de la composition des fumées dans la zone de détonation.

Par contre, lors de tirs avec un confinement modéré de la chargeles détentes sont freinées, ce qui a pour conséquence d'augmenter la longueur de la zone de détonation et également la température et la pression dans cette zone.

Enfin, lors de tirs avec un confinement important, les gaz subissent comme dans les tirs précédents une détente brutale à la fin de la zone de détonation, mais ici la détente est limitée à l'espace accessible aux fumées. Les équilibres chimiques peuvent alors s'établir avant que le confinement commence à céder. Tout au long de la détente, au fur et à mesure que le confinement cède, les réactions chimiques peuvent se développer. Quand le confinement a disparu, en fin de détente, les gaz font brutalement irruption dans l'atmosphère, ce qui fige leur composition.

Afin d'évaluer l'influence de ces deux types de réactions sur la toxicité des fumées, nous avons réalisé des essais en tirant divers explosifs dans différentes configurations de tir.

II - 1 - 2 - Essais réalisés :

Trois configurations de tir ont été retenues :

- Essais en charge suspendue : dans ces essais, la charge est suspendue horizontalement au centre de la chambre.
- Essais en mortier sans bourrage : dans ces essais, la charge d'explosif est tirée dans un mortier d'acier dont l'âme a un diamètre de 70 mm et une longueur de 1200 mm (voir figure 2). L'amorçage de la charge est postérieur (détonateur au fond du mortier).
- Essais en mortier avec bourrage : la seule modification par rapport aux essais précédents est l'obturation du mortier par deux bourres de sable de diamètre 65 mm et de longueur 300 mm.

Les essais ont portés sur trois explosifs :

- un explosif nitraté contenant 18 % de chlorure de sodium
- un explosif dynamite pulvérulente à 10 % de nitroglycérine-nitroglycol.
- un explosif bouillie sensibilisé par le nitrate de monomethylamine

Dans le tableau 1, sont données les productions totales de gaz secs mesurées avec les trois explosifs dans les trois configurations de tir.

| Mode de tir \ Explosifs | nitraté | dynamite | bouillie |
|---|---|---|---|
| Tir en charge suspendue | 269 | 208 | 286 |
| Tir en mortier sans bourrage | 304 | 353 | 367 |
| Tir en mortier avec bourrage | 377 | 414 | 458 |
| productions en litre/ kg d'explosif | | | |

TABLEAU 1 : Production totale de gaz secs.

Si l'on caractérise le taux de réactivité de l'explosif par la production totale de gaz secs, rapportée à la production maximale théorique, on observe qu'à l'air libre le taux de réactivité est faible (environ 50 %) et qu'il croît de facon importante avec le confinement.

Les réactions primaires ne permettent donc que la libération d'une part faible de l'énergie disponible allant de 50% à 75 % selon que ces réactions sont libres ou forcées. Par contre, lorsque les réactions secondaires peuvent se développer, en faisant un calcul de conservation des éléments, on constate que la quasi-totalité de l'explosif réagit. De plus, le confinement des produits de réaction permet aux équilibres chimiques de s'établir. La formation de monoxyde de carbone aux températures d'explosion des explosifs de mine classiques (≈ 2000 °K) est gouvernée principalement par l'équilibre dit " du gaz à l'eau":

$$CO + H_2O \rightleftharpoons CO_2 + H_2$$

Cet équilibre est déplacé vers la droite lorsque la température décroît, c'est à dire qu'il favorise la formation de $CO_2$ au détriment de CO. La combinaison d'une décomposition variable et de la rupture des équilibres à différentes températures permet d'observer des évolutions importantes selon la configuration de tir. Par exemple le rapport $CO/CO_2$ est peu différent lorsque le confinement est nul ou faible et augmente nettement lorsque le confinement devient important.

| Mode de tir \ Explosif | nitraté | dynamite | bouillie |
|---|---|---|---|
| Tir en charge suspendue | 0,22 | 0,10 | 0,16 |
| Tir en mortier sans bourrage | 0,25 | 0,04 | 0,13 |
| Tir en mortier avec bourrage | 0,34 | 0,28 | 0,36 |

TABLEAU 2 : Rapport CO/CO2.

Par contre, les réactions entre les oxydes d'azotes ne sont pas suffisamment rapides, aux temperatures inférieures à 3000°K, pour que les équilibres puissent être atteints. Toutefois, la formation d'azote et d'oxydes d'azote est le résultat de différentes réactions faisant intervenir des radicaux azotés. Suivant la configuration de tir, ces réactions sont plus ou moins importantes. Comme on peut le voir sur le tableau 3, la production de vapeurs nitreuses ( NOx = NO + NO2 ) décroît nettement avec l'augmentation du confinement.

| Mode de tir \ Explosif | nitraté | dynamite | bouillie |
|---|---|---|---|
| Tir en charge suspendue | 11,7 | 22,9 | 17,5 |
| Tir en mortier sans bourrage | 0,61 | 1,35 | 1,91 |
| Tir en mortier avec bourrage | 0,09 | 0,59 | 0,47 |
| productions en litre/ kg d'explosif | | | |

TABLEAU 3 : Production de vapeurs nitreuses.

II - 1 - 3 - Conclusions :

Les productions des principaux gaz toxiques ou nocifs dépendent étroitement des conditions de tir. Sous faible confinement, la production de vapeurs nitreuses est très importante. Par contre, elle diminue très rapidement avec le confinement. Quant à la production de monoxyde de carbone, elle évolue en sens inverse, mais de façon moins prononcée. Ces évolutions sont dues d'une part au taux de réaction faible dans la zone de détonation et d'autre part aux équilibres thermodynamiques et aux temps de réactions qui évoluent beaucoup selon les configurations de tir.

D'un point de vue pratique, le confinement réduit nettement la toxicité globale des fumées en permettant aux réactions chimiques d'aller jusqu'à leur terme.

**II - 2 - Relation entre la réactivité d'un explosif et la composition des fumées :**

II - 2 - 1 - Introduction :

Comme nous venons de le voir, le taux de réactivité d'un explosif est très faible lorsque le confinement est inexistant ou faible.

La réactivité d'un constituant solide est liée à sa surface spécifique : plus la surface spécifique est importante, plus le temps de réaction est court. D'autre part, dans le cas d'une détonation, un facteur important est la présence de pores fermés ou ouverts de faibles dimensions. En effet, l'onde de détonation comprime ces pores, ce qui crée des points chauds favorisant des décompositions locales.

La matière comburante couramment utilisée dans la fabrication des explosifs de mine -en raison notamment de son faible coût- est le nitrate d'ammonium.Comparée à d'autres constituants des explosifs en question, cette matière est peu réactive. Sa décomposition est donc médiocre. Afin d'apprécier l'influence de la variation de la réactivité de ce composant sur la réactivité globale de l'explosif et notamment sur la production de gaz toxiques ou nocifs, nous avons réalisé différents essais sur des mélanges explosifs fabriqués en laboratoire.

II - 2 - 2 - Essais réalisés:

La réactivité du nitrate d'ammonium est modifiée en faisant varier la porosité et la dimension des grains.

Deux nitrates de qualité différente ont été utilisés:

- nitrate d'ammonium dit" dense " employé pour la fabrication industrielle de dynamites et de nitratés(porosité ouverte mesurée avec un porosimètre à mercure: 30-150 mm3/g).
- nitrate d'ammonium dit "poreux" employé pour la fabrication d'explosifs nitrate-fioul ( porosité ouverte mesurée avec un porosimètre à mercure: 450-650 mm3/g).

Ces deux produits ont été broyés et tamisés et nous avons retenu les coupes granulométriques suivantes :

- 0,1 / 0,4 mm
- 0,4 / 0,63 mm

En utilisant ces différents nitrates d'ammonium, nous avons réalisé des explosifs du type nitraté composés de (% en poids):

| | |
|---|---|
| - Nitrate d'ammonium | 80,00 % |
| - Tolite ( trinitrotoluène) | 19,24 % |
| - Cellulose | 0,76 % |

Dans ce qui suit, nous désignons les mélanges comme indiqué dans le tableau 4.

| Désignation | Nitrate d'ammonium | Granulométrie |
|---|---|---|
| D1-G | "dense" | 0,4 / 0,63 |
| D1-F | "dense" | 0,1 / 0,4 |
| D7-G | "poreux" | 0,4 / 0,63 |
| D7-F | "poreux" | 0,1 / 0,4 |

Tableau 4 : Désignation des différents mélanges.

Divers essais de determination des propriétés explosives et de mesures de l'énergie permettent de classer ces explosifs par ordre de réactivité croissante suivant :
D1-G / D1-F / D7-G / D7-F

Dans le tableau 5, nous donnons les productions totales de gaz secs et les productions des principaux gaz toxiques ou nocifs, dans les tirs à l'air libre sans confinement, en charge suspendue.

| Mélange | Production totale gaz secs en l/kg | Productions en l/kg | | |
|---|---|---|---|---|
| | | NOx | CO | CO2 |
| D1-G | 304 | 14,2 | 15,0 | 145 |
| D1-F | 309 | 18,9 | 17,5 | 146 |
| D7-G | 350 | 17,9 | 11,5 | 140 |
| D7-F | 371 | 23,8 | 11,3 | 143 |

Tableau 5 : Resultats des tirs en charge suspendue.

On constate que le parametre déterminant est la porosité du nitrate d'ammonium. En passant de la qualité peu poreuse à la qualité poreuse, on observe une augmentation de la production de vapeurs nitreuses et une diminution de celle du monoxyde de carbone. Comme attendu, les bilans de conservation des éléments C et N

donnés dans le tableau 6 montrent que la réactivité du nitrate d'ammonium joue un rôle important dans la décomposition d'un tel explosif en charge suspendue.

| Elément | Valeurs calculées (en l) à partir des gaz dosés | | | | Valeurs calculées (en l) d'après la composition |
|---|---|---|---|---|---|
| | D1-G | D1-F | D7-G | D7-F | |
| C | 160 | 163 | 151 | 154 | 157 |
| N | 255 | 254 | 360 | 391 | 505 |

Les valeurs calculées sur les gaz dosés sont données avec une précision de : + ou - 7 l pour C
+ ou - 30 l pour N

Tableau 6 : Bilans C et N.

Si l'on admet que le déficit en azote est dû à une plus ou moins grande participation du nitrate d'ammonium, on obtient les taux suivants de réaction de ce dernier :

- D1-G : 44 %
- D1-F : 44 %
- D7-G : 68 %
- D7-F : 75 %

Par contre, lorsque que l'on confine la charge, l'influence de la reactivité du nitrate d'ammonium sur la production totale de gaz secs et sur les productions de gaz toxiques ou nocifs est trés faible. La seule exception, comme on peut le voir dans le tableau 7, est la production d'oxyde de carbone dans le cas d'un tir en mortier avec bourrage : plus le nitrate d'ammonium est grossier, plus la production d'oxyde de carbone est élevée.

| Mélange | Total gaz secs en l/kg | Productions en l/kg | | |
|---|---|---|---|---|
| | | NOx | CO | CO2 |
| D1-G | 464 | 0,6 | 36,4 | 114 |
| D1-F | 435 | 0,3 | 25,7 | 158 |
| D7-G | 444 | 0,5 | 38,1 | 126 |
| D7-F | 425 | 0,4 | 27,2 | 148 |

Tableau 7 : Résultats des tirs en mortier avec bourrage.

II - 2 - 3 - Conclusions :

Les résultats de ces essais montrent la grande influence des caractéristiques du nitrate d'ammonium sur la production de gaz toxiques.

En l'absence de confinement (charge suspendue), la quasi-totalité du constituant explosif -tolite- et du combustible -cellulose- réagit ainsi qu'une partie du nitrate d'ammonium. Le taux de réaction du nitrate d'ammonium passe de 40 % avec un nitrate peu poreux à environ 70 % avec un nitrate poreux.

Sous confinement (mortier avec bourrage), le nitrate d'ammonium, en grains grossiers, finit de se décomposer au cours de la détente des fumées dans le mortier. Dans ces conditions, lors de l'éjection du bourrage, l'équilibre chimique est rompu à une température plus élevée que lorsque les grains de nitrate d'ammonium sont petits, ce qui favorise la formation du monoxyde de carbone au détriment du dioxyde.

**II - 3 - Influence du milieu environnant (nature du gainage) :**

II - 3 - 1 - Introduction :

Lors d'un tir en trou de mine, l'onde de choc produite par la détonation de la charge d'explosif broie finement le terrain à proximité de la charge. Au-delà de la zone de broyage, l'onde crée des fissures radiales. Les gaz de détonation vont ensuite être mélangés aux particules provenant du broyage du terrain puis s'infiltrer dans les fissures. La nature du matériau autour du trou de mine est donc importante dans la production des fumées de tir.

En effet, dans le cas d'un matériau réactif comme le charbon, les particules intimement mélangées avec les gaz à hautes pression et température vont réagir et par conséquent modifier la composition des fumées de tir. D'après A.G. STRENG (9), la modification de la composition des fumées va dans le sens d'une augmentation relativement importante des produits de réaction incomplète ( CO, NO, NO2, etc... ), autrement dit de la toxicité.

Par ailleurs, une étude réalisée en URSS dont les résultats sont cités par A.G. STRENG, a montré que 54 % des gaz toxiques formés sont rejetés juste après le tir, 43 % sont piégés dans les déblais et peuvent être rendus à l'atmosphère lors du chargement et le solde reste piégé dans les déblais. Ces résultats montrent bien la différence entre les deux possibilités de piégeage des gaz après tir : soit ils sont emprisonnés dans les vides du tas abattu, soit ils sont adsorbés à la surface des matériaux. En ce qui concerne la deuxième possibilité, des essais réalisés en Allemagne par STOCHL et JISKRA(10) ont montré que l'adsorption varie suivant la nature des roches et suivant les gaz. Dans tous les cas, les quantités de gaz ainsi piégées sont très faibles et leur désorption est très lente ( de l'ordre de plusieurs jours). Par contre, pour les gaz emprisonnés dans les vides du tas abattu, comme l'a mis en évidence CLAEYS (11), lors de la reprise du tas, ces gaz diffusent dans l'atmosphère.

Pour apprécier l'influence du milieu environnant, nous avons réalisé différents essais en plaçant soit du charbon ,soit du sable autour de la charge d'explosif

II - 3 - 2 - Essais réalisés :

Deux des mélanges explosifs utilisés dans cette étude sont identiques à ceux présentés dans l'étude précédente, à savoir le plus réactif et le moins réactif. Une seule configuration de tir a été examinée. Il s'agit du tir en mortier avec bourrage en

plaçant autour de la charge un manchon de sable ou de charbon aggloméré. Ce manchon avait un diamètre intérieur de 40 mm, une épaisseur de 12,5 mm et une longueur de 300 mm. Par ailleurs, les bourres obturant le mortier étaient réalisées avec le même matériau aggloméré que la gaine.

Dans le tableau 8, nous donnons les rapports des quantités de gaz produits par l'explosif gainé de charbon aux quantités de gaz produits par l'explosif gainé de sable.

| | H2 | NOx | CH4 | CO | CO2 | Total gaz secs |
|---|---|---|---|---|---|---|
| D7-F + charbon / D7-F + sable | 9,4 | 0,2 | 168 | 7,8 | 1,1 | 1,5 |
| D1-G + charbon / D1-G + sable | 3,5 | 1,0 | 47,4 | 5,5 | 1,1 | 1,7 |

Tableau 8 : Rapport des quantités de gaz produits par l'explosif gainé de charbon aux quantités de gaz produits par l'explosif gainé de sable.

L'addition d'une gaine de charbon conduit donc quel que soit l'explosif, à une forte augmentation de la production de gaz secs. En évaluant la quantité de carbone présente dans les fumées en fonction de la nature de la gaine, on peut estimer l'épaisseur de la gaine qui a été décomposée. on suppose pour cela que l'explosif réagit complétement. On obtient ainsi une épaisseur de 4 à 6 mm selon la réactivité de l'explosif.

II - 3 - 3 - Conclusions:

La toxicité globale des fumées de tir peut-être caractérisée par exemple par l'indice de toxicité (I.T.):

$$I.T. = qCO + 5qNOx$$

avec qCO : production de monoxyde de carbone en l/kg
qNOx : production de vapeurs nitreuses en l/kg

La présence d'un matériau carboné au contact de l'explosif augmente de 5 à 7 fois cet indice, en raison notamment d'un fort accroissement de CO.

**II - 4 - Formation de vapeurs nitreuses à partir de l'air environnant:**

II - 4 - 1 - Introduction :

La production de vapeurs nitreuses est généralement attribuee aux constituants de l'explosif contenant de l'azote.

Il n'est pas exclu cependant que l'oxygène et l'azote atmosphèrique presents autour de la charge d'explosif participent aussi à leur formation.

D'un point de vue théorique, on montre par le calcul que cette hypothèse est plausible. Le modèle utilisé repose sur les équilibres chimiques suivants :

$$1/2\ O_2 \rightleftharpoons O$$

$$1/2\ N_2 \rightleftharpoons N$$

$$1/2\ O_2 + 1/2\ N_2 \rightleftharpoons NO$$

et assimile une onde de choc à une augmentation de température Pour chaque valeur de la température, on resoud les systèmes constitues par les équations de conservation des éléments et les équations d'équilibres, de façon à vérifier la relation de Rankine-Hugoniot pour la conservation de l'énergie dans le choc Avec un tel modèle, on obtient les résultats portés dans le tableau 9, dans le cas particulier de la chambre de 15 m3 du CERCHAR( atmosphère constituée de 7 moles d'oxygène, 27 moles d'azote et 1 mole d'argon).

| T (K) | U(M/S) | UP (M/S) | P (BAR) | V0/V | QNO (PPM) | D (M/S) |
|---|---|---|---|---|---|---|
| 1000 | 1300 | 1034 | 17.94 | 4.897 | 1.7 | 3146 |
| 1100 | 1389 | 1116 | 20.51 | 5.091 | 5 | 3385 |
| 1200 | 1473 | 1193 | 23.12 | 5.26 | 11.5 | 3611 |
| 1300 | 1553 | 1268 | 25.77 | 5.411 | 23 | 3827 |
| 1400 | 1631 | 1337 | 28.46 | 5.548 | 41.3 | 4035 |
| 1500 | 1706 | 1405 | 31.18 | 5.673 | 68.5 | 4236 |
| 1600 | 1778 | 1471 | 33.95 | 5.789 | 106.6 | 4430 |
| 1700 | 1849 | 1536 | 36.76 | 5.899 | 157.7 | 4620 |
| 1800 | 1918 | 1599 | 39.61 | 6.003 | 223.5 | 4805 |
| 1900 | 1985 | 1659 | 42.47 | 6.102 | 305.6 | 4983 |
| 2000 | 2051 | 1720 | 45.41 | 6.198 | 404.9 | 5161 |
| 2100 | 2115 | 1779 | 48.4 | 6.291 | 522.3 | 5335 |
| 2200 | 2179 | 1838 | 51.44 | 6.382 | 658 | 5508 |
| 2300 | 2242 | 1896 | 54.53 | 6.471 | 811.9 | 5678 |
| 2400 | 2305 | 1953 | 57.68 | 6.559 | 983.6 | 5846 |
| 2500 | 2366 | 2010 | 60.9 | 6.647 | 1172.3 | 6013 |
| 2600 | 2427 | 2067 | 64.18 | 6.734 | 1377 | 6179 |
| 2700 | 2488 | 2124 | 67.54 | 6.822 | 1596.1 | 6345 |
| 2800 | 2549 | 2180 | 70.98 | 6.91 | 1828.4 | 6511 |
| 2900 | 2610 | 2237 | 74.52 | 7 | 2072 | 6677 |
| 3000 | 2671 | 2294 | 78.16 | 7.091 | 2325.3 | 6844 |
| 3100 | 2732 | 2352 | 81.92 | 7.185 | 2586.4 | 7012 |
| 3200 | 2794 | 2410 | 85.8 | 7.281 | 2853.5 | 7183 |
| 3300 | 2857 | 2469 | 89.83 | 7.379 | 3124.7 | 7355 |
| 3400 | 2920 | 2530 | 94 | 7.48 | 3398.4 | 7530 |
| 3500 | 2984 | 2591 | 98.33 | 7.584 | 3673 | 7707 |
| 3600 | 3049 | 2653 | 102.84 | 7.691 | 3946.8 | 7888 |
| 3700 | 3115 | 2716 | 107.53 | 7.790 | 4218.7 | 8072 |
| 3800 | 3181 | 2779 | 112.28 | 7.909 | 4484.6 | 8254 |
| 3900 | 3248 | 2843 | 117.3 | 8.021 | 4748.2 | 8443 |
| 4000 | 3317 | 2909 | 122.51 | 8.135 | 5006.7 | 8634 |

*T : Température absolue en K.*
*U : Vitesse de propagation en m/s de l'onde de choc dans l'air.*
*UP : Vitesse en m/s de la matière derrière l'onde de choc.*
*P : Pression de l'onde de choc en bar.*
*V0/V : rapport des volumes avant et après choc.*
*QNO : Concentration finale de NO (exprimée en ppm) dans la chambre de tir*
*D : Vitesse de détonation em m/s de l'explosif qui induit le choc*

**Tableau 9 : Résultats du calcul .**

Par ailleurs, des essais réalisés en Allemagne (12) montrent qu'une faible quantité d'air présent autour de la charge augmente sensiblement la teneur en NO des gaz engendrés par la détonation.

Dans le but d'évaluer plus précisément la participation éventuelle de l'air à la production d'oxydes d'azote, nous avons réalisé des essais avec des explosifs ne contenant pas d'azote.

II - 4 - 2 - essais réalisés:

L'explosif utilisé pour ces essais est un mélange de chlorate de potassium, d'aluminium et de cellulose. Le bilan en oxygène de cet explosif est de -10 % et sa vitesse de détonation à l'air libre en cartouches de diamètre 30 mm est d'environ 2 km/s.

Nous avons effectué des tirs sous atmosphère contrôlée, avec les deux configurations de tir suivantes :

- Tir en charge suspendue en plaçant la charge dans un ballon de diamètre 1 m,
- Tir en mortier avec bourrage en balayant en continu l'âme du mortier.

Le tableau 10 donne les productions de gaz toxiques ou nocifs mesurées, lors des tirs en charge suspendue, en fonction de la nature du gaz contenu dans le ballon (air, argon, azote, oxygène).

| Gaz environnant la charge | Productions en l/kg | | | |
|---|---|---|---|---|
| | NOx | CH4 | CO | CO2 |
| air | 0,4 | - | 14 | 203 |
| argon | 0,06 | 0,9 | 52 | 179 |
| azote | 0,12 | 4,8 | 85 | 126 |
| oxygène | 0,13 | - | 3,4 | 227 |

Tableau 10 : Tirs en charge suspendue.

On constate une nette diminution de la quantité de vapeurs nitreuses produites par le tir lorsque l'air est remplacé par l'argon. On observe également une nette augmentation du rapport CO/CO2 due à l'absence d'air pour l'oxydation du CO en CO2. Au contraire, sous atmosphère d'oxygène, une grande proportion de CO est oxydée en CO2.

En mortier avec bourrage, comme on peut le voir sur le tableau 11, le remplacement de l'air par de l'argon ne modifie pas de façon sensible la production de vapeurs nitreuses.

| Gaz environnant la charge | Productions en l/kg | | | |
|---|---|---|---|---|
| | NOx | CH4 | CO | CO2 |
| air | 0,09 | 4,7 | 62 | 176 |
| argon | 0,08 | 4,0 | 60 | 199 |

Tableau 11 : Tirs en mortier avec bourrage.

II - 4 - 3 - Conclusions :

Dans le cas des tirs en charge suspendue, nous avons mis en évidence, avec un explosif ne contenant pas d'azote, la formation de vapeurs nitreuses. L'azote correspondant ne peut donc provenir que de l'azote atmosphèrique.

Dans le cas d'un tir en mortier avec bourrage, les quantités de vapeurs nitreuses sont plus faibles que dans les tirs en charge suspendue. Le balayage de l'atmosphère du mortier par de l'argon ne permet pas de diminuer notablement les quantités d'oxydes d'azote formés par le tir. La participation de l'air, dans cette configuration de tir, à la formation des vapeurs nitreuses est donc négligeable.

## III / CONCLUSION GENERALE :

La méthode pour l'analyse des fumées de tir retenue au CERCHAR permet de réaliser, de façon reproductible, des essais adaptés à la caractérisation de la toxicité des tirs en mine.

De plus, elle peut être utilisée pour la réalisation d'études plus fondamentales. Par exemple, il est possible d'apprécier l'effet de la nature du terrain ou l'influence de l'évolution de la réactivité de l'explosif sur la production de gaz toxiques.

Actuellement nous nous interessons à la caractérisation des explosifs de mine de la nouvelle génération (émulsions, nitrates-fiouls alourdis) dont le comportement semble être un peu différent, dans ces conditions de tir, du comportement des explosifs classiques.

## --- BIBLIOGRAPHIE ---

- (7) A review of laboratory and field test methods for studying fume characteristic of explosives, N.C. KARMAKAR and S.P. BANERJEE, Jour. of mines metals & fuels, august 1984, p.398-402.

- (2) Recherche CECA - Convention n° 7253-44/3/090 - Titre " Etude des risques présentés par les gaz toxiques produits par les tirs d'explosifs".

- (3) Recherche CECA - Convention n°7256-33-033 - Titre "Etude de l'influence de la nature des explosifs sur la production de gaz toxiques".

- (4) Recherche CECA - Convention n° 7260-02-010/03 - Titre "Etude de l'influence de la nature des explosifs sur les productions de gaz toxiques, lors des tirs".

- (5) Méthodes d'essais pour évaluer la toxicité des fumées de tir, P. CARBONEL et J. BIGOURD, Prop. and Expl. 5, 83-86 (1980).

- (6) Fumées de tir, P. CARBONEL J. BIGOURD et J. DANGREAUX, Ind. Min. 62, n° 7, juil. 1980, p.497-501.

- (7) Explosives research at CERCHAR, J.BIGOURD et C.MICHOT, à paraitre dans Prop, Explo and Pyro

- (8) Aspects particuliers de la détonation ou de la déflagration des explosifs de mine, J. DANGREAUX et J. BIGOURD, Journées P.VIEILLE, Paris, 26-27 sept. 1988

- (9) Evaluation of toxic after-detonating gases formed by industrial explosives, A.G. STRENG, Explosivstoffe n° 3/4 (1971).

- (10) Messung der am Grundenstaub absorbierten explosions produkte, STOCHL and JISKRA, Staub-Reinhalt-Luft 40 n° 6, juin 1980.

- (11) Les gaz toxiques d'explosion en milieu minier : le role de l'adsorption des vapeurs nitreuses, L. CLAEYS, Revue Medicale Minière n° 34/35 (1957).

- (12) Recherche sur les fumées produites par la détonation de divers explosifs, Dr. F. VOLK, Explosifs, p.72-80.

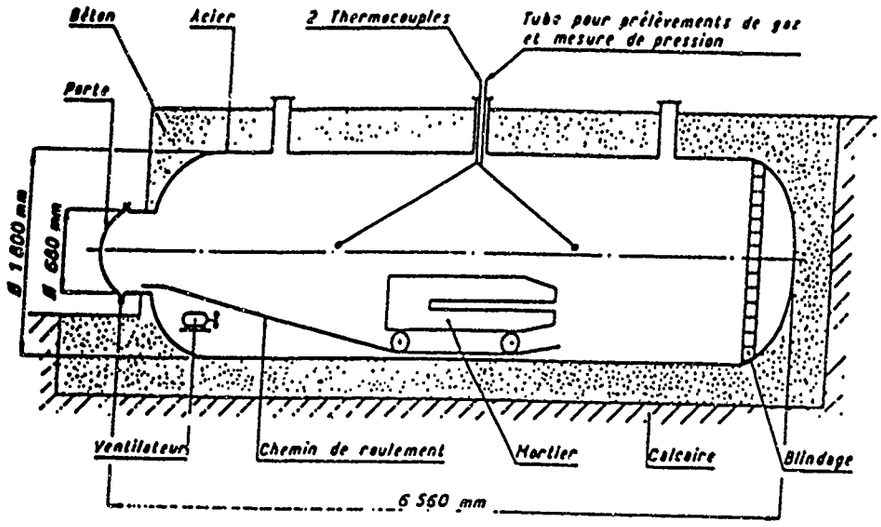


Figure 1 : Schéma de la chambre de 15 m3.

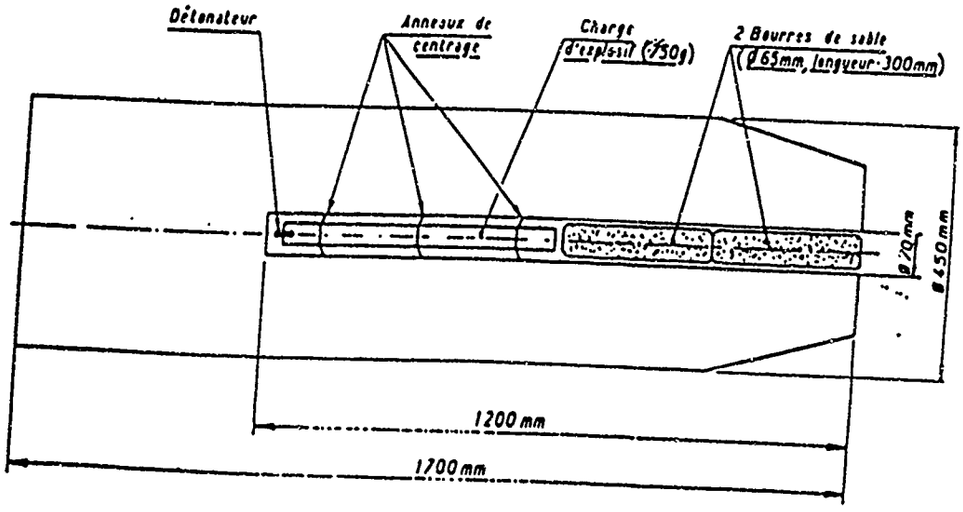


Figure 2 : Schéma du mortier d'acier.

# DETERMINATION OF NITROGEN OXIDES IN THE POST-DETONATION FUMES OF INDUSTRIAL EXPLOSIVES

Ralf B. Zimmermann
WBK-Bergbau-Versuchsstrecke
Dortmund - Derne, FRG

## ABSTRACT

In the fumes of industrial explosives the total content of toxic components such as CO and NOx should be as low as possible. To minimize the CO-content, the oxygen-balance of such explosives normally is set near zero, but is slightly in the positive region. In these cases fumes contain NO to a certain extent. After the expansion of the fumes and during the following diffusion and mixing with air, NO is oxidised to $NO_2$ and subsequently absorbed on wet or alkaline surfaces. These processes are so quick that the correct determination of the primarily developed NO in the gas-phase is prevented.

Modern analytical tools, like chemiluminescence detectors, allow the simultaneous plotting of a concentration- time- history of NO and NOx in the fumes cloud. By evaluating the kinetic laws of the rate-determining processes it should be possible to get an extrapolated value of the original NO-content at detonation time. This value can be used to compare the different explosive compositions and to estimate the effect of composition variations with respect to NO-concentrations.

## INTRODUCTION

In underground blasting operations toxic components in shotfiring fumes present a serious hazard especially under poor ventilation conditions. The main products in the post-detonation fumes of industrial explosives are nitrogen,

water vapor and carbon dioxide, but because of thermodynamics carbon monoxide and nitrogen oxides are always present to a certain extent. The amount of CO and NOx depends on a number of parameters, such as :

- composition of the explosive
- detonation characteristics
- mode of initiation
- diameter of charge and borehole
- mechanical strength of the confinement
- type of stemming

Some of the above parameters depend on the explosive's formula , others are influenced by regulations of usage. For the purpose of certification and approval of an explosive for underground use one needs a standard testing method to get comparable values.

As described in earlier papers (1), in the FRG this standard test is done by a small, but realistic blasting operation in a closed chamber in an experimental underground mine and chemical analysis of a sufficient number of fume samples. The results seem to have a close correlation to those, found under practical conditions. On the other hand the method is expensive, slow and gives little reproducibility. It should be supplied by a laboratory method, which will give hints for the development of an explosive with a minimum content of toxic fumes.

General requirements for this method have already been evaluated in previous work (2). The main result was, that the test charge used and the expansion factor of the fumes should be in the same order of magnitude as in practical blasting operation.

## EXPERIMENTAL

Explosive charges from 0.5 to 2 kg of normal cartridges in diameters of 25 to 40 mm are detonated either freely suspended or confined in a steel- or cardboard- tube in a closed concrete shell of 130 $m^3$ volume. The overpressure escapes through small diameter holes near the inlet door, so that only air is lost in the expansion process. The intensive mixing in the chamber volume is done by an axial flow fan with about 50 $m^3$/min. The sampling point is situated near the centre of the shell and is connected by a 4 mm i.d. polyethylene- tube with the gas analysers:

a) two non-dispersive IR-photometers for 2000 vpm CO full- scale or 20,000 vpm $CO_2$ full- scale (BINOS 1, Fa. Leybold- Heraeus)

b) NO-NOx-chemiluminescence analyser from 10 vpm to 10,000 vpm full- scale (NO/NOx-analyser, model 951, Fa. Beckman).

The readings of the analysers are monitored simultaneously by a three-channel-compensation-recorder. CO and $CO_2$ have their own channel on the recorder. The chemiluminescence analyser is switched every minute from the NO-mode to the NOx-mode and back by means of a catalytic converter and the output-signal is given to the third channel of the recorder. As can be seen from these diagramms, mixing is complete within less than 2 minutes and the CO and $CO_2$ concentrations are stable within a few percent for more than one hour (see fig. 1 and table 1).

The experiments reported below are carried out with charges of about 1.7 or 0.8 kg permitted explosive. Its cartridge diameter was 32 mm and it was confined in a cardboard tube of 40 mm i.d. with a wall thickness of 4 mm. The permitted explosive consists of about 10 % nitroglycerole, about 80 % of a near molar mixture of ammonium chloride and sodium nitrate and some ingredients to

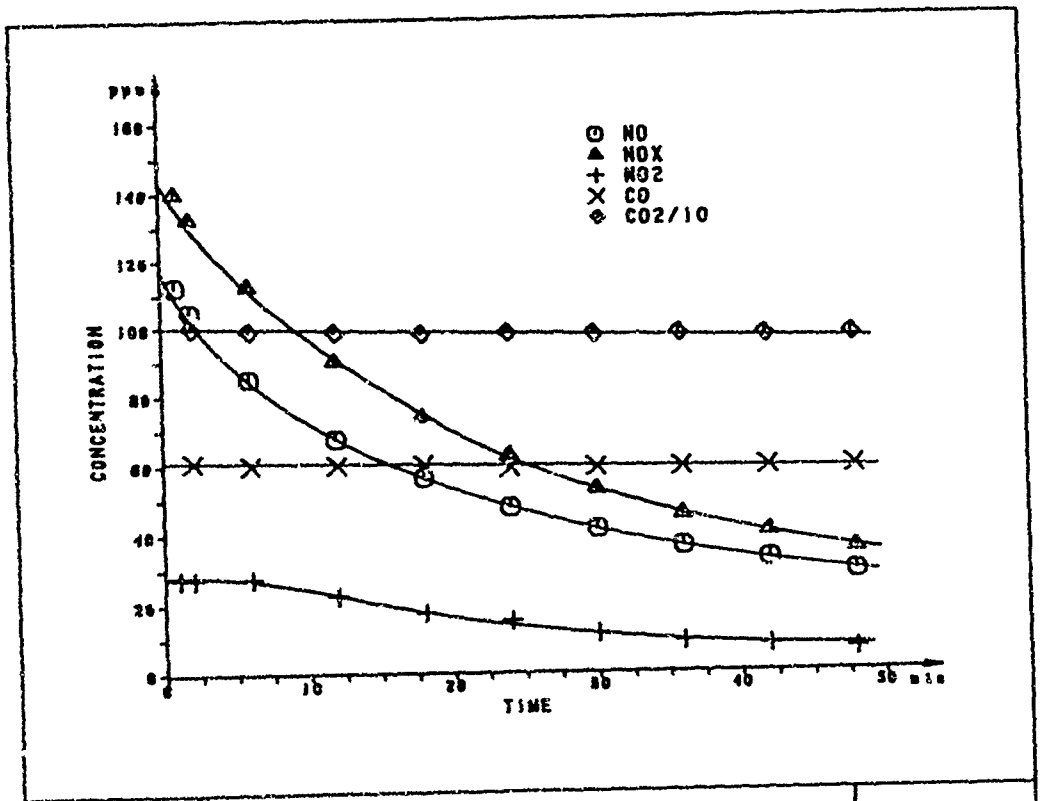


| WBK / BVS | Results of Test No. 9 | Fig. 1 |
|---|---|---|

improve anti-deflagration behavior and water resistivity. Its oxygen balance is +3,7 %; the velocity of detonation is 1700 m/sec and the detonation pressure about 1 GPa.

## RESULTS AND DISCUSSION

It is very easy, to get extrapolated initial values for CO and $CO_2$ concentrations from the concentration- time-diagramm for t = 0, the detonation time. The values for NO and NOx however decrease almost by one order of magnitude in less than one hour. As the decrease is not linear in time, it is impossible to get the initial values by a direct extrapolation. So a kinetic analysis of the data might be more appropriate.

It is well known that NO reacts to $NO_2$ in the gas phase by oxidation , which is absorbed on wet surfaces to the final stage of $NO_3^-$-ions. The reactions can be written as:

$$2\ NO + O_2 \longrightarrow 2\ NO_2 \qquad \text{(R-1)}$$

and

$$2\ NO_2 + \tfrac{1}{2}\ O_2 + 2\ OH^- \longrightarrow 2\ NO_3^- + H_2O \qquad \text{(R-2)}$$

As it was shown by BODENSTEIN in very careful experiments (3), the formation of $NO_2$ in R-1 is of second order with respect to NO and of first order with respect to $O_2$. So we get the kinetic law:

$$d[NO_2]/dt = -\ d[NO]/dt = 2\ k_1 \bullet [O_2]\,[NO]^n \qquad \text{(Eq-1)}$$

with n = 2 in the concentration range, experienced by BODENSTEIN (being about 100 to 1000 times higher than in the case of the fumes). By definition is:

$$[NOx] = [NO] + [NO_2] \qquad \text{(Eq-2)}$$

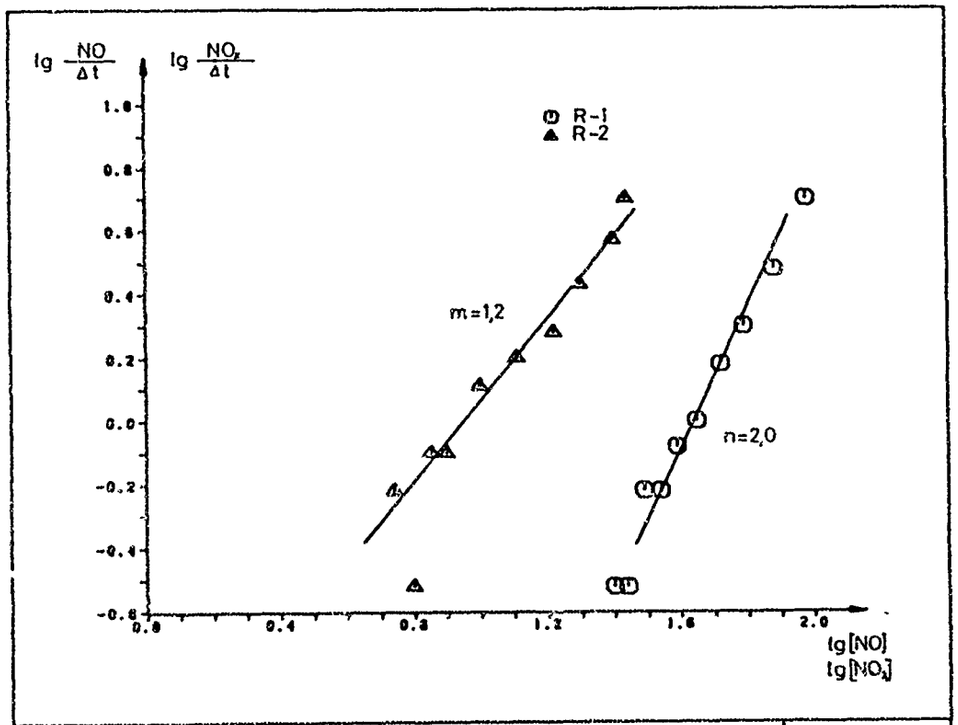


| WBK / BVS | Effective Reaktion Orders | Fig. 2 |
|---|---|---|

The concentration of NOx will be constant, if there is only R-1 in the gas-phase, but in case of surface reactions, for example R-2, it decreases. So the decrease of [NOx] is equal to the decrease of $[NO_2]$:

$$d[NO_2]/dt = d[NOx]/dt = -k_2 \cdot [O_2][NO_2]^m \qquad \text{(Eq-3)}$$

In order to get estimated values for the reaction orders m or n it is useful to begin with the differential form of the kinetic equations. Logarithming and replacing the differential ratios by difference ratios yields:

$$\lg(\Delta NO/\Delta t) = \lg(-2k_1^*) + n \lg[NO] \qquad \text{(Eq-4)}$$

resp. $$\lg(\Delta NOx/\Delta t) = \lg(-k_2^*) + m \lg[NO_2] \qquad \text{(Eq-5)}$$

In these equations the rate constant k is replaced by the constant $k^*$, which already implies the almost constant concentration of $O_2$.

Plotting the logarithms of $\Delta NO/\Delta t$ against [NO] or $\Delta NOx/\Delta t$ against $[NO_2]$ yields values for n = 2.0 and m = 1.2 (see fig. 2). This means that the decrease of NO is about second order and mainly follows the mechanism established by BODENSTEIN. Furthermore the absorption of $NO_2$ probably is of first order with respect to $NO_2$.

So we can use the kinetic equation Eq-1 in its integrated form. Assuming that $[NO]_i$ is the initial concentration of NO at the detonation time t = 0 and that the initial concentration of $NO_2$ is near zero, we obtain the following solution of the differential equation (4):

$$1/[NO] = k_1^* t + 1/[NO]_i \qquad \text{(Eq-6)}$$

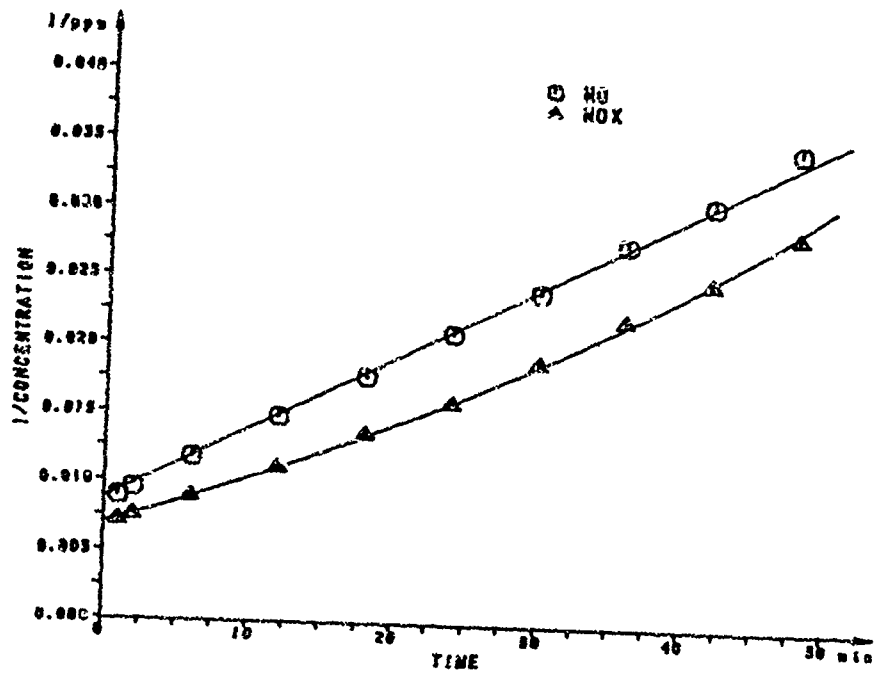


| WBK / BVS | Initial Concentrations | Fig.3 |
|---|---|---|

According to equation 6, a plot of 1/[NO] against the time t gives a straight line and a reliable extrapolation to t = 0 is now possible, which yields the initial concentration $[NO]_i$.

A similar plot of 1/[NOx] against t shows a slightly curved line, corresponding to an overall reaction order below 2 (see fig. 3). Nevertheless a reliable extrapolation to the initial concentration $[NOx]_i$ is also possible and yields a definitely higher value than that for $[NO]_i$, indicating an apparent small content of $NO_2$ in the initial fumes.

A similar result had already been reported by VOLK (5), obtained with a commercial explosive detonated in an argon-filled vessel, and it possibly could be attributed to a partial deflagration in this explosive. In our experiments, initial $NO_2$ also may be generated partly by deflagration. Another possibility is its formation by the rapid oxidation rate at the surface of the initial expanding fumes cloud and so the initial $NO_2$-concentration is only a virtual one.

A comparison of the results of three similar experiments, differing only in the mass of the explosive, shows a good reproducibility of the specific contents of NO, NOx, CO and $CO_2$, which are expressed in l/kg explosive (see table 2).

So the described method should be used in the development of a new generation of industrial explosives, the emulsion explosives, which will have in its fumes a much lower content of toxic components, especially of NOx, than conventional dynamites.

| Tab.1 Results of Test No.9 | | | | | | | |
|---|---|---|---|---|---|---|---|
| Time [min] | NO [ppm] | 1/NO [1/ppm] | $NO_x$ [ppm] | 1/$NO_x$ [1/ppm] | $NO_2$ [ppm] | CO [ppm] | $CO_2$ [ppm] |
| 1 | 112.5 | 0.0089 | 140.0 | 0.0071 | 27.5 | 62 | 1005 |
| 2 | 105.0 | 0.0095 | 132.5 | 0.0075 | 27.5 | 61 | 1000 |
| 6 | 85.0 | 0.0118 | 112.5 | 0.0089 | 27.5 | 60 | 990 |
| 12 | 67.5 | 0.0148 | 90.0 | 0.0111 | 22.5 | 60 | 985 |
| 18 | 56.25 | 0.0178 | 73.75 | 0.0136 | 17.5 | 60 | 980 |
| 24 | 47.5 | 0.0211 | 62.5 | 0.0160 | 15.0 | 59 | 980 |
| 30 | 41.25 | 0.0242 | 52.5 | 0.0190 | 11.25 | 59 | 975 |
| 36 | 36.25 | 0.0276 | 45.0 | 0.0222 | 8.75 | 59 | 975 |
| 42 | 32.5 | 0.0308 | 40.0 | 0.0250 | 7.5 | 59 | 970 |
| 48 | 28.75 | 0.0348 | 35.0 | 0.0286 | 6.25 | 59 | 970 |

| Tab.2 Results of Tests No.8-10 | | | | | | | | | | | |
|---|---|---|---|---|---|---|---|---|---|---|---|
| Test | NO | | $NO_x$ | | $NO_2$ | | CO | | $CO_2$ | | Charge Weight [g] |
| | l/kg | ppm/kg | l/kg | ppm/kg | l/kg | ppm/kg | l/kg | ppm/kg | l/kg | ppm/kg | |
| No. 8 | 7.9 | 60.5 | 10.2 | 78.2 | 2.3 | 17.7 | 4.5 | 34.8 | 44.1 | 339.4 | 1752.9 |
| No. 9 | 8.5 | 65.5 | 10.4 | 80.2 | 1.9 | 14.7 | 4.5 | 34.5 | 44.4 | 341.9 | 1769.8 |
| No.10 | 8.3 | 63.9 | 9.8 | 75.3 | 1.5 | 11.4 | 4.6 | 35.4 | 44.5 | 342.1 | 877.0 |

ACKNOWLEDGEMENT

This work was supported financially by the Federal Ministery of Research and Technology.

REFERENCES

(1) Eitz E & Zimmermann R, Explosifs 1977, p. 65/71
Carbonel P & Bigourd J, Explosifs 1979, p. 179/185
Koplin H, Nobel Hefte 1979, p.129/156
Crichton O, 19th Int. Conf. Mine Safety, Katowice (Poland) 1981, paper E-8

(2) Eitz E & Zimmermann R, Propell. Explos. 1978, p.17/19

(3) Bodenstein M, Z. phys. Chem. 1922, p. 68

(4) Frost A & Pearson R, Kinetics and Mechanism, New York 1962

(5) Volk F, Propell. Explos. 1978, p. 9/13

# DETERMINATION OF NITROGEN DIOXIDE GENERATED IN PROPELLANTS AND EXPLOSIVES BY POLAROGRAPHY AND HPLC WITH ELECTROCHEMICAL DETECTION

Arne Bergens
University of Uppsala
Dept. of Analytical Chemistry
P.O. Box 531
S-751 21 Uppsala, SWEDEN

Jan Asplund
Nobel Chemicals AB
S-691 85 Karlskoga, SWEDEN

## ABSTRACT

A method for the determination of nitrogen dioxide in propellants and high explosives has been developed, based on collection of nitrogen dioxides in a cartridge containing Florisil coated with diphenylamine. The nitrogen dioxide reacts with diphenylamine to form N-nitroso- and nitroderivatives. The nitroso- and nitroderivatives are eluted from the cartridge with methanol and analysed either by polarography or HPLC.

The amount of derivatives formed in the cartridge is related to the amount of nitrogen dioxide formed in the sample. Polarography was used for the determination of N-nitroso-diphenylamine in the cartridge. N-nitroso-diphenylamine was found to be the major derivative formed and accounted for more than 90% of the total amount of nitrogen dioxide.

HPLC with electrochemical detection can be used to monitor the formation of the different nitroderivatives in the cartridge exposed to nitrogen dioxide. After some modifications, the method should be possible to use for field sampling and determinations of nitrogen dioxide in propellant plants and storages.

## INTRODUCTION

The nitrate esters of single and double base propellants and high explosives decompose slowly. The cleavage of the weak nitrate ester bond involves a release of nitrogen dioxide and aldehydes.

$$RO-NO_2 \rightarrow RO^{\cdot} + NO_2$$

The $NO_2$ formed during this process can react further with the organic materials to form nitrogen oxide and other gases such as $N_2O$, CO, $CO_2$ and $H_2O$. The overall process can shortly be described as:

$$RO-NO_2 \xrightarrow{\Delta H} NO_x \qquad x = 1 \text{ or } 2$$

In the presence of air, any $NO_x$ formed can be oxidized to $NO_2$ which catalyses the cleavage of the nitrate ester bond. Hence, the decomposition process will be accelerated by the $NO_2$ formed.

By addition of a stabilizer compound, these reactions can be prevented. The function of the stabilizer is to react reasonably fast with the $NO_2$ formed and thereby protect the nitrate ester from exposure to $NO_2$. Common stabilizers are diphenylamine (DPA) and various derivatives of urea such as centralites and acardites.

A number of stability tests has been developed for the purpose of checking that a propellant has been properly stabilized and that it will be stable after many years of storage. The stability tests often involves a procedure for forced aging by storing propellant samples at different temperatures. Examples of such methods for stability determinations are:

- Determination of the loss in weight.
- Determination of stabilizer and stabilizer derivatives. The presence of nitro- and nitrosoderivatives is not in itself a sign of the propellant being unstable but discloses that the amount of stabilizer agent has decreased.
- Determination of the $NO_2$ by chemiluminescence. The chemiluminescent method is specific for NO and is used to measure $NO_2$ by catalytically reducing $NO_2$ to NO prior to reaction with $O_3$.
- Measurement of the heating power resulting from the exothermic decomposition reactions by micro calorimetry.

This work describes a method for the determination of $NO_2$ in propellants and high explosives based on collection of $NO_2$ in a cartridge containing Florisil coated with DPA. The $NO_2$ reacts with the DPA in the cartridge to form nitro- and nitrosoderivatives which are eluted from the cartridge and analysed by polarography or liquid chromatography with electrochemical detection (LCEC). The amount of nitroso- and nitroderivatives formed can be related to the amount of $NO_2$ generated by the sample. Investigations on quantitative collection of $NO_2$ in a cartridge containing Florisil coated with DPA has already been published[1,2]. These earlier publications has been aimed at ambient nitrogen dioxide monitoring.

Polarography and LCEC are two very suitable methods for determination of the nitro- and nitrosoderivatives formed in the Florisil cartridge. The only electroactive reducible compounds in the cartridge are the different nitro- and nitrosoderivatives of DPA. It is therefore possible to get a sensitive and selective detection of the compounds of interest by using one or both of these techniques.

An aromatic nitro group can be electrochemically reduced at a glassy carbon electrode or a mercury electrode. The extreme cathodic potentials required to reduce nitrodiphenylamines involves inconvenient operational problems because of the interference from dissolved oxygen in the mobile phase. The reduction products in acidic aqueous media are hydroxylamines which in their turn can be electrochemically oxidized at moderate potentials suitable to analytical determinations. Therefore, the electrochemical detector used in the LCEC system was equipped with two working electrodes mounted in a series configuration. The difficulties with oxygen interference can be overcome by using the first electrode as a generator electrode of easily oxidizable hydroxylamines. The hydroxylamines formed at the first electrode are detected at the second downstream electrode. Hence, it is the current at the second electrode that is monitored as the analytical signal.

## EXPERIMENTAL

### Apparatus for polarography.

The polarographic determinations were performed with a Metrohm Polarecord E 506. All potentials were measured and reported versus a Ag/AgCl reference electrode (Metrohm EA 427). The scan rate was 2.67 mV/s. Deoxygenation of sample solutions were performed by passing nitrogen through the solutions for ten minutes before the recording of polarograms.

**Apparatus for LCEC.**

The LCEC system consisted of a LKB 2150 HPLC double piston pump and a six port Valco injection valve with either a 20 µl or a 50 µl sample loop. Separations were made either on a 10cm x 4.6mm I.D. RP-18 Spheri-5 column with a 1.5cm x 4.6mm I.D. precolumn (Brownlee Labs, USA) or a 10cm x 3.0mm I.D. Chromspher-18 (Chrompack, The Netherlands). The amperometric detection system was controlled by two LC-4B potentiostats (Bioanalytical Systems Inc., USA). A cross section of the detector cell is shown in fig. 1. It consists of two blocks: one Kel-F block containing the two glassy carbon working electrodes and one block made of stainless steel which serves as the auxiliary electrode. The Ag/AgCl reference electrode (Bioanalytical Systems, USA) is placed downstream in the eluent. The potential settings for the two working electrodes were W1 = -1.0V and W2 = +0.6V. The detector cell was placed in stainless steel box to shield it from electrostatic disturbances. All tubing in the chromatographic system were of stainless steel since the commonly used teflon tubing at the pump inlet is easily penetrated by oxygen. The mobile phase was continously deoxygenated with argon.

Chromatograms were recorded on a Kipp & Zonen strip chart recorder or on a Spectra Physics (SP 4290) integrator.

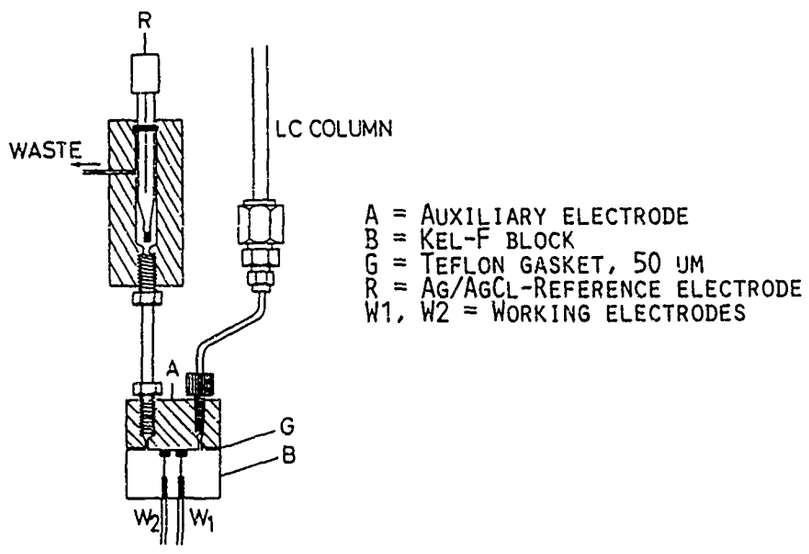


Fig. 1. Cross section of the dual electrode amperometric cell.

**Reagents.**

All solvents used were of pro analysi grade and purchased from Merck. 4-nitrodiphenylamine and 2-nitrodiphenylamine were purchased from Aldrich and used as received. Higher nitrated derivatives of DPA were supplied by Nobel Chemicals.

**Cartridges.**

The cartridges were constructed of a borosilicate glass tube with a diameter of 17mm. The glass tubes were equipped with conical ground joints (NS 14) and glass filters (porosity 2) according to fig. 2. The cartridges were packed with 2g 30/60 mesh Florisil (magnesium silicate, Fluka AG) coated with DPA. The coating was done by treating 10g of Florisil with 100ml methylenechloride containing 300mg DPA. After about one hour, the methylenechloride was slowly evaporated. The coated Florisil was then stored in dark ready for use in the cartridge.

**Collection of nitrogen dioxide.**

The cartridges were used during the Dutch stability test described in the Bofors textbook on analysis of explosives[3]. In this test, 4g samples are heated under standardized conditions in a test tube. The first 8 hours the test tube should be open to allow moisture to evaporate. After 8 hours the cartridge is placed on the test tube and the storage is continued. After every 24 hours a test tube with cartridge was removed and the cartridge was analysed for formed nitroso- and nitrodiphenylamine derivatives.

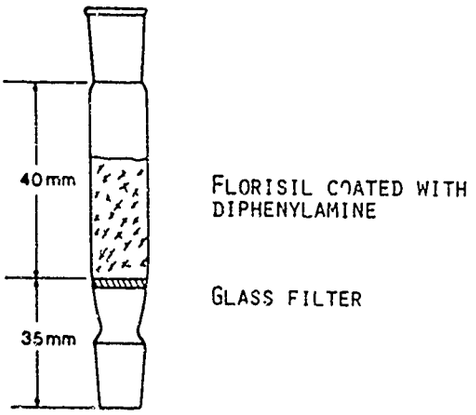


Fig. 2. Cartridge containing Florisil coated with diphenylamine.

**Preparations of samples.**

The cartridges were eluted with methanol and the received solutions were diluted to 100ml.

For the polarographic determinations, 20ml of the clear sample solution was diluted to 50ml with 10ml methanol, 5ml 1M ammonium acetate and distilled water. The methanol concentration in the sample solutions must be at least 60% in order to avoid precipitation of the analytes.

For the chromatographic analysis the sample solutions were diluted with mobile phase directly. Sufficient dilution factors for analysis were in the interval 10-50. Deoxygenation prior to injection into the LCEC system was necessary for samples requiring high sensitivity settings. This was accomplished by purging the samples with argon immediately before injection as described elsewhere[4]. The mobile phase composition was 60% 0.1M m-chloroacetic acid buffer (pH 2.7), 26% 2-propanol and 14% acetonitrile.

## RESULTS AND DISCUSSION

The reduction of the aromatic nitro group is an irreversible four electron process. The reduction gives hydroxylamines as the major products in acidic media[5-7]. N-nitrosoamines are also reduced to a hydroxylamine.

$$R-NO_2+4H^++4e^- \rightarrow R-NHOH+H_2O \qquad (I)$$

$$R-NO+2H^++2e^- \rightarrow R-NHOH \qquad (II)$$

The reductions can involve a further step giving an amine as product depending upon pH of the solution and its composition. DPA itself is not electrochemically reduced but it can be oxidized at potentials >0.8V[8].

The polarographic determinations can be performed either by direct current (DC) or differential pulse (DP) polarography. Linear calibration curves are obtained for N-nitrosodiphenylamine and the nitroderivatives in the medium specified in the experimental section.

The reaction mechanism for the reaction between $NO_x$ and DPA in the cartridge appears to be similar to the mechanism in aging propellants. In this mechanism, the first derivatives formed are N-nitrosodiphenylamine, 4-nitrodiphenylamine and 2-nitrodiphenylamine[9,10]. The major product in the early stages of aging is N-nitrosodiphenylamine. Fig. 3 shows DC- and DP-polarograms for a sample that has been stored for 150 hours at 110°C. The polarograms verifies that this mechanism is also valid for the DPA in the cartridge. The DC-polarogram reveals two reduction waves: the

first wave at -0.5V results from the reduction of 2- and 4-nitrodiphenylamine and the second wave at -1.0V results from the reduction of N-nitrosodiphenylamine. Fig. 3B illustrates the selectivity of DP-polarography. N-nitrosodiphenylamine can be analysed in the samples without involving a separation step by using DP-polarography. The peak at about -1.0V in fig. 3B shows that N-nitrosodiphenylamine is the major derivative formed and the double peak at -0.4 - -0.6V indicates the presence of 2- and 4-nitrodiphenylamine. Since the N-nitrosodiphenylamine is the major derivative formed, it was used as reference substance to evaluate the amount of $NO_2$ generated by the propellant sample. The nitroderivatives, however, has to be separated by liquid chromatography.

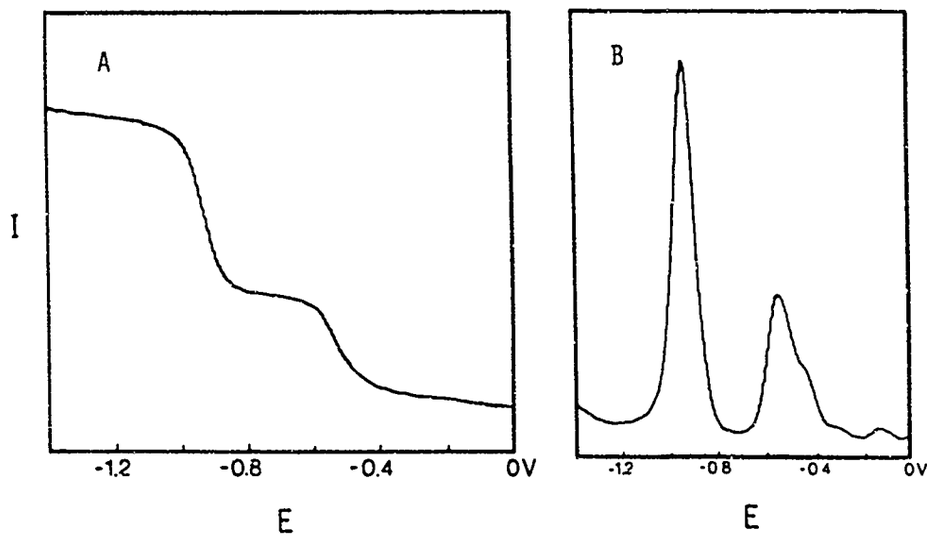


Fig. 3. Direct current polarogram (A) and differential pulse polarogram (B) from the determination of nitroso- and nitroderivatives.

The cartridges was also analysed by LCEC in order to study the formation of the different nitroderivatives. An example of a chromatogram of a sample stored at 105°C for 192 hours (8 days) is shown in fig. 4. At this point, higher nitrated derivatives has appeared. This could also be directly

observed by the change of colour on the cartridge. As the higher nitrated derivatives are formed the cartridges turned more and more yellow. Fig. 4 also shows the selectivity of the dual electrode amperometric detector. The only compounds in the samples that gives a measurable signal at +0.6V are the nitroderivatives which has been reduced to hydroxylamines at W1. The oxidation of the hydroxylamines at +0.6V is the reverse of reaction II above. The applied potential of +0.6V is not sufficient to oxidize the DPA present in the samples. The high amount of DPA gives only a minor disturbance on the baseline at about 7.5 minutes.

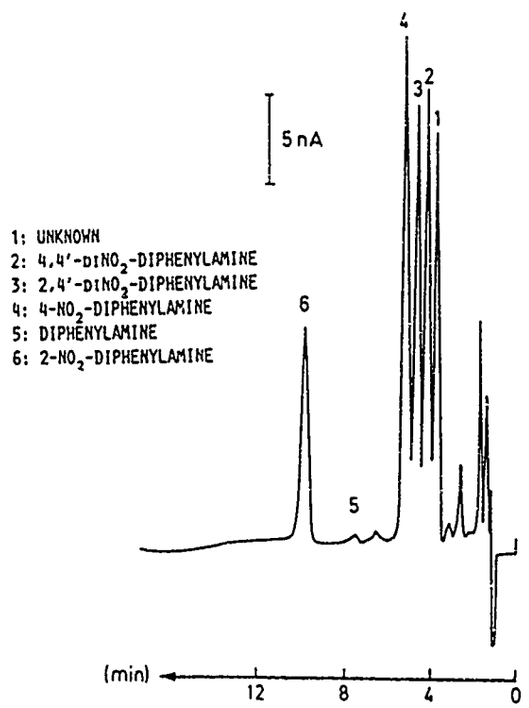


Fig. 4. Chromatogram from a double base propellant stored for 8 days at 105°C. Potentiostat settings: W1 = -1.0V and W2 = +0.6V, Column: Chrompack 10cm x 0.3cm I.D. Chromspher-18. Flow rate = 0.4ml/min.

The results from investigations of single base propellants are summarized in fig. 5. It can be seen from the results that a total loss in weight of 2% corresponds to a formation of about 2mg $NO_2$ per 1g single base propellant. It is also obvious that a relationship applies between the total loss in weight and the amount of formed $NO_2$. The results also indicate that a single base propellant stabilized with acardite II is more stable than a propellant stabilized with DPA. Note that the propellants are stabilized with different amounts of stabilizers.

This method is also applicable to field sampling and determination of $NO_2$ in ammunition plants and storages. At the moment, work is continued on this matter at Nobel Chemicals.

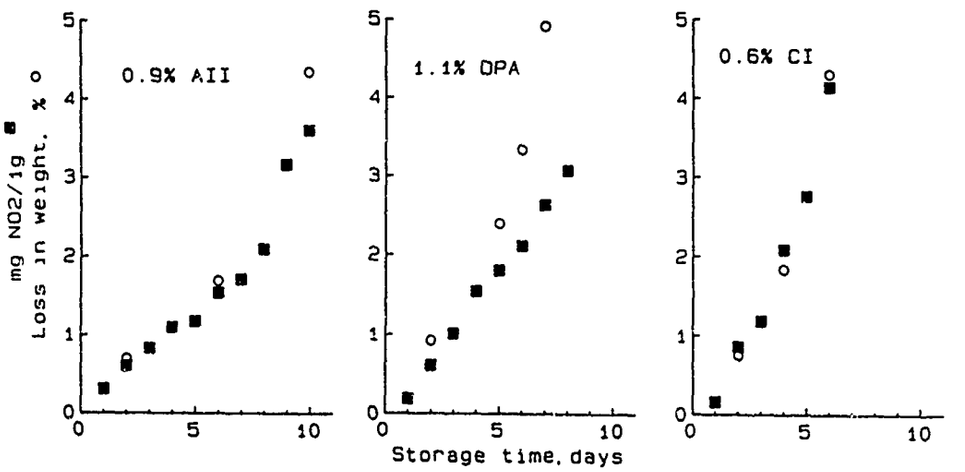


Fig. 5. Results from some determinations of loss in weight and $NO_2$ generated in single base propellants. AII = acardite II, DPA = diphenylamine, CI = centralite I.

## REFERENCES


1. F. Lipari, Anal. Chem., 56 (1984) 1820
2. J. Peschke, H. Stray and M. Oehme, Fresenius Z. Anal. Chem. 330 (1988) 581
3. Analytical Methods for Powders and Explosives, pp. 59-60, AB Bofors Nobelkrut, Bofors, Sweden, 1960
4. A. Bergens, J. Chrom. 410 (1987) 437
5. C.K. Mann and K.K. Barnes, Electrochemical Reactions in non-aqueous Systems, p. 348, Marcel Dekker, New York, 1970
6. D.A. Roston and P.T. Kissinger, Anal. Chem. 54 (1984) 429
7. R.O. Allendoerfer and P.H. Rieger, J. Am. Chem. Soc., 88 (1966) 3711
8. A. Bergens, K. Lundström and J. Asplund, Talanta, 32 (1985) 893
9. W.A. Schroeder, E.W. Malmberg, L.L. Fong, K.N. Trueblood, J.D. Landerl and E. Hoerger, Ind. Eng. Chem., 41 (1949) 2818
10. F. Volk, Propellants Explos., 1 (1975) 90

# PROCESSING THE POST-BLAST SCENE: AN INTEGRATED APPROACH

J.S. Deak, H. Clark, C. Dagens, J.J. Gaudet, B.W. Richardson

Royal Canadian Mounted Police, Ottawa, CDN

## ABSTRACT

The R.C.M.P. has recently created a National Response Team to attend the scene of major explosions in the jurisdiction of the federal police force.

Details of the R.C.M.P. approach will be discussed, including the roles of the various participants, as well as the development of an in-situ headspace sampling procedure and the use of photogrammetry to record the scene.

# IDENTIFICATION AND CHARACTERIZATION OF FLASH POWDERS

Charles R. Midkiff Jr.
Forensic Science Laboratory
National Laboratory Center
Bureau of Alcohol, Tobacco and Firearms
Rockville, MD 20850

## ABSTRACT

Flash powders are simple mixtures widely used in commercial fireworks and military simulators and increasingly being encountered in destructive devices. Although generally considered as low explosives, some formulations will detonate. Recently there has been interest in the potential hazards of these materials and approaches to their examination in the forensic laboratory are needed.

Formulations consist of a metal fuel, an oxidizer and/or additives and fillers. When sufficient sample is available, flash powders are identified with simple chemical tests for the fuel and oxidizer type. Characterization depends on identification of unusual oxidizers, additives and fillers present. Post-detonation residues pose a greater challenge, requiring more sensitive analytical methodology and familiarity with typical formulations and combustion/decomposition products. A variety of chemical tests and instrumental methods have been evaluated for specificity and sensitivity and those suitable for identification and characterization of intact powders and post-blast residues identified.

## 1. INTRODUCTION

In 1978 Meyers[1] described an approach to the identification and characterization of flash powders. Since that time, flash powders have been increasingly encountered in explosives evidence, in intact devices or as post-detonation residues. In addition, several recent cases have involved formulations differing from those normally seen.

Flash powders of the type usually encountered in the forensic

laboratory are designed to produce a flash of light accompanied by a loud report. In fireworks, for example, "Chinese Firecrackers" the filler may be described as flashlight powder. The term "photoflash powders" is better used to describe mixtures with lower levels of oxidizer and designed primarily for illumination. Among other materials that may be encountered as "flash powder" are whistle compositions. These are typically mixtures of an oxidizer, such as a perchlorate and a fuel; an organic compound or a salt of an organic acid (gallic acid, red gum, or a benzoate, biphthalate, or salicylate salt). Although apparently innocuous, these materials are reported to be very sensitive to ignition and should be handled accordingly.

Explosive type (sometimes referred to as "flash and sound") flash powders have a variety of compositions and applications, ranging from commercial fireworks and military training simulators to clandestinely manufactured explosive devices such as "Cherry Bombs" and "M-80's". In the United States, the latter are illegal in every state and each year are responsible for numerous injuries and some fatalities. The term M-80 rigorously describes a military training simulator containing about 3 grams of flash powder but is widely used as a name for a type of illicitly produced explosive device containing flash powder as the main charge. Larger versions of similar devices are frequently known as M-100's, M-1000's or "Quarter Sticks". These devices are easily and cheaply produced for a profitable underground market. Military training devices encountered are typically simulators for grenades and tank gunfire. These may contain up to two ounces (57 grams) of flash powder and when initiated in close quarters are capable of serious injury and property damage. A device resembling an M-80 in appearance is known as a "Pyro-pop"; however, internally the charge is contained in a gelatin capsule of the type used for medication. In these devices, only a small amount of neat flash powder is present and is physically separated from the bulk filler material, whereas in M-80 type devices the powder and filler material are admixed.

Flash powders are simple mechanical mixtures of an oxidizer and a metallic fuel such as aluminum or magnesium or an alloy of

these. Components may be added to facilitate ignition and a material to add bulk and prevent caking, referred to as the filler, is normally used in the M-80 type devices. Although flash powders have traditionally been considered as pyrotechnics or low explosives, it has been known for some time that certain formulations in small diameter tubes attain detonation velocities of 4600-4800 m/sec.[2] This is within the range of velocities (1,900-9,150 m/sec) of established high explosives. Flash powders can also be made to detonate unconfined if present in sufficient bulk[3] or by use of a blasting cap. Recently, the Bureau of Alcohol, Tobacco and Firearms has proposed that, for purposes of processing and storage, flash powders used in the fireworks industry be considered as high explosives[4]. An additional hazard with these materials is that, compared to conventional high explosives, flash powder formulations are more sensitive to initiation by friction and impact. When these materials are being examined in the laboratory, care should be taken to avoid static and friction as potential ignition sources.

## 2. TYPES OF FLASH POWDERS

Flash powders can be categorized by the oxidizer used or, less frequently, by the type of metallic fuel. Typical oxidizers and fuels are shown in Table 1. Of these, the most common is potassium perchlorate as the oxidizer and aluminum (flake and/or atomized) as the fuel. Several of the oxidizers shown are unlikely to be used in commercial or military pyrotechnics but could be encountered in the examination of improvised devices. Particle size and shape have a significant effect on the burning characteristics of flash powder. In general, for a given formulation, burning rate increases with increased surface area. This is attained either through a decrease in overall particle size or modification of particle morphology, e.g. thinning of the metal by rolling. Flaked aluminum has greater surface area per unit weight than atomized material and is preferable, although for certain applications, a mixture of particle sizes or shapes may be used. Potassium or sodium chlorate are infrequent in U. S.

domestic products because of the instability of mixtures of chlorates with sulfur.[5,6] Identification of chlorate as the oxidizer thus suggests either an imported or improvised product. Sodium nitrate is seldom used because of its hygroscopicity but is effective if kept moisture free. Although potentially useful as oxidizers, neither ammonium nitrate or perchlorate appear to have significant use in flash powders. Additives to facilitate ease of ignition include wood shavings, sulfur or antimony sulfide. Bulk additives for M-80 type devices are often cellulosic materials such as sawdust, wood shavings or meal, ground corn cobs (Grit-o-Cob) or grain hulls. Although these materials serve as additional fuel, they are principally fillers to add bulk and prevent caking. Several typical flash powder formulations are shown in Table 2.

## 3. ANALYSIS and CHARACTERIZATION

Intact flash powder is silvery-gray to black in color and under magnification can be seen to be a mixture of two or more components. A small portion of the sample can be placed on a spatula and heated to ignition, or more conveniently, folded into a piece of filter paper, held in forceps and ignited. Ignition gives a bright flash, occasionally with sparkles. When a few milligrams of sample are added to a vial containing water, a portion of the material dissolves while most of the metal and filler material, if present, float. The metal is held up by surface tension but the filler slowly becomes wetted and sinks.

When intact powder is available, a series of chemical tests serve to identify the material and provide characterizing information. With only small amounts of residues, however, greater sensitivity than available in simple tests may be required.

Chemical testing of neat flash powder begins by extraction of about 100 milligrams of the powder in a small vial with about 1mL of water. The sample is heated in a water bath to ensure solution of perchlorates, which have limited solubility at room temperature. The sample is filtered through #41 filter paper and the extract collected. Residue on the filter paper is washed with a few drops of hot water and the paper allowed to air dry. Cations are

development of a rose color is indicative of nitrates. Because of the reported carcinogenicity of alpha-naphthylamine, 1-naphthyl ethylene diamine has been used for several years in our laboratory with no apparent loss in sensitivity or specificity. Chlorate in solution is identified by the aniline sulfate test which forms a blue ring at the interface of acid and aqueous phases. This test resembles the brown ring test for nitrates which is also useful if further verification of nitrates is desired. For safety reasons, testing of solid chlorate samples as described in reference 9 is not recommended.

Although no longer as widely used in the forensic laboratory as in the past, microcrystalline tests are simple and fast, require no elaborate equipment and can have high specificity. A major limitation of many of these is sensitivity, however, when water extracts of flash powders are examined, adequate concentrations of chlorate, nitrate or perchlorate are available. One useful test is the formation of characteristic crystals with Nitron. A drop of the water extract is placed on a microscope slide and a drop of Nitron reagent added so that it flows into the test solution. Initially, blade-like crystals are formed with chlorate or perchlorate and these grow into clusters. Nitron also forms crystals with nitrate but these are fine needles in clusters. In the presence of high levels of nitrate, chlorate or perchlorate crystals may be obscured, however, if other tests have eliminated nitrate or chlorate as the oxidizer, Nitron is a useful indicator of perchlorate. Sensitivity of the test for perchlorate is about 1000 ppm. Chlorate sensitivity is somewhat less, probably only about 2500 ppm. No crystals are obtained with Nitron and 10,000 ppm of nitrite, sulfate, chloride, carbonate or bicarbonate alone, ions which might be expected in flash powder residues.

The cupric tetrapyridine perchlorate salt precipitates from aqueous solutions of perchlorates[5] at concentrations above about 2500 ppm. The crystals are lavender rhomboids, intially as single crystals but later forming clusters. Specificity of the test is good with no crystal formation with 10,000 ppm of chlorate, nitrate, nitrite, sulfate, chloride, carbonate or bicarbonate.

identified by a simple flame test of the aqueous extract using a platinum wire cleaned with dilute HCl prior to the test. Potassium gives a brief lavender flame color which is readily observed for extracts of potassium chlorate or perchlorate based mixtures. If; however, the flame color is bright yellow, a cobalt glass plate or blue optical filter should be used to remove obscuration by the intense 589nm emission of sodium. The violet color of potassium, if present, can be seen through the glass. Barium salts are indicated by a weak green color in the outer edge of the burner flame. Vogel[9] contains an excellent discussion of flame tests; concepts, conduct, and observed colors with and without a cobalt glass.

For intact powder extracts, simple spot tests supplement the flame test results. Many of these are routinely applied to explosive and explosive residue analyses.[10-12] Ammonium ion is identified by a Nessler test (red-brown precipitate) in a white spot plate. Barium produces a white precipitate or turbidity, depending upon concentration, when conc. $H_2SO_4$ is added to a few drops of the extract in a small vial. Formation of a red color with sodium rhodizonate, ethanol and HCl may also be used to detect/confirm the presence of barium.

Spot tests are also convenient to identify oxidizing anions, particularly with anion concentrations of about 1% (easily obtained with water extraction of the intact powder). Diphenylamine (DPA) in conc. $H_2SO_4$ gives a blue color with nitrate (immediate and permanent), chlorate (weak blue) and nitrite (blue which fades to yellowish). Mixtures containing perchlorate alone as the oxidizer give no blue color with DPA but, if mixed oxidizers are present, the development of a blue color does not exclude perchlorate. A useful test to distinguish chlorate and perchlorate is the formation of a colored complex with the dye Brilliant Green.[13] The perchlorate complex can be extracted from the aqueous phase into toluene whereas the chlorate complex is not extractable. Although sensitive, serious interference is caused by nitrate, nitrite and other strong oxidizing agents. The Griess test is specific for nitrites and, when modified by the addition of fine zinc powder,

Parker et al[8] reported no interference with bromide or iodide, however, levels of potentially interferring species studied were not indicated.

A violet precipitate with methylene blue and zinc sulfate is a useful spot test if perchlorate concentration is relatively high but better sensitivity and specificity are obtained when the reaction is used as a microcrystal test. At solution concentrations of about 500 ppm, thin violet needles are formed in 1-2 minutes and are a good indication of perchlorate. At this level, no interference in crystal formation was observed in the presence of 5000 ppm of chloride, sulfate, carbonate, nitrate, nitrite or chlorate. No crystals formed with the reagents alone and a 10,000 ppm solution of each ion. Interference by persulfate has been reported; however, if suspected, the solution can be boiled for several minutes to destroy the persulfate and retested.

At concentrations of about 500 ppm, perchlorate readily forms long white crystals with triphenylselenonium chloride (saturated solution in water).[13] Some of these will develop a distinctive fan structure. Specificity for perchlorate is good and no crystals form with 10,000 ppm of $Cl^-$, $ClO_3^-$, $NO_3^-$, $NO_2^-$, $CO_3^=$ or $SO_4^=$.

Perchlorate forms red mixed crystals of rubidium perchlorate and permanganate when solid rubidium chloride and potassium permanganate are added to a drop of a perchlorate solution.[14] The crystals are prisms or bipyramids with the intensity of the color related to the permanganate concentration. Although specific for perchlorate, the test is not highly sensitive. A lower range of 1,000 ppm appears optimistic and crystals are not reliably obtained below about 3,000 ppm.

Table 3 summarizes results obtained in the evaluation of spot/microcrystal tests for chlorate and perchlorate.

If confirmation of the cation is needed, sodium may be identified by the formation of pyramidal crystals, often twinned, with zinc uranyl acetate. The crystals exhibit yellow-green fluoresence under long-wave UV. No crystals are formed with potassium. Potassium is identified from the yellow precipitate formed with sodium cobaltinitrite.

A portion of the filtrate can be evaporated to dryness and the solid examined by infrared (IR) spectroscopy or by X-ray diffraction (XRD) to verify the identification of the oxidizer. Comparison is made with either laboratory generated or literature reference spectra. The former approach is preferable because spectra in the older literature were generated with instruments lacking the definition of current spectrometers. Even when sufficient sample is available for an IR or XRD, the approach works well only for mixtures containing a single water soluble oxidizer. Mixed oxidizers result in complex patterns to interpret and identification of the original compounds is difficult when two or more cations and anions are present in the extract.

The dried filter is treated with pyridine to dissolve sulfur, if present, and the pyridine extract collected. A few drops of 10% NaOH solution or sat'd $NaHCO_3$ are added to the pyridine extract. The development of a blue-green to brown color, depending on concentration, is indicative of sulfur. A small portion of the metal on the filter is mechanically transferred to a spot plate, tested with a few drops of 10% NaOH and observed under low magnification. Aluminum releases bubbles of hydrogen almost immediately. Zinc reacts very slowly and magnesium is unreactive. A second portion of the metal is tested with 1:1 HCl; zinc and magnesium often react promptly but aluminum has an induction period before bubbles are observed.

The Mg/Al (50:50) alloy used in some pyrotechnics reacts immediately and vigorously with 1:1 HCl but more slowly with NaOH than aluminum alone. When this behavior is observed, further testing of the metal should be conducted, either by chemical or instrumental tests. Atomic absorption, plasma or conventional emission spectroscopy, or atomic or X-ray fluorescence easily demonstrate that the metal is an alloy. With only a limited sample available, SEM/EDAX is attractive to characterize an alloy.

The filter is treated with several ml of 1:1 HCl to dissolve the metal remaining. If antimony sulfide is present, an odor of $H_2S$ may be noted and confirmed with moist lead acetate paper. Aluminum in the acid solution is identified by the fluorescent

complex with morin, magnesium by a blue precipitate with quinalizarin and antimony with triphenylmethylarsonium iodide or Rhodamine B.[15] An orange precipitate is formed by antimony in the presence of Triphenylmethylarsonium iodide (Pfaltz & Bauer M29900) whereas a violet precipitate is formed with Rhodamine B in conc. HCl. The material remaining on the filter will be essentially inert filler material and is identified by microscopic examination and comparison. A collection of common bulking/filler materials mounted on slides is useful for this purpose. Tables 4a and 4b comprise a flow chart or schematic suitable for the examination of intact flash powders.

For examination of post-detonation residues, the tests previously described are applicable when sufficient material is available; however, this is often not the situation. Typically, the evidentiary material, e.g. cardboard or plastic fragments, paper, pipe, etc is first examined under low magnification, (10-30X) and material of interest identified for testing. Residues are usually seen as a grey powder or traces of the metal deposited as a thin film on the surface of the device container or on objects adjacent to the device location. The powder may be removed by scraping but, although the film of shiny metal is readily observed under low magnification, it may be difficult to remove. After physical removal of residue particles for testing, the surface area is rinsed with warm water. If the metal is not removed by rinsing, it can be tested in-situ with drops of 10% NaOH or 1:1 HCl and the results observed under low magnification. The rinse solution is filtered and concentrated by slow evaporation if needed. A flame test gives preliminary identification of the cation. With the cobalt glass to remove obscuration, potassium is easily seen at 100 ppm or less. Because of the ubiquitous nature of sodium, it is difficult to assign significance to ppm levels of sodium unless suitable control samples are available for comparison. A spot test with $AgNO_3$ is useful as a screen for chloride ion, the major decomposition product of chlorate and perchlorate and may indicate the use of these as oxidizers. Weak tests, however, should be interpreted with caution and consideration given to the nature of

the surface from which the residue was extracted. One reference indicates, that while chlorates are detectable post-blast, "There is no possibility of detecting perchlorate after an explosion, because it is converted to chloride and oxide salts."[15]. Total inability to detect chlorates or perchlorates post-blast has not been our experience. Despite extensive conversion to chloride, either may be detected in residues from flash powder made with these oxidizers.

The filtrate or a warm water extract of physically removed particulate residue can be examined using the tests previously described. Because of the limited sensitivity of some of these, however, they are not as successful as more sensitive instrumental methods. As with the intact powder, the filter paper should be examined for the presence of the metal fuel. Little work has been reported on the identification of characteristic or typical combustion products of flash powders. Of potential interest would be aluminum oxide (major), antimony compounds (traces), carbonates from combustion of the bulk/filler material and sulfates from both sulfur and antimony sulfide.

Ion chromatography (IC) is well suited to the examination of post-blast residues of low explosives.[16] It provides working detectibility of about 10 ppm for $K^+$ and 5 ppm for $Na^+$ or $NH_4^+$. It is routinely used in our laboratory for examination of aqueous extracts of evidentiary debris. IC is equally suited to the examination of extracts for oxidizing anions such as perchlorate, chlorate or chloride.[17] We employ chemically suppressed ion chromatography to detect: $F^-$, $Cl^-$, $NO_2^-$, $Br^-$, $NO_3^-$, $HPO_4^=$ and $SO_4^=$ in a single injection. Perchlorate is determined in a second sample using a different eluent system and seperator column. The working range is below 20 ppm for each ion. Recent developments in single column ion chromatography suggest that it is applicable to these types of analyses and is a less expensive approach than methodology requiring a suppressor column.

## 4. CONCLUSION

Flash powders are simple, yet potent, explosives available from a variety of military or commercial sources. Because of their simple composition, they are easily improvised. As intact mixtures or as post-blast residues, flash powders are encountered as physical evidence in the forensic laboratory. Using a series of chemical spot, flame and microcrystal tests; the oxidizer, fuel, and additives may be identified. From this information, the powder may be placed in one of several classes. Minor components refine the classification while identification of the filler material, if any, assists in comparison of a known and questioned sample. Because of their availability, flash powders are present in a wide range of cases and may be received for analysis even by a laboratory normally doing few explosive-related examinations. With relatively simple techniques, available reagents and minimal instrumentation, even the smallest forensic laboratory should be able to successfully examine and characterize flash powder.

**REFERENCES**


1. Meyers, R.E.
"A Systematic Approach to the Forensic Examination of Flash Powder"
J. Forensic Sci. 1978, 23 (1) 66-73

2. Moiseenko, P.M.
"Explosive Characteristics of Mixtures of Ammonium Perchlorate and Ammonium Nitrate with Aluminum Powder"
Vzryvnoe Delo 1975, 75 135-141

3. Conkling, J.A.
Chemistry of Pyrotechnics Basic Principles and Theory
Marcel Dekker Inc. New York, NY 1985 pp. 176-177

4. Bureau of Alcohol, Tobacco and Firearms
Notice of Proposed Rulemaking: "Explosive Materials in the Fireworks Industry"
Federal Register 1988, 53 27452-27457 Wednesday July 20

5. Tanner, H.G.
"Instability of Sulfur-Potassium Chlorate Mixture"
J. Chem. Ed. 1959, 36 (2) 58-59

6. Conkling, J.A.
"Chemistry of Fireworks Old Industry, Long Unchanged, Starts to Move from Art to Science"
Chem. Eng. News 1981, 59 (26) 24-32 June 29

7. Lancaster, R.; Shimizu, T.; Butler, R.E.A. and Hall, R.G.
Fireworks Principles and Practice
Chemical Publishing Co. New York, NY 1972 231-234

8. Departments of the Army and Air Force
"Military Explosives"
TM 9-1300-214/TO 11A-1-34 28 November 1967

9. Svehla, G.
Vogel's Qualitative Inorganic Analysis
Longman Scientific & Technical/John Wiley & Sons
New York, NY 1987 pp. 4-7

10. Parker, R.G.; Stephenson, M.O.; McOwen, J.M. and Cherolis, J.A.
"Analysis of Explosives and Explosive Residues. Part 1: Chemical Tests"
J. Forensic Sci. 1975, 20 (1) 133-140

11. Washington, W.D.; Kopec, R.J. and Midkiff, C.R.
"Systematic Approach to the Detection of Explosive Residues V. Black Powders"
J. Assoc. Offic. Anal. Chem. 1977, 60 (6) 1331-1340

12. Crippin, J.B.
"Explosives Information (Residues - Spot Tests)"
Midw. Assoc. Forensic Sci. Newsl. 1985, 14 (1) 21-23

13. Feigl, F. and Anger, V.
Spot Tests in Inorganic Analysis 6th Ed.
Elsevier Publishing Co. London 1972 p.184

14. Benedetti-Pichler, A.A.
Identification of Materials
Academic Press New York, NY 1964 p.391

15. Jungreis, E.
Spot Test Analysis Clinical, Environmental, Forensic and Geochemical Applications
John Wiley & Sons New York, NY 1984 pp. 45-75

16. Rudolph, T.L.
"The Characterization of Some Low Explosive Residues by Ion Chromatography"
Proc. Int. Symp. Anal. Det. Explos. Dept. of Justice, F.B.I. Quantico, VA March 29-31, 1983 pp.213-219

17. Green, M.J.
"Ion Chromatographic Analysis of Perchlorate in Perchlorate/Sugar Explosive Devices"
LC Mag. Liq. Chromatogr. HPLC 1985, 3 (10) 894-896

Table 1

| | OXIDIZERS and FUELS | | | |
|---|---|---|---|---|
| Oxidizers | | | | |
| Common | $KClO_3$ | $KClO_4$ | $Ba(NO_3)_2$ | |
| Infrequent | $KNO_3$ | $NaNO_3$ | $NaClO_3$ | $NaClO_4$ |
| Rare | $CsNO_3$ | | | |
| Candidate | $NH_4NO_3$ | $NH_4ClO_4$ | $Ba(ClO_4)_2$ | |
| Fuels | Al | Mg | alloy (50:50) | |

Table 2

REPRESENTATIVE FLASH POWDER FORMULATIONS

| Formulation | | % by Weight | Reference | Usage |
|---|---|---|---|---|
| A | $KClO_4$ | 50% | 3 | simulator |
| | Magnesium | 17 | | |
| | $Sb_2S_3$ | 33 | | |
| B | $KClO_4$ | 64 | 3 | simulator |
| | Aluminum | 22.5 | | |
| | Sulfur | 10 | | |
| | $Sb_2S_3$ | 3.5 | | |
| C | $KClO_3$ | 43 | 7 | aerial display |
| | Aluminum | 31 | | |
| | Sulfur | 26 | | |
| D | $KClO_4$ | 50 | 3 | aerial display |
| | Aluminum | 23 | | |
| | Sulfur | 27 | | |
| E | $Ba(NO_3)_2$ | 78 | 8 | simulator |
| | Al (Grade A) | 3 | | |
| | Al (Grade B) | 12 | | |
| | Sulfur | 5 | | |
| | Castor Oil | 2 | | |

5/3/89

Table 3

**Sensitivity/Selectivity of Spot/Microcrystal Tests**

| Anion | Reagent(s) | Detection (ppm) reported | found | Interference |
|---|---|---|---|---|
| $ClO_3^-$ | Nitron | N/A | 2500 | $ClO_4^-$, $NO_3^-$ |
| $ClO_4^-$ | Copper tetra-pyridine | N/A | 2500 | ----- |
| | Methylene blue | N/A | 500 | $S_2O_8^{=}$ |
| | Nitron | N/A | 1000 | $ClO_3^-$, $NO_3^-$ |
| | Rubidium permanganate | 1000 | 3000 | ----- |
| | Triphenyl-selenium | 200 | 500 | ----- |

Table 4a

# INTACT POWDER ANALYSIS

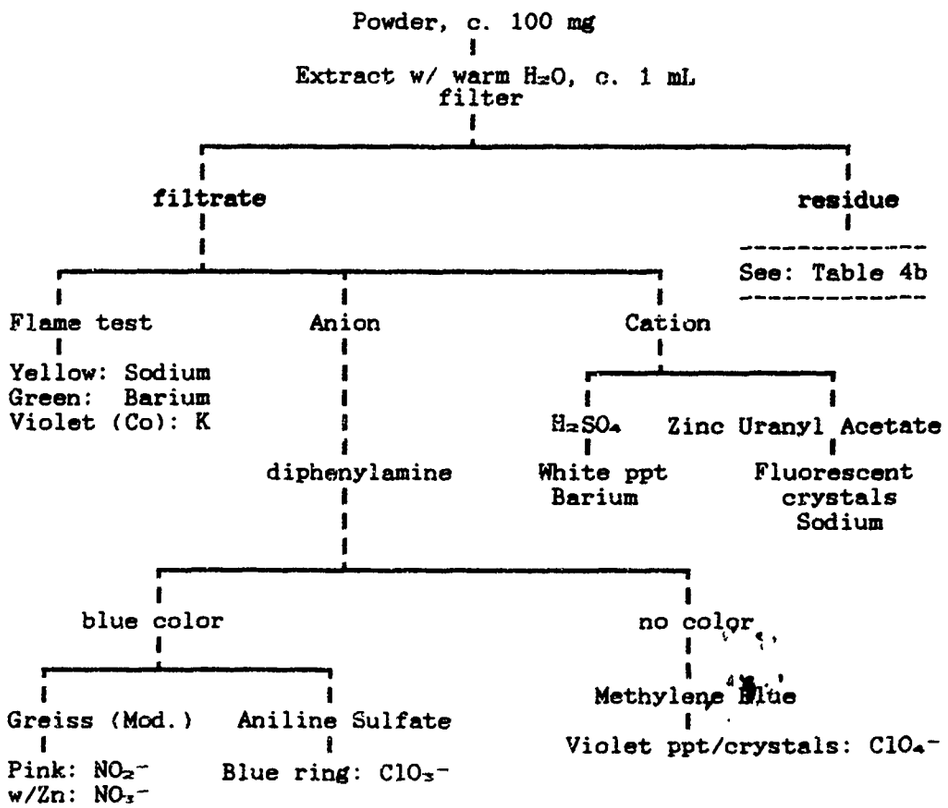


CRM 5/2/89

Table 4b

# INTACT POWDER ANALYSIS

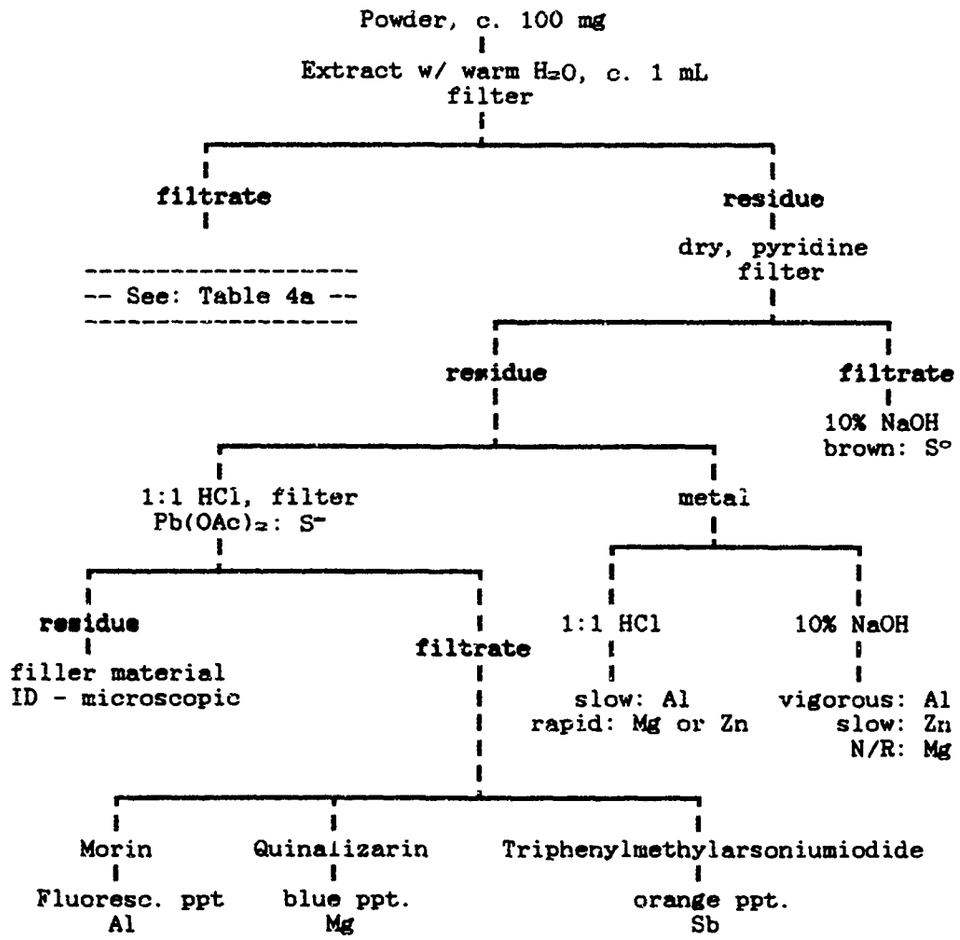


CRM 5/2/89

# POST - BLAST RESIDUE ANALYSIS IN THE R.C.M.P. LABORATORIES: SOME PRACTICAL OBSERVATIONS.

J.S. Deak, H. Clark, C. Dagenais, S. Jones, D. McClure, and B.W. Richardson

Royal Canadian Mounted Police,
Central Forensic Laboratory
Ottawa, Ontario, Canada

**ABSTRACT**

The Royal Canadian Mounted Police Forensic Laboratory Services has adopted a number of instrumental techniques for the analysis of post-blast debris. This paper outlines the techniques being utilized and offers some practical observations on these techniques. Information on an Explosives Transport Container and the recently-created National Post-Blast Response Team is also presented.

## Introduction

A number of major changes have occurred in the analysis of post-blast debris in the R.C.M.P. laboratories over the past three years. Until two years ago, explosive residue analyses were being conducted in each of the seven R.C.M.P laboratories across Canada using the analytical scheme developed by Beveridge 'et al' in the mid-70's.[1]

Since that time the decision was made to centralize explosives cases in two R.C.M.P. laboratories in Canada - Ottawa and Vancouver. The reasons for this centralization were three-fold:

1. there is not a large number of explosives incidents in Canada; therefore chemists in these two labs can more easily acquire and maintain expertise in this analysis;
2. the specialized equipment dedicated to explosives' analysis is expensive; and,
3. centralization allows for the correlation of related incidents across the country that may not be readily apparent if analyses were conducted in the various laboratories.

A number of instrumental analytical techniques have now been incorporated into our methodology to complement the established techniques. This paper reports on the practical applications of these techniques with respect to post-blast residue analysis. In addition, concerns with respect to the collection, preservation, and transportation of exhibit material will also be addressed.

## Thermal Energy Analyzer (T.E.A.)

The Central Forensic Laboratory is currently using a Thermedics Model 510 T.E.A. interfaced to a Hewlett-Packard Model 5880 G.C. equipped with a cool, on-column injector. The T.E.A. output is directed to a H.-P. Model 1000 Laboratory Automation System.

GC/TEA is used as a screening technique for the more common organic explosives, using a 15m x 0.32mm fused silica column with a 0.25µm DB-5 coating. In a 10 minute run (50°C, 0 min; + 20C°/min to 170°C ; 170°C for 4 minutes) the compounds in Figure 1 can be detected.

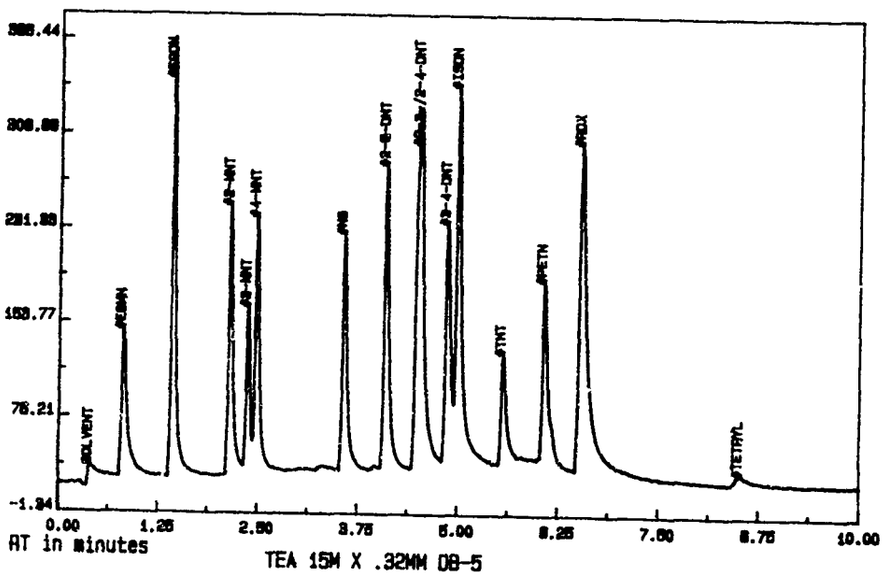


Figure 1 - GC/TEA chromatogram illustrating separation of some of the more common explosives (approximately 2 ng of each).

ISDN (isosorbide dinitrate) was chosen as an internal standard for the chromatography because it is a readily available pharmaceutical that elutes near the mid-point of the chromatographic run and has a lability similar to that of EGDN and NG.

The T.E.A. is operated in the nitroso mode with a G.C. interface

temperature of 280°C, a pyrolyzer temperature of 780°, and a total system vacuum optimized at 0.18 torr ( with an oxygen flow-rate of approximately 8 ml/min). The pyrolysis temperature of 780°C is a compromise that results in a decrease in sensitivity for the nitroaromatics but provides a lower level of interferences. Depending on the initial screening results, the pyrolysis temperature and the oven temperature programme can be optimized for the situation at hand.

Very early in our work it was discovered that the tedious acetone/liquid nitrogen cold trap could be replaced by a disposable, molecular sieve cartridge (available from Thermedics) without adversely affecting the detection of explosives of interest.

Another fact learned in the early stages of our work was that a guard column was absolutely essential for post-blast residue analysis. Our laboratory is currently using a 1m deactivated fused silica pre-column to trap any condensates before they reach the guard column. By breaking off a 10-25 cm length of contaminated guard column, the chromatography can be improved dramatically.

The obvious advantages of the use of GC-TEA have been documented elsewhere.[2,3,4] It is sufficient to state that it is a very effective technique for screening post-blast debris for explosives, as long as one is aware of its limitations:

1. it is still a chromatographic technique and by itself, cannot be used as positive identification unless confirmed by at least one more technique. One technique being investigated in our laboratory involves splitting the column effluent to the T.E.A. and to an electron capture detector and determining the relative detector response factors[5] for various explosives and potential interferences such as various nitrosamines.

2. certain non - volatile explosives cannot be readily analyzed by gas chromatography. Perhaps the most promising development to deal with these compounds is the use of SFC-TEA as documented by Douse.[8]
3. a number of non-nitro-based explosives are reportedly being used that cannot be detected by the T.E.A.[4]

Diamond Cell/Fourier Transform Infrared Spectrometry (DC/FTIR)

The high pressure diamond anvil cell (High Pressure Diamond Optics, Inc., Tucson, Arizona) as a sample holder for IR analysis of forensic samples has been used routinely in the R.C.M.P. Laboratories since the mid-60's.[7,22] When used in a state-of-the-art FTIR spectrometer, infrared spectra of residues and single crystals of unexpended explosives can be analyzed quickly and non-destructively. Once generated, the infrared spectrum can then be identified by searching a computerized spectral data-base of explosives and known residues (generated by the detonation of improvised, commercial and military explosives).

The R.C.M.P. Laboratories have standardized on the use of spectrometers equipped with dTGS detectors and cesium iodide optics rather than the faster MCT detector to allow us to obtain data in the 700 to 300 wavenumbers region of the infrared. This area is critical for the identification of a number of inorganics of forensic interest. Identification of commercial explosive constituents such as barium sulphate (encountered in certain classes of dynamites) can be readily identified by DC/FTIR. Similarly, single crystals of chlorates and perchlorates can be readily analyzed and differentiated by this technique (Figure 2). Liquid samples such as nitroglycerin can also be analyzed by the DC/FTIR technique.

The conventional high pressure diamond anvil cell used in our laboratories has been replaced in a number of locations by a mini-cell[21,23] which has the following advantages:

1. the unit is physically smaller and can be more readily accommodated by off-the-shelf, standard 6x beam condensers;
2. the diamond windows are thinner, therefore the energy throughput is considerably greater than through the high pressure cell;
3. because it is a low pressure cell, the diamonds are less apt to be damaged by inadvertantly applying too much pressure; and,
4. the mini-cell is less expensive than the high pressure version.

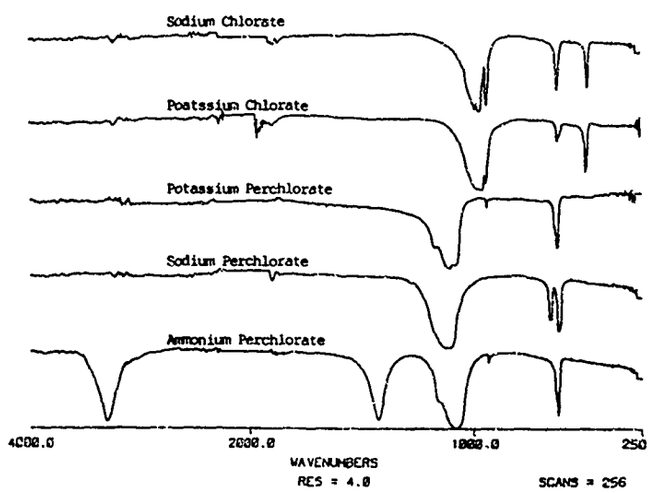


Figure 2 - Diamond Cell/FTIR spectra illustrating the discriminating power of IR for inorganic constituents. Samples consisted of single crystals pressed into a thin film between the diamond anvils.

## X-RAY DIFFRACTOMETRY (XRD)

Due to sample limitations, XRD has been traditionally limited to the use of powder cameras (either conventional Debye-Scherrer or Gandolfi cameras). Our laboratory has augmented these capabilities

with a Rigaku D/max-B automated diffractometer. The X-rays are produced using a 1.5 kw, fine-focus, copper tube run at 40 kv and 35 ma. A vertical goniometer as opposed to the horizontal one was chosen mainly to minimize the chances of minute, irreplacable samples falling off the sample holder.

Despite all of the advances in conventional XRD hardware over the years, it seems that the most useful advance is also the least costly. We have been using a low-background holder (made by The Gem Dugout, State College, Pennsylvania) for mounting samples for the past three years. These holders consist of quartz crystals cleaved in such a manner as to significantly reduce the background scatter, thereby allowing useful diffraction patterns on sample sizes of one mg or lower, depending on the nature of the material.

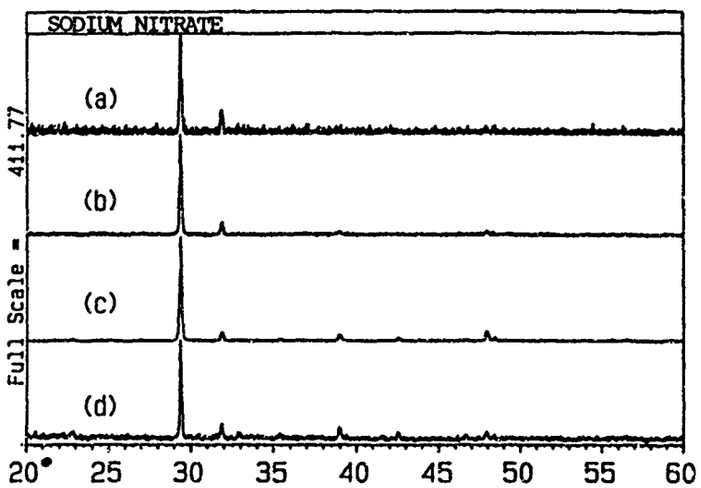


Figure 3 - X-ray diffraction patterns of sodium nitrate.
(a) 12 minute scan on one crystal, 0.1 mg.
(b) 10 12-minute scans on (a) co-added.
(c) 12 minute scan on standard 3 mg sample.
(d) 12 minute scan on 0.25 mg sample.

At the present time we are in the process of generating a searchable library of commercial and improvised explosive constituents, and also of residues of explosives generated on 1/2"-thick stainless steel substrates.

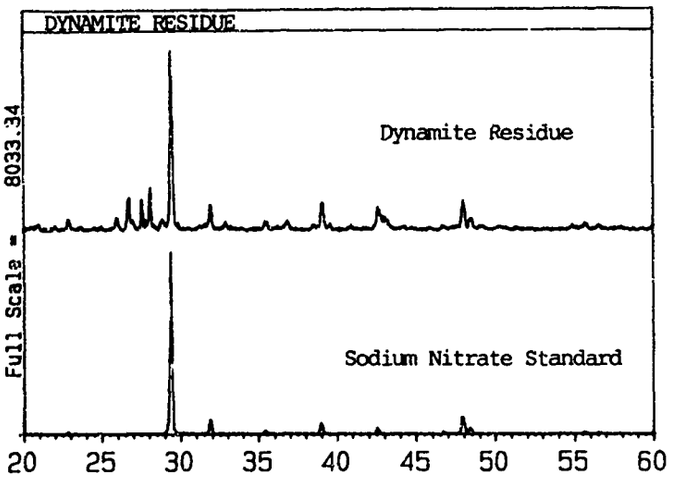


Figure 4 - Top: One milligram of dynamite residue on low-background holder. 5°(2θ)/min. 40 kv, 35 ma.
Bottom: 3 mg sodium nitrate standard.

The Rigaku system in our laboratory has an IBM PC-based operating system with both the Rigaku Search-Match software and the Fein-Marquart μ-PDSM (Micro-Powder Diffraction Search Match) software. Neither have yet been evaluted, however, preliminary indications suggest that for multi-component samples, the skill of the x-ray technologist is still the most critical factor in the successful interpretation of the data.

On samples that can be dispersed over an area of approximately 0.8 cm on the sample holder, a 5° - 90° diffraction pattern with data points collected every 0.02°(2θ) can be generated in a time frame as short as 2.5 minutes without adversely affecting the resolution. Figure 3 illustrates that using such a system, powder diffraction data can even be generated on single crystals without having to resort to Gandolfi cameras or to the more expensive microdiffractometers.

Figure 4 illustrates the diffraction pattern from approximately 1 mg of residue from a dynamite explosion scraped off a metal substrate.

## ION CHROMATOGRAPHY (I.C.)

The usefulness of ion chromatography in the examination of post-blast debris is well documented.[10-13] Our laboratories use a Dionex Model 2010i chromatograph interfaced to the H.-.P 1000 Lab Automation System. The operating conditions and typical chromatograms of the cations and anions of interest are illustrated in Figure 5.

A number of observations on the practical use of IC can be made. A micro-membrane chemical suppressor is used to enhance the eluant signal. The regenerant initially specified by Dionex for the cation suppressor was barium hydroxide. Problems with the precipitation of barium carbonate in the membrane prompted a switch to the tetrabutylammonium hydroxide (TBAOH) regenerant. Because of the cost of TBAOH, we recently procured an autoregenerant accessory (in essence, an ion exchange system) which will allow us to recycle this reagent.

Another very welcome addition is the Dionex AS9 separator column which will allow us to easily separate nitrate from chlorate as illustrated in Figure 6.

## GC/MS

GC/MS is used to confirm the identity of any nitro-organics detected by the GC/TEA screen. GC/MS analyses are conducted on a Finnigan Model 4510 Quadrupole Mass Spectrometer equipped with a Varian Programmable on-column injector.

Similar column and chromatograghic conditions described in the GC/TEA section were also applied here. The GC-MS interface temperature was dropped to 180°C for these analyses.

Positive Ion chemical ionization was adopted for this work using methane as the reagent gas. No problems were encountered identifying EGMN, EGDN, NG, RDX, TNT, or the DNT's at the 500 pg level. PETN is presenting problems at this concentration. As previously reported by Zitrin, the detection limit for PETN is

higher and it may be necessary to attempt to recover PETN via a preparative clean-up and introduce the sample to the MS via the direct probe inlet.[9]

## THE MICROSCOPE

The role of the microscope cannot be minimized. In post-blast situations (once the headspace analyses have been done) it is absolutely essential to conduct microscopic examinations for traces of explosive constituents and components of a device. Small particle identification (usually by DC/FTIR) before an aqueous extraction allows for the positive identification of the explosive constituents and/or residues. Once extracted with water, then evaporated to dryness, the complexity of the mixture and the production of mixed salts will greatly increase the complexity of the interpretation of any analytical data generated.

## SEM/EDX

Small particle analysis takes on an added dimension with SEM/EDX, which has proven useful for the identification of minute fragments of detonators (characterized as aluminum with traces of lead deposited on the surface) and for the detection of barium sulfate.[14] SEM is also useful for characterizing explosively-generated phenomena on metal surfaces. [15,16,17]

## EXTRACTION OF EXHIBITS

The analytical scheme developed by Beveridge 'et al' in the 70's has worked well with the traditional methods of analysis, however, with the advent of the more sensitive instrumental techniques, as well as with the use of a greater variety of sensitizers by the commercial explosives industry, it was necessary to revise our analytical extraction methodology. In the initial methodology, diethyl ether was the first solvent used. This is not suitable as

For anions
Sample volume : 50 ul
Conductivity : 30 uS
Guard column : HPIC-AG5
Separator column: HPIC-AS5
Eluant : 20 mM NaOH
Eluant flow rate: 1.5 mL/min.
Suppressor : anion micromembrane
Regenerant : 25 mM $H_2SO_4$
Regenerant flow : 5.0 mL/min.

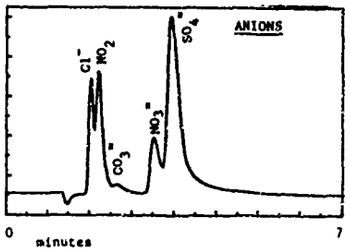


For monovalent cations
Sample volume : 50 ul
Conductivity : 30 uS
Guard column : HPIC-CG3
Separator column : HPIC-CS3
Eluant : 25 mM HCl/0.25 mM DAP·HCl
Eluant flow rate : 1.0 mL/min.
Suppressor : cation micromembrane
Regenerant : 20 mM TBAOH
Regenerant flow rate: 5.0 mL/min.

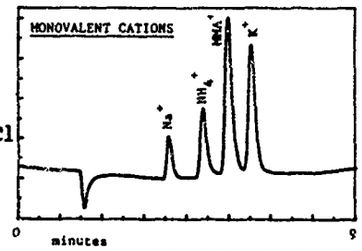


For divalent cations:
Sample volume : 50 ul
Conductivity : 30 uS
Guard column : HPIC-CG3
Separator column : HPIC-CS3
Eluant : 48 mM HCl/16 mM DAP·HCl
Eluant flow rate : 1.0 mL/min.
Suppressor : cation micromembrane
Regenerant : 100 mM TBAOH
Regenerant flow rate: 10.0 mL/min.

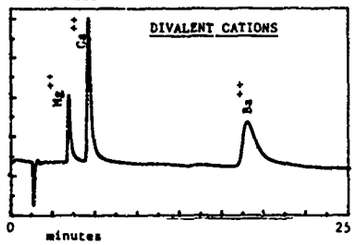


Figure 5 - Ion chromatograms illustrating elution of some ions of interest and the operating conditions used to generate them.

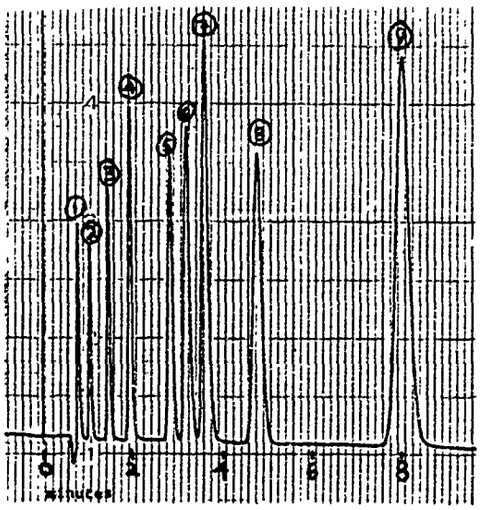

Eluent: 2mM $Na_2CO_3$/
C.75 mM $NaHCO_3$

Flowrate: 2 ml/min.

1) Fluoride
2) Chlorite
3) Chloride
4) Nitrite
5) Bromide
6) Chlorate
7) Nitrate
8) Phosphate
9) Sulphate

Figure 6 - Test chromatogram illustrating anion separation using the Dionex AS9 separator column.

a first step when using the GC/TEA due to the number of interferences that are co-extracted. Two techniques that will play prominent roles are the adsorption/elution headspace (A/E HS) or purge-and-trap technique and an extraction clean-up technique utilizing Porapak-T.[18,19]

## COLLECTION and PRESERVATION of EXHIBIT MATERIALS

Despite all of the advances in laboratory technology, if poorly selected and poorly preserved exhibits are submitted to the laboratory then the chances of detecting explosives or their residues will also be poor.

In order to ensure that appropriate materials are collected, the following steps are being taken:

A. Distribution of air samplers:

An air sampler system has been evaluated for use at the scene of an explosion that meets the following criteria:

1. the pump should be easy to use;
2. the adsorbent must be efficient and have a long shelf life;
3. the sampling flow-rate should be as large as possible, without exceeding the break-through volume of the adsorbent;
4. it should be relatively inexpensive.

A pump was designed to meet our specifications (Gilian Instrument Corporation, Wayne, New Jersey). This pump has a flow-rate of 2 litres/minute when attached to the sampling tube. It is operated by a simple on-off switch. To ensure that it can be ready at a moment's notice, it uses replaceable alkaline "C" cells rather than rechargeable batteries. The cost of this pump is approximately U.S.$150.

The sampling tubes are custom Orbo-tubes manufactured by Supelco containing two plugs of 60/80 mesh Tenax (100 mg and 50 mg)

separated by silanized glass wool. Because these tubes are sealed at the factory, shelf-life problems and contamination problems are minimized.

Tests conducted at this laboratory indicate that ethylene glycol mononitrate (EGMN), EGDN, and NG can be effectively trapped on Tenax at this flow-rate. Figure 7 illustrates the detection of EGDN and NG one day after the detonation of 5.5 kilograms of dynamite in a car. (EGMN is considerably more labile, and indications are that even under ideal circumstances it is difficult to recover by this method more than several hours after an incident.)

These air sampling units are being distributed to strategically selected sites across Canada to ensure that an air sample can be collected as soon as possible after an explosion has occurred. Using this relatively simple in-situ sampling apparatus, the laboratory will be able to very quickly determine if a nitroglcerin-based explosive (EGDN/NG) or an EGMN-based slurry explosive had been used.

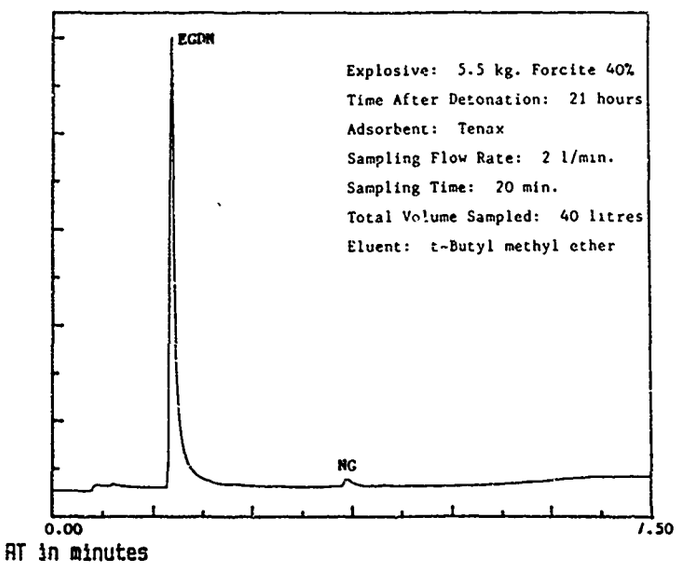


Figure 7 - GC/TEA analysis of air sampled in situ from the remains of a car, 21 hours after the explosion.

B. Post-Blast Scene Technician's Course

The Canadian Police College is starting a comprehensive, two-week course dealing with the processing of physical evidence at the scene of an explosion. Considerable time will be devoted to the proper collection and preservation of exhibits for laboratory analysis. One of the key points to be addressed is that an explosion scene is a crime scene that has to be methodically processed to obtain all of the physical evidence that may eventually link a suspect to the crime scene. There is a tendency for explosives' technologists at the scene to concentrate on the identification of the device and the explosive used. This often results in overlooking other physical evidence that could be crucial to identifying a suspect or to eventually linking a suspect to the explosion scene.

C. National Post Blast Response Team

A national response team has been assembled to assist any police force in Canada in processing the scene of a explosion. This team presently consists of the following core personnel:

Team Leader - works in conjunction with the local senior investigating officer in charge of the scene;

Post - Blast Consultant - an explosives technology expert to assist in determining the nature of an I.E.D., charge-size estimation, etc.;

Forensic Chemist - to assist in the collection and preservation of evidence for laboratory examination;

Police Service Dog - to help process the periphery of the scene (as required); and,

Identification Officer - to assist in documenting and recording the explosion scene.

These personnel would augment the locally-assembled unit

responding to an explosion. In addition to the traditional roles associated with an explosive response team several techniques are being considered:

1. the use of photogrammetry for documenting the scene;
2. the use of synthetic aperture radar to detect post-blast debris, particularly in remote, snow-covered areas;
3. the use of lap-top computers to document exhibit materials at the scene.

This Response Team would be immediately activated, in conjunction with the Canadian Aviation Safety Board, in incidents of in-flight, aircraft break-ups. In such incidents, the team members would examine the debris collected by the search teams for evidence of an in-flight explosion, the characteristics of which have been documented elsewhere.[15,16] It is worthwhile pointing out that a technique has been developed in Canada's National Research Council that would quickly allow one to determine if an in-flight explosion has occurred from an analysis of the cockpit voice recorder.[20] In the simplest terms, if an explosion occurs in an aircraft, the cockpit area microphone (CAM) mounted to the structure of the aircraft receives low frequency vibrational waves transmitted through the frame of the aircraft. The shape, spacing and frequency of these vibrations can determine if an explosive over-pressure has occurred, how far from the CAM the explosion was, and an estimation of the charge-size. This technique has been validated in a number of incidents.

## Explosives Transport Container

The analysis of live explosives often requires transporting them up to 2500 kilometers to a forensic laboratory. In order to do so safely, it was necessary to obtain a container that would be acceptable for transporting explosives by any convenient mode.

Such a container (weight = 39 kg; cost = U.S.$1100.) was

designed for us by the Canadian Explosives Research Laboratory (Energy, Mines and Resources, Ottawa). The container is essentially a safe containing a calcium silicate liner designed to hold seven teflon vials, each having a 10 gram capacity (Figure 7).

This container was tested for communication by detonating an explosive in the centrally-located vial. The surrounding vials contained various dynamites, PETN, RDX, etc. The detonation of the one 10 gram vial was contained within the safe. The explosion of the central vial did not communicate to any of the surrounding vials, regardless of the sensitivity of the explosives.

Loaded safes were also exposed to kerosene-fuelled fires for extended periods of time. The teflon vials were filled with 10 gram quantities of various explosives. No detonations occurred.

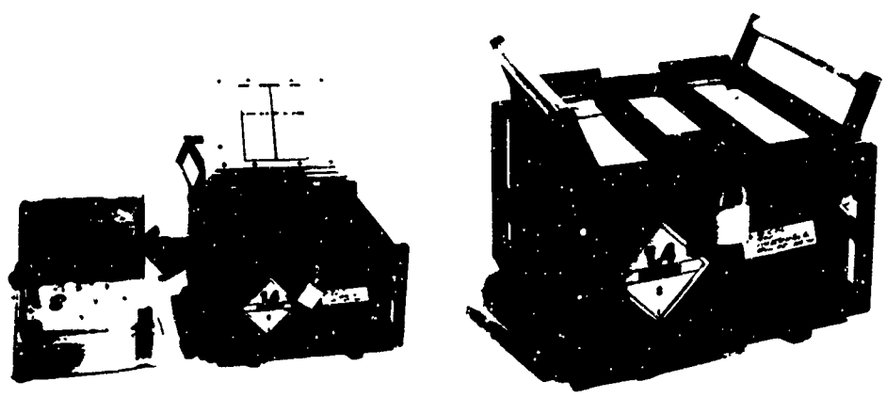

Figure 8 - Explosives Transport Container can be used to transport up to 70 grams of explosives by land, sea, or air. Samples are placed in seven PTFE vials each having a 10 gram capacity.

After the tests were completed, and the container was found to meet a number of standards, including I.C.A.O. standards, the safe was approved for use in Canada by ground, sea, and air transportation for up to 70 grams of explosives.

## SUMMARY

Developmental work in the area of explosive residue analysis is continuing. Recent emphasis has been on developing more sensitive methods of analysis. Such techniques are now in place and attention must be directed to the characterization and data-basing of commercial, military and improvised explosives and their residues utilizing the analytical data from these techniques. Attention must also be paid to ensure that investigators in the field are trained in the proper selection and preservation of physical evidence from explosion scenes.

## ACKNOWLEDGEMENTS

The authors would like to thank the following individuals who have provided continual support to our efforts : J. Garstang (Canadian Aviation Saftety Board) and R. Vandebeek (Canadian Explosives Research Laboratory). Thanks also to D. MacDougall for generating the IR spectra included in this paper and to F. Slingerland for the information on his structural acoustics research.

## References:

1.) A.D. Beveridge, S.F. Payton, R.J. Audette, A.J. Lambertus, R.C. Shaddick. Systematic analysis of explosive residues. J. For. Sci., 20, (1975), 431-454.

2.) D.H. Fine, W.C. Yu, E.U. Goff, E.C. Bender, D.J. Reutter. Picogram analyses of explosive residues using the thermal energy analyzer (TEA), J. For. Sci., 29 (July 1984), 732-746.

3.) J.M.F. Douse. Trace analysis of explosives at the low picogram level using silica capillary column gas chromatography with thermal energy analyzer detection. J. Chromatography, 256, (1983), 359-362.

4.) D.H. Fine., W.C. Yu, E.U. Goff. Applications of the nitro/nitroso specific detector to explosive residue analysis, Proc. of the International Symposium on the Analysis and Detection of Explosives. Quantico, Virginia, (1983), 169-179

5.) B.J. Perrigo, H.W. Peel, D.J. Ballantyne. Use of dual-column fused-silica capillary gas chromatography in combination with detector response factors for analytical toxicology. J. Chromatography, 341, (1985), 81-88.

6.) S. Zitrin, S. Kraus, B. Glattstein. Identification of two rare explosives, Proc. of the International Symposium on the Analysis and Detection of Explosives. Quantico, Va., (1983), 137-141.

7.) F.T. Tweed, R. Cameron, J.S. Deak, P.G. Rodgers. The forensic microanalysis of paints, plastics and other materials by an infrared diamond cell technique, For. Science, 4, (1974), 211-218.

8.) J.M.F. Douse. Trace analysis of explosives by capillary supercritical fluid chromatography with thermal energy analysis detection. J. Chromatography, 445, (1988), 244-250.

9.) S.Zitrin. Post explosion analysis of explosives by mass spectrometric methods J. Energetic Materials, 4, (1986), 199-214.

10.) P.D. Storey. The analysis of propellants, pyrotechnics and blasting explosives. Int. Jahrestag.-Fraunhofer-Inst. Treib-Explosivst, 17, (1986), 51-1 - 51-14.

11.) D.J. Reutter, R.C. Buechele. Ion chromatography of explosives and explosive residues. Proc. of the International Symposium on the Analysis and Detection of Explosives, Quantico, Va., (1983), 199-207.

12.) D. Barsotti, R. Hoffman, R. Wenger. The use of ion chromatography in the analysis of water gel explosives. Proc. Int. Symp. Anal. and Det. of Explosives, (1983), 209-211.

13.) T. Rudolph. The characterization of some low explosive residues by Ion chromatography. Proc. Int. Symp. Anal. and Det. of Explosives, (1983), 213-219.

14.) A.D. Beveridge. Personal communication.

15.) H.P. Tardiff, T.S. Sterling. Detection of explosive sabotage in aircraft crashes, Canadian Aeronautics and Space J., 15(1), (1969), 19-27.

16.) D.G. Higgs, E. Newton. A review of explosives sabotage and its investigation in civil aircraft J. Forens. Sci. Soc., 18, (1978), 137-160.

17.) M. Ueyama, I. Ishiyama. The characterization of fragments from electric blasting cap after detonation by scanning electron microscopy. For. Sci. Intl., 35,(1987), 219-230.

18.) J.B.F. Lloyd. Microcolumn clean-up and recovery techniques for organic explosives compounds and for propellants traces in firearms discharge residues. J. Chromatography, 330, (1985), 121-129.

19.) J.B.F. Lloyd. Adsorption characterstics of organic explosives compounds on adsorbents typically used in clean-up and related trace analysis techniques. J. Chromatography, 328, (1985), 145-154.

20.) F.W. Slingerland. Aircraft damage analysis by vibration spectrograms. J. Sound and Vibration, 110 '1), (1986), 166.

21.) D.W. Schiering. A beam condenser/minature diamond anvil cell accessory for the infrared microspectrometry of paint chips. Applied Spectroscopy, 42 '5), (1988), 903-906.

22.) R.J.Hrynchuk. Microsampling techniques with FTIR spectroscopy in forensic labs: The use of diamond cells. Presented at the Annual Meeting of the Can. Soc. of For. Sci., 18 October 1988, Toronto, Ontario, Canada.

23.) R.J.Hrynchuk. Optimized microtransmittance F.T.I.R. spectroscopy using a diamond anvil cell. Presented at the Annual Meeting of the Can. Soc. of For. Sci., September, 1986, Winnipeg, Manitoba, Canada.

# DETECTION AND ANALYSIS OF INORGANIC ANIONS IN EXPLOSIVES BY REVERSED-PHASE ION-PAIR CHROMATOGRAPHY

D. Woolfson-Bartfeld, Eli Grushka

Dept. of Inorganic and Analytical Chemistry,
The Hebrew University, Jerusalem, ISRAEL

Sara Abramovich-Bar and Yair Bamberger

Division of Criminal Identification,
National Police Headquarters, Jerusalem, ISRAEL

## ABSTRACT

The chromatographic methods that are used today in forensic laboratories to detect inorganic anions related to low explosives are neither quantitative nor sensitive. The majority of inorganic ions do not absorb in the UV range. Therefore, their detection presents difficulties. We report a method that can detect inorganic anions, which are commonly found in combustion residues of low explosives, by reversed-phase ion-pair liquid chromatography, using indirect UV detection. In our system the mobile phase consists of benzyltributylammonium chloride (4mM), phosphate buffer (pH 5) and hexane sulfonate (0.14mM). This system separates easily nitrate ions from chlorate ions, whose separation can present difficulties in conventional ion chromatography. In the method described here there is little sample preparation. No interferences were encountered while testing real samples from explosive residues. Detection limits are low and selectivity is high compared with existing techniques. Analysis time is short and it can be repeated immediately.

## 1. INTRODUCTION

The analysis of low explosive residues is difficult because most of these explosives use inorganic salts as oxidizers. The most popular oxidizers are usually nitrate and chlorate salts with potassium or ammonium as the co-ion (1,2). Since most of these explosives in Israel are improvised (home made), and since there is no way to predict the ingredients and their amounts in the bomb, they present a complex analytical problem. In addition, the analytical chemist has to face difficulties involved in a) handling the traces which are left for analysis after an explosion, and b) interferences that result from debris of buildings or other impurities that are collected together with the sample at the scene of the explosion (2).

In most forensic laboratories today the routine analysis of post explosion samples involves different analytical methods. These methods include extraction with water (for inorganic compounds) or acetone (for organic compounds), spot tests, IR spectroscopy (FT-IR), mass spectroscopy and ion exchange chromatography. Other methods are microscopic analysis and x-ray diffraction (3,4,5). Most of these methods are frequently not specific or sensitive enough for the analysis of inorganic anions. There is a great need today to develop a new analytical method that will be able to detect inorganic anions of explosives and explosive residues.

We report a method that can detect inorganic anions, which are commonly found in combustion residues of low explosives, by reversed-phase ion-pair liquid chromatography, using indirect UV detection. There is a difficulty in detecting inorganic anions by UV-detectors because they are UV transparent. In our method this problem is solved by using a mobile phase containing an ion-pair reagent (IPR) that absorbs in the UV range. The IPR adsorbs onto the stationary phase and turns the column into a dynamically coated anion exchanger. The inorganic anions are detected indirectly as a result of a detector response to a deficiency of IPR in the mobile phase. This deficiency occurs because of the interactions between the

ion-pair and the solutes in the column (6), which acts like an ordinary ion exchange column. The continuous flow of the IPR ensures the stability of the column and of the separation.

Reversed phase columns are commonly used in modern chromatography and are available at a reasonable cost. The instrumentation needed for this method consists of an HPLC, which is very common in many forensic laboratories. Thus, this new method can be used in many laboratories immediately and without any major expenses which are associated with new instrumentation or columns.

## 2. EXPERIMENTAL

Materials. The mobile phase was prepared using deionized water which was filtered through a 0.45-µm Schleicher & Schull membrane filter membrane. Benzyltributylammonium (BTA) chloride and hexane sulfonate were obtained from Sigma Israel (Tel-Aviv, Israel). All chemicals were of analytical reagent grade.

The column (50mm * 4.5mm I.D.) and the guard column (25mm by 4.5mm I.D.) were LiChrospher RP-18 cartridges (Merck, Darmstadt, F.R.G.). For the alternative system of thiocyanate and perchlorate we used a 50mm by 4.5mm I.D. column and a guard column (25mm by 4.5mm I.D.), both LiChrospher RP-8 cartridges (Merck, Darmstadt, F.R.G.).

The mobile phase consisted of 4mM benzyltributylammonium chloride (BTA), 0.14mM hexane sulfonate and 7mM phosphate buffer (pH 5). The alternative system for thiocyanate and perchlorate had a mobile phase that consisted of 4mM benzyltributylammonium chloride, 7mM buffer phosphate (pH 5) and 0.2M sodium chloride.

Instrumentation The chromatographic system consisted of a SP 8000 Spectra Physics HPLC with a Rheodyne injector (10-µl loop). The detector was Perkin-Elmer 85B UV-VIS variable wavelength detector. The recorder and integrator were part of the HPLC system. The column was thermostated at 35° C±0.1°C.

The spectrum of BTA was obtained with a Perkin-Elmer Lambda

5 UV-VIS spectrophotometer.

Sample preparation Samples containing post-explosive residues were extracted with water and then filtered and concentrated over a water bath. The solids which remained in the flask were weighed (between 15-30 mg) and diluted to 5-10 ml. Samples were filtered and injected immediately.

## 3. RESULTS AND DISCUSSION

In this study we have examined the behavior of nitrite, nitrate, chlorate, and sulfate (as sodium salts) ions, and thiocyanate and perchlorate (as potassium salts) ions as the inorganic anions. The chromatographic method was adapted from the literature (6) and was modified according to the needs for an analysis in a routine forensic laboratory.

The UV spectrum of BTA is shown in Figure 1. BTA has three absorption maxima: at 269, 262 and 257nm. We chose 262nm as the working wavelength of detection since at this wavelength BTA absorbs the most and it should provide the most sensitive detection. Another wavelength of 222nm was investigated to detect nitrite and nitrate. The high native absorbance of these anions at this wavelength ensures high sensitivities.

To maintain short analysis times, we used a 5 cm column. This short column did not affect the selectivity but shortened the retention times of most anions and gave sharper peaks. Phosphate buffer was used in order to further ensure sharp chromatographic peaks. The buffer was kept at pH 5 due to the better buffering capacity at that pH. To better control the analysis time and the selectivity of the column, hexane sulfonate was added to the mobile phase. Figure 2 shows a typical chromatogram of this system with a standard mixture of anions.

The last two peaks in the chromatogram belong, respectively, to thiocyanate and to perchlorate. Since their retention times were rather long, we decided to break down the analysis to two parts. We shall deal first with the separation of nitrite, nitrate, chlorate and sulfate and then we will discuss the separation of thiocyanate and perchlorate.

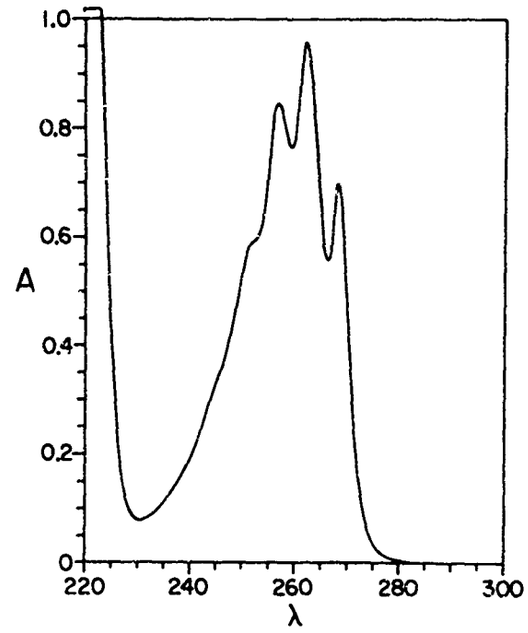


FIGURE 1 The UV spectrum of BTA. The solvent is water

The linearity and the detection limit of the present chromatographic system was examined by preparing calibration curves for all anions at both wavelengths. The response was linear for all anions. However, there was a difference in detection limits between the two wavelengths. Table I gives the regression parameters obtained from correlating the peak areas to the concentrations of nitrite, nitrate, chlorate and sulfate. Also given in the table are the detection limits of these four solutes in both wavelengths.

It has been reported(6,7) that the retention times of the solutes can be a function of their injected concentration. In general, as the concentration of the solute increased, the retention time decreased. This effect was observed in our system for the sulfate anion and it caused a problem in identifying and quantifying sulfate ions in samples where its

concentration was not known (as is the case in explosive residues). To overcome this problem, we have used the sulfate

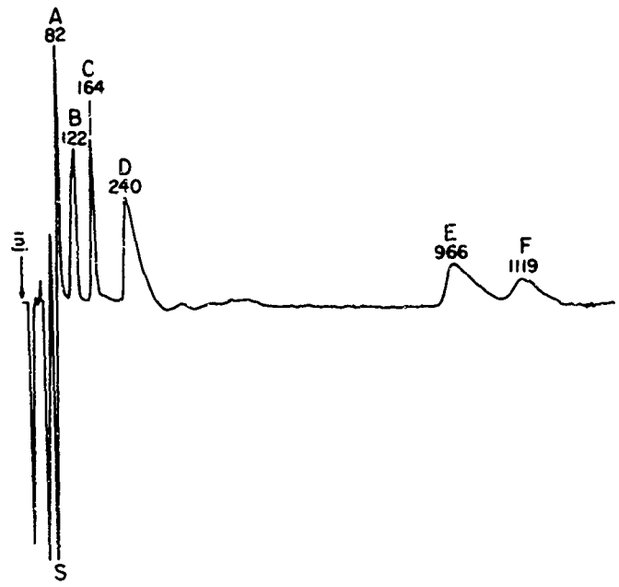


FIGURE 2 A chromatogram showing the separation of all six anions studied. The chromatographic conditions are given in the heading of Table I. Peaks identification: S=system peak, A=nitrite, B=Nitrate, C=chlorate, D=sulfate, E=thiocyanate, F=perchlorate.

calibration curve and another curve which is obtained by plotting the retention time of sulfate as a function of the injected concentration. The two curves are used as follows: The concentration of a suspected sulfate peak is ascertained by extrapolation from the retention time. This concentration is correlated to the peak area from the calibration curve. The calculated peak area is then compared with the experimental value. Agreement between the two values established the concentration and identification of the sulfate anion. In the

present work it was found that, at 222nm, the line correlating the retention to the concentration is described by the equation:

$$t_R = 267 - 5.24*C$$

and at 262 nm:

$$t_R = 269 - 4.84*C$$

In these two expressions, $t_R$ is given in seconds and the concentration in mM. The correlation coefficients are o.995 and 0.979, respectively.

TABLE I: REGRESSION PARAMETERS OF PEAK AREAS vs CONCENTRATION (mM)
Mobile phase contained 4mM benzyltributylammonium chloride, 7mM phosphate buffer (pH 5), and 0.14mM hexane sulfonate in water. Flow-rate was 2ml/min. Wavelength of detection was 222nm and 262nm. Temperature was 35±0.1°C. All anion were determined in the present of the other three.

| Anion | a | b | R | n | DL |
|---|---|---|---|---|---|
| Wavelength: 222nm | | | | | |
| Nitrite | 17.2 | -3.87 | 0.9997 | 10 | 2.8 |
| Nitrate | 12.4 | -4.07 | 0.9985 | 10 | 0.8 |
| Chlorate | 0.85 | -3.48 | 0.9906 | 6 | 21.3 |
| Sulfate | 1.15 | -4.80 | 0.9930 | 5 | 28.4 |
| Wavelength: 262nm | | | | | |
| Nitrite | 1.03 | -1.11 | 0.9996 | 5 | 48.3 |
| Nitrate | 1.16 | -2.01 | 0.9974 | 7 | 8.5 |
| Chlorate | 1.05 | -2.59 | 0.9976 | 7 | 10.7 |
| Sulfate | 1.59 | -3.23 | 0.9973 | 7 | 14.2 |

a = slope (divided by 10E+04).
b = intercept (divided by 10E+03).
R = Correlation coefficients.
n = number of different concentrations used to calibrate.
DL = detection limits in ppm.

To examine the utility of this system for identification and quantitation of post-explosive residues, we analyzed several explosive residues from actual cases. Figure 3 shows the chromatogram obtained from the the remains of an explosive charge which was discovered next to a bus stop in Jerusalem (file no. 3865/87). It was detonated and the remains from the explosion were sent for an analysis. Spot test identified

potassium chlorate and sulfur. The chromatogram confirmed the presence of these anions and the presence of nitrate as well.

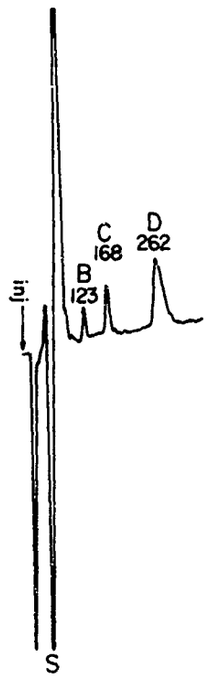


FIGURE 3 Chromatogram of water extract from Sample 1. The chromatographic conditions are given in Table I. Peaks identification: S=system peak, B=nitrate, C=chlorate, D=sulfate

Figure 4 shows a chromatogram of a sample which was obtained from the remains of a bomb discovered in Jerusalem (file no. 4498/87). The bomb was detonated by the police and the sample was extracted from parts of a pipe which made up the bomb. Conventional analysis found only traces of $KClO_3$. The chromatogram shows clearly the presence of chlorate ion as well as nitrate and sulfate ions.

Figure 5 shows a chromatogram of a sample obtained from the center of explosion of a bomb which exploded under a tanker truck not far from Rehovoth (file no. 3351/87). Spot test analysis indicated the presence of minute amounts of $KNO_2$ and

sulfur. The chromatographic analysis confirmed the presence of

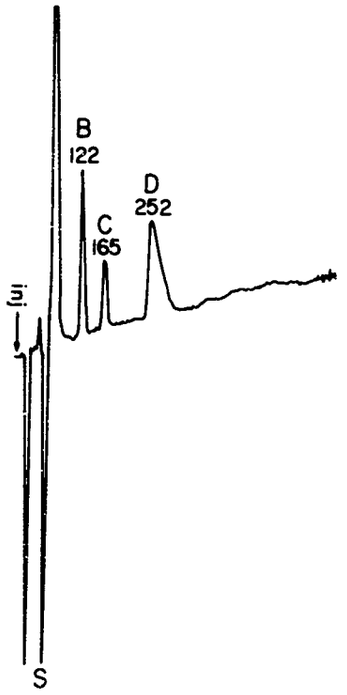


FIGURE 4 Chromatogram of water extract from Sample 2. Same conditions as in Figure 3. Peaks identification: S=system peak, B=nitrate, C=chlorate, D=sulfate

these two ions but also showed the existence of nitrate ion. Spot test and IR techniques can not differentiate between nitrate and nitrite. No such difficulty exists in the method described here. The presence of sulfate, nitrate and nitrite may be indicative of black gunpowder.

Figure 6 shows a chromatogram of a sample collected at the site of an explosion which occurred when a military vehicle passed by on the Ashkelon - Gaza road (file no. 6809/86). Spot test analysis found traces of potassium nitrite and sulfur. The chromatogram shows nitrite, nitrate and sulfate ions. In Figure 5 and 6 chlorate ion is missing. However, in both Figures there is an unidentified peak which elutes at 395 sec.

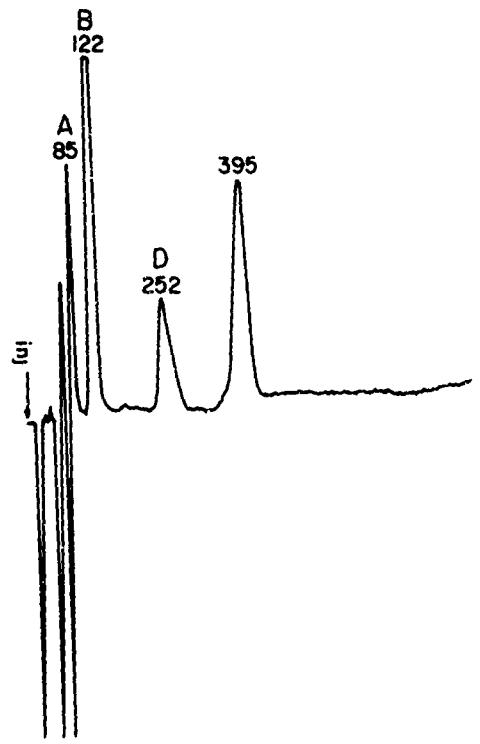


FIGURE 5 Chromatogram of water extract from Sample 3. Same conditions as in Figure 3. Peaks identification: S=system peak, A=nitrite, B=nitrate, D=sulfate

A comparison between Figures 3 and 4 and Figures 5 and 6 shows that different explosives where used in the two groups of explosions. In all chromatograms there is a clear picture of the various anions, and identification is immediate and without interferences. The sulfate anion was identified and quantified according to the method described above.

Table II shows the results of the quantitative analysis of the samples. The analysis was based on the calibration curves that were described in table I.

As mentioned earlier in this paper, the retention times for thiocyanate and perchlorate were much too long when the chromatographic system for nitrite, nitrate, chlorate and sulfate was used. Since thiocyanate and perchlorate are less common in explosive residues (at least in Israel) than the

other four anions, it was decided to develop a separate chromatographic system for those two anions.

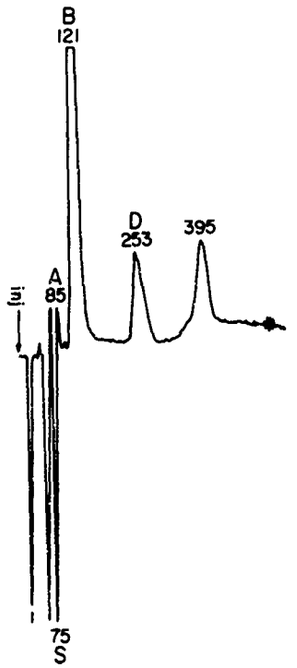


FIGURE 6 Chromatogram of water extract from Sample 4. Same conditions as in Figure 3. Peaks identification: S=system peak, A=nitrite, B=nitrate, D=sulfate

The new chromatographic system uses a RP-8 column. The mobile phase in this system was very similar to the previous one except that it did not contain hexane sulfonate, and its ionic strength was kept at a high level with the addition of 0.2M sodium chloride. This chromatographic system gave much shorter analysis times for both the thiocyanate and the perchlorate ions. In addition, this new system gave linear response for both anions. Figure 7 shows a typical chromatogram of the thiocyanate and the perchlorate ions using this chromatographic system.

TABLE II QUANTITATIVE ANALYSIS OF EXPLOSIVE RESIDUES
See table I for conditions.

| No. of sample | Nitrite | Nitrate | Chlorate | Sulfate |
|---|---|---|---|---|
| Wavelength: 222nm | | | | |
| 1 (fig. 3) | ----- | 0.11% | 1.70% | 5.27% |
| 2 (fig. 4) | ----- | 0.27% | 3.15% | 11.07% |
| 3 (fig. 5) | 0.53% | 6.61% | ----- | 18.85% |
| 4 (fig. 6) | 0.12% | 3.27% | ----- | 23.27% |
| Wavelength: 262nm | | | | |
| 1 (fig. 3) | ----- | ----- | 1.68% | 4.82% |
| 2 (fig. 4) | ----- | 0.69% | 3.73% | 12.22% |
| 3 (fig. 5) | ----- | 22.54% | ----- | 22.13% |
| 4 (fig. 6) | 0.63% | 29.89% | ----- | 20.63% |

Results are in % of the total sample weight.

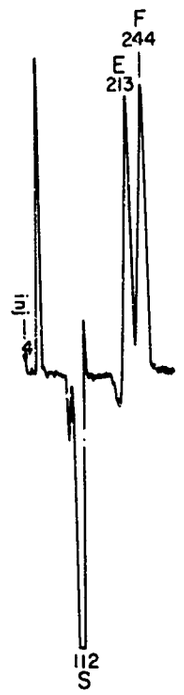


FIGURE 7 Chromatogram showing the separation between thiocyanate (peak E) and perchlorate (peak F). Chromatographic conditions identical to those in Table 1 except: Column=RP-8, no hexane sulfonate and the addition of 0.2M NaCl.

Attempting to test this system with real samples did not prove successful due to an interfering material which eluted at the same time as the thiocyanate and the perchlorate. Since we had only one sample where the presence of thiocyanate has been suspected, it was not clear whether this interference was inherent to the method or was related to the specific sample. At present, we are investigating the nature of the interference and methods for its elimination.

## 4. CONCLUSIONS

The new chromatographic method for the analysis of nitrite, nitrate, chlorate and sulfate ions in explosive residues is fast, selective and sensitive. The system has a linear response for all these anions. It shows selectivity toward nitrate and chlorate, which presents a problem in conventional ion chromatography. There is no need for elaborate sample preparation and the sample can be injected into the chromatograph immediately after water extraction from the bulk sample. Samples from explosive residues yield clean chromatograms with no interferences.

A chromatographic system that will identify and quantify thiocyanate and perchlorate is still under development.

## 5. ACKNOWLEDGMENTS

This research would not have been possible without the help and the support of the Israeli Police Force Forensic Laboratory and its team of analytical chemists.

## REFERENCES

1 J. G. Grasselli, Anal. Chem., 55 (1983) 1468A.

2 D. J. Reutter and R. C. Buechele, Proceedings of the International Symposium on the Analysis and Detection of Explosives, Quatico, Va. (1983) 199.

3 J. Yinon and S. Zitrin, The Analysis of Explosives, Pergamon Series in Analytical Chemistry. vol.3, Pergamon press (1981).

4 T. L. Rudolph, Proceeding of the International Symposium on Analysis and Detection of Explosives, Quatico, Va., (1983) 213.

5 D. D. Garner, M. L. Fultz and E. B. Byall, J. Energ. Mater., 4, (1986) 133.

6 W. E. Barber and P. W. Carr, J. Chromatogr., 260 (1983) 89.

7 B. Sachok, S. N. Deming and B. A. Bidlingmeyer, J. Liquid Chromatogr., 5(3) (1982) 389.

Tim Sheldon

Home Office Science and Technology Group
Woodcock Hill, Sandridge, St. Albans, UK

# A FIELD TRIAL OF EXPLOSIVES DETECTORS FOR PERSONNEL AND BAGGAGE SEARCH

## EXTENDED ABSTRACT

Explosives vapour detection is a well known technique for searching people, baggage, vehicles and buildings for concealed explosive devices. For the first two uses, it is necessary for the detector to have not only a high detection capability and low false alarm rate but a short response time. Since police forces and airport security personnel are frequently required to carry out this type of search, a trial was carried out by SRDB, assisted by the police, other government agencies and commercial organisations, to determine which of the instruments currently available was most suitable for the purpose.

The trial was carried out at the West Midlands Police training centre at Ryton-on-Dunsmore, West Midlands. Approximately 170 students took part in the trial. Six types of explosives detector were used, the Graseby Ionics PD5, AI Security Model 97, Graseby's PD4 (two examples of each of the above), the AI Exfinder 150, AI Model 85 explosives detecting doorway (which was not used for searching bags) and the Jasmin Simtec Exdetex 2, which was only used on bags because of its long response time.

Three types of explosives were used in the trial, namely Nobel's 1813, a nitroglycerin-based mining explosive, trinitrotoluene (TNT) and PE4, an RDX-based plastic explosive. Around 40 samples of each were packed into padded envelopes as were a similar number of inert samples. The trial was 'double blind'- sniffer operators and volunteers carrying the packages were not to know what was in them. This system is meant to avoid bias in the results which could occur if operators made a special effort to detect those packages which were known to be 'live". Precautions were taken to prevent the different explosives from cross-contaminating.

In the baggage trial, student's bags were labeled and laid out in a large hall. Some of them were then removed and replaced with bags in which explosives samples had been hidden. The bags were then searched with each type of detector and the response recorded.

For the personnel searching trial, students were given packages on a pseudo-random basis and were told to secrete them on their persons. After a waiting period, the students were subjected to search with each of the instruments on test. The instrument response was recorded as was the position on the body where any alarm occurred.

The results of the trial indicate that the Graseby PD5 gives the best combination of sensitivity, false alarm rate and speed. The AI 97 detected a wider range of explosives but had a very high false alarm rate. The Graseby PD4 had a very poor performance and the AI Exfinder 150 developed a fault during the baggage trial which prevented its further use. The AI 85 doorway showed some detection capability but its performance was generally poor and its false alarm rate high. The Jasmin Simtec Exdetex 2, (which is really designed for building search) proved to have a very high sensitivity and a very low false alarm rate but its response time is too long for rapid screening of large numbers of bags.

The overall conclusion was that none of the instruments tested fully meet the requirements of the police and airport security personnel, though the PD5 has some uses provided that its limitations are borne in mind. The format of the trial was satisfactory and any future trials carried out by SRDB are likely to be organised on similar lines.

# Nuclear Activation Analysis and Scanning Electron Microscopy in Forensic Gunshot Residues Determinations: a Critical Evaluation.

A. Brandone *, F. De Ferrari^, P. Pelizza^, M. Signori*, G. Terzaghi§

* Dipartimento di Chimica Generale dell'Universita' di Pavia, Viale Taramelli, 12. I 27100 Pavia. Italia.

^ Istituto di Medicina Legale dell'Universita' di Brescia. c/o Ospedali Civili, Piazza Ospedali. I 25100, Brescia - Italia-

§ Dipartimento di Chimica Fisica ed Elettrochimica dell'Universita' di Milano, Via Venezian. I 20100 Milano - Italia.

## S U M M A R Y

Experiments were carried out with Nuclear Activation Analysis (NAA) and with Scanning Electron Microscopy (SEM) equipped with Energy Dispersive X Ray Microprobe (EDX) in order to compare the features of the most employed techniques for evaluation of gunshot residues (GSR).

Two different techniques for sampling gunshot residues, were also tested:

i) Liquid paraffin dropped onto the skin of persons who fired a gun was employed for sample collection for quantitative Antimony determination by means of NAA as GSR indicator.

ii) Adhesive pads were tested for gunshot residues sampling from the skin: these samples were submitted for SEM individuation for GSR particles then for EDX microprobe for Antimony, Barium, Lead and Copper qualitative analysis.

Shots were fired with an automatic pistol and two revolvers and samples were collected from normal deposit sites of GSR from the shooters' hand.

Quantitative data for Antimony as revealed by means of NAA are reported together with the results of SEM - EDX.

A critical evaluation of the two techniques is reported.

## Introduction

At the present the most reliable and most widely applied techniques of gunshot residues (GSR) evaluation, are disigned to show their inorganic components.

Many techniques have been proposed and of these Nuclear Activation Analysis (NAA) (1, 2, 3, 4, 5, 6) and Scanning Electron Microscopy (SEM) (7, 8, 9, 10, 11) equipped with Energy Dispersive X-Ray Microprobe (EDX) are widely employed.

It is possible to carry out the instrumental quantitative determination of Sb and Ba, both GSR indicators, by means of NAA in many matrices such as paraffin, adhesive materials, cotton swabs etc., which are employed for sampling GSR from suspect hands.

Samples are generally taken from forefinger, thumb and from the back of the hand between these fingers since these are the usual sites where GSR deposits.

The SEM apparatus allows the observation of materials taken from suspect hands at different magnification in order to reveal GSR. Sampling is generally carried out by means of an adhesive pad which is pressed against the skin of the hands. The GSR particles are identified by their characteristic spherical shape.

The EDX test for the presence of Sb, Ba, Pb, and sometimes Cu deriving from the bullet jacket, confirm the existence of GSR on the sample. However both NAA and SEM-EDX have been subjected to many criticisms that may be summarized as:

1) NAA is unable to differentiate Sb and Ba deriving from GSR from Sb and Ba originating from professional activities, environmental contamination, industrial pollution, etc.

ii) SEM-EDX gives no quantitative informations, is time consuming, does not identify the part of the hand where GSR is revealed and, last but not least, it has been doubted wether the form of the particles is unique to GSR particles even when Sb, Ba, Pb are also found.

Experiments were carried out shooting with different firearms and collecting GSR from shooting hand with two different techniques, in order to compare the features of NAA and SEM-EDX for GSR evaluation. Arms handling experiments were also tested.

## EXPERIMENTAL

### Ammunition and fire arms.

The following ammunition was employed for experimental shots:

i) G. Fiocchi (Lecco, Italy) centre fire cartridges for 7.65 mm caliber automatic pistol (jacketed bullet).

ii) G. Fiocchi centre fire cartridges for .38" special caliber revolver (jacketed bullet).

iii) I.C.I. (U.S.A.) centre fire cartridges for .44" magnum caliber revolver (wad cutter).

The following firearms were employed for experimental shots:

i) P. Beretta mod. 70, 7.65 mm caliber automatic pistol.

ii) Smith & Wesson mod. 10, .38" special caliber revolver.

iii) Smith & Wesson mod. 29, .44" magnum caliber revolver.

### Sampling of GSR for testing

Two different techniques for sampling GSR were tried:

i) liquid paraffin dropped onto the skin of the shooter's hands in the usual GSR deposit sites: the back space of the hand between the forefinger and thumb for the automatic pistol and forefinger and thumb, separately sampled, for the revolvers.

ii) Adhesive pads apllied with a metallic holder: the sampling sites are the forefinger, thumb and the back of the hand between these fingers sampled with a single adhesive holder.

## Analytical methods

### Neutron Activation Analysis

The paraffin samples collected from firing hands, together with a Sb standard were irradiated at a neutron flux of c. $1x10^{12}$ n $cm^{-2}$ $sec^{-1}$ for 30 minutes in the TRIGA MARK II (250 KW) reactor at the University of Pavia.
After irradiation the samples were submitted to gamma spectroscopy using a 20 $cm^3$ Ge/Li detector connected to a 4096 channels pulse-height analyzer LABEN 701 coupled to a computer for data processing.
For Sb determinations the 0.564 Mev gamma ray of $^{122}Sb$ was compared to the standard after a cooling period of 24 hours.
The detection limits for Sb with the procedure adopted is /ug 0,005.

### Scanning Electron Microscopy and Energy Dispersive X ray Analysis

Sample adhesive pads were submitted to the SEM-EDX of the Department of Electrochemistry of the University of Milan.
The samples were first metallized using Au for SEM and their surfaces were then observed, region by region, using a Cambridge Stereoscan 150 electron microscope. Each single observation covered an area of about 50 x 50 /um.

EDX analysis is carried out at a pressure of about $10^{-7}$ Torr.; K, L, M characteristic lines of the excited elements are registered by means of a Si/Li crystal connected to a pulse-height analizer with a Link System 860 microprobe.

## RESULTS

The results of Sb quantitative determination and GSR particles identification are reported in tables 1, 2 and 3.

The quantitative results of NAA Sb determination show that this element was always found then confirming its role as a GSR indicator as indicated in our previous previous work (3, 6).

As may be seen from our experimental results SEM-EDX, by combining information about the morphology of GSR particle with its elemental composition, allows us to distinguish GSR from contaminating particles.

GSR particles are generally composed of Pb, Ba and Sb and show a spherical morphology, moreover they can be found on the surface of bigger and shapeless particles, or separately.

Their brightness, as observed with SEM, is a marker of these particles together with the characteristic shape; typical GSR particle is shown in fig. n^ 1.

The process used for SEM-EDX analysis consisted in searching for the presence of particles that, for shape and brightness, could be GSR. These particles were then analysed by means of EDX microprobe to know their elemental composition.

The simultaneous presence of Sb, Pb and Ba is a necessary, but not sufficient, condition for the identification of GSR because these elements are too diffused in environment to testify for GSR presence on their own.
It is worth underlining that the presence of Pb alone does not identify a particle as GSR.
The presence of Cu, Zn, Si, Ca on correctly shaped particles does not however assure positivity of the test, because these elements may also be due to environmental contamination and professional activities.
Furthermore, after the observation to SEM of c. 100 regions in which no particles have been revealed, the test can be considered negative.
Both analytical methodologies and their respective sampling techniques have shown their suitability for showing the presence of GSR by means the indicators choosen.
Nevertheless, SEM-EDX was unable to reveal GSR on samples taken from arms handling whereas all the samples analysed by NAA showed the presence of Sb.
Our work thus emphasis the advantages given by NAA that allows both quantitative determinations and the discrimination of the sites where Sb is present. In fact the site of finding and the respective quantitative data are very important to distinguish Sb, Ba, Pb of GSR origin from the presence of the same element due to environmental and casual contamination, or professional activities.

Moreover the sampling technique using liquid parafrin is very effective in picking up GSR and in our opinion it is better than adhesive pads.
This consideration seems to be confirmed by the finding that arms handling was not shown in adhesive pads analysed by SEM- EDX.
The scanning electron microscope has the advantage that it consents the observation of GSR particles which are recognized by their characteristic

shape. Furthermore EDX microprobe allows only a qualitative and not quantitative analysis.

Moreover, it is usual in criminal cases to make only one sample per hand, so it is impossible to identify the of GSR deposit site. This information is very important because in many cases it is possible to specify the type of firearms used.

A further problem is that SEM-EDX is time consuming and requires the costant presence of an experienced operator and this is probably the reason the Italian Police take only one sample per hand.

Summing up considering both the advantages and drawbacks of the two techniques experimented and on the basis of our work, it is our opinion that NAA is more reliable than SEM-EDX in GSR identification on suspect hands.

**REFERENCES**

1) V.P. Guinn "Non biological application of neutron activation analysis in forensic studies." Methods of Forensic Science, Interscience Publ. London III, 46 - 47, 1964.

2) R.K. Ruch, J.D. Buchanan, V.P. Guinn, S. Bellanco, R. Pinker "Detection of Gunpowdere Residuews by Neutron Activation Analysis." Am. Nucl. Soc. Transaction 5, 282, 1962.

3) G. Borra a. Brandone, G. De Bernardi, A. Fornari, M.A. Rollier "Gunshot Residues on paraffin drops: instrumental neutron activation assay of antimony, barium and copper." J. Radioanal. Chem. 15, 51, 1973.

4) A. Brandone, M. Tavani, "Sulle possibilita' di impiego della AAN nella pratica forense." Arch. Soc. Lomb. Med. Legale e delle Ass. 10, 8. 1974.

5) A. Brandone, T. Cerri. M. Tavani "L'analisi per attivazione neutronica nella pratica forense: determinazione della distanza di sparo." Arch. Soc. Lomb. Med. Legale e delle Ass. 14, 47, 1978.

6) P. Benedetti, A. Brandone, F. De Ferrari, D. Salza "Ulteriori esperienze sulla interpretazione del reperto di residui di polvere da sparo sulla cute delle mani." Rivista Italiana di Medicina Legale 1, 112, 1980.

7) E. Bohen "Application of the SEM in forensic medicine." SEM/1971, IIT Research Institute, Chicago, Il., 553, 1971.

8) H. Hantsche "Zur Anwendung des Raster-Elektronenmikroskops in der Kriminaltechnik". Direktabb. Oberfl. 4 (2),641, 1971.

9) R. Diederichs, M.J. Camp, A.E. Willmovsky, M.A. Hass, R.F. Dragen "Investigations into the adaptability of SEM/EDX to firearms related examinations." A.F.T.E. Journal 63, 1, 1974.

10) G. Judd, J. Sabo, W. Hamilton, S. Ferris, R. Horn "SEM micostriation characterization of bullets and contaminant particle identification". J. Forensic Sci. 19, 798, 1974.

11) J.L. Brown, J.W. Johonson " SEM-EDX microanalysis in forensic science". J. Ass. Offical Anal. Chem. 56, 930, 1973.

12) R.H. Keely, M.C. Robertson "The routine use of SEM and electron probe microanalysis in forensic science". SEM/1975 - IIT Research Institute, Chicago, Il. 479, 608, 1975.

Table n^ 1.- Comparison of NAA determinations of Sb and SEM - EDX Gunshoot Residues results. Firing tests with Beretta 7.65 mm caliber automatic pistol.

| Shoot n^ | /ug Sb | Gunshoot Residues | |
|---|---|---|---|
| 1 | 3.010 | Particles | found |
| 2 | 1.920 | " | " |
| 3 | 0.571 | " | " |
| 4 | 2.211 | " | " |
| 5 | 3.441 | " | " |
| 6 | 4.295 | " | " |
| 7 | 2.663 | " | " |
| 8 | 1.548 | " | " |
| 9 | 3.894 | " | " |
| 10 | 1.443 | " | " |
| 11 | 0.475 | " | " |
| 12 | 0.669 | " | " |
| 13 | 1.607 | " | " |
| 14 | 2.796 | " | " |
| 15 | 2.448 | " | " |
| 16 | 1.563 | " | " |
| 17 | 2.174 | " | " |
| 18 | 6.883 | " | " |
| 19 | 3.779 | " | " |
| 20 | 0.973 | " | " |

Table n^ 2.- Comparison of NAA determinations of Sb and SEM - EDX Gunshoot Residues results. Firing tests with Smith & Wesson caliber .38" special revolver.

| shoot n^ | /ug Sb forefinger | thumb | Gunshoot Residues | |
|---|---|---|---|---|
| 1 | 1.005 | 1.317 | particles | found |
| 2 | 1.439 | 1.615 | " | " |
| 3 | 0.790 | 1.645 | " | " |
| 4 | 1.431 | 1.645 | " | " |
| 5 | 1.322 | 0.585 | " | " |
| 6 | 0.910 | 0.564 | " | " |
| 7 | 1.319 | 0.650 | " | " |
| 8 | 0.563 | 1.208 | " | " |
| 9 | 1.172 | 0.573 | " | " |
| 10 | 1.622 | 1.033 | " | " |
| 11 | 1.780 | 0.765 | " | " |
| 12 | 1.364 | 1.035 | " | " |
| 13 | 1.005 | 0.553 | " | " |
| 14 | 1.695 | 0.657 | " | " |
| 15 | 1.968 | 1.190 | " | " |
| 16 | 1.102 | 0.444 | " | " |
| 17 | 2.033 | 0.745 | " | " |
| 18 | 0.882 | 1.106 | " | " |
| 19 | 0.960 | 1.118 | " | " |
| 20 | 0.683 | 0.427 | " | " |

Table n° 3.- Comparison of NAA determinations of Sb and SEM - EDX Gunshoot Residues results. Firing tests with Smith & Wesson caliber .44" magnum revolver.

| shoot n° | /ug Sb forefinger | thumb | Gunshoot Residues | |
|---|---|---|---|---|
| 1 | 0.227 | 0.031 | particles | found |
| 2 | 0.092 | 0.032 | " | " |
| 3 | 0.055 | 0.107 | " | " |
| 4 | 0.061 | 0.032 | " | " |
| 5 | 0.027 | 0.005 | " | " |
| 6 | 0.035 | 0.041 | " | " |
| 7 | 0.026 | 0.043 | " | " |
| 8 | 0.103 | 0.161 | " | " |
| 9 | 0.038 | 0.130 | " | " |
| 10 | 0.177 | 0.005 | " | " |
| 11 | 0.086 | 0.046 | " | " |
| 12 | 0.597 | 0.017 | " | " |
| 13 | 0.20 | 0.052 | " | " |
| 14 | 0.079 | 0.033 | " | " |
| 15 | 0.041 | 0.024 | " | " |
| 16 | 0.076 | 0.084 | " | " |
| 17 | 0.029 | 0.276 | " | " |
| 18 | 0.044 | 0.022 | " | " |
| 19 | 0.540 | 0.050 | " | " |
| 20 | 0.005 | 0.216 | " | " |

Table n° 4.- Comparison of NAA determinations of Sb and SEM- EDX Gunshoot Residues results relatives to arms handling.

| sample n° | /ug Sb forefinger | thumb | back space | G S R | |
|---|---|---|---|---|---|
| 1 | 0.127 | 0. 12 | 0.032 | not | found |
| 2 | 0.092 | 0.032 | 0.412 | " | " |
| 3 | 0.055 | 0.107 | 0.071 | " | " |
| 4 | 0.031 | 0.111 | 0.873 | " | " |
| 5 | 0.125 | 0.115 | 1.543 | " | " |
| 6 | 1.346 | 2.432 | 0.987 | " | " |
| 7 | 0.887 | 1.045 | 1.332 | " | " |
| 8 | 1.103 | 0.861 | 0.065 | " | " |
| 9 | 1.138 | 0.930 | 0.005 | " | " |
| 10 | 1.377 | 1.005 | 0.099 | " | " |

# THE FINGERPRINTING OF GUNPOWDER

A. Brandone*, F. De Ferrari**, P. Felizza**, M. Signori*

* Centro di Radiochimica ed Analisi per Attivazione C.N.R. c/o Dipartimento di Chimica Generale Universita' di Pavia, Viale Taramelli, 12. I- 27100 Pavia - Italia

* Istituto di Medicina Legale della Universita' di Brescia c/o Ospedali Civili. Piazza Ospedali. I- 25100 Brescia - Italia.

Summary

Modern physico - chemical methods allow reliable forensic analysis of gunshot residues (GSR) from the hands of suspected persons.

Inorganic components of primer such as Barium and Antimony and such elements as Lead and Copper contained in the bullets can be accurately revealed by means of many analytical techniques.

In order to improve the reliability of the method we doped some commercial cartridges with Samarium Oxide and tested, after shooting, its presence on the hands of the shooter.

The results show that Sm has never been found on the hands of non shooters, but it has been shown by Nuetron Activation Analysis on the hands which fired the gun, therefore suggesting the use of Samarium Oxide to dope gunpowder to make forensic research more reliable .

Ballistic tests were made using doped and non doped cartridges in order to asses the role of presence of $Sm_2O_3$ in the ammunition,

Introduction.

The problem of identification of gunshot residues (GSR) on the hands of suspect individuals is a question that has not yet been completely resolved in Forensic Sciences.

The presence of GSR is demonstrated, in fact, by finding the compounds deriving from the combustion of the gunpowder of the ammunition. For a long time this determination was effected by the identification of nitrite and/or nitrate ions produced from the combustion either of black powders or of the smokeless ones. Such compounds are removed from the skin of the hands by applying liquid paraffin (the so called paraffin glove) and demonstrated by means of colorimetric reagents (1, 2).

This method, however, is not as reliable as has been proposed: indeed many criticisms have been addressed to the specificity of the GSR indicators attributed to nitrite and nitrate ions, expecially given the large diffusion of chemical products which contain or may produce these ions (3, 4).

More recently, these colorimetric methods have been replaced by the identification of the inorganic components of the ammunition on the hands of the suspect shooters. These components are Antimony (Sb) and Barium (Ba), which are costituents of the cartridge primers, and by Lead (Pb) and Copper (Cu) which originates from the bullet (5, 6, 7, 8, 9).

Many analitycal methods have been proposed for quantitative determination of Sb, Ba, Pb and Cu for example atomic absorption spectroscopy (10, 11, 12), electrochemical techniques (13, 14, 15), X - ray fluorescence (9), neutron activation analysis (16, 17, 18, 19, 20. 21), scanning electron microscopy (22, 23, 24, 25, 26, 27).

In forensic science laboratories many of the above mentioned techniques are routinely used in criminal cases with better and more reliable identification of GSR, compared with the obsolete colorimetric methods for nitrite and nitrate evaluation.

However, as shown in our previous works (18, 21), Ba, Pb and Cu are generally present on the hands of non shooters, so that GSR identification must be effected considering only the Sb as a significant indicator. Nevertheless Sb seems to be not as specific as previously thought, since this element may also originate from professional activity, environmental contamination etc.. Thus in many cases the finding of Sb does not necessarily guarantee the actual presence of GSR on the skin of the hand examined.

Indeed the goal of scientific investigation in the ferensic field is to find reliable evidences that may be presented in Court and which would lead to conviction, not to conjectures or suppositions.

Bearing in mind this need, in this work we undertook to add a specific "fingerprinting" agent to gunpowder . This agent must not be present on the hands of normal individuals, so that its recovery on a suspected person constitues certain evidence of GSR presence.

## Eperimental

### Gunpowder Fingerprinting

Samarium (Sm), a chemical element belonging to the Rare Earths group, was choosen as "fingerprinting" agent. As was shown in preliminary work using the same technique, Sm is absent from the hands of normal

individuals. Moreover Sm is easily found by Neutron Activation Analysis, the analytical method we chose for determining GSR.

The fingerprintig agent Sm was added to the gunpowder of disassembled ammunitions as $Sm_2O_3$, to obtain a concentration of 0.15%. The cartridges were reloaded after accurate stirring to ensure an homogeneous distribution of $Sm_2O_3$ within the gunpowder. Preliminary firing experiments showed that the concentration of 0,15% was best for an efficient fingerprinting of ammunition.

The ammunition used for our experiments is of commercial production and thus with primers containing Sb; this element was therefore considered.

Ammunition and fire arms.

The following ammunition was employed for experimental fingerprinting with $Sm_2O_3$:

i) G. Fiocchi (Lecco, Italy) centre fire cartridges for 7.65 mm caliber automatic pistol (jacketed bullet).

ii) G. Fiocchi centre fire cartridges for .38" special caliber revolver (jacketed bullet).

iii) I.C.I. (U.S.A.) centre fire cartridges for .44" magnum caliber revolver (wad cutter).

The following firearms were employed for experimental shots:

i) P. Beretta mod. 70, 7.65 mm caliber automatic pistol.

ii) Smith & Wesson mod. 10, .38" special caliber revolver.

iii) Smith & Wesson mod. 29, .44" magnum caliber revolver.

Removal of GSR for testing.

The material used for removing GSR is liquid paraffin dropped from a lighted paraffin candle directly onto the skin of the shooting hand. The sampling site is the back of the hand between the forefinger and thumb for automatic pistol shots and the forefinger and the thumb, separately sampled, for firing tests carried out with revolvers. This sampling method removes GSR from the skin efficently and does not interfere in the analytical determinations.

Neutron Activation Analysis.

The paraffin samples collected from firing hands, together with Sb and Sm standards, were irradiated at a neutron flux of c. $1x10^{12}$ n $cm^{-2}$ $sec^{-1}$ for 30 minutes in the TRIGA MARK II (250 KW) reactor at the University of Pavia.

After irradiation the samples were submitted to gamma spectroscopy using a 20 $cm^3$ Ge/Li detector connected to a 4096 channels pulse-height analyzer LABEN 701 coupled to a computer for data processing.

For Sm and Sb determinations, the 0.103 MeV gamma ray of $^{153}Sm$ and 0.564 MeV gamma ray of $^{122}Sb$ were compared to the respective standards, after a cooling period of 24 hours.

The detection limits with the procedure adopted are 0,003 /ug for Sm and /ug 0,005 for Sb.

**Shooting tests**

The shooting tests carried out with the fingerprinted ammunition were as follows:

i) n° 170 shots with P. Beretta mod 70, 7.65 mm caliber automatic pistol.

ii) n° 26 shots with Smith & Wesson mod. 10, .38" special caliber revolver.

iii) n° 20 shots with Smith & Wesson mod. 29, .44" magnum caliber revolver.

All the firing test were effected at the firing range of the Tiro a Segno Nazionale of Pavia.

Evaluation of the speed of bullets have been carried out in order to asses possible change in ballistic properties of fingerprinted ammunition due to the presence of $Sm_2O_3$. A portable chronographer with photoelectric cells manufactured By Paini (Busseto, Italy) was emmployed for this purpose.

The speeds measured for bullets with fingerprinted cartridges were compared to those of bullets with original ammunition from the same production batch, as well as to those of bullets with reloaded, but not fingerprinted, cartridges.

Tests shots for bullet speed evaluations were as follows:

i) n° 50 shots with fingerprinted G. Fiocchi 7.65 mm caliber cartridges

n° 50 shots with original G. Fiocchi 7.65 mm caliber cartridges

n° 50 shots with reloaded G. Fiocchi 7.65 mm caliber cartridges

ii) n° 25 shots with fingerprinted G. Fiocchi .38" special caliber cartridges

n° 17 shots with original G. Fiocchi .38" special caliber cartridges

iii) n° 20 shots with fingerprinted C.C.I. .44" magnum caliber cartridges

n° 17 shots with reloaded C.C.I. .44" magnum caliber cartridges.

**Results and Discussion.**

The results of Sm and Sb determinations for experimental shots are reported in tables n° 1, 2 and 3, together with standard deviations.
The bullets speeds measured for fingerprinted, original and reloaded cartridges are shown in figures 1, 2 and 3.
Sm was found in the range from 0.013 to 1.127 /ug with a mean value of 0.102 /ug and s. d. = 0.152 in the paraffin samples of 161 of the 170 shots effected with 7.65 mm caliber fingerprinted cartridges; Sm was not found in 9 samples.
Sm was not found in GSR collected on forefinger and thumb of the shooting hands in paraffin samples from shots carried out with .38" special and .44" magnum caliber fingerprinted cartridges. The Sm traces sampled from the shots carried out with the revolvers are pratically the same shown for the 7,65 mm caliber pistol. The mean values for .38" spl. and .44" mgm. caliber are /ug 0.885, s.d.= 0,45 and 1.042. s.d. = 0.802 for the thumb, /ug 1.186 s.d. = 0.433 and /ug 1.692 s.d. = 1.52 for forefinger respectively. Sm was also not found in some paraffin samples for shots carried out with the revolvers. This fact is due, in our opinion, to the incorrect distribution of $Sm_2O_3$ in the gunpowder. This hypothesis seems to be confirmed by our finding Sb in the samples negative for Sm, which indicates GSR presence. The fingerprinting of gunpowder by the Manufacturer could make the distribution of the fingerprinting agent homogeneous.

Quantitative determinations of Sm and Sb in firing tests with the automatic pistol and with the revolvers testify that their traces in GSR are higly spread out, confirming the influence of the cartridges in GSR deposit.

The quantitative results obtained for the presence of Sb in the GSR shows that this element was always found thus confirming its role of GSR indicator, as pointed out in our previous work ( 21).

Measurements of bullet speed for the fingerprinted cartridges from 7.65 mm caliber ammunition showed lower values than those for bullets from the original ones. A comparable reduction of bullet speed was shown for reloaded, but not fingerprinted cartridges tested. This fact identifies the factor affecting the bullet speed in the reloading of the ammunition and especially in the operation of fixing the bullet to the cartridge case.

Summing up, the presence of Sm in the paraffin samples taken from the shoting hands of Sm fingerprinted ammunition shows the validity of our proposal for the fingerprinting of gunpowder.

In fact the presence of Sm on samples from suspected persons, acting as a reliable indicator of GSR togheter with Sb, could give Forensic Scientists the certainty of the presence of GSR on hands which could then presented in Court as evidence.

Moreover the ballistic properties of the fingerprinted ammunition are not affected by the presence of the fingerprinting agent, thus a practical application of the proposed fingerprint is possible.

The possibility of doping gunpowder with different elements taken from the Rare Earths group, or with mixtures of them, could furthermore allows the characterisation of the Manufacturer and of the caliber of ammunition used.

## References.

1) F. Benitez "Quelques consideration sur les taches produites par le projections d'armes a feu." Revue de Medicine Legale de Cuba, 11, 23, 1923.

2) I. Castellanos, R. Plasencia "The paraffin gauntlett: a new technique for the Dermo - nitrate test." J. of Crimininal Law and Criminol. 33, 465, 1941.

3) H.V. Turkel, J. Lipman "Unreability of dermal nitrate test for gunpowder." J. Crim. Law, Criminol. Police Sci. 46,282, 1955.

4) M.E. Cowan P.L. Purdon "A study on Paraffin Test". J. For. Sci. 12, 19, 1967

5) H.C. Harrison, R. Gilroy "Firearms discharge residues" J. For. Sci. 4, 184, 1959.

6) A. Shontag "Neue methode Bestinmung der Shussentfernung durk Spectrographische Spurenanalyse der "Schmanchelemenete" Antimon, Blei oder Barium." Archiv. für Kriminologie 120, 4, 1957.

7) R. Cornelis, J. Timperman "Gunfiring detection method based on Sb, Ba, Pb, Hg deposit on hands. Evaluation of the credibility of the test." Medicine Science and Laww. 14, 98, 1974.

8) M. Kijewsky, J. Lange "Neue aspekte in der Schessentfernungbestimmung durch anwendung der flammenlosen atom - absorption spektrophotometrie. Z. Rchtsmedizin." 74, 9, 1974.

9) G. Cave Bondi, E. Alexiv, G. Sacchetti "Identification of primer and gunpowder residues by the X - ray fluorescence technique: a preliminary research." Proceedings of the XIIth Congress of the Int. Academy of Forensic and Social Medicine. Vienna 1982.

10) F.P.J. Cahill, G.W. Van Loon "Trace analysis by atomic absorption spectroscpy and anodic stripping voltammetry". Am. Lab. 8, 11, 1976.

11) R.D. Cone "Detection of Ba, Sb and Pb in Gunshot Residues by flameless Atomic Absorption Spectroscopy". Proceedings of Southern Ass. of Forensic Scientist, Atalanta (USA), 1973.

12) S. Smith, J. Hwang " A new atomic absorption instrument applied to transient analysis". Proccedings of Pittsburgh Conference on Analytical Chemistry, Cleveland 1974.

13) R. Gagliano Candela, M. Colonna, L. Strada "Identificazione dei residui dell'esplosione di colpi d'arma da fuoco corta mediante polarografia di strippaggio anodico." Zacchia 51, 44, 1976.

14) F.Vydra, K. Stulik, E. Julakova "Electrochemical Stripping Analysis." Halsted Press, New York, 1976.

15) N.K. Konanur, G.V. Vanloon "Determination of lead and antimony in firearm discharge residues an hands by anodic stripping voltammetry." Atalanta 24, 184, 1977.

16) V.P. Guinn "Non biological application of neutron activation analysis in forensic studies." Methods of Forensic Science, Interscience Publ. London III, 46 - 47, 1964.

17) R.R. Ruch, J.D. Buchanan, V.P. Guinn, S. Bellanco, R. Pinker "Detection of Gunpowdere Residuews by Neutron Activation Analysis." Am. Nucl. Soc. Transaction 5, 282, 1962.

18) G. Borra a. Brandone, G. De Bernardi, A. Fornari, M.A. Rollier "Gunshot Residues on paraffin drops: instrumental neutron activation assay of antimony, barium and copper." J. Radioanal. Chem. 15, 51, 1973.

19) A. Brandone, M. Tavani, "Sulle possibilita' di impiego della AAN nella pratica forense." Arch. Soc. Lomb. Med. Legale e delle Ass. 10, 8. 1974.

20) A. Brandone, T. Cerri. M. Tavani "L'analisi per attivazione neutronica nella pratica forense: determinazione della distanza di sparo." Arch. Soc. Lomb. Med. Legale e delle Ass. 14, 47, 1978.

21) P. Benedetti, A. Brandone, F. De Ferrari, D. Salza "Ulteriori esperienze sulla interpretazione del reperto di residui di polvere da sparo sulla cute delle mani." Rivista Italiana di Medicina Legale 1, 112, 1980.

22) E. Bohen "Application of the SEM in forensic medicine." SEM/1971, IIT Research Institute, Chicago, Il., 553, 1971.

23) H. Hantsche "Zur Anwendung des Raster-Elektronenmikroskops in der Kriminaltechnik". Direktabb. Oberfl. 4 (2),641, 1971.

24) R. Diederichs, M.J. Camp, A.E. Wilimovsky, M.A. Hass, R.F. Dragen "Investigations into the adaptability of SEM/EDX to firearms related examinations." A.F.T.E. Journal 63, 1, 1974.

25) G. Judd, J. Sabo, W. Hamilton, S. Ferris, R. Horn "SEM micostriation characterization of bullets and contaminant particle identification". J. Forensic Sci. 19, 798, 1974.

26) J.L. Brown, J.W. Johonson " SEM-EDX microanalysis in forensic science". J. Ass. Offical Anal. Chem. 56, 930, 1973.

27) R.H. Keely, M.C. Robertson "The routine use of SEM and electron probe microanalysis in forensic science". SEM/1975 - IIT Research Institute, Chicago, Il. 479, 608, 1975.

**TABLE 1 : NAA - Sm results (µg)**

**fingerprinted G. Fiocchi 7.65 mm cal. cartridges**

| | | | | | |
|---|---|---|---|---|---|
| .120 | .059 | .077 | .050 | .028 | / |
| .044 | .055 | .306 | .020 | .100 | .056 |
| .033 | .058 | .032 | .026 | .282 | .064 |
| .068 | .061 | .042 | .015 | .305 | .036 |
| .127 | .062 | .350 | .046 | .492 | / |
| .145 | .057 | .353 | .051 | .448 | .063 |
| .186 | .070 | .030 | .015 | / | .049 |
| .100 | .039 | .024 | .049 | .031 | .034 |
| .116 | .084 | .056 | .047 | .028 | / |
| .064 | .081 | .095 | .028 | .033 | .037 |
| .112 | .047 | .065 | .069 | / | .018 |
| .040 | .051 | 1.127 | .097 | .030 | .019 |
| .110 | .050 | .950 | .068 | .027 | .049 |
| .088 | .022 | .126 | .026 | .066 | .013 |
| .165 | .055 | .795 | .060 | .020 | .032 |
| .230 | .038 | .085 | .379 | <0.005 | / |
| .036 | .038 | .145 | .140 | / | .016 |
| .090 | .080 | .032 | .239 | .043 | / |
| .160 | .057 | .052 | .092 | .016 | .023 |
| .060 | .118 | .124 | .266 | .041 | .027 |
| .150 | .082 | .062 | .145 | .043 | .090 |
| .130 | .044 | .045 | .091 | .040 | .014 |
| .096 | .039 | .070 | .207 | .039 | .056 |
| .090 | .038 | .028 | .171 | .034 | .052 |
| .060 | .100 | .062 | .158 | / | .031 |
| .070 | .068 | .029 | .224 | .073 | |
| .030 | .090 | .022 | .448 | .059 | |
| .040 | .075 | .059 | .621 | .089 | |
| .040 | .041 | .021 | .293 | .052 | |

**range:** .013 - 1.127

**mean value** .102

St. Dev. .152

/: not found $\leq$0.003 /ug

**TABLE 2 : NAA - Sb results (µg)**

**fingerprinted G. Fiocchi 7.65 mm cal. cartridges**

| | | | | | |
|---|---|---|---|---|---|
| 3.010 | 1.598 | .227 | 3.085 | .863 | .862 |
| 1.920 | 1.199 | 1.099 | 1.777 | 4.365 | 2.501 |
| .570 | 1.819 | 1.495 | 2.714 | 2.796 | 2.738 |
| 2.210 | 1.449 | 1.148 | 1.835 | 2.806 | 1.537 |
| 3.440 | 1.940 | .612 | 2.978 | .727 | .856 |
| 3.400 | 1.547 | .605 | 17.517° | 1.607 | 2.271 |
| 4.290 | 1.843 | 1.303 | 1.895 | 2.488 | 3.062 |
| 3.290 | .598 | .966 | 3.032 | .606 | 2.262 |
| 2.660 | 2.523 | 1.273 | 2.497 | .669 | 1.377 |
| 1.540 | 1.915 | 1.524 | 2.488 | .608 | 1.845 |
| 3.890 | 1.131 | .998 | .475 | 1.563 | .991 |
| 1.110 | 1.299 | 1.140 | .478 | .912 | 2.681 |
| 2.960 | 1.313 | 1.421 | .453 | .982 | .676 |
| 3.950 | .546 | 2.387 | .392 | 2.689 | 1.688 |
| 3.600 | 1.353 | 1.215 | .928 | .973 | .904 |
| 4.050 | 1.243 | 2.485 | 3.779 | 1.412 | 1.255 |
| 1.440 | 1.487 | 2.716 | .998 | .671 | .577 |
| 2.230 | .732 | 1.199 | 4.006 | 1.192 | 1.512 |
| 4.150 | 1.627 | .453 | 2.001 | 1.870 | 1.307 |
| 2.350 | 2.943 | 1.242 | 3.699 | 4.323 | 1.580 |
| 2.090 | 1.352 | 1.557 | 1.965 | 2.159 | .492 |
| 3.120 | 1.260 | 1.756 | 1.416 | 6.883 | 1.950 |
| 2.470 | 2.466 | 2.414 | 3.839 | 2.891 | 1.536 |
| 2.350 | 1.119 | 1.020 | 4.390 | 9.658 | 1.341 |
| 1.680 | 1.010 | .421 | 2.440 | 1.885 | 1.923 |
| 2.170 | 1.528 | 2.438 | 3.632 | 1.938 | |
| 1.540 | 1.831 | 1.986 | 2.524 | 2.164 | |
| 1.270 | 1.510 | 2.653 | 2.462 | 1.363 | |
| 1.380 | .992 | 1.280 | 1.317 | 3.237 | |

range: .227 - 9.658

mean value 1.940

St. Dev. 1.210

° not considered

**TABLE 3 : NAA - Sm results (µg)**
**fingerprinted G. Fiocchi .38" cal. cartridges**

| | | | | | |
|---|---|---|---|---|---|
| **THUMB** | .035 | .026 | .016 | .044 | / |
| | .049 | .032 | / | / | .024 |
| | .019 | / | .149 | .043 | .111 |
| | .022 | .020 | .044 | .052 | .020 |
| | / | / | .044 | / | .131 |
| | .025 | | | | |

**range:** .016 - .149
**mean value** .035
St. Dev. .039

| | | | | | |
|---|---|---|---|---|---|
| **FOREFINGER** | .018 | / | .033 | .018 | .054 |
| | .039 | .024 | .047 | / | / |
| | / | .019 | .031 | .077 | .152 |
| | .031 | / | / | .089 | .088 |
| | .040 | .030 | .058 | .067 | .076 |
| | .015 | | | | |

**range:** .015 - .152
**mean value** .039
St. Dev. .037

**NNA - Sb results (ug)**
**fingerprinted G. Fiocchi .38" cal. cartridges**

| | | | | | |
|---|---|---|---|---|---|
| **THUMB** | 1.317 | .650 | 1.035 | .444 | .427 |
| | 1.615 | 1.208 | .553 | .745 | 1.538 |
| | 1.645 | .573 | .657 | 1.106 | .299 |
| | 1.322 | 1.033 | 1.190 | 1.518 | .404 |
| | .564 | .765 | .340 | 1.310 | .233 |
| | .528 | | | | |

**range:** .233 - 1.645
**mean value** .885
St. Dev. .450

| | | | | | |
|---|---|---|---|---|---|
| **FOREFINGER** | 1.005 | .910 | 1.780 | 1.102 | .612 |
| | 1.439 | 1.319 | 1.364 | 2.033 | .645 |
| | .790 | .563 | 1.005 | .882 | 1.447 |
| | 1.431 | 1.172 | 1.695 | .960 | 1.546 |
| | .585 | 1.622 | 1.968 | .683 | 1.360 |
| | .910 | | | | |

**range:** .563 - 2.033
**mean value** 1.186
St. Dev. .433

/: not found $<$0.003 /ug

TABLE 4 : NAA - Sm results (µg)
fingerprinted C.C.I. .44" cal. cartridges

| | | | | | |
|---|---|---|---|---|---|
| THUMB | .031 | / | .130 | .033 | .022 |
| | .032 | .041 | / | .024 | .050 |
| | .107 | .045 | .046 | .084 | .216 |
| | .032 | .161 | .017 | .276 | .052 |
| | range: | .017 - .276 | | | |
| | mean value | .070 | | | |
| | St. Dev. | .074 | | | |
| FOREFINGER | .227 | .027 | .038 | .200 | .029 |
| | .092 | .036 | .177 | .079 | .044 |
| | .055 | .026 | .086 | .041 | .540 |
| | .061 | .103 | .597 | .076 | / |
| | range: | .026 - .597 | | | |
| | mean value | .127 | | | |
| | St. Dev. | .163 | | | |

NAA - Sb results (µg)
fingerprinted C.C.I. .44" cal. cartridges

| | | | | | |
|---|---|---|---|---|---|
| THUMB | .662 | / | 3.346 | .792 | 2.064 |
| | .502 | .779 | .791 | .516 | 1.793 |
| | .708 | .338 | .559 | .470 | 1.235 |
| | 1.085 | 1.018 | .486 | 2.345 | 1.343 |
| | range: | .338 - 3.346 | | | |
| | mean value | 1.042 | | | |
| | St. Dev. | .802 | | | |
| FOREFINGER | 951 | .593 | .813 | 2.566 | 2.717 |
| | .899 | .875 | 6 690 | 1.226 | .656 |
| | .735 | .363 | 2 668 | .690 | 2.824 |
| | .970 | 2 674 | 3 390 | .752 | .796 |
| | range: | .363 - 6.690 | | | |
| | mean value | 1.692 | | | |
| | St. Dev. | 1.520 | | | |

/: not found $\leqslant$0.003 for Sm and $\leqslant$ 0.005 /ug for Sb

FIG. 1 — BULLET SPEED

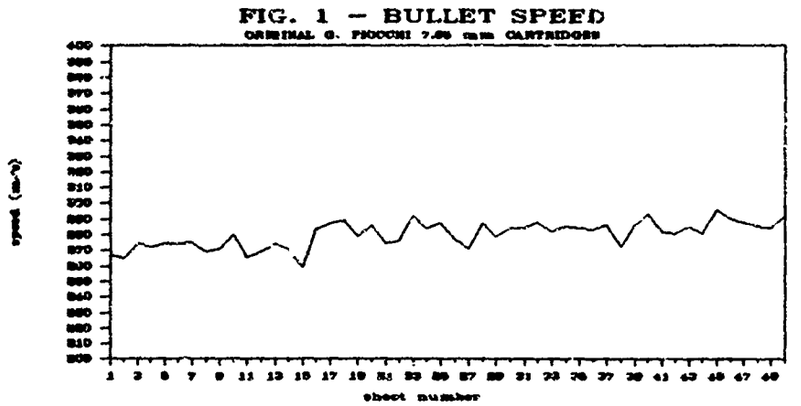


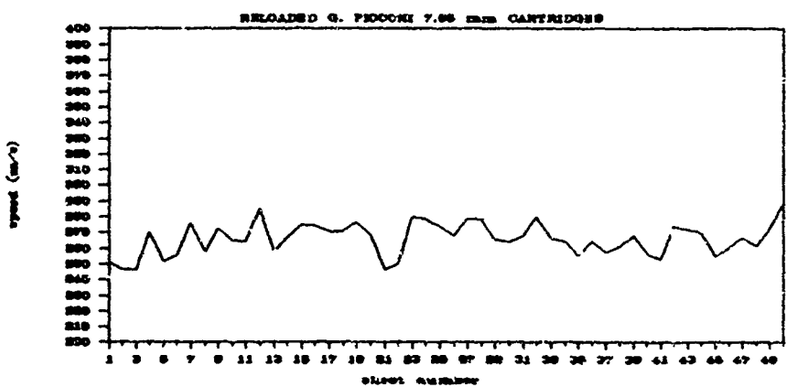


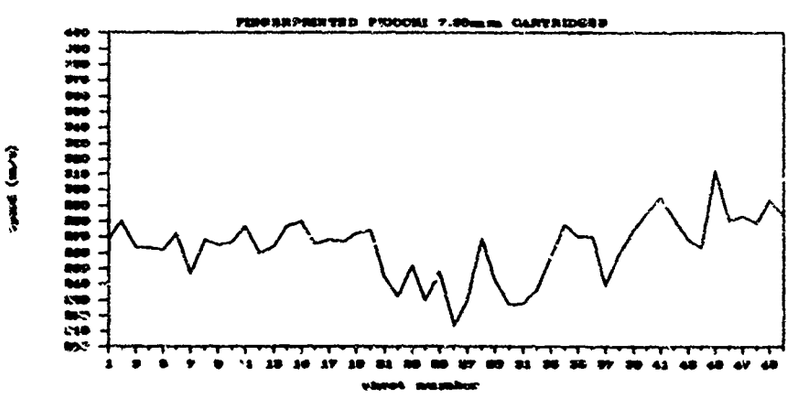

# FIG. 2 – BULLET SPEED

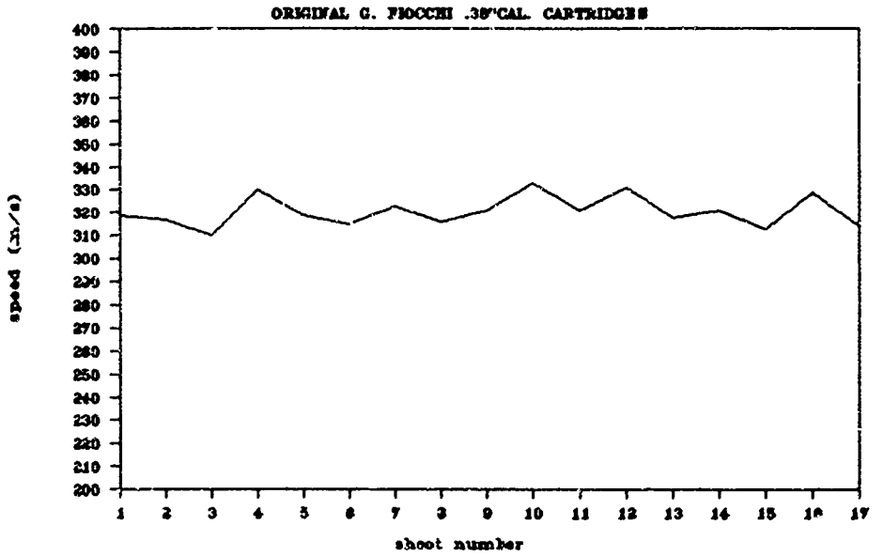


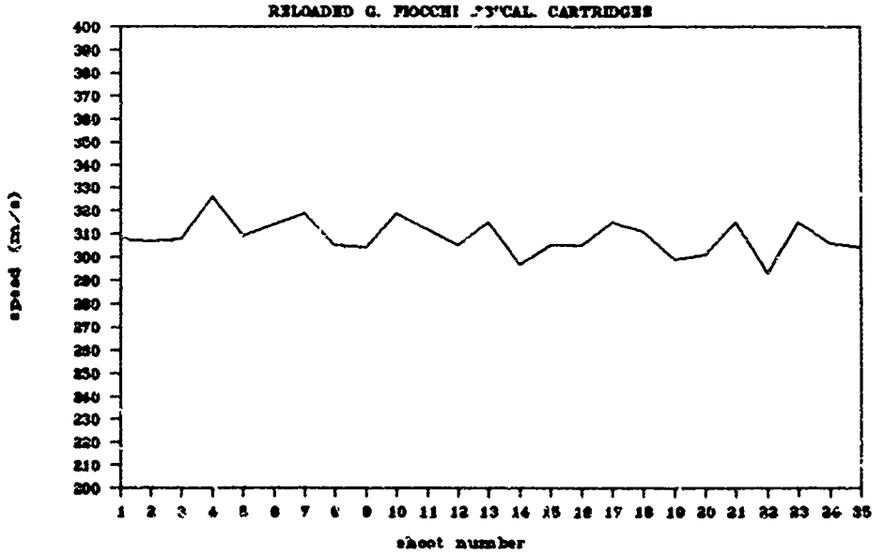

# FIG. 3 – BULLET SPEED

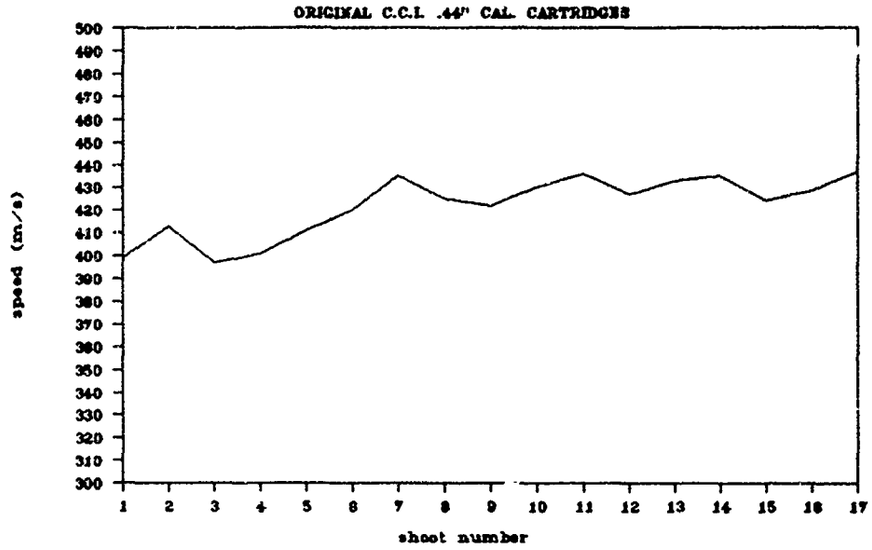


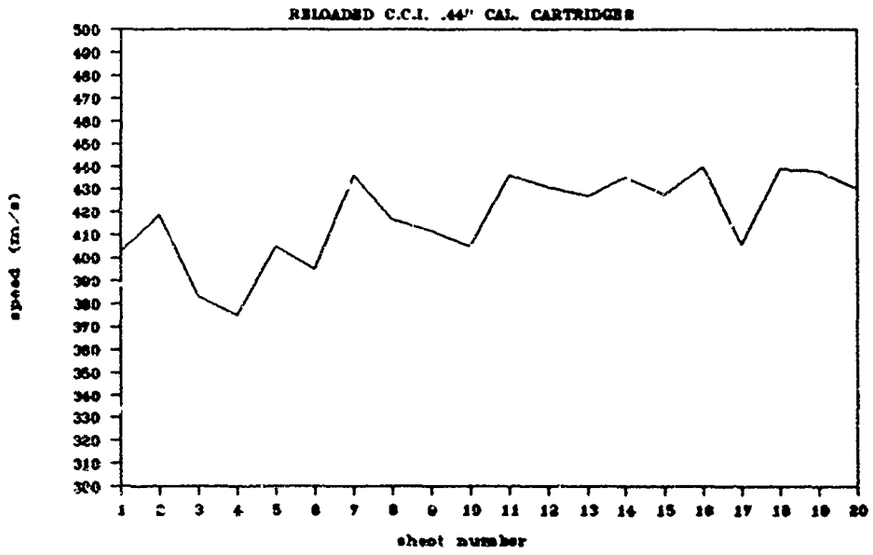

# QUANTITATIVE AND QUALITATIVE DETECTION OF α- AND β-HMX

Fredrik Hopfgarten
Nobel Chemicals AB
Department NEQ 3
S-691 85 KARLSKOGA
SWEDEN

## Abstract

HMX (Octahydro-1,3,5,7-tetranitro-1,3,5,7-tetrazocine) has four polymorphs α, β, γ and δ. These are stable at different temperature ranges and have different impact sensitivities. The most stable form at room temperature is the β-polymorph. The first three polymorphic forms are workably stable at normal pressure and temperature but the δ-polymorph transforms so readily that little has been done with it. The classification of the polymorphs has been derived from a consideration of physical properties. Only one melting point (280 °C) is known but solid transitions have been observed. The X-ray diffraction powder patterns of the polymorphs are quite distinctive and unique for the four different polymorphic forms.

In order to decide which analytical method is the most suitable for both quantitative and qualitative analysis of HMX different methods have been tested. The results from these analyses are discussed and the advantages of the different methods are described.

## 1. INTRODUCTION

HMX (Octahydro-1,3,5,7-tetranitro-1,3,5,7-tetrazocine) (fig 1) is known to exist in four polymorphic forms: α, β, γ and

δ. The first three are workably stable at room pressure and temperature but δ-HMX transforms so readily that little has been done with it. For the present study two of the four polymorphs were available, namely the α- and β-HMX. The classification as polymorphs has been derived from a consideration of physical properties. Only one structural formula is required to explain the properties of HMX in solution. Only one melting point (~280 °C) is known but solid-state transitions may be observed. The X-ray diffraction powder patterns of the polymorphs are quite distinctive although frequently during analysis of γ-HMX, there is evidence of total or partial transformation.

According to previous authors (ref 1), β-HMX contains a ring conformation such that the $NO_2$ groups adopt a chairlike arrangement. This gives the entire molecule a center of symmetry. The ring conformation of α-, γ- and δ-HMX is such that all the $NO_2$ groups are positioned on one side of the molecule, and the conformation possesses a two-fold axial symmetry. The discovery (ref 2) that the γ- form is actually a hydrate corresponding to the formula $2\ C_4H_8N_8O_8 \cdot 5\ H_2O$ is worth nothing. The question raised in our mind is how these differences between the polymorphs translate in terms of their heat capacity variations. δ-HMX is normally absent from samples that have been solution-processed because this form is thermodynamically favored only at high temperatures (>140 °C).

The following methods have been used for the examination of HMX: X-ray powder diffraction, IR-spectroscopy and DSC, and only α- and β-HMX have been studied. The infrared spectra of α- and β-HMX in pellet dispersion are quite distinctive. Indeed, the infrared differences are so striking that they serve as well as the X-ray diffraction patterns for identification.

## 2. EXPERIMENTAL

In x-ray powder diffraction work, the inherent precision of the Guinier camera geometry is of vital importance, not only for effective search-match and indexing procedures, but also for profile refinements and quantitative analyses. The collection of data on film has further advantages over other methods in that it is cheap and produces a durable record. Several computer-linked densitometer systems have been designed for crystallography. These systems were all designed for general, two-dimensional diffraction photographs, such as precession or oscillation films. The data collection from a Guinier photograph, however, is essentially a linear scan process, and the use of a drum densitometer is an unnecessary complication. The correction procedure has made it possible to avoid scaling errors from films of different exposure times. The new Guinier micro-densitometer has been designed as a single-beam instrument. Thanks to an interpolation procedure for finding peak positions and to the use of the internal standard technique, the differences between observed and calculated 2θ values are usually less than 0.01. Test runs with a step length of 0.02 mm have not improved the data quality, but have proved that the data are more dependent on camera adjustment, stability, internal standard and sample preparation technique than on the step length of the measuring device. The scanner mention above, is described in a Research Paper (Johansson, et al 1980, ref 16).

The IR-spectroscopy system used for obtaining spectra of HMX is a Perkin-Elmer model 781. All samples were run as potassium bromide pellets. Samples were prepared in the following manner: approximately 1.3-1.8 mg of HMX were weighed to the closest 0.02 mg and added to 300 ± 3 mg of potassium bromide. Mixing was accomplished by grinding in ball mill for 60 sec. The pellets are made as follows. Place the die assembly under a press (Perkin-Elmer 15 ton press). Evacuate die assembly for about 3 minutes, then

apply load to plunger sufficient to produce the desired quality of pellet (the load is 10 tons). Evacuation should proceed during the application of load and be maintained for a further 2 minutes. Release load on die but proceed with the evacuation another 2 minutes then release the vacuum. All samples were examined as potassium bromide pellets from 4000 to 600 $cm^{-1}$ in the transmission mode. For the quantitative classification the absorbance mode was used from 1060 to 780 $cm^{-1}$, with maximum ordinate scale expansion. Optimization of the instrument was accomplished following the vendor's recommended procedure. A polystyrene film was used to assess performance.

DSC, the instrument used was a Differential Scanning Calorimeter (DSC), Perkin-Elmer DSC-7. The DSC has the following specifications.

| | |
|---|---|
| DSC Type | Power compensated temperature null principle. Measures energy directly not differential temperature (T). |
| DSC Cell | Independent dual furnaces constructed of platinum-iridium alloy with independent platinum resistance heaters and temperature sensors. |
| Maximum Sensitivity | 8 μ W/cm |
| Dynamic Range | 8 μ W/cm to 28 mW/cm |
| Noise (RMS) | 0.002 mW |
| Calorimetric Accuracy | ± 1 % |
| Calorimetric Precision | ± 0.1 % |
| Temperature Precision | ± 0.1 °C |
| Temperature Accuracy | ± 0.1 °C |
| Temperature Display | 0.1 °C increments |
| Heating & Cooling Rates | 0.1 °C/min to 500 °C/min in 0.1 °C increments |

Optimization of the instrument baselines, curvature and

slope was accomplished by following the vendor's recommended procedure. The standard used for temperature and energy calibration was Indium, 156.60 °C melting point and 28 45 J/g transition energy. A sample of approximately 10 mg was used with a scanning rate of 2 °C/min. Samples used were of different types, including HMX. The sample size was kept as small as practicable (1-5 mg), scan rates were 20 °C/min.

A total of nine samples were tested. The composition of the samples were as following percent α-HMX/β-HMX: 0; 0.51; 0.90; 1.21; 1.35; 4.78; 7.49; 10.48 and 100 %. These nine samples were examinated both with X-ray powder diffraction and IR-spectroscopy for quantitative determination of α-HMX. The phase transition was studied with DSC, and this technique can also be used for qualitative analysis of HMX.

For the X-ray measurments of HMX the intensity of a reflexion from both α- and β-HMX were used. For the α-phase the reflexion with h,k,l-index 1,1,1 was used and for the β-phase the reflexion with h,k,l-index 1,0,1. The intensity of the reflexion depends on the concentration. All examinations were made with CuKα radiation with the wavelength: 1.54060 Å and with a camera radius of 40.16 mm.

Samples with the same composition were examined with IR-spectroscopy for the qualitative analyses the absorbance mode was used. The IR-absorbance is measured at the wavenumber 1030 $cm^{-1}$ where α-HMX has an absorbance peak, in contrast to β-HMX which has no absorption at this wavenumber. As reference line, the absorbance at the wavenumber 800 $cm^{-1}$ is used, where either α- or β-HMX have any absorbance (see fig 2 and 3). With the Perkin-Elmer model DSC-7, both transition temperature and transition energy are obtained simultaneously. The temperature is varied from +160 °C to +284 °C. The same nine sample compositions which have been examined X-ray and IR were

studied with DSC. Examples of thermogram describing phase transition (see fig 4).

## 3. RESULTS AND DISCUSSION

The calibration curve from the X-ray analyses is shown in fig 5 with the regression output. The X-ray powder diffraction data for α-HMX see Table 1 and for β-HMX see Table 2. In Table 3, the results from the automatic microdensitometer for X-ray powder diffraction photographs are presented. It is important to note that there has been no correction for absorption of the X-ray radiation in the crystals. But we expect to have the same absorption in α-HMX as in β-HMX and especially if we choose reflexions to measure on with almost the same θ. Another disadvantage with X-ray analyses of HMX for quantitative determination of α-HMX is that the calibration curve does not passed origo and this is because β-HMX has a weak reflexion at d=5.40 Å and we measured the α-HMX reflexion at d=5.37 Å. Another disadvantage is that at a low concentration of α-HMX gives a low intensity the determination of the background will be unreliable. Furthermore with these two problems, the theoretical line ought to be a little bent. The conclusion we can draw from this results is that we can make a quantitative determination of α-HMX from 1.0 % up to >10 % with an error range of ± 0.1 %.

The calibration curve from the IR analyses is shown in fig 6 with the regression output. The IR-absorbance spectra for β-HMX with 0.51 % α-HMX and pure α-HMX are shown in fig 7 and 8. The transmission spectra for β-HMX with 3 % α-HMX are shown in fig 9. From the transmission spectra, it is obvious that these spectra can not be used for qualitative analyses of HMX since a content of <3 % can not be indicated in these spectra, (see fig 9). From the absorbance spectra then there are no problems in making a quantitative analysis of α-HMX down to a concentration of

0.5 % α-HMX with an error range of ± 0.05 %. The following are important to take note of in IR-analyses of HMX using KBr pellets. RDX will interfere at the wavenumber 1030 $cm^{-1}$ with α-HMX, so correction for RDX must be made if the sample includes of some amounts of RDX. There can also be change in the spectra probably caused by stress relaxation in the KBr pellet or exchange between HMX and KBr such phenomena have been reported for inorganic compounds and KBr. It is also important to note that a lot of energy will be generated when the pellets are being made. The load is 10 tons and the pellet die has been dried at a temperature of +70 °C. So the pellet die will be a reaction chamber, which can make it possible to generate new or change phases in the HMX sample.

The identification and characterization of phase transitions in organic, inorganic and polymeric materials are obviously generally important. HMX thermograms obtained at a scan rate of 20 °C $min^{-1}$ showed a phase transition. See fig 10. This solid transition is shown as a broad (not sharp) peak. The transition endotherm spanned a temperature interval of c. 20 K, with initial temperatures in general agreement with the value of 459 K reported by Krien the enthalpy of transition (2.35±0.2 kcal $mol^{-1}$) may be compared with the value of 2.25 kcal $mol^{-1}$ for the β-δ transition quoted by Selig. The decomposition exotherm beginning at c. 540 K was interrupted by a sharp fusion endotherm at c. 551 K and an immediate rapid increase in the rate of decomposition. The energy of activation of 180-210 kcal $mol^{-1}$ for decomposition below the melting point is considerably higher than the value of 52.7 kcal $mol^{-1}$ reported by Rideal et al and may be compared with the DSC value of 228±24 kcal $mol^{-1}$ reported by Rogers and Morris. The temperature range corresponding to decomposition of HMX (c. 530-550 K) was also scanned at a rate of 0.5 K $min^{-1}$. It is possible that these high values for the acitivation energy for HMX is related to the

complexity of the decomposition reaction in the condensed state. The agreement between our results and those Rylance (ref 13), Krien (ref 12) and Hall (ref 11) is quite good (see Table 4). Thermogram from the test (see fig 10 and 11).

Table 4

HMX TRANSITION ENTHALPIES

| | | $\Delta H$ trans (kJ $mol^{-1}$) | | | |
|---|---|---|---|---|---|
| T(°C) | Transition | this work | Ref 11 | Ref 12 | Ref 13 |
| 193-204 °C | $\alpha \rightarrow \delta$ | 7.5 | 8.0 | 7.4 | 6.7 |
| 167-183 °C | $\beta \rightarrow \delta$ | 9.3 | 9.6 | 9.8 | 9.3 |

For pure α-HMX a higher transition temperature was obtained. As a conclusion I can say that it is always valuable to make a DSC-run in order to obtain a thermogram containing a lot of other information as well as the information about phase transition and energy of any phase transition. One will also obtain information about absolute purity for single component systems. For quantitative determination of α-HMX, I think it is best to compare the X-ray results with IR if possible. In the near fucure, we will start to examine HMX samples with a FTIR-spectrometer, there are three major advantages of Fourier transform infrared in comparision with dispersive instruments, including high signal-to-noise ratio, speed and wavenumber accuracy.

References

1 Eiland, P.F., and Pepinsky, R., Z. Kristallogr., 106, 273 (1954)

2 Howard, H.C., Larson, A.C., and Cromer, D.T., Acta Cryst., B30, 1918 (1974)

3 Cobbledick, R.E., and Small, R.W.H. Acta Cryst., C41, 1351 (1985)

4 Main, P., Acta Cryst., C41, 1351 (1985)

5 Licht, H.H., 2nd Symp Chem. Probl. connected stabil. Explos., (1970)

6 Mc Auley, C.D., Joubert, L.A., and Steyn, L.N., 7th Symp. Chem. Probl. connected Stabil. Explos., (1985)

7 Goetz, F., Brill, T.B., and Ferraro, J.R., J. Phys. Chem., 82, 17, 1912 (1978)

8 Holy, J.A., Firsich, D.W., and Walters, R.R., Int. Symp. Comp. Plast. Materials Explos. Prop. Pyrotech. (1988)

9 Brill, T.B., and Karpowicz, R.J., Am. Chem. Soc., 86, 21, 4260 (1982)

10 Karpowicz, R.J., and Brill, T.B., AIAA J., 20, 11, 1586, (1982)

11 Hall, P.G., Trans. Faraday Soc., 67, 556 (1971)

12 Krien, G., Licht, H.H., and Zierath, J., Thermochim. Acta., 6, 465 (1973)

13 Rylance, J., and Stubley, D., Thermochim. Acta., 3, 253 (1975)

14 Carignan, Y.P., Turngren, E.V., Cichinski, C.T., and Salo, J.K., 13th Proc, Symp. Explos. Pyrotech., (1986)

15 Cady. H.H., and Smith, L.C., LAMS-2652 (1962)

16 Johansson, K.E., Palm, T., and Werner, P-E., J. Phys. E. Sci. Instrum., 13,1289 (1980)

17 Selig, W., Explosivstoffe 4, 73 (1969)

18 Rideal, E.K., and Robertson, A.J.B, Proc. Roy. Soc. A, 195, 135 (1948)

19 Rodgers, R.N. and Morris, E.D., J. Org. Chem 32, 285 (1967)

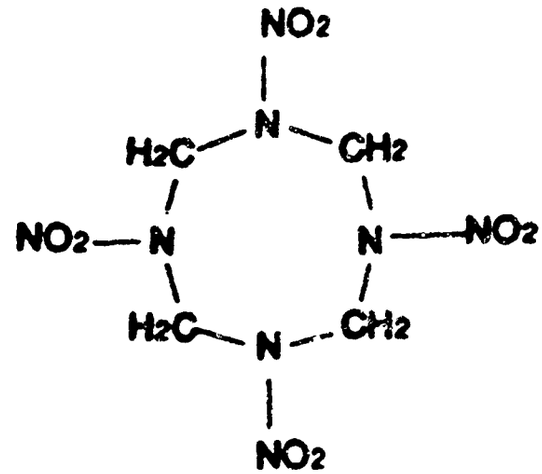


Figure 1 Structural formula of HMX

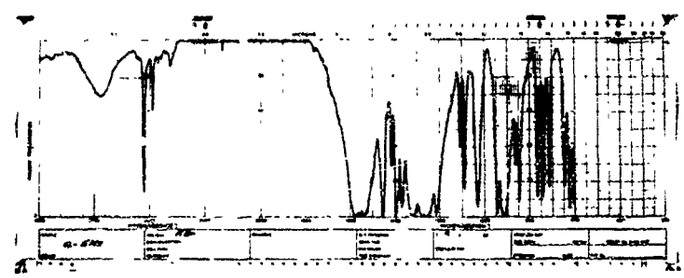

Figure 2 IR-transmission spectra of α-HMX

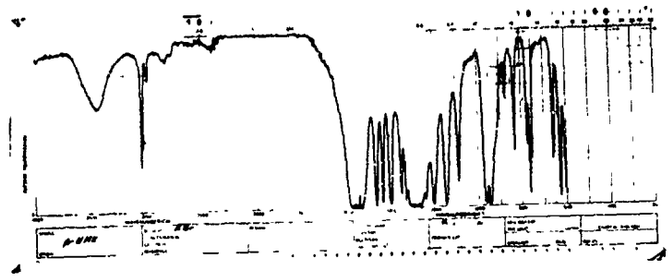

Figure 3 IR-transmission spectra of β-HMX

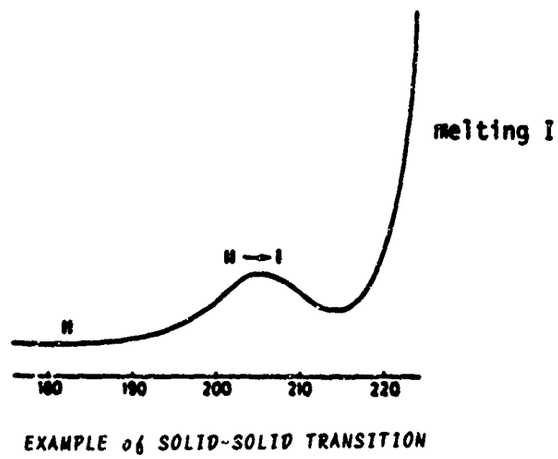


Figure 4 Example of a thermogram showing a solid-solid transition

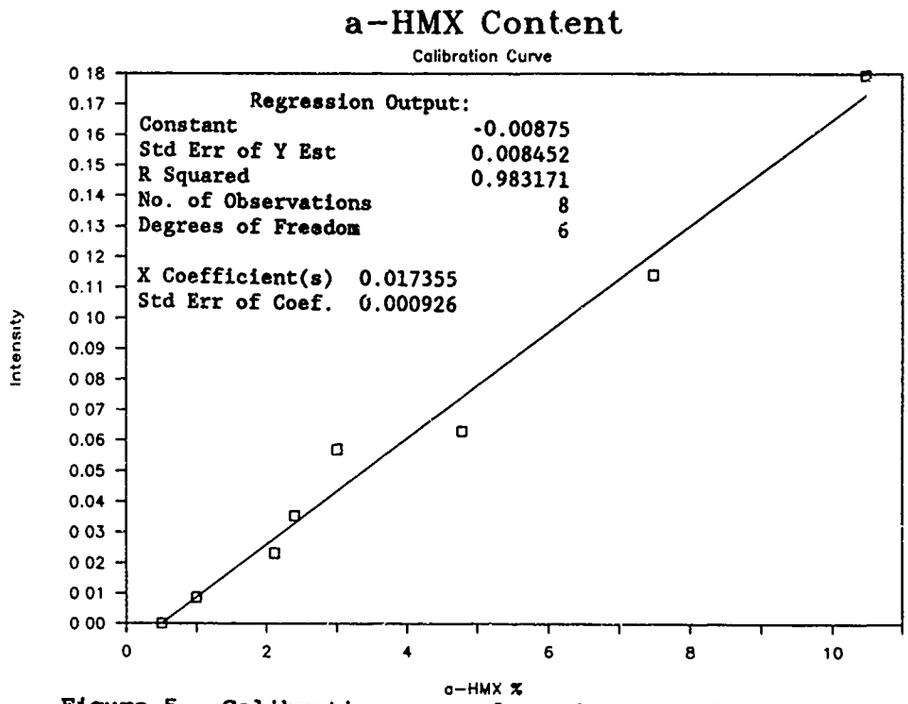


Figure 5 Calibration curve from the X-ray Analyses with the regression output

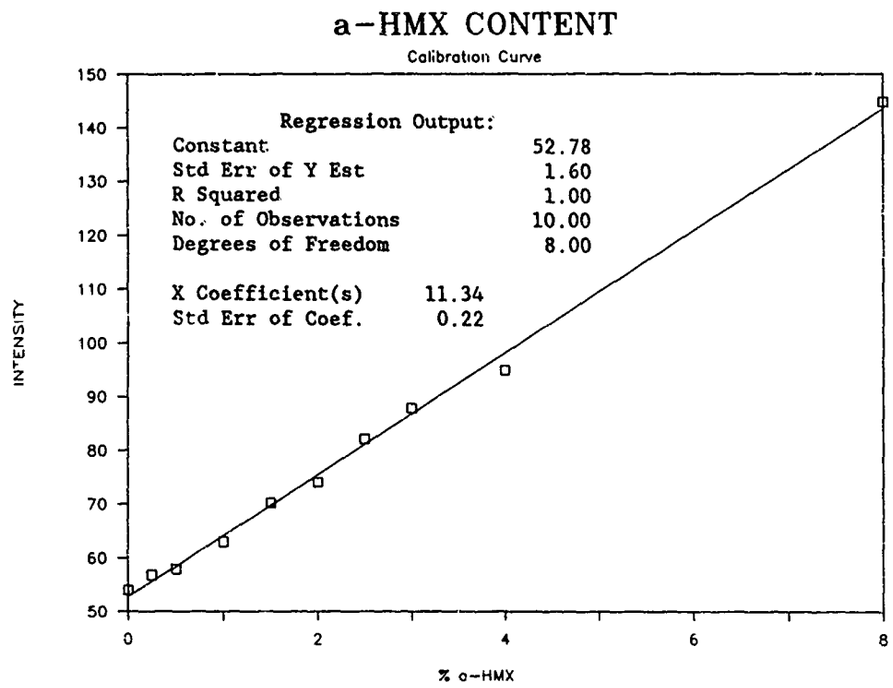


Figure 6 Calibration curve from the IR Analyses with the regression output

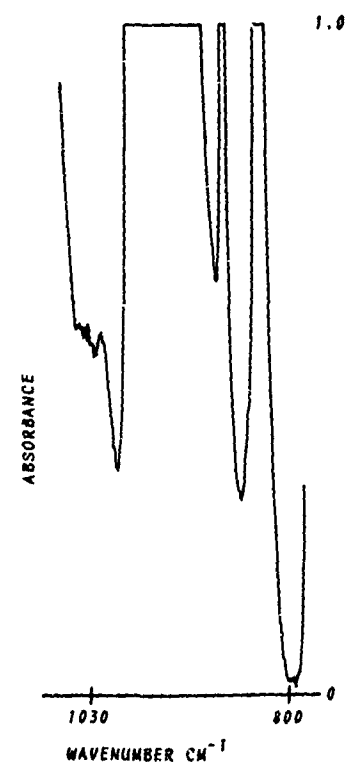


Figure 7 IR-absorbance spectra for β-HMX containing 0.51 % α-HMX

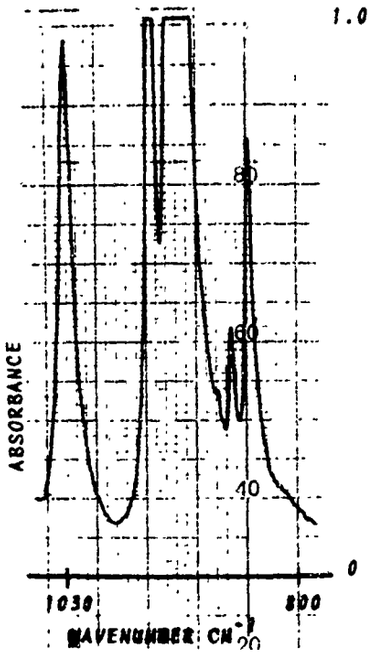


Figure 8 IR-absorbance spectra for α-HMX without β-HMX

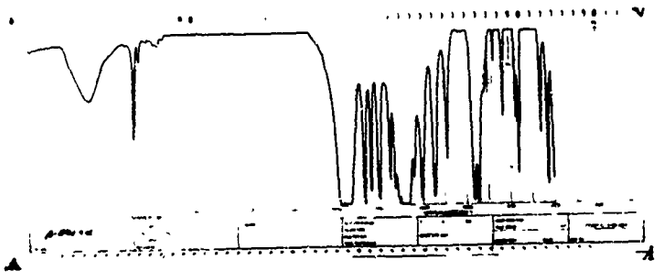

Figure 9 IR-transmission spectra for β-HMX containing 3 % α-HMX

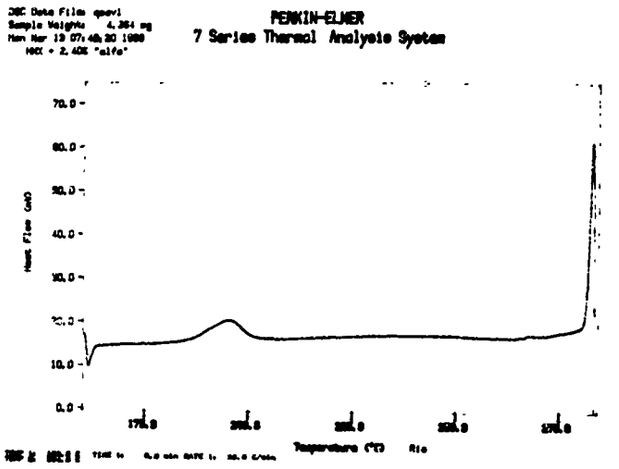


Figure 10 Thermogram of HMX with 2.40 % α-HMX showing the α-δ phase transition

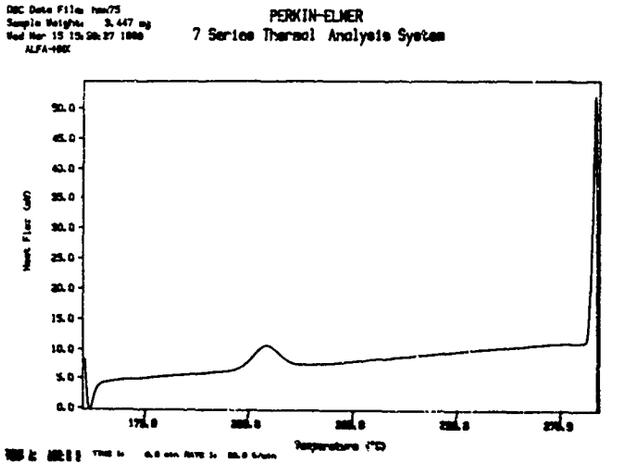


Figure 11 Thermogram of α-HMX showing the α-δ phase transition

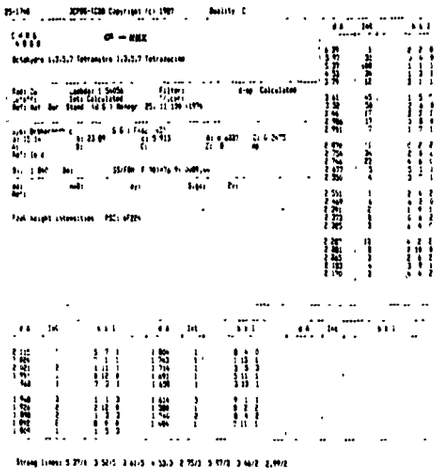

1.

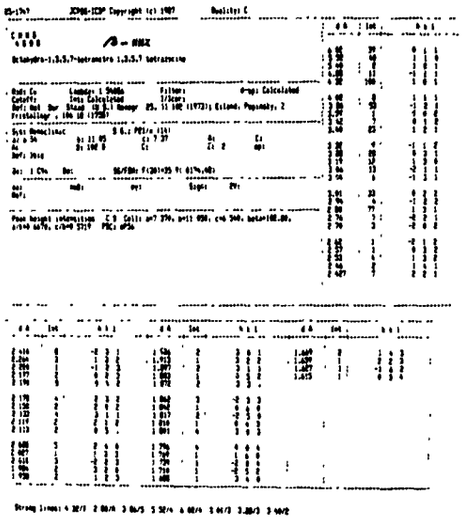

2.

Table 1 and 2 X-ray powder diffraction data for α-HMX and β-HMX

7.49 % α-HMX

CONTROL OF INPUT DATA

WAVELENGTH = [illegible] CARBON MONITOR = [illegible]

GUINIER GEOMETRY

MPF2 = MULTIPLICITY FACTOR TIMES F**2

I = INTEGRATED INTENSITY

SC*I = I SCALED TO I MAX = 100

THE SCALE FACTOR SC = [illegible]

| SC*I | I | MPF2 | I(OBS) | I(COR) | 2*THETA | SIN*SQ | D | CAT | NO |
|---|---|---|---|---|---|---|---|---|---|
| 20.96 | 457 | 74 | 20.68 | 20.68 | 14.749 | 0.01648 | 6.0013 | 1 | 1 |
| 30.46 | 664 | 129 | 22.55 | 22.55 | 16.086 | 0.01958 | 5.5055 | 1 | 2 |
| 9.04 | 197 | 40 | 23.13 | 23.13 | 16.540 | 0.02059 | 5.3688 | 1 | β-4 |
| 7.16 | 156 | 40 | 25.72 | 25.72 | 18.370 | 0.02543 | 4.8309 | 1 | 4 |
| 79.08 | 1724 | 565 | 28.86 | 28.86 | 20.590 | 0.03194 | 4.3101 | 1 | 5-β |
| 2.20 | 48 | 18 | 30.87 | 30.87 | 22.018 | 0.03647 | 4.0337 | 1 | 6 |
| 4.50 | 98 | 37 | 31.00 | 31.00 | 22.113 | 0.03678 | 4.0166 | 1 | 7 |
| 50.41 | 1099 | 460 | 32.39 | 32.39 | 23.100 | 0.04010 | 3.8469 | 1 | 8 |
| 27.98 | 610 | 434 | 36.79 | 36.79 | 26.244 | 0.05154 | 3.3930 | 1 | 9 |
| 9.08 | 198 | 115 | 37.83 | 37.83 | 26.984 | 0.05443 | 3.3017 | 1 | 10 |
| 30.83 | 672 | 490 | 38.27 | 38.27 | 27.301 | 0.05567 | 3.2649 | 1 | 11 |
| 0.76 | 191 | 140 | 39.31 | 39.31 | 28.045 | 0.05871 | 3.1791 | 1 | 12 |
| 6.95 | 217 | 149 | 40.76 | 40.76 | 29.081 | 0.06263 | 3.0538 | 1 | 13 |
| 31.28 | 682 | 487 | 41.70 | 41.70 | 29.744 | 0.06507 | 3.0012 | 1 | 14 |
| 100.00 | 2180 | 1818 | 44.08 | 44.08 | 32.012 | 0.07603 | 2.7936 | 1 | 15 |

DIFFRACTION DATA FILE NAME ?

Table 3 Output from the automatic microdensitometer for X-ray powder diffraction data. The sample examinated with X-ray powder diffraction consist of β-HMX with 7.45 % α-HMX

# POST EXPLOSION ANALYSIS BY NMR SPECTROMETRY

Y. Bamberger*, Y. Margalit** and S. Zitrin*

*Division of Criminal Identification, Israel National Police, Jerusalem, Israel.
**Israel Institute for Biological Research, Ness-Ziona, Israel 70450.

## ABSTRACT

In order to evaluate the applicability of NMR spectrometry to post-explosion analysis, the method was used in 24 cases handled by the Israeli Police. In 12 cases, explosives were identified by NMR in residues taken from post-explosion debris. In one case NMR was used successfully to identify traces of explosives on a vehicle.

The method, which was used without pre-separation or cleaning procedures was found to be reliable, fast, and identified explosives in about half of the cases.

## 1. INTRODUCTION

NMR spectra of common explosives and related compounds have been recorded (1,2), using 60 MHz instruments. NMR was also used to identify unknown samples of explosives (3,4). Our group tried to apply NMR to post-explosion analysis, using higher magnetic field. Following promising results (5), we broadened the scope of our previous work. The NMR spectra of 32 explosives and related compounds were recorded on a 250 MHz instrument, in order to serve as a reference library. Then the method was applied to 24 cases handled by the Israeli Police. Results obtained by other methods (TLC, LC and sometimes GC/MS) were compared with the NMR results.

---

**Author to whom correspondence should be addressed.

## 2. EXPERIMENTAL

The NMR spectrometer was a BRUKER WM-250, operating at 250 MHz for protons. The NMR measurements were done on protons.

The samples included pure explosives and post-explosion samples. Exhibits from post-explosion sites had been extracted with acetone. The extracts were dried on a water bath and re-dissolved in acetone-$d_6$, containing 0.1% TMS (internal reference).

The number of scans in each post-explosion spectrum was 100-400 (5-10 minutes). The amounts of the original explosives in the post-explosion samples were not known but could be estimated to be at least 10 micrograms of unexploded explosive material in the extract.

## 3. RESULTS AND DISCUSSION

NMR spectra of the following explosives and related compounds have been recorded and served as a basic library.

a) Nitroaromatic compounds:

1,3-dinitrobenzene; 1,4-dinitrobenzene; 2,4-dinitrophenol; 2,4-dinitrochlorobenzene; 2,4-dinitrotoluene (2,4-DNT); 2,6-dinitrotoluene (2,6-DNT); 1,3-dinitronaphthalene; 1,4-dinitronaphthalene; 1,5-dinitronaphthalene; 1,8-dinitro naphthalene; 1,3,5-trinitrobenzene (TNB); 2,4,6-trinitro phenol (picric acid); 2,4,6-trinitroresorcinol (styphnic acid); 2,4,5-trinitrotoluene (2,4,5-TNT); 2,4,6-trinitro toluene (2,4,6-TNT); 2,4,6-trinitrocresol; 2,4,6-trinitro anisole; 2,4,6-trinitrobenzoic acid; 2,4,6-trinitroxylene; 2,4,6-trinitrophenetol; 1,3,5-trinitronaphthalene; 1,3,8-trinitronaphthalene; 1,4,5-trinitronaphthalene.

b) Nitrate esters:

ethyleneglycol dinitrate (EGDN); diethyleneglycol dinitrate (DEGN); glycerine trinitrate ("nitroglycerine"); cellulose nitrate ("nitrocellulose"); pentaerythritol tetranitrate (PETN).

c) Nitramines:
1,3,5-trinitro-1,3,5-triazacyclohexane (RDX);
1,3,5,7-tetranitro-1,3,5,7-tetraazacyclooctane (HMX);
2,4,6, N-tetranitro-N-methylaniline (tetryl).

The NMR spectra of 24 extractions from explosive-related exhibits were recorded. The exhibits were collected by the Israeli Police and included debris from post-explosion sites. In one case, the exhibits included traces of explosives taken by wiping a suspect's car. The cases belonged to files handled by the Police during 1983-1989. Some of the explosions were connected to terrorist activity and the rest were connected to safe burglaries and other criminal activities. In all cases the NMR analyses were carried out after the samples had been identified by other analytical methods in the Israeli Police laboratories. The methods included TLC, LC and sometimes GC/MS.

In 11 cases the NMR results did not reveal the presence of the explosives found by the police laboratory (usually TNT or nitroglycerine).In the other 13 cases, summarized in Table 1, explosives were positively identified by NMR.

TABLE 1 - Identification of Explosives from Post-Explosion Residues by NMR

| File Number | NMR Results | Official Laboratory Results by other methods | Remarks |
|---|---|---|---|
| 1462/83 | PETN + lower nitrate esters (tri- and di-nitrates of PE*) | PETN | wiping the wheel and other parts of a suspect's car |
| 1459/83 | PETN + tri- and di-nitrates of PE | PETN | safe "cracking" |
| 1461/83 | PETN + tri- and di-nitrates of PE | PETN | safe "cracking" |
| 7105/84 | RDX | RDX + TNT | suspected package exploded by police |
| 1975/85 | RDX + PETN | RDX + PETN | explosion near apartment house in criminal act |
| 3687/85 | RDX + PETN | RDX + PETN | explosion near the Israeli Police HQ |
| 4302/85 | PETN + tri- and di-nitrates of PE | PETN | safe "cracking" in a Post Office |
| 2537/86 | RDX or HMX | HMX | accidental fatal explosion of a "LAW" missile |
| 11733/88 | RDX + TNT (1:1) | RDX + TNT + $NO_3^-$ + $ClO_3^-$ | explosion (terrorist act) |
| 9200/88 | RDX + TNT (traces) | RDX + TNT | explosion of a pipe (terrorist act) |
| 6738/88 | PETN + tri- and di-nitrates of PE | PETN | explosion of a car |
| 302/88 | PETN + tri-, di-, and mono-nitrates of PE | PETN | safe "cracking" |
| 100/89 | PETN + tri- and di-nitrates of PE | PETN | safe "cracking" |

*PE = pentaerythritol

It should be noted that the method could not distinguish between RDX and HMX, whose protons have the same chemical shift. Figures 1-3 show NMR spectra of three typical cases.

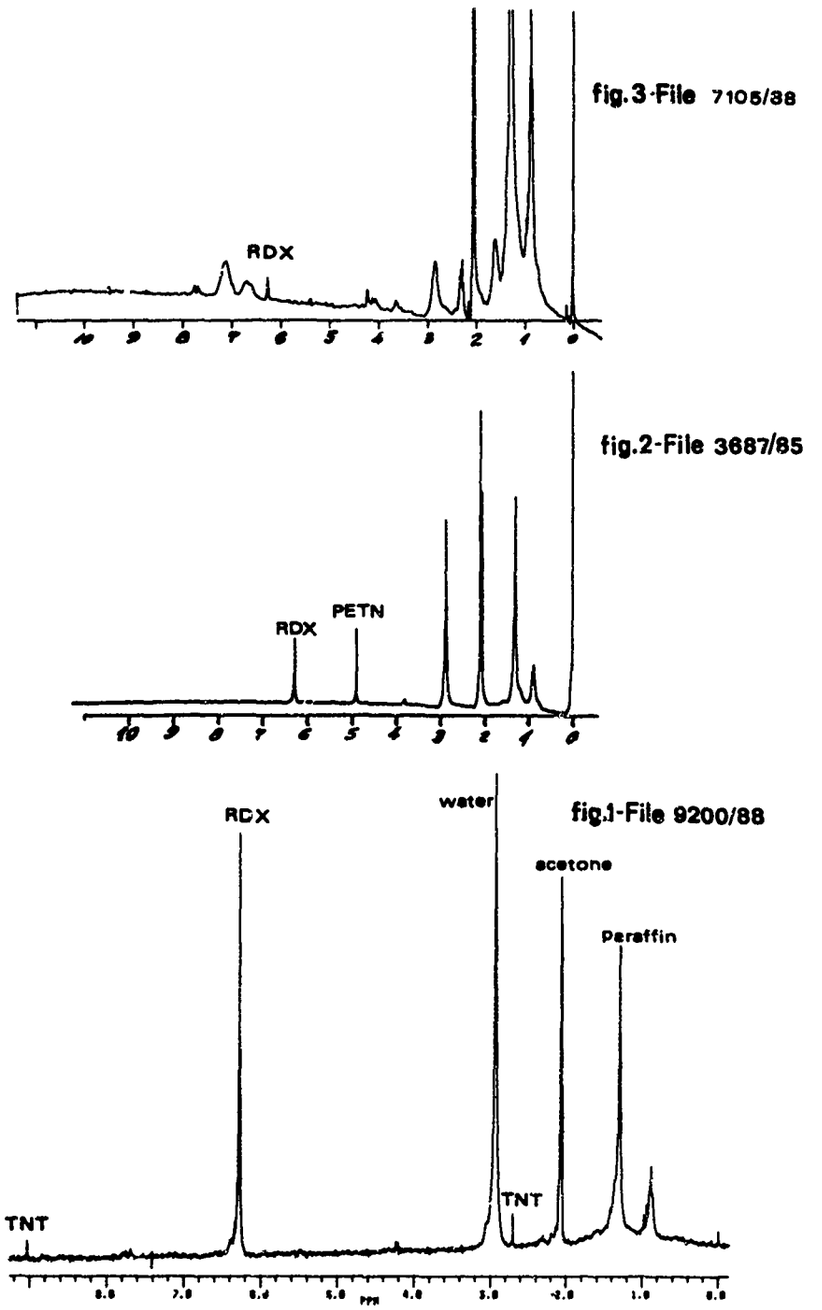


Fig.1,2,3 - Three examples of post-explosion cases identified by proton NMR analysis.

The appearance of the hydrolysis products of PETN in post-explosion extracts containing PETN was previously reported (6,7). They accompany PETN in most of its post-explosion extracts. Usually the trinitrate and dinitrate esters of pentaerythritol (PE) are detected. One case where the mononitrate ester of PE was firstly identified by NMR in a post-explosion extract is shown in Figure 4.

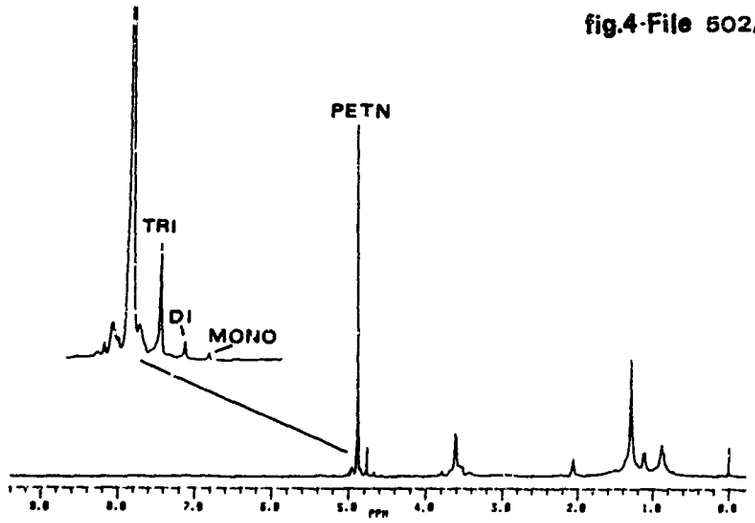


Fig.4 - NMR spectrum of a post-explosion extract containing PETN and tri-, di-, and mononitrate esters of PE.

The molar ratio between all the nitrate esters of PE in this case was: tetranitrate (PETN): trinitrate: dinitrate: mononitrate = 100:10:2:1, respectively.

The ratio between the different nitrate esters of PE could vary in different exhibits from the same explosion. This is demonstrated in a safe "cracking" (Figure 5) where extracts were taken separately from two metal pieces of the broken safe and from the area where the safe was placed. The molar ratio of the nitrate esters of PE was different in the three extracts.

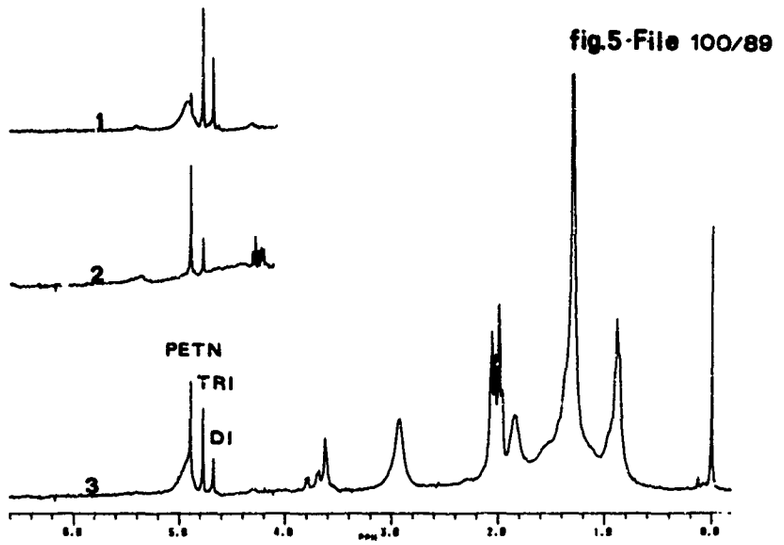


Fig.5 - NMR spectra of three samples collected from a safe cracking site. 1 and 2 are from metal pieces and 3 from the general area at the site.

## 4. CONCLUSIONS

While the reliability of NMR for the identification of organic compounds is well established, it is not considered a method of choice for post-explosion analysis. It seems that the sensitivity of the method would not suffice for the traces of explosive residues, and that other contaminants from the debris would interfere.

This paper demonstrates that in many cases (over 50% from the cases listed above) NMR can be successfully used for the identification of explosives after the explosion. The NMR method is fast, reliable and identifies several explosives in one run, without any pre-separation. The recent developments in NMR instrumentation increased remarkably the compatability of the method for post-explosion analysis.

**REFERENCES**


1. V.D. Hogan and T.A.E. Richter "A New Convenient Tool for Identifying Composite Explosives: Proton-Magnetic Resonance Fingerprinting" Technical Report No. 4790, Picatinny Arsenal, Dover, N.J. (1975).

2. A. Alm, O. Dalman, I. Frolen-Lindgren, F. Hulten, T. Karlsson and M. Kowalska "Analysis of Explosives" FOA Report C 20267-D1 National Defence Research Institute S-104 50 Stockholm, Sweden (1978).

3. H.-D. Schiele and G. Vordermaier, "Proceedings of the International Symposium on the Analysis and Detection of Explosives", Quantico, Va, ed. FBI, 1983 p. 367.

4. S. Zitrin, S. Kraus and B. Glattstein, "Proceedings of the International Symposium on the Analysis and Detection of Explosives", Quantico, Va, ed. FBI. 1983 p. 137.

5. Y. Margalit, S. Abramovitch-Bar, Y. Bamberger, S. Levy and S. Zitrin, J. Energetic Materials, 4, 363 (1986).

6. J. Helie-Calmet and M. Forestier, International Criminal Police Review, 38 (1979).

7. A. Basch, Y. Margalit, S. Abramovitch-Bar, Y. Bamberger, D. Daphna, T. Tamiri and S. Zitrin, J. Energetic Materials, 4, 77 (1986).

# EXPLOSIVES DETECTION WITH AN ION TRAP MASS SPECTROMETER

Scott A. McLuckey, Gary L. Glish, and Barry C. Grant
Analytical Chemistry Division
Oak Ridge National Laboratory
Oak Ridge, TN 37831-8121

## Abstract

The combination of atmospheric sampling glow discharge ionization with mass spectrometry/mass spectrometry provides a powerful approach to the detection of trace quantities of explosives in air. The ion source is operated in such a way as to make it relatively immune to ionization interferences. False alarms are minimized by mass spectrometry/mass spectrometry, which has orders of magnitude greater informing power than other analyzers used in explosives detection. The ion trap mass spectrometer is a promising new device for mass spectrometry/mass spectrometry. A glow discharge ion source has been coupled to an ion trap. Even in its early stage of development it has proved superior to devices that employ more conventional approaches to mass spectrometry/mass spectrometry. Improvements in ion injection into the ion trap, however, are desirable (and are likely).

## Introduction

We have been pursuing the rapid detection of trace quantities of explosives by atmospheric sampling glow discharge ionization (ASGDI) [1] in conjunction with mass spectrometry/mass spectrometry (MS/MS) [2]. Our initial efforts were devoted to the development of an MS/MS instrument with a quadrupole/time-of-flight (QTOF) geometry [3]. During the course of this work, new developments in the analytical capabilities of the three-dimensional quadrupole [4] made this device potentially useful as the MS/MS portion of an explosives detector. A number of critical questions, however, had to be answered before it could be concluded that an explosives detector based on the 3-D quadrupole could replace or even compete with one based on a more conventional MS/MS instrument.

This paper begins by briefly reviewing the ASGDI source as it relates to the ionization of explosives and the general aspects of MS/MS that make it particularly useful for this application. The commercial version of the 3-D quadrupole, Finnigan-Mat's ion trap mass spectrometer (ITMS), is then compared with the QTOF instrument with particular emphasis on relative merits for explosives detection. The remainder of the paper is devoted to illustrating important aspects of the ASGDI source/ITMS explosives detector we have noted over the past eight months. Particular emphasis is placed on the critical questions faced at the outset of this work and on the behavior of some of the common explosives in the ASGDI source/ITMS system.

## Atmospheric Sampling Glow Discharge Ionization for Explosives Detection

A *sine qua non* for mass spectrometry in general is a source of ions. The sample of interest must be converted from its normal state into gas-phase ions before mass analysis. The ionization method is therefore crucial to any analysis based on mass spectrometry. The explosives vapor detection problem requires the formation of ions characteristic of explosives when they are present in a complex mixture, ambient air. The relative concentrations of mixture components, particularly at the parts per million level and below, can vary widely with both location and time. Since it is desirable to detect explosives present at parts per trillion levels and below, an extremely selective ionization method is mandated. We analyze negative ions because, unlike most compounds in nature, explosives readily form anions. Indeed, several other approaches to explosives vapor detection take advantage of this characteristic. These include ion mobility spectrometry (IMS) [5], atmospheric pressure ionization mass spectrometry (APIMS) [6], and gas chromatography/electron capture detection (GC/ECD) [7]. There are, however, differences between the conditions used in the ASGDI source and those used in the other devices that have important ramifications for the ions that are

observed and the susceptibility for interferences. These points are discussed following a brief description of the ASGDI source and its operating conditions.

A side-view schematic of the ASGDI source attached to a quadrupole mass filter is shown in Figure 1. The ionization region is contained within a 6" Conflat flange. A 1 3/4" diameter hole is cut through the center of the flange. Four 1/2" pumpout ports are drilled through the side of the flange. Two aperture plates A1 and A2 are attached to either side of the Conflat flange and are electrically isolated from the flange by Viton O-rings. The O-rings also serve as vacuum seals. A1 contains a 200 μm aperture in its center and is attached to the atmosphere side of the flange. A2 contains an 800 μm aperture in its center and is attached to the vacuum side of the flange. The flange is typically pumped at a rate of ≈8 L/s which gives a pressure in the ionization region of ≈0.7 Torr. Under these conditions, ambient air is drawn into the flange at a rate of ≈5 mL/s. A potential of ≈-400 V is applied to A1 while A2 is typically grounded. Under these conditions a glow discharge spontaneously begins between A1 (cathode) and A2 (anode).

As indicated above, the conditions used in the ASGDI source are significantly different from those used in ionization at atmospheric pressure. These differences and their effects can be appreciated by considering simple pseudo-first order kinetics. Consider the reaction

$$X^- + M \longrightarrow X + M^- \qquad (1)$$

where M is present at a constant concentration throughout the period the reaction can proceed. The number of $X^-$ ions observed after some time t is given by

$$[X^-]=[X^-]_o e^{-k[M]t} \qquad (2)$$

and the number of $M^-$ ions that are formed is given by

$$[M^-]=[X^-]_o(1-e^{-k[M]t}) \qquad (3)$$

where $[X^-]_o$ is the number of $X^-$ ions present at t=0, k is the rate constant for the reaction, and [M] is the number density of M. Under API conditions, flow rates are typically on the order of 1

mL/s giving reaction times on the order of 1 s. Rate constants for fast ion/molecule reactions are on the order of $10^{-9}$ $cm^3$/molec-s. Rate constants for electron capture reactions, i.e.,

$$e^- + M \longrightarrow M^- \qquad (4)$$

can be as high as $10^{-7}$ $cm^3$/molec-s (100 times greater). Electrons are therefore quickly captured in the presence of an electronegative gas forming anions. (The number density of electronegative gases (primarily $O_2$) in air at atmospheric pressure and room temperature is $\approx 4 \times 10^{18}$ $cm^{-3}$.) The number densities of the reactants and the long reaction time result in a distribution of product ions that reflect thermodynamic equilibrium. Provided the rate constants are not too low, both the forward and reverse reactions for an ion/molecule reaction can occur a sufficient number of times to give an equilibrium distribution of reactants and products. Furthermore, number densities are high enough for third-body collisions to occur resulting in the observation of stable adduct ions as indicated below:

$$X^- + M + N \longrightarrow MX^- + N. \qquad (5)$$

In the ASGDI source, number densities are roughly three orders of magnitude lower than in API devices. Furthermore, the residence time of the molecules in the ionization region is typically less than 1 ms. Given such short residence times, ion/molecule reactions can only proceed to an appreciable extent if, assuming a rate constant of $10^{-9}$ $cm^3$/molec-s, the neutral number density is greater than about 20 parts per billion. Product ions only begin to rival the intensities of the background "reagent ions" in the source ($\approx$10% of the total ion current) when the concentration of the analyte is at least 20 parts per million. Therefore, for species present at levels less than 1 ppm the vast majority of negative ions come from electron capture and <u>not</u> ion/molecule reactions.

These differences in operating conditions have several significant effects on the data acquired with these ion sources. The first is that the ions characteristic of the explosive may be

different. For API sources it common to observe $(M-H)^-$ and $(M+X)^-$ ions whereas with the ASGDI source it is common to observe $M^-$ and/or fragment ions. The second effect manifests itself in the susceptibility for interferences. There are typically two types of interferences with most analytical techniques. One occurs when some species other than the analyte gives a signal that is indistinguishable from that of the analyte (MS/MS is used to minimize this interference). The second type occurs when some species alters the signal from the analyte either by suppressing its intensity or by moving it to another part of the spectrum where it is not recognized. An example of the latter would occur when some background species enters the API ionization region in sufficient quantity to change the ion/molecule reaction chemistry leading to a change in the identity of the analyte-related ions. This may involve a change, for example, from $(M+X)^-$ to $(M+Y)^-$. Since ion/molecule reaction chemistry plays essentially no role for low concentration analytes in the ASGDI source, the ions associated with the explosives do not change position on the mass scale despite the presence of large doses of compounds that alter ion/molecule reaction chemistry. The ASGDI source is vulnerable to this type of interference only insofar as it affects the number of electrons and distribution of their kinetic energies. An extreme example occurs when a heavy dose (> 10 parts per thousand) of a halocarbon is used to extinguish the discharge. Our experience with halocarbons at levels insufficient to extinguish the discharge but sufficient to completely alter the distribution of background ions in the ion source is a diminution in signal due to explosives of a factor of 2-3 but no change in the identity of the ions. The ASGDI source, therefore, is relatively immune to interferences of the second type.

## Mass Spectrometry/Mass Spectrometry for Explosives Detection

Explosives detection is a targeted compound analysis problem. MS/MS is now widely recognized as being particularly well-suited to this type of problem [2]. The MS/MS experiment most frequently used for explosives detection involves mass-selection of an

explosives related ion formed in the ion source, inducing collisions with a target gas, and mass analyzing the fragment ions that result from collision-induced dissociation (CID). This process is shown schematically in Figure 2. The combination of the ASGDI source with MS/MS provides for a highly specific form of analysis.

It is difficult to predict *a priori* the false alarm rate for any of the current explosives detectors in a real world scenario. However, it is possible to compare the techniques on the basis of the number of resolution elements in the analysis [8]. The number of resolution elements determines, in part, the informing power of an analytical technique. Informing power correlates with specificity. As a rule, as a mixture becomes more complex, greater informing power is required to distinguish between mixture components. A typical IMS spectrum is ≈20 ms wide and a typical peak width at half height is 1 ms. There are, therefore, ≈20 resolution elements for the ion mobility spectrometer. The overall specificity of the analysis relies heavily on the selectivity afforded by negative ion API. Similarly, for GC/ECD, the resolving power of the GC analysis is determined by the chromatographic resolution. For most GCs used in explosives detection there are, at best, a few hundred resolution elements in the typical chromatogram. The overall specificity of the analysis is enhanced by ECD. In MS/MS, the number of resolution elements is the product of the resolution elements of each stage of MS. For the ITMS, the resolution of each stage of MS is typically 650 (unit mass resolution throughout the mass range). The explosives ions generally fall below m/z 250 so that, realistically, there are about 250 useful resolution elements/stage of MS. The number of resolution elements for MS/MS is therefore ≈62,500. This number may be increased if additional resolution elements are added by varying the parameters that affect the reaction between stages of MS [8]. The specificity of the overall analysis is, of course, enhanced by analyzing negative ions. Informing power is also

determined by the dynamic range of the analysis [8] which further increases the informing power of MS/MS over the IMS and ECD. The informing power of MS/MS is therefore several orders of magnitude greater than any of the other commonly employed vapor detectors.

The sensitivity of an explosives detector employing MS/MS is determined in part by the throughput of the MS/MS instrument. This involves the efficiency of the first stage of MS, the efficiency with which fragment ions are produced from the parent ions, the efficiency of the second stage of MS, and the detection efficiency. These numbers are determined by the mass analyzers, ion optics, and the way in which CID is effected.

The ITMS as the MS/MS Instrument in an Explosives Detector

The figures of merit in comparing MS/MS devices in an explosives detector are sensitivity, specificity, speed, and size. Relative to the QTOF geometry, the ion trap is much smaller, has greater informing power (due to a factor of ten greater mass resolution in the second stage of MS) and therefore superior specificity, and comparable speed. The key to whether or not the ITMS can replace the QTOF is their relative sensitivities. A number of questions must be answered before it can be concluded that the ITMS is the best MS/MS instrument for this application. These questions are as follows:

1.) Does CID occur for the anions of interest under conditions used for MS/MS in the ITMS?

2.) Can ions be injected into the ITMS from the ASGDI source with sufficient efficiency to compete with the QTOF geometry?

3.) To what extent does CID and electron detachment upon ion injection into the ITMS compromise explosives detection?

Each of these questions is discussed below.

We demonstrated CID of polyatomic anions in a standard ITMS system [9]. We found, however, the conversion efficiency, the number of fragment ions formed by CID divided by the number of parent ions prior to CID, to vary widely with different anions.

For the nitroaromatics, for example the molecular anions fragment with conversion efficiencies greater than 10%. The $(M-H)^-$ anions showed conversion efficiencies <1%. (As indicated above, the ASGDI source produces molecular anions for the nitroaromatics.) Apparently electron detachment dominates for the deprotonated molecules. When this situation prevails, MS/MS provides no new information relative to a single stage of mass spectrometry. For the large majority of explosives related anions we have studied conversion efficiencies are seen to be well in excess of 10%. Illustrative examples are shown in the following section.

The second and third questions are related to ion injection into an ion trap. A schematic diagram of the side view of the system we have constructed for this purpose is shown in Figure 3. The figure shows an ASGDI source, a three element lens system, the three electrode ion trap structure, and a conversion dynode/electron multiplier combination. Details of the ion injection experiment with this device have been described [10]. Aspects most relevant to explosives detection are summarized here. The conventional approach to formation of ions in an ITMS is to inject electrons through an end-cap and to form ions by electron impact within the ion trap. This approach is unsatisfactory for explosives detection since electron impact is unselective. Negative ion formation within the ion trap is inhibited by the fact that electrons are not stored within the ion trap resulting in a relatively low electron number density for electron capture. Furthermore, the number density of explosives present in the ITMS after being leaked into the system along with the air matrix to a total pressure of $\approx 10^{-5}$ Torr is extremely low. Therefore, it is necessary to form anions from the explosives in a region with a high electron number density such as the ASGDI source.

We find that the injection efficiency, defined as the number of ions detected after being trapped in the ITMS divided by the number of ions that exit the ion source during the injection period, for the molecular anion of TNT is roughly 1% under optimum

conditions. This is comparable to the transmission of high mass ions through the quadrupole in the QTOF instrument. The conversion efficiency in the MS/MS experiment in the ITMS for the molecular anion of TNT is roughly 30%. The conversion efficiency in the QTOF for this anion is a few tenths of a percent. The improvement in MS/MS sensitivity is therefore several orders of magnitude. This indicates that, at least for some of the explosives, the ASGDI source/ITMS system is superior to the QTOF system since the former is smaller, more specific, more sensitive, and has comparable speed. The same conclusion cannot, however, yet be drawn for all of the possible explosives of interest. This is addressed by our third question.

CID has been observed to occur concurrently with ion injection into an ion trap for some ions. For anions, the competing reaction of electron detachment can also occur upon injection. We have noted that the relative amount of CID is minimized by the addition of He bath gas into the vacuum system to a pressure of a few mTorr. (This also significantly enhances injection efficiency.) Nevertheless, this does not eliminate CID. CID is most likely for particularly fragile anions. (Electron detachment is most likely for ions with low electron affinities. The anions from explosives tend to have quite high electron affinities. Electron detachment upon injection is not expected to be a problem for the explosives.) CID can affect the overall analysis by spreading the charge among several different ions and by decreasing the intensities of the high mass ions. The latter ions are most informative for MS/MS. To date, this appears to be a problem primarily for the nitrate esters. Ions from the nitrate esters tend to readily fragment to the $NO_3^-$ ion. As shown below, MS/MS of the $NO_3^-$ ion can be used to detect nitrate esters. However, for greater specificity, it is desirable to analyze higher mass anions.

We are learning more about CID in the ion trap and have proposed measures that may both increase injection efficiency and decrease CID upon injection. Future efforts will be made to test

these ideas. However, until they are demonstrated, we base our conclusions on the ASGDI source/ITMS combination upon its present configuration and operating procedures. The following section is devoted to describing some of our observations in explosives detection with the ITMS in its present configuration. Some of these data illustrate observations made in this section.

Behavior of Explosives in the ASGDI source/ITMS System

This section illustrates notable features of the ASGDI source/ITMS combination in the detection of explosives in ambient air. Figure 4 illustrates the high conversion efficiency in MS/MS frequently observed for explosives related anions. The top spectrum shows the $(M-NO_2)^-$ anion (m/z 176) from RDX, the major high mass ion formed in the ion source, isolated from all other ions after injection into the ion trap. The bottom spectrum shows the MS/MS spectrum. The m/z 102 fragment ion resulting from the loss of $CH_2NNO_2$ is by far the major product. The conversion efficiency is roughly 65%. This compares very favorably with the conversion efficiency of a few tenths of a percent in the QTOF instrument.

The base peak in the ASGDI mass spectrum of the nitrate esters EGDN, NG, and PETN is m/z 62, the $NO_3^-$ anion. Higher mass ions are also present in the QTOF instrument. However, the intensities of the higher mass ions in the ITMS system are greatly diminished, presumably due to CID upon injection. An ion at m/z 62 is always present in the background mass spectrum. We do not perform MS/MS on this ion in the QTOF instrument due to the relatively poor mass resolution of the TOF portion of the instrument. We have found with MS/MS in the ITMS system that the background ion at m/z 62 has a different structure than the m/z 62 formed from the nitrate esters. A comparison of MS/MS spectra is shown in Figure 5. The top spectrum is the spectrum obtained from the background ion. It fragments predominantly to give m/z 32, $O_2^-$. The bottom spectrum shows the MS/MS spectrum of the m/z 62 ion from EGDN. The major product ion appears at m/z 46 and is due to O loss to give $NO_2^-$. We have performed ab initio calculations on the $NO_3^-$ system [11] and

find two stable structures for $NO_3^-$. These observations make MS/MS of the m/z 62 anion useful for the detection of the nitrate esters. For example, Figure 6 shows the MS/MS spectrum of m/z 62 obtained from a vapor sampling of SEMTEX-H. The presence of PETN is clearly indicated by the appearance of the ion at m/z 46, $NO_2^-$. (The signal at m/z 60 is from $CO_3^-$ not removed in the initial mass selection stage and the signal at m/z 62 is undissociated $NO_3^-$.)

We have noted that black powder can be detected with this system by monitoring the signal in the mass spectrum at m/z 96. This is illustrated in Figure 7 which shows the mass spectrum over the region of m/z 50-130 in the absence of black powder (top) and when the head space of a vial of black powder is sampled (bottom). The m/z 96 anion is $S_3^-$. Black powder can therefore be detected by monitoring sulfur rather than detecting a nitro compound.

Figure 8 illustrates the current performance of the ASGDI source/ITMS combination with respect to sensitivity. The figure shows a partial mass spectrum obtained by sampling the head space vapor over a sample of TNT. Peaks appear at m/z 227 ($M^{-\cdot}$), m/z 210 $(M-OH^{\cdot})^-$, and m/z 197 $(M-NO^{\cdot})^-$. These signals are obtained in a single scan of the ITMS using an injection time of only 0.3 ms. Assuming that a TNT concentration of few ppb are sampled, the quantity of TNT drawn into the system during this period is roughly 50 fg. The TNT signals increase linearly with injection time over several orders of magnitude. Therefore lower concentrations give similar signals at longer injection times. Injection times can be extended up to several seconds.

## Conclusions

The combination of ASGDI with MS/MS is a powerful approach to trace explosives detection. The combination of sensitivity, specificity, and speed is unsurpassed in current approaches to vapor detection. Even in its early stage of development, the ASGDI source/ITMS combination is superior to the QTOF geometry device in most respects. Sensitivity is comparable or better, specificity

is significantly better, speed is comparable, and size is significantly reduced. A drawback is the extent of CID upon injection observed for some anions. This requires the nitrate esters to be detected using the $NO_3^-$ ion. The resolution of the second stage of MS makes this possible but the use of a higher mass ion would be preferred. As our understanding of ion injection into the ion trap grows we anticipate improvements in injection efficiency and better control over the extent of CID upon injection. Any improvements in these areas will enhance sensitivity and specificity.

## Acknowledgement

The authors acknowledge helpful discussions with Dr. Michael Weber-Grabau of Finnigan Corp. throughout this work. This research is supported by the U.S. Department of Energy, Office of Safeguards and Security, under Contract DE-AC05-840R21400 with Martin Marietta Energy Systems, Inc.

"The submitted manuscript has been authored by a contractor of the U S Government under contract No DE-AC05-840R21400 Accordingly the U S Government retains a nonexclusive, royalty-free license to publish or reproduce the published form of this contribution, or allow others to do so, for U S Government purposes."

## References

1. S.A. McLuckey, G.L. Glish, K.G. Asano, and B.C. Grant Anal. Chem., 60 (1988) 2220.

2. K.L. Busch, G.L. Glish, and S.A. McLuckey, "Mass Spectrometry/Mass Spectrometry: Techniques and Applications of Tandem Mass Spectrometry", VCH Publishers, New York, 1988.

3. G.L. Glish, S.A. McLuckey, and H.S. McKown Anal. Instrum., 16 (1987) 191.

4. R.E. March and R.J. Hughes, "Quadrupole Storage Mass Spectrometry", John Wiley and Sons, New York, 1989.

5. G.E. Spangler and M.J. Cohen in "Plasma Chromatography", T.W. Carr (Ed.), Plenum Publishing Corp., New York, 1984.

6. B.A. Thomson, W.R. Davidson, and A.M. Lovett, Environ. Health Perspectives, 36 (1980) 77.

7. J.R. Hobbs, U.S. D.O.T. Report No. FAA-RD-74-134, Transportation Systems Center, Cambridge, MA (1974).

8. D.D. Fetterolf and R.A. Yost, Int. J. Mass Spectrom. Ion Proc., 62 (1984) 33.

9. S.A. McLuckey, G.L.Glish, and P.E. Kelley, Anal. Chem., 59 (1987) 1670.

10. S.A. McLuckey, G.L. Glish, and K.G. Asano, Anal. Chim. Acta, In Press.

11. R.A. Flurer, S.A. McLuckey, and G.L. Glish. "Proceedings of the 37th ASMS Conference on Mass Spectrometry and Allied Topics", Miami Beach, FL, 1989, In Press.

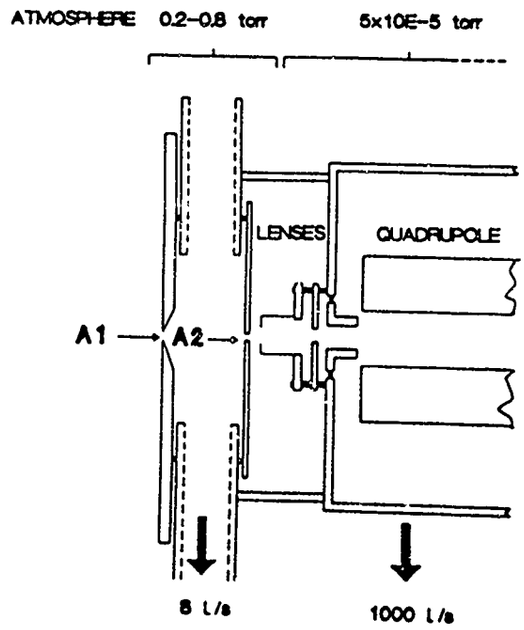


Figure 1- Side-view schematic of the atmospheric sampling glow discharge ionization source attached to a quadrupole mass filter.

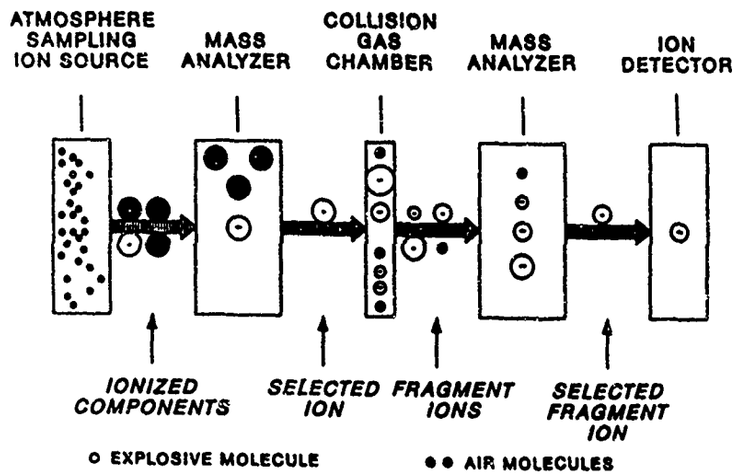


Figure 2- Generalized schematic approach to explosives detection using mass spectrometry/mass spectrometry.

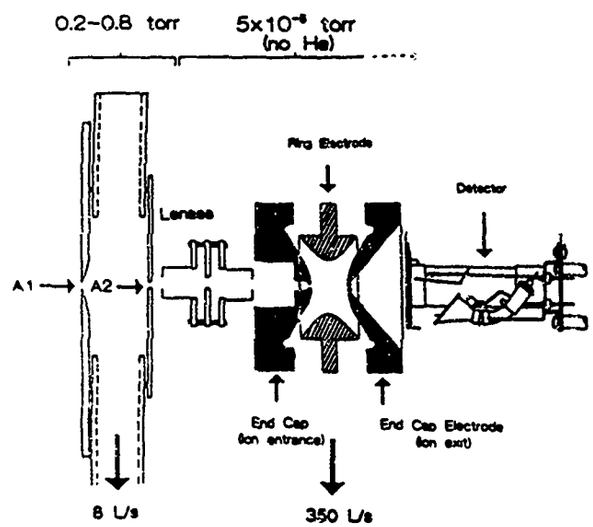


Figure 3- Schematic diagram of the ASGDI source/ITMS combination.

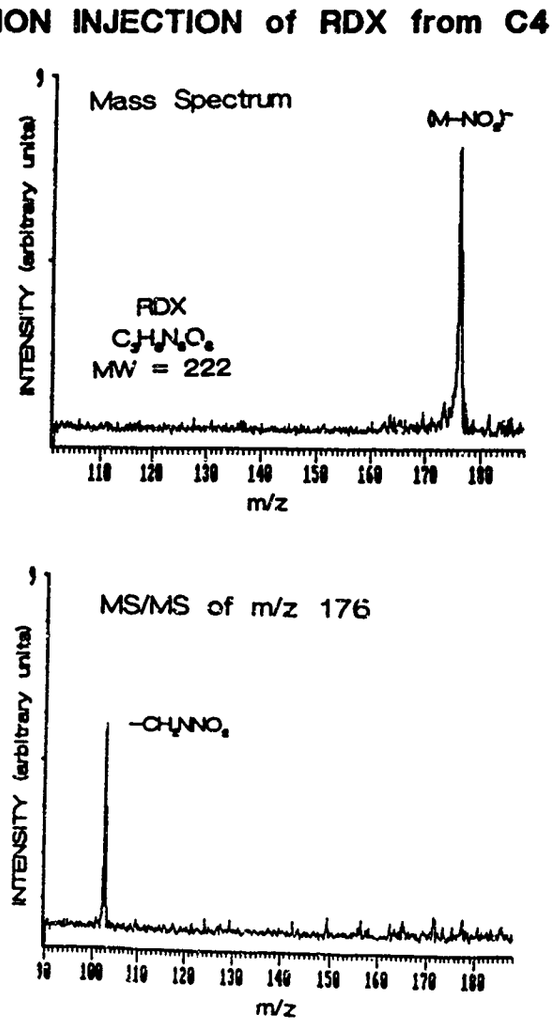


Figure 4- MS/MS of the m/z 176 anion from RDX $(M-NO_2)^-$. The top spectrum shows the m/z 176 ion injected from the ASGDI source isolated from all other ions. The bottom spectrum shows the m/z 102 anion from CID of the m/z 176 anion.

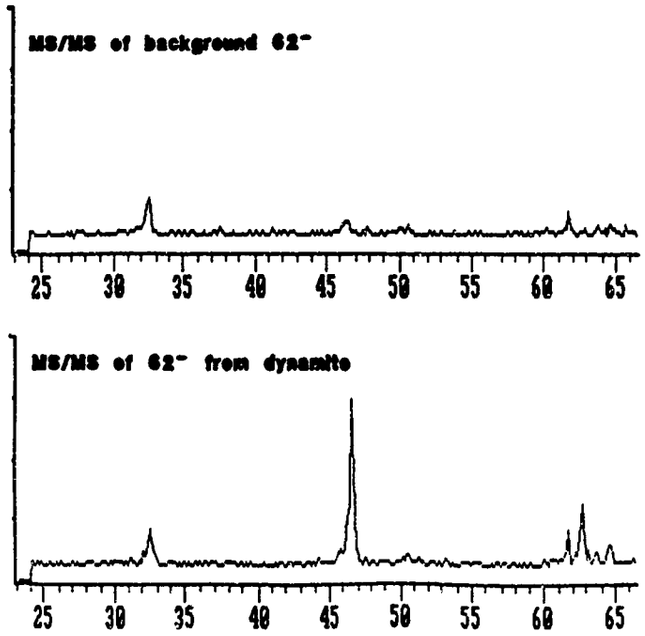


Figure 5- MS/MS spectra of m/z 62 anions: background $NO_3^-$ from the ASGDI source (top), $NO_3^-$ from nitrated dynamite (bottom).

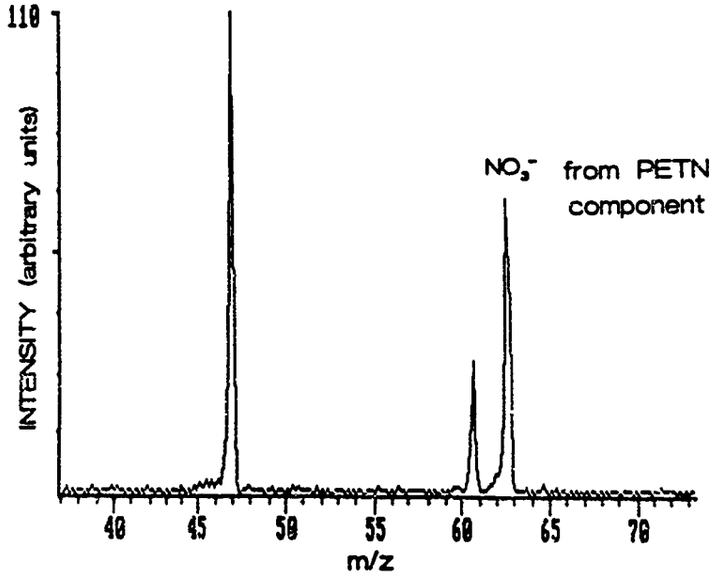


Figure 6- MS/MS spectrum of $NO_3^-$ from SEMTEX-H.

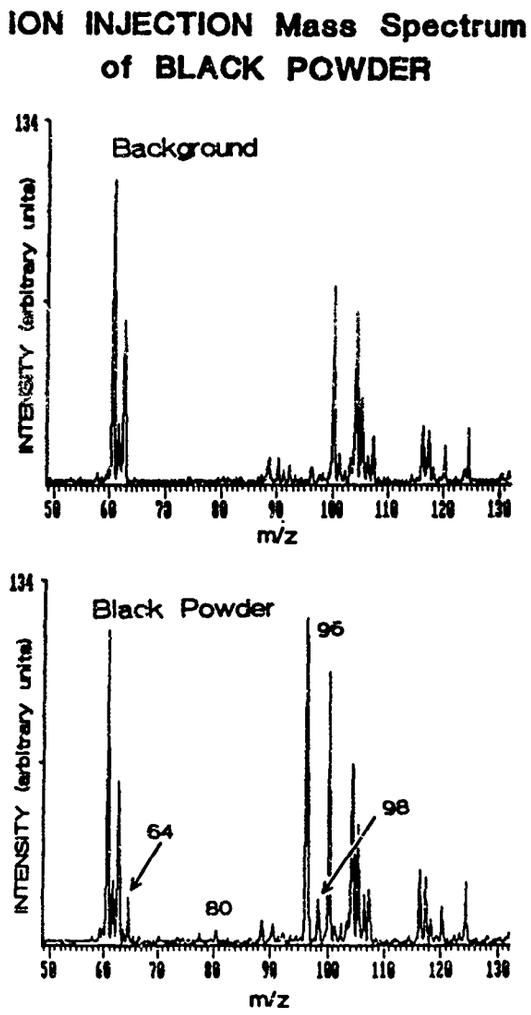


Figure 7- Mass spectra of background ions injected from the ASGDI source (top) and when vapors over black powder are sampled by the ion source (bottom).

## ION INJECTION Mass Spectrum of TNT

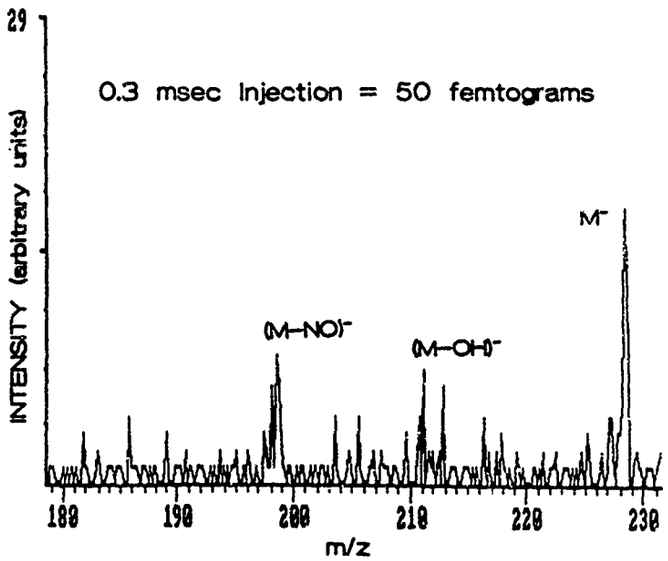


Figure 8- Mass spectrum of a few ppb of TNT in air obtained using an ion injection period of 0.3 ms.

# IDENTIFICATION AND CONFIRMATION OF SOME NITROCAGE COMPOUNDS AND EXPLOSIVES BY DEPMS

T.H. Chen and C. Campbell
U.S. Army Armament, Research, Development, and Engineering Center,
Picatinny Arsenal, N.J. 07806-5000

## ABSTRACT

In the synthesis of new, polynitrocage compounds, it is essential to identify and confirm the compound synthesized in each step. The techniques which are used most often include mass spectrometry, nuclear magnetic resonance, infrared spectrophotometry and x-ray diffraction technique. We found that the direct evaporation probe mass spectrometric technique (DEPMS) to be extremely useful in providing the molecular weight information and the structural features of the new nitrocage compounds. This technique was also found to be very useful in the identification of labile explosives and propellants.

This paper will describe the experimental conditions and discuss the results obtained.

## 1. INTRODUCTION

In the synthesis of new, polynitrocage compounds, it is essential to identify and comfirm the compound synthesized in each step. For this purpose, a mass spectrometric technique with a DEP in the positive ion chemical ionization (PICI) mode using methane is explored. Aside from our work[1], we are not aware of any investigations in this area. This technique, ideal for studying labile and nonvolatile compounds, enables the determination of molecular weight as well as structural features using only a minute quantity of sample. This technique was also found to be very useful in the identification of

nonvolatile explosives and labile propellants. This paper will briefly describe the experimental technique and discuss the results obtained including pseudomolecular ions, ions resulted from the compound of interest and reagent ions and other ions, and fragmentation patterns.

## 2. EXPERIMENTAL

A Finnigan Model 1020 B Mass Spectrometer was used in the low resolution study. In the DEP experiments, a small droplet of the sample solution in acetone with a concentration of approximately 1 μg/μl was carefully deposited on the loop of the heating wire. The solvent was allowed to evaporate at room temperature. In several instances where appropriate solvents for the samples could not be found, a very small speck of solid sample was deposited on the loop of the heating wire directly. This method did not work well due to easy loss of the sample during sample deposition and maneuvering of the DEP into the ion source.

The dried sample was introduced into the mass spectrometer through the direct solid insertion probe inlet and the scanning program initiated just prior to the insertion of the sample into the ion source in order to prevent loss of more volatile species. The ion source pressure was maintained at about 0.3-0.5 Torr. Immediately following the insertion of the sample into the ion source, the sample was heated rapidly at the rate of 10mA/sec, corresponding approximately to 10°C/sec to 1 A. The analysis time was approximately 100 seconds. The DEP was then backed off from the ion source and flashed for about 3 seconds at 1.2 A.

For PICIDEP high resolution MS (PICIDEPHRMS) using methane, Finnigan Model 8230 Mass Spectrometer was used. In this experiment, manual control of the desorption chemical ionization (DCI) emitter temperature and manual peak-matching versus an appropriate standard which was peak-matched vs. perfluorokerosene using electron ionization, were employed.

## 3. RESULTS AND DISCUSSION

The results of the DEP experiments are summarized in Figures 1 - 16. The identification and confirmation of a target compound in the synthesis was based on the assignment of the molecular weight-related ions, i.e., $MH^+$, $(M-H)^+$, $(M+C_2H_5)^+$, $(M+C_3H_5)^+$, and $(M+MH)^+$, the fragmentation pattern, and the comparison of the mass chromatogram of $MH^+$ or $(M-H)^+$ with the reconstructed ion chromatogram (RIC) of the compound being studied. BP denotes base peak.

Dinitrocyclopropane (DNCP) exhibits a simple mass spectrum (Figure 1) dominated by the $(M+1)^+$. Although quite weak in intensity, $(M+29)^+$ and $(M+41)^+$ were observed. The multimass chromatograms suggest that the $(M+1)^+$ fragments to m/e 86 by a loss of $HNO_2$ followed by a loss of oxygen to m/e 70. The peak at m/e 114 may be derived from $(M+29)^+$ by a loss of $HNO_2$. The peak at m/e 151 is likely to be $(M+H_3O)^+$.

1, 3, 3-Trinitroazitidine (TNAZ) also displays simple mass spectrum (Figure 2) with $(M+1)^+$ as the base peak. The $(M+29)^+$ and $(M+41)^+$, although low in abundance, support the $(M+1)^+$ assignment. Purity of TNAZ was quite high as the mass chromatogram of $(M+1)^+$ matches very well with the RIC of TNAZ. The $(M+1)^+$ fragments to m/e 146 by a loss of $HNO_2$, then to m/e 100 by a loss of $NO_2$. The peak at m/e 211 is probably $(M+H_3O)^+$.

1, 4-Dinitrocubane (DNC) undergoes considerable degradation forming a high abundance of low mass fragments with a base peak at m/e 90 (Figure 3). While the intensity of the $(M+41)^+$ is significant (~10%), the usually observed ion, i.e., $(M+29)^+$ is entirely missing from the spectrum. Instead, $(M+30)^+$ appeared in significant abundance (~10%). This apparent anomaly is noteworthy and arises most likely from the ion-molecule reaction of $NO^+ + M$ to form $(M+NO)^+$.

A PICIDEPHRMS experiment using methane was performed to measure the accurate masses of $(M+30)^+$ and $(M+41)^+$. The accuracy of the exact mass measurement was 20 ppm. The results are shown in Table 1. The results established m/e 224.0285 and 235.0714 to be

$C_8H_6N_3O_5$ and $C_{11}H_{11}N_2O_4$, respectively. This experiment confirmed the assignments of $(M+30)^+$ and $(M+41)^+$ as $(M+NO)^+$ and $(M+C_3H_5)^+$, respectively. The differences between the determined masses, i.e., 235.0285 and 235.0714, and corresponding theoretical values, 224.0307 and 235.0719 are -9.8 and -2.1 ppm, respectively, a good agreement. The mass spectrum obtained during this experiment is shown in Figure 4. It is not surprising that although the main features are identical, the ion abundances in Figure 3 and 4 are significantly different. The mass chromatogram of DNC resembles closely to its RIC indicating that the sample is quite pure.

The RIC of cubane 1, 4-bisammoniumtrinitromethide (CBATNM) is quite complex in contrast to the extremely simple mass chromatogram of $(M+1)^+$. Thus, the CBATNM sample appears to be quite impure. As might be expected in the case of a salt the multi-mass chromatograms revealed very weak $(M+1)^+$ and no $(M+29)^+$ and $(M+41)^+$ (see Figure 5). The fragments at m/e 269 (BP) and 134 can be ascribed to $[C_8H_6NH_2NH_3C(NO_2)_2NO]^+$ and $[C_8H_6(NH_2)]^+$, respectively.

The relatively close similarity of the RIC and the chromatogram of $(M+1)^+$ of 1, 2 dinitronoradamantane (DNNA) indicates the relatively high purity of the sample. The intensity of $MH^+$ is very high (~85%) and $(M+29)^+$ and $(M+41)^+$ can be easily observed (Figure 6). It should be noted that a high abundance of $(M+MH)^+$ (~50%) is also observed in this case. The $(M+MH)^+$ can be used as an additional evidence to identify the $MH^+$. The former fragments to 378 by the loss of $HNO_2$ while the latter fragments to m/e 166 by the loss of $HNO_2$, then to m/e 136 by the loss of NO. During this experiment, the effects of temperature and $(M+1)^+$ intensity on the relative intensities of $(M+MH)^+$, $(M+MH)^+-HNO_2$, $(M+41)^+$, $(M+1)^+$, and $(M+1)^+-HNO_2$ were observed. As the temperature rises with the corresponding increase in the relative intensities of the $(M+1)^+$ and $(M+41)^+$, the $(M+29)^+$, $(M+MH)^+$, $(M+MH)^+-HNO_2$, and $(M+1)^+-HNO_2$ decreased. In fact, at higher temperatures, the $(M+MH)^+$ and $(M+MH^+)-HNO_2$ disappears while $(M+41)^+$ increases to more than 50% of the $(M+1)^+$ (BP).

Comparison of the RIC and the mass chromatogram of the $(M+1)^+$ of 1-trinitromethyladamantane (TNMA) reveals the sample to be relatively pure. It should be noted that instead of $(M+1)^+$, $(M-1)^+$ is formed

predominantly and the $(M+29)^+$ was not observed while $(M+41)^+$ was observed in very low abundance (Figure 7). As in the case of DNC, the peak at m/e 315 probably arises from $(M+NO)^+$. It should also be noted that the peak at m/e 135 (BP) overshadows the other fragment ions. The $(M+1)^+$ fragments to m/e 239 by the loss of $HNO_2$, to m/e 193 by the loss of $NO_2$, to m/e 163 by the loss of NO, then to m/e 135 by the loss of CO.

The mass spectrum of 1-amino 3,5,7-trinitroadamantane (ATNA) is shown in Figure 8. Although the abundance of $MH^+$ is significant (~20%), the $(M+29)^+$ and $(M+41)^+$ were not observed. 316 probably results from $M+NO^+$ reaction. $MH^+$ fragments primarily to 240 (BP) by the loss of $HNO_2$.

The close resemblance of the RIC and the mass chromatogram of the $(M+1)^+$ of 1,3,5,7-tetranitroadamantane (TNA) indicated the sample to be quite pure. The profile of the RIC is unusual and this is attributed to the uneven sample coating thickness of the probe wire which gives rise to uneven heating of the sample. The mass spectrum of TNA (Figure 9) exhibits 270 as the base peak with significant abundance of $MH^+$, $(M+29)^+$, and $(M+41)^+$. The $MH^+$ fragments to m/e 270 by the loss of $HNO_2$, to m/e 240 by the loss of NO, to m/e 194 by the loss of $NO_2$, to m/e 164 by the loss of NO to m/e 148, then to m/e 132, $C_{10}H_{12}$, by the loss of O.

Figure 10 shows the mass spectrum of a sample submitted as a 8,8,11,11,-tetranitropentacycloundecane (TNPCU). However, the identifications of m/e 501, 291, 280, 279, and 251 respectively as $(M+MH)^+$, $(M+41)^+$, $(M+NO)^+$, $(M+29)^+$, and $MH^+$ establish the compound to be 8-keto, 11,11,-dinitropentacycloundecane. The $MH^+$ fragments to m/e 204 by the loss of $HNO_2$, to m/e 176 by the loss of CO, then to m/e 130 by the loss of $NO_2$.

The mass spectrum of 4,4,8,8,11,11,-hexanitropentacycloundecane (HNPCU) (Figure 11) shows rather low abundances of $MH^+$, $(M+29)^+$, $(M+30)^+$, and $(M+41)^+$. The $(M+30)^+$ is very likely to be $(M+NO)^+$. The $MH^+$ fragments to m/e 370 by the loss of $HNO_2$, then to m/e 294 (BP) by the losses of $NO_2$ and NO.

Figure 12 shows the mass spectrum of RDX. The molecular weight-related ions, i.e., the peaks at m/e 223, $MH^+$, m/e 252, $(M+NO)^+$, and m/e 263 $(M+C_3H_5)^+$ are relatively low in abundance, especially $(M+C_3H_5)^+$. Other low abundant ions include m/e 176, $(MH-HNO_2)^+$ and m/e 115. The abundant ions are m/e 75, $(CH_2NNO_2+H)^+$, m/e 149, $[(CH_2NNO_2)_2+H]^+$, m/e 103, and m/e 105 in the decreasing order of abundance.

In the case of HMX (Figure 13), only m/e 75, $(CH_2NNO_2+H)^+$ and m/e 105 are the relatively abundant ions. The other ions are low in abundance which include m/e 149, $[(CH_2NNO_2)_2+H]^+$, m/e 103, m/e 115, m/e 223, $[(CH_2NNO_2)_3+H]^+$, m/e 177 and m/e 297, $MH^+$. Except m/e 149 and m/e 103, the abundance of these ions are very low. The molecular weight-related ions for NG are m/e 228, $MH^+$, m/e 257, $(M+NO)^+$, and m/e 273, $(M+NO_2)$, all in significant abundance (Figure 14). The most abundant ion at the peak m/e 165, $(MH-HONO_2)^+$, results from the loss of $HONO_2$ from $MH^+$. The low abundant ions include m/e 212, m/e 183, and m/e 120.

Using the present technique, the structural features of NC can be readily obtained. In Figure 15 and 16, the mass spectra of NC samples with 12.0 and 14.0% nitrogen content are shown. The structural features can be explained in large part by assuming the peak at m/e 281 and m/e 131 to be $[CH_2ONO_2(CHONO_2)_2(CH)_2CHO]^+$, the totally nitrated glucose unit minus linking oxygens, and $[(CH)_2CHOH\ CHONO_2]^+$, respectively and the following fragmentation schemes. The m/e 281 fragments to m/e 251 by the loss of NO, or m/e 235 by the loss of $NO_2$, to m/e 206 by the loss of CHO, to m/e 189 by the loss of OH, to m/e 159 by the loss of NO, or m/e 143 by the loss of $NO_2$, then to m/e 97 by the loss of $NO_2$. Similarily, m/e 131 fragments to m/e 101 by the loss of NO, or to m/e 85 by the loss of $NO_2$, then to m/e 69 by the loss of an oxygen atom.

## 4. CONCLUSION

The DEPCIMS under our experimental conditions were found to be extremely useful in obtaining the molecular ion information and the structural features of the new nitrocage compounds studied. Thus,

in all cases except one, $(M+1)^+$ ions were observed. TNMA was the exception which formed $(M-1)^+$ ion. In almost all cases, the assignment of $(M+1)^+$ or $(M-1)^+$ were supported by the observations of the $(M+C_2H_5)^+$, $(M+NO)^+$, and $(M+C_3H_5)^+$. In a few cases, additional support was provided by the observation of $(M+MH)^+$. Furthermore, the fragmentation patterns revealed sufficient structural features of the compounds studied. This technique was also found to be useful in the identification of labile explosives and propellants, especially for nitrocellulose.

## ACKNOWLEDGEMENT

The authors are indebted to many of our colleagues and others for providing the precious nitrocage compounds; DNCP by Dr. P. Wade, TNAZ by Drs. O. Sandus and D. Stec, DNC by Dr. D. Stec, CBATNM by Dr. R.S. Damavarapu, DNNA, ATNA, and TNA by Dr. G. Sollot, TNMA by Dr. C. Capellos, TNPCU and HNPCU by Prof. A.P. Marchand. The authors are especially grateful to Dr. G. Collins of Finnigan MAT and Dr. T. Hartman of Rutgers University for the arrangement of high resolution experiment and to Dr. D. Burinsky and Mr. R. Dunphy for helpful discussions.

## REFERNCES

1. T.H. Chen and C. Campbell, "Identification and confirmation of Nitrocage and Related Compounds and Their Intermediates By Mass Spectrometric Techniques," Report of the Seventh Annual Working Group Meeting on Synthesis of High Density Materials, Parsippany, N.J., 162-192, 1988.

SSX: ELIST for DNC.DAT;3 using RICH.ELM;1
Finnigan MAT May 1 89 10:20:04 Page: 1

Spectrum Number 1

| Mass | Intensity BASE | Diff PPM | C 12 | H 1 | N 14 | O 16 |
|---|---|---|---|---|---|---|
| 224.0285 | 100.00 | -9.8 | 8 | 6 | 3 | 5 |
| 224.0285 | 100.00 | 40.3 | 9 | 6 | 1 | 6 |
| 224.0285 | 100.00 | -65.9 | 9 | 8 | 2 | 5 |
| 224.0285 | 100.00 | -15.8 | 10 | 8 | 0 | 6 |
| 235.0714 | 100.00 | 9.3 | 8 | 13 | 1 | 7 |
| 235.0714 | 100.00 | -92.0 | 8 | 15 | 2 | 6 |
| 235.0714 | 100.00 | -44.2 | 9 | 15 | 0 | 7 |
| 235.0714 | 100.00 | 51.4 | 10 | 9 | 3 | 4 |
| 235.0714 | 100.00 | 99.2 | 11 | 9 | 1 | 5 |
| 235.0714 | 100.00 | -2.1 | 11 | 11 | 2 | 4 |
| 235.0714 | 100.00 | 45.7 | 12 | 11 | 0 | 5 |
| 235.0714 | 100.00 | -55.6 | 12 | 13 | 1 | 4 |

*** ELIST Processing complete ***

Table 1. Accurate Mass Measurement of m/e 224 and m/e 235

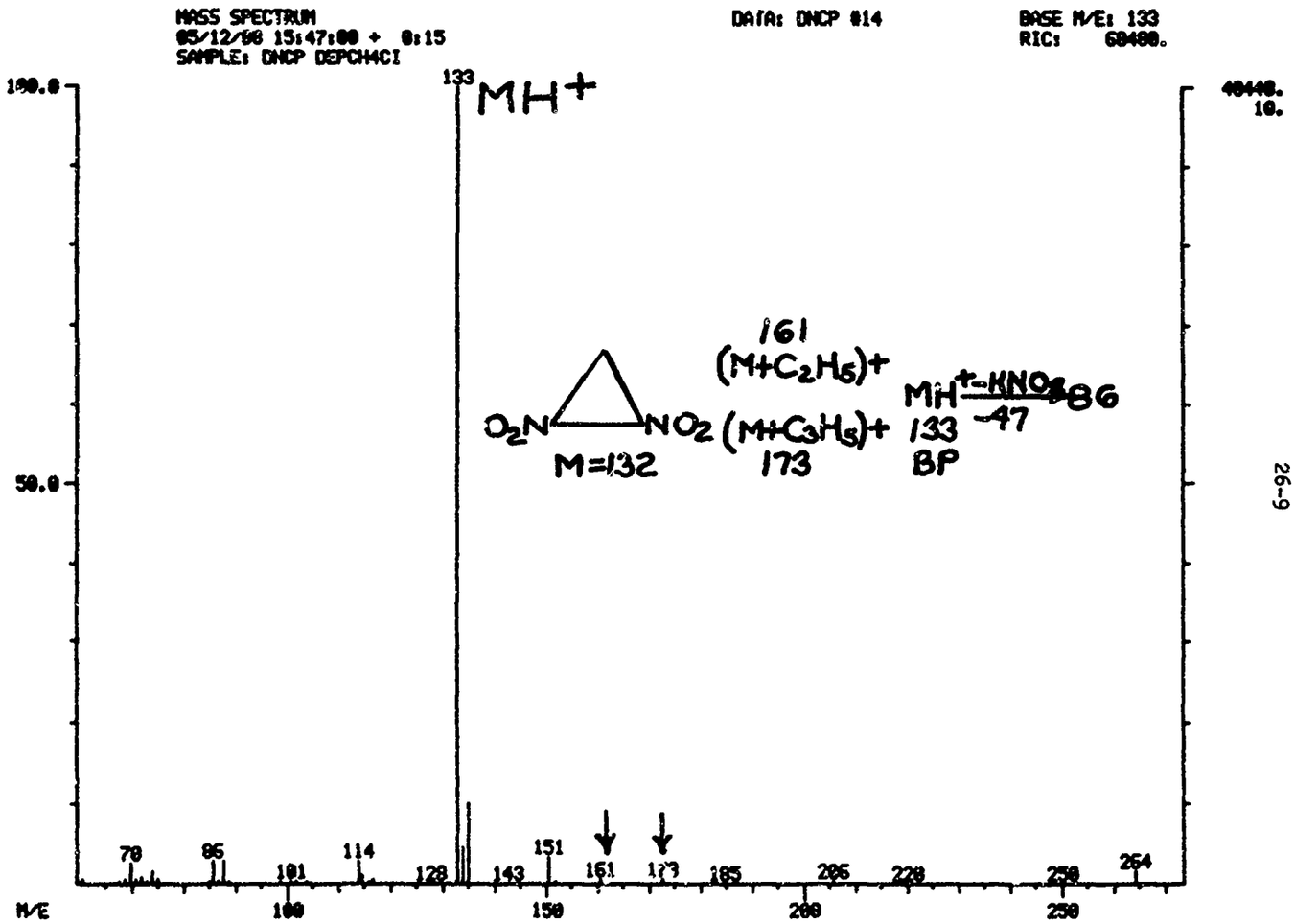


Figure 1. Mass Spectrum of DNCP, Scan # 14

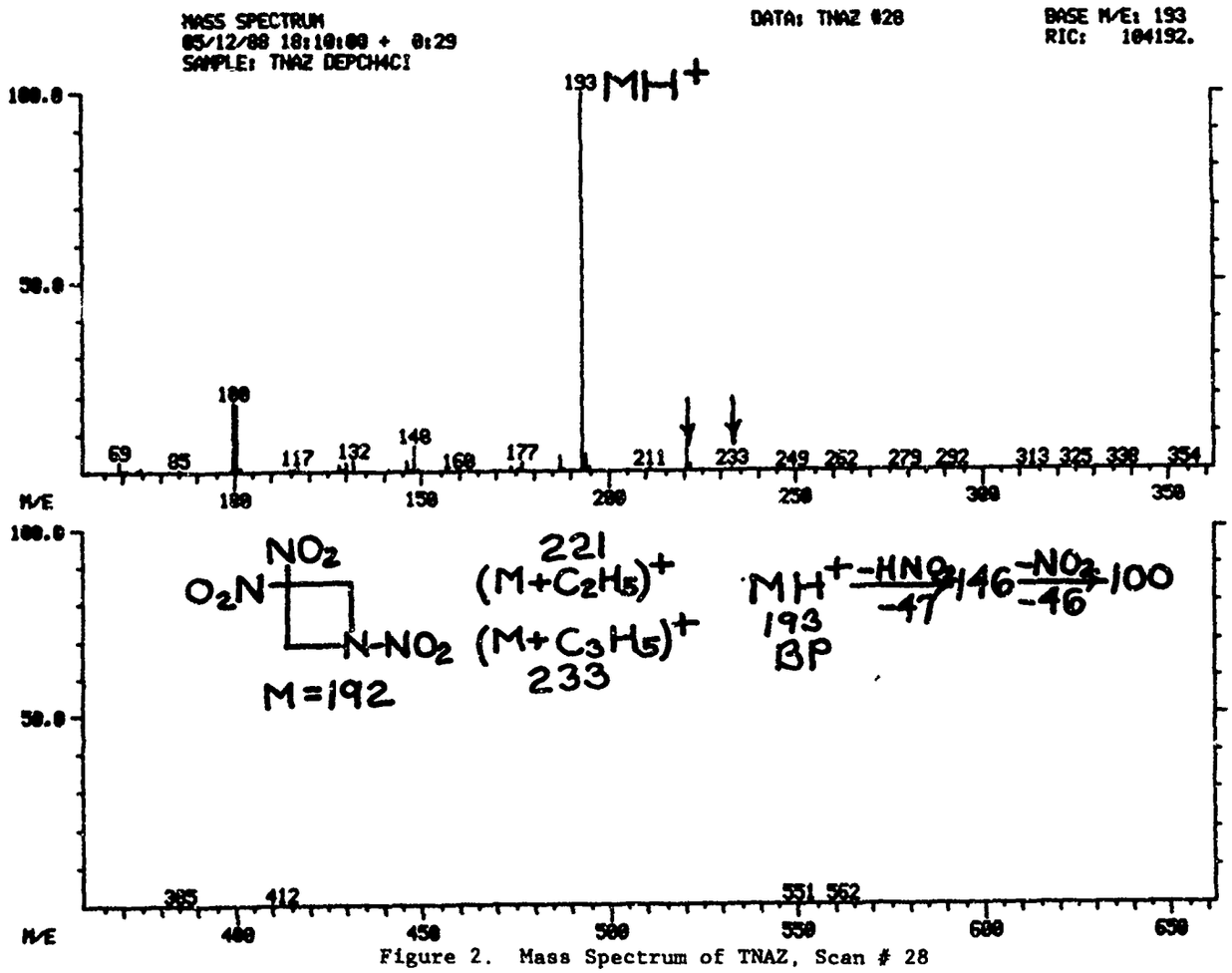


Figure 2. Mass Spectrum of TNAZ, Scan # 28

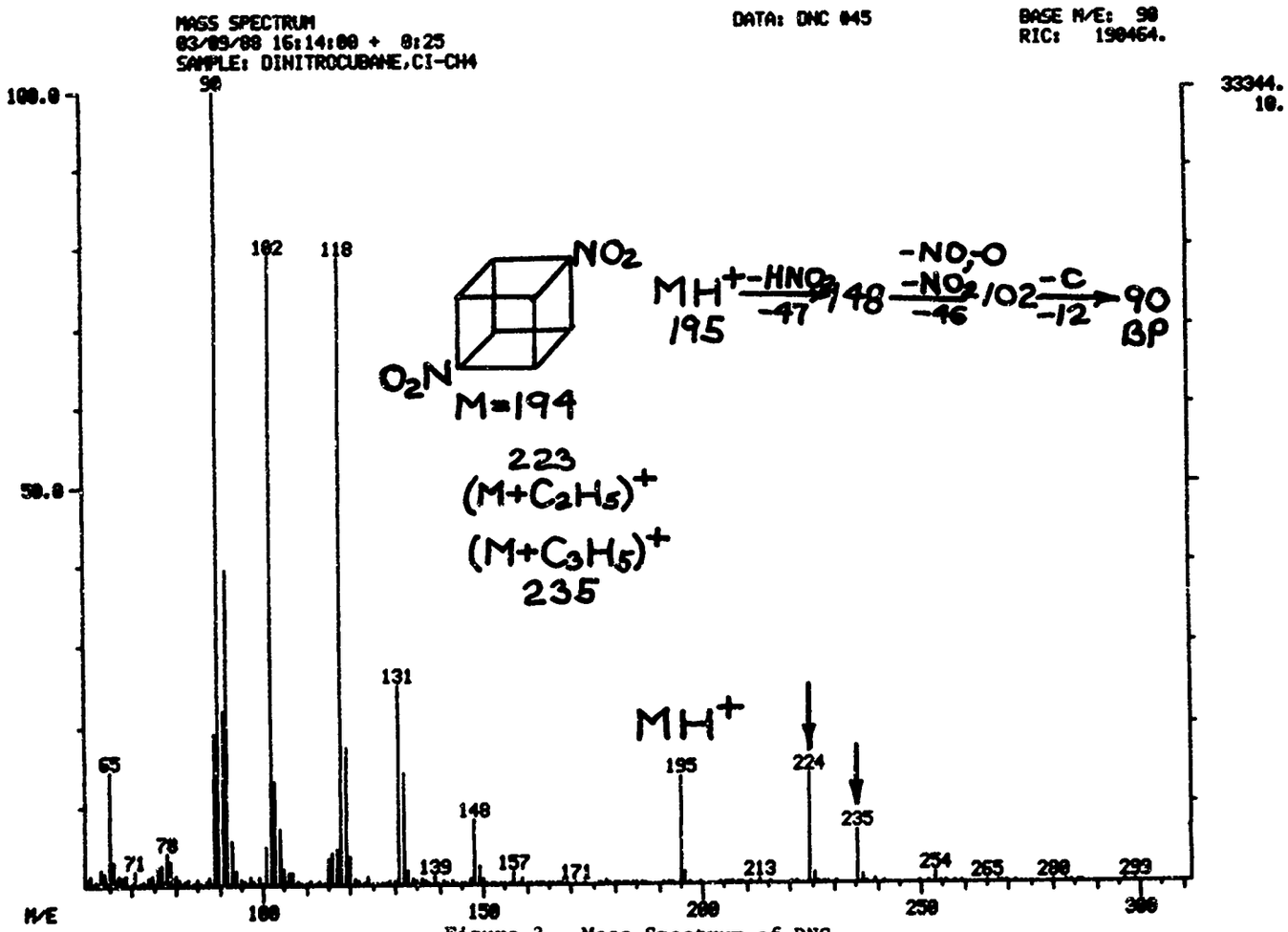


Figure 3. Mass Spectrum of DNC

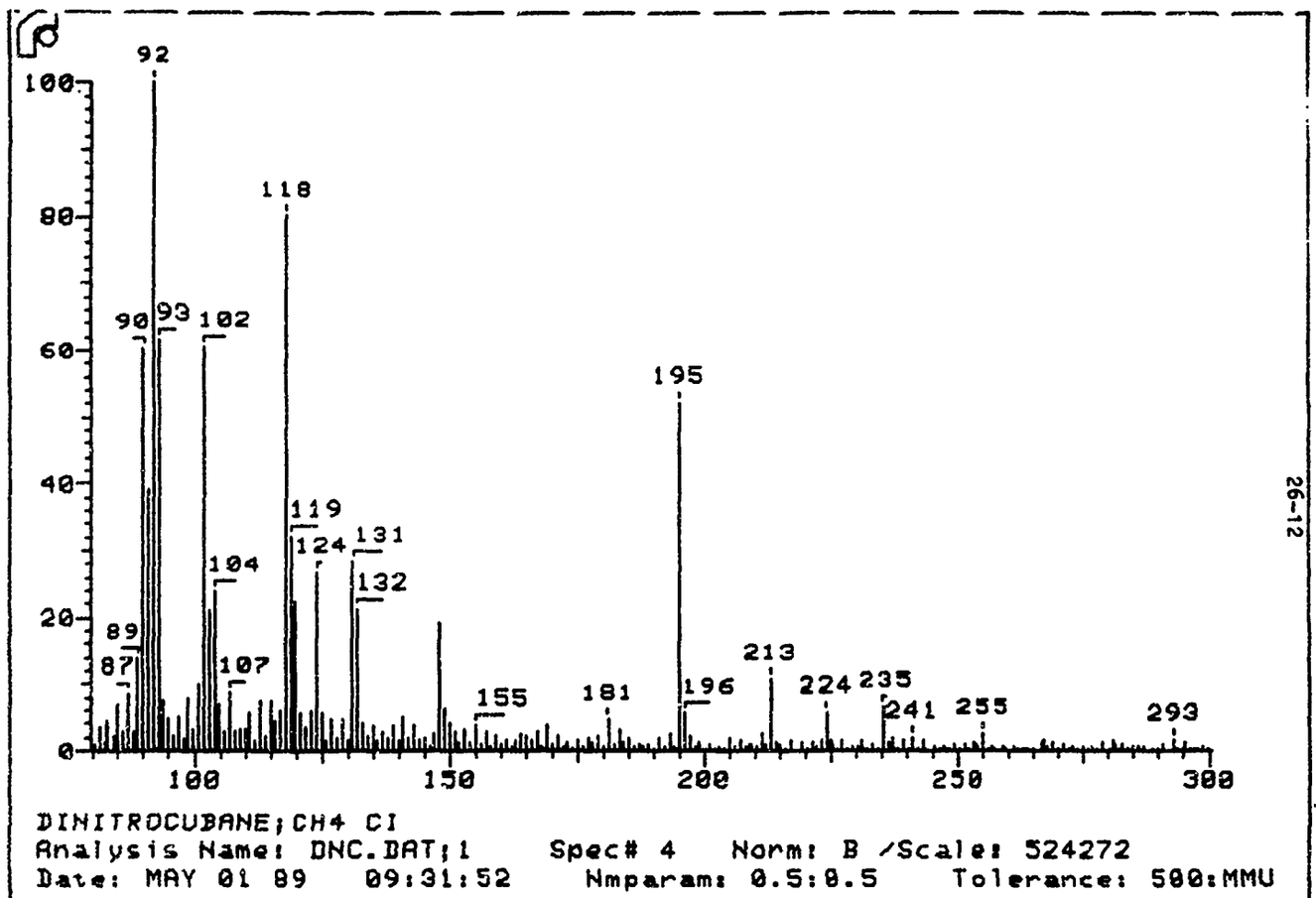


Figure 4. Mass Spectrum of DNC

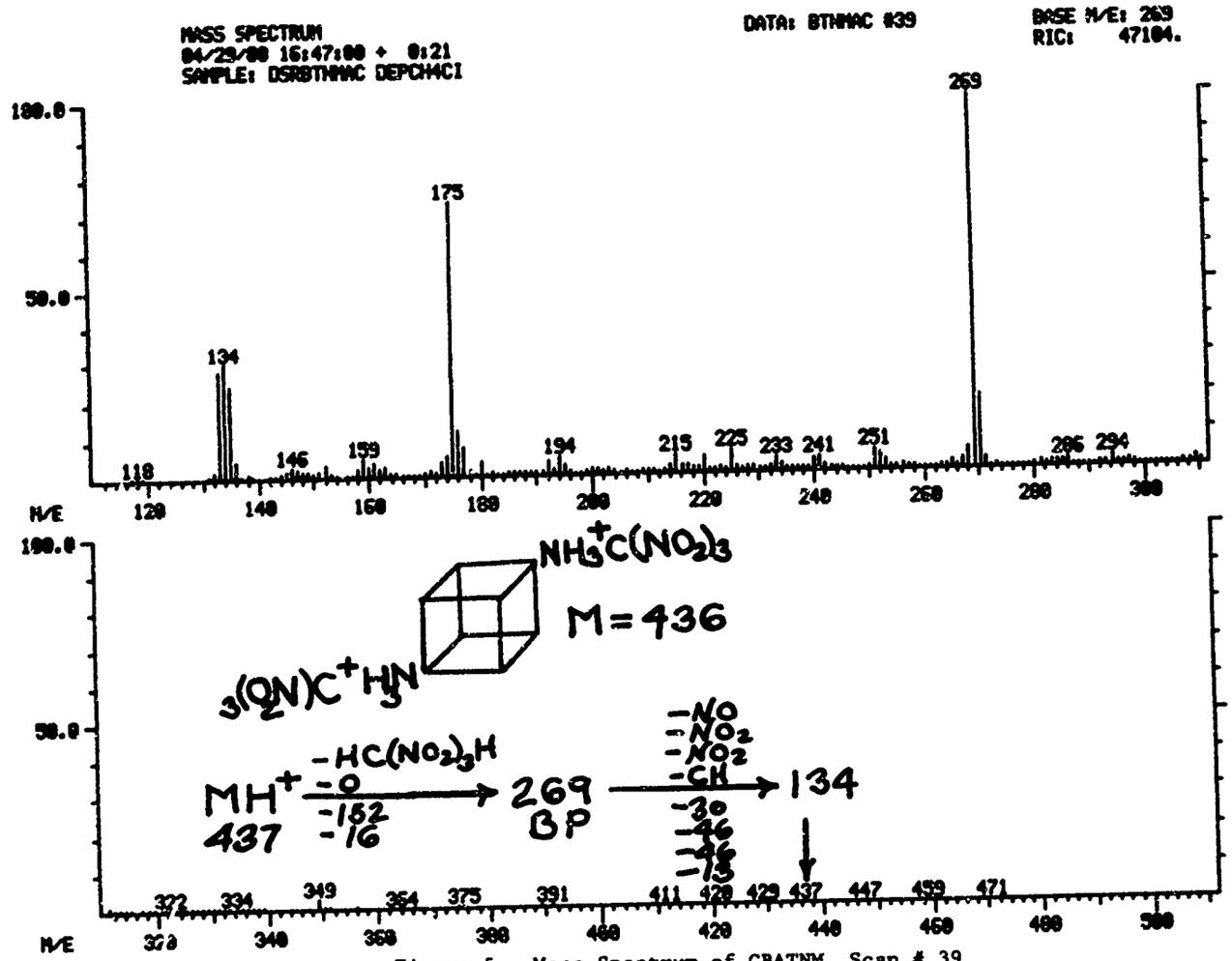


Figure 5. Mass Spectrum of CBATNM, Scan # 39

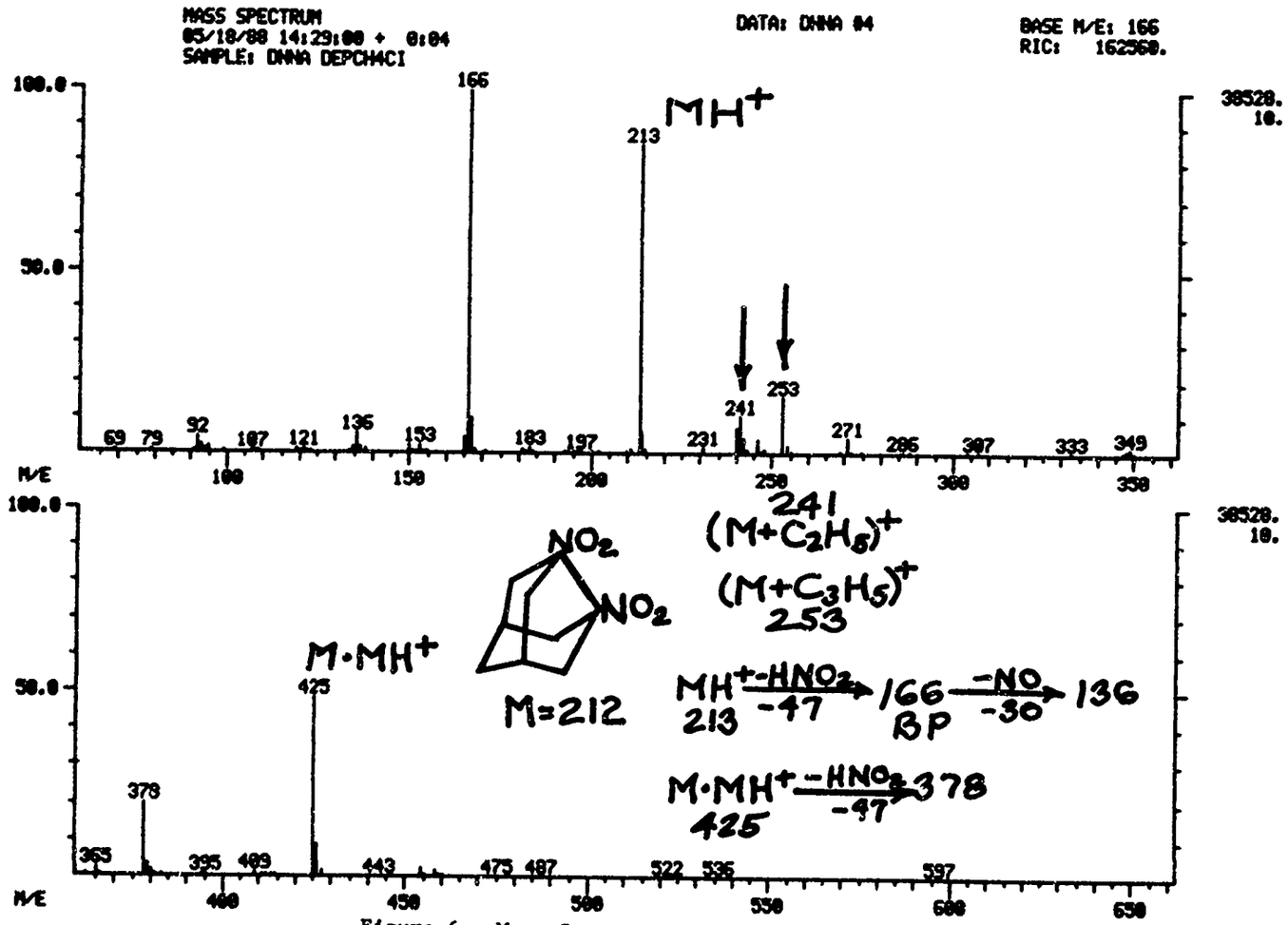


Figure 6. Mass Spectrum of DNNA, Scan # 4

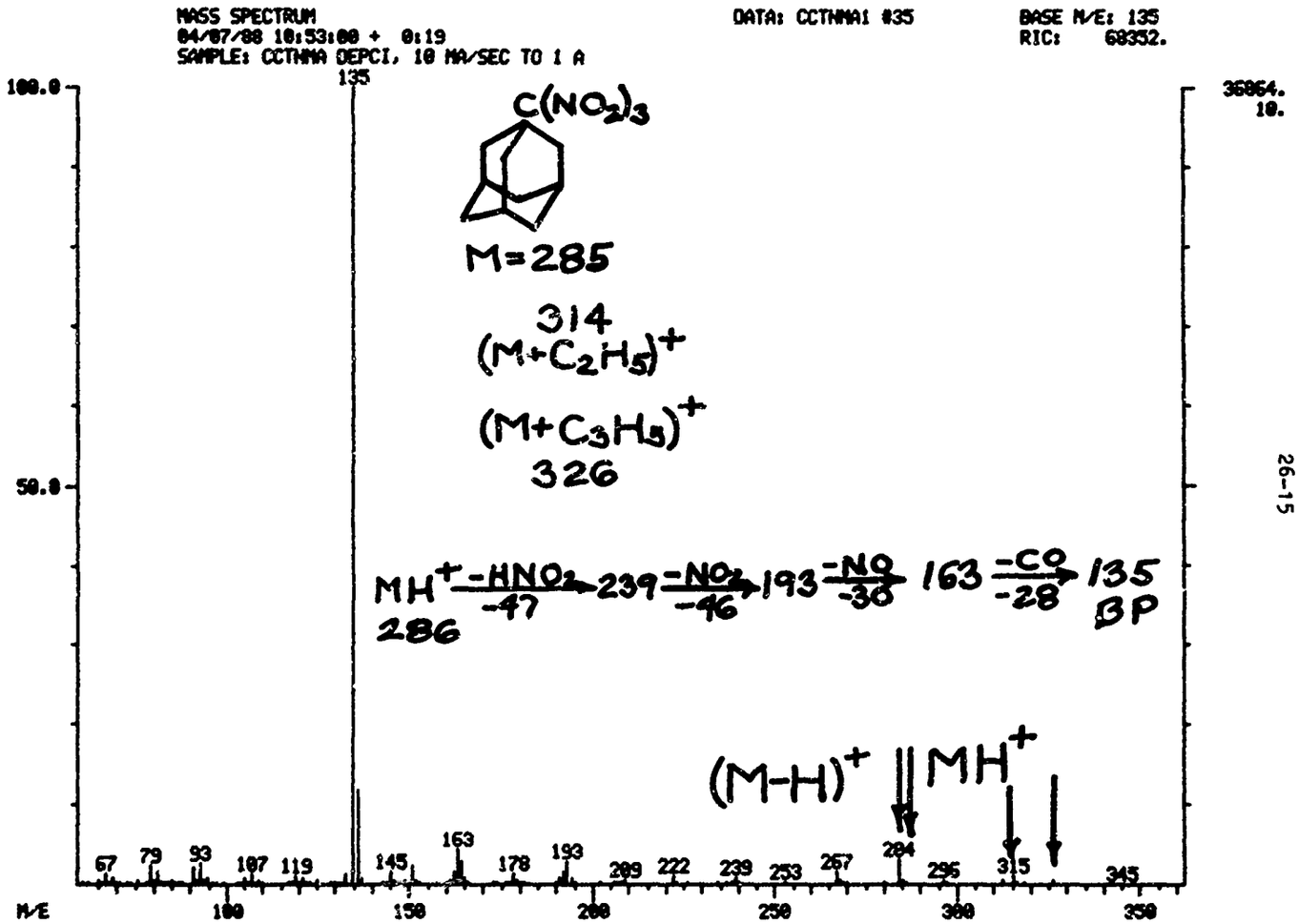


Figure 7. Mass Spectrum of TNMA, Scan # 35

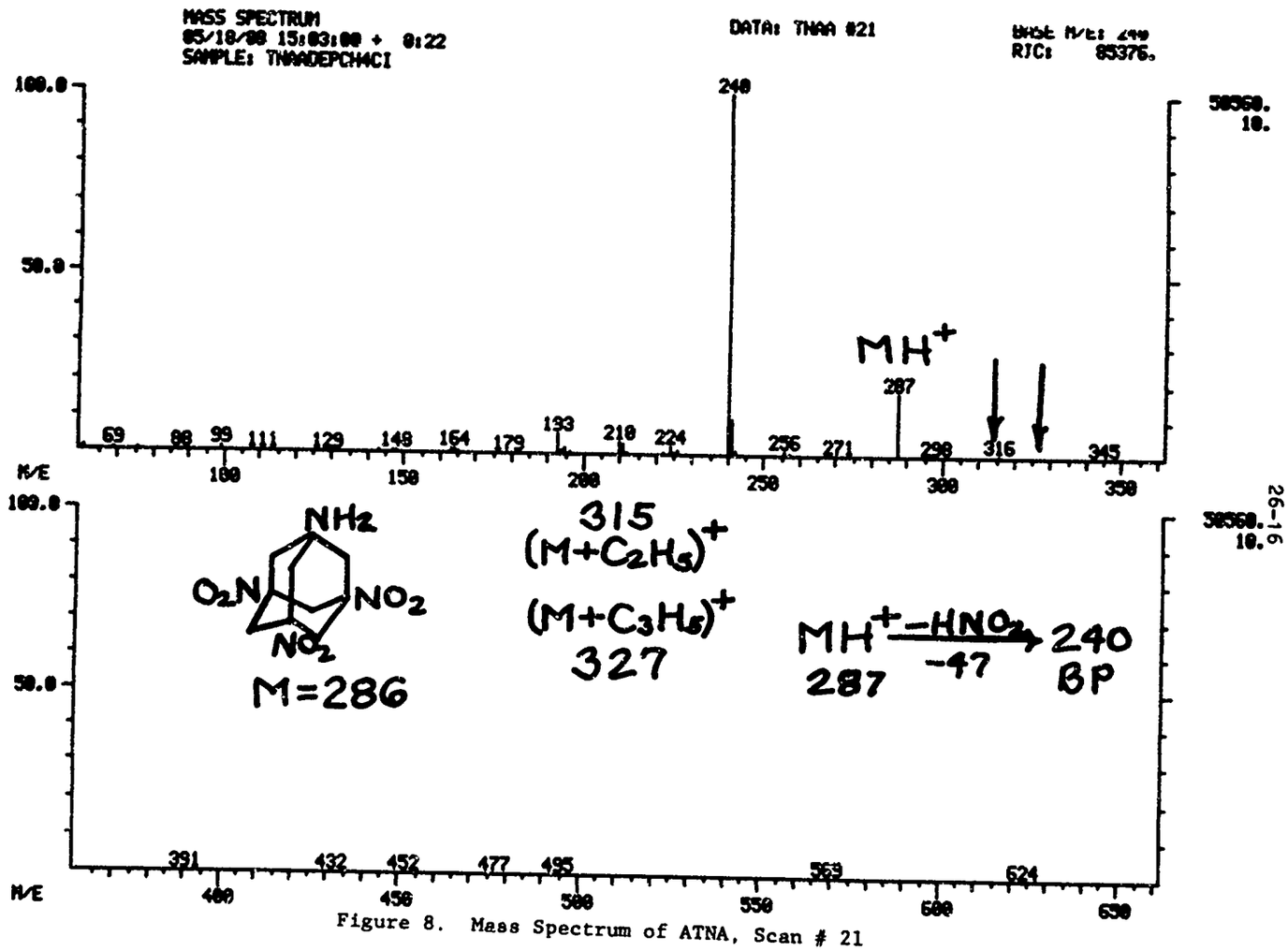


Figure 8. Mass Spectrum of ATNA, Scan # 21

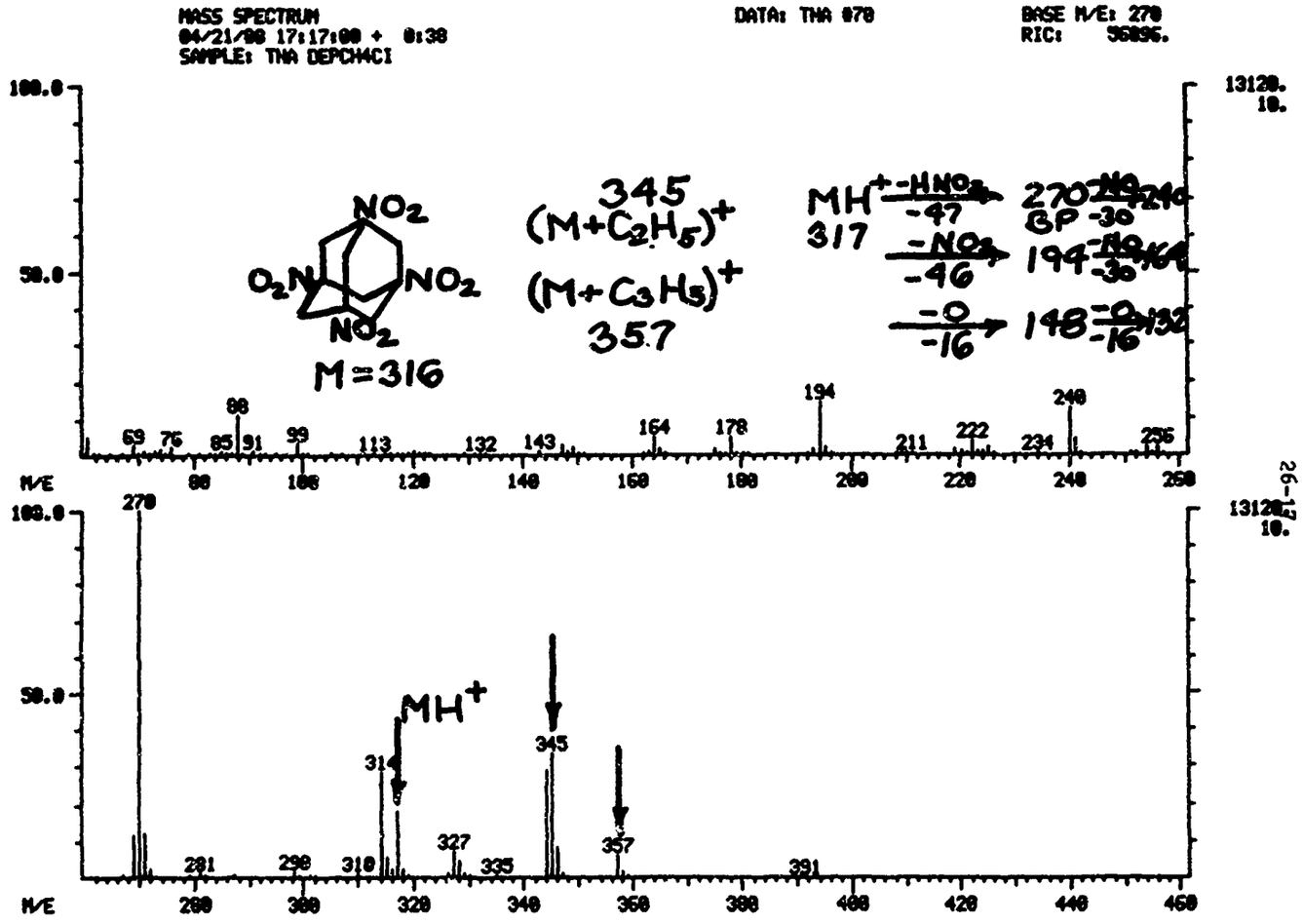


Figure 9. Mass Spectrum of TNA, Scan #70

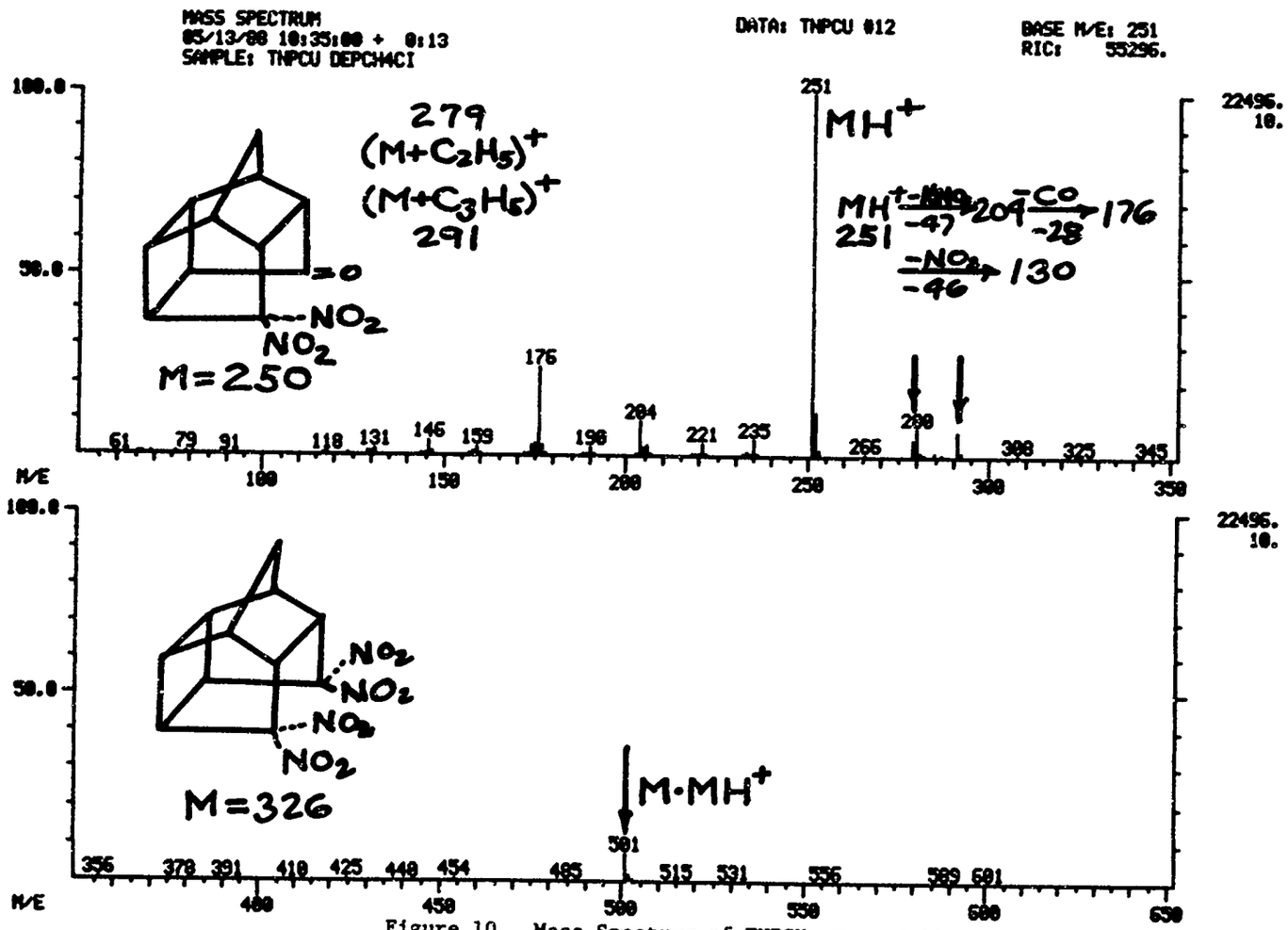


Figure 10. Mass Spectrum of TNPCU, Scan # 12

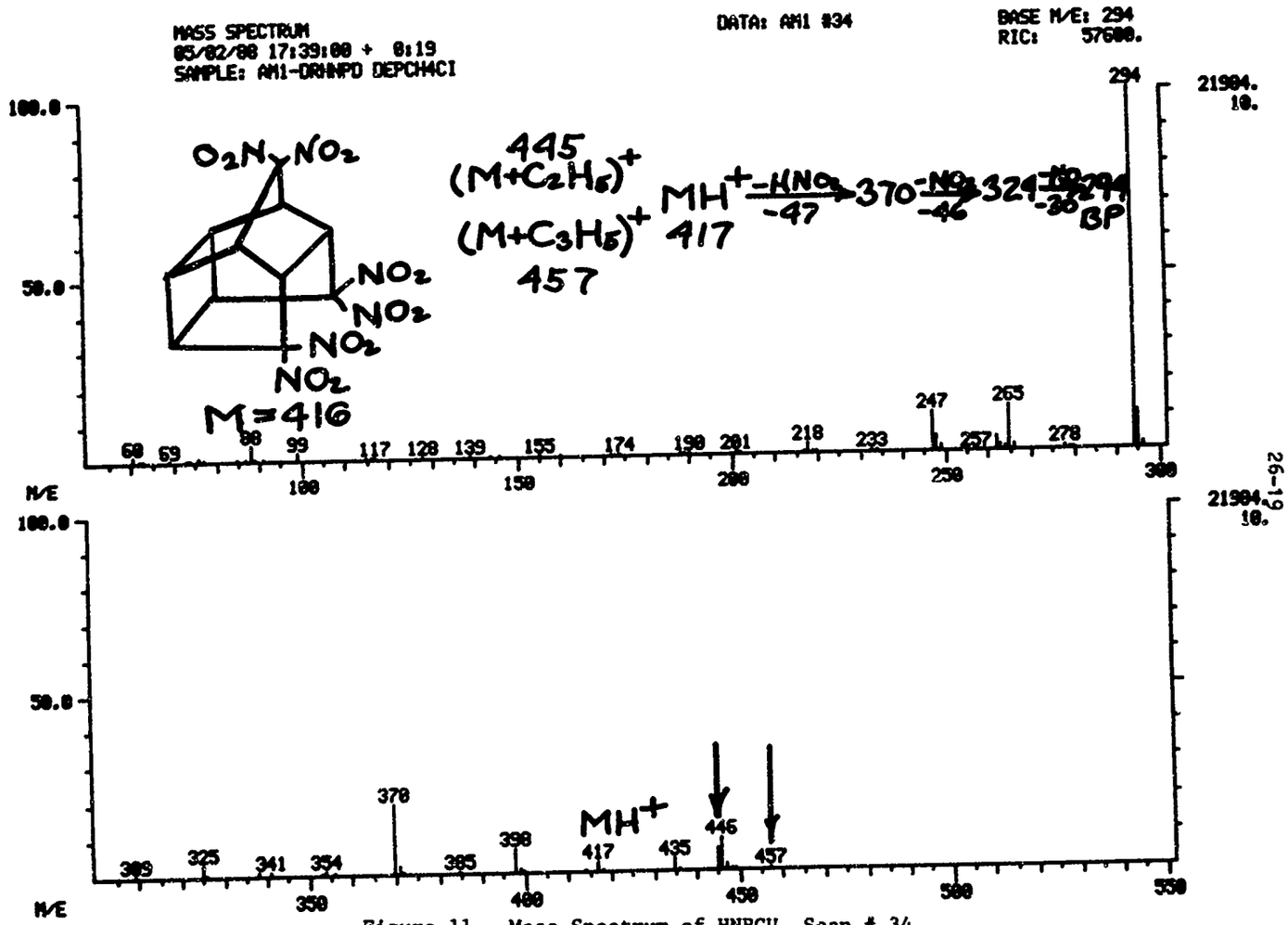


Figure 11. Mass Spectrum of HNPCU, Scan # 34

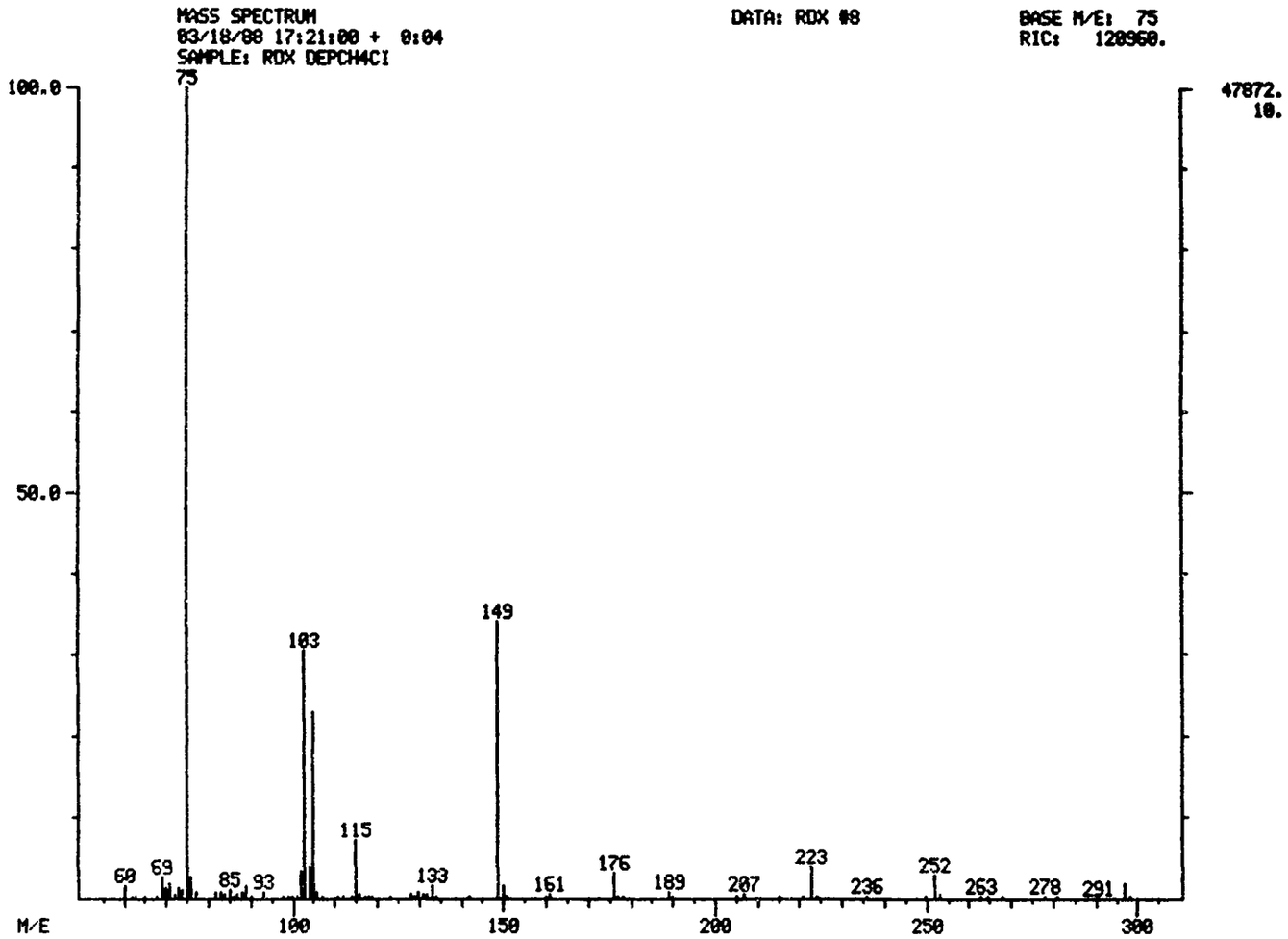


Figure 12. Mass Spectrum of RDX, Scan # 8

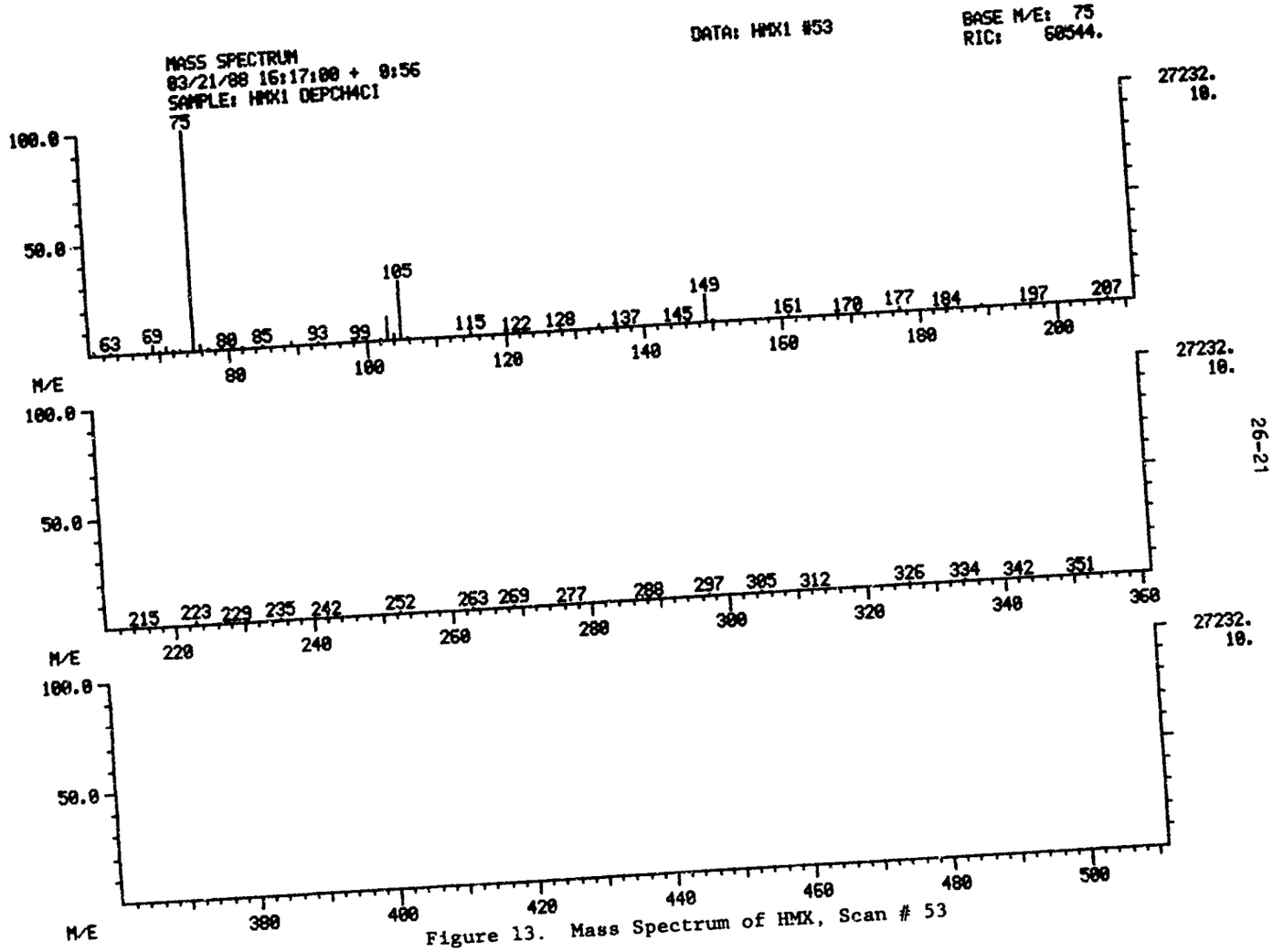


Figure 13. Mass Spectrum of HMX, Scan # 53

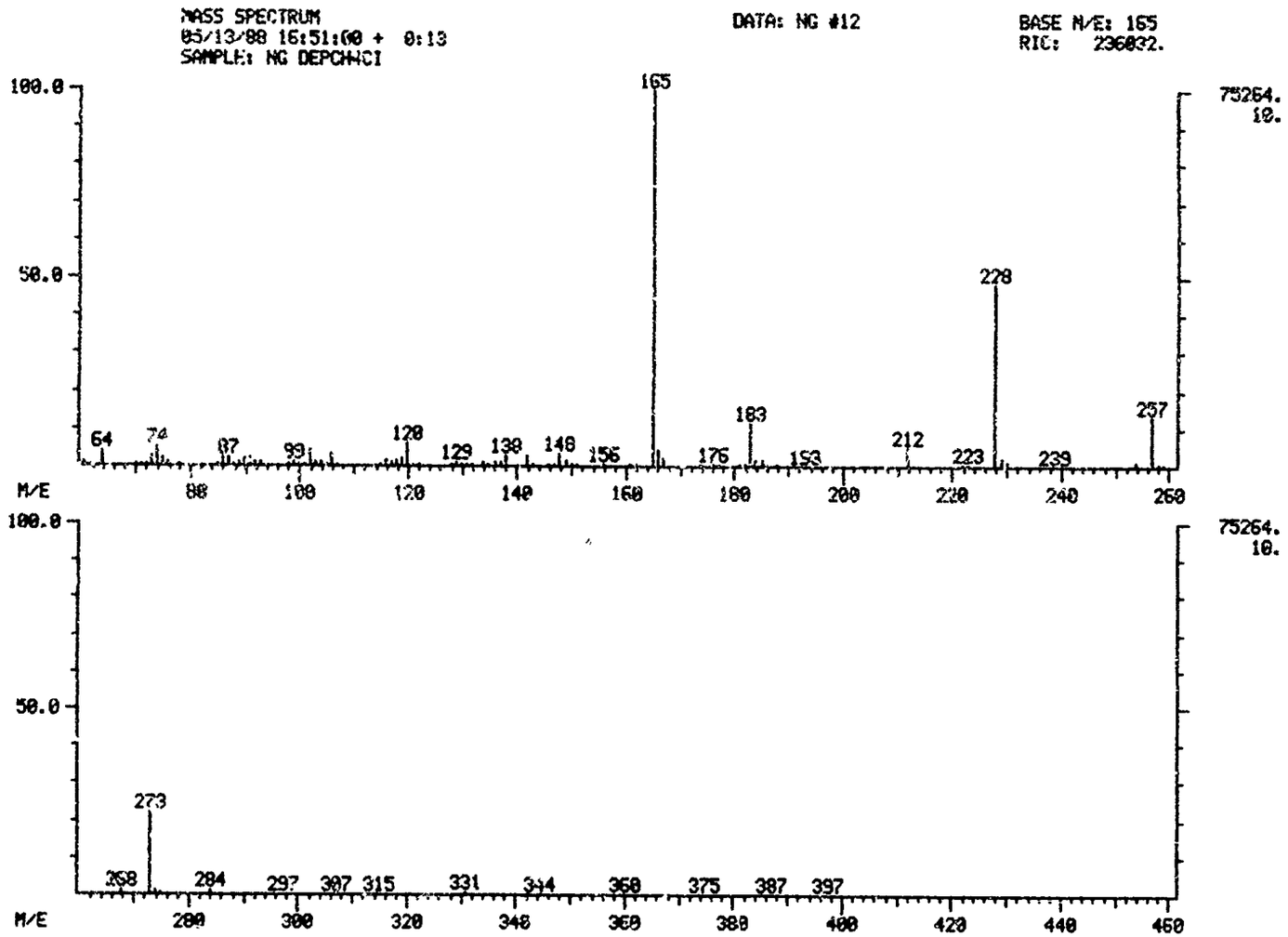


Figure 14. Mass Spectrum of NG, Scan # 12

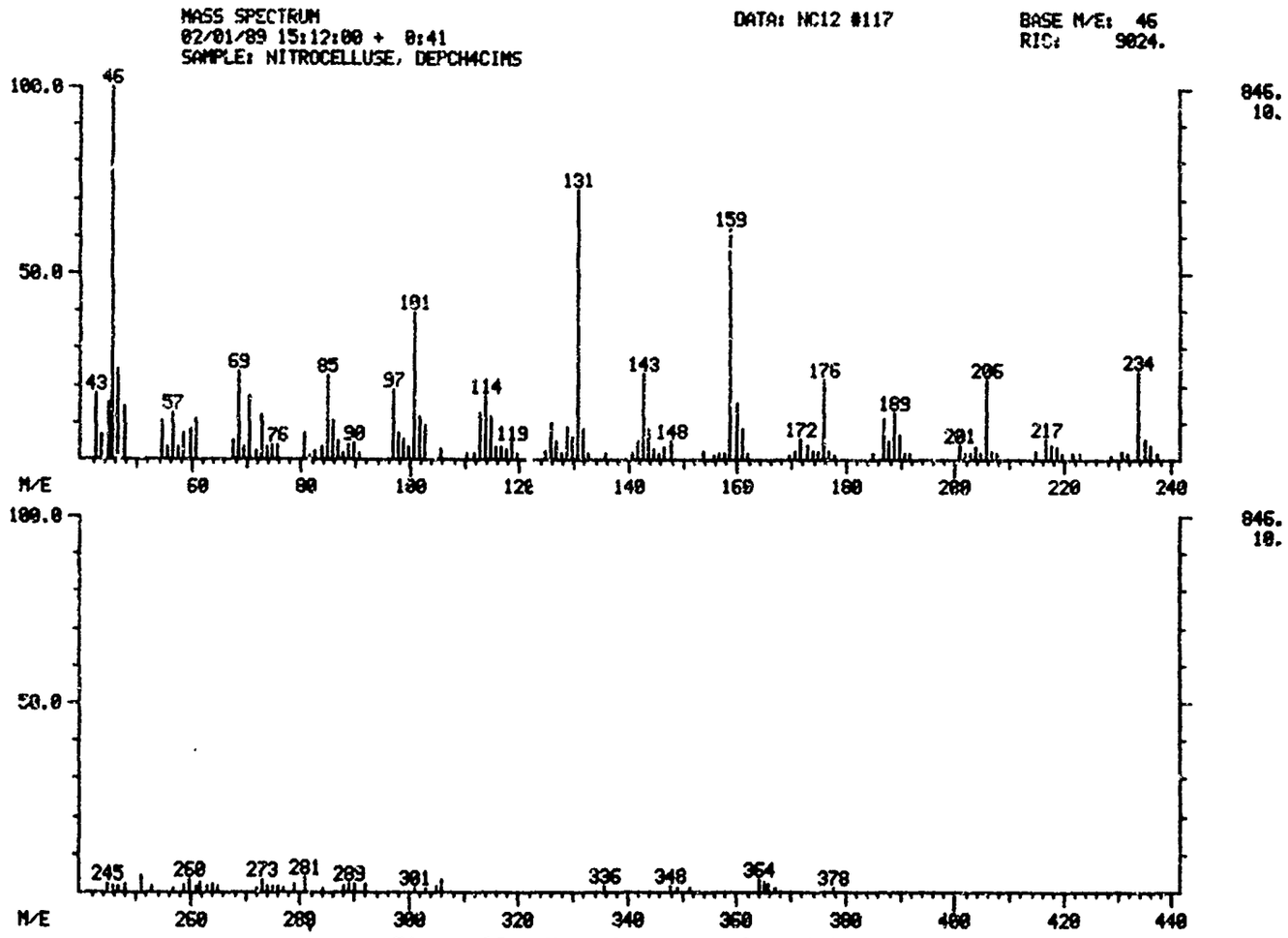


Figure 15. Mass Spectrum of NC (12.0% N), Scan # 117

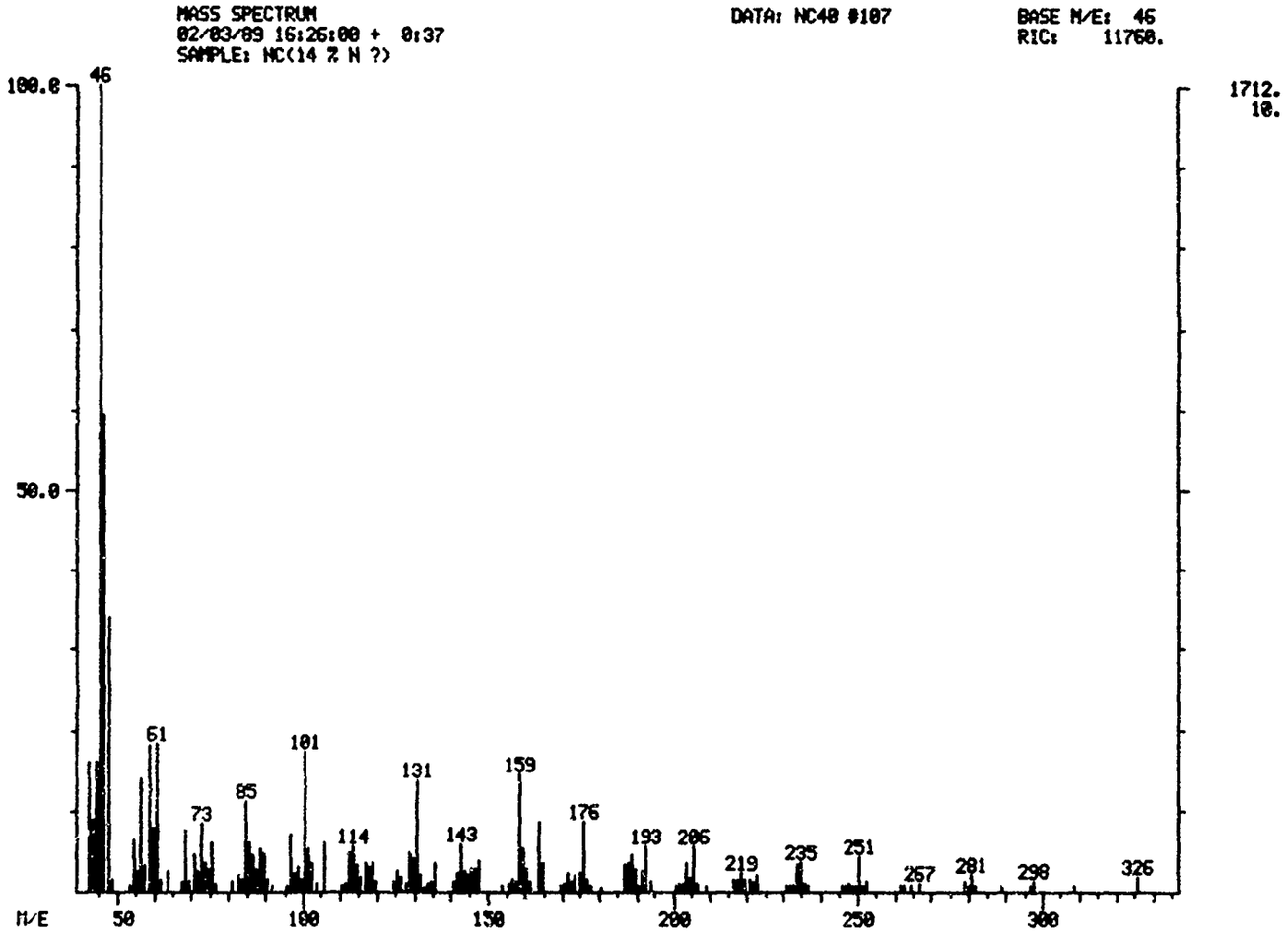


Figure 16. Mass Spectrum of NC (14.0% N), Scan # 107

# THE HPLC DETERMINATION OF SOME PROPELLANT ADDITIVES

P.A.M. De Bruyne*, J. Arijs, D.A.G. Vergauwe
and H.C.J.V. De Bisschop
Royal Military Academy - Department of Applied Chemistry
B-1040 Brussels - Belgium

ABSTRACT

To improve the properties of single and double based propellants, compounds such as diphenylamines and phtalic esters are often added.

In the present study a high pressure liquid chromatographic method has been developed. The method allows the simultaneous separation of the most important diphenylamine compounds and the commonly used phtalic acid esters in the presence of nitroglycerin. All compounds are separated and analysed using a C-8 reversed phase packed column and acetonitrile/water as mobile phase. Throughout most of the experiments solvent and concentration gradients are used. Compound identification is performed by a combination of a diode array detector and a data station; this allows automated identification of the compounds by means of spectral library data files.

Two solvent concentration gradient programs are elaborated in which solvent strengths are altered in such a way that a separation and detection of all the compounds considered can be done in two runs. The results indicate no interferences despite occasional poor peak separation and the data system can provide a quick chromatogram processing, which makes the interpretation of complex chromatograms no longer a time consuming activity. Furthermore, quantitative determination of all peaks is possible by using a single-point external calibration procedure.

The results of this study can be used to improve the analysis of minor propellant constituents dealt with in experiments on the behaviour of propellants subject to aging processes.

*Present address: Laboratory for Analytical Chemistry - State University of Ghent, Krijgslaan 281/S12, B-9000 Ghent.

## 1. INTRODUCTION.

Aging processes of nitrated compounds are important problems in the development of single and double based propellants. Nitroglycerin and nitrocellulose decompose under normal storing conditions, forming nitrogen oxides which catalyse further decomposition reactions[1]. These autocatalysed processes accelerate the aging of the explosive compounds in such a way that the propellant becomes unreliable within a relatively short time. In extreme cases this may lead to self ignition.

Diphenylamine is often added to the propellant in order to inhibit autocatalytic decomposition by reacting with the decomposition products to form stable compounds and thus preventing further catalytic action of the decomposition products. The inhibition process results in a series of nitrated diphenylamines that all remain present in the propellant.

The composition and the amount of the stabilizing agent together with its reaction products provide important information about the nature and the rate of decomposition of the propellant, and may give a better insight in propellant aging.

From these considerations it is clear that a reliable chemical analysis method is of major importance to propellant development. Because of the complexity of the solutions resulting from propellant extraction a chromatographic separation method is the most efficient technique, mainly due to its ability to perform a simultaneous identification and quantitative determination of a wide variety of chemical substances in a relatively short time under simple analysis conditions. Consequently, gas chromatography may be the most efficient and accurate separation chromatographic separation method. However, in the present study high pressure liquid chromatography, further referred to as HPLC, was preferred because of the thermal instability of diphenylamine and analogous compounds at the rather high operation temperatures of a gas chromatograph. Moreover we chose reversed phase HPLC mainly for its high selectivity over a wide variety of substances and for its short equilibration time needed to apply eluant gradients.

Reversed phase HPLC commonly uses packed bed separation columns filled with silica, chemically bound to chloro- or alkoxysilanes that often possess relatively large hydrocarbon chains, which represent the active chromatographic separation sites. An eighteen carbon chain provides the highest selectivity and the best separation capacity of the mixtures. However, traces of fats or other greasy matters, often encountered in propellant extracts, may block the column's exchange sites in such a way that the separation capacity is reduced dramatically after a few runs. Therefore we developped a separation technique based on a C-8 column. This column type has a lesser separation capacity than a C-18 column, but on the other hand interactions with non polar carbohydrates in the sample can be neglected.

An additional problem in propellant analysis is caused by the presence of alkyl phtalate esters which are extracted together with the diphenylamine compounds. These products are added to improve the thermoplastic behaviour of single and double based propellants. In spite of the large chemical difference between the phtalic acid esters and the diphenylamine compounds, both are found to elute in the same region . Such interferences complicate the interpretation of the analytical results.

Finally, in a few propellant types alkylated urea derivatives are added also to improve the propellant's properties. The presence of these compounds, co-eluting with some of the other components of the extraction mixtures, makes the resulting chromatograms even more complex to interprete.

From this it is clear that special analytical conditions are necessary in order to obtain fast and reliable detection and quantitative interpretation of the obtained chromatograms. For this reason in the present study, eluant gradients were applied to the system to improve peak separation. Furthermore, a diode array detector (DAD) has been integrated in our system because of its ability to provide additional information about the nature of the eluting compounds, and because it solves certain problems of co-elution still encountered even after optimizing solvent gradient separation.

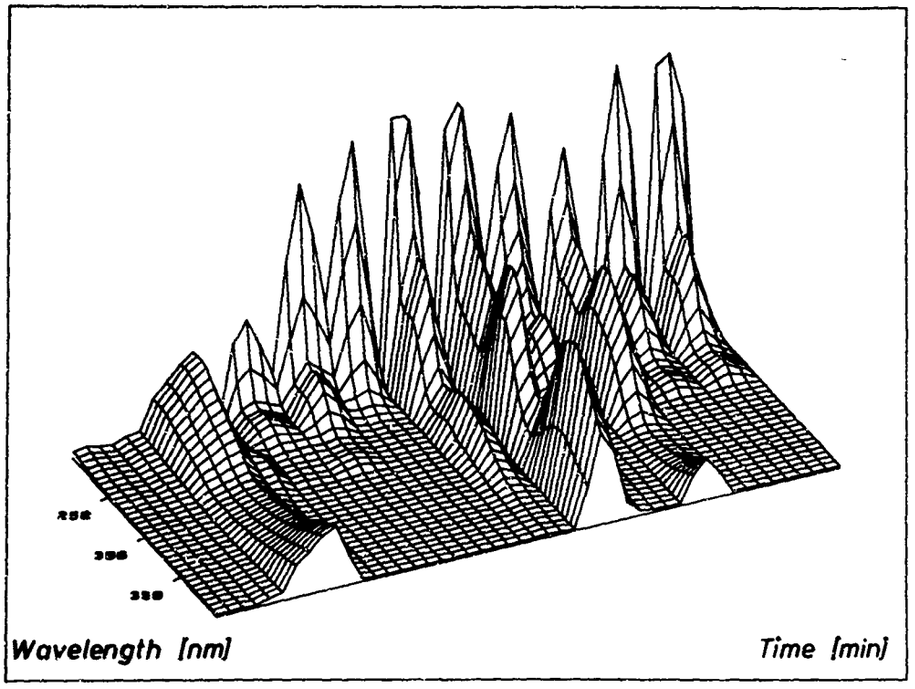


Figure 1a: Three-dimensional chromatogram recorded in a wavelength range between 200 and 400 nm.

## 2. EXPERIMENTAL.

The HPLC-system consists of two Waters type 510 liquid chromatography pumps coupled by means of an eluant gradient mixing chamber. Both pumps are controlled by an automated gradient controller. The gradient mixing chamber is connected to a Chromspher C-8 column (Chrompack). The detector is a Hewlett Packard 1040A Diode Array Detector (DAD). Detector signals are processed by a Hewlett Packard 9000/300 data system using the Chemstation Software features. The DAD allows to record UV/VIS spectra in the range between 190 and 600 nm. This results in a three-dimensional chromatogram that not only provides retention times but also gives typical uv/vis spectra of eluting compounds. In the present paper, all spectra were recorded in the wavelength range between 200 and 430 nm. In figure 1a a typical

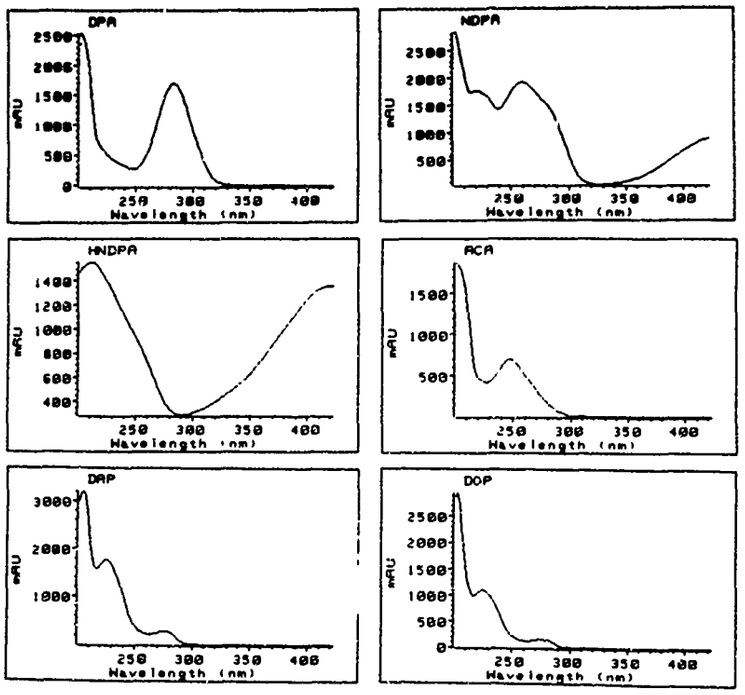


Figure 1b: UV/VIS spectra of DPA, NDPA, HNDPA, ACA, DAP, and DOP. (see Table 1 for abbreviations)

Table 1: Compounds present in the test mixtures in addition to nitroglycerin.

| |
|---|
| DIPHENYLAMINES |
| Diphenylamine (DPA) |
| 2-nitrodiphenylamine (NDPA) |
| 2,4-dinitrodiphenylamine (DNDPA) |
| 2,2',4,4',6,6'-hexanitrodiphenylamine (HNDPA) |
| N-nitrosodiphenylamine (NNDPA) |
| ALKYLPHTALATES |
| Dimethylphtalate (DMP) |
| Diethylphtalate (DEP) |
| Diallylphtalate (DAP) |
| Dibutylphtalate (DBP) |
| Dioctylphtalate (DOP) |
| UREAS |
| N-diphenyl,N'-methylurea (ACA, acardite) |
| N,N'-diethylurea (CEN, centralite) |

three-dimensional chromatogram is shown. Figure 1b shows some typical UV/VIS spectra of the compounds investigated in this paper.

Furthermore the DAD allows to identify the maxima of eluted peaks for up to eight different wavelenghts simultaneously. In this study peak height determination of all peaks was done at 210, 240, 275, 300 and 360nm. The recording band width was 10 nm and all signals were compared with the signal at a reference wavelength of 550 nm.

All eluants were prepared using Romil Far UV acetonitrile (for HPLC)and water, freshly generated from an Elgastat water system producing a water quality that corresponds to the standard requirements for HPLC water. Samples and standards were prepared from chemicals of analytical purity, in concentrated acetonitrile. Because of the lack of real propellant samples with known concentrations of all compounds present, test mixtures consisting of nitroglycerin [.01 M] and of each compound [.0001 M] listed in table 1 were prepared. These compounds are frequently encountered while analyzing propellants. By preparing thirteen component test mixtures we tried to anticipate every possible combination of compounds one could cope with in real propellant samples. All concentrations in the test mixtures were chosen in the same order of magnitude of the compound concentrations present in average propellant extracts.

## 3. RESULTS AND DISCUSSION.

### A. Separation conditions.

In HPLC , retention times of the eluted compounds depend on the strength of the eluant. In this study, where acetonitrile (ACN)/water mixtures are used as an eluant, retention times will increase with decreasing ACN content of the eluant. As seen from figure 2, in a test mixture eluted with 100% ACN, all compounds elute rapidly but on the other hand, almost no peak separation is observed. In figure 3, a chromatogram resulting from a 60/40 ACN/water isocratic elution is shown. Under these conditions some of the compounds present in the mixture are well resolved, but compounds, DAP and NNDAP, and, CEN, DPA and DNDPA, co-elute.

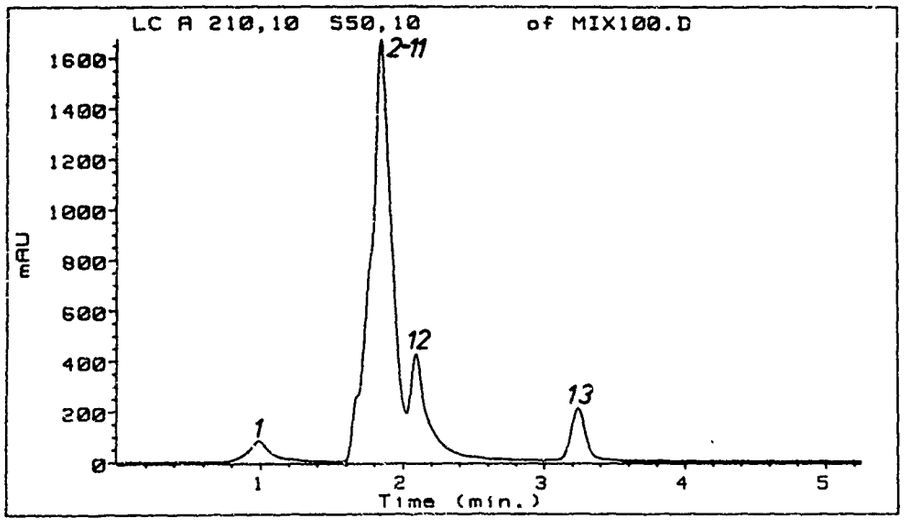


Figure 2: Chromatogram resulting from 100% acetonitrile isocratic elution. 1, HNDPA; 12, DBP; 13, DOP; 2-11, ACA, DMP, NGL, DAP, NNDPA, CEN, DPA, DNDPA, NDPA.

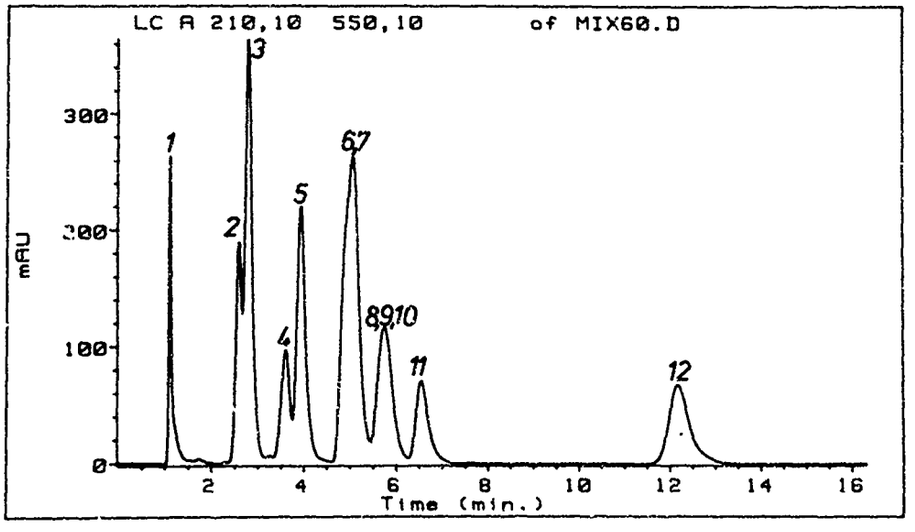


Figure 3: Chromatogram resulting from acetonitrile/water (60/40) isocratic elution. 1, HNDPA; 2, ACA; 3, DMP; 4, NGL; 5, DEP; 6, DAP; 7, NNDAP; 8, CEN; 9, DPA; 10, DNDPA; 11, NDPA; 12, DBP.

Furthermore, even after a one hour isocratic run, no evidence was found for the elution of DOP, probably due to low eluant strength. Moreover a 60/40 mixture is an eluant composition giving sharp and well resolved peaks that elute within acceptable run time. Thus it is clear that isocratic elution conditions are not suitable for efficient separation of the investigated compounds and that an acceptable chromatogram could only be obtained by applying eluant gradients. After a number of preliminary tests, we elaborated two eluant gradients that, together, are able to separate the test mixture allowing fast identification and accurate determination. The gradient elution conditions are summarized in table 2.

Table 2: Gradient conditions

| | Gradient 1 | | Gradient 2 | |
|---|---|---|---|---|
| | time | % ACN | time | % ACN |
| Initial condition | 0.00 | 30 | 0.00 | 40 |
| Sample injection | 5.00 | 20 | 5.00 | 20 |
| Isocratic elution | none | | 5.01 | 20 |
| Linear gradient start | 5.01 | 20 | 10.00 | 30 |
| Linear gradient end | 35.00 | 100 | 20.00 | 100 |
| Return to init. condit. | 35.02 | 30 | 20.02 | 40 |

In figure 4 a chromatogram recorded under gradient 1 conditions is shown; it is seen that the gradient program is able to perform an acceptable separation for nearly all the compounds in the test mixture. However, in HNDPA shows a peak splitting phenomenon. Furthermore ACA and DMP peaks are very broad and thus difficult to process. Therefore gradient 2 was elaborated: this gradient is unable to perform an acceptable separation for the majority of peaks but it provides good separation conditions for HNDPA, ACA and DMP. Consequently, an unknown mixture has to be eluted first with the gradient 1 program, and if the presence of HNDPA, ACA or DMP is indicated, a second run with gradient 2 is done. In figure 5 a typical chromatogram resulting from a gradient 2 elution is shown.

As indicated by figure 4, two couples are not separated by gradient program 1. These are DAP/NNDPA and DPA/DNDPA. As neither

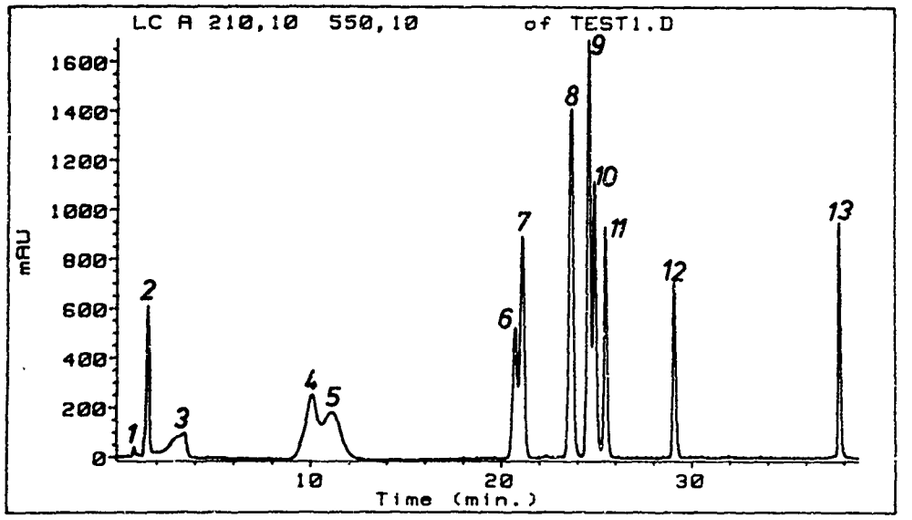


Figure 4: Chromatogram resulting from a gradient 1 run.1, solvent response; 2 and 3, HNDPA; 4, ACA; 5, DMP; 6, DEP; 7, NGL; 8, DAP and NNDPA; 9, DPA and DNDPA; 10, CEN; 11, NDPA; 12, DBP; 13, DOP.

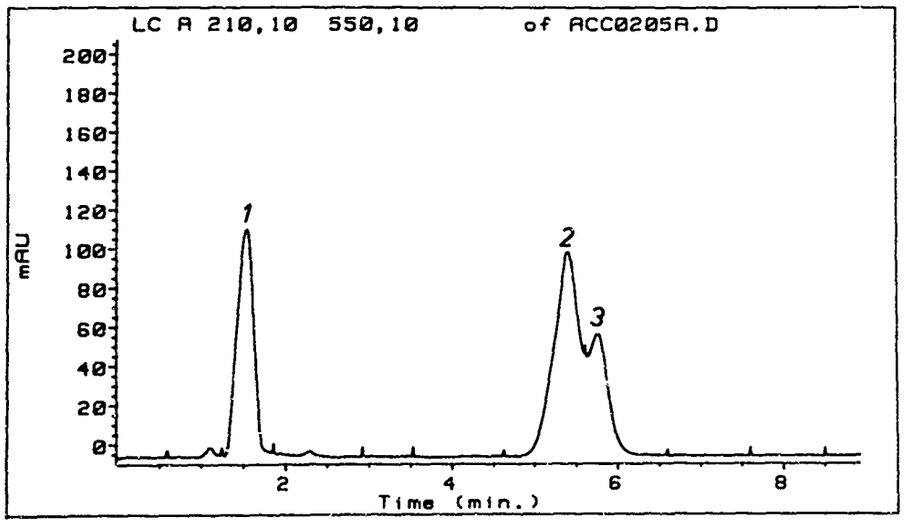


Figure 5: Chromatogram with gradient 2 to separate HNDPA, ACA and DMP.

gradient program 2, nor any other gradient elution condition is able to separate these compound couples, we used the DAD's detection capacities to identify and determine these compounds. This technique will be explained in the next section.

B. Compound identification

For the compound identification, UV/VIS spectra of the pure test mixture components were recorded by the DAD and stored in a spectral library . Automated identification of all eluted compounds is performed by the HP Chemstation: each recorded spectrum is compared with the spectra in the library; a positive identification is indicated when the spectrum in the library and the recorded peak spectrum match for more than 70% . Obviously, if more than one spectrum fulfills this condition, the one with the highest match percentage is chosen. In table 4, the data resulting from the identification run on the chromatogram from figure 4 are shown. The table indicates that although some compounds were successfully identified, DAP, DPA and DNDPA are not correctly identified by the program. Moreover, because of minor differences between the spectra of the phtalic acid esters (Figure 1b), the program is unable to distinguish between the various representatives of this class of compounds.

Table 4: Results of an identification run with spectral comparison performed on a test mixture chromatogram obtained with gradient 1.

| Peak nr. | Retention time (min) | Match (%) | Compound |
|---|---|---|---|
| 6 | 20.74 | 99.9 | DAP |
| 7 | 21.14 | 91.7 | NGL |
| 8 | 23.69 | 97.6 | NNDPA |
| 9 | 24.61 | 22.6 | ? |
| 10 | 24.90 | 99.0 | CEN |
| 11 | 25.49 | 100.0 | NDPA |
| 12 | 29.08 | 100.0 | DAP |
| 13 | 37.78 | 98.9 | DMP |

In a next step we introduced peak retention times as an additional identification feature in the program. Under these conditions, the program not only compares spectra, but it also

checks compound retention times: less than 10 % deviation from the stored retention time results in a positive identification. Table 5 summarizes the identification results of the chromatogram in figure 4 performed with both spectral and retention time checking. These results show that most of the peaks are correctly identified, but still, the co-eluting couple DAP/NNDPA is not distinguished and the couple DPA/DNDPA is not recognized at all.

Table 5: Results of an identification run with spectral and retention time comparison performed on a test mixture chromatogram obtained with gradient 1.

| Peak nr. | Retention time (min) | Match (%) | Compound |
|---|---|---|---|
| 6 | 20.74 | 99.9 | DEP |
| 7 | 21.14 | 91.7 | NGL |
| 8 | 23.69 | 97.6 | NNDPA |
| 9 | 24.61 | 22.6 | ? |
| 10 | 24.90 | 99.0 | CEN |
| 11 | 25.49 | 100.0 | NDPA |
| 12 | 29.08 | 100.0 | DBP |
| 13 | 37.77 | 98.9 | DOP |

In a final step, a peak purity checking procedure is introduced in the identification program. An impurity checking routine searches for differences in the recorded UV/VIS spectra at various locations in the area under the peak. If such differences are found, the program locates the position of the highest match between the library spectra and the recorded spectra. If both retention time and spectrum match at this point, a positive identification of the compound is registered. As seen from table 6, this procedure allows to identify all compounds to be analysed with gradient 1. In the same way an identification procedure with peak purity checking and spectral and retention time checking, a chromatogram resulting from an elution with gradient 2 can be performed. The results of a typical identification run on such a chromatogram is summarized in table 7.

Table 6: Results of identification run with peak purity checking and spectral and retention time comparison performed on a test mixture chromatogram obtained with gradient 1.

| Peak nr. | Retention time (min) | Match (%) | Compound |
|---|---|---|---|
| 6 | 20.74 | 99.9 | DEP |
| 7 | 21.14 | 91.7 | NGL |
| 8 | 23.59 | 95.7 | DAP |
| | 23.79 | 99.8 | NNDPA |
| 9 | 24.52 | 72.5 | DPA |
| | 24.66 | 88.0 | DNDPA |
| 10 | 24.90 | 99.0 | CEN |
| 11 | 25.49 | 100.0 | NDPA |
| 12 | 29.08 | 99.9 | DBP |
| 13 | 37.77 | 99.9 | DOP |

Table 7: Results of identification run with peak purity checking and spectral and retention time comparison performed on a test mixture chromatogram obtained with gradient 2.

| Peak nr. | Retention time (min) | Match (%) | Compound |
|---|---|---|---|
| 1 | 1.54 | 99.9 | HNDPA |
| 2 | 5.40 | 99.6 | ACA |
| 3 | 5.75 | 99.5 | DMP |

c. Quantitative determination

Since the main goal of this investigation is the development of a rapid quantitative determination of propellant additives, a single point external calibration method was preferred to assay the compounds in the test mixtures. However, preliminary experiments showed that such a procedure is successfully only if unknown and standard concentrations do not differ by more than 25%. Thus, an appropriate standard has to be calculated from a first run of the sample and by using the appropriate response factors for each compound at the selected wavelengths. To avoid possible interferences of extraction liquids (e.g. $CH_2Cl_2$), all peak heigths were determined in the wavelength range between 240 and 400 nm, since most of the commonly used solvents absorb between 190 and 235 nm.

It is clear that such a method does not allow the determination of co-eluting compounds. Therefore, in a first step, test mixtures were prepared which did not contain either DAP and

DNDPA or NNDPA and DPA. The repeateability of the assay of each compound was determined from five determinations of all compounds against independently prepared standard mixtures, according to the principles outlined in the preceding paragraph. The results are shown in table 8. It can be seen that the concentrations found do not differ significantly from the real concentrations at the 95% confidence level (Student t-test).

Table 8: Assay of propellant additives without co-eluting compounds

| Compound | Wavelength (nm) | Concentration (mmol/l) | Relative Standard Deviation ( % ) |
|---|---|---|---|
| HNDPA | 240 | 0.096 | 2.3 |
| NNDPA | 240 | 0.100 | 2.0 |
| DPA | 275 | 0.097 | 2.0 |
| DNDPA | 275 | 0.099 | 1.8 |
| NDPA | 275 | 0.100 | 1.6 |
| DMP | 240 | 0.099 | 2.1 |
| DEP | 240 | 0.100 | 0.8 |
| DAP | 240 | 0.098 | 2.6 |
| DBP | 240 | 0.099 | 1.0 |
| DOP | 240 | 0.097 | 2.6 |
| ACA | 240 | 0.098 | 1.0 |
| CEN | 240 | 0.098 | 1.5 |

When co-eluting couples DAP/NNDPA and DPA/DNDPA are present the following approach is possible: As seen from figure 6, NNDPA and DNDPA absorb considerably at 300 and 360 nm, respectively; at these wavelengths DAP and DPA do not absorb; this indicates that, even in the presence of DAP and DPA, concentrations of NNDPA and DNDPA may be calculated at 300 and 360 nm. Table 9 gives the calculated concentrations and accuracy estimates of NNDPA and DNDPA, determined at these wavelengths and of equal amounts of DAP and DPA. The concentrations of DAP and DPA were calculated by subtracting those fractions of the peak areas due to NNDPA or DNDPA from the total peak area of the co-eluting compounds at 240 or 275 nm. Those peak area contributions of NNDPA and DNDPA are obtained by transforming the detector signals at 300 and 360 nm to

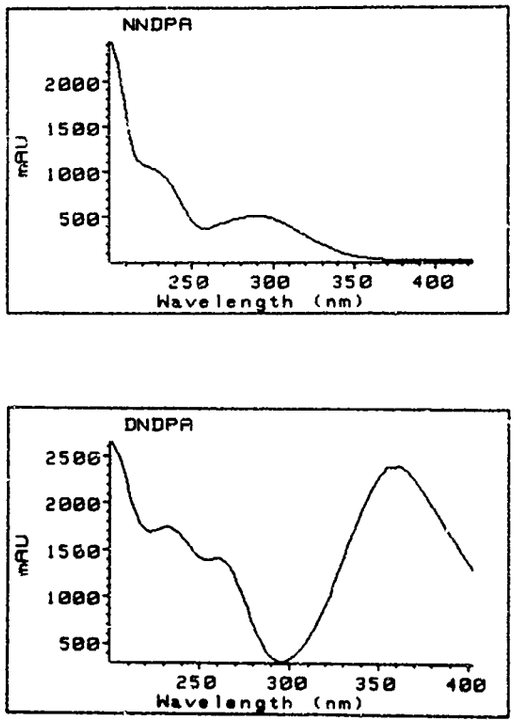


Figure 6: UV/Vis spectra of NNDPA and DNDPA

Table 9: Assay of NNDPA and DNDPA when co-eluting compounds are present. The concentration of the compounds present is 0.095 mmol/l each.

| Compound | Wavelength (nm) | Concentration (mmol/l) | Relative Standard Deviation ( % ) |
|---|---|---|---|
| NNDPA | 300 | 0.0943 | 3.2 |
| DNDPA | 360 | 0.0944 | 2.5 |
| DAP | 240 | 0.0899 | 5.0 |
| DPA | 275 | 0.0919 | 1.5 |

240 and 275 nm, respectively, using predetermined response factors at the various wavelengths. It is clear that the accuracy of the resulting values for DAP and DPA will depend on the relative concentrations of the co-eluting compounds. The determination of

the depedence of the accuracy on the relative concentrations of the co-eluting compounds is under investigation.

## 4. CONCLUSIONS

The results indicate the possibility of analysing complex mixtures resulting from propellant extracts using HPLC with a C8 reverse phase column and two gradient elution programs; the DAD detection and identification system allow the detection of various diphenylamines, phtalates and substituted ureas.

A single point external calibration standard allows the assay of the compounds within acceptable errors. Optimization of the calibration procedure and performance checking of the method developed on real propellant samples is actually under investigation.

## 5. REFERENCES

1. T. Urbanski, Chemistry and Technology of Explosives, Pergamon, 1965, Vol. 2, p.47.

# DETECTION AND IDENTIFICATION OF IMPURITIES IN RDX AND HMX BY NMR SPECTROSCOPY

M. Kaiser

Bundesinstitut für chemisch technische Untersuchungen beim Bundesamt für Wehrtechnik und Beschaffung, 5357 Swisttal 1, Großes Cent, Germany

## Summary

The $^1$H-NMR spectra of by-products in 1,3,5-trinitro-1,3,5-hexahydrotriazine (RDX) and 1,3,5,7-tetranitro-1,3,5,7-octahydrotetrazine (HMX) were measured in deuterated dimethylsulfoxide. Quantitative analysis of an NMR spectrum is shown in an example and compared with HPLC results. Characteristic by-products can be detected in RDX and HMX products of different manufacturers. The manufacturing process (Bachmann process, nitric acid process) is detected in the case of RDX from the occurance of characteristic by-products. The specific by-product of the Bachmann process for RDX is the compound 1-acetylhexahydro-3,5-dinitro-1,3,5-triazine (TAX) and for the HMX 1-acetyloctahydro-3,5,7-trinitro-1,3,5,7-tetrazine (SEX). The starting materials acetic acid, paraformaldehyde, and products which were formed from formaldehyde are more or less eliminated by the different manufacturers, who work according to the Bachmann process. Other impurities of RDX and HMX are aliphatic compounds, which could not be identified. The evaluation of all the impurities leads to an identification of the manufacturing process or of the manufacturer and also to a fingerprint of the manufacturing lot.

## 1. Introduction

Materials acquired for the German armed forces are subjected to the identification of their origin and nature of production processes. This demand is especially valid in the case of explosives because the manufacturing process may affect the properties which in turn influence the high degree of requirements for handling and function. The identification of explosives is also important in connection with acts of terrorism. As all other products of the chemical industry, explosives are not chemically pure compounds.

They contain characteristic by-products which are present in most cases only in very small quantities. The formation of the by-products depends on the manufacturing process. An identification and a quantitative determination of the characteristic impurities requires a high standard of chemical analysis.

The identification of different TNT species is essentially carried out by GC/MS. In the case of HMX and RDX it is not possible to use this method because of the thermal instability of these products. Instead of the GC method, proton NMR spectroscopy, which is of higher selectivity and higher detectability, is used to solve the problem. On the other hand, the sensitivity of NMR spectroscopy is not high. Therefore, a modern Fourier transform NMR spectrometer must be used to get a better signal to noise ratio by accumulation of a high number of spectra.

## 2. Experimental Conditions

In order to get a good NMR spectrum the substance must be dissolved in a deuterated solvent. The two deuterated solvents acetone and dimethylsulfoxide (DMSO), in which HMX and RDX are fairly soluble, are useful. For these measurements deuterated dimethylsulfoxide was used because of the higher solubility of RDX and HMX. Another reason was that there are no signals in the region from $\delta = 0.0 - 2.30$. If deuterated acetone would be used there would be an overlap of signals of the by-products with the acetone signal. Another reason for using dimethylsulfoxide is the overlap of the signals of RDX and HMX when using deuterated acetone as solvent.

The identification of by-products in the spectrum depends on the amplification and the signal to noise ratio. In NMR spectroscopy the signal to noise ratio is a function of the amount of substance and the number of accumulated spectra, as the signal to noise ratio improves with the square root of the accumulated spectra. For the experimental detection of the

by-products about 300 mg of RDX or HMX were dissolved in 0.8 to 0.9 ml of deuterated dimethylsulfoxide and about 1000 spectra were accumulated. The typical accumulation time with these parameters was about two hours per spectrum. For better comparability all spectra in the Figures 14 to 22 were plotted with the same height. The main RDX or HMX signal was set to a height of 1500 cm. The symmetrical spinning sidebands, which occur at this amplification, are marked with a dot. There is no information which could be extracted from these sidebands. The calibration was done by setting the signal of the dimethylsulfoxide to a value of $\delta = 2.49$. The solvent contains an impurity of water which occurs as a singlet at $\delta = 3.30$.

The compounds 1-acetyloctahydro-3,5,7-trinitro-1,3,5,7-tetrazine (SEX)[1] and 1-acetylhexahydro-3,5-dinitro-1,3,5-triazine (TAX)[2][3] were synthesized according to the literature. In the literature a variety of intermediate products of the RDX and HMX synthesis are proposed which were synthesized to a large extent. Elaborate and time consuming work for the synthesis of all proposed compounds was avoided and the by-products were hence isolated by preparative medium pressure chromatography.

The isolated unknown products were identified by $^1$H-NMR spectroscopy as 1,7-diacetoxy-2,4,6-trinitro-2,4,6-triazaheptane[4][5] and 1,9-diacetoxy-2,4,6,8-tetranitro-2,4,6,8-tetrazanonane[4]. The other examined by-products can be acquired commercially.

## 3. By-products in RDX and HMX

The possible by-products in RDX and HMX are:

1. starting materials for the process
2. products which were produced during the synthesis
3. solvents derived from recrystallisation

In the case of RDX there are two different production methods

(Bachmann process, nitric acid process) which differ in their starting materials. The starting materials of the Bachmann process[6], which can be present in the explosive, are acetic acid, acetic acid anhydride, ammonium nitrate, and paraformaldehyde. The occurance of acetic acid anhydride and ammonium nitrate is not possible due to the production process. Acetic acid and paraformaldehyde can be present if the product is insufficiently washed. The $^1$H-NMR spectra of these chemicals are shown in Figures 1 to 4. In the case of the nitric acid process these impurities cannot be present in the product since only hexamine and nitric acid are the starting compounds.

By-products which can be formed during synthesis are known in the literature. These are cyclic nitramines with an N-acetyl-group. The spectra of 1-acetyloctahydro-3,5,7-trinitro-1,3,5,7-tetrazine (SEX)[1] and 1-acetylhexahydro-3,5-dinitro-1,3,5-triazine (TAX)[2][3] are shown in Figures 5 and 6. Other types of by-products are open chain nitramines such as 1,7-diacetoxy-2,4,6-trinitro-2,4,6-triazaheptane[4][5] (Figure 7) and 1,9-diacetoxy-2,4,6,8-tetranitro-2,4,6,8-tetrazanonane[4] (Figure 8).

The solvents from recrystallisation are acetone[8] (Figure 9), cyclohexanone (Figure 10), γ-butyrolactone[9][10] (Figure 11) and dimethylsulfoxide[11]. Traces of dimethylsulfoxide cannot be detected under the conditions used in this work because the signal of the dimethylsulfoxide overlaps that of the deuterated dimethylsulfoxide. Fortunately, no European manufacturer is known who uses dimethylsulfoxide as solvent for recrystallisation.

## 4. Quantitative NMR Determination

A quantitative analysis of the NMR spectra is possible under some conditions[12]. There must be long waiting periods between the experiments, which are longer than 5 times the $T_1$-relaxation time. Nevertheless, a high digital resolution is re-

quired and the signals should be well separated. A good signal to noise ratio is required for exact measurements of the integrals. Under these circumstances, and assuming equal line broadening, not only the integrals but also the intensities can be determined according to the following equations:

$$\text{weight\% RDX} = \frac{I_{RDX} \cdot M_{RDX} \cdot F}{I_{RDX} \cdot M_{RDX} \cdot F + I_{HMX} \cdot M_{HMX}} \cdot 100$$

$$\text{weight\% HMX} = \frac{I_{HMX} \cdot M_{HMX}}{I_{RDX} \cdot M_{RDX} \cdot F + I_{HMX} \cdot M_{HMX}} \cdot 100$$

$$F = \frac{N_{HMX}}{N_{RDX}}$$

$I_{RDX}$ = integral or intensity of the RDX signal
$I_{HMX}$ = integral or intensity of the HMX signal
$M_{RDX}$ = molecular weight of RDX
$M_{HMX}$ = molecular weight of HMX
$F$ = factor
$N_{HMX}$ = number of protons of HMX
$N_{RDX}$ = number of protons of RDX

A quantitative analysis of RDX and HMX is shown in Figure 13. For a better resolution a Gauß/Lorenz transformation was done prior to the Fourier transformation and the determination was carried out without taking other by-products into account. The intensity and integral of the signals were determined and correlated to the HPLC analysis (Figure 13). The evaluation of the intensity shows a better result than the integral analysis. The difference of 1.8% is in good agreement with the HPLC result. The analysis of the integrals displays a lower precision because results depend on the setting of the integration margins. A quantitative determination of the by-products was not done because a HPLC method has yet to be developed. An estimation of the amount of by-products is in the order of max. 0.2 % for each compound.

## 5. Comparison of Different RDX and HMX Manufacturers

In Figures 12 to 22 the $^1$H-NMR spectra of different RDX and HMX samples are shown. The $^1$H-NMR spectrum of an RDX sample with normal intensities is shown. Only the signals of RDX and HMX are visible in the spectrum. The water signal results from the deuterated dimethylsulfoxide since water is an impurity in the solvent. Signals of the by-products could be observed only by a larger amplification of the spectrum. This was done by setting the main signal in the spectra (Figures 14 to 22) to a value of 1500 cm with the computer. With this amplification the spinning sidebands of large signals are visible. The spinning sidebands are marked with a dot. The by-products of RDX, which can be seen in the spectra, are acetone ($\delta$ = 2.07), TAX ($\delta$ = 2.16), open chain nitramine ($\delta$ = 2.05), acetic acid ($\delta$ = 1.90), cyclohexanone (for multiplet see clean substance), and aliphatic impurities ($\delta$ = 1.23 and 1,14). Besides these impurities there are also other signals at $\delta$ = 9.00, 8.25, and in the region of $\delta$ = 4.90. These signals result from paraformaldehyde and products which were formed from paraformaldehyde. There are no acetylated by-products in the RDX of the manufacturer D and no products which were formed from paraformaldehyde. This shows that this RDX is not synthesized in the Bachmann process, but in the nitric acid process. The recrystallisation from cyclohexanone is typical for manufacturer C and distinguishes him from all other manufacturers. Figure 18 shows a product which has been used in the production of an explosive. This spectrum can be analyzed as well. The signals at $\delta$ = 2.88 and 2.73 result from admixtures which were added during granulation.

HMX can be produced only by the Bachmann process. Therefore, acetylated by-products like SEX ($\delta$ = 2.26), open chain nitramines ($\delta$ = 2.05), acetic acid ($\delta$ = 1.90), and other products which were formed from paraformaldehyde could be observed in the spectra. As can be seen in the spectra, only SEX, open chain nitramines, as well as acetone ( $\delta$ = 2.05) from the recrystallisation and aliphatic impurities ($\delta$ = 1.14) occur (Figures 19 to 22). Also spectra of HMX/wax products

(Figure 22) can be analyzed adequately. Additional signals of the wax component in the NMR spectrum of the HMX/wax-product (manufacturer D) appear at $\delta = 3.51$ and in the region from $\delta = 1.50$ to 0.70.

The author thanks Dr. Langen and Dr. Gupta for revising the manuscript.

Referernces

1) C.D. Bedford et al., "Preparation and Purification of HMX and RDX Intermediates (TAX and SEX), Second Phase Final Report, U.S. Army Medical Research and Development Command, November 1980

2) C.D. Bedford et al., "Preparation and Purification of HMX and RDX Intermediates (TAX and SEX), Third Phase Final Report, U.S. Army Medical Research and Development Command, Dezember 1981

3) C.D. Bedford: "Preparation and Purification of Multigram Quantities of SEX and TAX", Final Report, U.S. Army Medical Research and Development Command, April 1983

4) W.E. Bachmann et al, J. Am. Chem. Soc, 73, 2769 (1951)

5) G.F. Wright, Canadian Journal of Research, Vol 27, Sec. B, 503 (1949)

6) W.E. Bachmann und J.C. Sheehan, J. Am. Chem. Soc. 71, 1842 (1949)

7) G.C. Hale, J. Am. Chem. Soc. 47, 2754 (1925)

8) T.C. Castorina, F.S. Holahan, R.J. Graybusch, J.V.R. Kaufman und S. Helf, J. Am. Chem. Soc, 82, 1617 (1960)

9) L. Svensson, J. Nyqvist u. L. Westling, J. Hasard, Mater, 13, 103 (1986)

10) L. Svensson, J. Nyqvist, Pat. DE 3520761A1, 25. März 1985

11) D.N. Thatcher, N.J. Sewell, US.Pat. 2900381, 18.08.1959

12) M.L. Martin, J.J. Delpuech und G.J. Martin, Partical NMR Spectroscopy, Heyden and Son (1980)

13) R.R. Ernst, Adv. Magn. Reson., 2, 1 (1966)

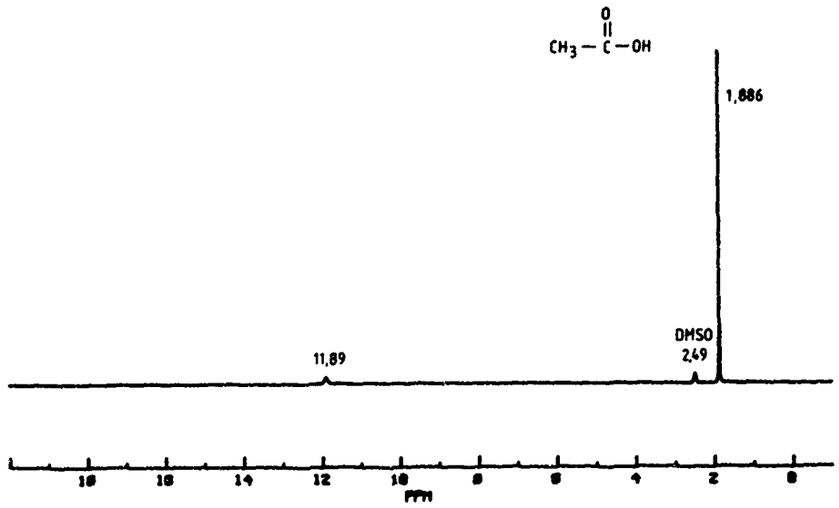


Figure 1: $^1$H-NMR spectrum of acetic acid. The signal at $\delta$ = 1.88 belongs to the methyl group. The acid proton at $\delta$ = 11.89 may shift if the concentration is changed.

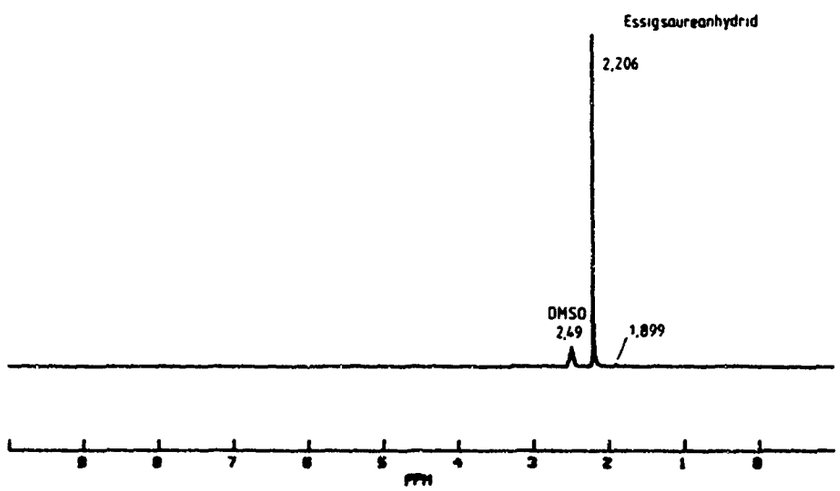


Figure 2: $^1$H-NMR spectrum of acetic acid anhydride. The signal at $\delta$ = 1.899 is an impurity of acetic acid.

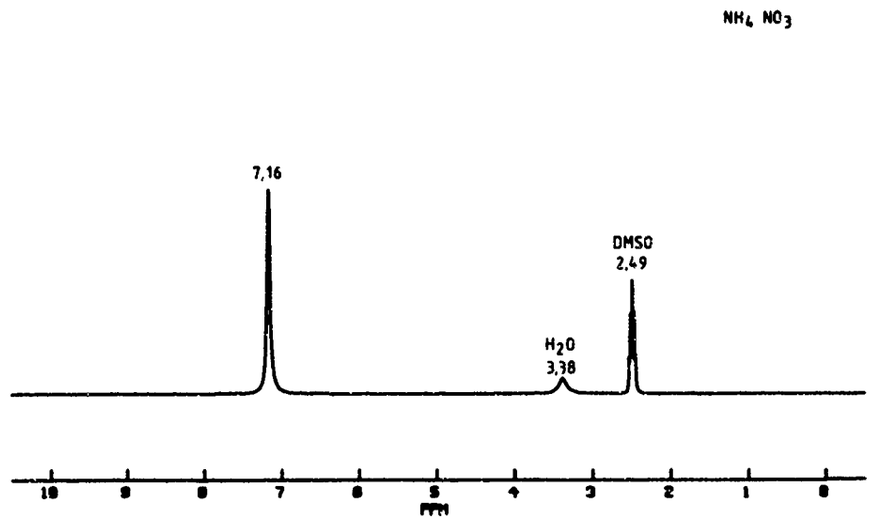


Figure 3: $^1$H-NMR spectrum of ammonium nitrate.

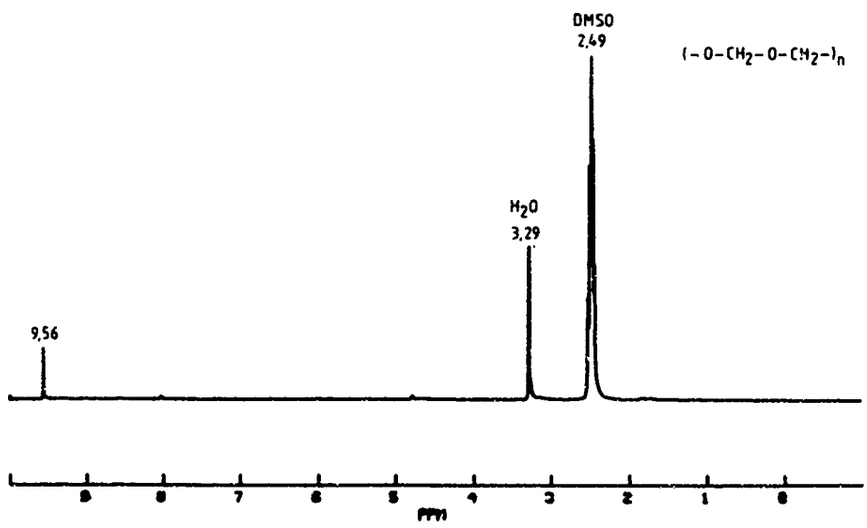


Figure 4: $^1$H-NMR spectrum of paraformaldehyde.

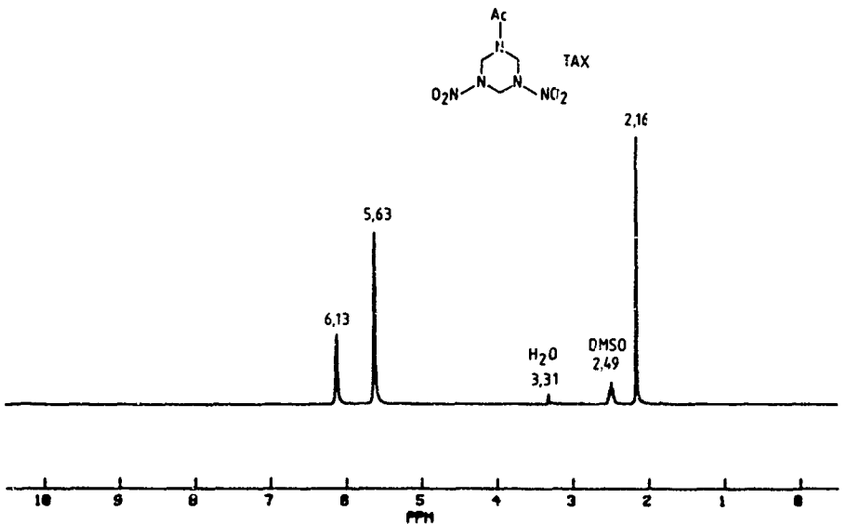


Figure 5: $^1$H-NMR spectrum of TAX.

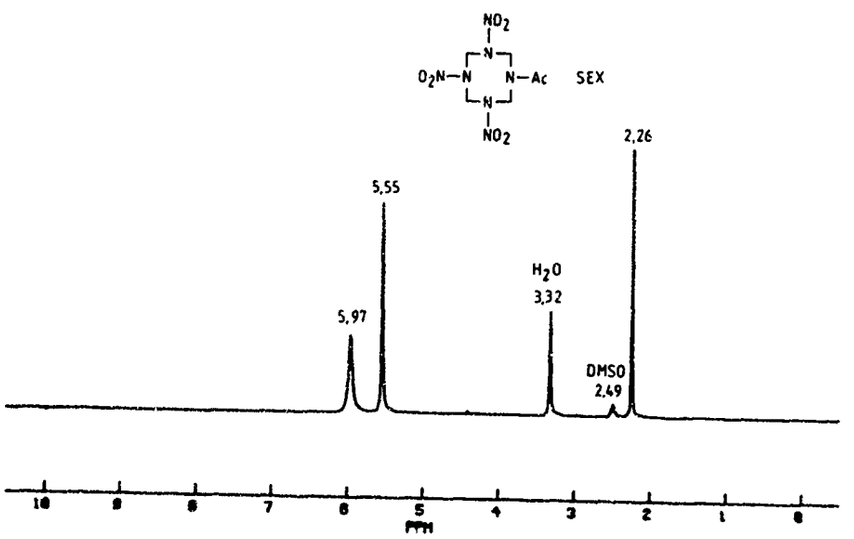


Figure 6: $^1$H-NMR spectrum of SEX.

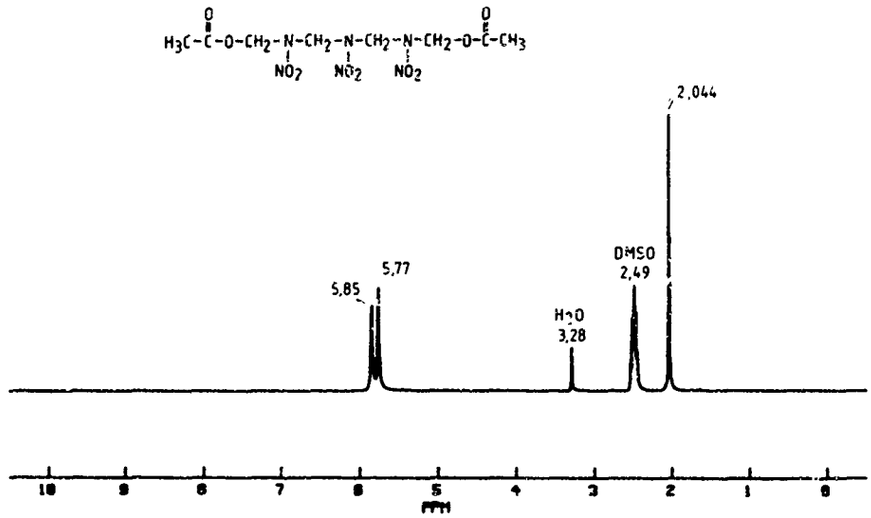


Figure 7: $^1$H-NMR spectrum of 1,7-diacetoxy-2,4,6-trinitro-2,4,6-triazaheptane.

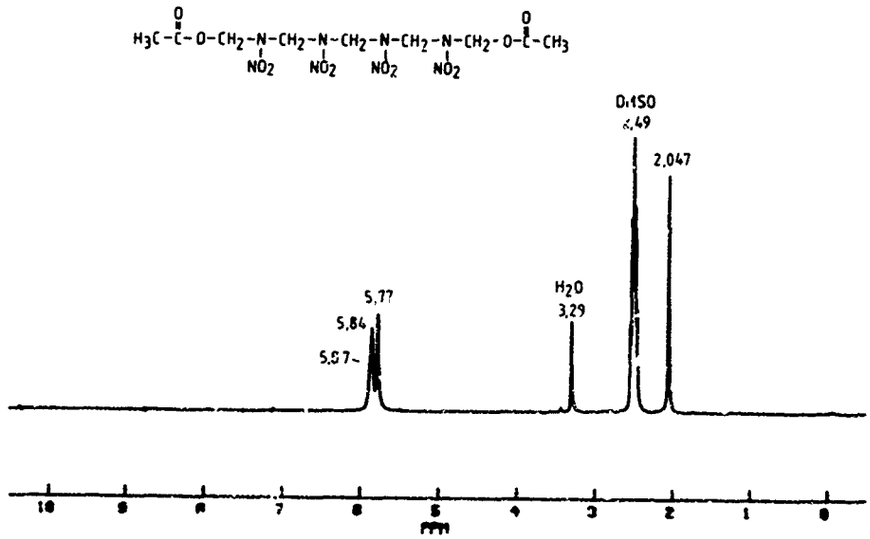


Figure 8: $^1$H-NMR spectrum of 1,9-diacetoxy-2,4,6,8-tetranitro-2,4,6,8-tetrazanonane.

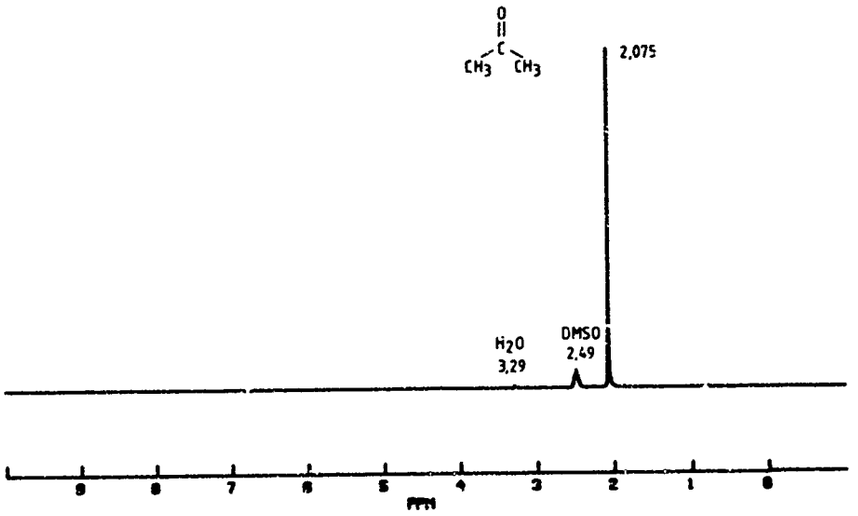


Figure 9: $^1$H-NMR spectrum of acetone.

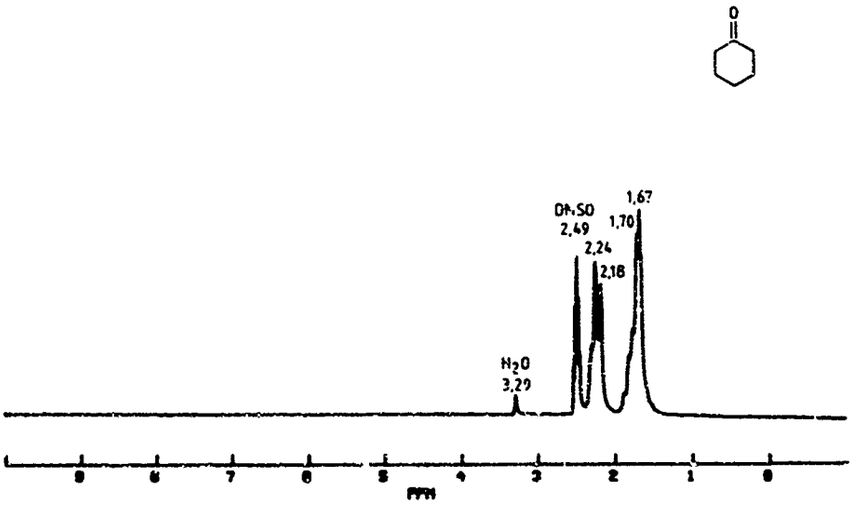


Figure 10: $^1$H-NMR spectrum of cyclohexanone.

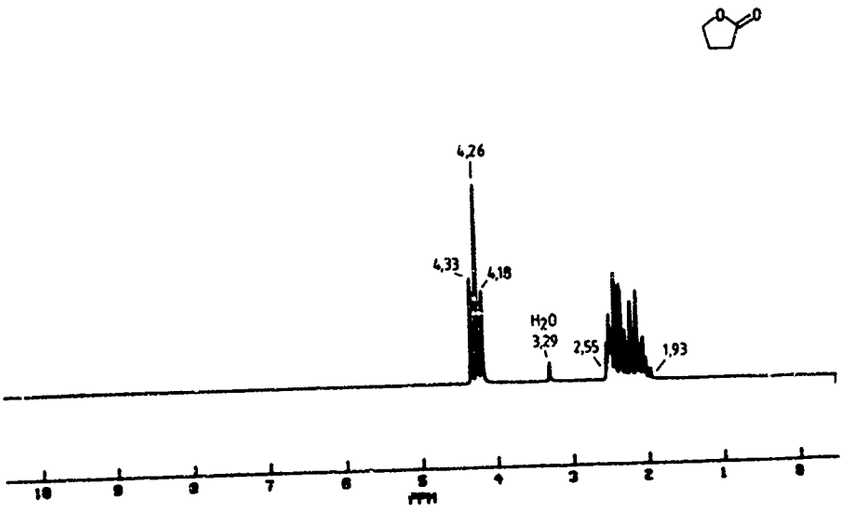


Figure 11: $^1$H-NMR spectrum of γ-butyrolactone.

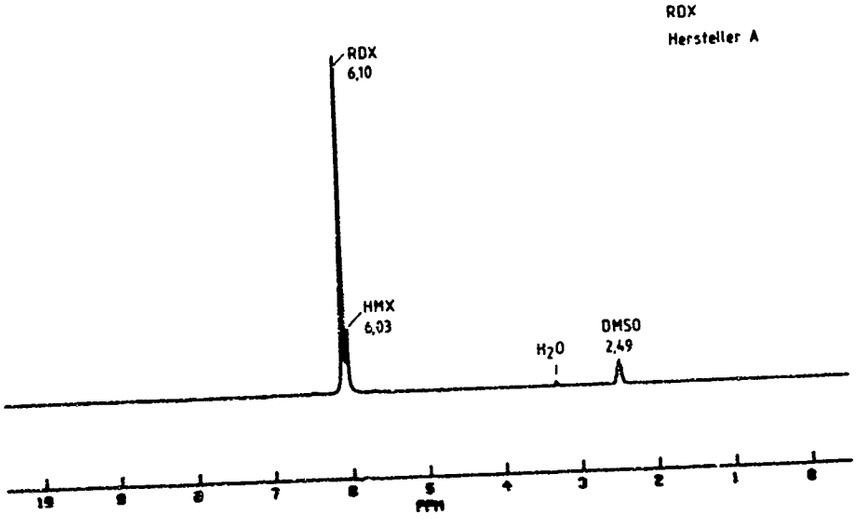


Figure 12: $^1$H-NMR spectrum of RDX of manufacturer A at normal amplification. The by-product HMX is detected at $\delta = 6.03$.

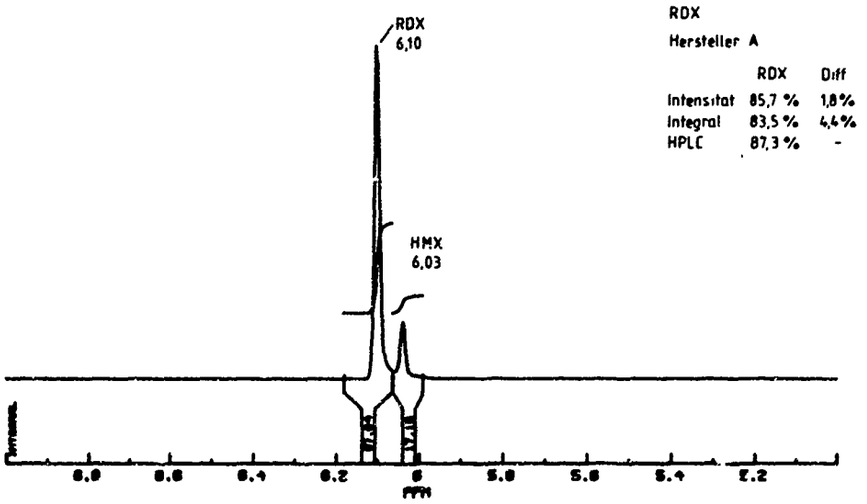


Figure 13: Quantitative determination of HMX in RDX by NMR spectroscopy. The comparison with HPLC is also shown.

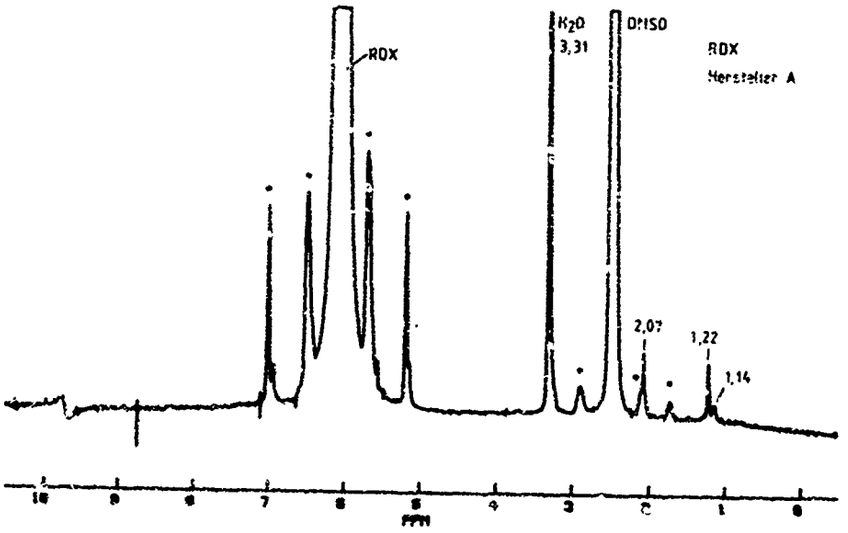


Figure 14: $^1$H-NMR spectrum of RDX of manufacturer A at high amplification. The detected impurities are acetone ($\delta$ = 2.07) and aliphatic compounds ($\delta$ = 1.22-1.14).

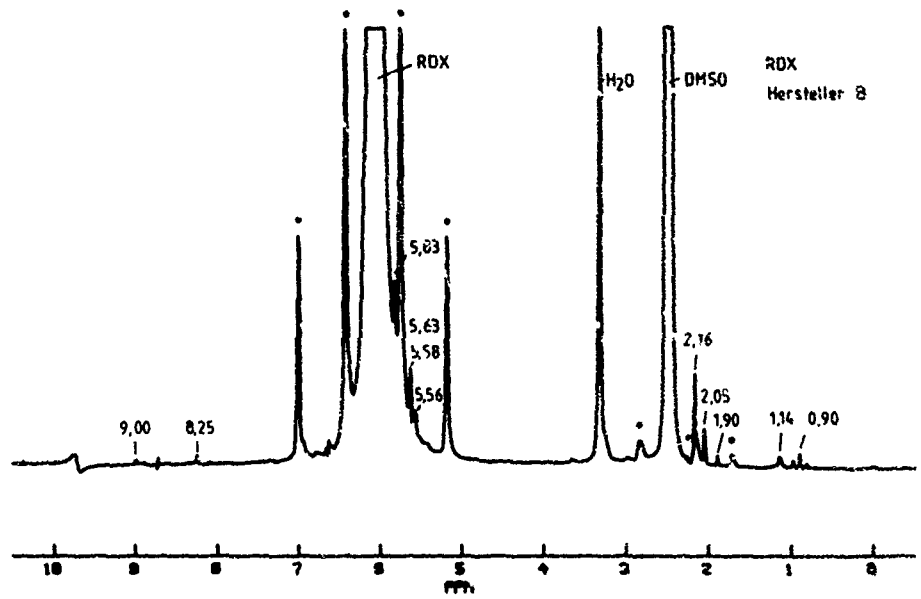


Figure 15: $^1$H-NMR spectrum of RDX of manufacturer B at high amplification. The detected impurities are TAX (δ = 2.16), open chain nitramines (δ = 2.05), acetic acid (δ = 1.90), aliphatic compounds (δ = 1.14-0.90) and products from paraformaldehyde (δ = 9.00; 8.25).

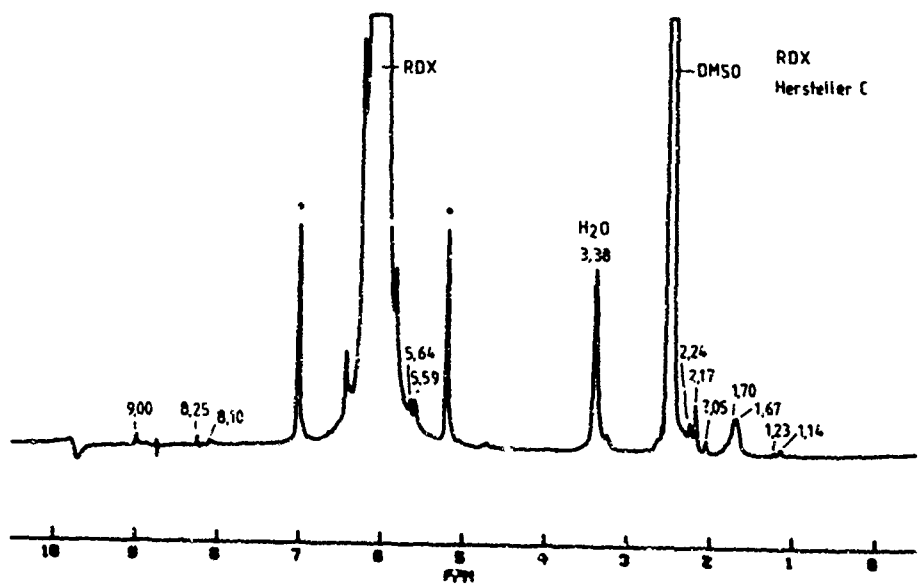


Figure 16: $^1$H-NMR spectrum of RDX of manufacturer C at high amplification. The detected impurities are cyclohexanone (δ = 1.50-2.30), open chain nitramines (δ = 2.05), aliphatic compounds (δ = 1.23; 1.14) and products from paraformaldehyde (δ = 9.00; 8.25; 8.10).

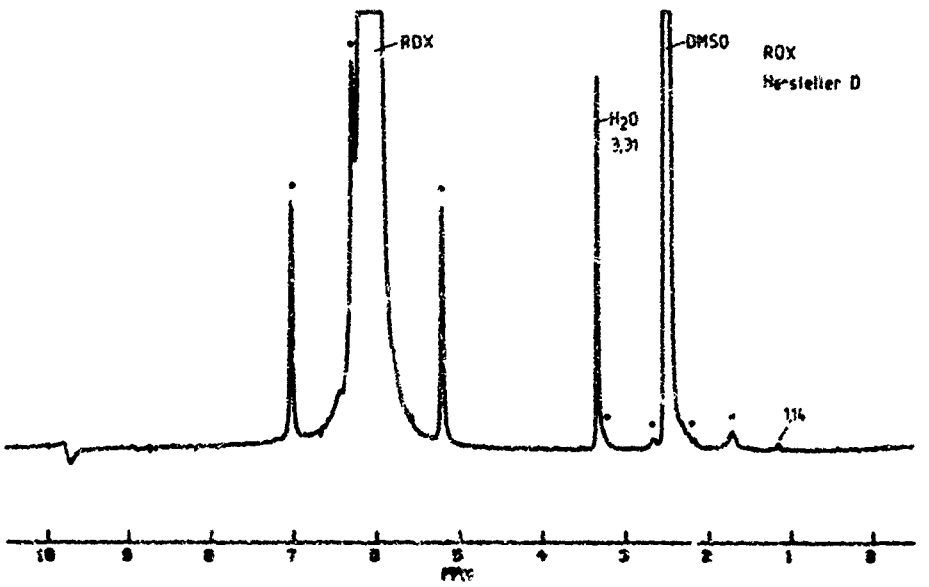


Figure 17: $^1$H-NMR spectrum of RDX of manufacturer D at high amplification. Only an aliphatic impurity (δ = 1.14) can be detected in the spectrum.

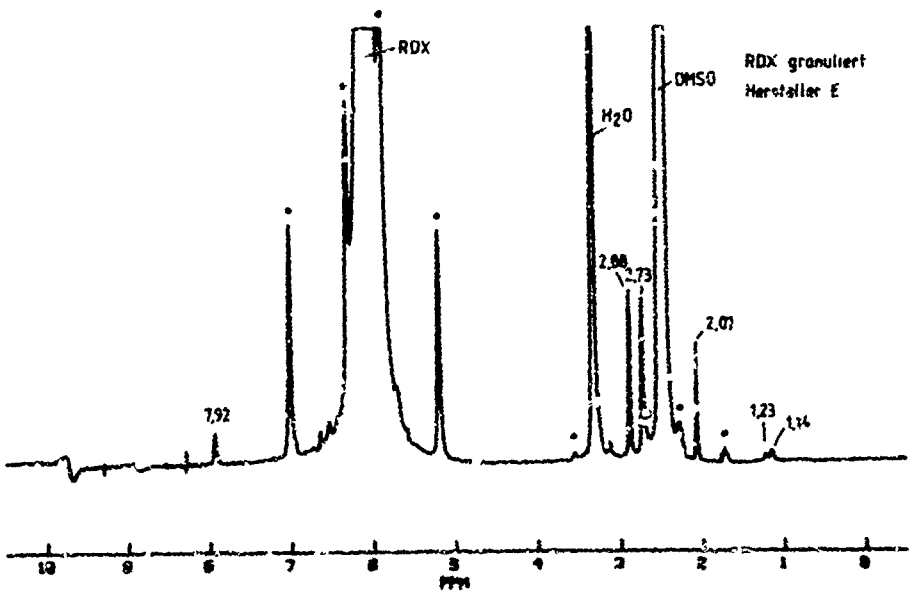


Figure 18: $^1$H-NMR spectrum of granulated RDX of manufacturer E. The detected impurities are acetone (δ = 2.07), aliphatic compounds (δ = 1.23; 1.14) and grenulation additives (2.88; 2.73; 7.92).

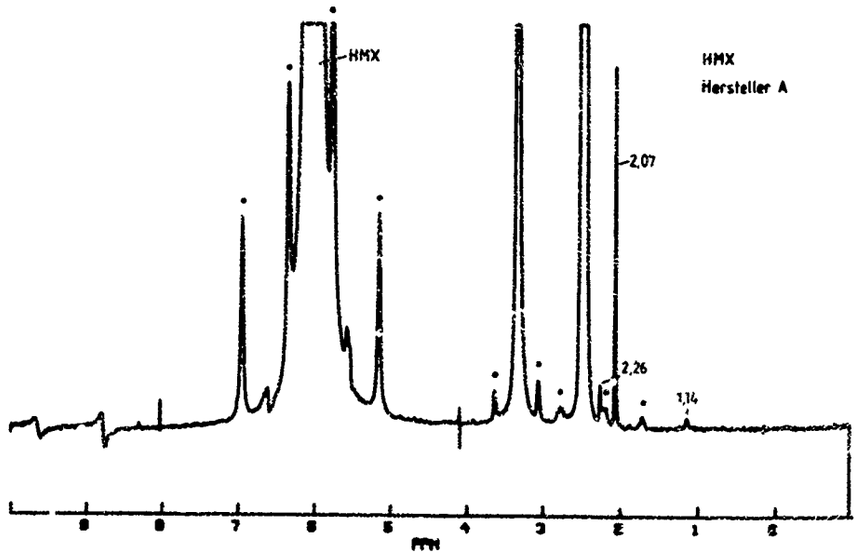


Figure 19: $^1$H-NMR spectrum of HMX of manufacturer A at high amplification. The detected impurities are SEX ($\delta$ = 2.26), acetone ($\delta$ = 2.07) and an aliphatic compound ($\delta$ = 1.14).

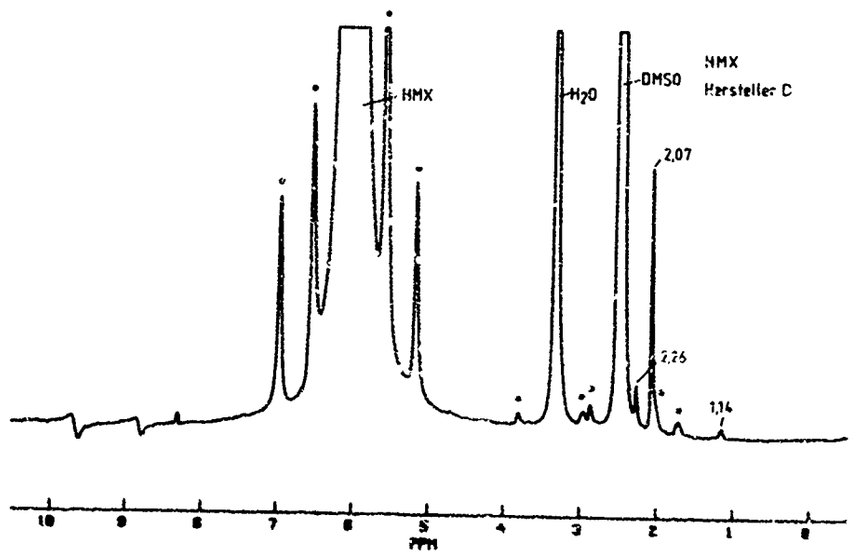


Figure 20: $^1$H-NMR spectrum of HMX of manufacturer B at high amplification. The detected impurities are SEX ($\delta$ = 2.26), acetone ($\delta$ = 2.07) and an aliphatic impurity ($\delta$ = 1.14)

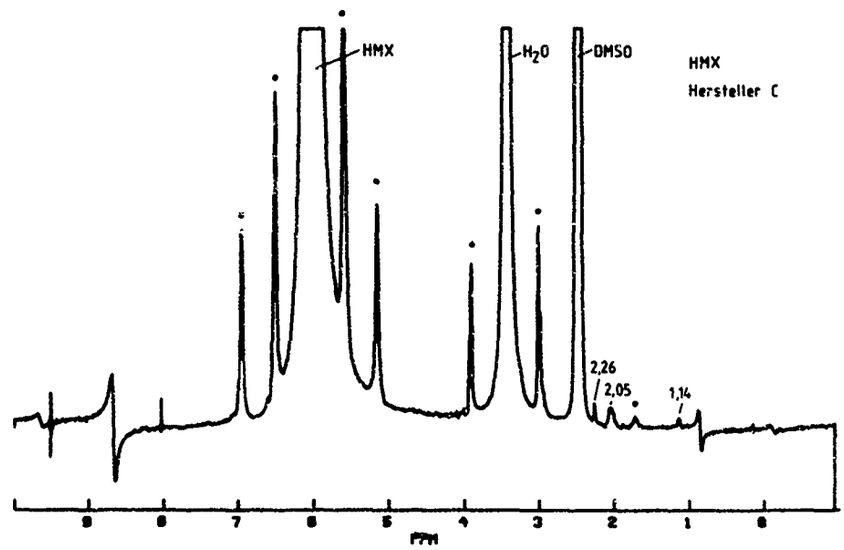


Figure 21: $^1$H-NMR spectrum of HMX of manufacturer C at high amplification. The detected impurities are SEX ($\delta$ = 2.26) and an aliphatic compound ($\delta$ = 1.14).

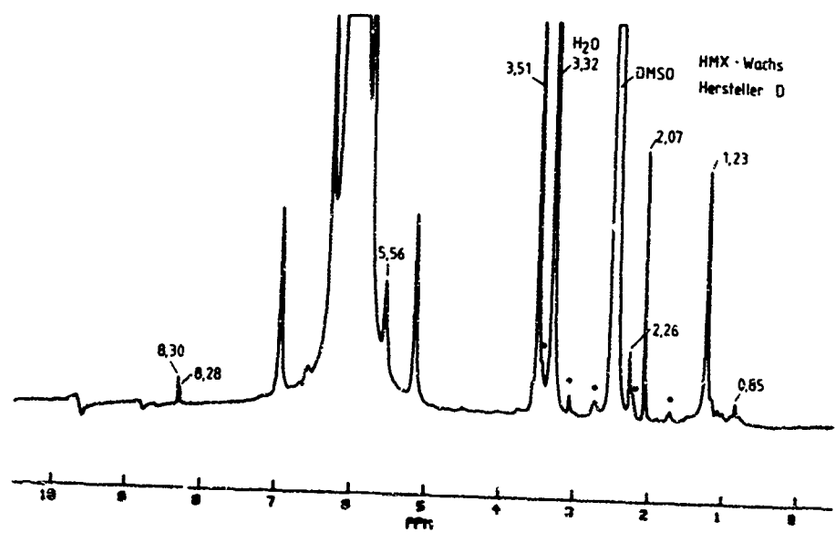


Figure 22: $^1$H-NMR spectrum of HMX/wax of manufacturer D at high amplification.

# MULTICOMPONENT ANALYSIS OF EXPLOSIVES

F. Ark and T.H. Chen
U.S. Army Armament, Research, Development, and Engineering Center,
Picatinny Arsenal, N.J. 07806-5000, U.S.A.

## ABSTRACT

This laboratory has been studying the multicomponent analysis of explosives using diode-array ultraviolet/visible spectrophotometry and Fourier transform infrared spectrophotometry (FTIR). The aim of this study is to replace the classical wet chemical methods which are tedious and time-consuming with the instrumental techniques with emphasis on speed of analysis, low toxicity of chemicals used, and future on-line process applications.

This paper will describe the experimental procedure used in the multicomponent FTIR analysis of Octol, composed of TNT and HMX, and discuss the results obtained.

## 1. INTRODUCTION

Many of the methods contained in the current military standards for the analysis of energetic and related materials were developed decades ago. They are usually tedious and time-consuming and quite often the toxic chemicals such as benzene and mercury are used in these methods. There has, therefore been, for sometime, a need to develop rapid, reliable, and safer analytical methodologies for the assay and composition analysis of energetic and related materials. This laboratory has been developing such methods for sometime using various instrumental techniques, especially the multicomponent diode-array ultraviolet/visible spectrophotometry[1,2,3] and multicomponent FTIR[4]. We are not aware of any efforts in this area. The aim of this study is to replace the classical wet chemical methods with rapid and reliable instrumental methods with emphasis on speed of analysis, low toxicity of chemicals used, and future on-line process applications. This paper will describe the experimental procedure

used in the multi-component FTIR analysis of Octol, composed of TNT and HMX, and discuss the results obtained.

## 2. EXPERIMENTAL

A Beckman Model FT 1100 FTIR Spectrophotometer with 4 $cm^{-1}$ resolution was used in the analysis. A liquid cell with 0.05 mm path thickness and NaCl windows was used in the recording of all spectra. The instrument was purged with nitrogen gas prior to and during the recording of spectral data.

The cyclohexanone used was Aldrich 99.8%, Gold Label Grade. The purities of HMX and TNT were better than 99%.

## 3. RESULTS AND DISCUSSION

Figure 1 shows the absorption charateristics of HMX; Figure 2, the absorption characteristics of TNT; Figure 3, the overlay of HMX and TNT; Figure 4, the overlay of HMX and cyclohexanone; Figure 5, the overlay of TNT and cyclohexanone; Figure 6, the overlay of HMX plus TNT and cyclohexanone in a standard solution; and Figure 7, the overlay of HMX plus TNT and cyclohexanone in a synthetic mixture. The scanning time for all spectra are approximately 100 seconds, corresponding to averaging of about 83 spectra. The concentrations of HMX and TNT in above figures were approximately 1.8 g and 0.6 g/100ml cyclohexanone, respectively. In Figures 1-3, the absorption of cyclohexanone was subtracted from the solution spectra. The sharp spikes result from the subtraction of cyclohexanone absorption from HMX in cyclohexanone and from TNT in cyclohexanone. (See Figures 4-7). The spikes occur at the strong absorption peaks of cyclohexanone. The significant absorption bands for HMX are at 1568, 1286, 1273, and 928$cm^{-1}$; and those for TNT are at 1545 and 1347$cm^{-1}$. In Figure 2, the hatched area, the dark area at 1347$cm^{-1}$, and the white area at 1545$cm^{-1}$ represent respectively, HMX absorption, TNT absorption above HMX, and TNT absorption below HMX. This means that HMX and TNT exhibit completely overlapping aborption except at 1347$cm^{-1}$ where the overlapping is slight. It would appear that based on the absorption characteristics of HMX and TNT, the wave number region of

1300-1600cm$^{-1}$ may be appropriate for the quantitation of HMX and TNT. In Figures 4-7, the dark area represents the absorption of cyclohexanone, the hatched area the absorption of HMX above cyclohexanone (Figure 4), the absorption of TNT above cyclohexanone (Figure 5), the absorption of HMX and TNT in a standard above cyclohexanone (Figure 6), the absorption of HMX and TNT in a synthetic mixture above cyclohexanone (Figure 7), and the white area represents the corresponding absorption of the solute in each solution below cyclohexanone.

It should be noted that the cyclohexanone absorption is quite strong in the vicinity of 928 and 1285cm$^{-1}$ where HMX and TNT exhibit significant absorption, the ratio of solvent to solute being about 1:1. Only the 1568cm$^{-1}$ region is essentially free from the interfering absorption of cyclohexane. This region was therefore included in the quantitative studies.

The quantitation was based on Beckman's Vector Quant software. The parameters studied include the starting index (SI), which enables the elimination of unwanted noise by choosing appropriate SI values, and the wave number region. In the quantitative analysis, five standard mixtures with composition of HMX ranging from about 71 to 79% and TNT from 21 to 28% (weight/volume)(Table 1) were prepared to bracket the concentration of the synthetic mixture (about 75 HMX and 25% TNT, w/v). The correlation coefficients of the standard curves were found to be 0.9963 for HMX and 0.9946 for TNT. This study established the optimum conditions for the analysis of Octol to be SI = 130 and the spectral region of 1617-1509cm$^{-1}$. The results are summarized in Tables 2 and 3. Table 2 is expressed in terms of the weight added and the amount found, whereas Table 3 is shown in terms of composition. The residual represents the unaccounted for portion of the spectrum. This amounts to less than 1% and arises most likely from the system noise. The results obtained are quite good with the % recovery of 99.51 and 99.42 for HMX and TNT, respectively. The precision in terms of RSD was 1.10%.

## 4. CONCLUSION

A rapid analytical method for the analysis of Octol by multicomponent FTIR has been developed. Cyclohexanone was used as the solvent and the starting index of 130 and the spectral region of 1617-1509cm$^{-1}$ were determined to be the optimum parameters. The results were quite satisfactory with 99.51 and 99.42 recovery % for HMX and TNT, respectively. The precision in terms of RSD was 1.1%.

## REFERENCES

1. T.H. Chen and F. Ark, "Rapid Analysis of Single Base Propellant by Multicomponent Ultraviolet Spectrophotometry", Paper No. 324, the 1984 Pittsburgh Conference and Exposition on Analytical Chemistry and Applied Spectroscopy, Atlantic City, New Jersey, March 5-9, 1984.

2. T.H. Chen and F. Ark, "Rapid Analysis of Explosives by Multicomponent Ultraviolet Spectrophotometry", the 187th American Chemical Society National Meeting, Paper No. 40, St. Louis, Missouri, April 8-13, 1984.

3. T.H. Chen and F. Ark, "Rapid Analysis of Nitroguanidine by Ultraviolet Spectrophotometry", the twenty-Third Eastern Analytical Symposium, Paper No. 114, New York, New York, November 13-16, 1984.

4. T.H. Chen and F. Ark, "Rapid Analysis of Explosives by Multicomponent FTIR", the 1986 Pittsburgh Conference and Exposition on Analytical Chemistry and Applied Spectroscopy, Paper No. 693, Atlantic City, N.J., March 10-14, 1986.

Table 1. Composition of Standard Mixtures

| Standard No. | Actual Weight g/25ml HMX | TNT | % (Weight/Volume) HMX | TNT |
|---|---|---|---|---|
| 1 | 0.4743 | 0.1216 | 79.00 | 21.00 |
| 2 | 0.4625 | 0.1382 | 76.99 | 23.01 |
| 3 | 0.4497 | 0.1497 | 75.00 | 25.00 |
| 4 | 0.4378 | 0.1622 | 72.94 | 27.06 |
| 5 | 0.4275 | 0.1725 | 71.25 | 28.75 |

Table 2. Analysis of HMX and TNT in Synthetic Mixtures

| Synthetic Mixture No. | Amount Added, g HMX | TNT | Amout Found,g HMX | TNT | Residual | % Recovery HMX | TNT |
|---|---|---|---|---|---|---|---|
| 1 | 0.4512 | 0.1514 | 0.4497 | 0.1500 | 0.0022 | 99.67 | 99.08 |
| 2 | 0.4503 | 0.1508 | 0.4487 | 0.1513 | 0.0013 | 99.64 | 100.33 |
| 3 | 0.4526 | 0.1522 | 0.4491 | 0.1505 | 0.0032 | 100.78 | 98.88 |
| 4 | 0.4507 | 0.1515 | 0.4498 | 0.1487 | 0.0050 | 99.80 | 98.15 |
| 5 | 0.4503 | 0.1497 | 0.4498 | 0.1493 | 0.0044 | 99.89 | 99.73 |
| 6 | 0.4493 | 0.1502 | 0.4475 | 0.1515 | 0.0022 | 99.60 | 101.07 |
| 7 | 0.4528 | 0.1580 | 0.4402 | 0.1560 | 0.0017 | 97.22 | 98.73 |
| | | | | | Average | 99.51 | 99.42 |
| | | | | | RSD, % | 1.10 | 1.10 |

Table 3. Analysis of HMX and TNT in Synthetic Mixtures

| Synthetic Mixture No. | Composition, Weight/Volume Added HMX | TNT | Found HMX | TNT | % Residual |
|---|---|---|---|---|---|
| 1 | 74.88 | 25.12 | 74.71 | 24.92 | 0.37 |
| 2 | 74.91 | 25.09 | 74.62 | 25.16 | 0.22 |
| 3 | 74.83 | 25.17 | 74.50 | 24.97 | 0.53 |
| 4 | 74.84 | 25.16 | 74.53 | 24.64 | 0.83 |
| 5 | 75.05 | 24.95 | 74.53 | 24.74 | 0.73 |
| 6 | 74.95 | 25.05 | 74.43 | 25.20 | 0.37 |
| 7 | 74.13 | 25.87 | 73.62 | 26.07 | 0.28 |

Table 3. Analysis of HMX and TNT in Synthetic Mixtures (cont'd)

| | Composition, Weight/Volume Added | | Found | | % Residual |
|---|---|---|---|---|---|
| | HMX | TNT | HMX | TNT | |
| Average | 24.79 | 25.20 | 24.42 | 25.10 | 0.48 |
| RSD, % | 0.41 | 1.21 | 0.49 | 1.91 | 0.21 |

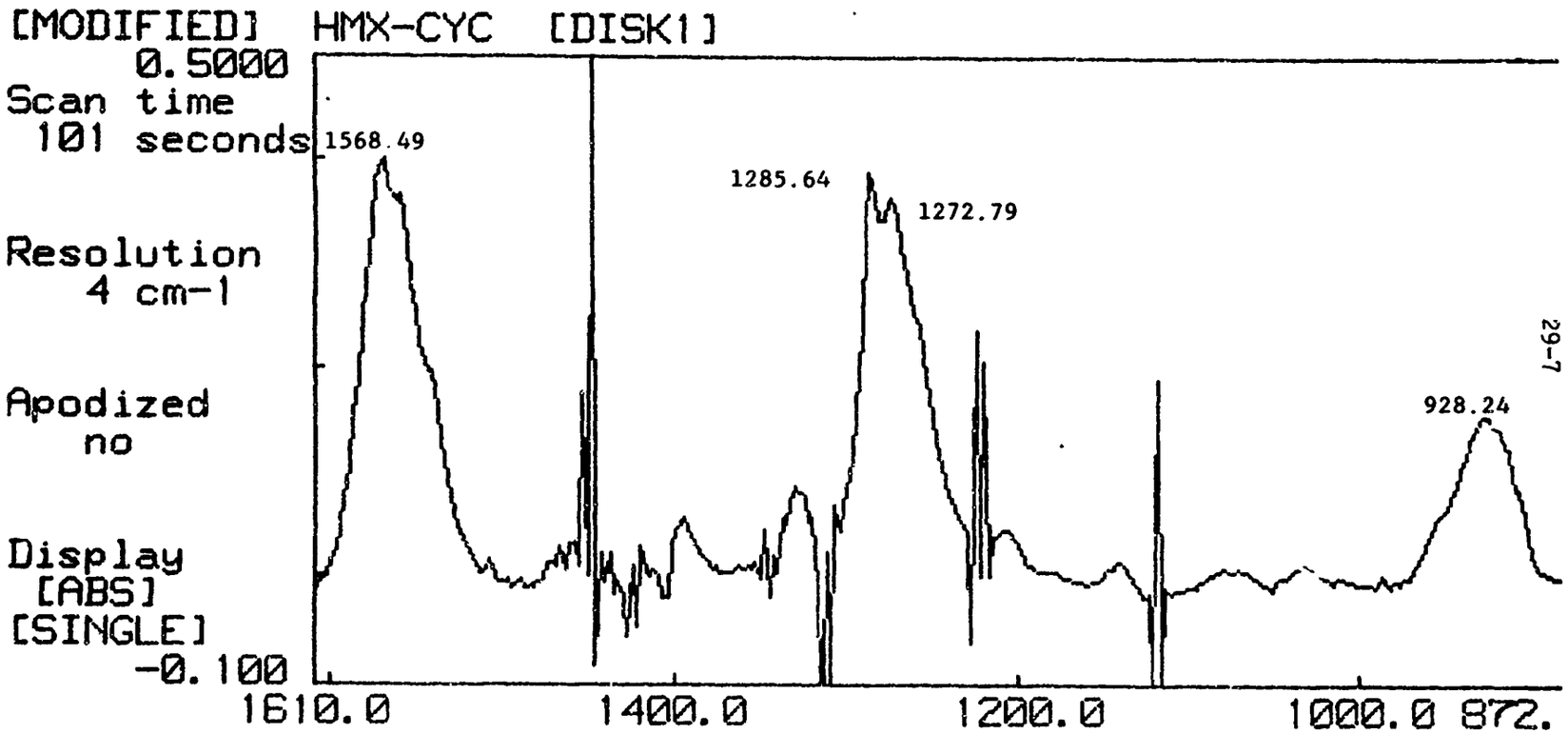


Figure 1. IR Spectrum of HMX

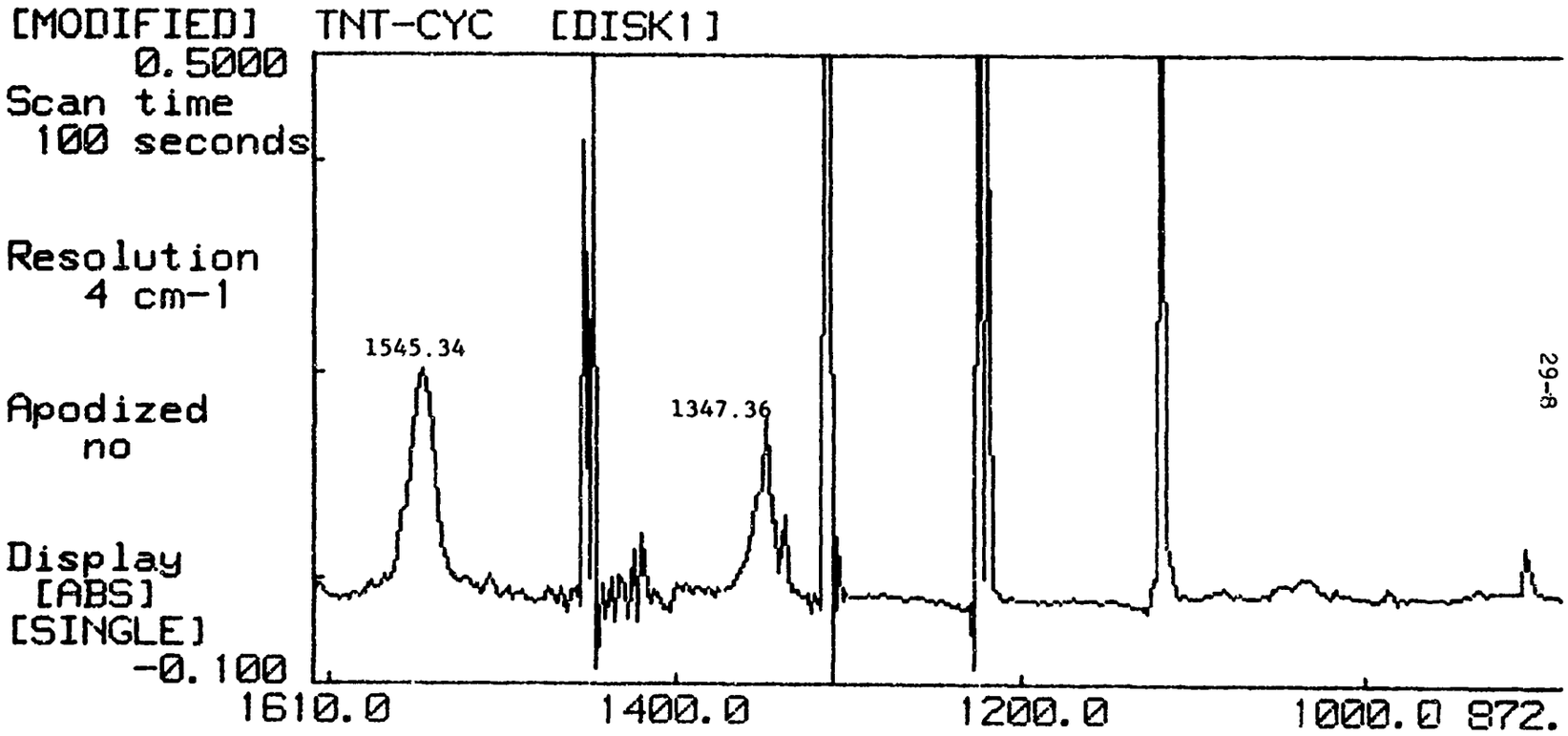


Figure 2. IR Spectrum of TNT

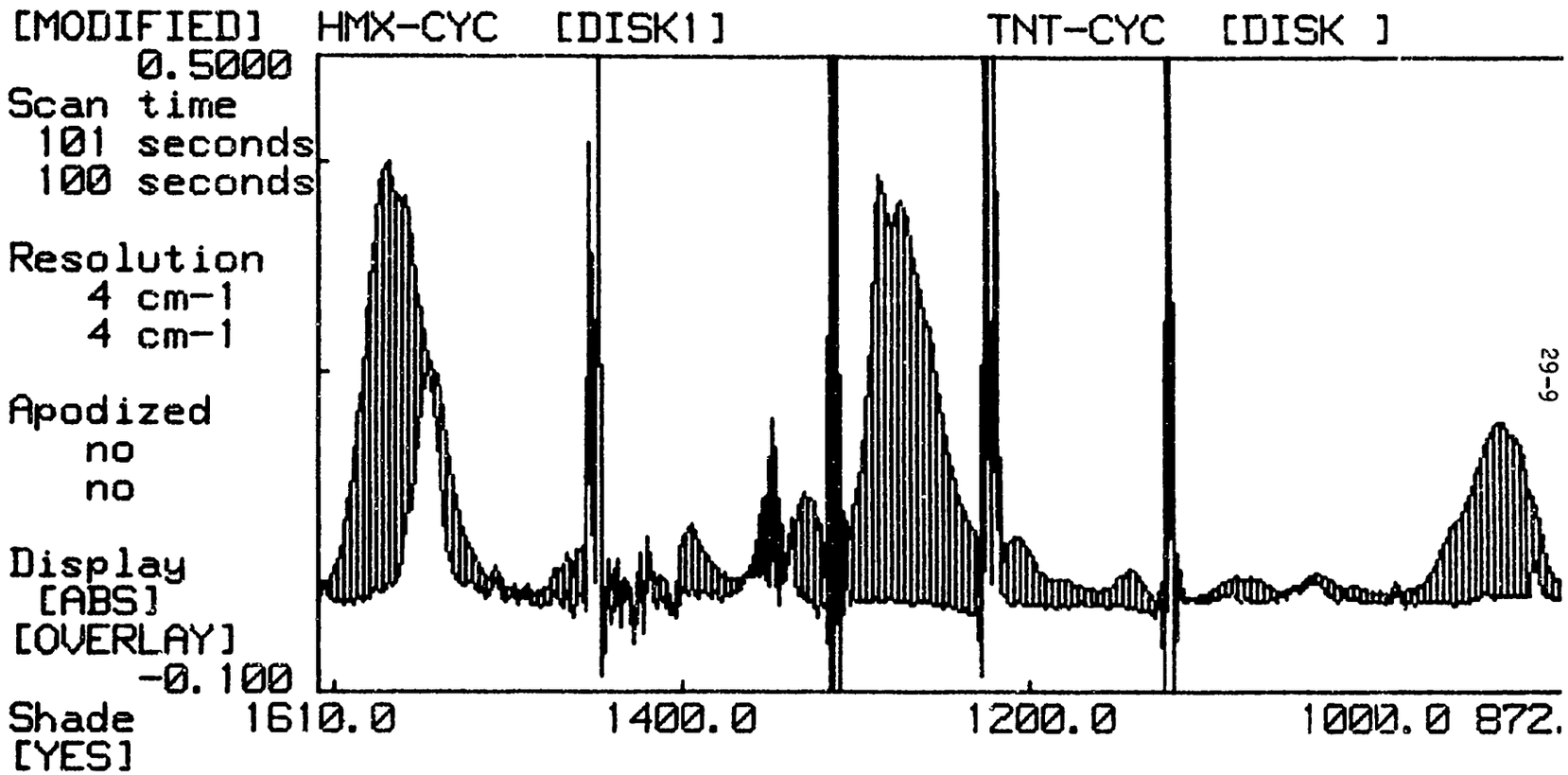


Figure 3. Overlay IR Spectra of HMX and TNT

Hatched Area: HMX Absorption

Dark Area at 1347 $cm^{-1}$: TNT Absorption above HMX

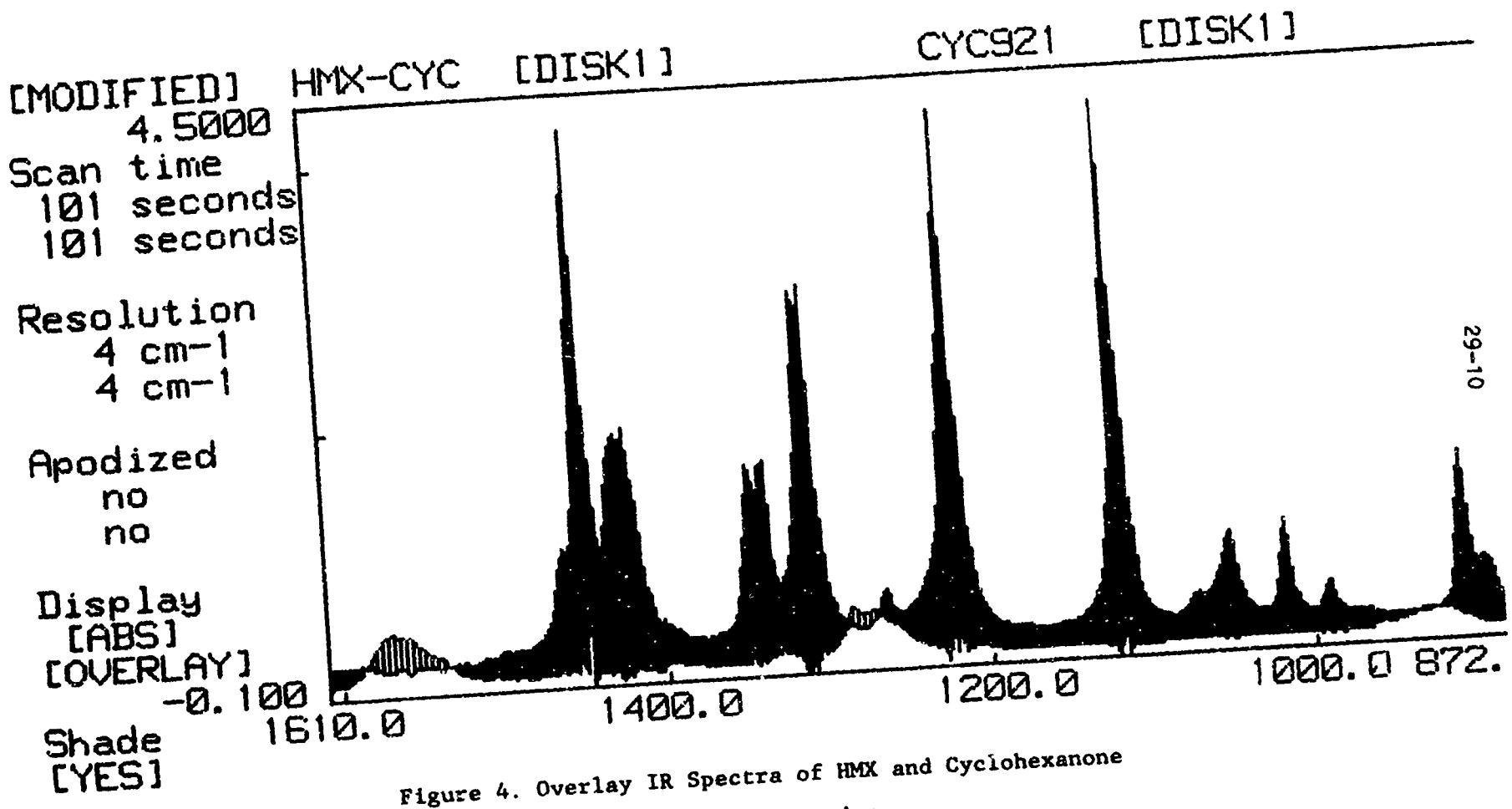


Figure 4. Overlay IR Spectra of HMX and Cyclohexanone

Dark Area: Cyclohexanone Absorption

Hatched Area: Absorption of HMX above Cyclohexanone

White Area: Absorption of HMX below Cyclohexanone

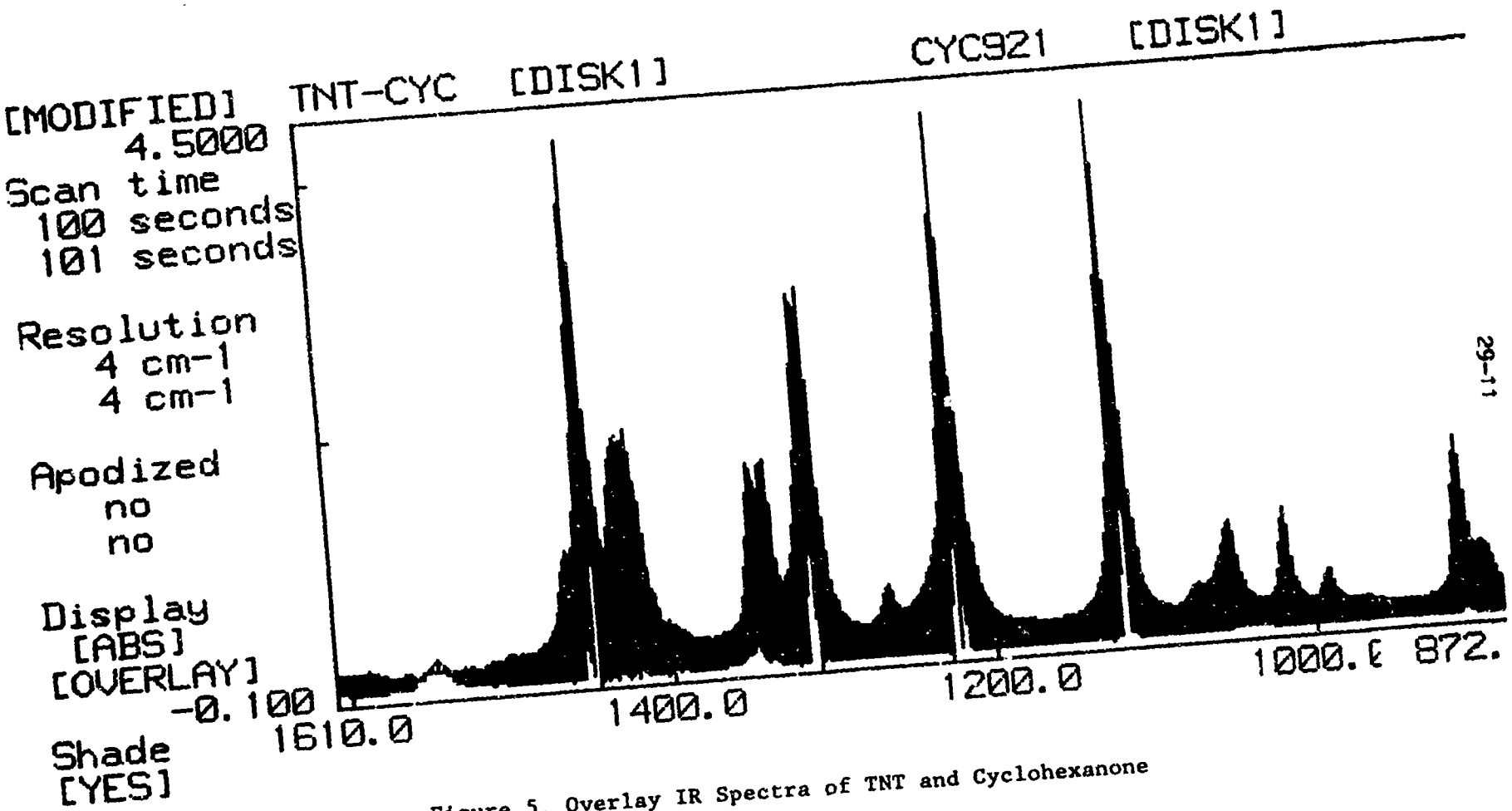


Figure 5. Overlay IR Spectra of TNT and Cyclohexanone

Dark Area: Cyclohexanone Absorption
Hatched Area: Absorption of TNT above Cyclohexanone
White Area: Absorption of TNT below Cyclohexanone

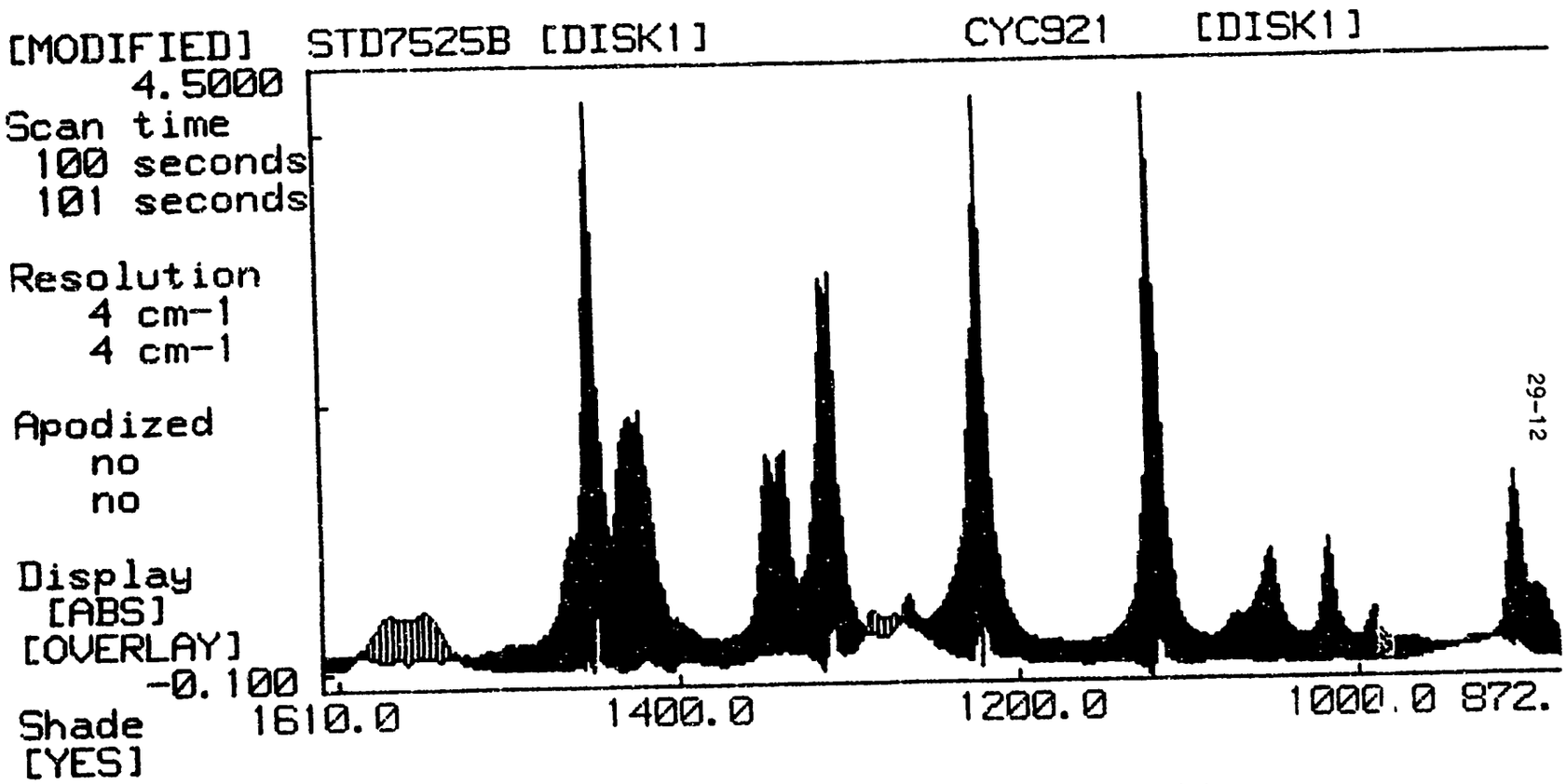


Figure 6. Overlay IR Spectra of HMX plus TNT in a Standard and Cyclohexanone

Dark Area: Cyclohexanone Absorption

Hatched Area: Absorption of HMX and TNT in a Standard above Cyclohexanone

White Area: Absorption of HMX and TNT in a Standard below Cyclohexanone

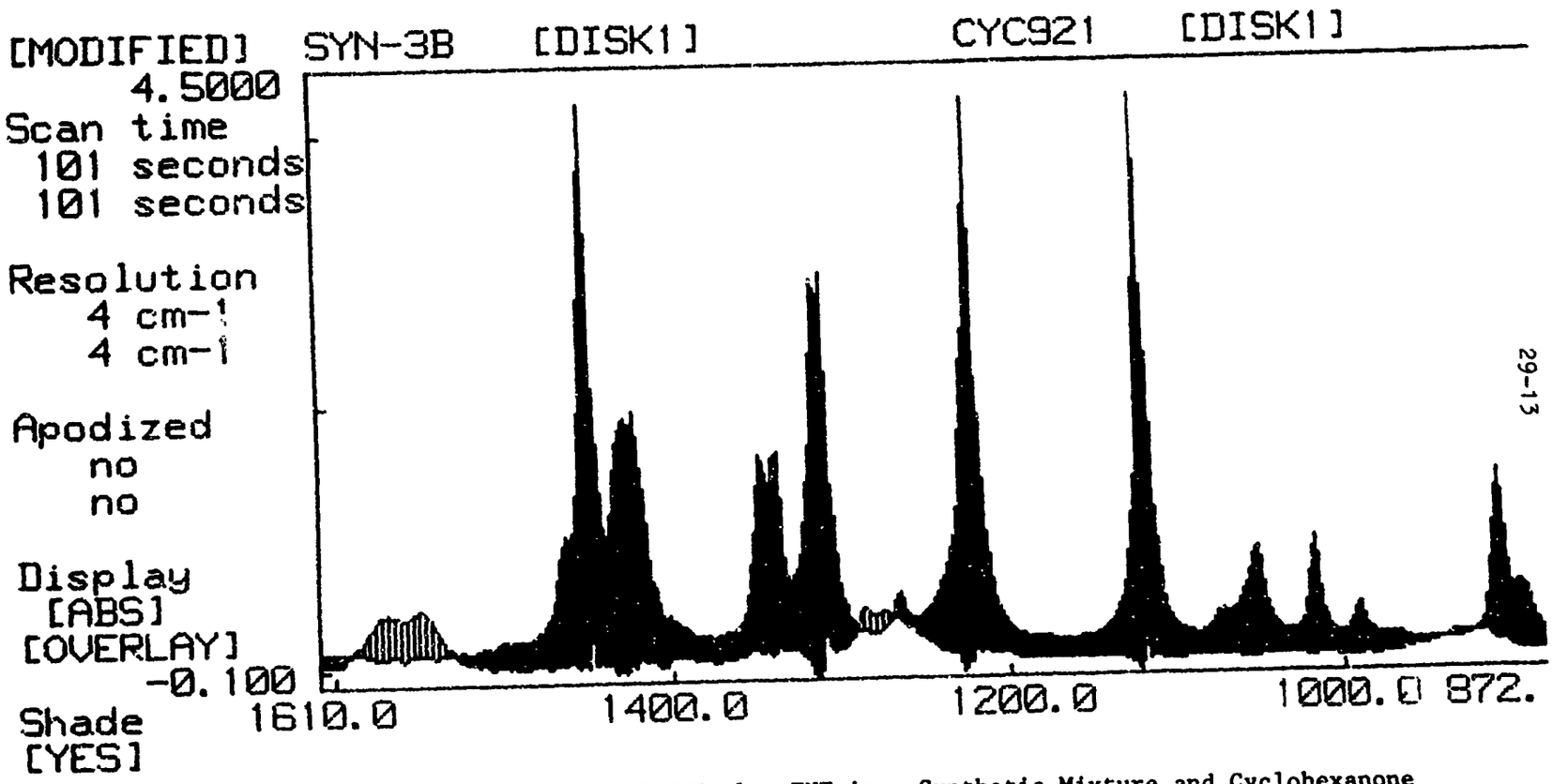


Figure 7. Overlay IR Spectra of HMX plus TNT in a Synthetic Mixture and Cyclohexanone

Dark Area: Cyclohexanone Absorption

Hatched Area: Absorption of HMX and TNT in a Synthetic Mixture above Cyclohexanone

White Area: Absorption of HMX and TNT in a Synthetic Mixture below Cyclohexanone

**ABSTRACT**

## DIFFUSION ASPECTS OF TRACEABLE MATERIALS FOR EXPLOSIVE DETECTION

by Dr J Gilbert (RARDE)

The use of dogs is still the most effective general method for searching for concealed explosives. The recent shift in illicit use from nitroglycerine based to plastic explosives has had consequences for both the dog handling and electronic detector based communities. The difference in vapour pressure between the solid and nitroglycerine based explosives has not only exacerbated the problems of detection, but also causes the facile contamination of the plastic explosives used for laboratory and training purposes.

This paper describes the background and work undertaken to quantify the sorption by and loss from plastic explosives of Ethylene Glycol Dinitrate and 3 Nitrotoluene commonly encountered constituents of commercial explosives. The knowledge of the diffusion coefficients for these materials enables estimates to be made of the rate of contamination of explosives stored with gelignites,together with the consequences for the detection of the contaminated material.

# GUNSHOT DISTANCE DETERMINATION BY MEANS OF INSTRUMENTAL NEUTRON ACTIVATION ANALYSIS AND AUTORADIOGRAPHY

A. Brandone, M. Signori
Dipartimento di Chimica Generale Università di Pavia
Via Taramelli 12, Pavia, Italia

F. De Ferrari, P. Pelizza
Istituto di Medicina Legale Università di Brescia
Spedali Civili, Brescia, Italia

V. Vidiri
Scuola di Polizia Giudiziaria - (Ministero degli Interni)
Via Vittorio Veneto 3, Brescia, Italia

## ABSTRACT

Forensic gunshot distance determination is a question not so easy to be resolved. As a matter of fact different techniques such as studies on tattoving of the skin, infrared photography, fluorescence tecniques, antimony determination on the target by means of Instrumental Neutron Analysis (INAA) etc. have been proposed.

We report here the quantitative determination of antimony on different target distances carried out by INAA coupled with the autoradiography of the neutron irradiated targets.

The target were fragments of cotton tissue (cm 10 x cm 10); firing distances were in the range from 5 cm to 100 cm; shots have been carried out with different firearms of the same calibre. The results are reported together with the advantages of the proposed techniques.

## 1. INTRODUCTION

Forensic activity during Judicial investigations of crimes in which firearms have been employed applies different criteria, among which great importance is attached to the determination of shooting distance.

The methods proposed and praticed are different in order to answer this serious question that, however, doesn't seem could be easily solved, especially when an accuracy of centimeters is required.

Even recently, numerous authors have tackled this problem; among the most meaningful works we can call to mind are the ones of Villanueva et al. (15) who have investigated gunpowder residues by Atomic Absorption

Spectrophotometry; the authors note that while iron, copper, cadmium and zinc have very irregular behaviour, lead, barium and antimony give very good results in agreement to other studies on this topic (2,12,16). Lekstrom and Koons (11) too have investigated this subject by colorimetric tests, studying in particular the Dithioxamide Test, also Known as the rubeanic acid (DTO test); this procedure based on the formation of colored precipitates with copper (dark green), nickel (pink or blue) and cobalt (brown) used in conjunction with the Modified Griess Test and with the Sodium Rhodizonate Test offers, according to the authors, a good reliability in the muzzle-to-target distance determination. Notable are also the experiments of Basu (1) on the use of Scanning Electron Microscopy equipped with energy dispersive X-ray fluorescence.

Among the different methods proposed, we think to be worthy the ones based on the determination of the levels of gunshot residues deposited on the target; more particularly, the quantitative analysis of antimony (Sb) by means of the Instrumental Neutron Activation Analysis (INAA) is the one that offers the best profit because it allows a low level of antimony's detection that, at the modalities explained later on, arrives at fractions of micrograms ($1x10^{-8}$gr). Furthermore the sample is not altered by chemical procedures and is available for further laboratory tests. We mustn't overlook the rapidity of analysis execution: in fact after 30 minutes of irradiation followed by 4-5 hours of cooling it's possible to obtain the quantitative datum of antimony.

The usefulness of this technique has been confirmed by many authors (7,10,14).

The proposed methodology is a novel application that has been previously tested by some of us (3,4,5) based on these experimentally proven considerations:

the gases generated at the moment of the shot by propellent charge deflagration come out from the muzzle, carrying away and dropping on the target, as far as 150-200 cm, gunpowder residues. Among these residues is the antimony that consequently will be detectable on the target itself. Therefore the amount of antimony present on the target varies according

to shooting distance, lowering as the distance increases. Comparing the results obtained from the sample with the ones obtained by testing shots at known distances possibly fired using the same fire arm and the same ammunition of the lawsuit in question, it's possible to find out the unknown distance.

Experimental investigations previously carried out by some of us (4,5) have evidenced the irreproducibility of the quantitative datum for shots fired at the same distance because of the cartridge in which the composition and the amount of the components, even if strictly standardized, can undergo light variations. Therefore stress is placed on the importance of recording the spatial distribution of gunshot residues that , independently of antimony level variations, is quite reproducible at a parity of distance.

In the present work we have made quantitative determinations of antimony on targets , for shooting distance from 5 to 100 cm, revealing its spatial distribution by autoradiography technique.

## 2. EXPERIMENTAL

Test shots were fired at the Judicial Police school of Brescia's indoor rifle range, using 9mm calibre fire arms that represent the usual equipment of the Police Force; these arms (Beretta mod. 51; Beretta mod. 92 SB; Beretta mod. 92 SB Compact; tommy-gun Beretta mod. M12S) are classified by the Italian law as war-arms, therefore not available to civilians. Ammunition consisted of 9mm calibre parabellum G. Fiocchi cartridges with jacketed bullet coming from the same production batch. For each pistol model, three different arms have been used, carrying out 15 shots from each of them. Shots have been executed at distances of 5,10,15,20,25,30,35,40, 45,50,60,70,80,90, and 100 cm in withe cotton target.

Following previously tested sampling modalities (3,4,5) 10 by 10 cm squares of cloth have been cut out around the entrance hole. Antimony level determination has been performed, according to tested methods (5,13) by the following scheme:

-1x $10^{12}$ neutron flux $cm^{-2}$ $sec^{-1}$ irradiation for 30 minutes in the TRIGA MARK II (250 Kw)reactor of The University of Pavia.

- $\gamma$ spectrophotometry for the 564 Kev radiation of the $^{122}Sb$ measured using a 20 $cm^3$ Ge/Li detector connected to LABEN 701 computerized scanner, after 48 hours' cooling period;
- autoradiography: this technique consists in laying the previously irradiated sample on a X-ray film for nearly 18 hours. The antimony decay radiations expose the film, producing an actual size image representing its spatial distribution.

3. RESULTS AND DISCUSSION

The results of antimony level determination are reported in the tables 1,2,3, and 4, and in the graphs 1,2,3, and 4. The examination of the data shows the variability of antimony deposits for shots at the same distance; this confirms the results of previous studies, demonstrating the important role carried out by the cartridge. This variability testifies to the possibility of mistakes in shooting distance identification by using the only quantitative datum relative to antimony, and to the usefulness of applying a second test suitable to evidentiate the distribution of the residues on the target, as will be further explained.

The analysis of the graphs seems to point out an exponential decrement for distances from 5 to 70-80 cm of Sb levels but doesn't show important differences among the four 9mm calibre pistol models. For longer distances, Sb amount remains steady because of bullet's cleasing. During its air trajectory. The adoption of the autoradiography test after the INAA test has allowed us to integrate the quantitative datum demonstrating the spatial distribution pattern of the residues. The worth of the autoradiography is not in only the film impression intensity but also in the dimension and the kynd of distribution of residues around the hole (photographs 1 to 12).

In previous studies (4,6) we have made a comparison with other kinds of photographic techniques (white light, infr red and ultraviolet photography ; autoradiography has demonstrated to be the best technique because of higher sensibility, producing a good visualization of the residues even for distances longer than 30-40 cm. Particularly significant is the constant presence of a shadow relevable around the bullet hole; it let investigators make differential diagnoses between entrance and

exit orifices, according to conclusions of many authors (8,9); Villanueva et al. (15) expecially have demonstrated the presence of antimony and lead residues for distances over 80 cm.

Also it must be stressed how the morphological datum is particularly useful in cases in which the target is a cloth made with fibers with a natural high content of antimony, lettin us differentiate the antimony originated by the shot from the antimony naturally present in the cloth.

4. CONCLUSIONS

In summary, according to our experience, we do consider autoradiography the complementary tecnique to the INAA.

4.1 In fact from an operative point of view, the material that has undergone neutron irradiation in one only session is first analyzed to determine its antimony content and later, by the use of autoradiography, the quantitive datum is completed with the image of the distribution of G S R. This double examination allows a reduction of the margin of error connected to the uncertain shooting-distance determination based only on the quantitative datum of Sb.

4.2 From an expert point of view, a further advantage offered by autoradiography must be stressed: the shape and the eccentricity of the deposit's shadow in relation to the entrance hole permit us to deduce the inclination of bullet's trajectory, similar to the classical smoke and tatooing marks.

4.3 The autoradiography images obtained from the exhibit and the test samples, enclosed in the expert's report, represent an element of immediate perception also to the non-specialists, giving the opportunity of verifying directly the investigation results to the judge and to the involved parties. We think this will have more importance in Italy because of the new code of penal procedure, expecially for that part of the trial known as preliminary inquiry.

4.4 Finally, we consider it possible to gain reliable conclusions on the determination of shooting distance by means of the proposed technique, even conscious that the optimum conditions of the experimental phase (perpendicular shot, wind absence, immediate sampling and optimum preservation

of the sample itself) are often very far from the ones pertinent to the actual case being investigated, and therefore we must stress the importance of collecting as much informations as possible even about the "story" of the exhibit itself untill the moment it has been given to the expert.

REFERENCES

1. S. Basu
Gunshot residue analysis in bullet wounds with the SEM-EDX
Microbeam. Anal., 21, p. 461, 1986

2. H. Booker, D.D. Schroeder, J.H. Propp
A note on the variability of Barium and Antimony levels in cartridge primers and its implications for gunshot residue identification
J. Forensic Sci., 2, p.81, 1984

3. A. Brandone, T. Cerri, M.Tavani
L'analisi per attivazione neutronica nella pratica forense: la valutazione della distanza di sparo
Arch. Med. Leg. Ass., 14, p. 47, 1978

4. A. Brandone, F. De Ferrari, P. Pelizza
Applicazione di diverse metodiche nella determinazione della distanza di sparo per armi da fuoco "corte"
Arch. Med. Leg. Ass., 10, p. 421, 1988

5. A. Brandone, F. De Ferrari, S. Salza
Ulteriori esperienze nella valutazione della distanza di sparo mediante l'analisi per attivazione neutronica
Riv. It. Med. Leg.,1 p.184, 1981

6. F. De Ferrari, A. Brandone
Determinazione della distanza di sparo per armi da fuoco "corte": prospettive offerte da diverse metodiche
Atti del Convegno di Balistica Forense, L'Aquila 25-28 Marzo 1981, Montagnoli ed., Roma

7. D. Dimitrov, D. Apostolov
Determination of the distance of a shot with firearms using Instrumental Neutron Activation Analysis
Yad. Energ., 19, p. 41, 1983

8. H. Kijewsky, J. Lange
Neue aspekte in der Schussentfernungsbestimmung durch Anwendung Flammenlossen Atomabsorption-Spektral Photometrie
Zeitschrift fur Rechtsmedizin, 74, p. 9, 1974

9. S.S. Krishnan
Firing distance determination by Atomic Absorption Spectrophotometry
J. Forensic Sci., 2, p. 351, 1974

10. S.S. Krishnan, R.E. Jerevis
Characterization of shotgun pellets and gunshot residues by trace element concentration patterns
J. Can. Soc. Forensic Sci., 4, p. 167, 1984

11. J.A. Lekstrom, R.D. Koons
Copper and Nickel detection on gunshot target by Dithiooxamide Test
J. Forensic Sci., 4, p. 1283, 1986

12. J.T. Newton
Rapid determination of antimony, barium and lead in gunshot residues via Automated Atomic Absorption Spectrophotometry
J. Forensic Sci., 2, p.302, 1981

13. M. Tavani, A. Brandone
La possibilità dell'impiego della Analisi per Attivazione Neutronica Nella pratica medico-forense
Arch. Med. Leg. Ass., 10, p. 281, 1974

14. H. Thieme
Shooting distance determination by energy dispersive x-ray fluorescence analysis in relatively close range shootings
Krim. Forensische Wiss, 53-54, p. 94. 1984

15. E. Villanueva, C. Hernandez-Cueto, J.A. Lorente, J. Garcia Quiles, M.A. Rodrigo
Study of inorganic residues around entrance and exit projectile orifices
J. Forensic Sci., 4, p. 1079. 1987

16. G.M. Wolten, R.S. Nesbitt
On the mechanism of gunshot residue particle formation
J. Forensic Sci., 3, p.533, 1980

BERETTA 92/SB SEMIAUTOMATIC PISTOL

FIG. 1

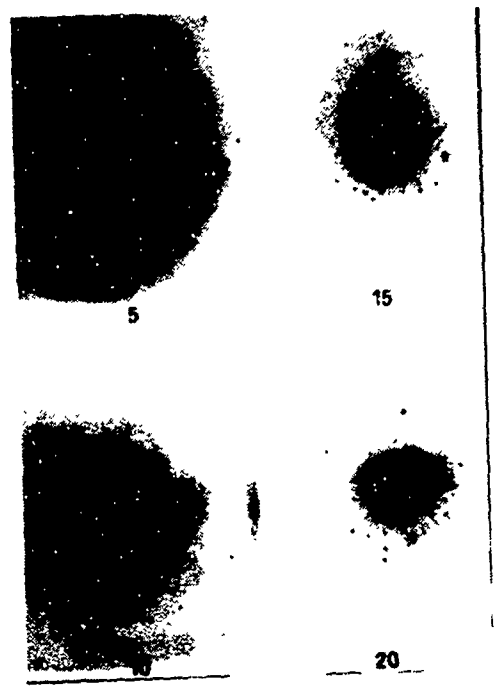


FIG. 2

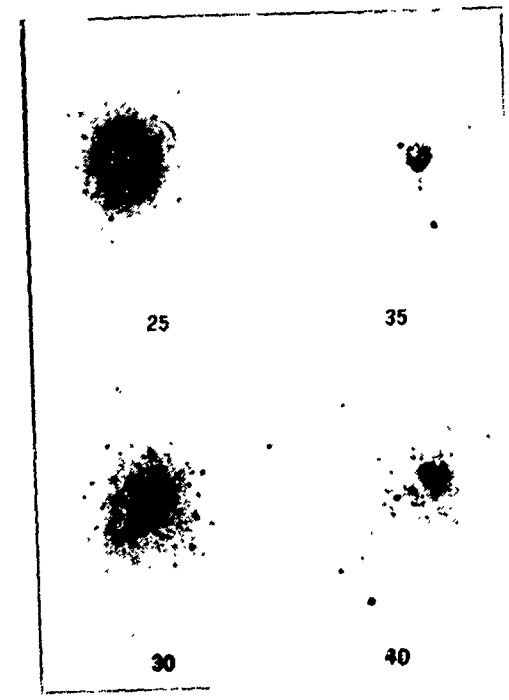


FIG. 3

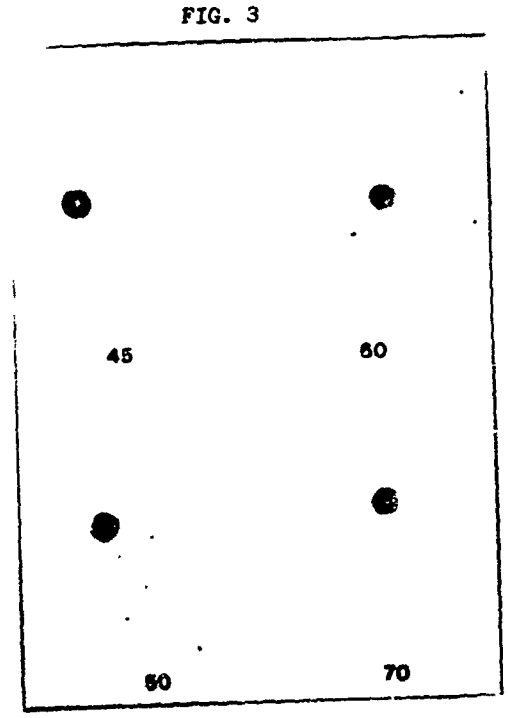


FIG. 4

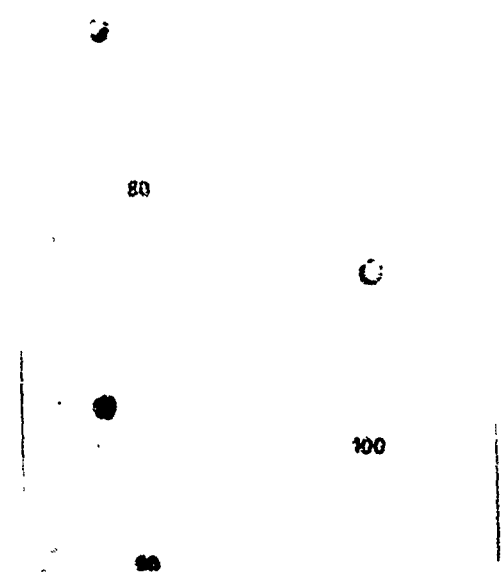

BERETTA 51 SEMIAUTOMATIC PISTOL

FIG. 5

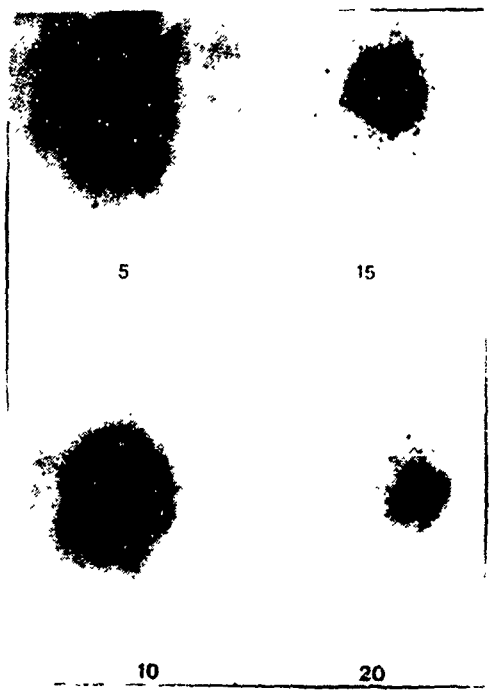


FIG. 6

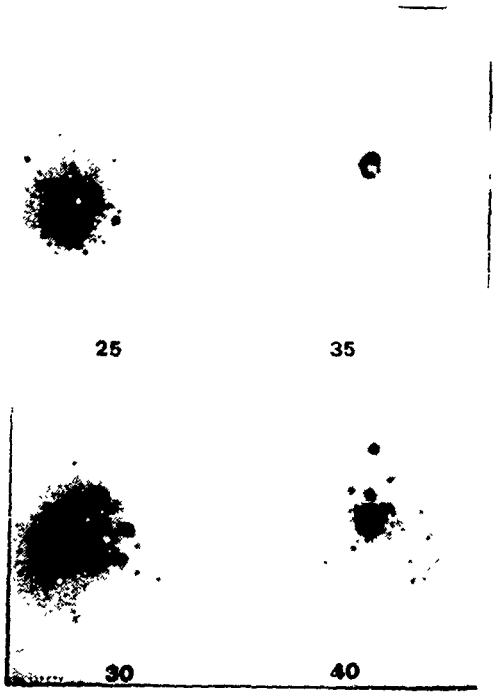


FIG. 7

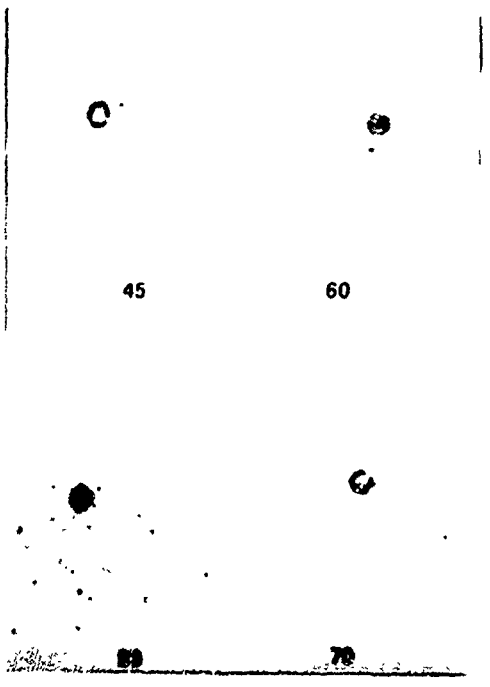


FIG. 8

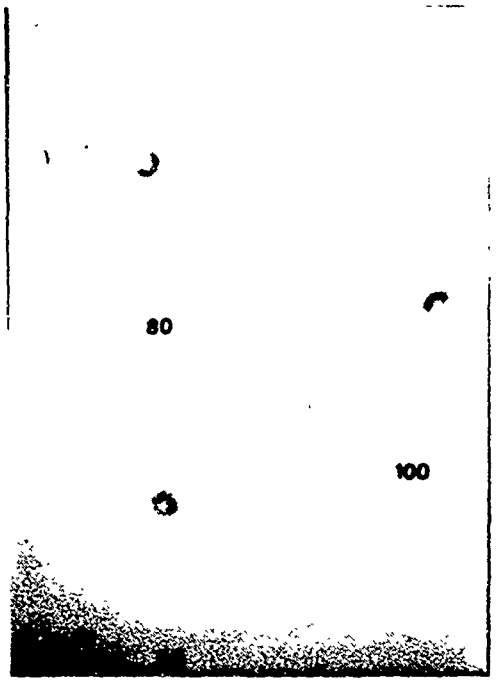

BERETTA M/12 S TOMMY-GUN

FIG. 9

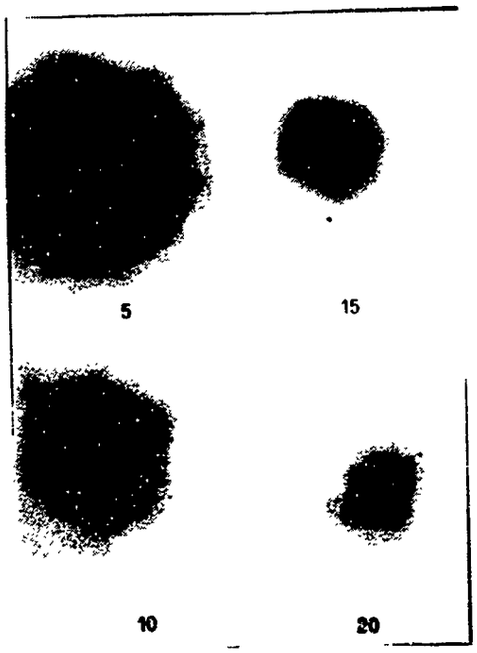


FIG. 10

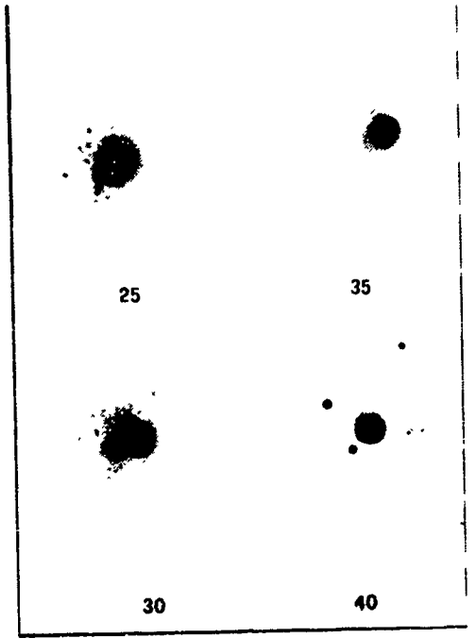


FIG. 11

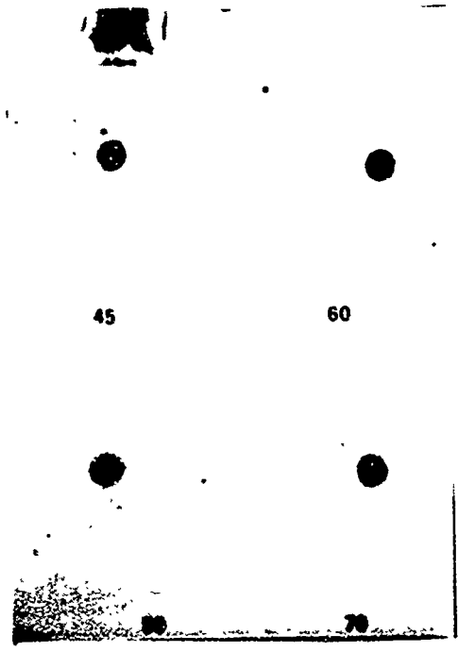


FIG. 12

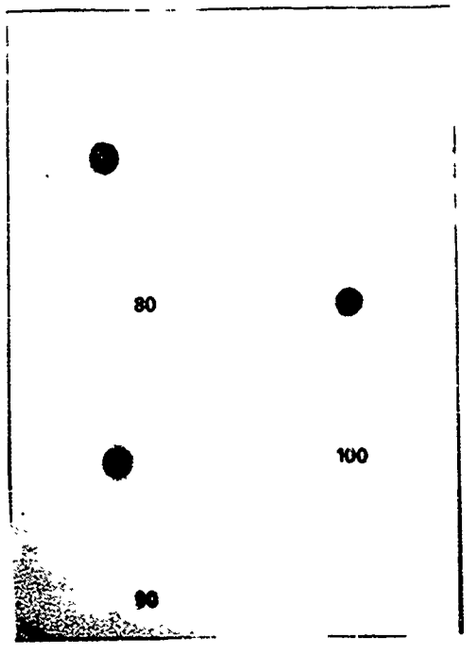

TABLE 1 : BERETTA 92/SB SEMIATOMATIC PISTOL

| REGISTRY NUMBER | x 36393Z | x 24598Z | x 65647Z | $\bar{M}$ | St.d. | V.C |
|---|---|---|---|---|---|---|
| SHOOTING DISTANCE (CM) | Sb LEVEL ON TARGET (µgr) | | | | | % |
| 5 | 188,06 | 214,92 | 226,00 | 209,66 | 22,41 | 10,68 |
| 10 | 112,43 | 133,55 | 166,52 | 137,51 | 31,95 | 23,23 |
| 15 | 74,24 | 70,98 | 95,20 | 80,14 | 14,30 | 17,84 |
| 20 | 59,34 | 60,28 | 95,09 | 71,57 | 21,12 | 29,50 |
| 25 | 44,13 | 79,27 | 76,91 | 66,77 | 20,76 | 31,09 |
| 30 | 35,16 | 58,26 | 60,15 | 51,19 | 14,76 | 28,83 |
| 35 | 26,64 | 37,81 | 41,04 | 35,16 | 8,50 | 24,17 |
| 40 | 28,13 | 26,57 | 24,86 | 26,52 | 1,93 | 7,27 |
| 45 | 28,88 | 28,04 | 19,57 | 25,48 | 5,50 | 21,58 |
| 50 | 13,98 | 14,61 | 14,23 | 14,27 | 0,37 | 2,59 |
| 60 | 7,04 | 8,27 | 10,79 | 8,70 | 2,21 | 25,40 |
| 70 | 4,18 | 6,18 | 5,06 | 5,14 | 1,18 | 22,95 |
| 80 | 4,75 | 3,16 | 3,51 | 3,81 | 0,93 | 24,40 |
| 90 | 3,39 | 3,04 | 4,70 | 3,71 | 0,98 | 26,41 |
| 100 | 3,38 | 3,27 | 3,80 | 3,63 | 0,33 | 9,09 |

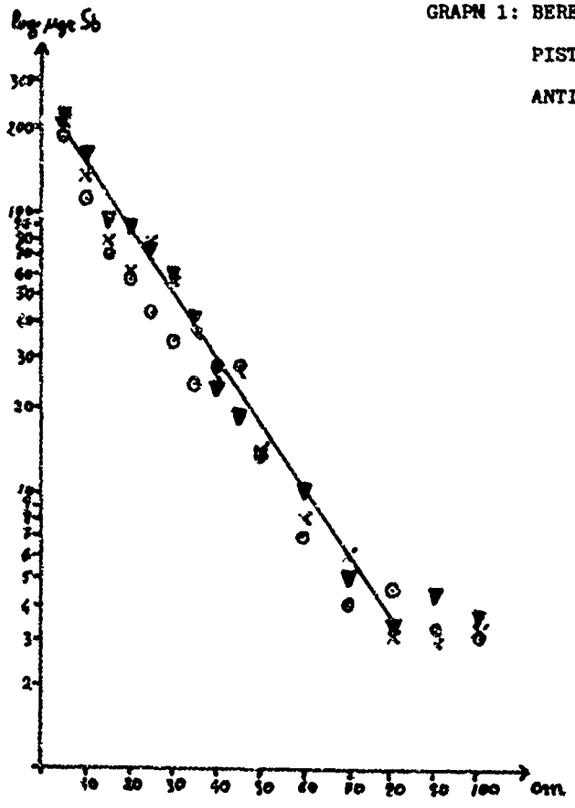


GRAPH 1: BERETTA 92/SB SEMIAUTOMATIC PISTOL - CORRELATION BETWEEN ANTIMONY LEVEL AND DISTANCE

TABLE 2 : BERETTA 92/SB COMPACT SEMIAUTOMATIC PISTOL

| REGISTRY NUMBER | x 61796Z | x 58597Z | x 57603Z | $\bar{M}$ | St.d. | V.C. |
|---|---|---|---|---|---|---|
| SHOOTING DISTANCE (CM) | Sb LEVEL ON TARGET (μgr) | | | | | % |
| 5 | 186,98 | 330,10 | 175,60 | 230,89 | 91,27 | 39,52 |
| 10 | 124,56 | 128,30 | 119,75 | 124,21 | 5,05 | 4,06 |
| 15 | 91,67 | 94,50 | 66,00 | 84,06 | 16,83 | 20,02 |
| 20 | 69,04 | 77,30 | 50,80 | 65,80 | 15,65 | 23,81 |
| 25 | 50,12 | 53,50 | 56,30 | 53,31 | 3,65 | 6,84 |
| 30 | 36,67 | 32,90 | 36,40 | 35,33 | 2,22 | 6,28 |
| 35 | 32,18 | 35,70 | 23,40 | 30,43 | 7,26 | 23,85 |
| 40 | 17,24 | 16,80 | 21,36 | 18,47 | 2,69 | 14,56 |
| 45 | 14,51 | 13,90 | 16,10 | 14,84 | 1,29 | 8,69 |
| 50 | 12,00 | 11,00 | 12,90 | 11,97 | 1,12 | 9,35 |
| 60 | 8,08 | 5,00 | 6,16 | 6,42 | 1,81 | 28,19 |
| 70 | 8,77 | 4,70 | 3,06 | 5,51 | 3,37 | 61,16 |
| 80 | 7,45 | 4,35 | 2,95 | 4,92 | 2,65 | 53,86 |
| 90 | 3,55 | 2,96 | 1,68 | 2,73 | 1,10 | 40,29 |
| 100 | 5,87 | 3,00 | 3,10 | 3,99 | 1,69 | 42,35 |

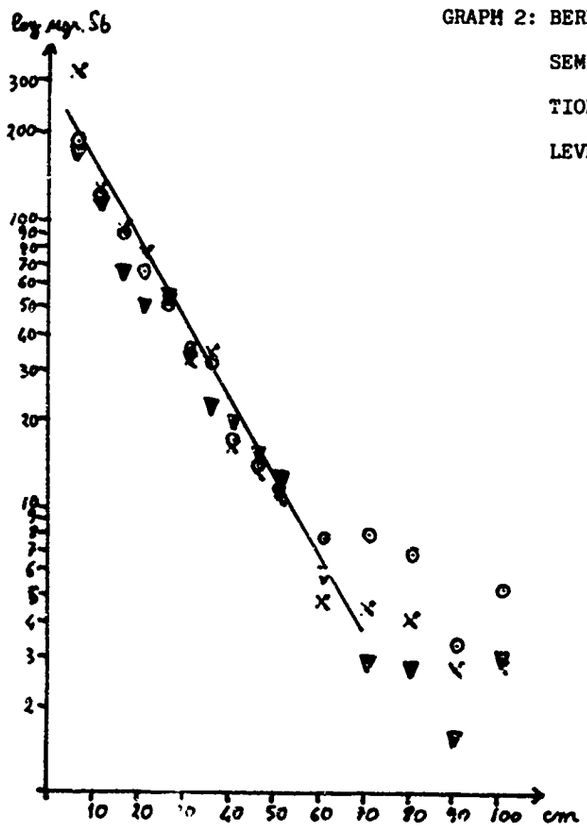


GRAPH 2: BERETTA 92/SB COMPACT SEMIAUTOMATIC PISTOL-CORRELATION BETWEEN ANTIMONY LEVEL AND DISTANCE

TABLE 3 : BERETTA 51 SEMIAUTOMATIC PISTOL

| REGISTRY NUMBER | 10232 | 14533 | 10454 | $\bar{M}$ | St. d. | V.C |
|---|---|---|---|---|---|---|
| SHOOTING DISTANCE (CM) | Sb LEVEL ON TARGET (μgr) | | | | | % |
| 5 | 311,54 | 307,06 | 231,50 | 283,37 | 47,28 | 16,68 |
| 10 | 117,47 | 131,75 | 121,18 | 123,47 | 8,43 | 6,82 |
| 15 | 77,08 | 79,72 | 82,45 | 79,75 | 3,17 | 3,97 |
| 20 | 56,59 | 62,64 | 51,39 | 56,87 | 6,64 | 11,67 |
| 25 | 68,46 | 56,38 | 48,40 | 57,75 | 11,85 | 20,51 |
| 30 | 52,45 | 36,16 | 40,16 | 42,92 | 9,62 | 22,41 |
| 35 | 45,96 | 42,61 | 27,28 | 39,95 | 11,03 | 27,60 |
| 40 | 23,01 | 31,84 | 21,87 | 25,57 | 5,89 | 23,03 |
| 45 | 21,45 | 15,24 | 13,04 | 16,58 | 4,96 | 29,91 |
| 50 | 12,62 | 20,05 | 12,15 | 14,94 | 4,66 | 31,19 |
| 60 | 7,27 | 9,07 | 12,61 | 9,65 | 3,15 | 32,64 |
| 70 | 5,30 | 4,32 | 5,64 | 5,09 | 0,77 | 15,12 |
| 80 | 4,82 | 4,49 | 5,74 | 5,02 | 0,73 | 14,54 |
| 90 | 3,95 | 3,39 | 3,44 | 3,59 | 0,33 | 9,19 |
| 100 | 5,85 | 3,73 | 4,74 | 4,77 | 1,25 | 26,20 |

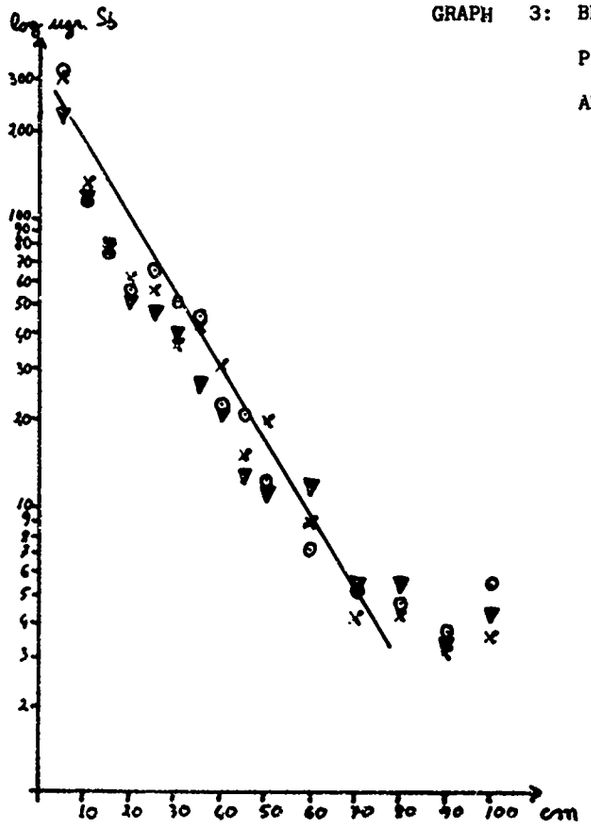


GRAPH 3: BERETTA 51 SEMIAUTOMATIC PISTOL-CORRELATION BETWEEN ANTOMONY LEVEL AND DISTANCE

TABLE 4 : BERETTA M/12 S TOMMY - GUN

| REGISTRY NUMBER | 19730-78 | 28193-79 | 03270-77 | $\bar{M}$ | St.d. | C.V. |
|---|---|---|---|---|---|---|
| SHOOTING DISTANCE (CM) | Sb LEVEL ON TARGET (μgr) | | | | | % |
| 5 | 175,77 | 255,69 | 146,25 | 192,57 | 64,65 | 33,57 |
| 10 | 164,31 | 149,74 | 207,29 | 173,78 | 34,00 | 19,56 |
| 15 | 121,92 | 111,04 | 89,08 | 107,34 | 19,40 | 18,07 |
| 20 | 93,56 | 73,88 | 66,31 | 77,91 | 16,09 | 20,65 |
| 25 | 84,19 | 49,68 | 59,46 | 64,44 | 20,38 | 31,62 |
| 30 | 62,12 | 52,78 | 48,81 | 54,57 | 7,86 | 12,72 |
| 35 | 40,65 | 42,75 | 40,59 | 41,33 | 1,27 | 3,07 |
| 40 | 41,41 | 28,39 | 43,26 | 37,68 | 8,78 | 23,3 |
| 45 | 29,50 | 18,31 | 24,69 | 24,16 | 6,61 | 27,35 |
| 50 | 16,53 | 21,54 | 19,08 | 19,05 | 2,95 | 15,48 |
| 60 | 15,71 | 19,02 | 14,65 | 16,46 | 2,58 | 15,67 |
| 70 | 8,91 | 10,32 | 8,01 | 9,08 | 1,36 | 14,97 |
| 80 | 6,77 | 6,43 | 6,17 | 6,45 | 0,35 | 5,42 |
| 90 | 7,12 | 5,64 | 8,15 | 6,97 | 1,48 | 21,23 |
| 100 | 8,89 | 4,12 | 7,22 | 6,74 | 2,81 | 41,69 |

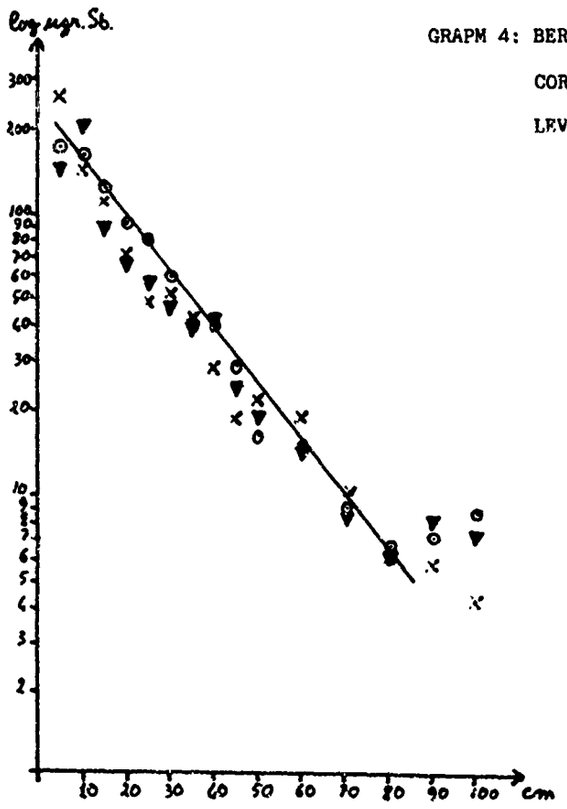


GRAPM 4: BERETTA M/12S TOMMY-GUN

CORRELATION BETWEN ANTIMONY

LEVEL AND DISTANCE

# DETECTION OF EXTREMELY LOW CONCENTRATIONS OF ULTRA PURE TNT BY RAT

S. Weinstein, Ph.D., R. Drozdenko, Ph.D., & C. Weinstein, M.A.

NeuroCommunication Research Laboratories, Inc.
36 Mill Plain Road, Danbury, Connecticut 06811, USA

Although much work has been performed using trained animals to detect the presence of explosive vapors, few attempts have been made to determine performance as a function of concentration. In our earlier work, rats were successfully trained to detect military-grade TNT with a high level of confidence. A typical example is rat-00-76 which detected military grade TNT with a statistical confidence level of better than 99.9%. In this early work, the concentration of explosive vapors was not measured, and subsequent vapor analysis by gas chromatography indicated that 2,4-DNT was the likely target vapor. In more recent work with highly-pure TNT, we collected samples of the test air and control air during measurements of a rat's performance. The concentration of TNT in test and control air streams was measured by gas chromatography (GC). In this manner, we investigated the ability of a rat to differentiate between concentrations of pure TNT.

Rat-79-88 was trained to press a bar when TNT-laden air was delivered, and to refrain from pressing a bar when nonTNT-laden air was delivered. The test apparatus (see Figure) was under computer control, and was used to deliver varying concentrations of TNT vapor. The computer additionally scored the rat's performance, controlled reinforcement contingencies, and controlled the air-sampling pumps for the GC.

Before the experiment to measure rat performance concurrently with TNT concentration, experiments were conducted to insure that the rat was indeed responding only to the presence of TNT, and not to some concomitant cue. In one series of experiments, the arms of the test apparatus that were used to deliver TNT or control air to the rat were switched. The rat responded to the delivery of TNT and not to the control air. In another series of experiments, the TNT source was removed from the test apparatus. For the first 50 trials, the rat detected TNT as if the source was still intact. For the second 50 trials, performance fell appreciably. Finally, during the last series of 50 trials, performance stopped. Because the reinforcement contingencies remained enabled, the rat could have received its reinforcement if it could have solved the detection task by alternate means. However, it did not. Detection during the first 100 trials was evidently due to residual TNT in the source chamber. In this manner, we verified that the rat responded only to the presence of TNT.

The experiment to measure performance as a function of concentration was conducted by measuring TNT concentrations by GC concurrently with the rat's performance. Both the test air and the control air were sampled concurrently during each session. The samples of air for GC analysis were collected from the same area that the rat sampled so that an accurate measure of what the rat was sampling would be gained. Rather than training the rat to specifically detect low levels of TNT, the rat was trained to detect saturated levels, and performance testing took place during titration of the concentration of TNT. During the titration experiments (600 trials), this rat evidenced 96% correct detection when challenged with TNT in the range of 2-3 ng/L; simultaneously, there were only 3 false alarms in the 309 challenges with

control air. Before titration, the rat averaged 95% correct behavior. The decrement in performance concomitant with titration was probably not due to fatigue, because the rat had a history of responding to up to 1171 trails in a few hours. That high work level was not exceeded during these experiments. The following Table provides data from the last three sessions.

TABLE

| Session | Trials | %Corr | %Detec | %FA | PERFORMANCE | TEST ng/L | CONTROL ng/L |
|---|---|---|---|---|---|---|---|
| 11 | 50 | 100 | 100 | 0 | 100 | 2.44 | 0.37 |
| 12 | 50 | 98 | 95 | 0 | 95 | 1.32 | 0.39 |
| 13 | 100 | 80 | 60 | 0 | 60 | 1.07 | 0.37 |

Key:

1. Session is a series of trails during which concentrations of TNT are collected.
2. Trails is the number of challenges presented.
3. %Corr is the percentage correct, which is the sum of the trails of detection and correct omission then divided by the total number of trials, expressed as a percentage.
4. %Detec is the percentage of detections.
5. %FA is the percentage of false alarms.
6. "Performance" is defined as the difference in percentages detection and false alarm.
7. "TEST" presents the concentration of TNT vapors (ng/L) in the test air.
8. "CONTROL" presents the concentration of TNT vapors (ng/L) in the control air (which is background noise).

Air Delivery System

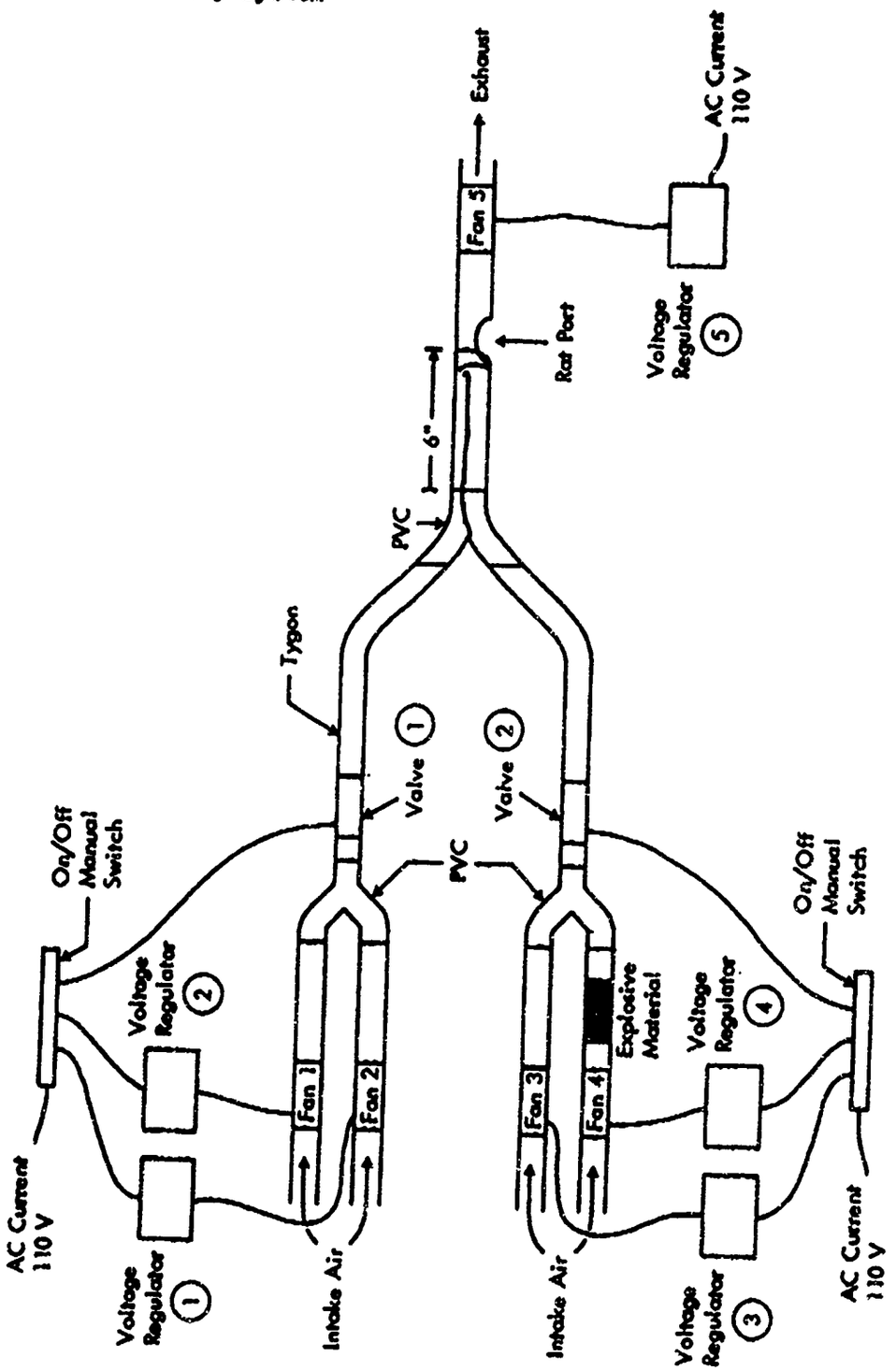

# FBI LABORATORY EVALUATION OF PORTABLE EXPLOSIVES VAPOR DETECTORS

Dean D. Fetterolf

FBI Laboratory, Forensic Science Research Unit
FBI Academy, Quantico, Virginia, 22135, USA

**ABSTRACT**

In March, 1988, the FBI Laboratory conducted an evaluation of commercially available explosives vapor detectors under operational scenarios typically encountered by law enforcement and security personnel. Three gas chromatograph/electron capture-based detectors, the Ion Track Model 97, the Scintrex EVD-1, and the Sentex Scanex Jr. as well as the ion mobility based Graseby PD-5 were evaluated.

The explosive detection and operational capabilities of each detector were examined by sampling laboratory reference standards, the test explosives and potential interferants. Bomb quantities of a variety of explosives were hidden in packages, briefcases, and luggage. Practical search problems also involved locating explosives hidden in automobiles, mail, motel rooms and a townhouse.

Only a few positive responses to potential interferants were recorded. Dynamite (NG and EGDN) was readily detected with only 2 hours soak time in the various test items and search scenarios. TNT was also found in some cases. The less volatile explosives including an $NH_4NO_3$ emulsion, PETN Deta Sheet and the C-4 were undetected in any test item after 18 hours soak time or in any of the practical search problems. Summarized test procedures and results are presented to allow the reader to evaluate the data with respect to his/her own operational requirements.

---

This is a publication of the Laboratory Division of the Federal Bureau of Investigation. Names of commercial manufacturers are included for information only and does not constitute or imply endorsement, recommendation of favoring.

## 1. INTRODUCTION

The rise in domestic and international terrorism in the last decade has generated an increasing interest by law enforcement and physical security personnel in the operational uses and capabilities of commercially available portable explosive vapor detectors. These uses include the security screening of personnel or items entering a building or secure facility. Law enforcement uses include such scenarios as bomb threats, suspicious packages or searching for secondary devices following an explosion.

A number of laboratory studies were carried out in the late 1970s by Sandia National Laboratories, the United States Department of Transportation, and the Naval Explosives Ordnance Disposal Facility. In April, 1981, a comprehensive field test of commercially available explosives detectors and dogs was carried out by the Research and Development Division of the Bureau of Alcohol, Tobacco and Firearms, U.S. Department of the Treasury.

This paper, condensed from a final report of 126 pages, summarizes the test procedures, provides a brief functional description of each detector, and presents the results from their evaluation under operational scenarios of interest to law enforcement and security personnel. The evaluation, conducted by the FBI Laboratory during March 21-24, 1988, was directed toward the needs of the "user" while maintaining a fair and impartial test environment.

It was made clear to the manufacturing representatives that participation in the test and the results thereof does not constitute or imply endorsement, favoring or recommendation by the U.S. Government or any agency or employee thereof. No specific recommendations regarding overall detector performance are made. The reader must evaluate the data with respect to his/her own operational requirements.

The explosive detection and discrimination capabilities of each detector were examined by sampling laboratory reference standards, the test explosives and potential interferants. Bomb quantities of a variety of explosives were hidden in packages, briefcases, and luggage. These test items were treated as suspicious items. The briefcases were also sampled using the EOD Technician procedure called "burping" which calls for the compression of the briefcase

forcing vapor-enriched air to escape, thus enhancing the probability of detection. This procedure was included at the request of some of the manufacturers. Practical search problems also involved searching for explosives hidden in automobiles, mail, motel rooms and a townhouse. These were directed searches in which several specific location were labeled and searched. This effectively eliminated the ability of the operator to conduct a proper search as an uncontrollable variable and placed the emphasis on the detector.

## II. TEST PROCEDURES AND GUIDELINES

Bomb quantities of live explosives were used in the packages, briefcases and suitcases. The explosives typically weighed from 1 to 1.25 pounds. Only 1/4 pound of dynamite was used due to the highly volatile nature of nitroglycerine (NG) and ethyleneglycol dinitrate (EGDN) and the fear of contamination. PETN Deta Sheet, Atlas 7D emulsion, TNT and C-4 explosives were selected from "sterile" (non-dynamite storage) bunkers. Hercules Red Dot smokeless powder was purchased a few days prior to the evaluation. The Hercules Unigel dynamite was stored in a separate bunker.

A soak time (time since package preparation and examination) of 18 hours was provided for packages and briefcases containing PETN, TNT, C-4, Atlas 7-D and smokeless powder. The soak time for dynamite was only 2 hours.

Great care was taken to avoid cross-contamination of the explosives and the test items during preparation, storage and handling. Double gloves were worn during the preparation. Storage was provided by double wrapping each item containing explosives in plastic garbage bags. These items were stored separately from blank items or those containing interferants. No dynamite or test items containing dynamite were permitted in the test facility until just before the testing began.

The manufacturing representatives were invited to attend the evaluation in January of 1988. A brief outline detailing which explosives would be used, the operational test scenarios, types of interferants, testing schedule, and figures of merit for the evaluation were provided.

Prior to the test, four operators were chosen by personnel of the FBI Laboratory because of their recognized expertise in explosives

and their familiarity with the requirements of explosives detection in the forensic and law enforcement communities. Their observations provided valuable insight into the state of the art in commercial explosives vapor detectors which would not have been obtained through the use of nonexperts or the manufacturing representatives.

Each manufacturer was provided an opportunity to describe their instrument to the operator and to provide training in its operation. As part of this training phase pure explosive compounds and the actual test explosives were sampled. Forms detailing the instrument model and serial number, operation within specifications, and satisfaction with the operator were completed by the manufacturing representatives. Following the training and on subsequent days the instruments were secured in locked laboratory space until the following day.

The actual search problems were done in teams. The search teams consisted of the trained operator, who made the decision as to a positive detector response; a scorer/observer, who recorded the results; and the manufacturing representative(s) who functioned as a witness. The tests were conducted in the blind mode so that none of these individuals had any knowledge of the explosives or their location. Simultaneous tests were conducted and the teams rotated.

Observers from over 40 U.S. Government and foreign agencies attending the test were segregated from the testing areas but had the opportunity to observe each instrument in the various phases of the evaluation. The manufacturers, the trained operators, and the observers were invited to provide written comments following the evaluation for inclusion in the final report.

## III. DETECTORS EVALUATED

Four detector manufacturers volunteered to participate in the evaluation. Table 1 provides a comparison of the various operating characteristics of each detector. A brief operational description of each is provided.

Graseby PD-5: The Graseby PD-5 is the only ion mobility spectrometer (IMS)-based portable explosives detector commercially available. This rechargeable, battery-operated detector is totally self-contained and requires no replenishing of carrier gas supply. After 2 minutes of warm-up and automatic calibration the instrument

operates in a continuous sampling mode with a 3-second response time. Two to 3 sampling intervals were used for each test item.

In operation, outside air is drawn in through a hand-held probe, by a pump contained within the briefcase unit. Air and explosives molecules diffuse through a membrane into a chamber where a sealed $^{63}Ni$ radioactive source ionizes the sample. Under the influence of an electrical field 20 millisecond bursts of ions drift toward the collector electrode. The larger and heavier explosive molecules drift more slowly than the air molecules. The microprocessor system recognizes these peaks at specific points in time and triggers an adjustable audible alarm. A digital display indicates the relative concentration of the explosive being detected.

Ion Track Instruments Model 97: The Ion Track Instrument (ITI) Model 97 is a dual gas chromatograph/electron capture-based detector. This portable detector is supplied with a rechargeable battery pack. Argon carrier gas is supplied from a 4 $ft^3$ refillable gas tank. After approximately 15 minutes of warm-up time this detector operates in the continuous mode with a 2-10 second response time.

Suspect vapor is drawn into the instrument through a membrane which isolates it from ambient air. The vapor is mixed with Argon, an inert carrier gas, and fed down both columns. One of the columns is coated with a chromatographic support which retards the progress of explosives molecules. Each column terminates in an electron capture detector (ECD).

If electronegative molecules, such as explosives are present they reduce the standing current in the ECD and trigger an alarm. The relative strength of the signal is displayed on a pseudo logarithmic bar graph display. The timing sequence of the signals from the twin ECDs discriminates between explosive vapors and those produced by similar nonexplosive substances.

Scintrex EVD-1: The Scintrex EVD-1 is a 2-component system consisting of a battery-powered, hand-held sampling unit and an analyzing unit which can be AC or battery operated. This analyzer unit consists of a desorber, chromatographic column and an ECD with a response time of 1.5 minutes.

The sampling unit consists of a battery-operated metering pump which draws air through a 7-cm quartz collection tube containing Tenax adsorbent at 600-800 ml/min for a preset time of 15 seconds.

The sample collection tube (containing the adsorbed vapor) is placed in the desorber portion of the analyzer. The tube is heated and purged with pure carrier gas. The vapor sample then enters the analyzer unit into a secondary adsorber, then to the chromatographic column and finally into the ECD. The electronic section of the detector monitors the standing current in the ECD. A microprocessor software algorithm decides whether there is a signal within preset retention time windows corresponding to an explosive. The results are then sent to a digital LCD display.

Sentex Sensing Technology Scanex Jr.: The Sentex Scanex Jr. manufactured by Sentex Sensing Technology is also sold under an exclusive license as the XID Corporation Model T-54. This portable detector consists of a preconcentrator, a gas chromatograph, an electron capture detector, and a rechargeable battery pack. Helium carrier gas is supplied from a refillable gas tank. Following 20 minutes of warm-up time the detector operates in the batch mode with an 8 to 20 second response.

The hand-held sampling probe is push button activated, drawing air into the unit as long as the button is depressed. According to the manufacturer the sampling pump should be activated between each item to clear any remaining material and to reestablish baseline operation. The sampling probe is connected to the briefcase unit by a 1 meter heated teflon tube.

An adsorbent material coated on a coiled platinum wire collects the explosive vapors if present. The platinum wire is then heated and the vapors desorbed onto a chromatographic column where seperation takes place. The sample then passes into a tritium foil ECD. The microprocessor decides whether there is a signal within a preset retention time window and triggers an audible alarm and an LED bar display.

TABLE 1. Detectors Evaluated

| DETECTOR | TYPE | CONCENTRATOR | OPERATION | EXPENDABLES | WARMUP | RESPONSE |
|---|---|---|---|---|---|---|
| Graseby PD-5[1] | IMS | Membrane | Continuous | None | 2 min | 3 sec |
| ITI Model 97[2] | GC/ECD | Membrane | Continuous | Ar Carrier | 15 min | 2-10 sec |
| Scintrex EVD-1[3] | GC/ECD | Tenax Tube | Batch | He Carrier | 30 min | 1.5 min |
| Sentex Scanex JR.[4] | GC/ECD | Pt Coil | Batch | He Carrier | 20 min | 8-20 sec |

1. Graseby Ionics Ltd., 6 Millfield House, Woodshots Meadow, Watford, Herts, England WD1 8YX
2. Ion Track Instruments, 109 Terrace Hall Avenue, Burlington, MA 01803, USA
3. Scintrex Security Systems, 222 Snidercroft Road, Concord, Ontario, Canada L4K 1B5
4. Sentex Sensing Technology, Inc., 553 Broad Avenue, Ridgefield, NJ 07657, USA

## IV. STANDARDS, TEST EXPLOSIVES AND INTERFERANT RESULTS

Pure Explosive Compounds: Samples of laboratory reference explosives listed in Table 2 were sampled in near contact by each detector. It is quite clear from this data that the detectors evaluated respond to the higher vapor pressure NG and 2,6 DNT without any difficulty. In general, and as expected, the lower vapor pressure pure explosives (TNT, RDX and PETN) provide an increasing challenge to these detectors.

The response of the Sentex/XID detector to pure PETN and RDX is unique and deserves a brief discussion. It has been demonstrated at Sandia National Laboratories that explosive vapors will adsorb on any surface. There is a rank-order of preferential adsorption by the various explosive compounds. In simple terms this means that EGDN or NG adsorbed on surfaces can be preferentially replaced by RDX or PETN. The released EGDN or NG reaches the detector and provides a response. The result is that one falsely believes that the detector is responding to RDX or PETN directly. Such behavior has been observed experimentally at Sandia on short pieces of teflon tubing. The Sentex Scanex Jr. is equipped with 1 meter of teflon tubing between the sample pump and the briefcase unit.

TABLE 2. Laboratory Standards Results

| PURE COMPOUNDS | GRASEBY | SCINTREX | ITI | SENTEX |
|---|---|---|---|---|
| NG Tablets | + | + | + | + |
| Ammonium Nitrate | - | - | + | - |
| 2,6 DNT | + | + | + | + |
| TNT | - | - | + | + |
| PETN | - | - | - | + |
| RDX | - | - | - | + |

Test Explosives: Small pieces of each of the test explosives were sampled in near contact by each detector. Great care was taken to prevent cross contamination of the explosives or contamination of the instruments or test facility during this stage of testing. For this reason no Hercules Unigel dynamite was sensed in this phase as all detectors responded to NG tablets. The results of sampling the test explosives are shown in Table 3. Some important points can be made by comparing the data from Tables 2 and 3.

All instruments readily responded to the Hercules Red Dot, a double-based smokeless powder which contains a relatively high percentage of NG. No detectors responded to the military explosive C-4. These responses were consistent with Table 2.

Several noteworthy differences can be seen between Table 2 and Table 3. For example, the Graseby PD-5 and the Scintrex EVD-1 alarm on military TNT is due to the higher vapor pressure 2,6-DNT impurity and not the TNT itself. In addition, while all detectors responded to the Dupont Deta Sheet they failed to directly detect the pure PETN with the exception of the Sentex Scanex Jr. The detectors are most likely responding to a volatile component in the formulation.

The response between the ammonium nitrate and the Atlas 7-D appear to be inconsistent. The ITI detector responded to the pure ammonium nitrate but failed to alarm on the test explosive. The Scintrex and Sentex detectors failed to respond to the pure ammonium nitrate but alarmed on the uncontaminated Atlas 7-D. It should be noted that the Atlas 7-D also contains a sensitizer, ethylenediamine dinitrate. However, without laboratory evaluation of each detector it is difficult to determine if this caused the detectors to alarm.

TABLE 3. Test Explosive Results

| TEST SAMPLES | GRASEBY | SCINTREX | ITI | SENTEX |
|---|---|---|---|---|
| Hercules Red Dot Smokeless | + | + | + | + |
| Atlas 7-D | - | + | - | + |
| TNT | + | + | + | + |
| C-4 | - | - | - | - |
| Dupont Deta Sheet (PETN) | + | + | + | + |

NOTE: Dynamite not tested to avoid contamination.

Interferant Results: Twenty-five potential interferants were analyzed in a laboratory environment. These samples were chosen because of their chemical composition and past experiences with various detectors by a number of individuals. Table 4 shows the interferant results for the detectors.

Most notable is the fact that the Scintrex EVD-1 and the Sentex Scanex Jr. recorded no positive responses to any of the interferants

chosen. Both instruments operate on a preconcentration step which involves adsorption of the explosives vapors prior to analysis. These volatile vapors are not adsorbed or chromatographic and detection conditions are such that these compounds do not co-elute or alarm as explosive molecules.

The 2 positive responses by the Graseby PD-5 are easily explained. The Skoal Wintergreen Smokeless Tobacco contains methyl salicylate (the wintergreen flavoring). This detector is programmed to respond to this chemical as this is the same basis used to check for decontamination in chemical warfare training exercises by the British military. The microprocessor could be reprogrammed to eliminate this alarm. The response to the diesel fuel sample was, as later determined in laboratory tests, due to contamination on the plastic cap and not the diesel fuel within the vial. The p-Cresol alarm was unique to the Graseby and unexplainable.

The ITI Model 97 responded to the Coty Wild Musk and Obsession colognes both which contain musks. The chemical structure of musks is similar to that of TNT. The response to the Cepacol mouthwash cannot be explained without further laboratory investigation. The Super Glue response was due to the fact that the glue was still wet, an unlikely event in real situations. The response to the Skoal Wintergreen Smokeless Tobacco is most likely due to the flavoring chemicals.

Table 4. Interferant Results

| | GRASEBY | ITI | SCINTREX | SENTEX |
|---|---|---|---|---|
| Men's/Women's Toiletries | | | | |
| Shield Deodorant Soap | - | - | - | - |
| Kiwi Shoe Polish (Black) | - | - | - | - |
| Cepacol Mouthwash | - | + | - | - |
| Coty Wild Musk Cologne Spray | - | + | - | - |
| Gilette Right Guard Spray | - | - | - | - |
| Obsession Cologne | - | + | - | - |
| Household Chemicals | | | | |
| PineSol Cleaner Disinfectant | - | - | - | - |
| Enoz Moth Balls | - | - | - | - |
| Lysol Spray Disinfectant | - | - | - | - |
| Raid Ant and Roach Killer | - | - | - | - |
| Pledge Dusting/Waxing Polish | - | - | - | - |
| Super Glue | - | + | - | - |
| Food Stuffs | | | | |
| Chicken of Sea Tuna (Oil) | - | - | - | - |
| Fisherman's Net Sardines | - | - | - | - |
| McCormick Ground Cloves | - | - | - | - |
| Smoking Materials | | | | |
| Captain Black Pipe Tobacco | - | - | - | - |
| Skoal Wintergreen Smokeless Tobacco | + | + | - | - |
| Laboratory Chemicals | | | | |
| Perchloroethylene | - | - | - | - |
| Acetone | - | - | - | - |
| Gasoline | - | - | - | - |
| Diesel Fuel | + | - | - | - |
| Potassium Chlorate | - | - | - | - |
| Chloroform | - | - | - | - |
| p-Cresol | + | - | - | - |
| Dioctyl phthalate | - | - | - | - |

## V. TEST ITEM RESULTS

Package Results: Twenty-five 1-ft$^3$ sealed, and paper-wrapped cardboard boxes were used in this test segment. These packages were treated as a typical law enforcement scenario, the unidentified suspicious package. The operator, scorer/observer, or manufacturing representative was not permitted to touch the packages. Sampling was permitted along the taped edges of the package. No penetration or puncturing of the test item by needles or probes was permitted.

The packages were placed in a sample grid within a 250-seat auditorium. Great care was taken to surround the package containing the 1/4 stick of dynamite with blank boxes. This proved useful as in less than 1 hour it was not possible to approach this package without alarming the Graseby PD-5 detector. The packages were moved outdoors to avoid contaminating the test facility or the other packages.

The package test consisted of 10 blanks boxes, 6 explosives, and 9 interferants. The interferants chosen from Table 4 were perchloroethylene, Coty Musk Perfume, Kiwi Shoe Polish, mixed tobacco products and moth balls. Results of the test for the explosive containing packages are shown in Table 5 for the Graseby PD-5, the ITI Model 97 and the Scintrex EVD-1. The Sentex Scanex Jr. which failed to operate correctly was withdrawn from the evaluation.

The only explosive detected by all the detectors was dynamite in package number C8. Only the ITI Model 97 responded to the package containing TNT. All other explosives were undetected. The Graseby PD-5 provided the only positive response to a blank or an interferant package. The Graseby response to package number G8 is unexplained.

TABLE 4. Package Results

| ITEM | CONTENTS | GRASEBY | ITI | SCINTREX |
|---|---|---|---|---|
| A14 | PETN Sheet | - | - | - |
| C8 | Dynamite | + | + | + |
| E1 | C-4 | - | - | - |
| E14 | Atlas 7D Emulsion | - | - | - |
| H14 | Smokeless Powder | - | - | - |
| J11 | TNT | - | + | - |

Briefcase Results: Twenty-five new molded plastic briefcases were used in the examination. Seven briefcases contained explosives, while 8 contained interferants and 10 were empty or blanks. The briefcases were placed at least 8 feet apart in the 3rd-floor hallway of the test facility.

This test involved 2 examinations, the first being a sampling of the briefcase along the metal-lined edges, locks and hinges. This search procedure would be typical of a suspiciously placed briefcase. To simulate a physical security scenario, the second sampling involved "burping" the briefcase by the scorer/observer in order to release trapped air from the briefcase. This procedure was included at the request of some of the manufacturing representatives.

The results of the briefcase test are shown in Table 6. The Graseby PD-5 correctly alarmed on the Hercules Red Dot smokeless powder and the 2 dynamite briefcases. A positive response was recorded for the Skoal Wintergreen Smokeless Tobacco. Unexplained responses to Musk and Pledge were recorded.

The ITI Model 97 correctly located the TNT and the 2 dynamite briefcases. Positive responses were recorded for 3 interferant briefcases 1 with Skoal Tobacco and 2 containing Coty Musk Perfume. These responses are consistent with the interferant study results. A positive response was also recorded to a blank briefcase.

The Scintrex EVD-1 correctly located the TNT, smokeless powder, 2 dynamites, and the Atlas 7-D briefcases without the need for "burping." No positive responses to blanks or interferants were recorded.

TABLE 5. Briefcase Results

| ITEM | CONTENTS | GRASEBY | ITI | SCINTREX |
|---|---|---|---|---|
| 3 | TNT | - | + | + |
| 7 | Smokeless Powder | +B | - | + |
| 11 | PETN Sheet | - | +/- | - |
| 13 | Dynamite | + | + | + |
| 16 | Atlas 7-D Emulsion | - | - | + |
| 20 | Dynamite | + | + | + |
| 23 | C-4 | - | - | - |

Note: (+) denotes positive response without burping; (-) denotes negative responses; (+B) denotes positive response on burping only; (+/-) denotes positive response without burping and negative response on burping.

Luggage Results: An assortment of 10 pieces of luggage of various types (soft sided, carry on, etc) filled with clothing were sampled. One item, a soft-sided zippered, bag contained dynamite. The Graseby PD-5, ITI Model 97 and the Scintrex EVD-1 correctly identified the bag. No other alarms were recorded.

**VI. Practical Search Exercise Results**

The practical search problems were set up in the FBI Hogan's Alley training complex located at the FBI Academy. This multiuse facility was designed to provide a realistic environment for law enforcement training exercises. It also houses office space and additional Academy-related services.

The search problems were set up to evaluate the capability of each detector in routine physical search scenarios. This test was designed not to evaluate the operator/detector combination but the detector itself. Each item or area to be searched was clearly labeled with a 3x5 card as to where and what was to be searched. For example, if a desk drawer was to be searched it would already be partially open (1/4 inch) and clearly labelled as to search along the open edge. No test area could be opened, moved, or otherwise disturbed by the search team. This directed search eliminated the operators' ability to conduct a thorough search as an uncontrolled experimental variable and ensured an equal opportunity for all detectors to respond to the hidden explosives. The Sentex Scanex Jr. was voluntarily withdrawn from these searches by the manufacturer due to instrument failure the previous day.

Post Office: This search scenario centered around a typical small town post office. A service window and locked mail boxes were located here. The purpose of this scenario was to simulate a search of mail. A letter, a manila envelope, and a package addressed to the test coordinators were individually searched. A standard exterior mail box was also searched.

The manila envelope contained PETN sheet explosive. The Graseby PD-5, the ITI Model 97 and the Scintrex EVD-1 failed to locate the PETN explosive. It is of interest to note that all 3 of these detectors responded to the PETN test explosive in Table 3, when in near contact with the [illegible]le. No false alarms were recorded by the detectors on the other test items.

Telephone Booth: A suspicious black gym bag was left in a sidewalk-style telephone booth outside of the bank. A porous brown paper lunch bag containing Hercules Red Dot double-based smokeless powder was placed on top of the clothes in the gym bag. For safety reasons the powder was not placed in a metal pipe as would be the typical case if an improvised explosive device was used. No detector responses were recorded. It should be noted that all 3 detectors responded to the test explosive when in near contact with the sample. No false alarms were recorded in the area.

Automobile No. 1 Exterior Search: A late model Chevrolet sedan was searched from the exterior. Such a search might be undertaken of vehicles entering a secure facility. Only selected areas of the automobile were searched. Two wheel wells, cracks of the hood, trunk, and passenger side front door were searched. An interior air sample was taken through the partially open drivers' window. A quarter (1/4) stick of Hercules Unigel Dynamite was placed in the trunk on top of the spare tire.

The Graseby PD-5 and the ITI Model 97 correctly responded to the dynamite while searching along the crack of the trunk after about 1 hour soak time. No other alarms were recorded by these 2 detectors. The Scintrex EVD-1 performed this analysis in the afternoon and also correctly responded to the dynamite in the trunk. The only other positive response was recorded in the afternoon by the EVD-1 on the interior air sample. This is most likely due to explosives vapors penetrating the rear seat or through the speaker area due to the longer soak time.

Automobile No. 2 Interior Search: The interior of a late model Lincoln Towncar was searched. Samples from inside the trunk, glove box, under the passenger and drivers' seat and the interior air were obtained. One-sixth pound of TNT was placed under the driver's seat.

The Graseby PD-5 and the ITI Model 97 correctly responded to the presence of the TNT under the driver's seat. An unexplained intermittent alarm was recorded in the trunk near the right rear speaker and in the glove box by the ITI detector. The Graseby PD-5 also alarmed under the passenger seat. No alarms were recorded by the Scintrex EVD-1. This was atypical of the performance of this instrument in other portions of the evaluation where it successfully located TNT.

Motel Room 117 Search: This standard single occupant motel room was labeled with 3x5 cards at six locations. Based upon our experience the previous day with dynamite vapors, only a small piece of dynamite wrapper was used. A 2x2-inch piece of dynamite wrapper was placed inside a styrofoam coffee cup in an office size garbage can. The lid was placed on the cup with the tear back drinking hole exposed. The garbage can was partially filled with trash (soda cans, snack food bags, etc.). The cup was placed near the top of the garbage can being partially covered by a snack food bag.

Both the ITI Model 97 and the Scintrex EVD-1 correctly located the dynamite wrapper in the garbage can. The Graseby PD-5 alarmed on room air upon entering the room but failed to alarm on the dynamite wrapper in the garbage can. The Graseby alarm on the desk drawer is inconsistent with its response in other empty desk drawers. The alarms by the Graseby PD-5 and the Scintrex EVD-1 on a clock on one of the tables are unexplainable.

Motel Room 118 Search: An identical adjoining room was sampled in six locations including desk drawers, a night stand, under the bed and a chair cushion. One desk drawer contained 1/4 pound of C-4 explosive. The desk drawer was partially open. This explosive was not detected by any of the detectors in this scenario. This is consistent with each detector's failure to detect the C-4 explosive itself. No other positive responses were recorded in this room.

Motel Room 125 Search: Motel Rooms 125 and 126 were prepared in such a manner as to simulate an overnight guest. The shower was run for a few minutes and the toilet flushed and deodorized. The room preparer shaved, brushed his teeth, gargled with a mouthwash and used an underarm deodorant. Several bursts of a room deodorizer were sprayed into the room. Windows within the motel rooms were also cleaned with Windex.

Hercules Red Dot smokeless powder in an open ziplock bag was placed in a dresser drawer. For safety reasons the powder was not placed in a pipe as would have been the case if an improvised explosive devise were present. No detector responded to the smokeless powder in the drawer. No other alarms were recorded to searches of a different drawer, the sink or toilet area.

Motel Room 126 Search: This adjoining room was prepared in an identical fashion to Room 125. There was no explosive material located in this room.

One dresser drawer contained a small amount of Skoal Wintergreen Smokeless Tobacco. The Graseby PD-5 alarmed on this drawer. This alarm is consistent with previous exposure (Table 4) to Skoal Wintergreen Smokeless Tobacco during the interferant test. The Scintrex alarms on the tobacco drawer and a heater vent are unexplained.

The ITI Model 97 alarm under the bed was also unexplained. The ITI also failed to alarm on the Skoal Wintergreen Smokeless Tobacco as it had during the interferant test.

Townhouse Search: The living room, kitchen, and a second floor office of a 3-story townhouse were searched. A piece of dynamite wrapper (approximately 2"x 3") was placed under one of the sofas in the living room. No explosives were placed in the kitchen. A one pound stick of Atlas 7-D emulsion was placed in a desk drawer in the office.

All three detectors correctly located the dynamite wrapper under the sofa in the living room. The Graseby detector produced no other alarms in this room. Intermittent and unexplained alarms were observed on a second sofa by the ITI Model 97 detector. The Scintrex EVD-1 also alarmed on the room air and near a table drawer holding a video cassette recorder. These alarms on air samples are consistent with this detectors response when sampling air in the areas where dynamite or dynamite wrappers were located.

No explosives were located in the kitchen. Recent plastering in the kitchen produced an unexpected background odor which did not interfere with the operation of any of the detectors. Samples were obtained under a sink which had household chemicals stored there, behind a washing machine, in a china cabinet, and room air. The only alarm recorded in the kitchen was the Graseby PD-5 alarm in an old unused refrigerator. This alarm is unexplained.

A stick of Atlas 7-D was placed in the desk drawer in the second floor office. No detector located this explosive. No other alarms were recorded on the file cabinet, a trunk, under a chair or from the air sample.

## VII. SUMMARY

This evaluation was designed to examine the commercially available explosives vapor detectors in operational scenarios. The scenarios chosen were typical of those encountered by law enforcement and security personnel. No specific conclusions or recommendations are made. The readers must judge the data with respect to their own specific operational requirements. Several general conclusions are apparent from the data.

The 2 electron capture detectors, the ITI Model 97 and Scintrex EVD-1 and the ion mobility based Graseby PD-5 detector completed the entire evaluation without experiencing instrumental failure. In general, these detectors readily and reliably detected the higher vapor pressure ethyleneglycol dinitrate (EGDN) and nitroglycerine (NG) containing explosives in the test items (packages, briefcases, suitcases) and the area searches in Hogan's Alley. In fact, only a small amount of residual particulate matter or a piece of wrapper from the dynamite was necessary for detection. Military TNT containing the more volatile DNT component was also detectable in some cases.

The lower vapor pressure inorganic explosives (water gel/slurries and emulsions) such as Atlas 7-D and the organic (PETN and RDX) plastic explosives such as PETN Deta Sheet and C-4 were undetected in the various area search scenarios even though the detectors were directed to search specific areas. It should be noted that both of the inorganic explosives are widely used commercially in the United States. PETN and RDX-based explosives are commonly used by militarys throughout the world. It should be pointed out that these explosives were obtained from "sterile" sources and not exposed to contamination from the nitrated esters EGDN and NG.

Over the last 10 years or so there appears to have been a general improvement in sensitivity of the commercial detectors toward NG, EGDN and TNT. The challenge still remains to find a small portable hand-held detector able to reliably detect the inorganic and plastic explosives in operational scenarios.

To meet this important challenge, it will be necessary for explosives manufacturers, instrument companies, forensic scientists and law enforcement personnel to work together.

# AIRPORT TESTS OF FEDERAL AVIATION ADMINISTRATION THERMAL NEUTRON ACTIVATION EXPLOSIVE DETECTION SYSTEMS

Chris C. Seher
Department of Transportation
Federal Aviation Administration Technical Center
Atlantic City Airport, NJ 08405 - USA

## ABSTRACT

A system for detecting explosives in airline passenger baggage or cargo has been developed and tested by the Federal Aviation Administration (FAA) under a contract with Science Applications International Corporation (SAIC) located in Santa Clara, California. Luggage or cargo is moved on a conveyor into a region of neutron radiation. The neutrons easily penetrate the luggage and cargo, where some are absorbed by atoms, which emit elementally distinctive gamma rays. Thus by monitoring the high energy gamma rays that escape the luggage with detectors placed in a ring around the inspection cavity, one can determine the composition of the luggage contents. Nitrogen is found in many materials, but only explosives have relatively high concentrations thus allowing the nitrogen concentration and distribution in a bag to be the primary signature used by the completely automated thermal neutron activation (TNA) system to make a decision on whether an explosive is present.

In parallel, but independent of the TNA stand-alone testing, an X-ray machine was used to inspect the suspicious bags (as determined by the TNA technique), and the X-ray image was correlated with the three dimensional nitrogen density distribution from the TNA system to yield an improved automated decision. The results of comprehensive airport testing of the X-ray Enhanced Neutron Interrogation System (XENIS) and the TNA system performed during 1987-88 are summarized.

## 1. INTRODUCTION

A system for detecting commercial and military type explosives in airline passenger baggage and in individual air cargo parcels has been developed by the Federal Aviation Administration (FAA) under a contract with Science Applications International Corporation (SAIC) in Santa Clara, California. The FAA operational requirements for any explosive detection system (EDS) dictate that several pounds of commercial type explosives such as dynamites, watergels, slurries, and emulsions as well as military C-4 and plastic sheet type RDX/PETN

(Semtex) based explosives be detected with a greater than 95 percent probability with less than a 1 percent or 2 percent probability of false alarm. The performance probabilities must be achieved while processing at least 10 pieces of luggage a minute using a technique that is independent of explosive shape. In addition an EDS must: cause no damage to inspected items; be non-hazardous to passengers, operators, and the environment; be reliable, easily maintainable, and operable by relatively unskilled personnel; cause no unwarranted financial burden on airlines, airport operators, or passengers; and commensurate with all other requirements it should occupy the smallest volume of space and have the lightest weight possible.

The FAA has developed and tested two thermal neutron activation (TNA) EDS. One system uses a Californium 252 radioisotope as a source of neutrons with an energy spectrum from near zero to 10 million electron volts, 10 MeV. The second prototype called the DD EDS uses an accelerator to bombard deuterium, absorbed in a scandium target, with deuterium ions of sufficient energy to cause nuclear fusion which produces neutrons of a nearly constant energy of 2.5-3 MeV with a peak neutron intensity of $5 \times 10^8$ n/sec. Both systems have performed equally well in terms of detection/false alarm probability. The advantage of the accelerator is that radiation is produced only when the accelerator is turned on and not having the higher energy spectrum reduces the radiation shielding required for the system. The main disadvantage of the DD system is that the accelerator is a complex and costly device that requires much more service and maintenance than a Californium source. Fast neutrons from either source are slowed down "thermalized" by hydrogenous moderating material that make up the walls of the integrating cavity to create a cloud of low-energy neutrons. The neutrons diffuse into the luggage or cargo to be screened and produce characteristic gamma rays that are promptly emitted following neutron capture. A detector array of up to 80, 4" x 4" NaI (TI) inorganic scintillators arranged in C-shaped rings around the neutron source in each system detect the gamma-ray spectra obtained from up to a 16" x 26" x 36" sample in the cavity. The cross sectional area and depth of the detectors were optimized to trade-off good spatial resolution versus high background counts.

## 2. DISCUSSION

Figure 1 is a plot of the gamma spectrum obtained from a luggage sample with an explosive simulant attached. It should be noted here that explosives simulants were made to match the response of real explosives in the TNA system, through "side by side" comparisons in the lab, so as to avoid taking live explosives onto the airport. Simulants for each of the different types of explosive threats were made, and, in particular, the sheet explosive simulant was made in a thin sheet. Each simulant was the minimum amount of explosive considered to be a threat. The few hundred counts to the extreme right of the spectrum in Figure 1 arise from nitrogen. Nitrogen gamma rays are the most energetic prompt gamma rays in nature, having an energy of 10.8 MeV. Most of the rest of the spectrum arises from shielding and other materials in the suitcase. The dominant feature is the 2.2 MeV gamma ray from hydrogen. Weaker peaks are seen from carbon, silicon, aluminum, irons, and sodium iodide. Above 10 MeV, only nitrogen should be seen, but the spectrum shows what looks like a smooth, high energy tail. This tail arises from an electronic artifact called pileup which occurs when two gamma rays impinge on a detector at so nearly the same time, that the electronics treats them as one event and sums the energies. Special electronics were developed especially for the EDS to handle count rates an order of magnitude greater than commercially available electronics could achieve. The EDS construction materials were carefully selected to minimize background, and corrections for the remaining backgrounds are applied to each detector. A spectrum as in Figure 1 is taken for each detector every second, which represents about four inches of travel of the inspected baggage. The spectra are fed into a MicroVax II computer, which uses the nitrogen concentration and distribution in a bag as the primary signature as its basis for making a completely automated decision as to the presence of explosives. The TNA EDS are designed to be operated by a baggage handler. All analysis, processing, and control is automated. The operator need merely start conveyors, and monitor the exit alarm for the possible presence of an explosive threat.

## 3. RESULTS

Extensive laboratory optimization measurements were followed by an intensive period of airport testing (June 1987 - March 1988), which included measurements with both the radioisotopic and electronic neutron sources. Six separate airport tests to detect simulated bulk and sheet

and sheet explosive simulants at the operationally required throughput rate were performed at the San Francisco and Los Angeles International Airports in California on both domestic and international baggage and cargo sets to many different destinations. The results of the tests are summarized in Table I.

TABLE I

AIRPORT TEST RESULTS FOR THE TNA EXPLOSIVE DETECTION SYSTEM FOR MORE THAN 40,000 SCREENED ITEMS

| Item | Probability of Detection (PD%) | Probability of False Alarm (PFA%) |
|---|---|---|
| Luggage | 90 - 96 | 3 - 8 |
| Cargo | 90 - 95 | 1 - 4 |

The range of PD and PFA values results from variations in performance due to the content of the luggage items as a function of the destination and the season of the year. The trade-off in PD vs PFA to match a particular situation is programmed into the system decision-making process.

A disturbing result of the airport tests was the large fraction of items, particularly in the international sample, that contained more than one threat equivalent of nitrogen, meaning greater than 300 grams of nitrogen (see Figure 2). This illustrated the need to measure other independent, distinguishing features besides nitrogen to reach the lowest possible PFA. To achieve this, a large number of discriminants were determined, the most significant of which are the average density of each bag, the neutron flux attenuation in the bag, and the spatial distribution of nitrogen. Whenever trade-offs were required, the systems were always optimized toward the operationally determined, higher risk international baggage and plastic type sheet explosives. Figure 3 shows the performance curve from which system operating points maybe set. Slightly more than the minimum explosive threat greatly increases detectability performance. Conversely, less of any explosive target will reduce the system performance.

A second independent program was run in parallel with the development of the TNA EDS. A commercially available two-view X-ray machine, with two separate X-ray tubes and arrays, was used to inspect the suspicious bags (as determined by the TNA technique). The two machines were linked together with an image processor and separate computer, which correlated the elemental information from the TNA system

with the density image produced by the X-ray system. Image correlation and enhancement algorithms were developed, as was an automated decision module. Thus, this dual sensor or, "XENIS" system, could take a "second look" at a suspicious bag with the X-ray machine, decide if an explosive really could be present, and identify the physical object which had the threatening signature. In operation, it was set to not lose any proper detections, but to cut the false alarm rate as much as possible. It achieved a 50 percent reduction in false alarm rate with no loss in detection rate. The X-ray images were also stored on an optical disk for later use.

During the field testing of these units, a number of other important tests were done. All bags exiting the system were monitored for induced radiation, a measurement required by the California Radiologic Health Branch. No significant induced radioactivity was found. Two different film makers and the National Bureau of Standards ran tests to see if the radiation levels would fog film; none was detected in ten passes of the film through the system.

## 4. CONCLUSIONS

The two EDS TNA systems met or exceeded all of the requirements specified by the FAA in on-line tests. In addition, the added dual sensor approach of enhanced X-ray inspection of TNA suspect baggage was demonstrated to be highly effective in automatically reducing and finally resolving false positive signals from the TNA EDS alone. Based on these results, the FAA has awarded a follow-on contract for up to ten operational prototypes, to be deployed at high risk international airports for Government sponsored 1 year on-line operational evaluations. The first system was installed last month at JFK International Airport in New York. The new systems have been reduced in size to an overall length of about 13 feet, maximum width of 8 feet, and height of about 6 feet as depicted in Figure 4. In addition, the add-on XENIS technique will be used to reduce operational false positives. The XENIS installation approximately doubles the length of the overall system. Because of the short-lived usefulness of the target and the overall unreliableness of the electronic sources currently available for the TNA application, the first six prototypes delivered through January, 1990 will use radioactive sources. Continued research and development is being directed toward longer-lived, more reliable, and advanced electron neutron sources. Specifically an electrostatic generator and a

radio frequency quadrupole (RFQ) linear accelerator system are currently being evaluated for application to TNA EDS.

SAIC has received device registration for the TNA system and the Nuclear Regulatory Commission (NRC) has found no significant impact to the environment for airport ramp level baggage inspection use. The FAA has received a materials license (Number 29-13141-05) to use TNA registered devices at high-risk United States airports. The NRC is currently evaluating the possible use of TNA system deployment at or nearby ticket counters in the airport concourse areas.

Research and development is needed and will continue in the areas of non-nitrogenous explosive detection and smaller and smaller explosive threat detection through multi-elemental analysis, perhaps specifically through hydrogen-nitrogen ratios.

In addition, work is underway to enhance or replace the current discriminant analysis techniques for automated threat detection, with artificial neural networking.

## 5. ACKNOWLEDGEMENTS

The cooperation of the host airlines and airports was instrumental in the success of these system demonstrations. I would like to especially thank the managements of Los Angeles and San Francisco International Airports and the entire staffs of United, Trans World, and Pan American Airlines for their cooperation and support in helping to make aviation safer and more secure.

# Gamma Ray Spectrum

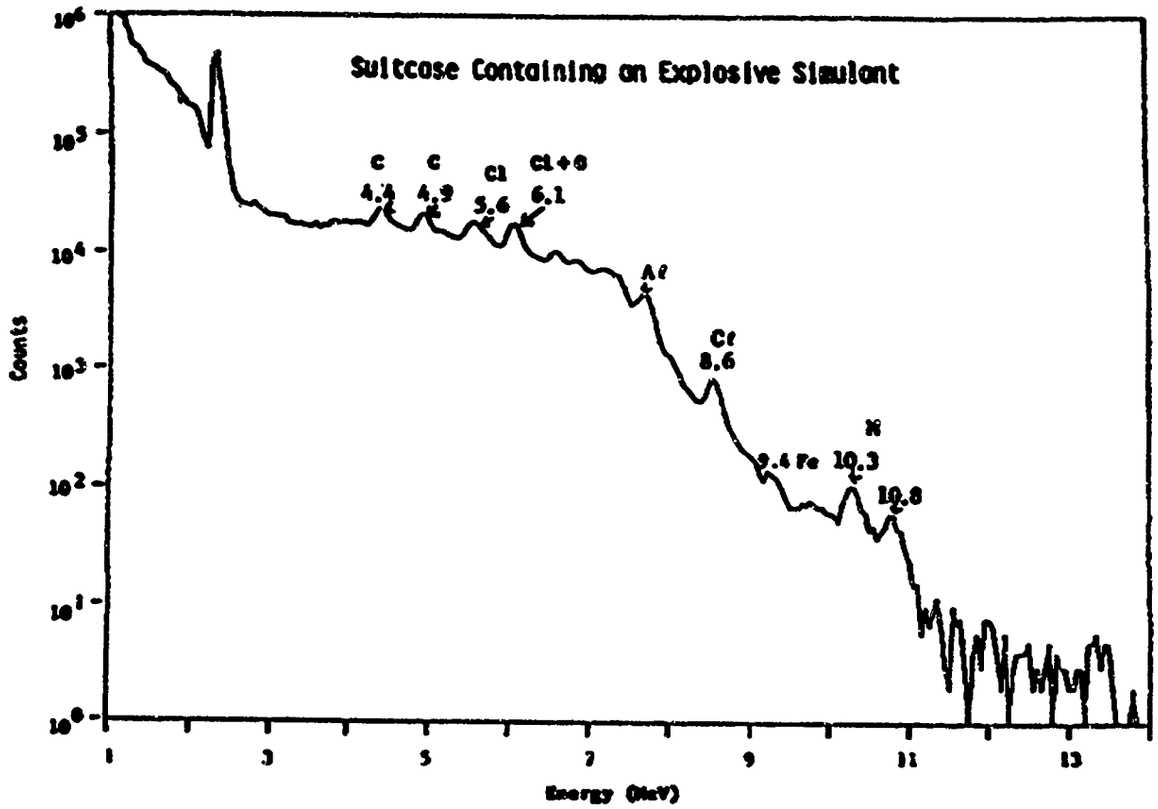


Figure 1

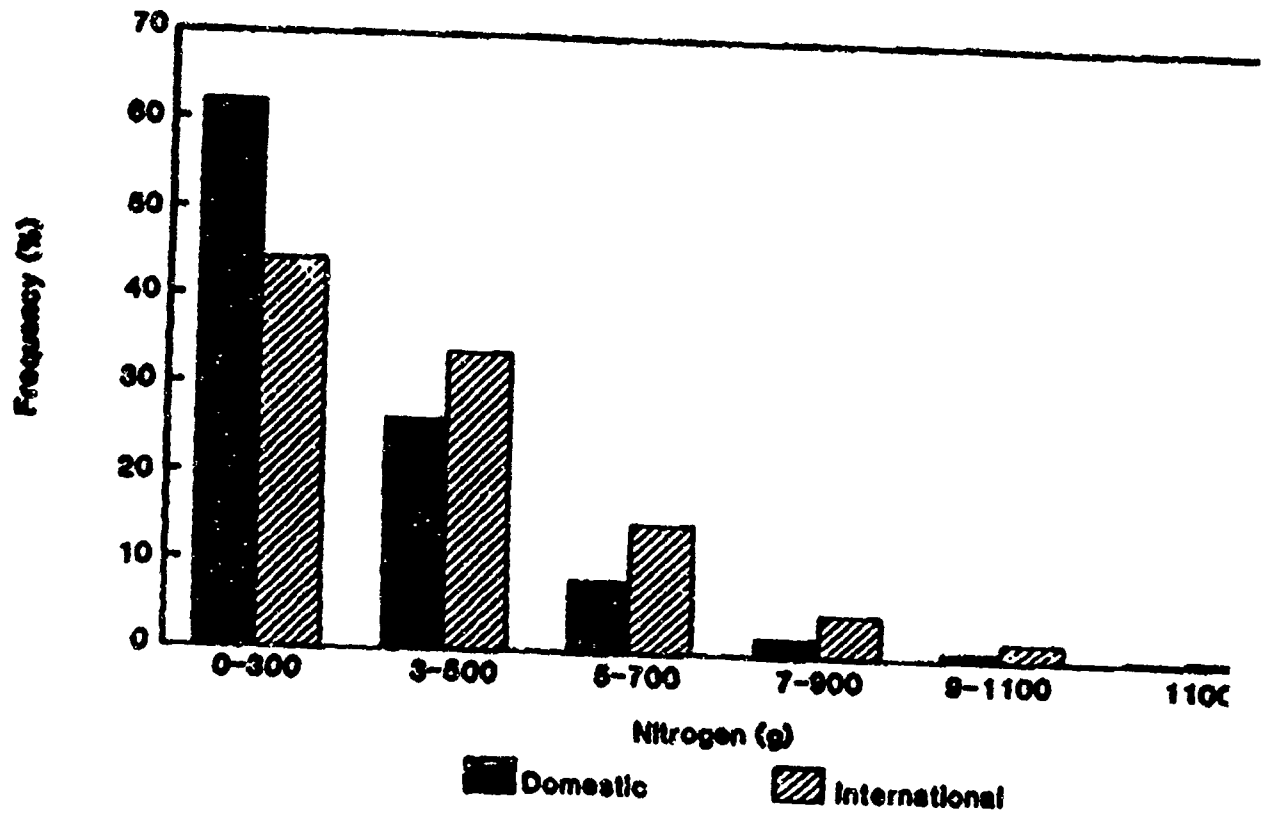


*Domestic vs international nitrogen distribution.*

## Performance of Explosive Detection System Weighted over All Explosives

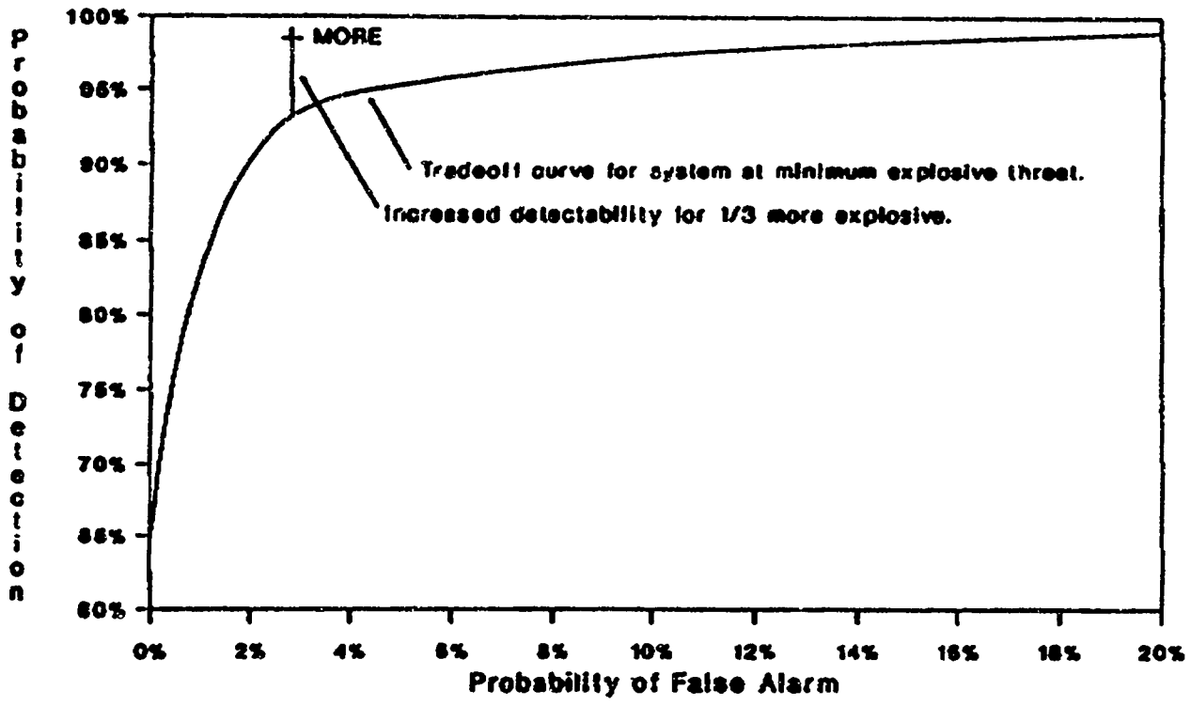

# System for Nuclear On-line Observation of Possible Explosives (SNOOPE)

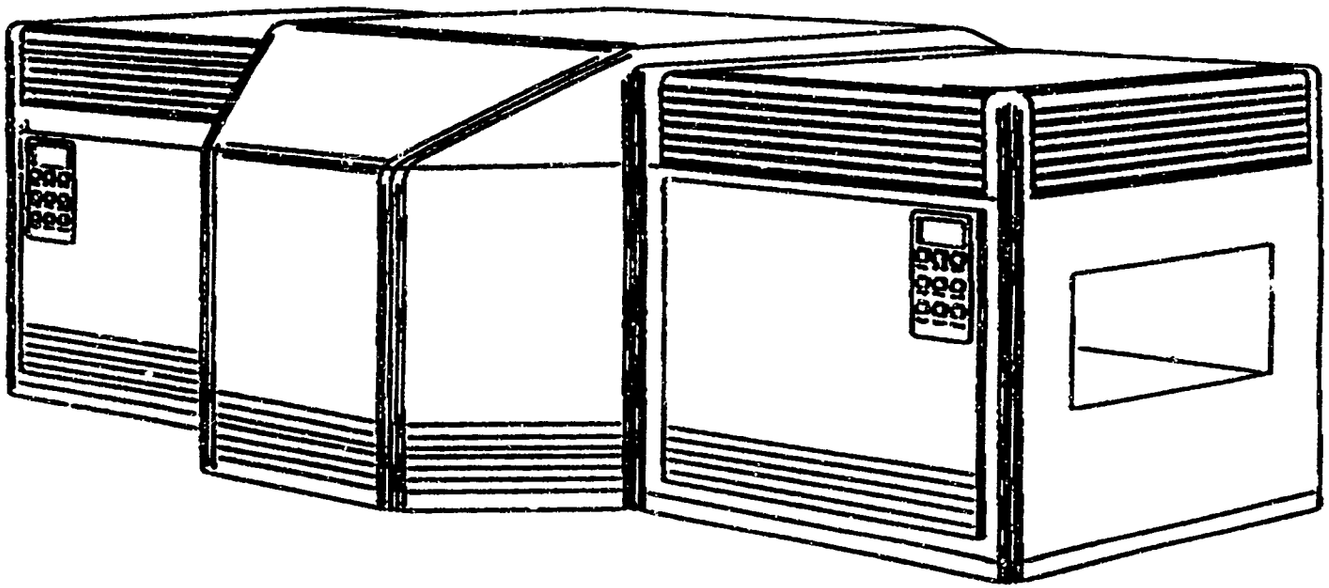

Chris Seher

BIOGRAPHY

* Graduated from Drexel University in 1971 with Bachelor of Science degree in Physics
* Masters in Aviation Management in 1985
* Employed by FAA since 1967 at the FAA Technical Center in Atlantic City, New Jersey
* Worked in Aviation Security Program area for 11 years
* Currently, Manager of Bulk Explosives Detection R&D Program
* Directed the contract effort in thermal neutron activation detection of explosives for the past 6 years

# EVALUATION OF THE OAK RIDGE MS/MS EXPLOSIVES DETECTOR*

F. J. Conrad and D. W. Hannum

Division 5248, Sandia National Laboratories, Albuquerque, NM 87185

B. C. Grant, S. A. McLuckey, H. S. McKown, and G. L. Glish,
Analytical Chemistry Division, Oak Ridge National Laboratory,
Oak Ridge, TN 37831-8121.

## ABSTRACT

**Results are presented for the evaluation of the Oak Ridge National Lab (ORNL) MS/MS as an explosives detector. This instrument is a beam instrument containing a quadrupole and a time-of-flight detector section (QTOF). The tests include a Limit of Detection for the instrument, an interferent study, a test of personnel sampling for explosives, a test involving mail sampling, and detection tests with bomb quantity explosives.**

## INTRODUCTION

Since the vapor pressures of the explosives compounds of interest are extremely low at room temperature and pressure[1], greater and greater sensitivities are being required of the detection instruments[2]. As a result, many different instruments are being investigated to determine their suitability as detection instruments. One such instrument is the Mass Spectrometer/Mass Spectrometer (MS/MS) unit developed at Oak Ridge National Lab (ORNL) specifically for the detection of explosives in mail by vapors.

## APPARATUS

The mass spectrometer/mass spectrometer used in these tests was a special unit constructed for the security section of

* This work was supported by the U.S. Department of Energy under Contract DE-AC04-76DP00789.

ORNL by the mass spec section to inspect the incoming mail. The unit is a quadrupole/time-of-flight (QTOF) beam instrument using a special atmospheric sampling glow discharge ionizer (ASGDI) developed by ORNL. The unit is large measuring 2.23 meters long by 0.8 meters wide by 1.88 meters tall.

The unit comes with a remote sampler which is a quartz tube with a quartz wool plug. The sampling tube measures 10 mm OD by 8 mm ID by 15.3 cm long and the loosely packed quartz wool measures approximately 4 cm. This sampler is used to collect sample by preconcentration before analysis. The preconcentrator with its sample is inserted into the heated inlet where the explosives sample is desorbed into the glow discharge ionizer.

A Thermedics Inc. Vapor Generator was used as the standard RDX vapor source for establishing the Limit Of Detection of the unit.

**OVERVIEW OF THE MS/MS APPROACH TO EXPLOSIVES DETECTION**

What follows is an overview of the approach to explosives detection taken with the ORNL quadrupole/time-of-flight instrument fitted with an atmospheric sampling glow discharge ionization source. This instrument is referred to herein as a beam-type instrument wherein ions that exit the ion source traverse the instrument in a beam. The overall approach to explosives detection is illustrated schematically in Figure 1 which indicates an ion source and two mass analyzers in sequence. Initially, air containing explosives molecules is drawn into the ion source where some of the explosives molecules are converted to negative ions by one of several mechanisms. Unlike the majority of compounds in nature, the molecules of organic high explosives readily form stable negative ions. Analyzing the negative ions that issue from the ion source therefore provides an important degree of discrimination against most of the species that are present in air in much higher numbers than the explosives. The negative ions that exit the ion source pass through two stages of mass analysis. There are several possible modes of operation of the tandem mass spectrometer which are discussed below. The mode indicated in Figure 1 shows the most common form of MS/MS whereby anions formed in the ion source are mass-selected by a first stage mass analyzer

and are subjected to collisions with a gas admitted into a region between the mass analyzers as discussed in Appendix A. The anions that pass through the first stage of mass analysis are referred to as the parent ions and the region where the target gas is admitted is referred to as the collision region. The anions that issue from the collision region are then mass analyzed by a second stage of mass analysis. These ions typically include both parent ions that either did not fragment after collision or did not undergo a collision and fragment ions or so-called daughter ions that result from collision-induced dissociation. This overall procedure provides very high specificity since a positive indication for an explosive requires the formation of negatively charged parent ions, parent ions with mass/charge (m/z) ratios corresponding to those known to be formed from explosives, and daughter ions of characteristic m/z values.

## MATERIALS

Military grade C-4, pure RDX, military grade TNT, Pure TNT, Detasheet C, PrimaCord, PBX 9404 pellets, flake TNT, pistol powder, rifle powder, black powder, and "old" 40% dynamite were available at Sandia.

Eastman cyclohexanone was used as the simulant C-4 solvent.

The interferents used were diesel fuel, "Skoal" smokeless tobacco, "Coty Musk for Men" cologne, "Kiwi" shoe polish, banana skin, and Fisher Certified A.C.S. Methylene Chloride and Methanol.

## PROCEDURES

### Qualitative Survey of Explosives and Interferents.

Before detailed testing was attempted a qualitative survey of the explosives and interferents was run. This survey was conducted by presenting vapors from the different explosives and interferents directly to the inlet of the MS/MS and noting if a detection was made. If a detection was made no further testing was done in the qualitative survey with this explosive or interferent. If no detection was made the explosive or powder was sampled with the quartz sampling tube, and checked for a detection.

The compounds that were used as interferents are delineated above. Methylene chloride and methanol also were used to

investigate the stability of the glow discharge source with respect to suppression.

**Limit Of Detection (LOD)**

The basic instrument LOD was established for each of the modes of operation of interest by inserting the outlet of the Thermedics Inc., RDX vapor generator directly into the inlet of the MS/MS. Since explosives molecules are sticky it is necessary to insert the generator outlet and let the adhered molecules bake off the tip to equilibrium before taking a reading on the concentration. This effect is shown in Figure 2. Note the starting level, the peak level, and the equilibrated level. The reading is taken as the difference between the starting level and the equilibrated level.

The quartz tube preconcentrator assisted instrument LOD was established for the most usable modes of operation of the MS/MS. The equilibrated output of the vapor generator was drawn into the quartz tube with quartz wool preconcentrator using a modified "Dust Buster" sampler. This drawing of the sample was performed out in the open with no attempt to shield from the air conditioner air currents in the room other than to sample at a flow rate into the sample tube which was greater than the output of the vapor generator and to sample at approximately 3.2 mm from the exit of the tube. The tubes were then inserted into the heated inlet to the MS/MS and the outputs recorded in the different modes of operation on the instrument.

**Bomb Quantity Testing**

The procedure for executing the bomb quantity tests was to present each of the materials to the inlet of the MS/MS to determine if a detection was possible. If no hit was made, then a sample was taken close to the surface of the explosive material (within approximately 3.2 mm) with the quartz sampler and the sampler was inserted into the MS/MS for analysis. If the surface of any of the explosives was touched by the sampling tube, the tube had to be baked out for a considerable time and another sample taken.

**Personnel Sampling**

To date no standard procedure has been defined and accepted

for personnel sampling. Since this instrument uses the quartz sampler, the samples taken from personnel in this test were taken as one might sample with a metal detector hand-sampler. The quartz tube was attached to the hand-sampler and the unit turned on. The sampling was started by placing the tip of the tube under the arm at the pit using the vapor-touch method. This method requires the vapor sample to be taken while touching the clothing or sampled surface with one side of the tube tip at approximately a 45 degree angle. The sampler was moved down the side of the individual to the belt, across the belt area to the other side, and up to the arm pit on that side. The sampling was jumped back to the belt area where the pocket area was searched and downward on the outside of the leg. Then the opposite pocket area and leg were sampled in the same manner. The individual was turned around, and the sampler run down the middle of the back to the belt area. One pass was made back-and-forth across the belt area and down the inside of each leg to the shoe top. This total sample required only 25 seconds to complete. The sample was then inserted into the MS/MS for analysis.

A sample of C-4 measuring 6.3 x 8.3 x .32 cm was placed outside the "T" shirt and under the summer weight western shirt in the belt area of the one of the authors and after 1 hour and 26 minutes the sampling technique described above was used to make the search.

**Mail Sampling**

Segregated letters at some installations are delivered in a tray that is approximately 30.5 cm long and has the letters closely packed and standing on edge. This uniformity allows the letters to be sampled easily. The chosen method of sampling this configuration was to install the quartz tube sampler in the pump, start the pump, and pass the tip of the sampler along the tops of the envelopes and down between each letter while riffling the envelopes using the vapor-touch method. The sampling of the tray was completed by sampling around the tray perimeter.

Our test simulated the above sampling procedure in that the previously used small C-4 sample was placed in an envelope and after 10 minutes the outside of the envelope was sampled by the

vapor-touch method. After an additional 16 minutes, a 4-second sample was taken at the top of the same envelope using the same sampling method.

## RESULTS AND DISCUSSION

### Qualitative Survey

All of the bare explosives were detected with ease at the inlet of the MS/MS except the Deta Sheet C and this material was detected easily with the quartz sampler.

TABLE 1

| Type Powder | - | Detected |
|---|---|---|
| Pistol | - | NG |
| Rifle | - | DNT |
| Black | - | Mass 192 and 96 |

The powders such as pistol, rifle, and black were checked. Pistol powder had a peak at mass 62 which is $NO_3$ minus from degraded NG. The main peak in rifle powder was mass 182 which was DNT. Figure 3 shows the mass spectrum of black powder. The peak of importance is the small peak at mass 192 which was always present in the spectra. Until now it has been assumed that black powder could not be detected. Additional work has proven that this peak could be sulfur which is used in the formulation of the black powder. Elemental sulfur can decompose into many molecular configurations from $S_8$ down to lower numbers of sulfurs. The peak at mass 192 appears to be $S_6$ and the peak at mass 96 appears to be $S_3$.

### Interferents

We envision that there are two types of interferents for explosives detectors. One type of interferent is the compound that causes a false alarm (indicates it is an explosive when it is not). The other class of interferent is the compound that changes or negates the sensitivity of the instrument (in the case of this MS/MS instrument this could be a glow discharge suppressant or a substance that can change the ion chemistry of the source).

The materials diesel fuel, "Skoal" smokeless tobacco, "Coty"

Perfume, "Kiwi" shoe polish, and a banana skin that were possible false alarm agents gave no interference.

The two solvents that were used to test the stability of the ASGDI source were methyl alcohol and methylene chloride. It had been noted previously at Sandia that if a softer ionization source is used it is possible to completely change the ion chemistry of explosives molecules like RDX and PETN when the ion chemistry changes from oxygen minus to chloride minus because these molecules add the reactant ions to the explosive molecule thereby resulting in a completely different ion mobility time or m/z. Neither of the solvents tested changed the reaction ion chemistry of the source. The only noticeable change was a slight suppression of the glow discharge and thereby the current but no detrimental effect was noted.

**Limit Of Detection**

The LOD for RDX was established for the Single Ion Monitoring mode of operation of the Quadrupole/Time-of-Flight (QTOF) (see Appendix A - Modes of Operation of the QTOF) and using a mass resolution of approximately 400 the LOD was found to be 3 parts per trillion (cc/cc).

The LOD for the Time-of-Flight (TOF) mode of operation at a mass resolution of approximately 400 was found to be 30 ppt (cc/cc).

The LOD for the Targeted Daughter Ion mode of operation was found to be 3 ppt (cc/cc).

The LOD of the instrument was lowered by a factor of 10 by the use of the quartz tube sampler. This procedure was run by sampling with the quartz sampler, then desorbing into the unit and integrating the signal over a 10 second time period. This integrated area was then divided by the factor of 10 to get the grams per second. The LOD of the Targeted Daughter Ion mode of operation by this method became 0.3 ppt (cc/cc).

**Bomb Quantity Testing**

The explosive C-4, 375 grams, was sampled both at the inlet of the instrument and with the tube sampler with positive results. Military TNT, 275 grams, was sampled only at the inlet because the response at the inlet was so great that we did not want to saturate

the instrument by sampling with the quart tube. Tetryl, which was in the form of pressed pellets which were 2.54 cm O.D. right circular cylinders and 1.9 cm long, was detected both at the inlet and with the tube sampler. The vapor from the cut end of a 275 gram sample of PrimaCord could not be detected at the inlet but was easily detected with the tube sampler. Figure 4 shows the magnitude of the signal for the detection of PrimaCord. Deta Sheet C, 275 gram, could only be detected by the use of the sample tube. The Deta Sheet material seems to be the hardest explosive material to detect of the explosives materials tested. PBX 9404 pellets, which contains only a small trace of RDX, could only be detected using the sampling tube[3].

**Personnel Sampling**

The C-4 sample had been placed under the shirt and allowed to remain for 1 hour and 26 minutes before sampling. The sampling procedure listed above was used to sample the individual in a vapor-touch method. The first sample that was taken saturated the instrument at the sensitivity setting of the detector used in these studies. The sampling tube was changed to a new tube. The C-4 sample was removed immediately and 3 hours and 20 minutes later another 8 second sample was taken of the area using the vapor-touch method. This sample also saturated the instrument. It will be discussed below in the mail sampling test that a faint outline of the C-4 sample seemed to be evident while the sample was in the envelope and remained after the sample had been removed. It was in this area that large signals were recorded. It is possible that the RDX material is actually being transported through the shirt material just as with the envelope.

**Mail Sampling**

The response of the first vapor-touch sample of the envelope containing the C-4 sample was tremendous. Figure 5 shows the response of the Single Ion Monitoring (SIM) method of sampling the envelope with the quartz tube sampler. This measurement involves monitoring m/z 176 in a single ion monitoring mode as a function of time. The area under the curve is related to the quantity of material collected. When the same small C-4 sample was placed in the envelope and the sides of the envelope allowed to touch the

sample, it appeared that the outline of the sample could be discerned on the envelope. This indicates that it is possible that the RDX explosive was transported through the paper of the envelope by the motor oil, the polyisobutylene, the solvent cyclohexanone, or a combination of these.

After an additional 16 minutes, the top of the envelope was sampled by the vapor-touch method for 4 seconds. The response was large. Since the top of the envelope had been slit open to remove the contents and had not been taped closed for the test, some of the vapor must have been pumped out to the sampler without touching the walls of the envelope.

## CONCLUSIONS

The MS/MS Explosives Detector designed and built by Oak Ridge National Laboratory has been evaluated by a combined team of Sandia and ORNL personnel. This device with its remote sampler, although produced as an explosives detector for sampling mail, could be used in many other sampling scenarios, such as searching personnel, searching mail, searching buildings, etc.

The limits of detection for the SIM mode, the TOF mode, the Targeted Daughter Ion Mode, and the Targeted Daughter Ion Mode with sampler were determined to be 3 ppt, 30 ppt, 3 ppt, and 0.3 ppt, respectively. All of the bare explosives samples that were used were detected by the unit using the sampler.

## REFERENCES

1. B. C. Dione, D. P. Rounbehler, E. K. Achter, J. H. Hobbs, D. H. Fine, J. Energetic Materials 4, 447 (1986).
2. F. J. Conrad, J. of the Nuclear Materials Management, Proceedings Issue, Columbus, Ohio, 212 (1984).
3. B. J. Yelverton, J. Energetic Materials, 6, 073-080 (1988).
4. S. A. McLuckey, G. L. Glish, K. G. Asano and B. C. Grant, Anal. Chem., 60, 2220 (1988).

## APPENDIX A

### General Description of the ASGDI Source/QTOF Instrument

The explosives detector evaluated in this study relies upon Atmospheric Sampling Glow Discharge Ionization (ASGDI) as the means for converting explosives molecules to anions and a quadrupole/time-of-flight (QTOF) tandem mass spectrometer as the instrument to provide MS and MS/MS data. These have been described previously.[4]

## Modes of Operation of the QTOF Instrument

Meaningful data can be acquired from the QTOF instrument in a variety of ways. Each mode of operation has certain characteristics that make it more or less useful than another possible mode for a particular application. A brief qualitative description of each operating mode that may be useful in explosives detection is described below along with some comment as to its relative merits.

Quadrupole Mass Scan. The mass spectrum provides information on the relative intensities and masses of the ions formed in the ASGDI source. The mass spectrum can be obtained using the quadrupole mass filter by holding the TOF deflection plate voltages at the same potential as the flight tube and scanning the quadrupole mass filter. The mass resolution, scan speed, and scan range are all defined by the operator. This method is useful for screening purposes to check for the presence of parent ions characteristic of explosives. The specificity of this mode is lower than that of MS/MS but is still good with respect to other explosives detectors. A disadvantage associated with this mode is the loss in sensitivity associated with scanning the mass spectrometer. Most of the analysis time is spent in areas of the mass spectrum where no explosives-related ions are present.

Single Ion Monitoring. This mode refers to the situation in which the quadrupole mass filter is set to pass only ions of one m/z ratio and the TOF is not employed. In the absence of chemical interferences at the m/z of interest, this mode provides the greatest sensitivity since all of the time is spent on a region in the mass spectrum where explosives-related ions are expected, overcoming the problem associated with scanning. The disadvantage, of course, is that only one explosive can be monitored at a time. The specificity and sensitivity of this mode can be varied via the mass resolution. Transmission through the quadrupole can be increased by degrading the resolution thereby increasing sensitivity and decreasing specificity. A variation on this mode is multiple ion monitoring or peak hopping in which the quadrupole is alternately moved to pass different m/z values in sequence. This allows for several explosives to be monitored with some

compromise in ultimate sensitivity for each explosive. The multiple ion monitoring mode is intermediate in sensitivity between single ion monitoring and the full mass scan.

TOF Mass Spectrum. The other method of obtaining a full mass spectrum is to put the quadrupole mass filter in the rf-only mode using a low peak-to-peak rf voltage on the rods, thereby passing all ions through the quadrupole, and acquiring the TOF spectrum. The mass resolution in TOF is generally poorer than with the quadrupole mass filter so that the specificity is generally poorer than with a quadrupole scan. Furthermore, the quadrupole mass filter, when operated in the rf-only mode, does not pass all ions with equal efficiency introducing what can be severe discrimination against some ions. Furthermore, the TOF mode suffers from a compromise in sensitivity due to the fact that the TOF gate is only "on" 1 per cent of the time. This is analogous to the losses experienced by scanning the quadrupole. With the quadrupole, however, the time spent on any mass is generally less than 1 per cent and the transmission is also lower than in the TOF. Therefore, the sensitivity of the TOF mode is expected to be better than that of the quadrupole mass scan. Nevertheless, the improvement in sensitivity is generally not deemed to overcome the loss in specificity so that the TOF mode is rarely used for explosives detection and was not used during these tests.

Conventional Daughter Ion MS/MS. The mode with by far the greatest specificity is conventional daughter ion MS/MS whereby daughter ions are mass analyzed by TOF after the parent ion is mass-selected with the quadrupole at unit mass resolution. Relative to single ion monitoring, the sensitivity of this mode is lowered by the 1% duty cycle of the TOF. That is, only 1% of the parent ions are subjected to MS/MS. This might lead to a decrease in detection limit by a factor of 100. This, however, is not usually observed due to the well-known reduction of "chemical noise" afforded by MS/MS. The background ions at the same m/z value as the parent ion generally do not give the same daughter ions so that even though the signal level is decreased, the background noise level is decreased even further. In practice, the limit of detection in the MS/MS mode is lower than that in the single ion

monitoring mode, but not by two orders of magnitude. The greatest combination of specificity and sensitivity is obtained via the combination of single ion monitoring with MS/MS using unit mass resolution parent ion selection. Again, this only permits one explosive to be monitored at a time. A usual operating procedure, therefore, is to combine the multiple ion monitoring mode of the quadrupole with MS/MS. The quadrupole can be hopped over a series of predetermined m/z windows and when a signal is obtained that exceeds a threshold level for one of the m/z windows, the MS/MS spectrum can be obtained for that m/z. An explosive is then indicated if daughter ions characteristic of the explosive is detected above a predefined threshold. The extent to which the sensitivity for any given explosive is compromised is, of course, determined by the number of different m/z windows that the quadrupole must monitor.

Targeted Daughter Ion MS/MS. A possibly useful mode of operation for explosives detection was identified during these tests that compromises some specificity relative to conventional daughter ion MS/MS but promises to greatly enhance the overall sensitivity of the analysis. This mode, referred to here as the targeted daughter ion mode, uses the quadrupole mass filter in a very low resolving/high transmission mode in conjunction with TOF. The quadrupole is operated so as to pass only high mass ions, e.g. ions of mass greater than m/z 180, and the TOF is operated in the normal way. Operationally, this is very similar to the TOF method for obtaining a mass spectrum. The difference is that in the targeted daughter ion mode, the quadrupole is used to filter out low mass ions that issue from the ion source whereas all ions are transmitted in the normal TOF mass spectrum mode. When the low mass ions from the ion source are not transmitted through the quadrupole, i.e. in the targeted daughter ion mode of operation, the only low mass ions that can be detected via TOF are those that arise from fragmentation of the high mass ions that pass through the quadrupole. In this way, all of the characteristic daughter ions that arise from explosives can be monitored while all of the high mass parent ions are passed through the quadrupole simultaneously and with relatively high transmission. In general,

transmission in the rf-only mode for an ion of a given m/z ratio is over an order of magnitude greaterthan in the single ion monitoring mode. Furthermore, the advantage in the reduction of chemical noise by MS/MS is retained. This mode, therefore, might be competitive in sensitivity with single ion monitoring. An additional advantage comes into play when considering monitoring for several explosives. This approach obviates peak hopping with the quadrupole as is necessary in the multiple ion monitoring mode coupled with MS/MS. The specificity of the targeted daughter ion mode, although lower than that of the conventional MS/MS mode, should still be high relative to other means for explosives detection. The following must be true in order to register a positive signal; i) the molecule must form a negative ion, ii) the negative ion must have a m/z value greater than 180 or so, and iii) the ion must give daughter ions of the characteristic m/z values. The difference in these criteria from those in effect for conventional daughter ion MS/MS is that the parent ion must have a defined m/z value in conventional MS/MS. The presence of a parent ion of a specified m/z that produces a specified daughter ion upon MS/MS analysis allows the specific explosive to be unambiguously identified. In the targeted daughter mode, the fact that an explosive is probably present is indicated by the presence of a targeted daughter ion but the specific explosive is not identified (although the compound class may be). This information may still be inferable, however, without recourse to conventional MS/MS since the parent ions are also present in the TOF spectrum. The presence of both a characteristic daughter ion and parent ion increases specificity over the presence of a daughter ion alone. The targeted daughter ion mode of operation as performed on the QTOF had not yet been implemented and characterized. None of the testing was there- fore performed with this mode of operation. However, most of the testing in this report was performed with the quadrupole in a low resolving mode in combination with TOF. This mode is intermediate between conventional MS/MS and the targeted daughter mode using the quadrupole in the rf-only mode. The results of these tests were very promising and have encouraged the development of the targeted daughter ion mode. Even if the

specificity of this approach proves to be unacceptably low, it might be useful as a high sensitivity rapid screening procedure to indicate if conventional MS/MS is necessary.

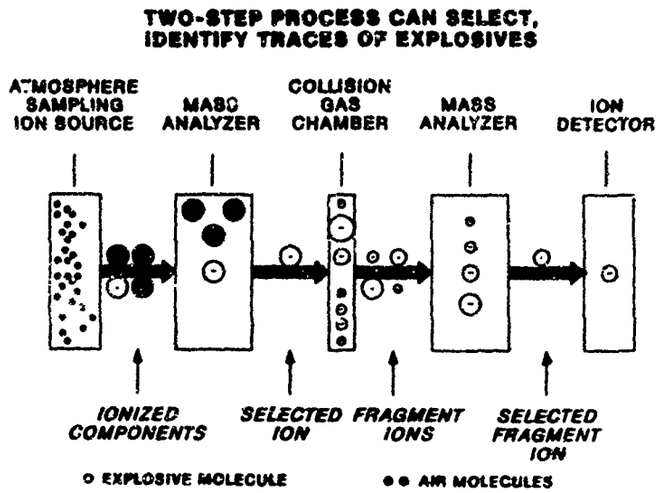


**Figure 1.**

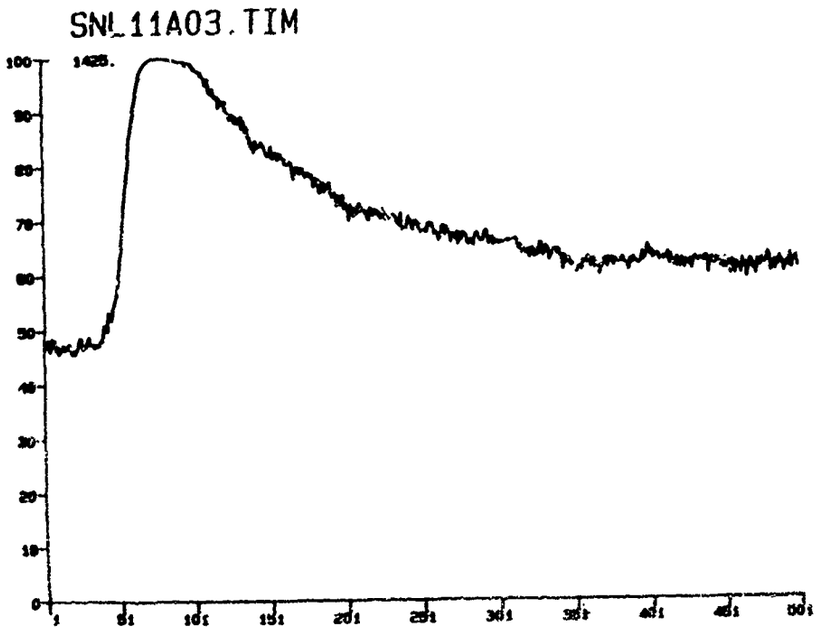


**Figure 2.**

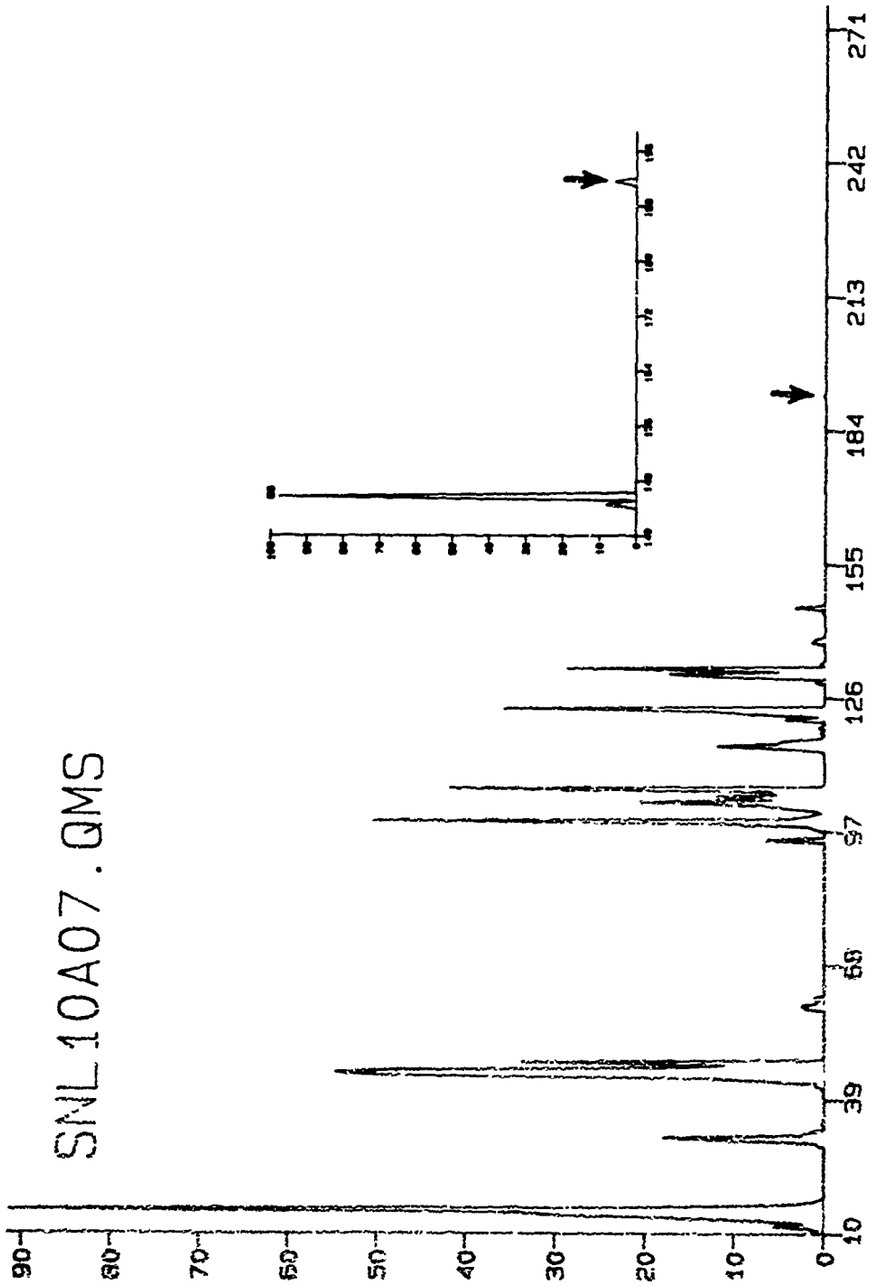
SNL10A07.QMS
90
80
70
60
50
40
30
20
10
0
10
39
68
97
126
155
184
213
242
271

**Figure 3.**

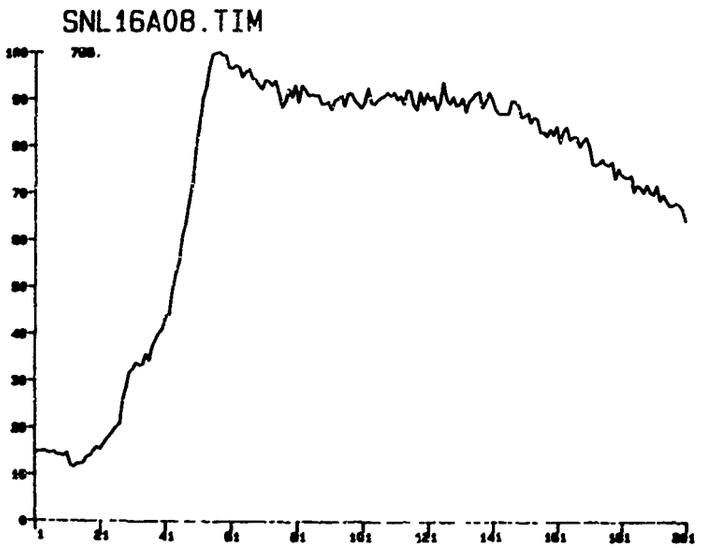


**Figure 4.**

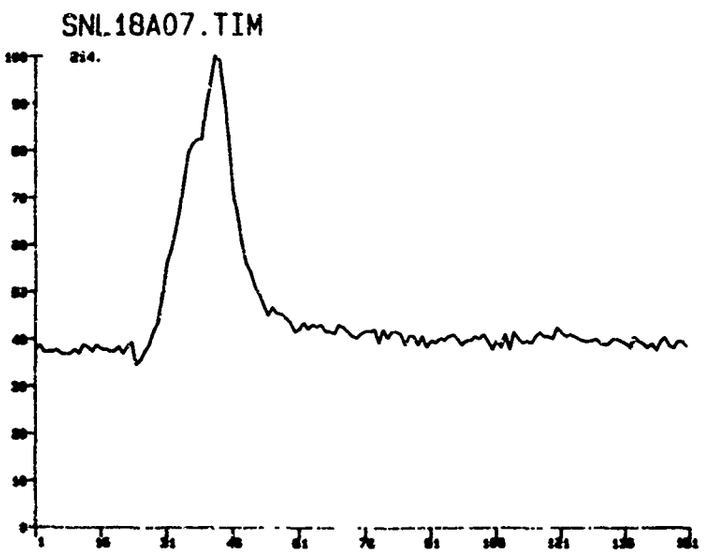


**Figure 5.**

# NUCLEAR BASED EXPLOSIVE TECHNIQUE - 1989 STATUS

Tsahi Gozani
Science Applications International Corporation
2950 Patrick Henry Drive
Santa Clara, CA 95054, U.S.A.

C. C. Seher
Department of Transportation
Federal Aviation Adminstration Technical Center
Atlantic City, NJ 08405, U.S.A.

Richard E. Morgado
Los Alamos National Laboratory
Los Alamos, NM 87545, U.S.A.

## ABSTRACT

Very significant progress in the detection of bulk explosives has been achieved since the last meeting in 1986. The thermal neutron activation (TNA) technique has been conclusively shown in extensive airport tests under Federal Aviation Administration (FAA) supervision, to be very reliable and a highly sensitive method for detection of all commercial and military explosives in luggage and cargo, regardless of shape and method of concealment. Several TNA based explosive e detection systems (EDS) are currently under construction and will be installed at selected U.S. airports starting in the early summer of 1989. The results of the comprehensive airport testing of the TNA systems during the period of 1987-88 are summarized. The success of the TNA technique, which is virtually the only method to detect concealed explosives, does encourage research in other nuclear based detection techniques which are complementary to TNA. These are fast neutron activation (FNA), the associated particle, nuclear resonance absorption and photoneutron activation techniques. The principles and highlights of the research and development of these techniques will also be reported.

## 1. INTRODUCTION

Three years ago we presented the rationale for the detection of bulk explosives based on nuclear techniques that addressed the requirements of civil aviation security in the airport environment [1]. Since then efforts have intensified, culminating in the successful airport demonstrations of two

prototype thermal neutron analysis (TNA) systems. The Pan Am 103 disaster in late December 1988 has accelerated the design of the first production models of the TNA based explosive detection system (EDS). The first of these is currently being readied for routine operation at the TWA international terminal at John F. Kennedy Airport (JFK) in New York. Five additional systems will be installed between August 1989 and January 1990 in various international airports in the U.S.A. and Europe.

The TNA based EDS's have proven to be very successful in meeting the civil aviation security requirements, and large scale production of these systems is anticipated. While TNA systems are being implemented, R&D is continuing to improve this type of system. Other nuclear techniques are also being investigated in the lab in order to assess their potential to provide further enhancements in EDS performance, e.g., faster response time, lower false positive rate, smaller size, lower cost, etc.

We will briefly review the status of the on-going activities in the arena of nuclear based EDS's. To provide a more complete perspective, we will commence with a brief review of the non-nuclear EDS techniques or procedures that are being employed.

## 2. BRIEF REVIEW OF NON-NUCLEAR DETECTION METHODS FOR EXPLOSIVES

Methods employed for detecting the presence of explosives include manual search as well as a variety of methods based on technologies that observe and measure one or more specific properties common to explosives.

### 2.1 Manual Search

This approach, although limited in practical use, has achieved impressive results especially when combined with profiling (e.g., as used by El Al). An attractive feature of this approach is that it has a strong deterrent effect on would-be perpetrators. However, it suffers from several deficiencies. In particular, its efficacy is highly dependent on the operator's skill and experience. Some of the new plastic explosives can be molded into extremely thin layers ("sheet explosives") and camouflaged so as to confound even experienced searchers. The method is also labor intensive, tedious, and time consuming, seriously inconveniencing passengers. Full scale implementation of this method in a busy airport such as JFK, Heathrow, or the like, is practically impossible.

### 2.2 Vapor Detection

Several detection methods focus on sensing the minute amounts of vapor emitted by explosives ("sniffers"). Some of these techniques are more sensitive

to specific classes of explosives than others. However, substantial improvements in the overall detection sensitivity and the processing times of these instruments are necessary to make them acceptable in an on-line screening mode. In fact, military explosives are characterized by extremely low vapor pressures. As a consequence, unless a contaminate or by-product of the manufacturing process is detectable, the amounts of vapors emitted by these explosives are several orders of magnitude below the sensitivity thresholds of present day equipment rendering them undetectable by these methods. In addition, many vapor sensing techniques can optimize their sensitivity for specific explosive compounds while sacrificing sensitivity to the rest of the spectrum of explosive threats, thus giving a false sense of overall performance. Common knowledge to the terrorist community is the fact that explosive "sniffers" are easily thwarted by wrapping the explosive itself in plastic. Dogs are also used for explosive vapor detection, primarily on an emergency basis, but their use is limited by the relatively short attention span that they are able to maintain. Little information is available on independent double blend tests to indicate the true performance of dogs even on a limited use basis. These techniques, however, are probably the only practical ones for scanning humans and/or animals.

## 2.3 X-Ray Densitometry

X-rays have become the accepted procedure for inspection of carry-on luggage for the presence of weapons. Matter absorbs part of any X-ray beam that passes through it. The degree of absorption of an object is determined by the atomic number and the density times the overall thickness of these objects, which is why metals absorb more than for example, cloth. When an object is placed between an X-ray source and an array of detectors a 2-dimensional projection or a silhouette of the object is obtained. An enhancement of this technique is the "dual energy radiography" approach, where a second, lower energy scan of the object, provides crude information on the atomic numbers of the composite elements of the object. With such a device two 2-dimensional images of the object are obtained, one portraying the low atomic number (Z) components (e.g., those having hydrogen, carbon, nitrogen and oxygen), and the other showing the higher atomic numbers (metallic) components. Dual energy radiography reduces the clutter in the image, by separating the metallic objects from the low Z objects. However, it cannot distinguish between many benign low Z objects and explosives, since they have similar compositions and appearances. X-ray computed tomography (CAT scanning) goes one step beyond conventional radiography by generating a 3-dimensional density image of the object by performing many scans.

In general, X-ray images cannot differentiate between different materials of similar overall densities. These methods are very time consuming and extremely dependent on the operator's skill and experience. They require a human to inspect each parcel. Such systems can be very useful as complementary to other methods (described below), by helping to resolve the few cases that are not automatically cleared of suspicion by the TNA based EDS.

## 3. FUNDAMENTALS OF NUCLEAR-BASED EDS

The shortcomings of the previous common techniques form the main reason for the development of nuclear-based techniques. Nuclear-based detection techniques probe the screened items with penetrating radiation, notably neutrons and photons. An array of detectors positioned near the screened item senses the high-energy gamma-ray reaction products induced by the probe (see Figure 1). The intensity, energy, and spatial distribution of the detected radiation; their relationship to the probing radiation; and any additional information concerning the object are used to determine the presence or absence of an explosive.

Nuclear interrogation involves detecting reaction products from target elements (or isotopes) that are reliably and sufficiently present in all explosives. The discriminating features of explosives are summarized in Table 1 according to their specificity and sensitivity as a basis for detection. The universal occurrence of these same elements in nonexplosives, however, limits the attainable level of detection sensitivity, and, invariably, increases the probability of false positives.

The operational criteria limit the choice of techniques to those probing reactions that can meet the criteria in a practical way. These criteria include availability, cost, size, and shielding requirements. The dose rate imparted to the object and the induced radioactivity in the contents of luggage and the potential exposure to the public are also very important considerations in selecting appropriate probes.

Table 2 lists the available nuclear reactions. Brief comments given in the table are based either on actual experimental results or other assessments. These comments focus attention on the potential and limitations of the various techniques. The table clearly underlines why TNA is the most successful nuclear-based technique: nitrogen has a unique, very high energy gamma-ray (10.8 MeV), it is relatively easy to obtain high enough thermal neutron fluxes, and this flux does not create any significant radiation exposure to the public.

## 4. STATUS OF THERMAL NEUTRON ANALYSIS (TNA) TECHNIQUE

The TNA technique is based on detecting primarily nitrogen and some secondary elements. High density nitrogen is a rather specific signature, but by no means the only one, of all commercial and military explosives. Upon capturing thermal neutrons nitrogen nuclei emit 10.8 MeV gamma-rays, which are practically the highest possible in such reactions. Thus, the intensity and spatial distribution of this high energy gamma-ray provide a strong indication of the presence of explosive. The spatial distribution of the 10.8 MeV (i.e., of nitrogen) is provided by a complex image reconstruction afforded by the efficient detector arrays employed in the current TNA-EDS built by SAIC. The TNA technique is somewhat sensitive to backgrounds from other interfering elements and from benign materials that contain some of the same elements as explosives. The demonstrated ability of TNA-EDS to distinguish between explosive and other benign materials in many difficult conditions is a testimony to the advanced stage of the TNA technique, and it sets the standard for comparison with other techniques.

In the SAIC TNA-EDS, the neutron source is either the radioisotope $^{252}Cf$ or an electronic neutron generator with a neutron intensity of less than $10^9$ n/s. Fast neutrons from the source are slowed down by moderating materials that make up the walls of the interrogating cavity and around the source to create a cloud of low-energy neutrons. The overall size of the system is determined by the requirements for sufficient moderating material to produce a high neutron flux in the interrogating cavity, plus additional shielding to reduce radiation exposure to personnel (see Figure 2). The neutrons diffuse into the screened object to produce characteristic gamma-rays that are promptly emitted following neutron capture. The SAIC detector array consists of tens of inorganic scintillators with the neutron source at the center.

Figure 3 depicts the typical gamma-ray spectra obtained from a luggage sample with a threat amount of explosive simulant. These spectra are characterized by a large background of low- and intermediate-energy gamma-rays arising from suitcase contents and from cavity construction materials. The construction materials were carefully selected to minimize backgrounds, and corrections for the remaining backgrounds are applied to each detector. Additional corrections are applied to the high-energy gamma-rays from chromium, chlorine, and nickel that interfere directly with the gamma-rays from nitrogen.

High-speed analog-signal-processing electronics were developed to measure precisely the energy of each gamma-ray at the data rates necessary to

meet the system throughput requirement. The detected gamma-ray signals are converted into pulses suitable for computer processing. If a predetermined set of conditions is fulfilled (one among them a localized region of high gamma-ray rate from nitrogen), the system's alarms indicate the possible presence of an explosive threat.

Extensive laboratory optimization measurements were followed by an intensive period of airport testing (June 1987 - March 1988), which included measurements with both the radioisotopic and electronic neutron sources. Tests to detect simulated bulk and sheet explosive at the operationally required throughput rate were performed at the San Francisco and Los Angeles International Airports in California on both domestic and international baggage sets. The results of the tests [3] are summarized in Table 3.

The range of PD and PFA values results from variations in performance due to the contents of the luggage items as a function of the destination and the season of the year. The trade-off in PD versus PFA to match a particular situation is programmed into the system decision-making process.

The success of the two prototype TNA-EDS has lead to a design of a more compact Cf-based EDS (see Figure 2). This system measures 4 m long, 2.4 m at the widest point, and 1.8 m high. It is a straight-through system, where the luggage is conveyed on a straight belt through it. The system can screen 600 bags per hour. The system decision is done fully automatically. However, when a suspect bag is identified, a list of reasons for that decision is presented to the operator with possible suggestions for further investigation in order to clear or confirm the suspicion.

Six Cf-based compact EDS systems are being manufactured by SAIC for the FAA. The first of these is currently being implemented at TWA International terminal at JFK in New York.

## 5.0 X-RAY ENHANCED NEUTRON INTERROGATION SYSTEM (XENIS)

The XENIS system is an optional addition to the basic TNA-EDS. XENIS identifies and displays the specific object causing an alarm. The system was developed in conjunction with EDS and was subject to the same rigorous airport testing program.

XENIS allows alarm bags from the EDS to be "double checked" without exposing personnel to the hazards of physical inspection. The number of false positive from the EDS can be reduced by much as 50% when the power of the special x-ray system is coupled to the basic EDS.

The XENIS system is composed of a dual-view x-ray machine, an image processor, an optical disk drive and a computer. XENIS combines the lower spatial resolution image of the TNA with the higher resolution density image of the x-ray machine. Once this information is collected, sophisticated image processing techniques are used to combine and analyze the resultant correlated image. This image is passed on to the XENIS decision algorithm where a suspect/no suspect decision is made by the computer. The specific object which caused the alarm is automatically identified and highlighted on the display screen.

## 6. FAST NEUTRON ACTIVATION EXPLOSIVE DETECTION SYSTEM (FNA-BASED EDS)

To extend the advantages and overcome some limitations of the TNA approach, SAIC is investigating a new technique that relies on the inelastic reactions of fast neutrons (FNA) on carbon, nitrogen, and oxygen. A continuous flux of fast neutrons (14 MeV) is produced in the reaction resulting when a beam accelerated deuterons (at 150 keV) impinges onto a tritium (T) target, liberating alpha particles ($^4$He) and neutrons. Subsequent neutron collisions produce characteristic gamma-rays from inelastic reactions with the main constituents of explosives. Thus, most of the characteristic components of explosives can, in principle, be detected and imaged. The overall improvement in PD and PFA can be estimated once the system's signal-to-background ratios are determined for each element.

The main difference between the TNA and the FNA-induced gamma spectra is illuminated in Figure 4. The main signals in FNA, coming from oxygen (6.13 MeV) and carbon (4.44 MeV) are of significantly lower energy than the 10.8 MeV resulting from TNA of nitrogen thus lowering the signal to background ratio. However, the interaction of fast neutrons in the detector crystal generate continuum of gamma-rays extending to very high energies. This feature of the spectrum aggravated by pulse pile-up considerably complicated the development of FNA as a practical tool. By judicial use of composite shieldings, combinations of detector arrays and fast electronics, FAA technique has come closer to proof of practicality.

## 7. THE ASSOCIATED PARTICLE TECHNIQUE

The associated particle technique [1][2] further extends the idea of FNA to produce three-dimensional images of gamma-rays produced by fast neutron inelastic interactions.

The technique exploits the temporal and spatial correlation between the 14-MeV neutron and its associated alpha particle ($^4$He) produced in the d-T

fusion reaction described in the previous section. At low deuteron energies the alpha particle and neutron are produced back-to-back. Thus, by localizing the alpha particle, the direction of the neutron is determined. The neutron's subsequent interaction point is determined by measuring the total time between the detection of the alpha particle and the detection of the gamma-ray produced in the neutron interaction.

As an example, measurements conducted at the Advanced Nuclear Technology Group at Los Alamos National Laboratory demonstrated the ability to obtain spatial depth.

The time distribution of three 2.5 cm thick objects made of aluminum, carbon, and iron, respectively, positioned 10 cm apart along the neutron path, is illustrated in Figure 5. The fourth, broadened object in the timing spectrum results form elastically scattered neutrons that interact directly in the gamma-ray detector. The choice of location of the gamma-ray detector and the shielding surrounding it are important parameters that can be tailored to the geometry of the problem. The inelastic gamma-rays produced by 14.7 MeV neutrons provide unique signatures for most low- and intermediate-Z elements of interest to explosive detection. In particular, carbon, nitrogen, and oxygen can be readily identified either individually, as depicted in Figure 6a, 6b, and 6c, or in a compound simulating high explosives, as shown in Figure 6d.

The Los Alamos group is assembling a computer system based on the VME-bus to provide real-time parallel processing for data acquisition and analysis. The system will have the capability to acquire data for all combinations of multiple alpha particle detectors and gamma-rays detectors. Data will be stored in two-dimensional matrices for each detector combination and will incorporate the ability to sum gamma-ray spectra corresponding to each alpha detector pixel. By storing data in this way, it will be possible to project gamma-ray energy data in real time for any time slice, resulting in real-time three dimensional imaging. Parallel processing is planed with one CPU sorting data, while another processor is matching detector gains, summing gamma-ray spectra, and generating projections from pre-selected energy or time windows for individual or groups of elements.

In summary, the main advantage of the technique is the capability of providing one-sided, three-dimensional imaging of the main elemental constituents of explosives. Its ultimate usefulness is primarily limited by low sensitivity, resulting in interrogation times measured in several minutes rather than a few seconds, required for practical airport applications.

## 8. HIGH-ENERGY PHOTON PROBES - PHOTOACTIVATION REACTIONS

Photoactivation reactions involve the production of relatively short-lived radioisotopic beta emitters predominantly via the (gamma, n), (gamma, p), and (gamma, 2n) reactions. The reaction threshold for the elements of interest to explosive detection require a very intense beam of high-energy photons (mostly 10 MeV and above) in the form of bremsstrahlung produced by electron accelerators. The detection signal is derived from either the 511 keV gamma-rays from the annihilation of the low-energy positron or from bremsstrahlung emitted by high-energy electrons. In either case, timing can be used to improve the signal to background. For very short lived emitters (a few milliseconds), sensing begins promptly after the photon pulse; for longer-lived emitters (seconds to minutes), interrogation is delayed until other shorter-lived backgrounds have died away. Coincident detection of the back-to-back 511 keV gamma-rays from positron annihilation is inherently imaging in three dimensions, but has extremely low efficiencies. The detection sensitivity ultimately depends on the photoactivation cross section (a few millibarns) and the half-life of the isotope, while selectivity will also depend on the half-life and the threshold energy of the production reaction relative to thresholds for competing backgrounds. Technique numbers 3, 9, 11, 22, and especially 13 (see Table 2) fall into this category. Unfortunately, all these techniques are wholly inappropriate for luggage inspection. The foremost reason is the extremely high dose rate they impart to the screened luggage, going far beyond damaging all photographic and some magnetic media. The unavoidable accompanying neutron background, induced activities, and complexity render this avenue of development unwarranted.

## 9. CONCLUSION

We have briefly reviewed the current status of nuclear-based EDS. The research development, production, and field implementation since the last report in 1986 demonstrated the viability of the nuclear techniques in general and TNA in particular. While TNA has become a practical reality, providing the only technology aids to effectively combat civilian aircraft sabotage, limitations and potential of other techniques have been sharply recognized allowing to focus effort on the most promising techniques for possible next generation systems.

## REFERENCES

1. T. Gozani, R. E. Morgado, C. Seher
Nuclear Based Techniques for Explosive Detection, J. of Energetic Materials, Vol. 4, 377-414, 1986.

2. R. E. Morgado, T. Gozani, C. Seher
The Detection of Bulk Explosives Using Nuclear Based Techniques, Inter. Congress of Applied Criminology, Gent, Belgium, 8/29-9/2/88.

3. P. Shea, T. Gozani
Airport Tests of SAIC/FAA Explosive Detection System Based on Thermal Neutron Activation Technique, American Defense Preparedness Assoc. Meeting, Cambridge, MA, 10/26/88.

| Characteristic Feature | Specificity |
|---|---|
| Nitrogen density | High |
| Oxygen density | High |
| Carbon density | Moderate |
| Hydrogen density | Moderate |
| N:H, N:C, C:O, and C:O+N ratios | Very high |
| Trace metals | Moderate-high |
| Total density | Moderate |
| Physical shape | Low |

Table 1: Generic Discriminating features of explosives

| No. | Isotope | Probe Energy* | Reaction | Comments |
|---|---|---|---|---|
| 1 | $^{1}H$ | $n_{th}$ | $^{1}H(n_{th},\gamma)^{2}H^{*}$ | Low specificity |
| 2 | $^{1}H$ (and $^{10}B$) | n (slowing down spect.) | thermalization absorption | Low specificity |
| 3 | $^{2}H$ | $\gamma$(>2.2 MeV) | $^{2}H(\gamma,n)^{1}H$ | Low specificity, very low sensitivity |
| 4 | $^{2}H$ | n(14 MeV) | $^{2}H(n,2n)^{1}H$ | Low specificity, very low sensitivity |
| 5 | $^{12}C$ | $n_{th}$ | $^{12}C(n_{th},\gamma)^{13}C$ | medium specificity, low sensitivity |
| 6 | $^{12}C$ | n(14 MeV) | $^{12}C(n,n'\gamma)^{12}C^{*}$ | medium specificity, low sensitivity |
| 7 | $^{12}C$ | n(14 MeV) | $^{12}C(n,p)^{12}B^{*}$ | medium specificity, low sensitivity |
| 8 | $^{12}C$ | n(14 MeV) | $^{12}C(n,\alpha)^{9}Be^{*}$ | medium specificity, low sensitivity, high background |
| 9 | $^{12}C$ | $\gamma$(>19 MeV) | $^{12}C^{x}(\gamma,N)^{11}C$ | medium specificity, low sensitivity, unacceptable very high dose rate, complex |
| 10 | $^{13}C$ | $n_{th}$ | $^{13}C(n_{th},\gamma)^{13}C$ | medium specificity, very low sensitivity |
| 11 | $^{13}C$ | $\gamma$(>5 MeV) | $^{13}C(\gamma,n)^{12}C$ | medium specificity, very low sensitivity, probably unacceptable high dose rate |
| 12 | $^{14}N$ | $n_{th}$ | $^{14}N(n_{th},\gamma)^{15}N^{*}$ | specific, most practical basis for TNA to date |

Table 2: Assessment of accessible nuclear reactions for neutrons or high-energy photon interrogation

| No. | Isotope | Probe Energy* | Reaction | Comments |
|---|---|---|---|---|
| 13 | $^{14}N$ | $\gamma$(>11 MeV) | $^{14}N(\gamma,n)^{13}N$ | specific, low sensitivity, very high dose rate, high induced activity, neut. background, complex unacceptable |
| | | $\gamma$(>30 MeV) | $^{14}N(\gamma,2n)^{12}N$ | specific, low sensitivity, very high dose rate, high induced activity, high neut. background, complex unacceptable |
| 14 | $^{14}N$ | n(14 MeV) | $^{14}N(n,n'\gamma)^{14}N^*$ | specific, high background |
| 15 | $^{14}N$ | n(14 MeV) | $^{14}N(n,\alpha\gamma)^{11}B^*$ | specific, high background |
| 16 | $^{14}N$ | n(14 MeV) | $^{14}N(n,p\gamma)^{14}C^*$ | specific, high background |
| 17 | $^{14}N$ | n(14 MeV) | $^{14}N(n,d\gamma)^{13}C^*$ | specific, high background |
| 18 | $^{14}N$ | n(14 MeV) | $^{14}N(n,2n)^{13}N$ | specific, high background low sensitivity |
| 19 | $^{16}O$ | n(14 MeV) | $^{16}O(n,n'\gamma)^{16}O^*$ | specific |
| 20 | $^{16}O$ | n(14 MeV) | $^{16}O(n,p)^{16}N^*$ | specific, low sensitivity |
| 21 | $^{16}O$ | n(14 MeV) | $^{16}O(n,\alpha)^{13}C^*$ | specific, low E signatures |
| 22 | $^{16}O$ | $\gamma$(>16 MeV) | $^{16}O(\gamma,n)^{15}O$ | specific, low sensitivity, very high dose rate, high neut. background, complex, unacceptable |

Table 2: Assessment of accessible nuclear reactions for neutrons or high-energy photon interrogation (continued)

| Item | Probability of Detection (%) | Probability of False Alarm (%) |
|---|---|---|
| Luggage | 90-96 | 3-8 |
| Cargo | 90-95 | 1-4 |

Table 3: Airport test results for the TNA Explosive Detection System for more than 30,000 screened items

## Schematic Of Nuclear Based EDS

How Hidden Objects Are Detected In Luggage

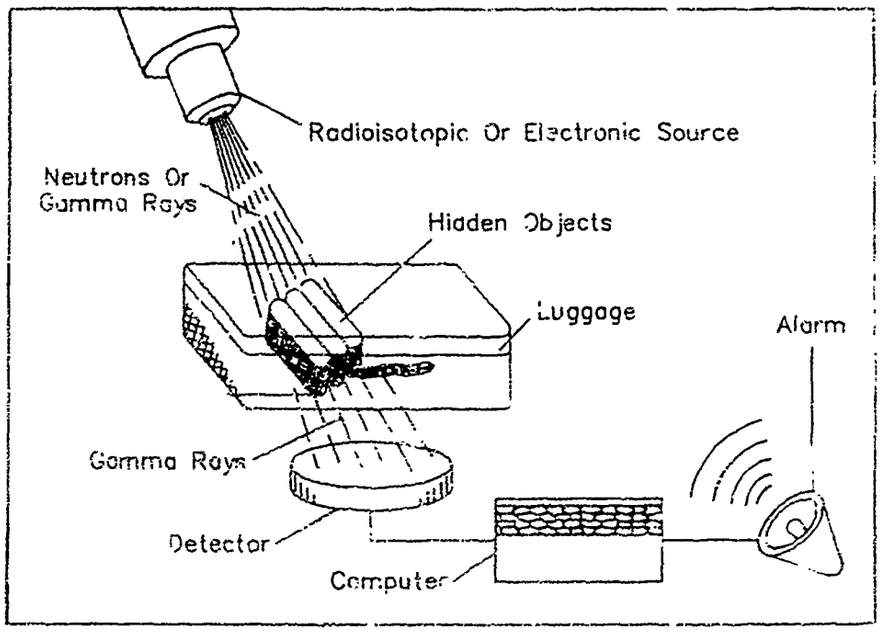


Figure 1

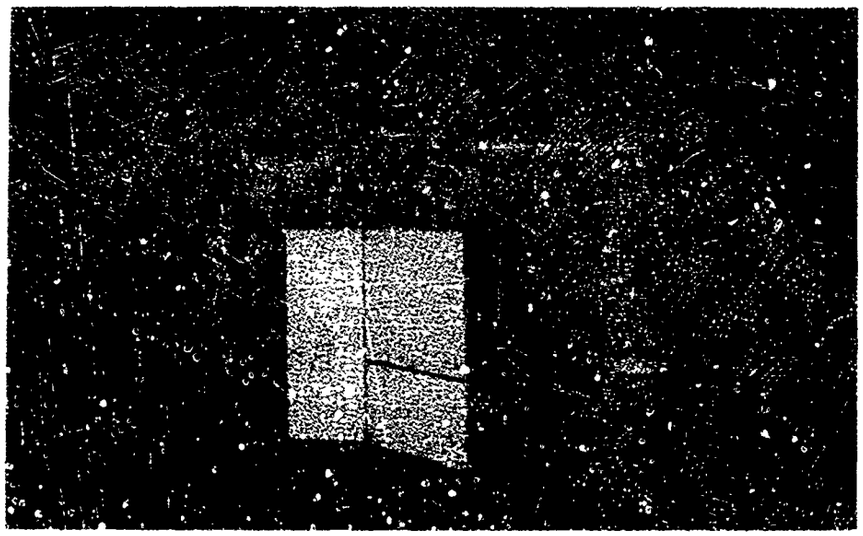

TNA - EDS (production model)

FIGURE 2: SAIC explosive-detection system.

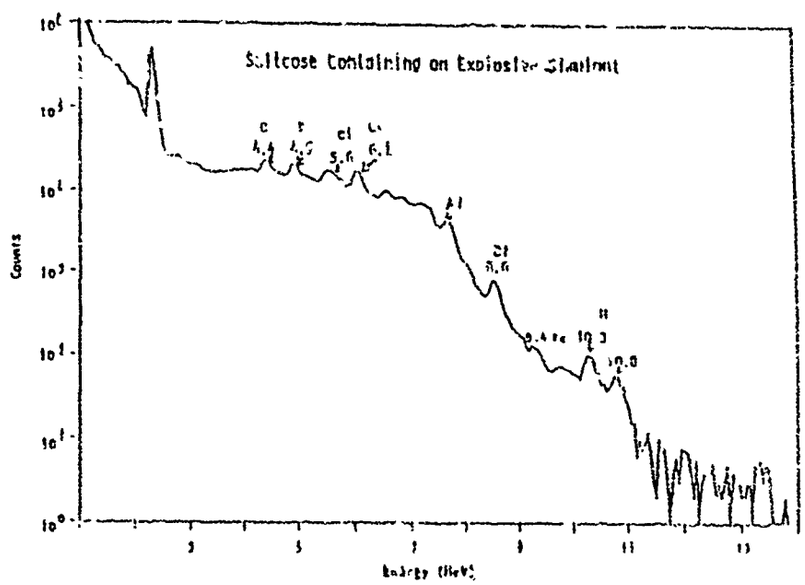


FIGURE 3: Pulse height distribution of suitcases containing explosive.

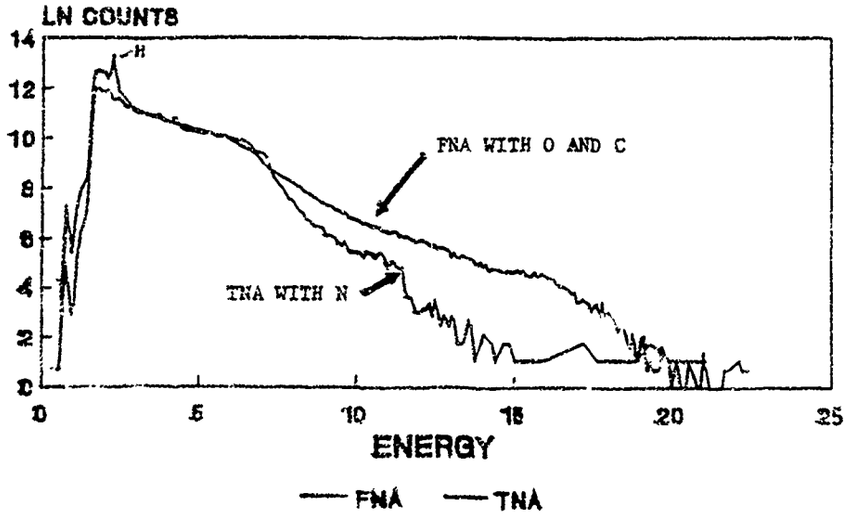


FIGURE 4: Comparison of pulsed height distribution (in sodium iodide detector) between TNA and FNA.

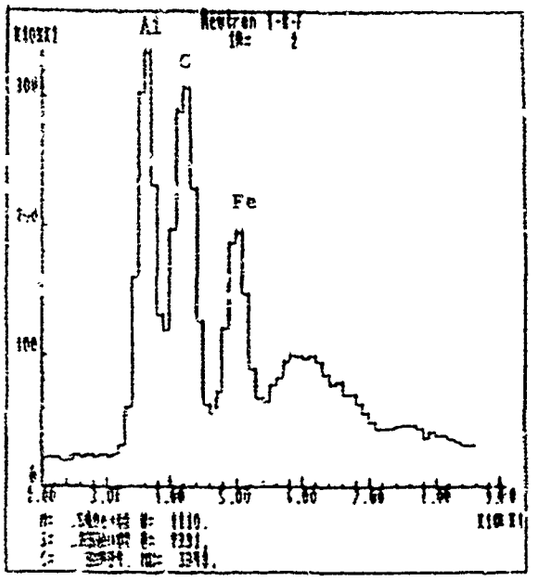


PROJECTION ON TO TIME OF FLIGHT AXIS

FIGURE 5: Time-of-flight spectrum for aluminum, carbon, iron objects.

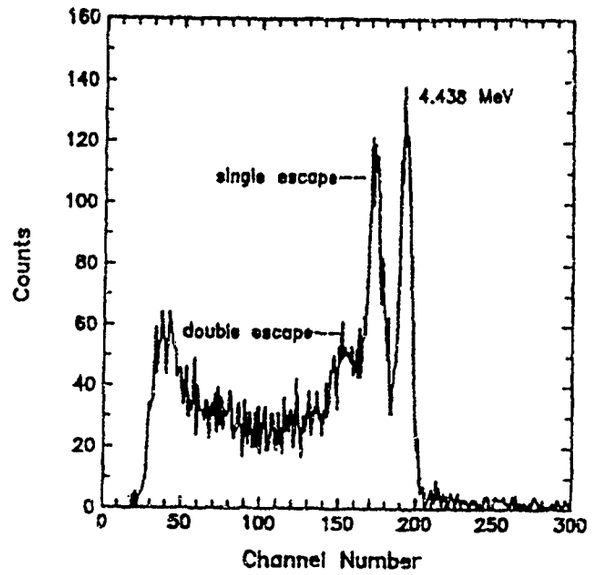


FIGURE 6a: Time-gated energy spectrum for a 7.6 by 7.6 cm $BaF_2$ detector using a 10.2 cm thick carbon target.

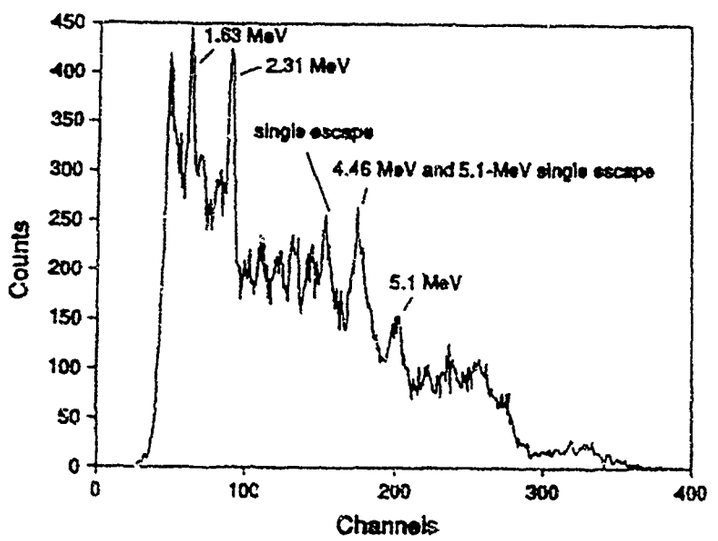


FIGURE 6b: Time-gated energy spectrum for liquid nitrogen.

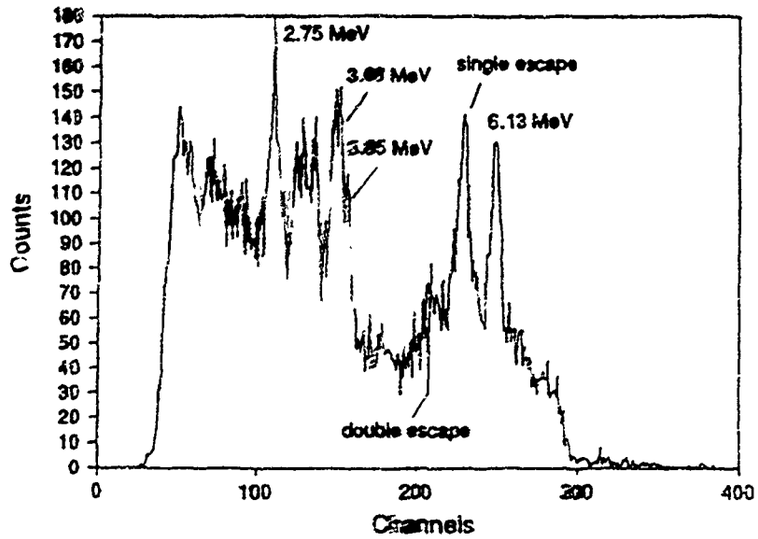


FIGURE 6c: Time-gated spectrum for oxygen.

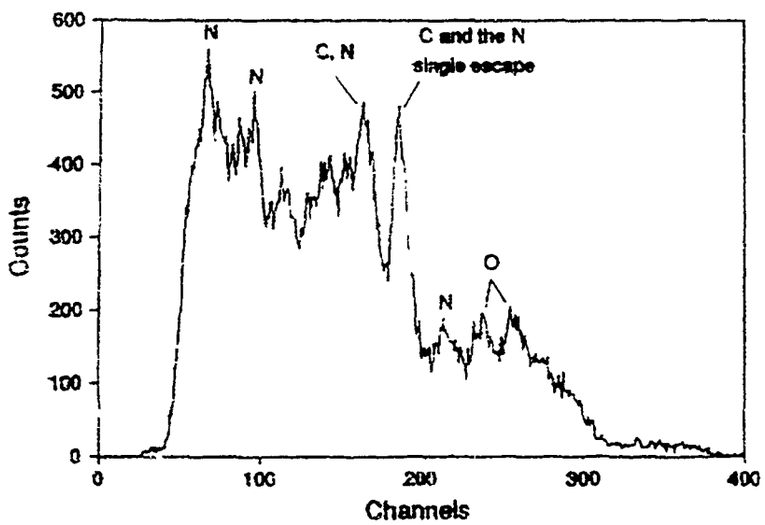


FIGURE 6d: Time-gated spectrum for simulated explosive.

# APPLICATION OF A DESORPTION-CONCENTRATION DEVICE (D.C.I. PLATINE) TO EXPLOSIVES DETECTION

*J.C. SARTHOU*
*Commissariat à l'Energie Atomique*
*Centre d'Etudes du RIPAULT - B.P. N° 16 37260 MONTS - FRANCE -*

## ABSTRACT

The D.C.I. "platine" presented in this article is used as a sampling interface in the design of an explosives vapours detector. Consistent with every kind of gas chromatograph, this device operates as well transference as enrichment by reconcentration of trapped vapours. Results achievements with PETN, TNT and RDX allow to estimate such an interface efficiency. For TNT, amounts in the nanogram range have been detected with FID. In a parallel way, mass spectrometry tests of sensitivity show a possible improvement of sensitivity level.

## INTRODUCTION :

We are presently setting up an explosives vapours detection system which final shape will be as follows :

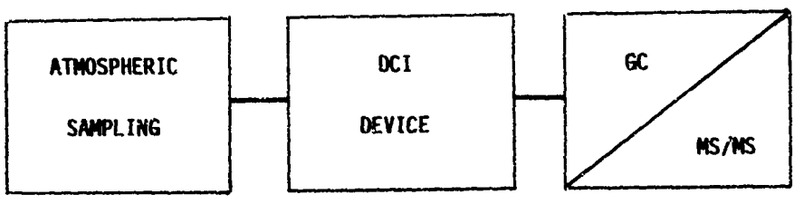


As indicated on the diagram, the final shape of the system will be profiting by new generation mass spectrometers (ITD and TSQ) which sensitivity is now consistent with usual explosives vapours pressures. [1.2.3.] However, high detection sensitivity access is conditionned on adequate resolving of the collecting and transfering duplicate problem. Therefore, it was significant that this stage should be profited by the most efficient fitting ; for this reason, D.C.I. "platine" - DELSI INSTRUMENTS. FRANCE - was selected. [4] The presented experimentation shows how and why this device an interesting solution for the problem is . The D.C.I. "platine" principle is as follows :

1 - Explosive vapours desorption with gas flow.
2 - Cold trapping of these vapours on adsorbent.
3 - Injection of trapped compounds into analyser.

The results registered with TNT, RDX and PETN, show satisfying efficiency mainly resulting from following factors :

- the lack of any chemical operation on the sample,
- the strong equilibrium displacement towards total desorption,
- the efficiency of injection.

Moreover, cold trapping used during reconcentration step allows measuring precision and reproducibility to be increased. With intent of early quantifying the DCI "platine" response, we directly operated with disolved explosives ; however it is important to remember that, in real detection operation, the oven will receive an atmospheric sampling catridge.

We successively present in this article :

1 - System description and operating.
2 - Experimental conditions and results.
3 - Results discussion.

## 1°) - DCI "PLATINE" : DESCRIPTION AND OPERATING

As indicated on figures n°1 and n°2, the DCI "platine" is connected in parallel derivation of a gas chromatograph carrier gas. On figure n°1, the system is in desorption-concentration step, on figure n°2, in introduction step. The operating of the device is as follows :

### DESORPTION :

A known weight of disolved explosive is set in the oven container. At 160° C, and under reduced pressure, gas flow (He in present case) displaces equilibrium towards total desorption of targetted compounds.

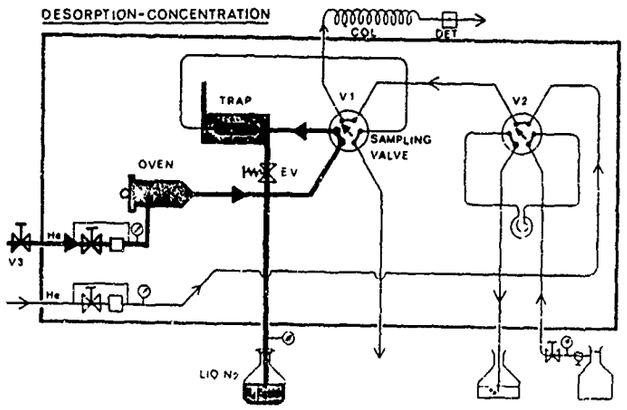


**FIGURE 1 : DCI : DESORPTION - CONCENTRATION STEP**

**CONCENTRATION :**

The volatiles diluted in carrier gas by thermal desorption are carried out onto the concentrator filled with Tenax. The volatiles adsorption reconcentrating is "optimized" by a cold trapping at - 40°C. These concentration two variables are desorption temperature and duration. Their respective optimal values are a function of targetted compounds volatility ; for explosives case, we have defined a compromise to avoid too high decomposition of the product.

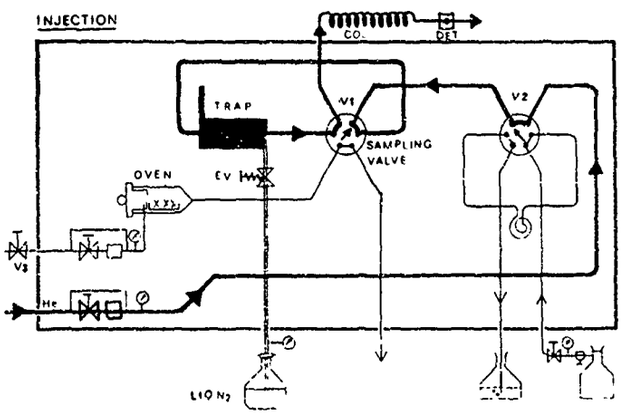


**FIGURE 2 : DCI : INJECTION STEP**

**INJECTION :**

After changing the connection of the line into position 2, the injection is instigated by an ultrafast heating rate at 2 500°C./min. that induces instantaneous desorption and injection. Excepted caution against oven contamination, there is no difficulty to operate the DCI "platine" ; from what good reproducibility is obtained as shown in further on results.

**EXPERIMENTAL AND RESULTS**

**Experimental**

Performed trials have permitted the setting of following experimental conditions :

**DCI**

| | | |
|---|---|---|
| Desorption temperature | : | 160° C |
| Desorption time | : | 10 min. |
| Desorption pressure | : | 0,3 bar |
| Trap temperature | : | - 40° C |
| Injection temperature | : | 200° C |
| Line temperature | : | 160° C |

**GC**

| | |
|---|---|
| Model | : Girdel "Serie 30" |
| Column | : SE 52 - WCOT 0,25 mm - 25 m. length |
| Carrier gas pressure | : 1,4 bar |
| Detector | : FID |
| Detector temperature | : 180° C |

**Results**

We have carried out two series of experimentations, one qualitative, the other quantitative.

Qualitative trials intented to identify explosives by their retention times in satisfying analysis duration. For this purpose, the GC was operated with temperature programming from 140° C to 200° C at heating rate of 10° C/min. These trials have been performed on several explosives mixtures. Thereafter presented on figure n°3, the chromatogram obtained with a PETN,TNT and RDX mixture, in respective amounts of $5.0 \times 10^{-6}$ g., $2.1 \times 10^{-8}$ g. and $2.5 \times 10^{-6}$ g. . Corresponding retention time reproducibility has been believed sufficient (± 3 sec.) for allowing, if necessary, targetted explosives identification.

PROGRAMMED TEMPERATURE

FROM 140°C. TO 200°C. at 10°.min.

1 PETN $5.0 \times 10^{-6}$ g.

2 TNT $2.1 \times 10^{-8}$ g.

3 RDX $2.5 \times 10^{-6}$ g.

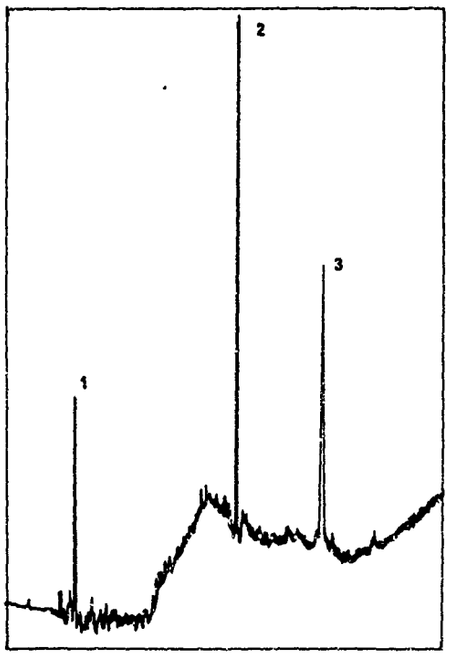


FIGURE 3 : TEMPERATURE PROGRAMMATION CHROMATOGRAM

Quantitative trials were more especially assigned for DCI "platine" efficiency measurements. In that case, we operated at fixed temperature like established with preliminary tests :

120° C for PETN
180° C for TNT + RDX mixture.

In both cases, we have got following retention times :

- 4 mn 45 s ± 2 sec. for PETN
- 7 mn 03 s ± 2 sec. for TNT
- 11 mn 03 s ± 2 sec. for RDX

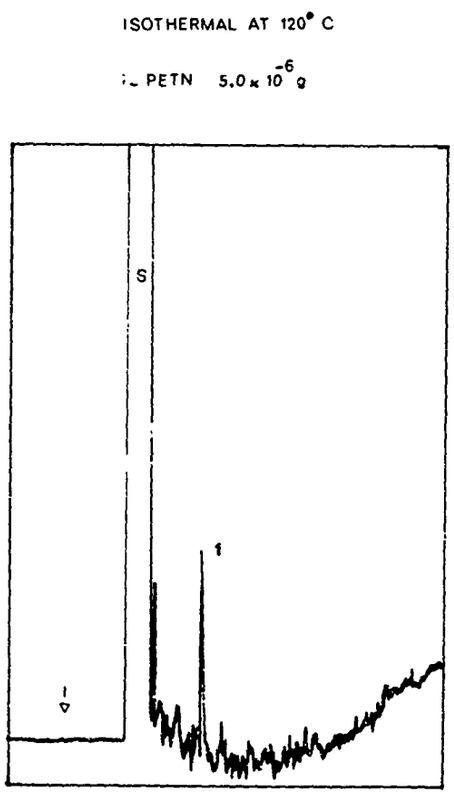


**FIG. 4** : PETN at 120° C (fixed temperature)

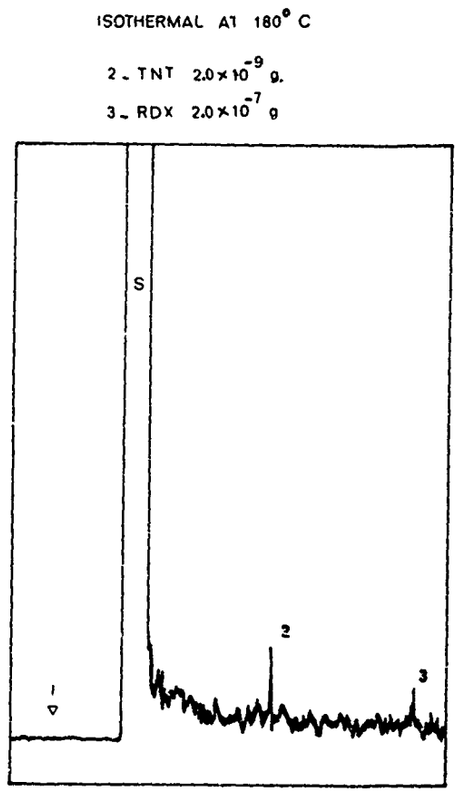


**FIG. 5** : TNT + RDX at 180° C (fixed temperature)

Figure n°4 represents a chromatogram carried out with $5.0 \times 10^{-6}$ g. of PETN, and figure n°5, those of $2.0 \times 10^{-9}$ g. of TNT and $2.0 \times 10^{-7}$ g. of RDX. These values are representing sensitivity limits of the system with described analytical conditions.

## DISCUSSION

Considering with experimental conditions, above results indicate a good capability of DCI "platine" on transferring and reconcentrating explosive vapours. As well as complementary trials, these results allow to suppose that better adjustment of experimental conditions should induce higher efficiency appreciation. For example, in consideration with analytical conditions, the detection of $2.0 \times 10^{-9}$ g. of TNT, indicates that DCI device is able, at least, to transfer such an explosive amount. Besides, we estimate that only modification of few parts of the system will permit to increase the response in several orders of magnitude.

### DCI :

It is possible that TENAX should not be the best explosive adsordent ; in this case, we suggest a different phase, like glasswool, for example.

### GC :

The use of a shorter column like DB5-15 meters of length, for example, must improve the sensitivity by thermal decomposition reducing.[5]

### DETECTOR

Especially here, sensitivity can get best improvement. This affirmation is based on two complementary experiments. The first, consisted in cutting off DCI, and directly injecting on the GC column, what has permitted to check that $2.0 \times 10^{-9}$ g. of TNT were not DCI transference limit, but did represent FID sensitivity limit. The second experiment, performed with mass spectrometry, allows to wait for a three orders of magnitude improvement, like shown on figure n°6 and figure n° 7 diagrams.

Figure n°6 represents the 210 ion fragmentogram of TNT carried out on GC/MS - ITD 700 - with $4 \times 10^{-10}$ g. injected ; signal/noise ratio being higher than 100.

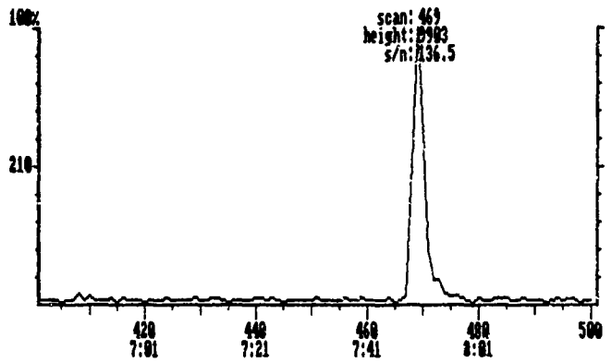


**FIGURE 6 : SELECTED ION 210 FRAGMENTOGRAM WITH 4.10 x $10^{-10}$ g. OF TNT - GC-MS (ITD 700)**

The figure n°7 represents total ion current carried out in GC/MS - TSQ 46 - with 2.0 x $10^{-11}$ g. of TNT ; signal/noise ratio being higher than 1 000. These both last cases still seem to stay far from sensitivity limits of spectrometers, what allows to expect an additional improvement.

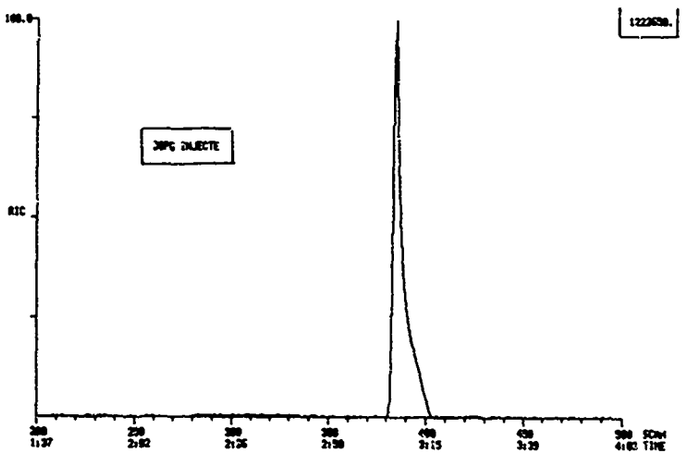

**FIGURE 7 : TOTAL ION CURRENT WITH 2.0 x $10^{-11}$ g. OF TNT GC.MS (TSQ 46)**

**CONCLUSION :**

In this article, our object was to demonstrate DCI "platine" consistence with an explosives vapours detection system. We could be measuring the transference factor to allow easy reaching of FID limits and that, for its part, mass spectrometry will permit to find a better factor. We are thinking we can say that, from its conception, performances and easy operating, DCI device promotes fast building of an operational transference interface, thanks to reconcentration and injection efficiency that facilitates access to the high sensitivity range of the most performant analysers.

## BIBLIOGRAPHY

1°) - **B.C. GRANT ; K.G. ASANO ; G.L. GLISH and S.A. MAC LUCKEY.**
*TRACE ANALYSIS FOR ORGANICS IN AIR USING ATMOSPHERIC SAMPLING GLOW DISCHARGE IONIZATION SOURCE.*
Proceedings of the 36th ASMS Conference on Mass Spectrometry and Allied Topics - 1988 - San Francisco - Cal. - USA.

2°) - **R.A. YOST.**
*THE ROLE OF TAMDEM MASS SPECTROMETRY IN RAPID DETECTION AT TRACE LEVELS.*
Scientific Conference on Chemical Defense Research - USA - Nov. 20-86

3°) - **G.A. EICEMAN ; J.H. KREMER ; A.P. SNYDER and J.K. TOFFERI**
*QUANTITATIVE ASSESSMENT OF A CORONA DISCHARGE ION SOURCE IN ATMOSPHERIC PRESSURE IONIZATION MASS SPECTROMETRY FOR AMBIENT AIR MONITORING.*
Intern . J. Environ. Chem. V:33. 1988.

4°) - **J. GREGOIRE and A. SAMOUN.**
*DYNAMIC HEADSPACE ANALYSIS WITH DCI GAS CHROMATOGRAPHIC DEVICE.*
33th PITTSBURGH Conference - March 1982 - Atlantic City - USA.

5°) - **T. TAMIRI and S. ZITRIN.**
*CAPILLARY COLUMN GC/MS OF EXPLOSIVES.*
Journal of Energetic Materials - Vol. 4 - 1986.

# A MODEL OF EXPLOSIVE VAPOR CONCENTRATION

T.A. Griffy
Department of Physics
University of Texas
Austin, Texas, USA

## ABSTRACT

Many instruments which are employed to locate improvised explosive devices are designed to detect the vapor emitted by the explosive. The effectiveness of such instruments clearly depends on both the sensitivity of the equipment and the amount of vapor present. The model presented here can be used to predict the explosive vapor concentration one might expect for various detection scenarios. In the model are the effects of the amount of explosive, room volume, air exchange rate and deposition of explosive on the surfaces present. Example calculations are given for various detection scenarios such as room searches and portal inspection systems.

## 1. INTRODUCTION

The improvised explosive device is the preferred tool of the terrorist. In 1987, 56.7 per cent of the terrorist incidents were bombings[1]. Clearly a reliable method of locating explosives, whether during transportation, hidden in a cache or placed at the intended target would be a significant deterrent to such attacks. Consequently, much effort has been devoted to developing effective explosive detectors. Many of the devices currently in use depend on the detection of the vapor emitted by the explosive. It is thus important to understand the vapor concentration which might be expected under the varied search conditions likely to be encountered. A simple

[1] *Patterns of Global Terrorism : 1987*. United States Department of State Publication 9661, August 1988.

method which can be used to estimate the vapor present in various detection scenarios is described here. For concreteness we present results for vapor emitted by a "one pound" (0.45 kg) block of TNT into a room with a volume of 30 $m^3$. The mathematical formulation is of course more general and can be easily used for other situations simply by changing the appropriate parameters such as equilibrium vapor pressure, molecular weight etc. We list below the symbols in the following calculation as well as the values assigned to these parameters in the example calculation.

| | |
|---|---|
| $A_B$ | Surface area of explosive block (0.03 $m^2$) |
| $A_W$ | Surface area of room "walls" (50 $m^2$) |
| D | Diffusion coefficient of explosive in air ($3 \cdot 10^{-6}$ $m^2/s$) |
| G | Evaporation rate constant in Hertz-Knudsen equation $\left(1.5 \cdot 10^{-6} \frac{kg}{m^2 s}\right)$ |
| M | Molecular weight of explosive ($227 \cdot 10^{-3}$ kg/mole) |
| m | mass of explosive |
| p | Vapor pressure of explosive |
| $p_o$ | Equilibrium vapor pressure of explosive ($4 \cdot 10^{-4}$ Pa $\approx 3 \cdot 10^{-6}$ mmHg) |
| R | Gas constant, 8.31 J/mole°K |
| T | Temperature |
| $\alpha_{(v)}$ | Rate constant associated with evaporation in air (vacuum) |
| $\beta_{(v)}$ | Rate constant associated with adsorption by walls in air (vacuum) |
| $\gamma$ | Rate constant associated with room air exchange |
| $\varepsilon$ | Ratio of effective mixing velocity to kinetic velocity |
| $\rho$ | Density of explosive |
| $\sigma$ | Mass per unit area of explosive monolayer ($1.2 \cdot 10^{-6}$ $kg/m^2$) |

$\tau_D$ Diffusion time

$\tau_V$ Time for air exchange

$\tau_W$ Time to cover the walls with a monolayer

## 2. THE CALCULATION OF VAPOR PRESSURE

The calculation of evaporation from a solid *into a vacuum* can be derived from kinetic theory and is given by the Hertz-Knudsen equation,[2]

$$\frac{dm}{dt} = GA_B$$

where $\frac{dm}{dt}$ is the mass per unit time evaporating from a solid block with surface $A_B$ and G is a rate constant:

$$G = \left(\frac{M}{2\pi RT}\right)^{1/2} p_o.$$

For example, the rate constant for TNT ($M = 227 \cdot 10^{-3}$ kg/mole, $p_o = 4 \cdot 10^{-4}$ Pa) at room temperature (T= 290° K) is

$$G = 1.5 \cdot 10^{-6}\ \mathrm{kg/m^2\,s}.$$

The amount evaporating from a "one pound" block is then

$$\frac{dm}{dt} = (1.5 \cdot 10^{-6})\,(0.03) = 4.6 \cdot 10^{-8}\ \mathrm{kg/s}$$

The rate of evaporation into a vacuum is significantly higher than the actual evaporation rate into air. Corrections to the Hertz-Knudsen coefficient to account for this are discussed below.

---

2 H. Hertz, Ann. Physik, 17, 177 (1882)
H. Knudsen, Ann. Physik, 47, 697 (1915)

If a mass m of the vapor fills a volume V, the vapor pressure can be obtained from the ideal gas law

$$p = \frac{RT}{MV} m.$$

This relation can be used to calculate the rate of change of the vapor pressure when the explosive is evaporating into a vacuum

$$\frac{dp}{dt} = \frac{RT}{MV}\frac{dm}{dt} = \frac{RT}{MV} GA_B = \left(\frac{RT}{2\pi M}\right)^{1/2} \frac{A_B}{V} p_o = \alpha_v p_o$$

This result follows from the assumption that the evaporated vapor is uniformly and instantaneously mixed throughout the volume V. Clearly this is a rather drastic assumption and modification will be discussed below.

There are other factors which influence the time rate of change of the vapor pressure. As the vapor pressure approaches its equilibrium value the evaporation rate will go to zero. Vapor can be lost when the molecules of explosive stick to the "walls" (i.e., any surface) of the room. Vapor can also be lost by air exchange caused by the ventilation system in the room. These effects can be incorporated in the rate equation:

$$\frac{dp}{dt} = \alpha_v (p_o - p) - \beta_v p - \gamma p.$$

As above, the first term in this equation describes evaporation of the vapor. The second term describes loss due to coating of the walls. The initial value of the rate constant $\beta_v$ can be calculated in the same way that $\alpha_v$ was above with the result

$$\beta_v(t=0) = \left(\frac{RT}{2\pi M}\right)^{1/2} \frac{A_W}{V}.$$

Clearly $\beta_v$ will go to zero as all of the "walls" within the volume become coated with explosive. However this time is long compared with $\alpha_v^{-1}$, so we can take $\beta_v$ to be a constant for small times.

The constant in the third term in the rate equation, which describes air exchange, can be taken to the reciprocal of the time required for one complete exchange of air in the room, i.e. $\gamma = \tau_V^{-1}$.

Before proceeding to discuss solutions of the rate equation we need to remove the rather drastic assumption that all of these processes are taking place in a vacuum. A suggestion as to how this might be done comes from recognizing that the rate constants $\alpha_v$ and $\beta_v$ can be written as

$$\alpha_v = \frac{1}{4}\bar{v}\,\frac{A_B}{V} \quad \text{and} \quad \beta_v = \frac{1}{4}\bar{v}\,\frac{A_W}{V}$$

where $\bar{v}$ is the average molecular speed predicted by kinetic theory:

$$\bar{v} = \left(\frac{8RT}{\pi M}\right)^{1/2}$$

To a first approximation we can remove the vacuum assumption by simply replacing this average speed by a (much slower) effective diffusion velocity

$$v_{eff} = \varepsilon\,\bar{v}$$

The value of the rate constants are similarly magnified:

$$\alpha = \varepsilon\,\alpha_v \text{ and } \beta = \varepsilon\beta_v$$

The solution to the rate equation is now easily attained.

$$p(t) = \frac{\alpha}{\alpha+\beta+\gamma}\,p_o\,(1-e^{-(\alpha+\beta+\gamma)t})$$

Since the factor $e^{-\beta t}$ goes to zero rapidly, the vapor pressure in the room quickly reaches the value

$$p(t) = \frac{\alpha}{\alpha+\beta+\gamma} p_o$$

Since $\alpha$ and $\gamma$ are usually much less than $\beta$

$$p(t) \cong \frac{\alpha}{\beta} p_o = \frac{A_B}{A_w} p_o$$

This rather surprising result indicates that *until such time as the "walls" of the room are coated with explosive, the vapor pressure remains substantially below the equilibrium value.* Inserting the values for the typical example (a one pound block of TNT in an average room) gives $p = 6 \cdot 10^{-4} p_o$. Note that since this result depends on the ratio of $\alpha$ to $\beta$ it is independent of the effective diffusion velocity.

We can estimate the time required to coat the walls by assuming the walls are coated with a monolayer of explosive. For TNT the mass per unit area of this monolayer is $\sigma = 1.2 \cdot 10^{-6}$ kg/m$^2$. The total mass of explosive on the "walls" is then $\sigma A_w = 6 \cdot 10^{-5}$ kg for a room with a surface area of 50 m$^2$. The time required to coat the walls can be obtained by dividing this number by the evaporation rate predicted by the Hertz-Knudsen equation

$$\tau_w = \frac{\sigma A_w}{\frac{dm}{dt}} = \frac{6 \cdot 10^{-5}}{4.6 \cdot 10^{-8}} = 1.3 \cdot 10^3 \text{s}.$$

Clearly this is a lower limit on the time required to coat the walls since the true evaporation rate will be significantly less than the evaporation rate into a vacuum which is given by the Hertz-Knudsen equation.

## 3. THE ROLE OF DIFFUSION

Thus far we have assumed that the explosive vapor is mixed with the air at a rate determined by some effective mixing velocity. It is interesting to ask what role diffusion might play in this mixing process. The diffusion equation which determines the spatial and time dependance of the vapor concentration c(r,t) is

$$\frac{\partial c}{\partial t} = D\nabla^2 c.$$

The diffusion coefficient can be estimated from the formula for rigid elastic spheres.

$$D_{12} = \frac{3}{8(n_1+n_2)\,\sigma_r^2}\left(\frac{kT\,(m_1+m_2)}{2\pi m_1 m_2}\right)^{1/2}$$

where n is the molecular density of the two gasses, m the molecular mass and $\sigma_r$ the effective collision diameter. Inserting the numbers appropriate to TNT diffusing in air gives

$D \cong 3 \cdot 10^{-6}.m^2/s.$

For a point source which begins diffusing at t = 0 an analytic solution to the diffusion equation can be obtained

$$c(r,t) = \frac{1}{(4\pi Dt)^{3/2}} \exp\left(-r^2/4Dt\right).$$

Taking the derivative of this result allows us to estimate the time required for the peak in the vapor concentration to reach a distance r from the source

$$t_D = \frac{r^2}{6D}.$$

If diffusion alone were responsible for the vapor transport, this result tells us it would take about 15 hours for the vapor to move a distance of one meter from the source! Clearly diffusion is not the dominant transport mechanism.

The diffusion rate can also provide some insight into how the Hertz-Knudsen equation might be modified to account for the fact that that evaporation process takes place in air rather than in a vacuum. Assume the explosive is transported by diffusion through the boundary layer of thickness $\delta$ surrounding the explosive. The effective velocity is then

$$v_{eff} \cong \frac{D}{\delta} = \varepsilon \bar{v}$$

For a one millimeter thick boundary layer*

$$v_{eff} = \frac{3 \cdot 10^{-6}}{10^{-3}} = 3 \cdot 10^{-3} \text{ m/s.}$$

This gives a value of $\varepsilon \sim 10^{-4}$.

This result can also be used to estimate the effectiveness of some of the portal detection schemes which have been proposed. The <u>maximum</u> amount of explosive which can be detected at a portal inspection is given by the formula

$$m = D\frac{1}{5}\left(\frac{\rho_a v_o}{l\mu}\right)^{1/2}\left(\frac{M}{2\pi RT}\right)^{1/2} p_o A t$$

where A is the surface area of the explosive, t is the inspection time and other symbols have their usual meaning. This formula will give a significant over estimate of the amount of explosive reaching the detector since no account is taken of the "packaging" of the explosive and it is assumed that all of the explosive that

---

* The boundary layer thickness can be estimated using the equation (H. Rouse, *Elementary Mechanics of Fluids*, J. Wiley N.Y. 1946)

$$\delta \approx 5\left(\frac{l\mu}{p_a v_o}\right)^{1/2}$$

where $\mu$ is the viscosity ($18 \cdot 10^{-6}$ Pa · s for air at 20°C), p is the density (1.29 kg/m$^3$ for air), l is a characteristic length and $v_o$ is the free stream velocity

evaporates is collected by the detector. It is nevertheless useful since it gives an upper bound on the amount of explosive one can expect. As an example, if the airstream velocity is 5 m/s, the effective length 0.1 m and the area of the explosive is taken to be 0.05 $m^2$, for TNT the maximum amount of explosive one might collect is 0.5 μg.

## 4. SUMMARY AND CONCLUSIONS

A simple model can be used to estimate the amount of explosive vapor which one might find in various detection scenarios. In many situations the explosive vapor pressure predicted by this model is significantly less than the equilibrium vapor pressure. This result suggests vapor detectors will require substantially increased sensitivity if they are to be effective in locating explosives.

# DESIGN OF A HIGH-PERFORMANCE GAS-PHASE EXPLOSIVES VAPOR PRECONCENTRATOR

D.P. Lucero

IIT Research Institute
4600 Forbes Boulevard
Lanham, Maryland 20706 USA

ABSTRACT

The vapor preconcentrator/detector module is an adsorption-desorption device that obtains preconcentration factors in excess of 500 in less than a 9-sec cycle. It comprises an adsorption chamber and matrix, a detector compartment, and special-purpose inlet and outlet valves that minimize the chamber dead volume. A TNT vapor adsorption efficiency near 98 percent can be obtained with a 2832-l/min sample flow rate and a desorption efficiency near 88 percent with a 2-l/min purge gas flow rate. It uses an orthogonal flow geometry to obtain comparable efficiencies for the adsorption and desorption processes despite the large disparity in the adsorption-desorption gas flow rates. The preconcentrator and the essential elements of the detector are configured in an integrated module design comprising a concentric array of circular tubes containing the adsorption matrix in an annular chamber and, at the core of the assembly, a detector module such as an electron capture detector or the ionization chamber of an ion mobility spectrometer.

## 1. INTRODUCTION

Engineering analysis shows that an adsorption-desorption preconcentrator model using orthogonal flow geometry for the sample (adsorption) and purge (desorption) gas streams can produce preconcentration factors in excess of 500 over a 9-sec processing period. The preconcentrator device is VapaZorb: an assemblage of circular concentric tubes. Longitudinal and radial gas flows are used sequentially for the vapor molecule adsorption and desorption processes, respectively. A 98 percent adsorption process efficiency and an 88 percent desorption process efficiency can be obtained for TNT with a 2832-l/min sample air stream flow rate and a 2-l/min purge gas stream flow rate.

Special-purpose sample inlet and sample outlet valves are used that minimize sample losses and pressure drop during the adsorption process and minimize the void volume of the adsorption chamber during the desorption process. All other active elements of VapaZorb are contained within the

module except those components related to sample and purge stream controls. An integrated VapaZorb and detector can be designed by locating a detector module or the inlet to the detector module in the central core of the VapaZorb assembly. This design approach minimizes explosives vapor molecule losses usually encountered with the preconcentrator-detector interface.

Gas-phase explosives vapor detector modules with lower detection limit (LDL) characteristics near the part per trillion (ppt, v/v) level have been available commercially for several years.[1] To obtain sub-ppt LDL response in the field, most detectors require special sample processing, e.g., analyte separation and the removal of water vapor, oxygen, or other interferents. The detection alarm set point concentration levels of many scenarios for the detection and location of a clandestine explosives cache, however, is believed to be at sub-ppt levels.[2,3] Thus, to function in a practical explosives vapor detection system with reasonably low false-alarm probabilities, the detector module LDL must be below the alarm set point concentration. For this requirement, most detector modules must be provided with an explosives vapor preconcentrator.[4-6]

The utility of a detector module operating with a preconcentrator is extended significantly with large (> 100) sample preconcentrations over relatively short time cycles (< 15 sec). Explosives exhibiting lower vapor pressures (approximately 1 ppt) are more detectable with the use of a high-performance preconcentrator.

Detection systems of lower detection limits will consequently perform with lower false- and missed-alarm probabilities.[3] Most explosives vapor preconcentrators are intermittent adsorption-desorption type devices. Their performance limitation is ascribed principally to the incompatibility of the pneumatic design constraints that lead to a performance exhibiting either a high adsorption and a low desorption efficiency, or the converse, or both low adsorption and desorption efficiencies. The unique design features of VapaZorb promote a preconcentration action with relatively high (> 88 percent) adsorption and desorption efficiencies with a large disparity in adsorption and desorption gas flow rates.

## 2. PRECONCENTRATION FACTOR

The performance of intermittent adsorption-desorption type preconcentration modules including VapaZorb is described as follows:

$$P_f = (Q_s T_s / Q_p T_p) \eta_a \eta_d \qquad (1)$$

where

$P_f$ = preconcentration factor, dimensionless;

$Q_s$ = sample gas stream flow rate, l/min;

$T_s$ = adsorption time increment, sec;

$Q_p$ = purge gas stream flow rate, l/min;

$T_p$ = desorption time increment, sec;

$\eta_a$ = adsorption process efficiency, dimensionless; and

$\eta_d$ = desorption and transport process efficiency, dimensionless.

An examination of equation 1 reveals the design constraints and problems associated with producing a preconcentration module with a high preconcentration factor. The time increment for the entire preconcentration cycle is limited primarily by the detection application. For the inspection of baggage items and personnel at transportation terminals, the maximum time for a single examination, which includes sample processing, detection, and alarm, is 6 to 10 sec. Thus, in considering the time to close and open the valves and heat and cool the adsorption matrix, it is evident that parametric flexibility in the preconcentrator design is associated mainly with the gas stream ratio, $Q_s/Q_p$.

Attendant to manipulating $Q_s/Q_p$ is the constraint of maintaining the adsorption and desorption efficiency product, $\eta_a\eta_d$, at reasonable levels such that increases in $Q_s/Q_p$ are not offset essentially by corresponding decreases in $\eta_a\eta_d$. A close examination of the hardware required to handle both large and relatively small flow rates and the attendant pressure losses with high adsorption and desorption efficiencies indicates clearly that these design constraints operate at cross purposes. Therein lies the primary problem in the design of an adsorption-desorption preconcentrator that produces preconcentration factors in excess of 20.

## 3. VAPAZORB

VapaZorb is a gas-phase discontinuous adsorption-desorption vapor preconcentrator comprising five functional subsystems as depicted in Figure 1: the adsorber-desorber (A/D) module, sample stream inlet valve, sample stream outlet valve, sample stream flow control network and sampling vacuum pump, and purge gas supply and flow control network.

The operation of VapaZorb is typical for most discontinuous adsorption-desorption preconcentration devices with the exception of the heating and cooling processes. The heating elements are powered constantly. Cooling is accomplished by the sample air stream, at ambient temperature, flowing

through the A/D module. Likewise, heating is accomplished by thermal conduction from the heating elements and the preheated purge gas flowing through the A/D module. A high adsorption efficiency is obtained by utilizing an adsorption matrix in the A/D module that (1) promotes a large explosives vapor molecule mass transfer coefficient to the adsorbing surface and (2) provides a large adsorption surface area. In addition, the adsorption matrix is of a relatively small thermal mass, which permits adequate heating and cooling as described above. A high desorption efficiency is obtained over a short time period (< 3.4 sec) by minimizing (1) the number of adsorption chamber volume gas exchanges required for the desorption process, (2) the adsorption chamber volume with a compact adsorption matrix, and (3) the void volume introduced by valves and the valve A/D module interfaces.

A special feature of VapaZorb is the pneumatic design and operation of the A/D module. The module promotes a uniform wide front flow of purge gas through the adsorption matrix in a fashion that minimizes the number of adsorption chamber volumetric gas exchanges required to obtain efficient transport of the desorbed explosives vapor molecules to the detector.

4. PRECONCENTRATION CYCLE

There are five basic steps in the VapaZorb preconcentration process. With the A/D module at thermal equilibrium, the purge gas pneumatic lines pressurized fully, and the sampling vacuum pump in operation, the following steps compose the preconcentration cycle:

(1) VapaZorb is activated into the adsorption mode: the inlet and outlet sample valves open, and sample gas stream enters the A/D module;

(2) The sample gas cools the adsorbing matrix surface contained within the A/D module, and explosives vapor molecules are transported to and adsorbed on the matrix surface;

(3) The desorption process is activated: the sample stream inlet and outlet valves are closed;

(4) The adsorbing surface is heated to the explosives molecules desorption temperature; and

(5) The purge gas enters the A/D module where it is preheated and flows into the adsorption chamber and out through the purge gas stream exhaust to the detector; the desorbed explosives vapor molecules are carried to the detector with the purge gas.

5. ADSORBER-DESORBER MODULE

Figure 2 is a cut-away illustration of the A/D module showing radial symmetry about the center line (℄). Only the basic functional elements of the module are depicted. The sample stream inlet and outlet valves are not shown.

The module envelope is a short right-circular cylinder approximately 1.02 cm (0.4 in.) long and 14.6 cm (5.75 in.) in diameter. It comprises three tubes arrayed concentrically: an inner thin wall perforated metal tube, a thick wall porous metal tube, and an outer solid metal tube. The annular spaces between the solid metal tube and porous tubes are closed at both ends to form an annular plenum chamber. Both ends of the porous tube are faced with thin solid metal segments that seal the ends and prevent longitudinal gas flow. The annular space between the porous metal and perforated metal tubes is the adsorption chamber containing the adsorption matrix: 10 thin-wire screen elements stacked and evenly spaced normal to the sample gas stream flow. Heating elements and a temperature sensor for control purposes are embedded in the porous tube, which is maintained at 200°C. (These are not shown in Figure 2.)

To minimize adsorption losses[7,8] in transporting desorbed molecules from VapaZorb and the detector module, the front end of the detector module, e.g., the ionization chamber of an electron capture device, ion mobility spectrometer, atmospheric pressure ionization mass spectrometer, etc., can be located in the VapaZorb detector compartment. One end of the detector compartment is sealed with a bulkhead fitting through which electrical and pneumatic feed-throughs leading to the detector module are located.

The sample gas stream enters and leaves the adsorption chamber and flows longitudinally as shown. Purge gas enters the plenum chamber through the gas port shown in the solid metal tube wall of the module. By design, the porous tube is an element of relatively large pneumatic impedance. Thus, as the purge gas enters, it will distribute itself uniformly throughout the plenum chamber and subsequently flow radially with maximum uniformity through the porous tube over its entire length, through the adsorption chamber and the perforated tube, and into the detector compartment. This gas flow mode minimizes the number of adsorption chamber volume exchanges required to remove the sample molecules from the chamber in the desorption process.

5.1 Sample Stream Inlet and Outlet Valves

During the explosives vapor desorption process, the sample stream inlet and outlet valves are closed, i.e., they will prevent the flow of purge gas out the adsorption chamber ends. To achieve a high desorption efficiency, it is essential, as stated previously, that the void volume of the adsorption chamber and the void volume between the adsorption chamber and both inlet and outlet valves are minimal. Special-purpose valves are designed to accomplish the closure with the constraints listed. The inlet valve is depicted in Figure 3 and the outlet valve in Figure 4. The sealing element of each valve is a toroidal plunger. Figure 3 shows the inlet valve in the closed position, and Figure 4 shows the outlet valve in the open position. Both valves are activated into either the closed or opened condition by pneumatic forces that arise from vacuum or purge gas pressure, respectively. Each is transmitted to the toroidal plunger, through the pneumatic connection from the plunger to the solenoid valve and, thus, to either the vacuum sampling pump or the purge gas supply. Note Figures 1 and 2 show that the purge gas stream network contains only an inlet port at the A/D module.

In the inlet valve configuration, the toroidal plunger is hard-mounted structurally by a frame webbing to the A/D module outer solid metal tube. Forces exerted by the plunger on the A/D module sealing surfaces are transmitted through the frame to the A/D module outer solid tube. The toroidal plunger is fabricated of two concentric collapsible metal bellows tubes sealed by a flat metal annular bulkhead at one end and by a toroidal truncated cone at the opposite end. A lamination of relatively soft material is attached to the conical surface as shown in Figure 3 to make the seal. Gas pressure or vacuum is introduced to the toroidal assembly through the bulkhead fitting and the gas line at the base of the plunger. The 3-way solenoid valve is connected pneumatically and alternately to the purge gas supply and the vacuum side of the sampling pump.

The operation of each valve is described as VapaZorb proceeds through a preconcentration cycle starting with Step 1, in which VapaZorb is activated into the adsorption mode: the sampling vacuum pump is engaged by the sample stream flow control network. Simultaneously, the 3-way valve (Figure 3) opens to the pneumatic line from the vacuum side of the sampling vacuum pump. A vacuum is pulled on the toroidal plunger through the 3-way solenoid valve. The vacuum causes the toroidal plunger to collapse away

from the A/D module. The displacement is sufficient to expose a large gap to the sample stream to minimize sample loss and sample stream entry pressure loss. As VapaZorb proceeds to Steps 2 and 3, the 3-way solenoid valve is switched from open to the sample vacuum pump to open to the purge gas supply. In this mode, VapaZorb is in the desorption stage of the cycle, and the plunger is pressurized by the purge gas supply through the 3-way solenoid valve. The pressure causes the toroidal plunger to distend toward the A/D module. The plunger sealing surface fits into the annular entrance of the A/D module adsorption chamber, and a seal is made at the edges of the porous and perforated tubes against the plunger sealing surface. Note that by design as depicted in Figure 3, the void volume between the adsorption chamber and the inlet valve is minimized.

The sample stream outlet valve plunger and seal is identical and operates in exactly the same fashion as the inlet valve. However, a toroidal chamber surrounds the plunger, which itself is hard-mounted to the inner perforated metal and outer solid metal tubes shown in Figure 4. The valve plunger is hard-mounted to the toroidal chamber through the frame webbing. In the open position (Figure 4), sample gas flows out the adsorption chamber into the toroidal chamber and to the vacuum pump. In the closed position, the sealing forces are transmitted from the plunger to the surrounding toroidal chamber. Note that by design, as depicted in Figure 4, the void volume between the matrix component and the valve is minimized.

5.2 Adsorption Matrix and Adsorption Efficiency ($\eta_a$)

The adsorption process is primarily a transfer of explosives vapor molecules from the sample gas stream to the adsorbing surface. It is primarily a diffusional process. For conditions at which the explosives molecules adsorbed with a unity sticking coefficient,[9] the adsorption efficiency is described as follows:

$$\eta_a = 1 - \exp(-k_m A_s/Q_s) \qquad (2)$$

where

$k_m$ = explosives vapor molecule average mass transfer coefficient, cm/sec, and

$A_s$ = matrix adsorbing surface area, $cm^2$.

The product $k_m A_s$ is maximal with a wire screen matrix: a series of 10 annular thin wire screen elements stacked normal to the gas sample stream flow direction. Thin wires or bodies of small dimensions placed normal to the flow exhibit a relatively large $k_m$ because the small wire dimension

prohibits the development of a thick gas boundary layer.[10,11] The rate-limiting diffusional impedance in the transport of molecules from the sample gas stream of the adsorption surface is proportional to the thickness of the gas boundary layer adjacent to that surface. Thus, the thinner the boundary layer, the larger the $k_m$ obtained. For turbulent gas sample stream flow in the adsorption chamber, $k_m$ for the wire screen is approximated as follows:[12,13]

$$k_m = (3.91/\epsilon)(D/D_w)(\mu/\rho D)^{1/3}(\rho Q_s D_w/\mu A_c)^{0.425} \qquad (3)$$

where

$\epsilon$ = void fraction of the screen element, dimensionless;

D = explosives vapor molecule diffusion coefficient in the sample gas at ambient temperature, $cm^2/sec$;

$D_w$ = screen wire diameter, cm;

$\mu$ = sample gas viscosity, g/sec-cm;

$\rho$ = sample gas density, $g/cm^3$; and

$A_c$ = adsorption chamber entrance area, $cm^2$.

Equations 2 and 3 were used to examine the mass transport characteristics of TNT molecules from an air sample stream to a series of 10 stacked wire screens of various wire diameters and meshes available commercially, contained in an annular cylindrical adsorption chamber 1.02 cm (0.4 in.) long with 9.53-cm (3.75-in.) and 7.0-cm (2.75-in.) outside and inside diameters, respectively. The screen layers are separated by approximately 0.56 mm (0.022 in.). A $k_m$ of 192 cm/sec is obtained with a 50-mesh screen of 0.023-mm (0.009-in.) diameter wire to yield a 98 percent TNT adsorption efficiency at a 2832-l/min (100-scfm) sample air stream flow rate near 20°C.

5.3 Desorption and Transport Efficiency ($\eta_d$)

The desorption process occurs in two steps: (1) desorption of explosives vapor molecules from the wire screens and (2) transport of explosives vapor molecules into the purge gas and to the detector compartment.

As an example, TNT molecules adsorbed on the matrix surface, as described later, begin desorbing abruptly at approximately 120° to 130° C. The heating time required to obtain the temperature level and thus accomplish desorption from the surface is approximately 3 sec.

When the wire screen matrix attains the desorption temperature, the explosives molecules are transported rapidly (< 40 msec for TNT) into the purge gas filling the adsorption chamber. For a 2-l/min purge gas flow

rate, the gas flow mode is laminar, thus permitting a second molecular diffusional process to affect significantly the desorption transport efficiency. In over-simplified terms, molecular back diffusional flow is induced by the concentration gradient at the interface between the purge gas and the chamber residual gas containing explosives molecules. The effect is similar to peak broadening obtained in gas chromatography. It is assumed as a worst-case condition that the back-diffusion in the VapaZorb adsorption chamber is similar to peak broadening, and the resulting explosives molecule concentration gradient developed by the process is described by a normal probability curve.[14] For example, for TNT molecules in a 28.6-$cm^3$ adsorption chamber volume and a 33.3-$cm^3$/sec purge gas flow rate, the interface broadens from a theoretical plane of zero thickness to a layer of mixed TNT and purge gas molecules thicker than 0.406 cm after one adsorption chamber volume exchange or 0.846 sec.

For this worst-case condition, 60.6 percent of the remaining TNT molecules in the adsorption chamber are removed after each successive gas volume exchange. On this basis, it is estimated that 98 percent of the TNT molecules desorbed from the matrix surface will be transported to the detector compartment after 4 volume exchanges and a 3.4-sec time increment.

The porous tube is in effect a special-purpose port for the purge gas to enter the adsorption chamber at a uniform velocity with a relatively wide front. Nonuniform flow is attendant to pneumatic configurations in which gas enters a chamber through small tubes or openings, e.g. valves, and subsequently expands abruptly into a much larger volume. The adsorption chamber void volume is minimized by the configuration of the sample gas stream inlet and outlet valves shown in Figures 3 and 4, i.e., the large entrances and flat sealing surfaces. A worst-case arbitrary estimate of the void volume attendant to the adsorption chamber-valve configuration is 10 percent of the total adsorption chamber volume.

The adsorption and transport overall efficiency is estimated as the product of the vapor desorption efficiency from the matrix surface (100 percent), - purge gas efficiency of transporting the vapor into the detector compartment (98 percent), and the fraction of the excess void volume in the adsorption chamber with the inlet and outlet valves closed, i.e., $\eta_d$ = 88 percent.

5.4 Matrix Heating and Cooling

Cooling the wire screen matrix is accomplished by the convective action of the sample gas stream, which is near ambient temperature (10° to 40° C).

The heat transfer coefficient in the cooling phase is estimated at 0.156 $W/cm^2\text{-}^oC$ (274 $Btu/hr\text{-}ft^2\text{-}^oF$).[15] To reduce the thermal mass of the matrix and increase thermal conductance, the wire screens are fabricated of aluminum. The wire screen thermal mass is 1.68 $cal/^oC$ ($1.2 \times 10^{-2}$ $Btu/^oF$). Cooling the matrix from 130° to 40°C in 1 sec will require an average heat transfer rate of 2.05 kW (7000 Btu/hr). The average energy removal rate by the air is $1.48 \times 10^4$ Btu/hr, which cools the wire screens to ambient temperature in approximately 0.4 sec.

The VapaZorb heater elements are located in the body of the porous tube. Power is supplied constantly to maintain the tube to at least 200° C. The porous tube also serves as a heat exchanger; it heats the purge gas as it flows through the tube. Thus, heating the adsorption matrix is accomplished by conduction from the heated porous tube through the metal wires and the convective action of the hot purge gas flowing past the screens. The thermal conductance for 0.23-mm (0.009-in.) diameter wire and 50-mesh screen from the porous tube to 10 stacked screens is approximately 1.3 $W/^oC$ (8 $Btu/hr\text{-}^oF$), while the convective heat transfer conductance is $9.66 \times 10^{-4}$ $W/^oC$ (1.7 $Btu/hr\text{-}^oF$). The low heat transfer convection conductance reflects the much lower gas flow rate of the purge gas stream relative to the sample air stream. The overall heat transfer conductance from the heated porous tube and the hot purge gas is 1.57 $W/^oC$ (9.66 $Btu/hr\text{-}^oF$). For a porous tube maintained at 200° C and a screen wire temperature at 10° C, the wire screen matrix will heat to the 130° C desorption temperature in less than 3 sec.

5.5 Pressure Losses

The characteristics of the sampling vacuum pump and the components of the sample stream flow control network of Figure 1 will depend on the detection system maximum allowable signal instability and the pressure losses incurred by the sample stream in flowing through the matrix adsorption chamber. For the annular dimensions listed earlier, the pressure losses in passing 2832 l/min (100 scfm) of air through the wire screen adsorption matrix is 0.072 atm (1.06 psi).[16]

The characteristics of the components in the purge gas flow rate control network will depend on the flow rate and the pressure losses incurred in flowing radially through the porous tube. For the tube dimensions listed earlier and with a pore size of 0.5 μm, the pressure drop for a 2-l/min (0.071-scfm) purge gas flow rate is 3.4 atm (50 psi). This pressure loss constrains the purge gas flow regulator absolute

pressure at the purge inlet and perhaps at the torodial plunger of the inlet and outlet valves to 4.42 atm (65 psi).

5.6 Adsorption Surface

It is important to ensure that the adsorption matrix surface obtains the adsorption and desorption characteristics described earlier. Surface treatment of the aluminum wire screen will ensure a unity adsorption probability (i.e., unity sticking coefficient), or at least high and constant adsorption probability for each explosives vapor molecule adsorption surface collision. Likewise it will ensure a high desorption probability above a specific temperature level.

To reduce heating and cooling times, the maximum and minimum desorption temperature level difference should be reasonably small, e.g., 20° to 50° C or smaller if permitted by the thermal characteristics of the adsorbing/desorbing surface and the temperature controller. To minimize the matrix heating time, the desorption temperature level should be reasonably close to the maximum ambient operating temperature yet above the explosives vapor adsorption temperature of all other materials, e.g., stainless steel, aluminum, etc., used in the fabrication of the A/D module and exposed to the explosives vapor molecules. In addition, the thermal characteristics of the adsorption matrix are constrained to maximum operating temperatures below the decomposition temperatures of the explosives vapors.

It is probable that the most uncertain long-term operational aspect of VapaZorb is associated with the repeatability of the adsorption surface performance. Its empirical relationships with its operating parameters must be defined to a practical degree to establish repeatable performance. This includes defining coating fabrication, preconditioning, storage, and operational parameters. Experimental data must be obtained to define the thermal adsorption-desorption cycle and the practical cycle life of the coating.

For explosives preconcentrators in general and specifically for VapaZorb, a thin coating of fused silica on the aluminum wire screens is a suitable adsorbing surface.[17,18] Fused silica is selected primarily as the adsorbing surface because it exhibits high adsorption and desorption probabilities at reasonably low temperature levels (< 80° C and > 130° C, respectively) for formation of a tightly bonded monolayer of explosives molecules.

A significant design engineering problem associated with a fused silica coating on the aluminum wire screen arises from the difference in thermal expansion coefficients and the repeated heating and cooling cycles. It is very possible that because of the thinness of the fused silica coating, the stresses on the coating will be minimized such that cracking and peeling can be avoided over long operating periods. For a 16-hr day, VapaZorb will experience 4800 heating-cooling cycles between a 80° and 130° C, or larger, temperature difference. The sheering stress on the aluminum-silica bond will oscillate between 500 to 1000 psi 4800 times each working day.

An alternate coating that may be acceptable is TFE Teflon.[8] The coating must be very thin because TFE dissolves explosives vapor molecules and will induce a time delay in the desorption process proportional to the square of the TFE coating thickness. For example, a 0.001-in. coating of TFE will introduce a 0.3- to 0.4-sec delay in desorbing.[19]

## 6. PERFORMANCE

### 6.1 Specifications

The basic VapaZorb dimensional, operating, and performance specifications are listed in Table 1. These specifications were developed for arbitrary requirements established by a 10-sec maximum allowable preconcentration process cycle and a preconcentration factor in excess of 500. In addition, TNT vapor was selected on the model explosives vapor molecule to estimate transport properties and adsorption and desorption efficiencies.

### 6.2 Tradeoffs

Adjustments to these specifications for specific applications will be primarily between preconcentration factor cycle time as determined by VapaZorb control temperature, matrix heating time, and purge time. Constraints on the maximum allowable sample stream flow rate and/or sample air velocity affect the preconcentration factor directly.

ACKNOWLEDGEMENTS

The author thanks Susan Hendrickson of the IITRI-East Engineering staff for technical editing and management of the manuscript preparation.

REFERENCES

1. W.D. Williams and J.K. Syverson, "Explosives Detector Field Tests," Research and Development Division, Bureau of Alcohol, Tobacco and Firearms, U.S. Department of the Treasury, April 1981.

2. C.T. Pate, "Characterization of Vapors Emanating from Explosives," LEAA Contract J-LEAA-025-73, Analytical Research Laboratories, Inc., June 1976.

3. D.P. Lucero, "User Requirements and Performance Specifications for Explosives Vapor Detection Systems," J. Test. and Eval. 13, 222 (1985).

4. A. Linenberg in "Proceedings, New Concepts Symposium and Workshop on Detection and Identification of Explosives," 1978.

5. L.W. Hrubosh, R.L. Morrison, R.W. Ryan, E.G. Walter, and M.M. Fulk, "Study of Conventional Preconcentration Techniques for Explosive Vapors," Report No. UCID-16766, Lawrence Livemore Laboratory, August 1973.

6. P.J. Thoma, J.M. May, D.E. Elisco, and T.J. Conrad in "Proceedings, New Concepts Symposium and Workshop on Detection and Identification of Explosives," 1978, p. 81.

7. D.P. Lucero in "Proceedings, New Concepts Symposium and Workshop on Detection and Identification of Explosives," 1978, p. 65.

8. P.K. Peterson and F.J. Conrad in "Proceedings, New Concepts Symposium and Workshop on Detection and Identification of Explosives," 1978, p. 85.

9. H. Eyring and E.M. Eyring, "Modern Chemical Kinetics," Reinhold Publishing Corporation, 1963, p. 73.

10. H. Schenck, "Heat Transfer Engineering," Prentice Hall, Inc., 1959, p. 92.

11. A.H.P. Skelland, "Diffusional Mass Transfer," John Wiley and Sons, 1974, p. 222.

12. A.S. Gupta and G. Thodos, A. I. Ch. E. J. 9, 751 (1963).

13. A.H.P. Skelland, "Diffusional Mass Transfer," John Wiley and Sons, 1974, p. 12.

14. F. Daniels and R.A. Alberty, "Physical Chemistry," 3rd edition, John Wiley and Sons, 1967, p. 403.

15. W.H. McAdams, "Heat Transmission," McGraw-Hill Book Co., 1954, pp. 258, 273.

16. R.H. Perry and C.H. Chilton, "Chemical Engineers Handbook," McGraw-Hill Book Co., 1969, p. 5-35.

17. B.T. Kenna and F.J. Conrad, "Studies of the Adsorption/Desorption Behavior of Explosive Molecules," SAND 86-0141J, Sandia National Laboratories, Albuquerque, New Mexico, unpublished.

18. M.A. Henderson, T. Jin, and J.M. White, Appl. Surf. Sci. 27, 127 (1986).

19. D.P. Lucero, Anal. Chem. 40, 707 (1968).

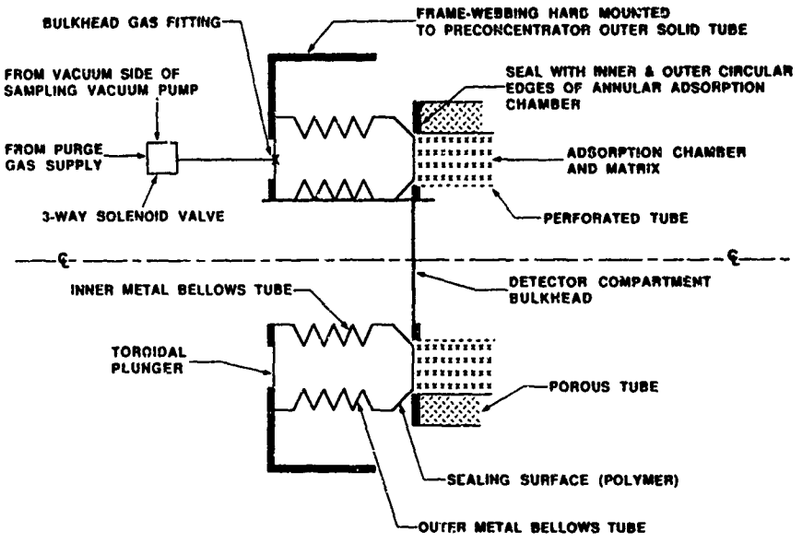


FIGURE 3. Sample Stream Inlet Valve

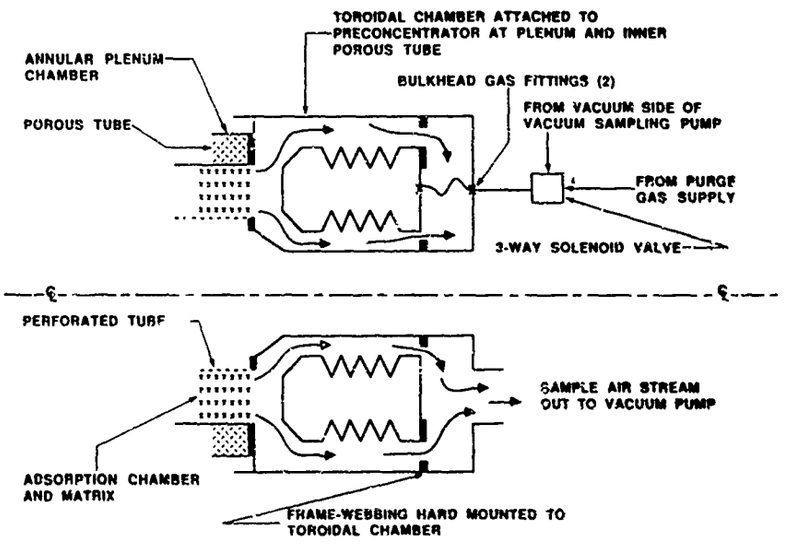


FIGURE 4. Sample Stream Outlet Valve

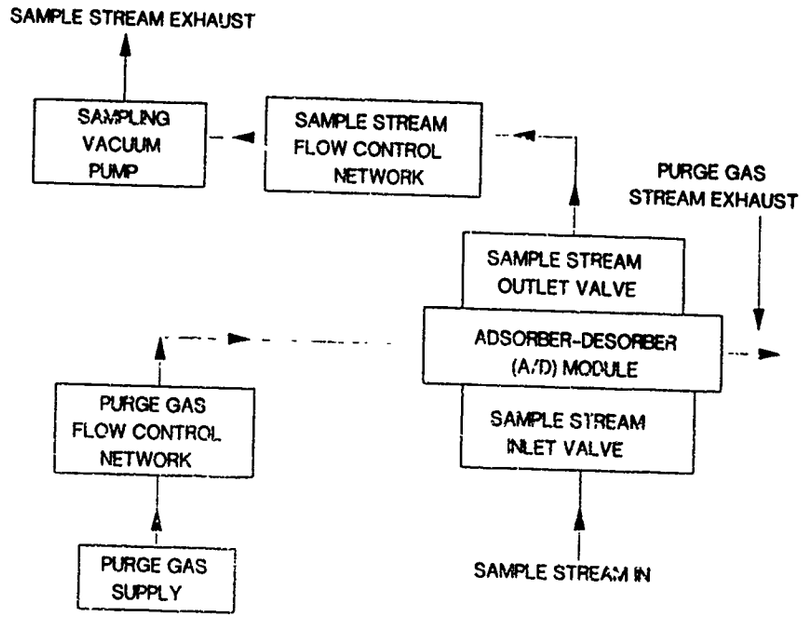


FIGURE 1. VapaZorb Pneumatic Network

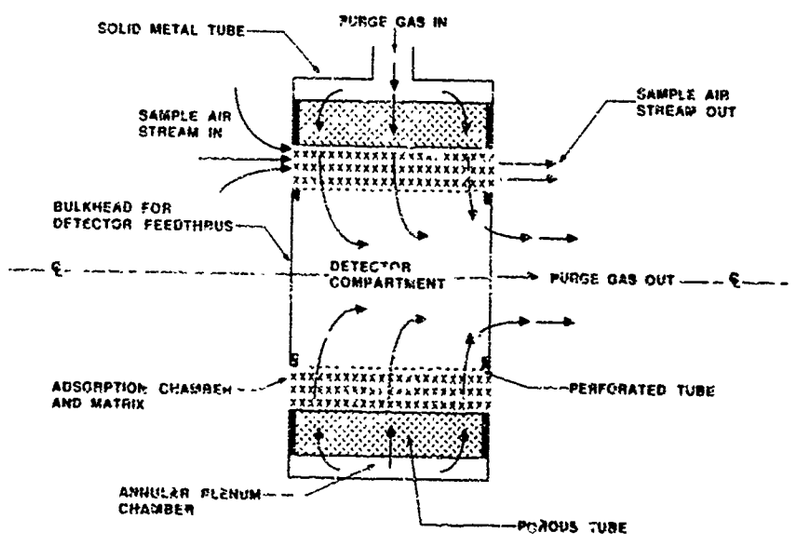


FIGURE 2. Adsorber/Desorber Module

TABLE 1. VapaZorb Operating and Performance Specifications

The specifications listed apply to a TNT explosives vapor species and VapaZorb using air sample gas and dry nitrogen purge gas between 10° and 40° C.

| | |
|---|---|
| Preconcentration Factor: | 720 |
| Cycle Time (s): | 8.9 |
| Sampling Time (s): | 2 |
| Sample Gas Flow Rate (l/min): | 2832 |
| Purge Time (s): | 3.4 |
| Purge Gas Flow Rate (l/min): | 2 |
| Matrix Cooling Time (s): | < 0.5 |
| Matrix Heating Time (s): | 3.0 |
| Adsorption Efficiency: | 0.98 |
| Desorption and Transport Efficiency: | 0.88 |
| Control Temperature (°C): | 200 |
| Adsorption Temperature (°C): | < 50 |
| Desorption Temperature (°C): | 120-130 |
| Warm Up Time (min): | 30 |
| Heating Power (W): | 1000 |
| Sample Gas Pressure Loss (atm): | 0.072 |
| Purge Gas Pressure Loss (atm): | 3.4 |

# A BIOLUMINESCENT EXPLOSIVES VAPOR DETECTION AND IDENTIFICATION SYSTEM

E.M. Boncyk

U.S. Army Belvoir RD&E Center
Fort Belvoir, Virginia 22060-5606 USA

## ABSTRACT

A breadboard TNT vapor detection system utilizing an enzyme that catalyzes the reduction of TNT molecules has been developed by the U.S. Army. It has a TNT-in-air minimum detectable concentration of 0.01 ppt (v/v), which can be achieved in a total analysis time of 10 min. An examination of the enzyme catalysis rate shows that the system is highly specific to TNT. The system shows a 0.028 relative response to DNT and a zero relative response to PETN, RDX, EGDN, NG, DEGDN, HMX, and Semtex. The primary interferent species appear to be nitroheterocyclic compounds. Nitrofuran and nitropyrine have an equivalent interferent response near that of DNT. This development shows that a multi-explosives vapor detection and identification system can be developed. Its operation is based on using an array of reaction cells, each containing a single immobilized enzyme specific to an individual explosives vapor molécule and a single cell comprising a co-immobilized mixture of all the explosives molecule enzymes.

## 1. INTRODUCTION

The U.S. Army Belvoir Research, Development and Engineering Center (BRDEC) has developed a breadboard bioluminescent trinitrotoluene (TNT) detection system using an enzyme and liquid reagents with a response specific to TNT (1,2). A reaction cell containing the enzyme immobilized on a solid substrate reacts with a liquid sample stream to subsequently produce a bioluminescence in a second reaction cell with an intensity that is inversely proportional to the TNT concentration in air (3). The system can be used to detect gas-phase TNT vapor molecules at low-level concentrations in enclosures.

Based on the breadboard TNT detection system developed, an identical design approach can be used to detect and identify vapors from several different explosives. The approach uses specific enzymes responsive to specific explosives to perform the bioluminescent transduction.

Work is planned to develop enzymes responsive to other explosives, such as nitroglycerine (NG) and ethylene glycoldinitrate (EGDN), to catalyze similar type reactions between the reagents and the NG and EGDN molecules. Enzyme development for other explosives, such as 1,3,5-trinitro-1,3,5-

triazacyclohexane (RDX), 1,3,5,7-tetranitro-1,3,5,7-tetrazacycloctane (HMX), and pentaerythritol tetranitrate (PETN) will follow.

2. EXPLOSIVES VAPOR MONITORING

Vapor monitoring systems that detect the presence of a clandestine explosives cache will require ultra-low-level detection capabilities (4) as summarized in Table 1. After examining the user requirements and the performance characteristics of the explosives vapor detection and identification systems, it is obvious that the utility of the bioluminescent detection system is restricted primarily to enclosure monitoring applications and suspect site predetonation examination. The requirements most critically affecting the performance specifications of the bioluminescent system are the processing time to perform the detection and identification and the false- and missed-alarm probabilities.

Further examination of the detection requirements and consideration of the practical aspects of the detection procedures (4,5) suggest a minimum detectable concentration (MDC) of 0.001 ppt and an alarm set point concentration level near 0.005 ppt.

Online gas stream monitoring systems operating at ultra-low-level detection limits, e.g., < 1 ppt (v/v), require extractive analytical techniques with a special-purpose sample train and a vapor-generating gas calibration device in support of the detector module. The bioluminescent sample train provides extensive sample processing (4,5) in the form of large sample preconcentration and can effect a gas- to liquid-phase interface. A vapor-generating calibrator is used to periodically and quantitatively assess, by a vapor challenge, the system signal and zero instabilities such that periodic system response readjustments can be made to null these instabilities. Frequent calibrations will reduce the system false-alarm probability. Figure 1 illustrates these modules in the basic configuration of an ultra-low-level vapor monitoring system.

A review of the MDC and other performance characteristics of explosives detector modules available commercially (6-9) and in development indicates that the sample train must transport explosives vapor molecules efficiently to the detector module, i.e., with a minimum sample loss, and produce massive explosives vapor bioluminescent preconcentration (4). In the bioluminescent TNT detection system, these functions are performed by the sample train in the TNT detection system, thus permitting the detector module to attain a TNT MDC near 0.01 ppt (v/v) in air in a 10-min detection cycle. An MDC near 0.001 ppt can be attained by improvements to the system liquid stream transport components and signal processing. In addition, it is estimated by engineering

analysis that these improvements to the bioluminescent TNT detection system will permit operation near 0.018 ppt alarm set point concentration levels with false- and missed-alarm probabilities of 0.27 percent over 8-hr operating periods with a single 30-min calibration episode.

3. TNT EXPLOSIVES VAPOR DETECTION SYSTEM

Operation of the bioluminescent TNT explosives vapor detection system is based on the action of the individual modules of Figure 1 on a sample airstream.

In general, the bioluminescent signal is obtained by a series of chemical reactions (10,11), which occur in the detector module. Two primary reactions can occur: one reaction with TNT absent and the second with TNT present. The reagents react in the $TNT_{ase}$ reaction cell of Figure 2 as follows:

$$NADH + FMN + H^+ \text{----}> NAD^+ + FMNH_2 \qquad (a)$$

The second reaction occurring with TNT molecules is the reduction of TNT promoted by the catalytic action of the TNT enzyme, with the TNT reductase:

$$TNT + NADH + H^+ \text{----}> TNT_{red}^+ + NAD^+ + H^+ \qquad (b)$$

Reaction (b) competes directly with reaction (a) for NADH, resulting in a proportional decrease in the amount of $FMNH_2$ and, subsequently, a decrease in the intensity of bioluminescence produced in the second reaction cell or bioluminescence reaction cell as described below by reaction (c). The TNT concentration in the liquid stream is inversely proportional to the decrease of bioluminescent intensity (1,12) as measured by a light detector (photomultiplier tube).

The reaction products and the remnants of the three liquid streams of Figure 2 are transported in a single stream to the second reactor, the bioluminescence reaction cell as shown in Figure 2, where the following reaction occurs:

$$FMNH_2 + RCHO + O_2 \text{----}> FMN + RCOOH + H_2O + h\nu \qquad (c)$$

Reaction (c) is catalyzed by an oxidoreductase and by bacterial luciferase (2,13). It utilizes the $FMNH_2$ in the presence of a long chain aldehyde and oxygen to produce the bioluminescence ($h\nu$). Both catalysts are co-immobilized on the reaction cell matrixes (14,15).

The overall process is described by tracing the flow of the TNT molecules through the network of Figure 2.

3.1 Sample Train

The sample train performs the gas-phase sampling, preconcentration, and detector module interface functions. Its operation is based on the action of a liquid gas extractor (16,17). The preconcentration factor obtained is approximately 107,000 operating with a 150-l/min sample airstream for 5 min

with a 50 percent extraction efficiency. This produces a 3.5-ml liquid water sample.

The system operates in an automated batch mode over a specific time period. A sample airstream passes continuously through the sample train. Simultaneously, a recirculating liquid water stream flowing in the sample train extracts a large fraction of the TNT molecules from the airstream and stores and accumulates them in liquid solution. At the end of the sampling period, the liquid solution is removed from the sample train and is transported to the detector module for analysis (5). In effect, a gas-phase sample is transformed into a liquid sample to interface with the liquid-phase detector module. In addition, the TNT sample is preconcentrated.

3.2 Detector Module

Figure 2 is a schematic network of the detector module. It comprises the hydrodynamic network, reagent reservoirs, liquid sample stream, $TNT_{ase}$ and bioluminescence reaction cells, and light detector.

Practical implementation of this detector module is based on the fabrication of the $TNT_{ase}$ and bioluminescence reaction cells. It is accomplished with a heterogeneous reactor bed onto which the $TNT_{ase}$ enzyme is efficiently immobilized in the $TNT_{ase}$ reaction cell, while the bacterial luciferase and oxidoreductase enzymes are co-immobilized in the bioluminescence reaction cell. A microbore guard column packed with activated sepharose 4B matrix comprises the $TNT_{ase}$ reaction cell. It is a CTFE rod with a drilled hole 1 mm in diameter and 2 cm long. The bioluminescence cell is a 10- 1 Drummond Microcap column packed with activated sepharose 4B matrix (14,15). Figure 3 depicts the bioluminescence reaction cell assembly.

As described earlier, the sample liquid stream converges continuously with reagent streams at a heterogeneous chemical reactor, the $TNT_{ase}$ reaction cell of Figure 2. The TNT and reagent reaction is catalyzed by the TNT enzyme immobilized on the surface of the reactor bed as described by reaction (b). Subsequently, the reaction product stream flows to the bioluminescence reaction cell, where the bioluminescence occurs, reaction (c), producing bioluminescence as one of the reaction products. The bioluminescence intensity is inversely proportional to the TNT vapor concentration in air (15).

Table 2 (18) lists data on the performance of the TNT bioluminescence detector module breadboard. A 0.25-ppt TNT concentration level in air is detectable, i.e., MDC = 0.25 ppt, after a 20-min sample time by the sample train. The performance specifications of the modules in the system are adequate for the TNT vapor monitoring application described earlier. The

detector module total time required to perform the transduction is less than 103 sec. Most of the time required for the detection is in the preconcentration process.

Experimental work is currently in progress to determine the detector module zero and span instabilities. The span and zero instabilities obtained to date show that additional work is required to stabilize both reactions (a) and (c) or reaction (c) alone. Obtaining low zero and span drifts is of significant importance in minimizing the system false-alarm probability (18).

3.3 Calibrator

A system explosives vapor challenge is performed periodically by a calibrator. Calibration gas is produced in a thermally controlled, packed-bed column containing a pure TNT coating on the bed particles (17,19).

3.4 Specificity and Interferent Responses

A quantitative indication of the $TNT_{ase}$ specificity to TNT was obtained by subjecting a variety of explosives and possible interferent species to a prescreening process by the methods of the Michaelis-Menton kinetic assessment (20). This method provides a valid assessment for zero relative response measurements, i.e., a zero relative response measurement with the Michaelis-Menton surely means a zero relative response of the TNT vapor detection system. A greater than zero response, however, usually requires further quantitative verification obtained from the detection system response.

A Cary Spectrophotometer model was used to measure the relative responses of various explosives and possible interferents to that response obtained from the TNT exposure to the TNT enzyme. The reference cell contained buffer (50 mM acetone, 50 mM MES, 100 mM TRIS at pH = 7.0, total volume of 990 µl) plus 10 µl of the TNT enzyme. The sample cell contained buffer, 10 µl TNT enzyme, 10 µl 30 mM NADH, and 10 µl of the explosive or interferent.

PETN, RDX, EGDN, NG, diehtylineglycol dinitrate (DEGDN), HMX, and Semtex showed zero relative response to TNT. Nitropyradine had a 0.028 relative response to TNT. Dinitrotoluene (DNT), nitrofuran, and nitropyradine. The relative response measurements showed an adequate specificity to TNT, thus excluding a response to other types of explosives. A small but measurable relative response to nitroheterocyclic compounds appeared. Further work is required to determine the interferent TNT equivalent response of these compounds.

4. MULTI-EXPLOSIVES VAPOR DETECTION AND IDENTIFICATION SYSTEM

The prescreening process provided the expected results. The enzyme was specific, as anticipated, and reacted only with compounds of similar structure to TNT, but with less intensity. The specificity of enzymes suggests the

possible development of a multi-explosives vapor detection and identification system. By developing separate enzymes for each explosive or family of explosives, the detection system will also be able to identify which explosives are present and in what quantity.

The U.S. Army is examining the feasibility and utility of a multi-explosives vapor detection and identification system using enzymatic bioluminescent techniques. It appears that the system can be of significant utility in pre- and post-bomb detonation inspection scenarios (21). A system exhibiting performance specifications similar to those of Table 2 for the bioluminescent TNT detection system is adequate for monitoring enclosures (as summarized by Table 1) for the explosives most favored by terrorists or underworld bombers.

The multi-explosives detection and identification system comprises the modules of Figure 1. A calibrator or vapor generator carrying a multitude of explosives sources will be required, otherwise the system is identical to the TNT vapor generator (17,19), including the sample train (16,17).

An array of enzymatic reaction cells are required by the detector module, each specific to a corresponding type of explosive. For example, one configuration of the detector module is shown by Figure 4. Four reaction cells are arrayed in parallel hydrodynamically: an $EXPLO_{ase}$ reaction cell, a $TNT_{ase}$ reaction cell, a $PETN_{ase}$ reaction cell, and an $RDX_{ase}$ reaction cell. Each reaction cell of Figure 4 is identical to the $TNT_{ase}$ reaction cells described earlier and differs only in that each is provided with the corresponding immobilized enzyme responsive to individual types of explosives. The $EXPLO_{ase}$ reaction cell carries all the enzymes co-immobilized on the substrate.

Reagent and sample streams flow continuously and converge at the inlet of each reaction cell. Each stream thereafter flows through its corresponding reaction cell and 3-way valve ($V_E$, $V_T$, $V_P$, and $V_R$). At this juncture, the resulting streams are diverted by each valve to waste (W) or to the bioluminescence reaction cell.

For the no-general-alarm condition, i.e., TNT, PETN, and/or RDX vapors are absent in the sample or are present at concentration levels below the MDC of the system, the liquid sample and reagent streams flow continuously through the network of Figure 4. The stream emanating from the $EXPLO_{ase}$ reaction cell is diverted by $V_E$ to the bioluminescence reaction cell and ultimately to waste. Concurrently, the liquid streams emanating from the $TNT_{ase}$, $PETN_{ase}$, and $RDX_{ase}$ reaction cells are diverted to waste by $V_T$, $V_P$, and $V_R$, respectively.

In the event of a general alarm, the module 3-way valves are programmed into a sequential diversion of each reaction cell stream from waste to the bioluminescence reaction cell. During the entire sequential stream diversion process, $V_E$ diverts the $EXPLO_{ase}$ stream to waste. An identification of the explosives vapor species is obtained by the stream that initiates a specific alarm, i.e., specific to the stream flowing through the bioluminescence cell at the time of the alarm.

The system is not limited to the three explosives species shown in Figure 4. Additional reaction cells may be added to the network as is deemed practical.

For the four stream networks depicted by Figure 4, the total sample flow rate is approximately 0.148 ml/min or 0.037 ml/min per stream, and the total reagent flow rate is 0.296 ml/min or 0.074 ml/min per stream. On the basis of the bioluminescent TNT vapor detection system, the time required to perform the entire sequence is approximately 515 sec (103 sec per stream). An additional 103 sec is required to clear the lines at the start of each sequence. A time increment of 103 sec is added to the sequence for each additional stream added. The minimum total volume of liquid sample required per cycle is 1.27 ml, and the total processing time is 8.58 min.

## 5. CONCLUSIONS

With the completion of the prescreening tests on the TNT enzyme, and based on the results obtained, BRDEC concludes that a multi-explosives vapor detection and identification system can be successfully developed. It will require replacing several components currently comprising the TNT detector module, such as sample and reagent stream flow rate control components and cooling the photomultiplier tube to reduce the detector module noise level (22). Rigorous production control techniques must be developed and implemented in the assembly of the $EXPLO_{ase}$ and bioluminescence reaction cells to minimize zero and span drift.

Work on a multi-explosives vapor detection and identification breadboard system will be deferred until reaction cells are produced that incorporate co-immobilized enzymes for several types of explosives. Interferent tests will be performed with the chosen explosives catalysts with verification by a reference technique.

## ACKNOWLEDGEMENT

Special thanks to S.K. Hendrickson of Germantown, Maryland, for editing and managing the preparation of this manuscript.

REFERENCES


1. H.C. Egghart, "The MERADCOM In Vitro Biosensor Program," Report 2364, U.S. Army Mobility Equipment Research and Development Command, Fort Belvoir, Virginia, June 1982.

2. M. DeLuca and D. Vellom, "Detection of Low Levels of TNT Using Immunologic and Bioluminescent Techniques," U.S. Army Contract DAAK-70-79-C-0174, University of California at San Diego, October 1, 1979, through September 30, 1982.

3. C. Bryant and T. Martin, University of California, San Diego, "Bimonthly Progress Report," Contract No. DAAK70-86-K-0031, June 1987.

4. D.P. Lucero, "User Requirement and Performance Specifications for Explosives Vapor Detection Systems," J. Testing and Evaluation 13, 1985, p. 222.

5. D.P. Lucero and E.M. Boncyk, "Transport and Preconcentration of Explosives Vapors by Liquid Sampling Modules," J. Energetic Materials 4, 1986, p. 473.

6. W.D. Williams and J.K. Syverson, "Explosives Detector Field Tests," Research and Development Division, Bureau of Alcohol, Tobacco and Firearms, U.S. Department of the Treasury, Washington, D.C., April 1981.

7. The Aerospace Corporation, "Reassessment Survey Report on Explosives Detection and Identification Techniques," Report ATR 77(7911-04)-1, April 1977.

8. Proceedings, New Concepts Symposium and Workshop on Detection and Identification of Explosives, NTIS No. PB290055, Washington, D.C., 1978, p. 37.

9. "Symposium on Explosives Detection for Security Applications," J. Testing and Evaluation 13, May 1985, p. 210.

10. D. Vellom, J. Hinkley, A. Loucks, H. Egghart, and M. DeLuca, Analytical Applications of Bioluminescence, The Academic Press, Inc., 1984, p. 133.

11. L.J. Kricka and D. Vellom, Methods in Enzymology 133, 1986, p. 229.

12. H.C. Egghart in Proceedings, New Concepts Symposium and Workshop on Detection and Identification of Explosives, NTIS No. PB290055, Washington, D.C., 1978, p. 169.

13. L.J. Kricka, G.K. Wienhauser, J.E. Hinkley, and M. DeLuca, Analytical Biochemistry 129, 1983, p. 392.

14. G.K. Wienhauser, L.J. Kricka, J.E. Hinkley, and M. DeLuca, Applied Biochemistry and Biotechnology 7, 1982, p. 463.

15. M. DeLuca and D. Vellom, "Detection of Low Levels of TNT Using Immunologic and Bioluminescent Techniques," Report No. DAAK70-79-C-0174, University of California at San Diego for U.S. Army Mobility Equipment Research and Development Command, Fort Belvoir, Virginia, 1982.

16. Midwest Research Institute, "Design and Develop a Vapor/Liquid Interface," for U.S. Army Belvoir RD&E Center Procurement and Production Directorate, Fort Belvoir, Virginia, Contract No. DAAK70-83-C-0068, August 3, 1985, to August 3, 1986.

17. Midwest Research Institute, "Design and Develop a Vapor/Liquid Interface," Final Report, May 1988.

18. E.M. Boncyk and D.P. Lucero, "Bioluminescent TNT Detection System," in Proceedings of International Congress on Applied Criminology, Gent, Belgium, 1988.

19. P.A. Pella, Anal. Chem. 48, 1976, p. 1632.

20. L. Stryer, Biochemistry, 3rd edition, W.H. Freeman and Company, New York, 1988, pp. 187-195.

21. J. McBride, Philadelphia Police Department, Philadelphia, Pennsylvania, private communication with E.M. Boncyk, U.S. Army Belvoir RD&E Center, Fort Belvoir, Virginia, April 1988.

22. G.C. Young, "Photomultiplier Tubes and Their Applications," R/P055T72, International Symposium on Microscopy, Oxford, England, April 1972.

**Figure 1.**
**Vapor Detection System**

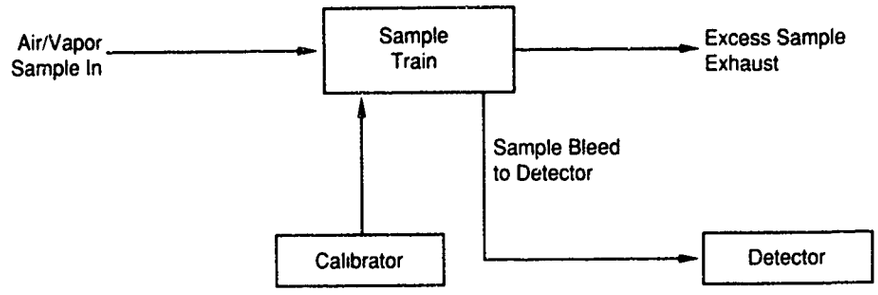


**Figure 2.**
**Bioluminescent TNT Detector Module**

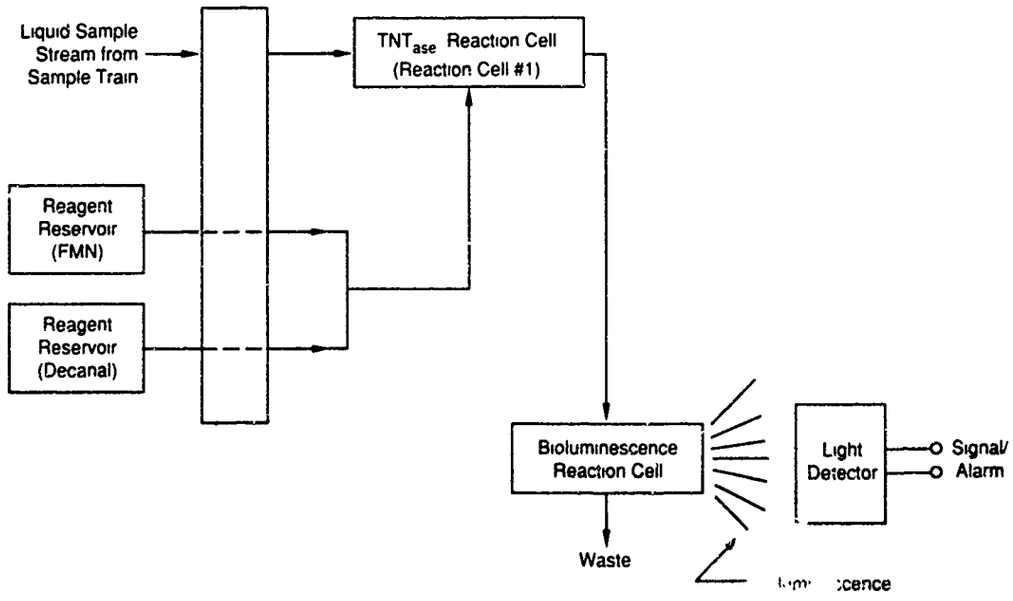

**Figure 3.**
**Bioluminescence Reaction Cell[11]**

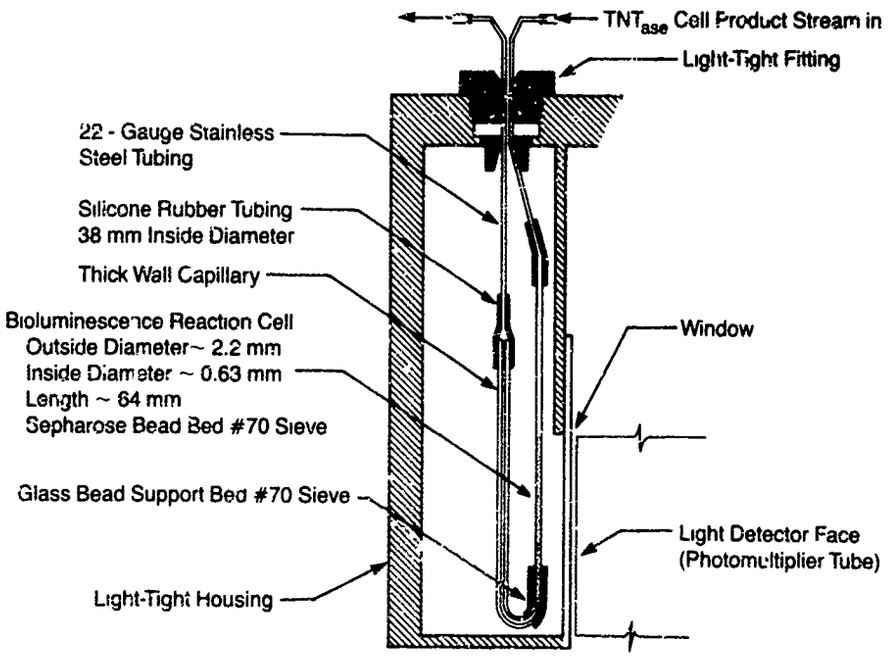

**Figure 4.**
**Bioluminescent Explosives Vapor Detection and Identification Module**

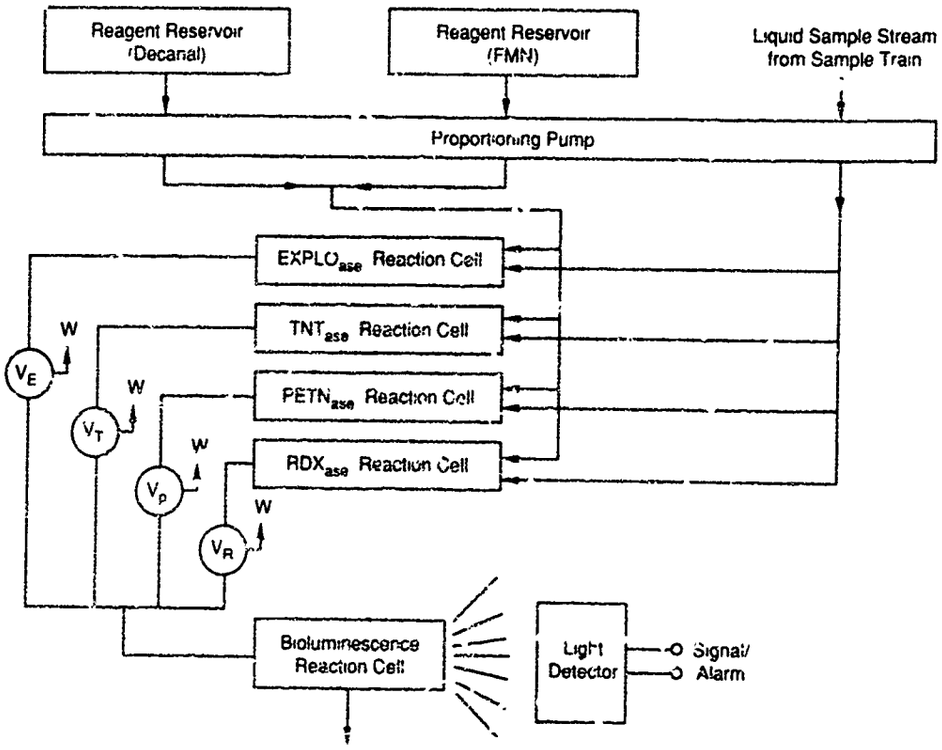

**Table 1.**
**Explosives Vapor Detection System User Requirements and Performance Specifications [4,5]**

| Application/Requirement | Processing Item/Personnel Examination @ Processing Station | Searching Area Search and Examination | Monitoring Enclosure Monitoring |
|---|---|---|---|
| Maximum Missed-Alarm Probability | $< 5 \times 10^{-4}$ | $< 5 \times 10^{-4}$ | $< 5 \times 10^{-4}$ |
| Maximum False-Alarm Probability | $< 5 \times 10^{-4}$ | $< 0.05$ | $< 5 \times 10^{-4}$ |
| Processing/Examination Rate | 15 (Item-People/Min) | 28m$^3$ (1000 Ft$^3$/Min) | Continuous |
| Minimum Detectable Concentration @ Sample Train Inlet, ppt | [illegible] | 1 | 0.001 |
| Maximum Allowable Alarm Set Point Concentration, ppt | 5 | 5 | 0.005 |
| Maximum Allowable False-Alarm Probability @ 5 ppt | $< 10^{-4}$ | $< 0.04$ | $10^{-4}$ |
| Maximum Allowable Missed-Alarm Probability @ 10 ppt | $< 10^{-4}$ | $< 0.04$ | $< 10^{-4}$ |
| Maximum False-Alarm Probability with Interferent @ 1 ppt | $2.3 \times 10^{-3}$ | $< 0.06$ | $2.3 \times 10^{-3}$ |
| Maximum Missed-Alarm Probability with Interferent @ 1 ppt | $2.3 \times 10^{-3}$ | $< 0.06$ | $2.3 \times 10^{-3}$ |

Table 2. Operating Specifications*

The system operating parameters are selected to obtain a system response to TNT-in-air samples. To generate the TNT concentration samples over the 0.01- to 1.0-ppt range, the output TNT concentration of the calibrator must be varied by a combination of changes to the calibrator output flow rate and TNT column temperature. Specifications were obtained from independent module tests.

| | |
|---|---|
| **Sample Train (18)** | |
| Sample flow rate (l/min) | 150 |
| Liquid volume discharge (ml) | 3.5 |
| Sampling time (min) | 5, 10, 15, 20 |
| TNT input concentration (ppt)** | 0.014 to 0.28 |
| Preconcentration: | |
| (1) 5-min sample time | 107,000 |
| (2) 20-min sample time | 429,000 |
| **Calibrator (18)** | |
| Column temperature (°C) | 5 to 20 |
| TNT output concentration (ppb) | 0.7 to 3.5 |
| Carrier gas flow rate (ml/min) | 3 to 12 |
| **Detector Module+** | |
| Detanal flow rate (ml/min) | 0.037 |
| EMN flow rate (ml/min) | 0.037 |
| Sample flow rate (ml/min) | 0.037 |
| Noise equivalent TNT concentration++ in liquid solution (nM/l) | 2.4 |
| Minimum detectable concentration (ppt): | |
| (1) 5-min sample time | 1 |
| (2) 20-min sample time | 0.25 |
| Average time rate-of-response (s): | |
| (1) rise time | 53 |
| (2) fall time | 53 |
| (3) lag time | 50 |
| (4) total time | 103 |
| Linearity (percent) | Experiments in progress |
| Span drift (percent full scale/h) | Experiments in progress |
| Zero drift (percent full scale/h) | Experiments in progress |
| Interferent equivalent response (ppt) | Experiments in progress |

* D.P. Lucero, J. Testing and Evaluation 13, 1985, p. 222.

** Resultant TNT input concentration after mixing calibrator output gas flow (3 to 12 ml/min) and sample train sample flow (150 l/min).

\+ Federal Register 40, 33, 1975, pp. 7053-7057.

++ Noise equivalent concentration of TNT in air has no direct meaning because MDC is determined by preconcentration. Noise reduction is related only to liquid detector module.

# COMPARISON OF DIFFERENT TECHNIQUES FOR THE HEADSPACE ANALYSIS OF EXPLOSIVES

John R. Hobbs and Edward Conde

Transportation Systems Center
Research and Special Programs Administration
U. S. Department of Transportation
Kendall Square, Cambridge, Mass. 02142, USA

## ABSTRACT

Various sampling and analysis methods were used to analyze the headspace vapors over various explosives samples in order to characterize them. Sampling techniques such as direct headspace sampling, trapping on Tenax with thermal release, and sampling onto coated platinum wire with subsequent thermal release were investigated. Detection techniques used included Ion Mobility Spectrometry, Capillary Gas Chromatography with Electron Capture Detection, and Capillary Gas Chromatography with Mass Spectrometry. The results show that certain sampling techniques and certain detection techniques can provide more information than other techniques, and that some methods can provide faster preliminary information.

## 1. INTRODUCTION

The characterization of the headspace volume above explosives continues to be of interest to those attempting to detect explosives by sampling their emitted vapors. In the course of the measurement of TNT vapors in soil samples over

buried land mines, the method of choice was extraction of the soil with acetone and analysis of the extract by capillary gas chromatography with detection by thermal energy analysis (GC-TEA). When no TNT was found from samples buried for one year, it was decided to sample the soil headspace with the ion mobility spectrometer (IMS). The results of this sample clearly revealed the presence of TNT. Based on this result, the soil extracts were then re-examined using capillary gas chromatography with electron capture detection (GC-ECD), and the TNT was detected in all the earlier samples that did not show TNT by GC-TEA. This result clearly shows that much time and effort could have been saved had the correct technique been used initially. It is the purpose of the work reported in this paper to present a comparison of various headspace techniques that were utilized and the results obtained by each. Of the methods investigated, trapping on Tenax and thermal release directly into the injector of a gas chromatograph with electron capture detection appeared to offer the best results. The advantages and disadvantages of the methods studied will be discussed.

## 2. EXPERIMENTAL

### 2.1 Sampling Methods

The explosives samples were placed into glass jars equipped with plastic lids lined with teflon. Two holes were drilled into the lid and teflon liner so that two sealed disposable pipets could easily be inserted and removed from the lid. Sampling onto

the coated platinum wire was done using the Xontech Model 7101 portable sampler and cartridge shown in Figure 1. The sampler inlet was placed into the jar with explosives and the sampler turned on for the desired sample time. The Tenax traps were Chemical Data Systems (CDS) stainless steel traps 6" long x 1/4" OD, packed with Tenax and threaded on one end with 10/32 threads. Sampling onto the Tenax traps was accomplished using a constant volume sampler (1) connected to the Tenax trap. The trap was placed into the explosives sample jar through one of the drilled holes and helium purge gas was flowed into the jar through the other drilled hole. The flow of the constant volume sampler and the helium purge flow were adjusted for proper flow through the Tenax trap. After the proper sample time, the Tenax trap was removed for analysis.

## 2.2 Desorption Methods

Two thermal desorption methods were used. The first apparatus was the Chemical Data Systems Model 320 Thermal desorption unit. In this unit the stainless steel Tenax trap was thermally desorbed at 146 C with helium gas at 30 milliliter per minute. The desorbed sample was then trapped internally in the unit on another, longer Tenax trap. From this trap, the sample was again thermally desorbed onto the front of another Tenax trap where it was finally desorbed and backflushed through a heated transfer line to the gas chromatograph for analysis.

The second thermal desorption apparatus consisted of a Luer-Loc fitting with a 10/32 male thread and an O-ring which was screwed into the threaded end of the stainless steel Tenax trap. Next, a syringe needle was attached to the Luer-Loc fitting and the other end of the trap was connected to a Teflon connector which in turn was connected to a 10 milliliter per minute helium flow (Figure 2). This entire assembly was inserted through a hole drilled in an aluminum block that was heated by a temperature controlled heating mantle and into the septum of the gas chromatograph. A thermocouple to measure the desorption temperature was placed into the aluminum block next to the Tenax trap (Figure 3).

The desorption method used for the Xontech platinum wire concentrator is shown in figure 4 and has been described in detail elsewhere (2).

## 2.3 Analytical Methods

A Hewlett Packard 5890 gas chromatograph was used both with the electron capture detector and and with a Hewlett Packard 5970B mass selective detector coupled via a direct interface. In both cases the samples were introduced into a split injector, with the total split flow set to 2 milliliter per minute. The column used with the electron capture detector was a 15 meter Supelco SPB-5 held at 40 C for ten minutes, temperature programmed to 140 C at a rate of 10 C/min, and finally held a 140 C for 30 minutes. The column used with the mass selective detector was a 30 meter J&W Scientific DB-5, operated as above.

A Franklin GNO Beta 7 Ion Mobility Spectrometer (IMS) was used in the atmospheric sampling mode to analyze vapors trapped on the Tenax traps. The same stainless steel Tenax traps were used without the needle and the O-ring. Medical air was flowed through the Tenax trap at 10 milliliters per minute, and the entire trap was placed in the heated quartz inlet of the IMS. The IMS was operated at atmospheric pressure and 200 C. The drift gas was air at a flow rate of 500 milliliters per minute, the carrier gas was air at a flow rate of 100 milliliters per minute, and the exit vacuum flow was set at 700 milliliters per minute. As a result of these conditions, 200 milliliters per minute of room air were continuously drawn into the heated inlet. The trapped material from the Tenax trap was desorbed into this air stream and analyzed.

IMS studies were also made when sampling the headspace vapors directly into the heated inlet of the IMS unit operated as above.

## 3. RESULTS

The explosives samples studied in this investigation were Semtex, Hercules 40-percent dynamite, Atlas NCN slurry explosive, and Hercules Unique double-based propellant. These explosives were chosen because they represent a wide variety of explosives and offer a wide range of vapor pressures to investigate. The data will be discussed in terms of the headspace method used and results for each explosive will be compared.

### 3.1 Xontech Platinum Wire Concentrator

The Xontech platinum wire concentrator only worked marginally for the 40 percent dynamite sample. Although a capillary column was used, the peaks were broad and the resolution was poor. These results are probably due to the large diameter of the sampling head causing peak broadening and sample loss. In addition, either the concentration of headspace vapors from the other explosives was too low for detection or, the coating on the platinum wire was not optimum for their adsorption. This headspace concentrator was the least effective of the three investigated.

### 3.2 Chemical Data Systems Model 320 Concentrator

The results using the Chemical Data Systems Model 320 concentrator are shown in Figures 5 through 8. Figure 5 shows the GC-ECD capillary chromatogram of a 5 second headspace sample above the 40-percent Hercules dynamite. The peaks at retention times 16.2 and 22.1 minutes were identified by retention time measurements as ethylene glycol dinitrate (EGDN) and nitroglycerine (NG), respectively. The other peaks in the chromatogram have not be identified.

The GC-ECD chromatogram of the headspace vapors above Atlas NCN slurry explosive is shown in Figure 6. The peak at retention time 16.2 minutes is a trace of EGDN contamination as determined from data previously reported on this sample (2). The other peaks have not be identified. There is some indication from

retention time measurements that the peak at retention time 2.3 minutes may be due to nitromethane, but this has not been confirmed.

The GC-ECD chromatogram of Hercules Unique double-based propellant headspace vapors is shown in Figure 7. Again the characteristic peak for EGDN is seen at retention time 16.2 minutes and there is a small peak at retention time 22.2 corresponding to NG. Other peaks have not been identified.

Finally, the chromatogram for the headspace analysis of Semtex is shown in Figure 8. The vapors were collected for one hour and only very small peaks were found. The EGDN peak at 16.2 minutes is evident and was also observed in the bulk analysis of this particular Semtex sample. Obviously, the vapor pressures of PETN and RDX are quite low and do not appear in the chromatogram.

### 3.3 Tenax Needle Method

The results using the Tenax needle apparatus are shown in Figures 9 through 12. The GC-ECD chromatogram of a 1-second sample of the headspace above the 40 percent Hercules dynamite is shown in Figure 9. The large peak at retention time 16.2 minutes has been confirmed to be EGDN. Based on retention time measurements, the peak at 22.1 minutes is NG. The peak at 21.1 minutes corresponds to an impurity found in the chromatogram of NG taken from a transdermal nitro patch. The other peaks have not been identified.

Figure 10 shows the GC-ECD chromatogram of a 20-minute headspace sample above the Atlas NCN slurry explosive. EGDN is again identified as the peak at retention time 16.2 minutes.

A 30 minute headspace sample of vapors above Hercules Unique double-based propellant produced the GC-ECD chromatogram shown in Figure 11. Again a strong EGDN peak is seen at retention time 16.2 minutes and the characteristic NG peak at retention time 22.1 minutes. The large peak at 18.4 minutes has not been identified. A large peak is also observed at retention time 21.1 minutes corresponding to the impurity peak mentioned above. The large peak at retention time 23.0 minutes has not been identified.

Figure 12 shows the GC-ECD chromatogram of a 30 minute headspace sample from Semtex explosive. A very large EGDN peak is observed at retention time 16.1 minutes. The small peak at 22.0 minutres is due to a trace of NG. There is also a trace of the NG impurity mentioned above at retention time 21.1 minutes. The peak 27.1 minutes has been identified by retention time measurements as 2,4-Dinitrotoluene (2,4-DNT). The peak at retention time 24.8 has not been identified.

### 3.4 Ion Mobility Spectrometry Studies

IMS data were taken by two methods. In the first method the headspace vapors were trapped on the Tenax traps as described above and desorbed into the heated inlet of the IMS. In the secondr method, the headspace vapors above the explosives were sampled directly into the heated inlet of the IMS instrument.

The Tenax trap method presented some difficulty in that the background in the IMS was constantly changing and often quite complex. More work needs to be done with this technique, but it should prove to be quite sensitive, based on the direct headspace sampling described below.

The results of the direct headspace sampling of the explosives samples are shown in Figures 13 through 16. Figure 13 shows the IMS spectrum of the headspace vapors above the Hercules 40-percent dynamite. The single peak at drift time 8.43 msec corresponds to the NO3- Ion with reduced mobility 2.53.

Figure 14 shows the IMS spectrum of the headspace vapors above the Atlas NCN slurry explosive. The predominant peak occurs at 8.31 msec and reduced mobility 2.59 and probably corresponds to the NO3- ion.

The IMS spectrum of the headspace vapors above Hercules Unique double-based propellant is shown in Figure 15. Again, the major peak appears at drift time 8.61 msec and reduced mobility 2.53, corresponding to the NO3- ion. There are two small drift peaks at 13.59 msec and 14.22 msec with reduced mobilities of 1.61 and 1.63, respectively that have not been identified.

Figure 16 shows the IMS spectrum of the headspace vapors above Semtex explosive. The predominant peak occurs at drift time 8.42 msec and reduced mobility of 2.53 corresponding to the NO3- ion. The peak at drift time 14.46 msec and reduced mobility 1.48 matches the peak from RDX, while the peak at drift time 15.20 msec and reduced mobility 1.40 matches the predominant peak from pentaeryithol tetranitrate (PETN).

### 3.5 GC-MS Studies

The Tenax needle trap was installed on a Hewlett Packard 5890 capillary gas chromatograph connected to a Hewlett Packard 5970B mass spectrometer via a direct capillary interface. This technique worked well with high vapor pressure explosives such as the 40 percent dynamite, but did not have sufficient sensitivity to detect the trace explosives vapors above the low vapor pressure explosives such as Semtex and C4. The total ion chromatogram of the vapors from a 1 hour headspace sample of Semtex explosives showed only hydrocarbons coming from the oils, dyes, and plasticizers used in the explosives. In this scanning mode no nitrated explosives compounds were found. However, in the single ion monitoring mode, scanning masses 30, 46, 76, and 120, the resultant total ion chromatogram shown in Figure 17 was obtained. Peaks are due to m/z=30, NO ion; m/z=46, NO2 ion; m/z=76, CH2NO2 ion; and m/z=120, CH2N(NO2)2 ion. The m/z= 30 and 46 ions can come from any nitrated explosives, while the m/z=76 ion comes from EGDN and NG, which have already been shown to be present in this sample. The m/z=120 ion is a predominant ion in the mass spectrum of RDX which is present in this sample. PETN was not detected specifically since the mass spectrum of PETN shows mainly m/z= 30 and 46, and is hard to distinguish from the mass spectrum of the nitrate esters. The method lacks the overall sensitivity of the GC-ECD technique, but could provide useful information under the right circumstances.

## 4.0 DISCUSSION AND CONCLUSIONS

Of the headspace techniques investigated, the Tenax needle trap with GC-ECD detection proved to be the most sensitive and to provide the most useful information. Headspace vapors were able to be collected and analyzed for the four different types of explosives that varied widely in vapor pressure. The Tenax needle tarp apparatus could also be used with GC-MS with limited success in the single ion monitoring mode, although it was not as sensitive as the GC-ECD. With further work, the Tenax needle apparatus could also be used with the IMS detector. With this detector, shorter trapping times are required and this technique could provide useful, preliminary information that could direct one to the appropriate analytical technique for the complete analysis of a particular explosive. For example, debris from a bomb scene investigation could be sampled either using the Tenax needle trap or directly with the real time inlet into the IMS detector, and this preliminary analysis might indicate the types of explosives one should search for in a complete analysis.

The two commercial systems, the Xontech platinum wire concentrator and the Chemical Data Systems Model 320 concentrator, are not adequate for the low vapor-pressure materials, but performed adequately for high vapor pressusre materials, such as dynamite. The CDS-320 was designed for environmental applications and works well for vapors at the part-per-billion level, but suffers from dead volumes, long transfer lines, and poor GC resolution when looking for much lower levels associated with analysis of headspace vapors above explosives.

In conclusion, the Tenax needle trap has been shown to work very well with the capillary GC-ECD system and should be able to be made to work with the IMS detector. Used with GC-MS in a single ion monitoring mode and, in particular, with either chemical ionization or atmospheric pressure ionization, should provide useful data from the headspace analysis of explosives.

## REFERENCES


1. John R. Hobbs, Darryl Howes, and Steve Kellner
   An Explosives Vapor Generator For Calibration of Explosives Vapor Detectors, U. S. Department of Transportation, Federal Aviation Administration Report No. FAA-RD-80-131, 1980.

2. John R. Hobbs and Edward Conde
   Vapor Characterization of Water Gel Explosives
   Presented at the Second International Symposium on the Analysis and Detection of Explosives, Israel, 1986
   Published in Journal of Energetic Materials, 4, Nos. 1-4, 511, 1986.

Figure 1. Xontech Model 7101 Sampling Pump.

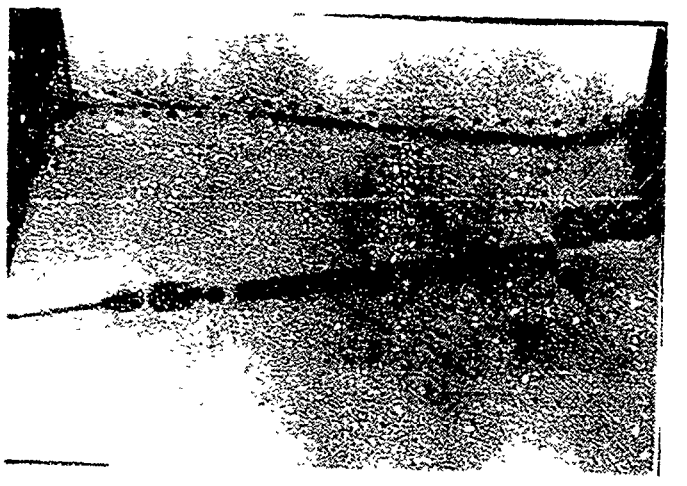

Figure 2. Tenax Needle Trap.

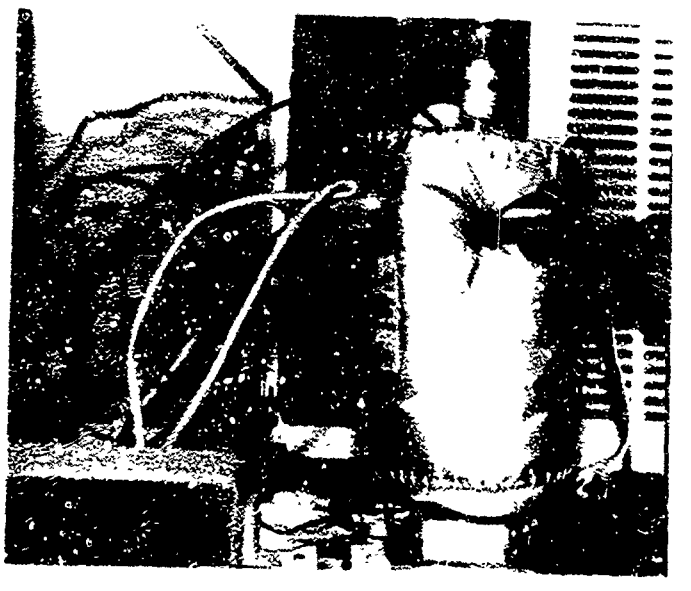

Figure 3. Tenax Needle Adsorber Apparatus

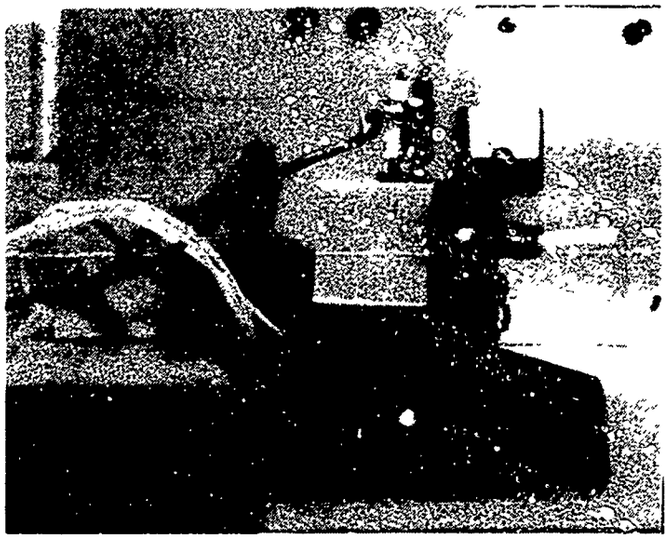

Figure 4. Xontech Platinum Wire Desorber

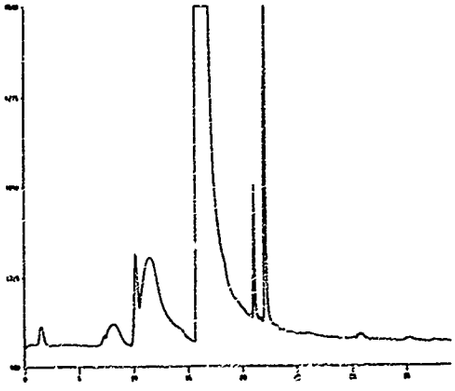

Figure 5. GC-ECD Chromatogram of Hercules Dynamite by CDS-320 Concentrator.

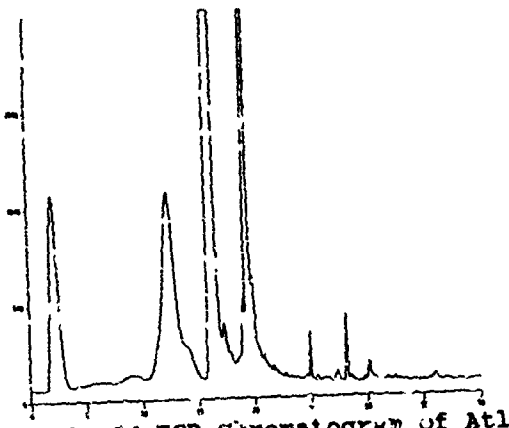

Figure 6. GC-ECD Chromatogram of Atlas NCN Slurry by CDS-320 Concentrator.

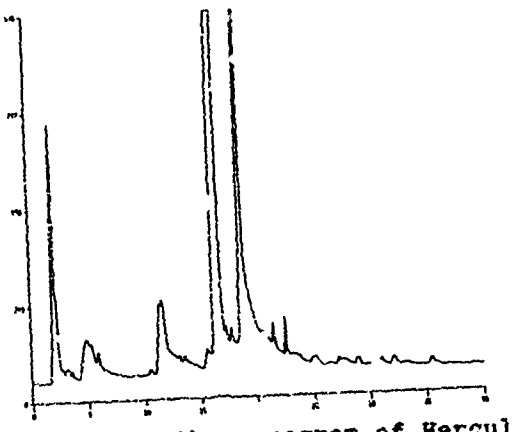

Figure 7. GC-ECD Chromatogram of Hercules Unique Double-based Propellant by CDS-320 Concentrator.

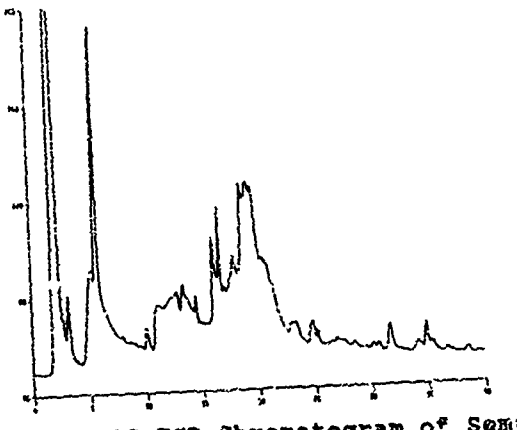

Figure 8. GC-ECD Chromatogram of Semtex by CDS-320 Concentrator.

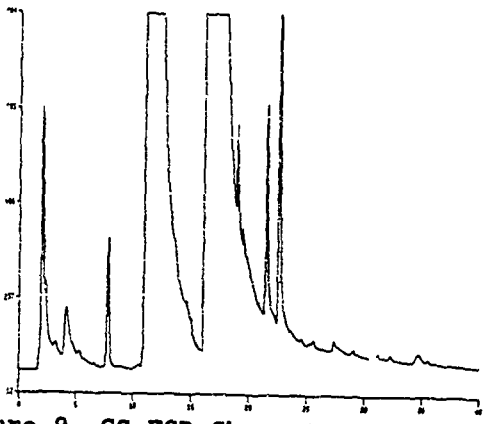

Figure 9. GC-ECD Chromatogram of Hercules Dynamite by Tenax Needle Trap.

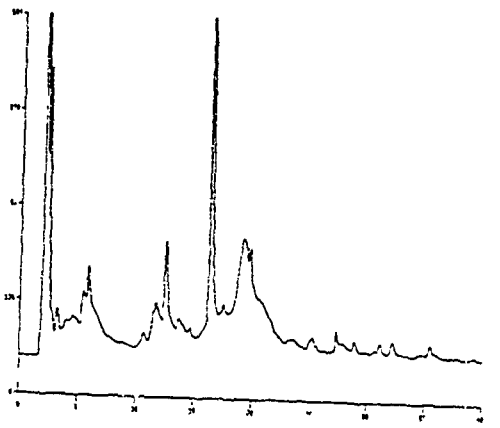

Figure 10. GC-ECD Chromatogram of Atlas NCN Slurry Explosive by Tenax Needle Trap.

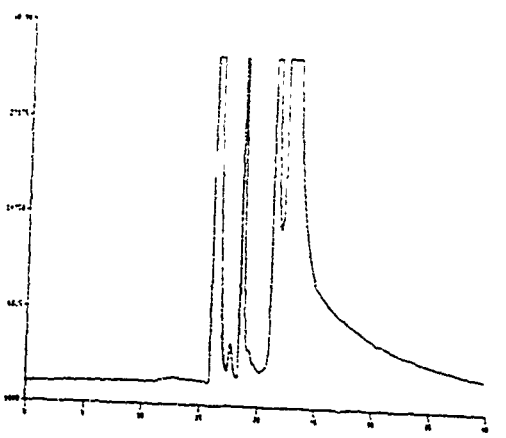

Figure 11. GC-ECD Chromatogram of Hercules Unique Double-based Propellant by Tenax Needle Trap.

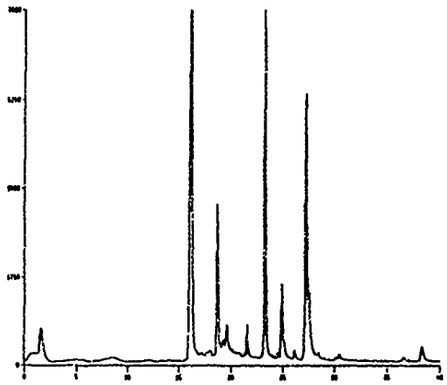

Figure 12. GC-ECD Chromatogram of Semtex Explosive by Tenax Needle Trap.

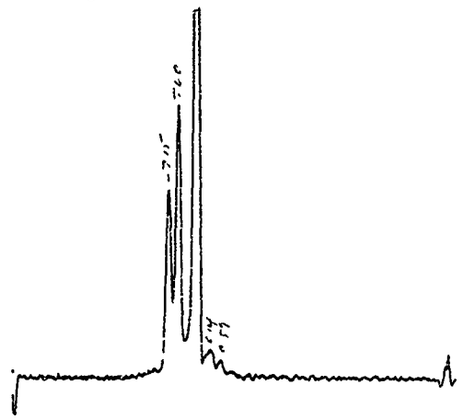

Figure 13. IMS Spectrum of hercules Dynamite.

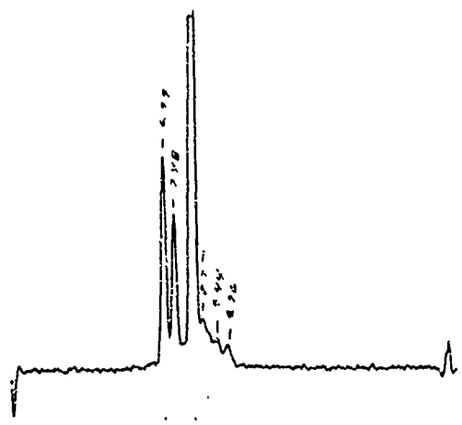

Figure 14. IMS Spectrum of Atlas NCN Slurry Explosive.

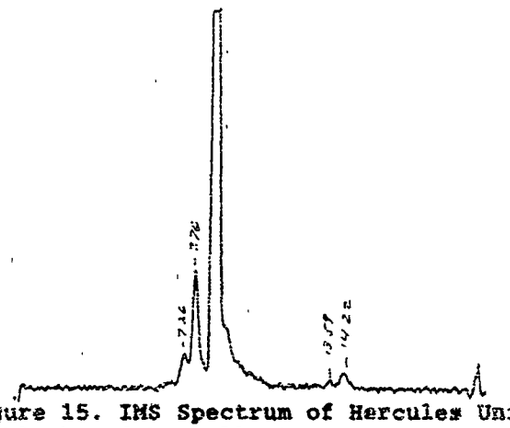

Figure 15. IMS Spectrum of Hercules Unique Double-based Propellant.

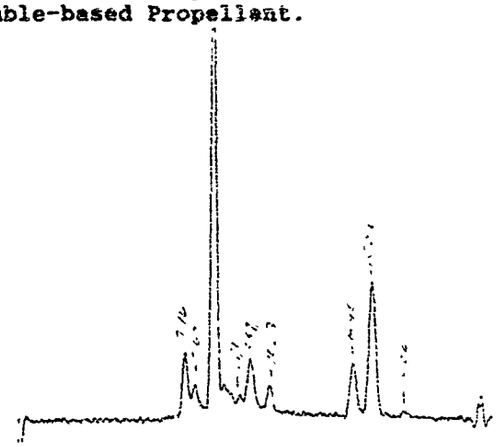

Figure 16. IMS Spectrum of Semtex Explosive.

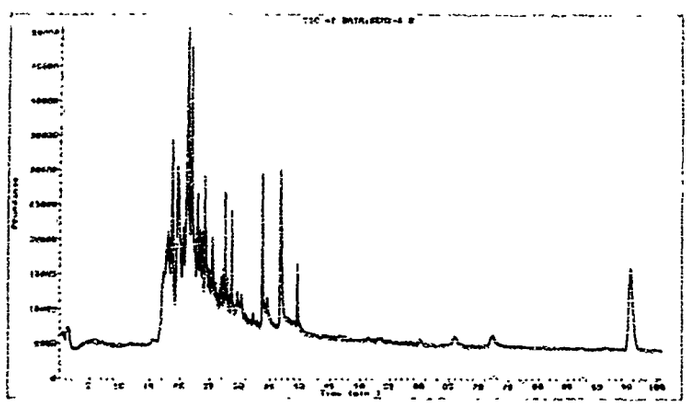

Figure 17. Total Ion Chromatogram from Single Ion Monitoring of Semtex Headspace Sample.

# DEVELOPMENT OF A PORTABLE EXPLOSIVES DETECTION SYSTEM

Rudy Jackson
Dipomatic Securities Division
U. S. Department of State
Washington D. C.

Edward E. A. Bromberg
Thermedics, Inc.
470 Wildwood St.
Woburn, MA 01888

## Abstract

The U. S. Department of State, as part of its continuing effort to increase the safety of its personnel overseas, has funded the development of a portable explosives detector. This detector consists of two sections, a sampling device and an analysis unit. The system self calibrates, alarms when an explosive is found, and identifies the type of explosive. Water is the only consumable. The system is rugged and weather resistant, and able to operate in severe environmental conditions. Operation of the device to screen vehicles, packages, personnel and buildings will be described.

## Introduction

Unfortunately, terrorists activities, especially against civilian targets, have increased over the past few years. Government and military installations and personnel have also been targeted. Many of these attacks, PAN AM 103 for example, involved the use of sophisticated explosive devices, and have led to high casualty rates. In response to these attacks, security at airports, embassies, government offices, and military installations has

increased. The security methods used are personnel-intensive, subjective in implementation, and time consuming. The increased security is inconvenient to those having to pass through the security stations. It is recognized, however, that the inconvenience is a small price to pay for the added security.

Research and development in the security field has been accelerated in recent years in order to automatic screening devices to detect the presence of explosives.[1] These devices include enhanced X-rays, TNA (thermal neutron activation)[2] and vapor detection. Unfortunately, no device can be used by itself for all scenarios where explosive detection is required. These devices must be looked upon as an additional weapon to increase the security of the public, which must be properly integrated into the security techniques currently being used.[3]

This paper will focus on the description of the development and use of a sophisticated explosives vapor detector. The main work described herein was performed under contract with the United States Department of State (DOS) to develop an explosives detector (EGIS®) to screen vehicles and packages (see design goals below). Further work was performed under contract to the United States Federal Aviation Authority (FAA), especially the development of a personnel walk-in device (SecurScan™), and the evaluation of EGIS to screen luggage.

EGIS, a portable vapor detection explosives device, Figure 1, is a highly sensitive and selective device that has been developed to detect many types of explosives,

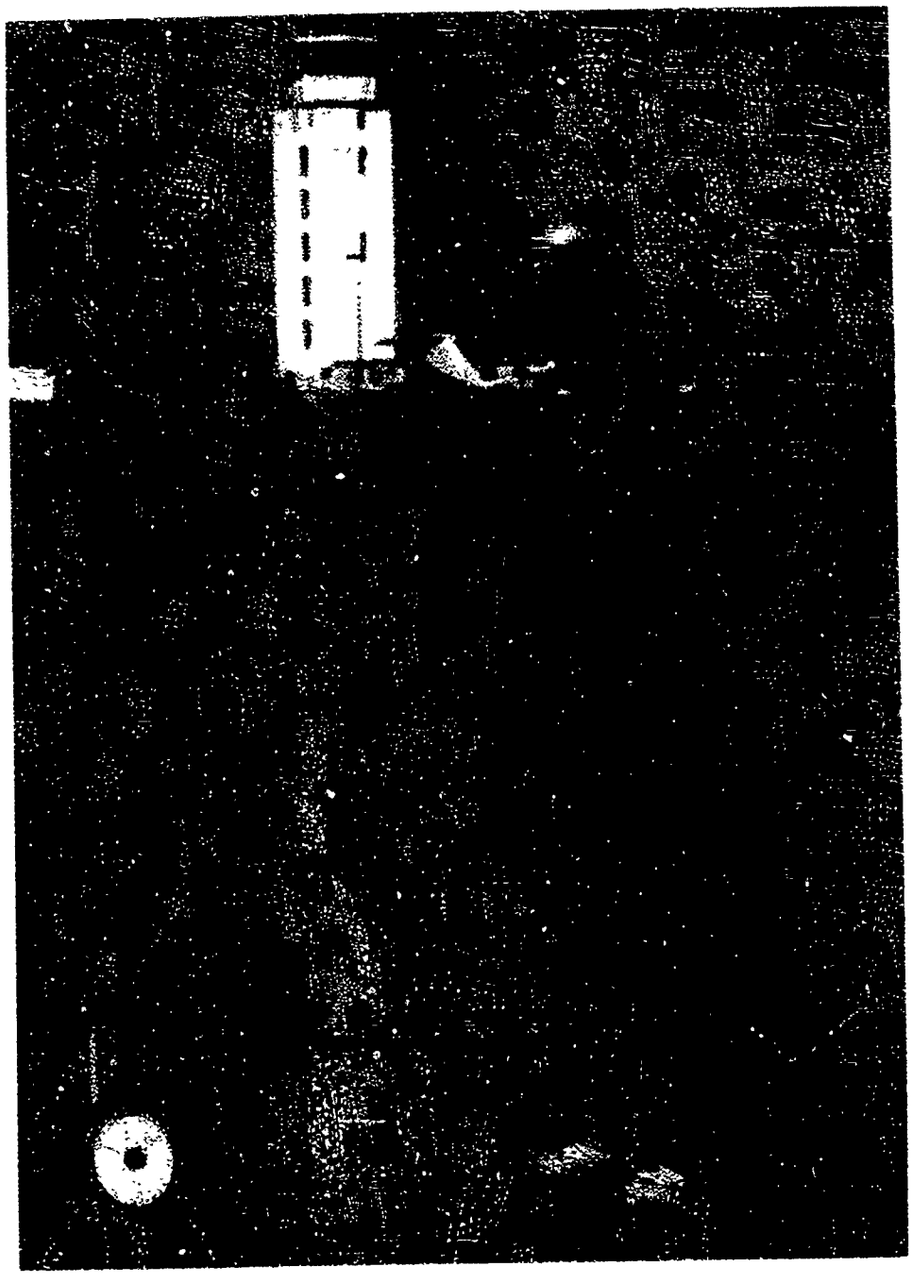

FIGURE 1.

EGIS EXPLOSIVES DETECTOR

including NG, TNT, DNT, PETN, RDX, EGDN. EGIS has been designed to compliment explosives screening techniques currently in use, to increase security at high-risk installations such as airports, jails, and embassies.

SecurScan, Figure 2, contains the same analysis device as EGIS. The sampling area is about the size of a telephone booth. The person to be screened, walks into the booth, waits about 6 seconds in the booth for a proper sampling, turns around and walks out. The sample analysis begins after the person walks out of the sampling area. A second person can be screened, while SecurScan completes the analysis of the first person's sample.

Due to the classified nature of some parts of the device and the test data, it is not possible to provide a detailed description of the chemistry section of EGIS and SecurScan, or of the ultimate sensitivity of the unit.

It should be noted in passing, that the same technology used in EGIS and SecurScan to detect explosives, has been modified in a device (SENTOR™) to detect drugs such as cocaine and heroin.

## General Comments on Vapor Detection

Vapor detection, as is true of all explosive detection techniques, has its strengths and weakness. The equilibrium vapor pressure of an explosive is determined by the type of explosive and the ambient temperature. Assuming that enough explosive is present, a realistic scenario, to reach equilibrium, the vapor pressure is not affected by the amount of explosive present. The rate at which equilibrium

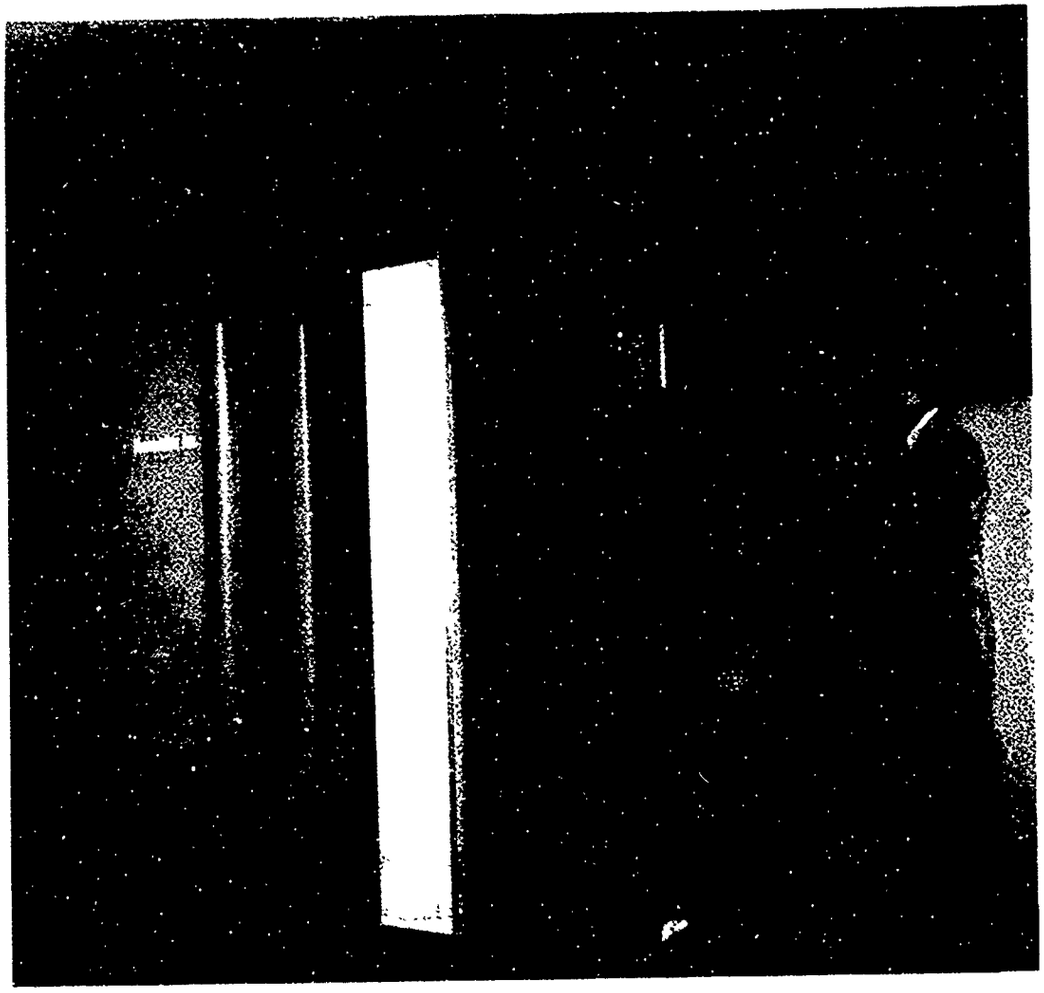

FIGURE 2. SECURSCAN - Portal Explosives Detection System

is reached is a function of surface area, and other secondary effects. Thus, from a purely vapor pressure point of view, a 0.1 kilogram explosive device and a 10 kilogram explosive device, of the same explosive, would have equal probability of being found. From the point of view of size, the 0.1 kilogram device would be easier to hide than the 10 kg device. Additionally, since the vapor detection device should be part of a general security screening system, the 10 kilogram device has a greater probability of being found by other means, visual for example, than the 0.1 kg device.

Table 1 summarizes the equilibrium vapor pressure data, at room temperature, for some of the explosives of interest.[4] This table points out challenges to the development of a vapor detection based explosives detector. First, the large dynamic range required in sensitivity, i.e. seven orders of sensitivity difference between RDX and EGDN. Second, the extremely low vapor pressure for RDX. Note, that the vapor pressure data given in table 1 are the equilibrium vapor pressure. In practice, the probability is that the actual vapor pressure present is significantly below that listed in Table 1. Without divulging the actual lower detectable limit of EGIS, EGIS has been demonstrated to have a sensitivity well below that listed in Table 1 (less than one part in $10^{14}$). Thus EGIS becomes a practical device to be used as part of an explosives screening protocol.

TABLE 1 - Vapor Pressure at Room Temperature

| Explosive | Equilibrium vapor pressure at room temperature Concentration PPT (v/v) |
|---|---|
| EGDN | 100,000,000 |
| NG | 580,000 |
| DNT | 55,700 |
| TNT | 9,400 |
| PETN | 18 |
| RDX | 6 |

Another critical issue, when discussing any detector and sensitivity, is selectivity. Clearly a highly sensitive, but poorly selective, device would be of no practical use since the number of false alarms would be extremely high. EGIS is an extremely selective device, with a very low false alarm rate, determined both by laboratory challenges with many potential interferences, as well as by field trials. EGIS not only alarms that an explosive has been found, but also notifies the user as to which exact explosive, or explosives, have been found.

## DOS Design Goals

Based upon the years of experience that Thermedics had developed in designing and building trace level analyzers, Thermedics was awarded the contract to develope a breadboard explosives detector. The contract goal was to develop an explosives detector whose primary function was to screen vehicles for explosives at the entrance to U.S. embassies overseas. The layout of each embassy is different, and so are the needs at each embassy. In general, automobiles and trucks entering the compound either belong to workers at the

embassy, or trades people, or are official vehicles.

The first prototypes of these detectors were delivered in July of 1986, with some units being installed in embassies overseas to gain operational experience. Based upon the experience gained with these prototype units, clearly defined specifications for the final design of EGIS were developed. The usage goals were expanded to include searching packages, rooms, buildings, and in some cases people. Mobility was also considered a necessary feature, since the unit could then be moved from one location to another, for example, from the embassy compound to a hotel to check individual rooms. Detailed specifications of weight, size, power consumption, environmental, and performance characteristics were also developed, Table 2 is a summary list of the specifications.

EGIS Specifications

The design goals of Table 2 were determined prior to the completion of all of the evaluation testing. Subsequently, several of the targets were found to be incompatible, and compromise adjustments were made. Adjustments were made to the ruggedness, weight and large voltage variation targets. In order to achieve large voltage variation immunity, power conditioning equipment has to be added at additional weight. Ruggedness was also achieved by additional weight to the chassis. In order to make these properties compatible with the desire for a portable unit. the unit was designed in the configuration of a two wheeled cart, which can be disassembled into two readily transportable units.

The third column in table 2 lists any adjustments

Table 2 - Target Specifications for EGIS

| PARAMETER | SPECIFICATION | EGIS |
|---|---|---|
| <u>Performance</u> | | |
| Analysis time | 15 seconds | 30 seconds |
| False alarm rate | 1% | (1) |
| Miss rate | 1% | (1) |
| Lower detectable limit | Confidential | (1) |
| Overload recovery | | |
| Miscellaneous | No harmful gases or substances | meet |
| <u>Operational</u> | | |
| Adjustments | None by user | meet |
| Calibration and span | Automatic | meet |
| Clean cycle | Automatic | meet |
| Diagnostics | Automatic by computer | meet |
| <u>Service and Maintenance</u> | | |
| Electrical reliability | 20,000 hours MTBF | (2) |
| Mechanical reliability | 5,000 hours MTBF | (2) |
| Total system reliability | 1,000 hours MTBF | (2) |
| Mean time for repair | 1 hour | (2) |
| Daily maintenance | 10 minutes | meet |
| Weekly maintenance | 30 minutes | meet |
| Monthly maintenance | 1 hour | meet |
| Semi annual maintenance | 4 hours | meet |

Table 2 - Target Specifications for EGIS
(cont.)

| PARAMETER | SPECIFICATION | EGIS |
|---|---|---|
| Electrical | | |
| Voltage | 90-135 or 180 to 270 field set | meet |
| Frequency | 47-65 Hz | meet |
| Power consumption | 2000 VA | meet |
| Voltage transients | 3 KV maximum | meet |
| Mechanical | | |
| Dimensions | Less than 25 cubic feet | 18 cu ft |
| Weight | Less than 200 pounds | 300 pounds |
| Transportability | In small station wagon, 2 people | meet |
| Environmental | Snow and rain proof | meet |
| Shock and vibration | 6 inch corner drop | (2) |
| Shipping uncrated | 35 kilometers in automobile | (2) |
| Shipping crated | 15,000 kilometers airplane | (2) |
| Environmental | | |
| Storage temperature | -20 to 180 F (-29 to 82 C) | meet |
| Operational temperature | 0 to 120 F (-18 to 50 C) | meet |
| Operational humidity | 0 to 95% noncondensing | meet |
| Warm up time, above 0C | 1 hour | meet |
| Warm up time, below 0C | 2 hours | meet |
| Miscellaneous | | |
| Power failure above 0C | Battery backup computer | meet |
| Power failure below 0C | Battery powered water heater | meet |
| Power failure warm up time | 10 minutes to cold start warm up | meet |
| Remote | Remote annunciator up to 1500 ft | meet |
| Security | Unauthorized, forced entry only | meet |

(1) Exact result dependent upon test protocol
(2) Being evaluated by an independent laboratory

between the original target goal and the final performance specifications of EGIS. It should be noted that some parameters are still under evaluation, MTBF (mean time between failure) for example. Others parameters are classified. The false alarm rate, for example, is dependent upon the exact test protocol used. This protocol is classified.

The EGIS performance results listed here are based upon tests which Thermedics has performed. Independent testing has been arranged for by the Department of State. Those results will be reported separately at a future date.

## EGIS Detailed Description

In use, the guard uses the sampling device to sample the object in question, person, package, vehicle, airplane, or room. The amount of sampling time can vary from a few seconds to several minutes, depending upon the object, security risk and the amount of time available. After sampling, the guard connects the sampling device to the analysis unit, and begins the analysis by pushing the start button. In less than 30 seconds, the analysis is complete; the analysis unit gives either a clear signal, or an alarm signal. If an alarm signal is given, the type of explosive found and the relative strength of the signal is indicated.

EGIS consists of two units, the sampling device and the analysis unit. The sampling device, shown in greater detail in figure 3, consists of a coil, lamp, pyrometer and rubber gasket on the front. The interior contains the blower and

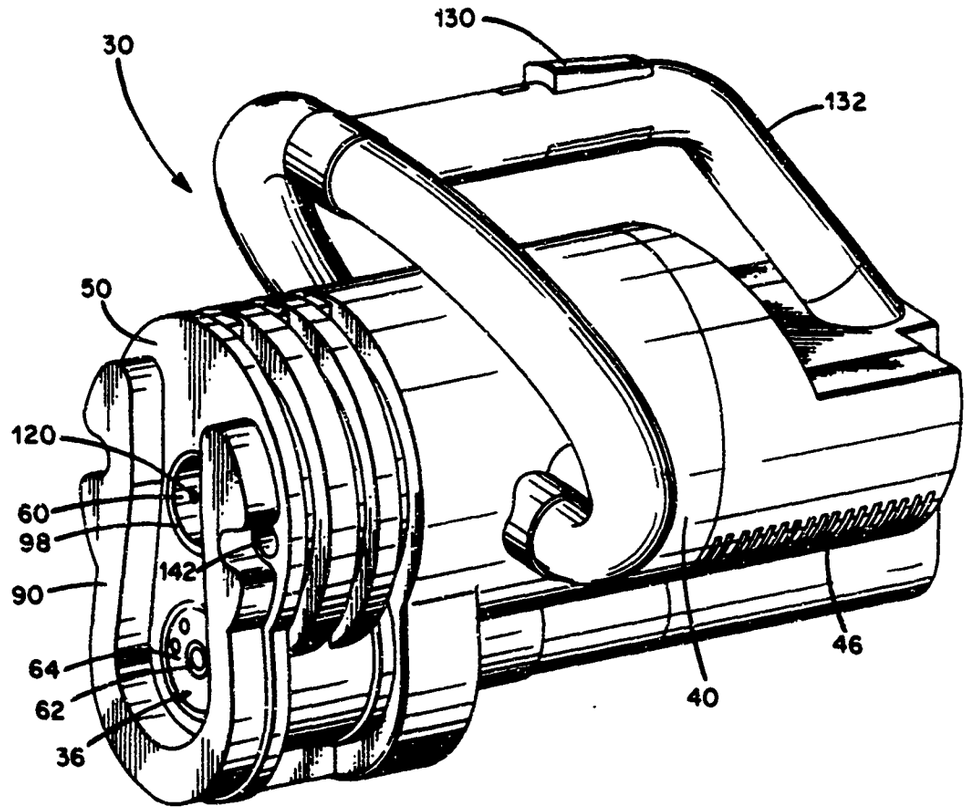


FIGURE 3. SAMPLING DEVICE
36 collector; 60 lamp; 90 rubber gasket;
130 power switch

electronics. Rechargeable batteries are connected at the rear of the unit. The unit can be operated in an air-only sampling mode, or in a heating, air sampling mode. If the sampling device is touching a surface when the trigger is pulled, as indicated by the closure of microswitches built in to the rubber gasket. the lamp comes on along with the blower. If the micro switches have not been closed, only the blower comes on. The pyrometer monitors the surface temperature to make ensure that the lamp does not overheat a surface, causing damage.

The analysis unit consists of an interface, which connects the sampling device to the analysis unit; the chemistry module, which houses the sophisticated classified chemistry; the chemiluminescence detector, pumps, heaters and electronics. The complete system is under computer control. Although the chemistry used is very sophisticated, the analysis is easy, since the on board computer handles all the data reduction and interpretations. Non-technical personnel can be successfully trained to use the device. Minimal interpretation is required by the user.

In order to take a sample, the user brings the sampling device up to the object to be sampled. The trigger is then pulled, and the sampling device automatically takes a sample. The sampling device shuts off when an adequate sample has been taken, typically 5-7 seconds. Multiple samples can be taken prior to an analysis. For example in order to properly sample a vehicle, samples should be taken at different parts of the vehicle. In sampling luggage, all luggage associated with a given passenger could be sampled

prior to performing the analysis.

Upon completion of the sampling, the sampling device is connected to the analysis device. The analysis begins with the sample being transferred to the analysis device, where the sophisticated chemistry takes place. Currently the analysis time is approximately 30 seconds. Encouraging preliminary work has been performed that indicates that the target goal of 15 seconds should be achievable. Ten seconds after the beginning of an analysis, the sampling device may be removed, and, used to take additional samples. After the analysis is completed, either a clear, alarm, or retest message is given on the display panel. If an alarm is given, the type of explosive found is indicated, as well as the relative strength of the signal found. As previously discussed, the strength of the signal and the size of the explosive device do not necessarily correlate. EGIS contains many transducers, and sophisticated internal diagnostics which continually monitor the operation of the unit, giving an error message if a malfunction is determined.

## EGIS Evaluation

Extensive evaluation of EGIS has been performed at Thermedics using vapor generators. By very careful preparation, it has been possible to produce pure samples of each individual explosive, and thus to determine the absolute lower detection limit for each of the explosives of interest. These tests are performed by bringing the EGIS sampling device up to the vapor generator, sampling for a

given time, typically 5 - 10 seconds, and then analyzing the sample collected. From the known discharge rate of the vapor generator, and the sampling time, the lower detectable limit can be calculated. Based upon these tests, it has been demonstrated that EGIS meets or exceeds the requirements implied by Table 1.

In order to test for selectivity, EGIS has been challenged with different types of potential interferences as listed in Table 3. EGIS was tested by sampling the potential interferences alone, and with explosives, in order to determine both positive and negative response to the potential interferent. (A negative response would occur if the expected response to an explosive is reduced due to the presence of the potential interferent along with the explosive.) Any effects were below the lower detectable limit of EGIS.

In addition to testing for vapors, more practical, but also less objective tests were performed by constructing simulated bombs. Simulated bombs were assembled using actual explosives, without detonators. These bombs were assembled into luggage, radios, boxes etc. Some of these tests were double blind. Many were performed at Thermedics, while some were performed by independent observers. The results of these tests confirm that the technology used is capable of detecting even small amounts of plastic explosives hidden in suitcases. Based upon the test results, the most effective sampling protocols have been developed.

Table 3 - Representative List of Potential Interferences

| Substance | Where found |
|---|---|
| nitrogen oxides (gas) | Engine exhaust gases, air pollution, smog, tobacco smoke |
| sulfur dioxide (gas) | air pollution, smog |
| hydrogen sulfide (gas) | air pollution, smog rotten eggs |
| ammonia (gas) | smelling slats, cleaning agents |
| carbon dioxide (gas) | soft drinks, exhaust gases, tobacco smoke |
| fluorinated gases | rotten fish, industrial solvents |
| chlorinated solvents | dry cleaning fluids, degreasing materials |
| hydrocarbons | gasoline, jet fuel, lighter fluid, waxes |
| nicotine products | tobacco, snuff, chewing tobacco |
| nitro musks | perfumes, shampoos, after-shave, hairspray |
| nitrobenzenes | shoe polish |
| acetone, ketones | nail polish |
| ethanol | alcoholic beverages |
| methanol | gas, antifreeze |
| nitrosamines | pesticides, herbicides, tobacco smoke |
| amines | rotten fish, industrial solvents |
| acetic acid | vinegar, salad dressings |
| water vapor | high humidity |
| carbon monoxide (gas) | exhaust gases, tobacco smoke |
| organic esters | synthetic flavors |
| ethylene glycol | engine antifreeze |
| glycerol | lubricants |
| methane, propane | natural gas |
| naphthalene | moth balls |
| urethanes | varnish |
| ureas, uric acid | urine |
| hydrazines | anti-corrosion agent, rocket fuel |
| sodium nitrite | food preservatives |

## Applications of EGIS

While the initial, primary goal in developing EGIS for the Department of State was for use in screening vehicles, EGIS can also be used to screen packages, luggage, rooms, buildings and people. Thus in addition to being used to screen the entrance to embassies, EGIS is well suited for use at passenger and luggage check-in areas at airport or at any other high risk area.

In order to develop a search protocol for vehicles, computer models were generated to determine the optimum sampling sequence, which would minimize sampling time and that would lead to a reasonable probability of detecting a hidden bomb. An appropriate sampling sequence would involve using both the air and surface (lamp on) sampling modes. In screening a vehicle, one would sample surfaces such as the door, trunk lid, hood, and steering wheel, using the surface mode. One would also sample the trunk, passenger compartment, engine compartment, and wheel wells, using the air mode. Multiple samples of the vehicle would be taken prior to beginning the analysis. The total time to sample the vehicle is strongly dependent upon how thorough a search is being made.

In sampling packages and luggage, the outside surface of the item would be sampled using the surface mode. Experience has shown that if the package or luggage is opened, with a sample also being taken from the inside, the probability of finding any hidden device increases. In order to increase throughput, more than one item may be sampled prior to performing the analysis.

In sampling large areas such as rooms, one would take many air samples from different parts of the room. In addition, taking surface samples of areas likely to have been touched would increase the probability of finding any hidden devices.

In screening people, the sampler would be used in the air-mode only with a few samples taken from different areas of the persons clothing.

## Conclusions

With the development of EGIS, it has been demonstrated that vapor detection can be used to screen for explosives, including, but not limited to, plastic explosives. These conclusions are based upon the results of detailed tests performed by Thermedics, as well as performance and application testing performed by outside laboratories. Thus, EGIS can be added to the arsenal of weapons used against the rising terrorism to increase the security of the general public.

## Acknowledgements

Most of the work described here was performed under contract to the DOS, contract number 2038-563371. Additional funding was provided by FAA under contract number DTRS-57-84-C-00063. We would also like to thank Massport and the Massachusetts State Police, and Patrolman Jim Spriggs in particular, for providing the explosives used in the testing of the units, and for the input of much technical information.

## REFERENCES

1) M. M. Waldrop, Science, 243, (1989)

2) T. Gozani, R. E. Morgado and C. C. Seher, J. of Energetic Materials, 4, 377 (1986)

3) P. Neudorfl and L. Elias, J. of Energetic Materials, 4,415 (1986)

4) B. C. Dionne, D. P. Rounbehler, E. K, Achter, J. R. Hobbs and D. H. Fine, J. of Energetic Materials, 4, 447 (1986)

# LABORATORY EVALUATION OF PORTABLE AND WALK-THROUGH EXPLOSIVES VAPOUR DETECTORS

Lorne Elias and Pavel Neudorff

National Research Council Canada
National Aeronautical Establishment
Ottawa, Ontario K1A 0R6

## ABSTRACT

A total of thirteen different explosives vapour detectors has been quantitatively tested for their responce to certain nitroorganics, as part of an assessment of their overall efficacy in field use. Eleven of these instruments are housed in carrying cases for portability, two are designed as fixed-installation portals for personal screening. The methods used to determine the sensitivity or lower detection limit of the equipment is described, and the results presented.

The sensitivity to EGDN of the 'continuous', rapid-response (<5s) detectors ranged from about 1-100 ppb, while that of the batch-sampling, slow-response devices varied from 5-100 ppt. For the walk-through detectors, a vapour emission rate on the order of 50 µg/min was required to elicit a response, roughly comparable to the emission from an openly exposed stick of commercial dynamite.

## 1. INTRODUCTION

Explosives vapour detectors (EVDs), or bomb 'sniffers', have been in production now for nearly two decades. Intended to emulate the trained search dog in uncovering concealed explosives, it is evident that EVDs enjoy a captive, if somewhat limited, market, particularly in the area of aircraft security. It is also apparent, however, that the devices have met with only partial success in gaining widespread acceptance by security people as a reliable countermeasure to the bomb threat.

One reason for this reluctant acceptance probably has to do with the preconceived expectation, suggested by the term 'bomb detector', of an instrument that can unerringly respond to any and all explosive fillers, from matchheads to Semtex - an expectation, as it

turns out, far removed from reality. Another reason, though, may lie in the enthusiastic claims touted by some manufacturers of the equipment, which in practice have proven to be overly optimistic. Nevertheless, advances in EVD technology have been made, and sniffers are seen as a viable complement or, in some applications, as an alternative to trained canines.

In assessing the efficacy of a particular vapour detector, an evaluation independent of the manufacturer's information is clearly desirable. A number of simulated field studies involving the simultaneous testing of several EVDs have been conducted to provide this type of evaluation *(1-5)* , one of the more recent studies being reported at this Symposium *(6)*.

In addition to simulated field trials, we have found that laboratory evaluation of EVDs is a useful and important prerequisite in gauging the ultimate utility of an instrument. Laboratory testing, for example, allows the quantitation of the sensitivity (lower detection limit) of the detector, probably the single most important parameter, and can reveal any idiosyncrasies of the device prior to field use, under controlled conditions.

This paper details the testing protocol used in our Laboratory, and presents results of the evaluation of thirteen different EVD systems *(7)* carried out over a span of several years. In the present context laboratory evaluation encompasses determination of sensitivity to certain explosives, speed of response and the effects of potential interferants. Two classifications of EVDs are included, the man-portable, hand-operated type and the fixed-installation, automated portal system for personal screening.

## 2.0 EXPERIMENTAL

### 2.1 General Procedure

Sensitivity is measured by subjecting the instrument under test to known and controllable levels of the explosives vapours from a dynamic vapour source. In the case of the portable EVDs, sensitivity is defined as the minimum *concentration* for which a positive response is elicited at least 80% of the time, while with the walk-through systems sensitivity is better represented in terms of the minimum *mass flow* or emission rate of explosives vapour.

The explosives used in the quantitative work were ethylene glycol dinitrate (EGDN), nitroglycerine (NG) and 2,4-dinitrotoluene (DNT). The vapour pressures of these materials at 22°C as determined earlier in this Laboratory *(8)* are:

| | | |
|---|---|---|
| EGDN | - | 80,000 ppb(v/v) |
| NG | - | 300 |
| DNT | - | 250 |

NG and DNT were normally employed at room temperature, EGDN was usually maintained at 0°C, where its vapour pressure is 8,500 ppb (1 ppb = $10^{-9}$).

As part of the evaluation, the instruments also underwent some limited qualitative testing, by sampling air in close proximity to various commercial and military explosives as well as commonly encountered non-explosive, odorous substances.

## 2.2 Trace Vapour Source

A key element of the present evaluation procedure makes use of the headspace vapours generated by a test sample of explosive; the vapours are swept by a carrier flow of air which may be diluted by mixing with one or more auxiliary air streams, or used undiluted. With the explosive sample thermostated and the air flows metered, a continuous explosive vapour-in-air stream is provided in which the concentration level is controllable through adjustment of the air flow rates and temperature of the sample. A dynamic vapour generator of this type was first reported in *(9)*, and a more elaborate design operating on a similar gas-blending principle in *(10)*.

The test sample is housed in a glass U-tube holder between plugs of silanized wool, as shown in Figure 1. About 1/2 g of explosive sample in granular form or, in the case of liquid explosives, on rolled-up filter paper is packed loosely in the tube to allow intimate but unrestricted flow of the carrier gas. A multi-orifice jet outlet such as that indicated is effective in providing good mixing of the vapour-laden stream with the diluent stream. The holder is immersed in a water bath to the level of the tapered glass joint of the cap.

The design of the vapour source is relatively simple, yet versatile, inasmuch as it enables the use of both pure samples as well as real explosives; a similar design, for example,

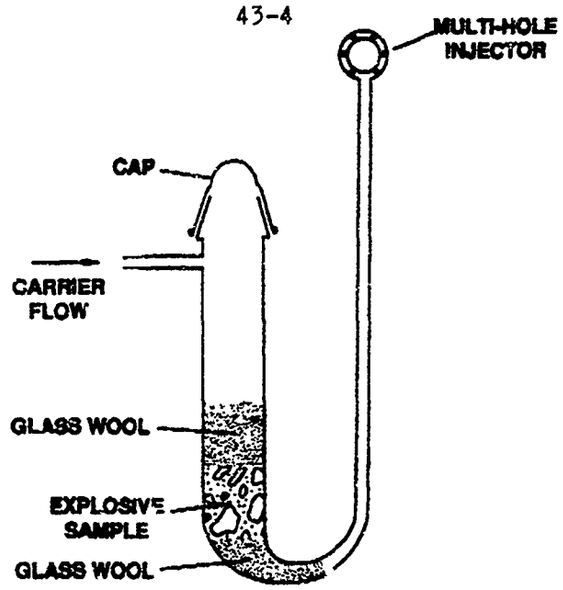


FIG. 1: GLASS U-TUBE SAMPLE HOLDER

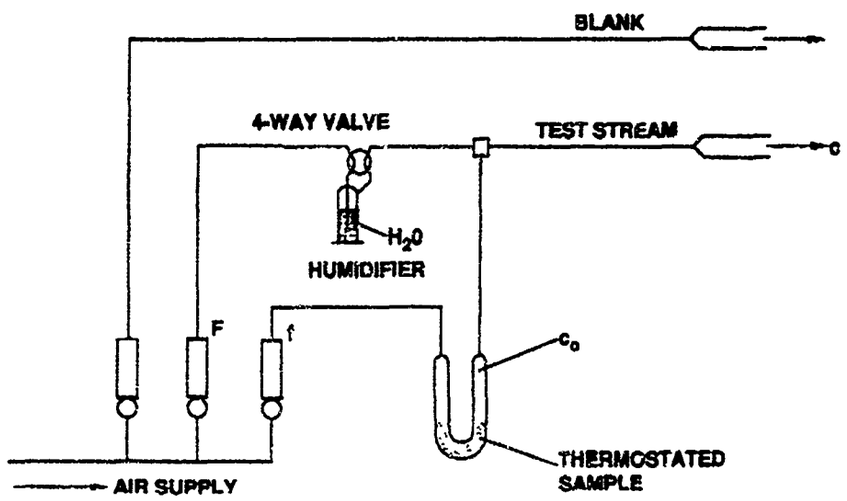


FIG. 2: SINGLE-STAGE TRACE VAPOUR SOURCE

$$c = c_o \frac{f}{F + f}$$

was used recently to study the volatile effluents from C4 and other plastic explosives *(11)*. It also has advantages over permeation-type sources in re-equilibrating more quickly following temperature changes in bath temperature, a wait period of 10 min usually being sufficient.

The carrier flow through the source is nominally in the range 1-100 mL/min. At these flow rates a quasi-equilibrium static vapour pressure is maintained over samples of EGDN, NG or DNT, as confirmed repeatedly by GC analysis of the effluent stream.

2.3 Single-Dilution Vapour Generator

When the effluent stream from the sample source is mixed with a larger air flow (of 2-20 L/min) as shown in the schematic arrangement of Figure 2, the concentration of explosive vapour $c$ in the test stream is given simply by

$$c = c_0 f/(F + f),$$

where $c_0$ corresponds to the equilibrium vapour headspace concentration at bath temperature, $F$ and $f$ are the diluent and carrier flow rates, respectively.

This single-stage dilution vapour generator could be used to provide test stream vapour levels in the low-to-high ppb range; for example, with EGDN in the sample holder immersed in an ice bath and flow settings adjusted to $f$ = 3 mL/min and $F$ = 15 L/min, a test stream concentration $c$ = 1.7 ppb is generated. Or, NG and DNT test streams in the low-to-sub ppb region could be obtained operating at 22°C bath temperature.

Water-filled gas wash bottles could be switched into the diluent line by means of a 4-way stopcock to simulate a high-humidity environment, which was of interest in evaluating the response of some of the instruments. An auxiliary clean air reference stream was useful for 'zeroing' purposes.

In testing the portable EVDs for minimum detectable concentration, the flow rate of the test stream was maintained well in excess of the intake flow rate of the detector, to avoid dilution by ambient air. The test stream sampling port, into which the probe of the EVD is barely inserted, is about 3 cm in diameter, large enough so as not to be restricted by the presence of the probe.

## 2.4 Double Dilution Vapour Generator

Some detectors, particularly those with a preconcentrator feature, require EGDN test streams of ppt concentrations (1 ppt = $10^{-12}$). While such low values are achievable with the previous single-dilution generator by employment of cryogenic bath temperatures, a more convenient method is one based on a two-stage dilution process, which requires only an ice bath thermostat.

The configuration depicted in Figure 3 allows the attainment of EGDN concentrations from less than 1 ppt to 1 ppb. The first-stage mixture, comprised of $(F_1 + f_1)$, is maintained at constant pressure, independent of the flow settings, by the 1 psig (*ca.* 7 kPa) check valve; most of the flow, in fact, is vented through the check valve and only a small fraction flows through the calibrated flow restrictor at a rate $f_2 = 4.0$ mL/min to mix with the second diluting stream $F_2$. For EGDN at 0°C, the test stream concentration (to a close approximation) is given by $c_2 = 34 f_1/F_1F_2$; a few examples of the flow settings used are indicated in the following table.

| $F_1$ | $F_2$ | $f_1$ | $c_2$ |
|---|---|---|---|
| 10.0 L/min | 17.0 L/min | 2.5 mL/min | 0.5 ppt |
| 2.0 | 4.2 | 2.5 | 10 |
| 2.0 | 4.2 | 25.0 | 100 |
| 0.5 | 1.7 | 25.0 | 1000 |

As with the single-dilution generator, all flow lines in contact with the explosives vapours, including the calibrated leak, are made of glass.

Both the single- and double-dilution generators operate with purified laboratory air as the carrier and diluent gases. The response of an EVD determined under the ideal conditions presented by these sources therefore represents the maximum sensitivity of the instrument to explosives vapours.

## 2.5 Single-Stage/Ambient-Air Vapour Generator

EVDs, of course, are intended for use in various field situations where they must contend with the prevailing background matrix of other vapours and gases. To gain insight on the capability of a detector in real-air sampling situations, recourse is frequently made in our Laboratory to a third design of vapour generator (*12*), a diagram of which appears as Figure 4.

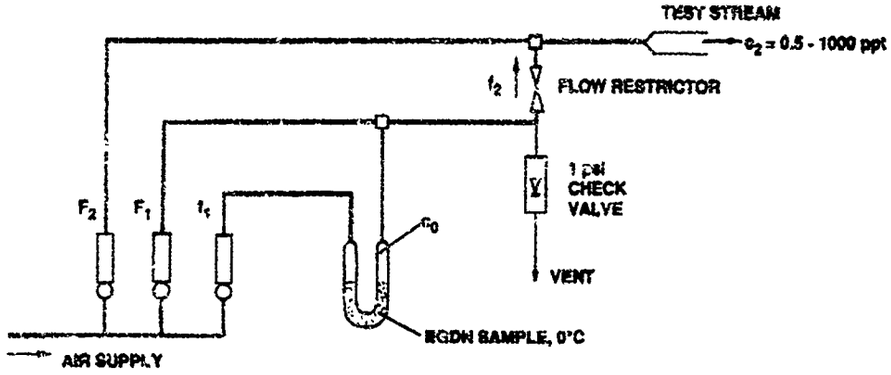


FIG. 3: DOUBLE-DILUTION EGDN VAPOUR SOURCE

$$c_2 = c_0 \frac{f_1 f_2}{F_1 F_2}$$

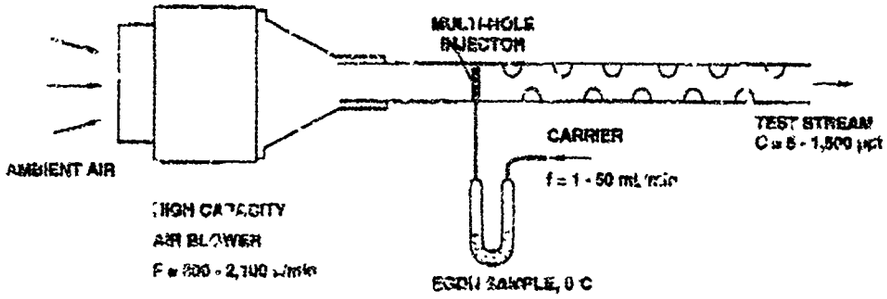


FIG. 4: SINGLE-STAGE/AMBIENT AIR VAPOUR SOURCE

This apparatus, originally constructed as a means to quantify the olfactory ability of trained canines, channels ambient air through a 5.5 cm O.D. glass pipe by means of a variable-speed, high-volume pump. A metered vapour stream is introduced into the flow as indicated, to provide a real-air test stream with a controlled explosive vapour content. Self-contained as a unit (except for power) and set on casters for ease of mobility, the 'dog box' generator can be located in a machine shop, warehouse or other area for a more realistic assessment of detector performance.

The importance of real-air *vs.* purified-air sampling has been observed particularly with the high-sensitivity EVDs employing vapour preconcentrators. One model when tested with the purified air stream of the double-dilution source exhibited a detection limit to EGDN of as little as 4 ppt; when subjected to the spiked air stream from the 'dog box', however, its performance degraded more than ten-fold because of background noise, and its sensitivity was found to be around 75 ppt.

## 2.6 Portable EVDs

The portable instruments tested were of two types: (a) the continuous, fast-acting devices based on electron-capture detection (ECD) or ion mobility spectrometry (IMS), usually in conjunction with semi-permeable membranes, and (b) the slower, batch-sampling, gas chromatographic (GC) equipment with ECD, utilizing vapour preconcentrators. The air sampling flow rate in most cases was of the order of 1 L/min, and readily accommodated with any of the three vapour generators above.

The response to some common spoofing agents, including toilet, cleaning compounds, foods and solvents, about 40 in all, was qualitatively investigated by sniffing the openly exposed material.

Seven different EVDs of type (a) and four of type (b) have been tested and are reported on here.

## 2.7 Walk-Through EVDs

The variety of walk-through detectors is far less than that of the portable devices, although the concept is attractive for airport and power plant security purposes, and several development projects in the area are underway. The airport scenario presents considerable

detection challenge, in that sampling time is limited (*e.g.*, 6 s/passenger) and sample dilution is very large.

Two portal screening systems have been evaluated to date, both utilizing a high-volume air curtain to transfer explosives vapours from the 'passenger' under scrutiny to the analyzer. Because the flow rates involved in each case (>2,000 L/min) are larger than could be supplied by the above vapour generators, detector sensitivity is measured in terms of the mass flow of vapour rather than the steady-state concentration emitted by the generator. Moreover, not all the vapour emitted by the source is entrained by the air curtain and swept into the analyzer. Depending on the proximity of the source to the sample intake openings of the portal, an indeterminate proportion of the vapour is lost to the ambient atmosphere.

In evaluating the walk-through systems, an EGDN-filled source as shown in Fig.1 was used, without dilution and operated at room temperature. Carrier gas flows of 10-100 mL/min provided EGDN mass flows in the required μg/min range. The source was carried by the 'passenger' into the portal and maintained at some fixed position in the air curtain for the prescribed sampling time, 6 or 12 s; source position was varied vertically and laterally to assess the uniformity and efficiency of the portal sampling. Step changes in vapour emission rate were effected during the tests by simply unattaching then re-attaching a charcoal trap to the outlet of the U-tube as required, while maintaining the carrier flow.

Tests were also conducted with the walk-throughs using hundred-gram quantities of real explosives carried by the subject. The types of explosives used were determined from preliminary trials measuring the inherent sensitivity of the analyzer, in which the vapour source was placed directly in the sampling manifold of the detector. Only those materials which produced a sizable signal in these preliminary runs were used in the walk-through tests.

## 3.0 RESULTS AND DISCUSSION

### 3.1 Portable EVDs

Table 1 summarizes the test results on instrument sensitivity, speed of response and specificity, in respect of EGDN vapour. The sensitivity ratings for the portable devices, as indicated earlier, are given in terms of the minimum detectable concentration of explosive.

Models A-G are the continuous-sampling (fast) type, Models H-K are the discrete-sampling (slow) detectors. The response time of the fast models is the time required to elicit a positive signal following introduction of a stepwise concentration of the vapour into the sampling probe of the device. The response time of the slow EVDs refers to analysis time only, following injection of the collected sample; for the latter four cases shown, a sampling time of 15 s was used. With all EVDs (A-K) the criterion for positive response at a given vapour level was 8 'hits' out of 10 trials.

The 'Relative Specificity' of the detectors to EGDN is based on qualitative testing conducted with some non-explosive materials, mainly those known from past experience to trigger an 'Alarm' response in EVDs, which include cosmetic products (perfumes and deodorants), dry cleaning solvents and oils and waxes.

With the exception of Models A, B and K, all EVDs are comprised of two main components, a sampling head and valise-size analyzer unit, interfaced by means of an umbilical line (1-2m long) housing electrical leads and gas lines.

TABLE 1. PORTABLE EVD RATINGS FOR EGDN DETECTION

| *Model Code* | *Operating Principle* | *Min. Detectable Concentration* | *Response Time* | *Relative Specificity* |
|---|---|---|---|---|
| A | IMS | 110 ppb | 1 s | poor |
| B | IMS | 25 | 1 | poor |
| C | mb/ECD/ECD | 30 | 2 | fair |
| D | mb/ECD | 2.5 | 1 | poor |
| E | pr/ECD | 0.9 | 3 | fair |
| F | mb/IMS | 0.8 | 3 | good |
| G | mb/ECD/ID | 0.7 | 1 | poor |
| H | pr/GC/ECD | 0.1 | 25 | very good |
| I | pr/GC/ECD | 0.05 | 30 | very good |
| J | pr/GC/ECD | 0.05 | 25 | very good |
| K | pr/GC/ECD | 0.005 | 150 | excellent |

Abbreviations:

| | | | | | |
|---|---|---|---|---|---|
| IMS | - | Ion Mobility Spectrometry | pr | - | Preconcentrator |
| mb | - | Membrane | GC | - | Gas Chromatography |
| ECD | - | Electron Capture Detector | ID | - | Ionization Detector |

The tradeoff in sensitivity and specificity for speed of response is clearly evident in comparing the data of the fast- and slow-response detectors, and within the class of slow types alone. The continuous EVDs have response times of a few seconds, poor-to-good selectivity, and a lower detection limit in the 1-100 ppb range; the GC-based instruments, on the other hand, are a few orders of magnitude more sensitive, considerably more specific, but require 0.5 - 3 min per analysis. Model K, the most sensitive and specific of the EVDs tested, is also the slowest.

The continuous samplers are generally equipped with a manual- or auto-zero adjustment to compensate for background contamination levels (such as may be encountered in a smoky area or sealed room), a feature which is not necessarily advantageous. When the contamination levels are significant these models suffer a deterioration in sensitivity, as observed on occasion when testing with the ambient-air vapour source (*cf.* Sec. 2.5).

Models A,B and F are IMS-based detectors. A and B were the most compact and simplest to use of all the EVDs, but were found to be the least effective in terms of poor selectivity and sensitivity, being of rudimentary design. In contrast, the more sophisticated IMS unit Model F provided a comparatively low limit of detection combined with good specificity. When subjected to high-humidity testing, the latter underwent some loss in sensitivity. Figure 5 illustrates the loss in response of detector F due to humidity, and the loss from prolonged sampling due to auto-zeroing.

Model F, and Model C which employs a novel twin-ECD configuration, are designed to respond to NG and DNT vapours as well as EGDN; the measured sensitivities are shown in Table 2.

TABLE 2. MODELS *C* AND *F* RESPONSES TO EGDN, NG AND DNT

| | *Sensitivity* | |
|---|---|---|
| *Vapour* | *Model C* | *Model F* |
| EGDN | 30 ppb | 0.8 ppb |
| NG | 0.5 | 2 |
| DNT | 3 | 3 |

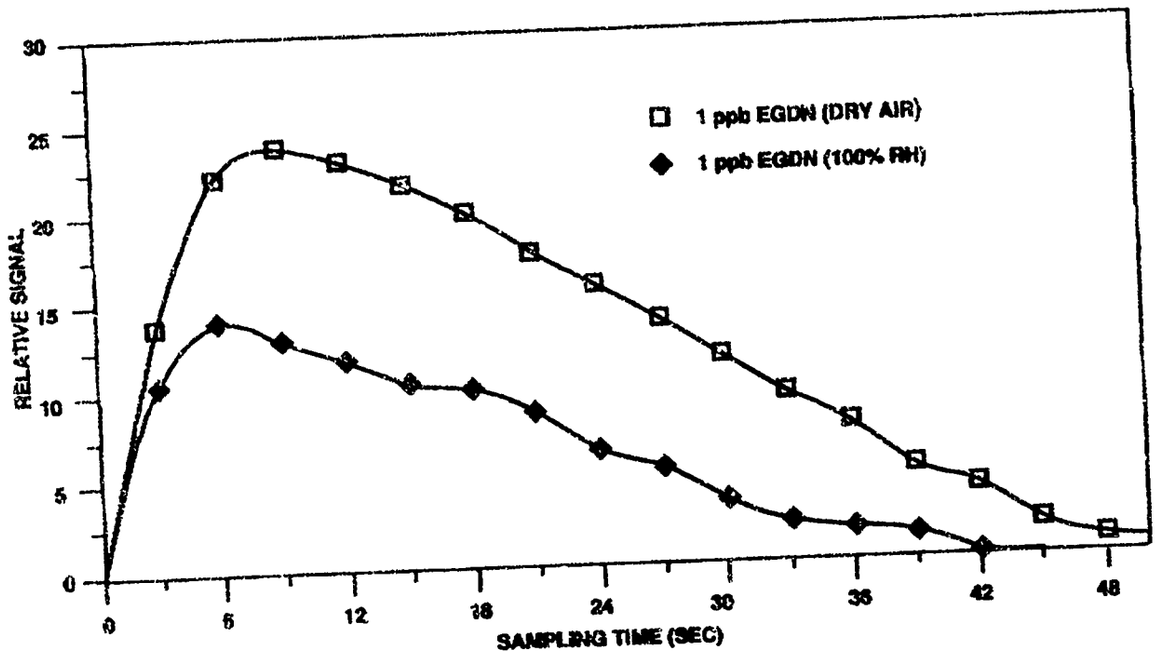


FIG. 5: EFFECT OF HUMIDITY AND SAMPLING TIME ON DETECTOR RESPONSE TO EGDN, MODEL F

The use of an ionization detector in series with an electron-capture detector (ECD) as embodied in Model G resulted in a four-fold improvement in sensitivity over a similar device with ECD only, Model D, but no improvement in specificity.

A common feature of the GC Models H,I and J is the use of a wire preconcentrator having a specially treated surface. This form of vapour adsorber has the advantage of effecting a simple, rapid means of thermal desorption through resistive heating. The wire preconcentrator, however, has a somewhat limited collection and retention efficiency. A series of runs was made with Model J in which sampling was alternated between a vapour stream from the Double-Dilution Generator (Sec. 2.4) and room air; these tests were intended to simulate the non-homogeneous, real-air conditions in a search scenario where, for instance, a 15 s 'sniff' of suspect luggage may encompass an explosives vapour plume in one localized area and explosives-free air in another. The results of this testing are presented in Figure 6, showing a 'washing-out' effect of the collected vapours by explosives-free room air. By comparison, the packed adsorber tube utilized in Model K to preconcentrate the vapours requires a longer desorption cycle but is not subject to such losses.

The batch-sampling EVDs, despite the time penalty associated with them, may offer advantages in certain applications. Model K, for example, is designed with a lightweight hand probe separate from the analyzer to facilitate off-sensor sampling; Model J can also be adapted to operate in this fashion. Further, Models H and J provide an option for unattended operation in a continual cycling mode, *i.e.*, repetitive sampling and analysis, for fixed-position monitoring applications.

### 3.2 Walk-Through EVDs

The results for the two systems evaluated in this study are summarized in Table 3 (*cf.* Table 1 for abbreviations).

TABLE 3. WALK-THROUGH EVD RATINGS FOR EGDN DETECTION

| *Model Code* | *Operating Principle* | *Min. Detectable Mass Flow* | *Response Time* | *Relative Specificity* |
|---|---|---|---|---|
| L | nib/ECD | >60,000 ng/min | 6 s | poor |
| M | pr/ECD | 38,000 | 12 | fair |

**FIG. 6: SENSITIVITY TESTING OF EXPLOSIVES DETECTOR MODEL J:**
**SAMPLING VIA PRECONCENTRATOR/VAPOUR COLLECTOR**

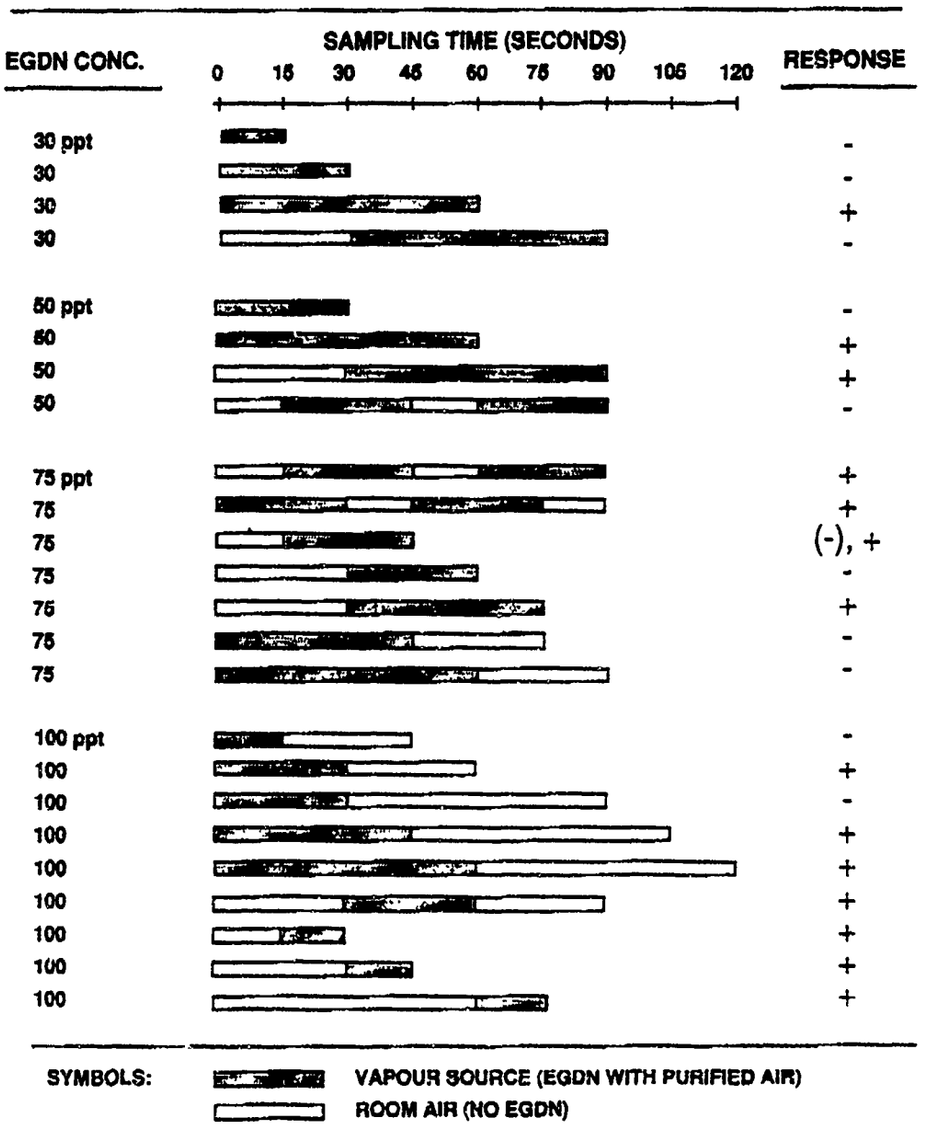

The sensitivity, reckoned as the Minimum Detectable Mass Flow of EGDN needed to trigger an 'Alarm' indication, was highly position-dependent; both systems, particularly Model L, exhibited 'blind' spots where no detection was possible within the emission range of the vapour source. For comparison, the emission rate of EGDN from an average stick of commercial dynamite, openly exposed, is approximately 50 µg/min (*13*).The values shown above represent the sensitivity of the EVDs at which the probability of detection was *ca.* 80%. Figure 7, depicting some test results for Model M, exemplifies the non-uniform sampling field of the portals and the dependence of detection on the quantity and location of the explosive in the air curtain.

Both EVD systems rely on a high-volume air curtain flowing transversely across the subject to sweep any explosives vapours to the analyzer located on the downwind side of the flow. Model L utilizes a series of fans on both sides of the portal operating in a push-pull fashion to move a total volume of air of about 10,000 L/min, with three sensor heads being arranged vertically between the fans to sample a portion of the curtain. Model M channels the air flow from a single large blower having a capacity of 2,400 L/min through manifolds to vertical slits on the sides of the portal in a similar push-pull manner, but in this case, the entire flow is sampled through the sensor, which consists of an on-line preconcentrator and ECD.

A comparison of the total system sensitivity given above with the inherent sensitivity of the sensor may be drawn for each unit. The minimum mass flow of EGDN detectable when the vapours were introduced directly into the intakes of the analyzer heads were 0.03 ng/min and 1,100 ng/min, respectively for Models L and M. However, the greater inherent sensitivity of the former is offset by a dilution factor (and sampling inefficiency) of more than $10^6$-fold in portal operation, whereas the disparity between the basic and overall sensitivity of Model M is less than a factor of 40.

Nevertheless, the effects of dilution in high-volume sampling impose severe limitations on sensitivity even in the case of Model M, when compared to the sensitivity achieved with the low-volume, portable EVDs. Table 4 lists the minimum detectable mass flows of EGDN and the sampling flow rates used for these two classes of continuous-sampling detectors. A general trend toward degrading sensitivity (and specificity) with increasing sampling flows is apparent.

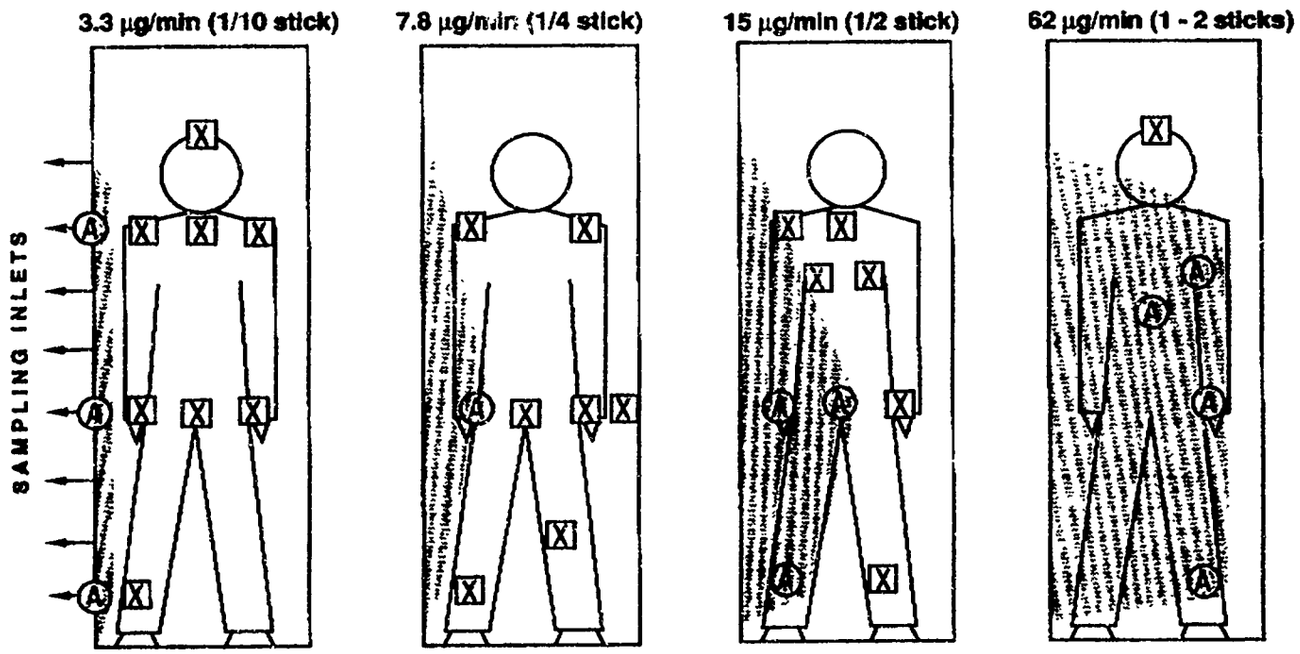


**FIG. 7: SENSITIVITY TESTING OF WALK-THROUGH EXPLOSIVES DETECTOR MODEL I.**

EGDN RELEASED FROM VAPOUR SOURCE AT DIFFERENT LOCATIONS INSIDE PORTAL GENERATED ALARM (A), OR NO ALARM [X], DEPENDING ON EMISSION RATE. FOUR EMISSION RATES (µg/min) SHOWN, WITH APPROXIMATE QUANTITIES OF DYNAMITE REQUIRED TO PRODUCE SIMILAR EMISSION; SHADED AREAS INDICATE WHERE GIVEN QUANTITY OF DYNAMITE COULD BE DETECTED WITH > 90% PROBABILITY.

TABLE 4. COMPARISON OF WALK-THROUGH AND PORTABLE EVDs

| *Model Code* | *Sampling Flow Rate* | *Min. Detectable Mass Flow* | *Relative Specificity* |
|---|---|---|---|
| L | 10,000 L/min | >60,000 ng/min | poor |
| M | 2,400 | 38,000 | fair |
| A | 10 | 6,200 | poor |
| B | 10 | 1,500 | poor |
| C | 0.4 | 76 | fair |
| D | 1 | 16 | poor |
| E | 1.5 | 9 | fair |
| F | 1 | 4 | good |
| G | 1 | 4 | poor |

## 4.0 CONCLUDING REMARKS

The laboratory testing described above has been useful in revealing the strengths and weaknesses of the various EVDs. Rating them in terms of sensitivity, specificity and speed of response, no one instrument emerges as the ideal, universal detector suitable for all field situations, one that is both fast *and* sensitive to explosives. The requirement of real-time detection obviously exacts a sizeable penalty in the lower limit of detection and selectivity achievable when the time factor is not a constraint.

The time factor, however, is always a prime consideration in bomb detection, and, therefore, a choice must be made as to the relative importance of speed of response and reliability (*i.e.*, sensitivity and specificity) of detection in a particular scenario. In screening individual items such as baggage or parcels prior to loading on a departing flight, for instance, it can be argued that a number of false positives is a reasonable tradeoff for the speed of screening provided by the continuous-sampling EVDs; the counter argument, on the other hand, is that the sensitivity of the real-time instruments is such as to limit their utility to the detection of rather large dynamite bombs which may be concealed in the baggage.

Even the 'ideal' detector, however, may be no better in field use than a less-than-ideal device, depending on the skill and dedication of the operator. The development of automated walk-through EVDs represents an attempt designed, at least in part, to eliminate the reliance on operator skill. The two models evaluated in this study, however, appear to be of marginal effectiveness, and if this type of screening is desirable a radical new concept is required.

Most of the evaluation work reported here has centered on EGDN as the target vapour, for two reasons. For one, EVDs are effective primarily as EGDN detectors, owing to the relatively high vapour pressure of the material. Secondly, EGDN is probably the single most commonly encountered vapour characteristic of explosives, abundant in the headspace of commercial dynamite and also associated in trace amounts with many non-dynamite explosives, including plastics (*11,14*). This last fact takes on new relevance in light of the current concern with Semtex and other plastic explosives.

In the authors' opinion, detection of plastic explosives based on vapour detection of the parent compounds, *e.g.*, RDX or PETN, is an approach unlikely to succeed in actual search applications, where dilution and barrier effects can significantly reduce the available headspace levels (*ca.* 10 ppt), probably by 3-5 orders of magnitude. A more viable approach may be to focus efforts on detection of the more volatile EGDN contaminant.

Of course, EVD technology, with all its foreseeable advances, is not a panacea to the hidden bomb threat, but one more technical aid in an arsenal of countermeasures that merits continuing development.

## 5.0 ACKNOWLEDGMENTS

We are grateful to Transport Canada for their longtime support of this work, and to D. Wilson of that department for his help in conducting the tests. Our thanks also to J. Arnold of the Public Safety Management Office of NRC.

## 6.0 REFERENCES

1. G. Seman and L. Elias, "Detection of Hidden Explosives on Passeng Aircraft Using Hand Searchers, Biosensors and Vapour Detectors", in Proc. New Concepts Symposium and Workshop on Detection and Identification of Explosives, sponsored by U.S Depts. of Treasury,Energy, Justice, and Transportation, Reston, VA., p. 119-138 (1978).

2. G.A. Wild, "Comparative Trials of Some Commercial Explosives Detectors", RARDE Technical Report 10/80, Royal Armament Research and Development Establishment, Fort Halstead, U.K., 1980.

3. W.D. Williams and J.S. Syverson, "Explosives Detector Field Tests", Report of Research and Development Division, BATF, U.S. Dept. of Treasury, Washington, D.C., 1981.

4. M. Asselin and R. Voyzelle, "Evaluation of Three CommercialExplosives Detectors", DREV Report 4195/81 (Restricted), Dept. of National Defence, Ottawa, Canada, 1981.

5. R.J. Mathews, "Survey of Explosives Vapour Detectors", Report of Materials Research Laboratories (Commercial-in Confidence), Dept. of Defence, Melbourne, Australia, 1987.

6. D. Fetterolf, "FBI Laboratory Evaluation of Portable Explosives Vapor Detectors", presented at 3rd Int. Symp. on Analysis and Detection of Explosives, Mannheim-Neuostheim, FRG, July, 1989.

7. The EVD models tested in this study were or are commercial units; the names are not specified for proprietary reasons, but can be made available on a need-to-know basis.

8. M. Authier-Martin, M. Krzymien and L. Elias, "GC Determination of the Vapour Pressures of Explosives", NRC Report LTR-UA-60, National Research Council, Ottawa, Canada (in preparation).

9. M. Krzymien and L. Elias, "A Continuous-Flow Trace Vapour Source", J. Phys. E: Scientific Inst., Vol. 9, p. 584-86 (1976).

10. P.A. Pella, "Generator for Producing Trace Vapor Concentrations of 2,4,6-Trinitrotoluene, 2,4-Dinitrotoluene, and Ethylene Glycol Dinitrate for Calibrating Explosives Vapor Detectors", Anal. Chem., Vol. 48, p. 1632-37 (1976).

11. G. Scaiano and L. Elias, "Characterization of Explosives Vapours", NRC Report LTR-UA-XX, National Research Council, Ottawa, Canada (in preparation).

12. P. Neudorfl and L. Elias, "Research Programme on Explosives Vapour Detection at NRC", J. Energ. Materials, Vol. 4, p. 415-446 (1986).

13. C. Pate, " Characterization of Vapours Emanating from Explosives", Final Report No. J-LEAA-025-73, U.S. Dept. of Justice, p. 90 (1976).

14. A. Linenberg, "Detection of Vapors of Explosives by Tracing aTypical Common Vapor Using Preconcentration Gas ChromatographyTechnique", in Proc. New Concepts Symposium and Workshop Identification and Detection of Explosives, sponsored by U.S. Depts of Treasury, Energy, Justice, and Transportation, Reston, VA p. 269-276 (1978).

# PYROTECHNIC FLASH COMPOSITIONS

U. Krone
NICO Pyrotechnik, Hanns-Jürgen Diederichs GmbH & Co. KG, Trittau

H. Treumann
Bundesanstalt für Materialforschung (BAM), Berlin

## ABSTRACT

In general, pyrotechnic compositions are more sensitive than commercial explosives, regardless the type of the stimulus. On the other hand, their explosive strength is considerably smaller. But some of the pyrotechnic compositions come close to the explosive effects of commercial explosives, flash compositions for example.

Flash compositions are used in fireworks as well as in pyrotechnic articles for technical purposes like report signals, battle simulation and practice devices, birdscaring ammunition and anti-riot-devices for instance.

The special hazards in manufacture and use of these compositions result from the above-mentioned combination of both a high sensitivity and a strong explosive effect. The paper presents the safety characteristic data of some flash compositions (thermal and mechanical sensitivity and sensitivity to detonation shock). In particular, the explosive strength of flash compositions is compared with some values found for commercial explosives.
Furthermore a comparison between a potassium perchlorate-aluminium-mixture and trinitrotoluene is made on the basis of shock wave measurements.

The conclusion is that the public security may be considerably endangered by the abuse of pyrotechnic flash compositions, because they are able to explode even without confinement, but do not need a detonator.

Problems of detection and analysis of the flash compositions and their reaction products will be discussed.

# VERFAHREN ZUR ENTSCHÄRFUNG VON BOMBEN NACH DER LOW-ORDER-SPRENGTECHNIK

Martin Volk, Wolfgang P. W. Spyra

Der Polizeipräsident in Berlin
Direktion Polizeitechnische Untersuchungen
D - 1000 Berlin 62

## Z U S A M M E N F A S S U N G

Die Kampfmittelräumdienste finden auch heute noch Munition aus früheren Kampfgebieten. Besonders gefährliche Rüstungsaltlasten sind Bombenblindgänger. Zur Entschärfung dieser Bombenblindgänger stehen dem Feuerwerker eine Vielzahl von Methoden zur Verfügung über deren Einsatz allein die Zweckmäßigkeit entscheidet. Gegenüber der Behandlung eigener, bekannter Munition birgt unbekannte und oftmals ungleichartige Fundmunition für die Kampfmittelräumdienste zusätzliche Risiken in sich. Insbesondere weisen die Produkte des letzten Weltkriegsjahres erhebliche Abweichungen auf.
Aus Gründen der Arbeitssicherheit ist der Einsatz von Fernentschärfungsmethoden vorrangig. Es wird eine modifizierte Low-Order-Sprengtechnik vorgestellt, die den Fernentschärfungsmethoden zuzuordnen ist. Diese Methode sieht vor, daß die Hauptladung angebohrt, geprüft und mit einer definierten Sprengladung so angeregt wird, daß die Bombenhülle lediglich geöffnet wird. Eine Volldetonation (High-Order) der Hauptladung tritt nicht ein.

...

## 1. EINFÜHRUNG

In der Bundesrepublik Deutschland einschließlich Berlin (West) werden jährlich durchschnittlich 1 000 t Rüstungsaltlasten durch die Kampfmittelräumdienste von Bund und Länder geborgen und vernichtet. Darunter befinden sich eine Vielzahl von Sprengkörpern, meist Blindgänger, die wegen der Transportunsicherheit durch Feuerwerker vor Ort gesprengt oder entschärft werden müssen.

Der Zustand von Bomben, die als Hauptladung 50 kg Sprengstoff und mehr enthalten, stellt nach mehr als 4 Jahrzehnten unkontrollierter Ablagerung eine lebensbedrohende Gefahr dar.

Bereits der bestimmungsgemäße Umgang mit Munition ist gefährlich und erfordert Sachkunde. Das Gefahrenmoment steigert sich erheblich, wenn Munition, wie Bomben, Granaten, Minen, u. a. m. unkontrolliert Umwelteinflüssen über eine lange Zeit ausgesetzt sind. Chemische Reaktionen der eingebrachten Komponenten können zur Bildung von besonders empfindlich reagierenden Substanzen führen, wie Azide und Pikraten.

## 2. THEORETISCHER ANSATZ

Die Überlegungen, die zu dieser Entschärfungsmethode geführt haben, basieren auf Beobachtungen aus der Kampfmittelbergung. Allgemein bekannt sind Blindgänger, die von außen keine Deformation der Bombenhülle erkennen lassen. Daneben gibt es Funde von Bombenblindgängern, bei denen die Bombenhülle geöffnet ist und die Hauptladung sich offenkundig nicht umgesetzt hat. Die Erklärung findet sich in der Regel darin, daß der Bombenkörper auf eine harte Materie aufgeschlagen ist und so die Materialdehnungsgrenzen überschritten wurden.

...

In der Praxis spricht man von sogenannten Zerschellern. Das klassische Beispiel eines Zerschellers zeigt das Bild 1. Dieser Blindgänger, eine MC 1 000 (US)-Bombe, traf auf eine Gleisanlage. Die Öffnung der Bombenhülle ist in der gezeigten Weise mit den klassischen physikalischen Vorgängen eines Auftreffens der Bombe auf die Eisenkante der Gleisanlage erklärbar. Die Elastizitätsgrenze des Materials wurde überschritten.

Bild 1: Bombenblindgänger Typ Zerscheller

Dieser vielfach uneingeschränkt vertretenen Zerscheller-Theorie stehen Erkenntnisse aus anderen Funden von Bombenblindgängern entgegen.

...

Seltener ist ein Fund, wie er in dem Bild 2, einer Collage einer britischen GP 1 000-Bombe, gezeigt wird. Der Körper wurde nahezu senkrecht im Boden steckend aufgefunden. Das Kopfteil der Bombe ist unversehrt, während das bezünderte Heckteil geöffnet ist. Die Hauptladung ist ebenfalls offenkundig unumgesetzt. Die ursprüngliche Bombenform einschließlich des Bodenzünders ist zeichnerisch dargestellt.

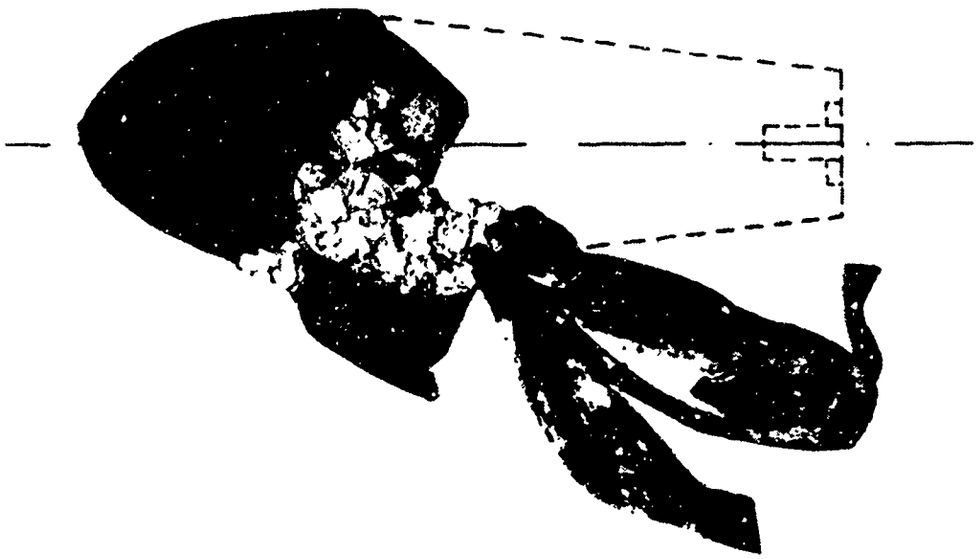

Bild 2: Collage, Geöffneter Bombenblindgänger und Bombenschema

Das gezeigte Schadensbild ist mit den Vorstellungen zu der Zerscheller-Theorie nicht mehr erklärbar.

...

Bei genauerer Untersuchung stellt man fest, daß die Boosterstufe in der Zündkette: Anzündhütchen, Bleiazid (Übertragungsladung) und Tetryl (Verstärkerladung, Booster) nicht bestimmungsgemäß gearbeitet hat. Bekannt ist, daß es technisch bedingt zu Ausfällen in der Ablauffunktion von Zündketten kommen kann. In dem vorgestellten Fall hat die freigesetzte Energie aus einer Teilreaktion ausgereicht, um den Bombenkörper teilweise zu zerlegen. Sie war jedoch zu gering, um die Hauptladung zur vollen Umsetzung anzuregen. Die Bombe wurde durch eine Teilreaktion unwirksam. Diese Beobachtungen haben zu der Vorstellung geführt, daß die gezielte Herbeiführung des in Bild 2 gezeigten Schadensbildes ein gewünschtes Ergebnis bei der Unschädlichmachung von Bombenblindgängern sein könnte.

Dieses Ergebnis könnte unter folgenden Bedingungen bzw. bei der Realisierung folgender Randbedingungen erreicht werden:

a) Im Bombenkörper wird ein Druck erzeugt, der so groß ist, daß die Materialdehnungsgrenzen schlagartig überschritten werden.

b) Die Öffnung der Bombenhülle soll gezielt erfolgen, und zwar derart, daß der Sprengstoff der Hauptladung frei zugänglich ist. Splitterbildung ist unerwünscht.

c) Der Energieeintrag soll so gering gehalten werden, daß keine initiale Anregung der Hauptladung erfolgt.
Der Druck im Bombenkörper kann durch Sprengstoff erzeugt werden.

...

Wenn der Ansatz zu dieser Methode grundsätzlich richtig ist, müßte eine äußerst geringe Menge an Sprengstoff - bezogen auf die Hauptladung - ausreichen, um das Öffnen der Bombenhülle ohne Detonation der Hauptladung zu erreichen.
Um der Forderung nach schlagartigem Druckaufbau zu entsprechen, wurde zur Erzeugung der Aufbruchenergie ein Sprengstoff mit hoher Detonationsgeschwindigkeit gewählt: Tetranitropentaerythrit (PETN). Die Detonationsgeschwindigkeit beträgt 8 400 m/s, bei Schnuranwendung ca. 7 000 m/s. Zum einen sollte erreicht werden, daß die Anregung der Hauptladung möglichst kurz ist und zum anderen, sollte die Hauptladung entgegen der Absicht durch den noch vorhandenen Zünder zur Detonation angeregt werden, wäre die Bombenhülle zum Zeitpunkt der Initiierung der Explosion der Hauptladung durch den noch vorhandenen Zünder bereits geöffnet. Ein eintretender Schaden würde geringere Ausmaße haben.

## 3. DURCHFÜHRUNG DER ENTSCHÄRFUNGSMETHODE NACH DER LOW-ORDER-SPRENGTECHNIK

Den grundsätzlichen Aufbau dieser Methode zeigt die Prinzipskizze, Bild 3.

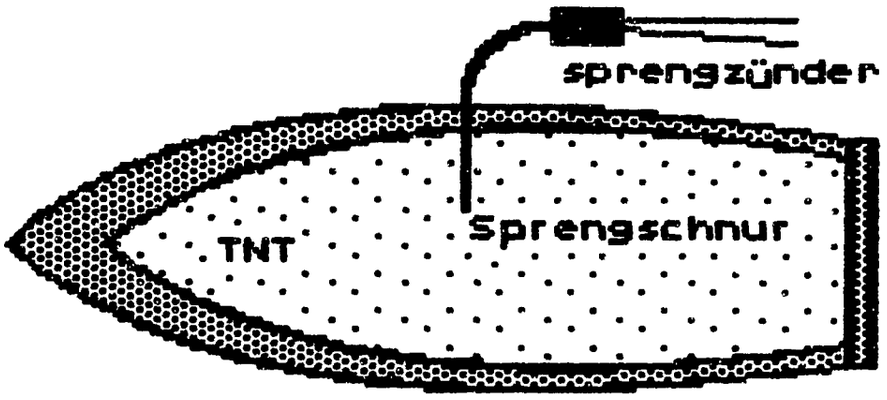


Bild 3: Prinzipieller Aufbau zur Entschärfung von Bombenblindgängern nach der Low-Order-Sprengtechnik

...

Jeder Entschärfung ist die zweifelsfreie Identifizierung der Munition voranzustellen. Gegebenenfalls auch durch Untersuchungsmethoden, die im Fall von Fremdmunition einen Aufschluß über den inneren Aufbau des Bombenkörpers, insbesondere des Zünders, erlauben.

Die zu erprobende Methode wurde fast ausschließlich an Bomben durchgeführt, die Trinitrotoluol (TNT) als Hauptladung enthielten.

Nach der beschriebenen Methode wird in den sicher gelagerten Bombenkörpern asymmetrisch, quer zur Längsachse, eine 8 mm-Bohrung niedergebracht. Eine Kühlung des Materials beim Bohrvorgang erscheint nicht erforderlich. Vergleichbare Belastungen des Hauptsprengstoffes waren in dem Herstellungsverfahren ebenso üblich, wie bei der Beseitigung von Großbomben mittels eingeführter Bombonschneidgeräte. Der Bohrvorgang kann ferngesteuert durchgeführt werden. Die Bohrung wird je nach Mantelstärke 100 - 300 mm in den Hauptladungssprengstoff geführt, wobei das Material der Hauptladung ausgetragen wird.
Damit erhält man zweifelsfrei Aufschluß über den tatsächlichen Ladungsinhalt.

Trifft man beim Bohren auf einen sogenannten Lunker, einen Hohlraum in der Hauptladung, so ist der Bohrvorgang an anderer Stelle zu wiederholen, sofern nicht die vorgenannte Kontaktstrecke von 100 - 300 mm erzielt werden konnte.
In das 8 mm-Bohrloch wird der Bohrtiefe entsprechend Standardsprengschnur geführt. Die verwendete Standardsprengschnur enthält 12, 5 g PETN pro Meter. Damit beträgt die eingebrachte Menge an PETN anteilmäßig 1,25 g bis 3,75 g.
Für die Kapselmontage außerhalb der Bombenhülle belassene Schnurlängen bleiben in der Berechnung unberücksichtigt. Die für eine funktionsfähige Booster-Ladung notwendige PETN-Menge liegt dem derzeitigen Erkenntnisstand zufolge bei mehr als 4 g, sofern TNT-Sprengstof festgestellt wurde.

...

Das Ergebnis einer Entschärfung nach der Low-Order-Sprengtechnik zeigt das Bild 4

Bild 4: Ergebnis einer Entschärfung nach der Low-Order-Sprengtechnik

In fast allen Experimenten wurde bei dieser Entschärfungsmethode der Zünder von der Hauptladung getrennt. Die Öffnung der Bombenhülle erfolgte stets in der Form, daß die Hauptladung frei zugänglich und in Stückenform vorlag. Die Öffnungslinie führte in jedem Versuch durch das Bohrloch.
Seit Oktober 1987 wurden 25 Bomben unterschiedlichster Herkunft nach der vorgestellten Methode entschärft.
Eine Übersicht gibt die Tabelle.

...

**Tabelle** - Versuchsergebnisse der Low-Order-Entschärfungsmethode, Polizei Berlin

| Versuch Nr. | Bombentyp | | Herkunft | Versuchs-Datum | Hauptladung (Optische Prüfung) | Order | Sprengstoff-PETN (g) |
|---|---|---|---|---|---|---|---|
| 1. | GP | 500 | (GB) | | TNT (typ.) | low | 3,5 |
| 2. | SD | 250 | (D) | 08.10.1987 | Ammonsalpeter weiß | low | 3,5 |
| 3. | Demo | 500 | (USA) | 08.10.1987 | TNT (typ.) | low | 3,5 |
| 4. | MC | 500 | (GB) | 08.10.1987 | TNT (typ.) | low | 3,5 |
| 5. | FAB | 250 | (SU) | 08.10.1987 | TNT (typ.) | low | 3,5 |
| 6. | GP | 500 | (GB) | 08.10.1987 | TNT (typ.) | low | 3,5 |
| 7. | FAB | 70 | (SU) | 08.10.1987 | TNT (typ.) | low | 2,0 |
| 8. | FAB | 70 | (SU) | 08.10.1987 | Granulat dunkelbraun | high | 2,0 |
| 9. | Demo | 300 | (USA) | 08.10.1987 | 1. TNT (atyp.)gelb-grün | high | 3,5 |
| 10. | FAB | 70 | (SU) | 08.1987 | TNT (typ.) | low | 2,0 |
| 11. | FAB | 70 | (SU) | 08.10.1987 | TNT (typ.) | low | 2,0 |
| 12. | FAB | 100 | (SU) | 12.04.1988 | TNT (typ.) | low | 3,0 |
| 13. | GP | 500 | (GB) | 12.04.1988 | TNT (typ.) | low | 3,5 |
| 14. | GP | 500 | (GB) | 12.04.1988 | TNT (typ.) | low | 3,5 |
| 15. | Demo | 500 | (USA) | 12.04.1988 | TNT (typ.) | low | 3,5 |
| 16. | SD | 250 | (D) | 09.08.1988 | TNT (typ.) | low | 3,5 |
| 17. | SC | 250 | (D) | 14.09.1988 | TNT (typ.) | low | 3,5 |
| 18. | SD | 75 | (D) | 21.09.1988 | TNT (typ.) | low | 2,0 |
| 19. | FAB | 125 | (SU) | 18.10.1988 | TNT (typ.) | low | 3,0 |
| 20. | GP | 500 | (GB) | 30.11.1988 | TNT (typ.) | low | 3,5 |
| 21. | MC | 500 | (GB) | 30.11.1988 | TNT (typ.) | low | 3,5 |
| 22. | FAB | 125 | (SU) | 30.11.1988 | TNT (typ.) | low | 3,5 |
| 23. | MC | 1 000 | (GB) | 22.03.1989 | TNT (typ.) | high | 5,5 |
| 24. | GP | 500 | (GB) | 29.03.1989 | TNT (typ.) | low | 1,0 |
| 25. | GP | 500 | (GB) | 23.05.1989 | TNT (typ.) | low | 1,25 |

In 3 Fällen erfolgte eine detonative Umsetzung, d. h. die Hauptladung wurde durch die eingebrachte, geringe Menge an Sprengstoff zur vollen Umsetzung gebracht. In 2 Fällen war eine von TNT abweichende Sprengstoffbeschaffenheit festgestellt worden. Die dritte Anordnung war mit einem höheren PETN-Anteil (5,5 g) versehen.

## 4. DISKUSSION DER VERSUCHSERGEBNISSE

In erster Linie ist auszuwerten, welche Erklärungen es dafür geben kann, daß in 3 Fällen von 25 die Methode nicht zu dem gewünschten Erfolg führte. Dazu ist es notwendig, einige nähere Betrachtungen zum Mechanismus der Methode aufzustellen.
Der ursprüngliche Gedanke der Methode liegt in der Annahme, daß die Erzeugung der Druckwelle in einem inkompresorblen Medium durch die angegebene Menge an Hochleistungssprengstoff ausreicht, um den Bombenkörper zu öffnen. Grobe Abschätzungen der Drucke, die bei einer Detonation in einem Bombenkörper entstehen, haben ergeben, daß - Materialdefekte außer acht gelassen - die Bombenhülle dem entstehenden Druck widerstehen müßte. Die Berechnungen wurden durch Experimente bestätigt.

Wir leiten daraus ab, daß die Hauptladung an dem Aufbau des notwendigen Druckes zur Überwindung der Materialkräfte beteiligt ist. Der Energieeintrag in das gegossene Trinitrotoluol ist an dem Zustand der Hauptladung erkennbar. Es ist wahrscheinlich, daß Vorgänge ablaufen, die den Anfängen einer Deflagration entsprechen. Die Anregung der Hauptladung bleibt aber unterhalb des notwendigen Energieeintrages für eine volle Anregung zur Umsetzung des Trinitrotoluols (TNT).

...

Wertet man die Versuchsergebnisse der Tabelle unter diesem Gesichtspunkt aus, so sind bei den Versuchen Nr. 8 und Nr. 9 andere Bedingungen zu unterstellen, als in allen anderen Fällen, ausgenommen Versuch Nr. 23. Die Hauptladungen der Versuche Nr. 8, dunkelbraunes Granulat bzw. Versuch Nr. 9: TNT Struktur mit gelb-grüner Farbgebung konnten nicht identifiziert werden.
Im Versuch Nr. 23 handelte es sich um die in Berlin nur noch sehr selten gefundene 1 000 lbs-Bombe britischer Herkunft. Zur Öffnung der Bombenhülle wurden ca. 5,5 g PETN eingebracht. Die Menge war damit mindestens doppelt so hoch, wie in allen übrigen Versuchen und reichte aus, um die Hauptladung zur Umsetzung anzuregen.
Die Auswertung dieses Versuches hat gezeigt, daß bei einer Ladungsmenge von 2 - 3 g PETN, wie sie bei der Versuchsreihe sonst üblicherweise verwendet wird, ein zufriedenstellendes Ergebnis im Sinne einer Entschärfung erwartet werden darf. Die Versuche für Bomben mit Hauptladungsmengen von über 250 kg Sprengstoff sind nicht abgeschlossen.

## 5. FAZIT

Die vorgestellte Methode der Entschärfung unter Anwendung der Low-Order-Sprengtechnik erscheint uns geeignet, hinreichend abgesichert zu sein für Bomben mit Trinitrotoluol (Hauptkomponente) als Hauptladungsmenge bis zu Ladungsmengen von 250 kg Sprengstoff. Sie trägt den Unwägbarkeiten von Fundmunition in besonderer Weise Rechnung.